Experimental Performance and Recommendations for Qualification of Post-installed Anchors for Seismic Applications

Von der Fakultät Bau- und Umweltingenieurwissenschaften
der Universität Stuttgart zur Erlangung der Würde eines
Doktor-Ingenieurs (Dr.-Ing.) genehmigte Abhandlung

Vorgelegt von

Philipp Mahrenholtz

aus Braunschweig

Hauptberichter:	Prof. Rolf Eligehausen
Mitberichter:	Prof. Tara Hutchinson
	Prof. Jan Hofmann

Tag der mündlichen Prüfung: 1. Juni 2012

Institut für Werkstoffe im Bauwesen der Universität Stuttgart

2012

Abstract

Ensuring the technical suitability of post-installed concrete anchors by means of pre-qualification has proved of great value over the last decades. A large variety of pre-qualified anchor products are available and designers, authorities and contractors can pick the most suitable and economic anchor product for the targeted use. While this system gained in general a high degree of refinement, the seismic application of anchors is still not well covered. For this reason, increased efforts were recently put on the research of seismic anchor performance.

The research presented in this thesis contributed its share. This thesis constitutes a systematic and comprehensive approach to seismic anchor qualification based on extensive investigations. The goal of this work is to close the gap in knowledge relating to seismic anchor behaviour to enable amendments to existing qualification guidelines by meaningful tests allowing the assessment of the seismic performance.

The initial scope of this thesis is to provide the foundation necessary to come up with a comprehensive scheme for the seismic qualification of post-installed anchors. After a brief introduction of the motivation, background and objectives of the research on anchors for use in seismic applications (Chapter 1), the state of the art of current qualification guidelines is discussed (Chapter 2). The extensive investigations carried out to overcome identified deficits in knowledge are presented and the key results are discussed (Chapter 3). Points identified as critical for seismic anchor performance supported the development of the seismic amendment of the European qualification guideline which testing protocols were verified by tests (Chapter 4).

While the aforementioned tests were conducted under simulated seismic conditions, the tests presented in the second part were conducted under real seismic conditions. Therefore, shake table tests were carried out which enabled the comparison of the anchor behaviour on component and system level. The target was to evaluate whether the concept of future seismic pre-qualification tests sufficiently replicate the characteristic demands of a real earthquake. The test data was compared with the stipulated requirements and assessment criteria of the proposed pre-qualification tests (Chapter 5). Based on all test investigations, recommendations for seismic anchor pre-qualification are given and important aspects of seismic design are highlighted (Chapter 6). To predict the displacement behaviour, which is often critical for seismic qualification, a model to estimate the anchor displacement for a given load and crack demand is proposed (Chapter 7). Finally the findings are summed up and open questions requiring further research are formulated (Chapter 8).

Kurzfassung

Der Nachweis der technischen Eignung von nachträglich im Tragwerk installierten Dübeln mit Hilfe von Zulassungsverfahren hat sich in den vergangenen Jahrzehnten etabliert und bewährt. Aus einer großen Auswahl an zugelassenen Dübeln können sich Planer, Behörden und Bausausführende für die jeweilige Anwendung geeignete und wirtschaftliche Produkte auswählen. Während dieses System im Allgemeinen sehr ausgereift ist, werden die besonderen Belastungen, die im Falle von Erdbeben auf Dübeln wirken, bis dato noch nicht ausreichend berücksichtigt. Dies hat in den letzten Jahren zu einer verstärkten Anstrengung in der Erforschung des Verhaltens von Dübeln unter Erdbebeneinwirkungen geführt.

Die in dieser Promotionsarbeit vorgestellte Forschung leistet hierzu einen Beitrag. Sie stellt eine systematische und umfassende Behandlung der seismischen Qualifikation von Dübeln dar und basiert auf umfangreiche Untersuchungen. Das Ziel dieser Arbeit ist es, Wissenslücken über das Verhalten von Dübeln unter Erdbebenbelastung so zu schließen, dass bestehende Qualifikationsrichtlinien um sinnvolle Versuche für die Beurteilung der Erdbebentauglichkeit ergänzt werden können.

Im Rahmen der Promotionsarbeit werden zunächst die Grundlagen erarbeitet, die für einen fundierten Ansatz zur seismischen Qualifikation notwendig sind. Nach einer kurzen Einleitung über die Motivation, Hintergründe und Ziele der Erforschung von Dübeln unter Erdbebenbelastungen (Kapitel 1), wird der gegenwärtige Stand der Qualifikationsrichtlinien erörtert (Kapitel 2). Die zur Beseitigung der daraus abgeleiteten Kenntnisdefizite durchgeführten Untersuchungen werden anschließend präsentiert und diskutiert (Kapitel 3). Jeder Aspekt, der als maßgeblich zur Charakterisierung des Verhaltens von Dübeln unter Erdbebeneinwirkung erkannt wurde, unterstützte die Erarbeitung einer entsprechenden Ergänzung der europäischen Qualifikationsrichtlinie, deren Prüfprotokolle anhand weiterer Versuche verifiziert wurden (Kapitel 4).

Während die vorgenannten Versuche unter simulierten Erdbebenbedingungen durchgeführt wurden, wurden die Dübel bei den im zweiten Teil der Promotionsarbeit beschriebenen Versuchen unter realen Erdbebenbedingungen untersucht. Hierfür wurden Rütteltischversuche durchgeführt, die einen Vergleich des Verhaltens eines im Tragwerk eingebauten Dübels mit dem eines im Versuchskörper eingebauten Dübels ermöglichen. So konnte geklärt werden, ob das Konzept der zukünftigen Qualifikationsrichtlinien die charakteristischen Anforderungen eines echten Erdbebens widerspiegeln. Die Versuchsergebnisse wurden den vorgeschlagenen Anforderungen und Bewertungskriterien gegenübergestellt (Kapitel 5). Basierend auf den gewonnenen Erkenntnissen werden Empfehlungen für die seismische Qualifikation von Dübeln abgeleitet und wichtige Bemessungsaspekte aufgezeigt

(Kapitel 6). Um das für die seismische Qualifikation oftmals maßgebende Verschiebeverhalten besser vorhersagen zu können, wird ein Modell zur Abschätzung der sich aus zyklischen Lasten und sich zyklisch öffnenden und schließenden Rissen ergebenen Dübelverschiebung vorgeschlagen (Kapitel 7). Abschließend werden die wesentlichen Erkenntnisse zusammengefasst und offene Fragen formuliert, die weitere Untersuchungen erfordern (Kapitel 8).

Acknowledgement

First of all I would like to thank my PhD advisor Professor Rolf Eligehausen for his strong commitment to my doctoral work which continued steadily beyond his retirement. As my work at the Institut für Werkstoffe im Bauwesen, Universität Stuttgart (IWB) covered a broad range of anchor technology, I benefited from Professor Rolf Eligehausen's remarkable expertise in this field of engineering. His support of my ideas for investigational approaches was very encouraging and resulted ultimately in a very challenging, but in many aspects rewarding stay at the University of California, San Diego (UCSD), a lighthouse of eathquake engineering.

Professor Tara Hutchinson (UCSD) was not only a wonderful host on a professional and private level; she also served as a reputable source of knowledge in seismic engineering during my research career. Her apparently inexhaustible drive was always an inspiration to me and I am thankful for her enthusiastic acceptance to be a co-reviewer of my PhD thesis.

I appreciate the instant support I experienced by co-reviewer Professor Jan Hofmann (IWB) when proposing the visiting stay at the UCSD and for giving me the opportunity to wrap up the research I conducted along five years of laboratory work, graduate teaching, computer administration and other obligations. I thank him to be member of the reviewing committee. Sincere thanks are given to Professor Manfred Bischoff for taking the chair of the examination board.

I also would like to express my thanks to Professor Hans-Wolf Reinhardt (IWB) for his fortunate support in applying for governmental research funding. My thanks also go to Dr. Jörg Asmus (IEA Engineering Office) and Dr. Werner Fuchs (IWB) for the advice on friction tests, Professor Rob Dowell (San Diego State University) for the exchange on ductility, and Dr. Dieter Lotze (MPA Governmental Material Testing Institute) for his consultancy on group testing. Dr. Thilo Pregartner (formerly at IWB) is thanked for the fruitful discussions on many specific topics.

Administrative staff of both universities had worked in the background to get things organised. The support of Heidi Bauer, Gisela Baur, Silvia Choynacki and Regina Jäger from the IWB, Simone Stumpp from the MPA, as well as Lynda Tran and Lindsay Walton from the UCSD is gratefully acknowledged. The dedicated and persistent support by IWB librarian Monika Werner is also highly appreciated.

Laboratory staff of both universities was a pleasure to work with in a team. Eugen Lindenmeier and Peter Scherf are thanked for helping me with my always extraordinary servo control systems and test setups in the Anchor Lab, and Paul Greco is thanked for his outstanding commitment and diligent work style which was an important factor for the successful accomplishment of the shake table tests in the Powell Lab. Both laboratory managers, Bernd Schlottke and Andrew Gunthardt, are thanked for making their lab an enjoyable place to work.

To a great extent, the research incorporated in this dissertation was funded by the company Hilti. For the financial support, but also for the mutual trust, I would like to thank Dr. Ulrich Bourgund, John Silva, and particularly Dr. Matthew Hoehler. Opinions, conclusions, and recommendations expressed in this thesis, however, are those of the author, and do not necessarily reflect those of the sponsor. The stay at the UCSD was also co-funded by the German Academic Exchange Service (DAAD) which is greatly appreciated.

I also owe my thanks to my colleagues at the IWB and fellow students at the UCSD for whatever they taught me or for backing me on the long run to the end – this holds in particular for the sandwich generation who helped me to endure when I had to chew more than I bit off: Walter Berger, Ronald Blochwitz, Josipa Bošnjak, Barbara Chang, Stefan Fichtner, Yangyang Gao, Cenk Köse, Michael Potthoff, Saurabh Prasad, Dénes Sándor, Marina Stipetic, Wentao Zhu. Particular thanks go to Dr. Derrick Watkins (formerly at UCSD) and Dr. Richard Wood (formerly at UCSD), as well as to Dr. Christoph Mahrenholtz (formerly at IWB) and Akanshu Sharma (Bhaba Atomic Research Centre (BARC) and IWB) for sharing their professional experience and friendship over the years, and for proofreading my thesis.

Finally, I would like to thank my wonderful wife and daughter for their many years' patience when their husband and father left home in the crack of dawn and returned late-night.

Table of Contents

Notation

Acronyms and Abbreviations

AC	Acceptance Criteria
ACI	American Concrete Institute, standard developing organization, also taken as shortform for respective US-American normative standard
ADP	Accumulated Damage Potential
ASCE	American Society of Civil Engineers
ASPC	Anchor Seismic Performance Categories
ASTM	American Society for Testing and Materials
BA	Bonded Anchor
BM	Bundesministerium (German Federal Government Department)
BSSC	Building Seismic Safety Council
BZS	Bundesamt für Zivilschutz (Swiss Federal Office for Civil Defense)
C	Concrete | Concrete failure
CEB	Comité Euro-International du Béton
CSA	Canadian Standards Association
Cs	Secondary Concrete failure
CC	Concrete Capacity
CCD	Concrete Capacity Design
CEN	European Committee for Standardization
CoG	Centre of Gravity
CUAP	Common Understanding of Assessment Procedure
CV	Coefficient of Variation
DAfStb	Deutscher Ausschuss für Stahlbeton
DAQ	Data Aquisition
DBD	Displacement Based Design
DIBt	Deutsches Institut für Bautechnik (German Institute for Civil Engineering (Federal Construction Authority))
DIN	Deutsches Institut für Normung (German Institute for Standardisation)
EA	Expansion Anchor
EC	Eurocode, European normative standard for structural design and construction work developed by the CEN
EERI	Earthquake Engineering Research Institute
EN	European Norm (European Standard)
EOTA	European Organisation for Technical Approvals
ESR	ES-Report (US technical approval warranting by the ICC-ES)
ETA	European Technical Approval
EU	European Union
FE	Finite Element
FEMA	Federal Emergency Management Agency
FFT	Fast Fourier Transformation
FIB	Federation International du Béton (International Federation for Structural Concrete) often spelled fib
FM	Floor Motion
FRP	Fibre Reinforced Polymer
GM	Ground Motion
GSHAP	Global Seismic Hazard Assessment Program
HB	Headed Bolt
HCF	High Cycle Fatigue
HS	Headed Stud

HVAC	Heating, Ventilating and Air Conditioning
ICC-ES	International Code Council – Evaluation Service, ICC-ES Report also taken as technical approval
IDA	Incremental Dynamic Analysis
ISO	International Standardisation Organisation
IWB	Institut für Werkstoffe im Bauwesen (Institute of Construction Material of the University of Stuttgart)
LCF	Low Cycle Fatigue
Ld	Load-displacement
LP	Linear Potentiometer
LRFD	Load and Resistance Factor Design
LTM	Load Transfer Mechanism
LW	Load Washer
MEP	Mechanical, Electrical and Plumbing
MPA	Materialprüfanstalt (Governmental Material Testing Institute)
NA	National Annex of a European Standard
NEHRP	National Earthquake Hazard Reduction Program
NCS	Non-structural Components and Systems
NZS	New Zealand Standard Council
P	Bond failure in case of adhesive anchors
PBD	Performance Based Design
PC	Precast Concrete
PFA	Peak Floor Acceleration
PFM	Predominant Failure Mode
PIA	Peak Input Acceleration
PNA	Peak NCS Acceleration
Po	Pull-out | Pull-out failure
PTFE	Polytetrafluoroethylene
PrEN	Pre-standard European Norm
Pt	Pull-through | Pull-through failure
RC	Reinforced Concrete
S	Steel | Steel failure
Sa	Spectral acceleration
SA	Screw Anchor
SDCP	San Diego Crack Protocol
SDLP	San Diego Load Protocol
SDSU	San Diego State University
SEAOC	Structural Engineers Association of California
SEAOSC	Structural Engineers Association of Southern California
SLS	Serviceability Limit State
SP	String Pot
TB	Technical Board
TC	Technical Committee
TS	Technical Specification
UB	Uniform Bond
UC	UnderCut anchor
UCSD	University of California, San Diego
ULS	Ultimate Limit State
US	United States of America

Common Subscripts

ave	Average
c	Concrete | Concrete failure mode
cr	Cracked
cube	Cube
cyc	Cyclic | Cycle
cyl	Cylinder
d	Design
eff, ef	Effective
eq	Earthquake (seismic) | Equivalent
k	Characteristic
m	Mean
max	Maximum
min	Minimum
n, nom	Nominal
p	Pullout | Pullout failure mode
R	Resistance
req	Required
s	Steel | Steel failure mode
test	Value obtained from test
u	Ultimate
ucr, uncr	Uncracked
y	Yield | Yield failure mode
5%	5 % fractile (i.e. quantile)

Prefix

cal.	Calculated
req.	Required

Latin Uppercase Letters

A	Accidental action (EC) | Cross sectional area | Strain after rupture
A_a	Response amplification factor
A_c	Cross section of concrete member
A_{eff}	Effective cross sectional area
A_g	Strain before necking
A_{gross}	Gross cross sectional area
A_h	Bearing area of anchor head
A_s	Area of steel
C	Compression
D	Dead load (ACI)
E	Earthquake load (ACI) | Effect of action (EC) | Modulus of elasticity
F	Load or force, action (EC)
F_{red}	Reduced loading
F_u	Ultimate load, either tension load ($\rightarrow N_u$) or shear load ($\rightarrow V_u$)
$F_{u,res}$	Residual ultimate load capacity
F_{exp}	Expansion force
$F_{Ru,m}$	Mean ultimate strength
$F_{5\%}$	Characteristic strength as 5 % fractile (i.e. quantile) of the ultimate loads
F_0	Unreduced loading
H	Building height measured from the top of a rigid basement
I	Moment of inertia of a cross-section

L	Length
L_o	Original reference length before testing
L_u	Reference length after testing
M	Moment
N	Tension | Axial load or force Nominal strength (ACI)
N_{ave}	Average anchor load level measured during shaking
N_{max}	Maximum or target load for tension load cycling tests
N_{min}	Minimum load during tension load cycling tests
N_p	Permanent load
N_{pp}	Load in the post-peak
N_{target}	Target load for system level tests
N_u	Ultimate tension load
$N_{u,group}$	Ultimate anchor group load
$N_{u,cr}$	Ultimate (single) anchor load for cracked concrete
$N_{u,cyc}$	Residual ultimate (single) anchor load for cyclically cracked concrete
$N_{u,cyclic}$	Residual ultimate (single) anchor after load cycling for cracked concrete
$N_{u,uncr}$	Ultimate (single) anchor load for uncracked concrete
N_w	Sustained axial load | Permanent load
N_y	Load at (pseudo) yield point
$N_{5\%}$	Nominal capacity as 5 % fractile
N^*	Maximum anchor load measured during shaking
R	Resistance (EC)
R_p	Response modification factor
S	Internal forces (EC) | Soil factor
S_o	Original cross sectional area
T	Period | Tension
T_p	Predominant period
V	Shear load or force
V_u	Ultimate shear load
V_{max}	Target load for shear load cycling tests
W	Weight

Latin Lowercase Letters

a_{floor}	Floor acceleration
a_g	(Design) ground acceleration
a_{NCS}	NCS acceleration
c_{nom}	Nominal concrete cover
d, d_{nom}	Diameter of anchor or threaded rod
d_0	Diameter of drill bit / drilled hole
f	Frequency
f_c	Compressive cylinder strength of concrete
$f_{cc,150}$	Compressive (150 mm) cube strength of concrete
f_{cm}	Mean value of concrete cylinder compressive strength
f_{ct}	Tensile strength of concrete
f_u	Ultimate strength of steel
f_y	Yield strength of steel
g	Gravity
h	Overall depth of a cross-section
h_{ef}	Effective embedment depth
h_{nom}	Nominal embedment depth
h_t	Pitch of thread

h_s	Length of the end without full height of thread
k	Empirical coefficient for determining concrete capacity | k-factor (statistics) | Stiffness | Transmission ratio of anchor to expansion force
k_{cr}	Stiffness of anchor located in a crack
k_s	Secant stiffness
k_{uncr}	Stiffness of anchor located in uncracked concrete
ℓ	Length
ℓ_p	Plastic hinge length
n	Number of anchors in a group
n_{cyc}	Number of cycles
p	Load level factor | Bearing pressure
q_a	Behaviour factor of a non-structural element
s	Spacing | Centre to centre spacing of anchors
s(N)	Anchor displacement as a function of load
s_{ave}	Average crack spacing
s_{cr}	Critical anchor spacing
s_{cyc}	Anchor displacement accumulated during cyclic actions
s_i	Initial anchor displacement
s_{max}	Maximum crack spacing
t	Time
Δw	Difference in lower and upper crack width in crack cycling tests | Crack width, additive to the initial hairline crack
w	Crack width
w_1	Crack opening width, sometimes also denoted Δw_1 or w_{max}
w_2	Crack closing width, sometimes also denoted Δw_2 or w_{min}
w_{ave}	Average crack width
w_k	Characteristic crack width
w_{max}	Target crack width for crack cycling tests
z	Height of a non-structural element above the level of application of the seismic action

Greek Uppercase Letters

Δ	Difference | Displacement
Δ_m	Maximum deformation
Δ_y	Yield deformation
Σ	Sum
Ω_0	Amplification factor to account for overstrength of the seismic resisting system

Greek Lowercase Letters

α	Empirical coefficient for determining steel capacity in shear | Reduction factor | Angle of cone | Correlation factor | Scale factor
α_{eq}	Reduction factor for earthquake applications
β	Stiffness of load-displacement curve between 0.1 and 0.3 $N_{u,m}$
δ	Displacement | Angle of friction
δ_{1000}	Displacement after 1000 crack cycles
ε	Strain
ζ	Damping Ratio
γ	Angle of undercut | Partial safety factor (EC)
γ_a	Importance factor of a non-structural element

γ_{inst}	Installation partial safety factor
γ_F	Partial safety factor of force
γ_G	Partial safety factor of permanent action
γ_Q	Partial safety factor of variable action
γ_M	Partial safety factor of material
γ_{Mc}	Partial safety factor of concrete failure
γ_{Mp}	Partial safety factor of pullout/pull-through failure
γ_{Ms}	Partial safety factor of steel failure
κ	Curvature
κ_{LV}	Reduction factor for adverse load distribution
μ	Mean value | Coefficient of friction | Ductility factor
μ_m	Mean margin of safety
ρ	Reinforcement ratio of longitudinal tension reinforcement
σ	Stress | Standard deviation
σ_s	Steel stress
$\tau_{b,m}$	Mean bond stress
τ_u	Ultimate bond stress
ϕ	Diameter of reinforcement bars | Load reduction factor (ACI)
ψ_w	Strength reduction factor for cracked concrete

1 Introduction

Nations frequently suffer tremendous economic damage due to earthquakes. Apart from the direct damage to infrastructure, building and equipment, indirect damage or follow-up costs occur, mainly caused by fires, power interruptions, or by loss of production, environmental pollution, and also social repercussions. Most attention is given to the direct effects of earthquakes and spectacular collapses of structures, however, the consequential effects of apparently minor damage can also be serious (Figure 1.1a). Proper anchorage can reduce the damage. To ensure an adequate performance under the adverse conditions of an earthquake, however, the anchor has to be qualified for the intended use.

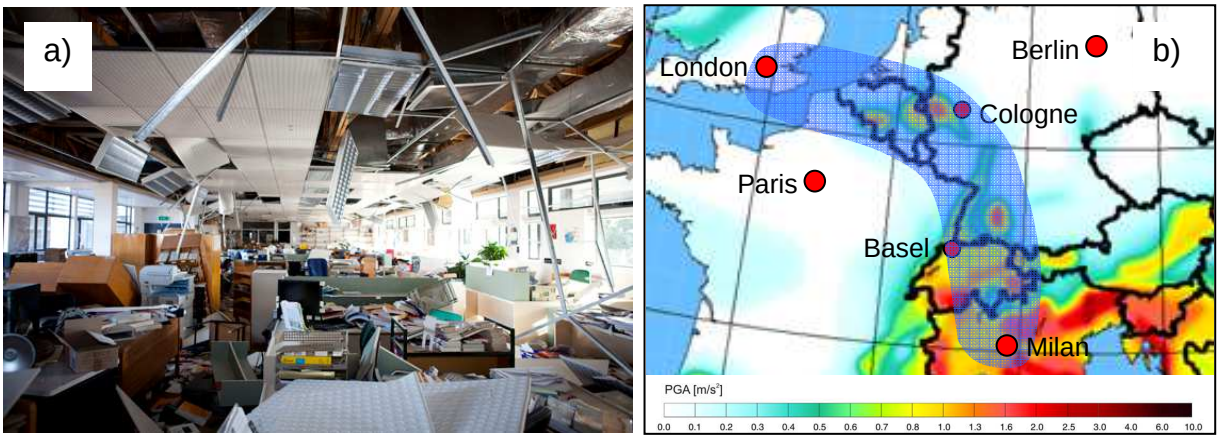

Figure 1.1 a) Collateral damage in office after the Darfield Earthquake 2010 (The Press, Christchurch); b) Seismic risk map of central Europe (after *Grünthal, G.; Arvidsson, R. et al. (2004)*), and "Blue Banana" indicating high concentration of people and assets (after *Brunet, R. (2002)*)

1.1 Motivation for Research on Anchors for Use in Seismic Regions

The probability to experience an earthquake is deemed to be comparatively low for many regions in the world. However, the level of risk to potential damage depends not only on the level of hazard, but also on the asset value and its vulnerability of the considered area. Studies have shown that the risk of earthquakes is actually high not only for areas traditionally well known as earthquake prone areas like California, Japan, New Zealand etc. but also for Switzerland and Germany (*Schwarz, J.; Maiwald, H. et al. (2005)*; *Schuler, D. (2007)*) where the seismic provisions are traditionally less stringent. Because these areas have been spared of strong earthquakes in the last century, people lack of personal experiences. As a result, the

awareness of the immense risk of an earthquake is not widespread among the general public and decision makers (*Götz, A. (2003)*).

Due to the significant increase in value of urban building and infrastructure, as well as increase in population and standard of living over the past decades, even minor seismic events would result in significant damage. In *Schwarz, J.; Maiwald, H. et al. (2005)* it is pointed out that German urban centres are outside of areas of high seismicity. However, a recurrence of the Cologne earthquake of 1841 could result in an economic loss of about 500 Million EUR (665 Million USD). The worst case scenario of a maximum credible earthquake affecting also the surrounding regions could even cause a damage of 60,000 Million EUR (80,000 Million USD) (*Schwarz, J.; Langhammer, T. et al. (2004)*). Likewise, a major event today like the 1356 Basel earthquake could result in costs as high as 50,000 Million CHF (55,000 Million USD) (*Schuler, D. (2007)*). Earthquake resistant construction is not expensive, in particular when it is considered early in the design process. In this context it is pointed out that half of all earthquake damage costs in buildings is caused by non-structural damage (*Herdman, R. (1995)*, *Taghavi, S.; Miranda, E. (2003)*, *Schuler, D. (2007)*).

While the seismic hazard level has to be accepted as constitutional and together with the concentration of asset values as unchangeable (Figure 1.1b), increased awareness has drawn the attention to the need of more stringent requirements for building codes in Europe to reduce the vulnerability (*Meskouris, K.; Hinzen, K.-G. (2003)*). The revised design codes *SIA 261 (2003)* for Switzerland, *DIN 4149 (2005)* for Germany and later the release of the *Eurocode 8 (2006)* reflect the efforts undertaken to introduce more realistic seismic design scenarios. Together with the design codes for concrete structures *SIA 262 (2003)* and *Eurocode 2 (2005)* it was possible to raise the European code standards similar to the long existing and continuously improved design codes in the US (*ACI 318 (2011)*) and New Zealand (*NZS 3101 (2006)*).

The resolute application of earthquake resistant construction methods developed over past decades reduces drastically the number of potential earthquake victims and the amount of damage caused by earthquakes. New structures situated in developed countries are generally well designed and generally show good seismic performance. However, anchorages especially of non-structural components and systems (NCS) are often neglected in the design process (*Masek, J.; Ridge, R. (2009)*, *Griffin, M.; Winn, V. (2009)*). The practice on seismic anchoring of NCS lags considerably behind the design practice for structural elements and their connections, as it is often not clear who is responsible for their design. Reconnaissance reports on the latest major earthquakes confirm the unclear distribution of responsibilities (e.g. *EERI SER Maule (2010)* or *EERI SER Christchurch (2011)*) and identified insufficient anchorage as a substantial cause for earthquake damage. In contrast, the costs for earthquake resistant anchorages are

very low in relation to the possible damage reduction (high cost-benefit ratio), making the use of earthquake-proof anchor systems a method with considerable potential. Figure 1.2 and Figure 1.3 show some examples of typical damages caused by anchor failure.

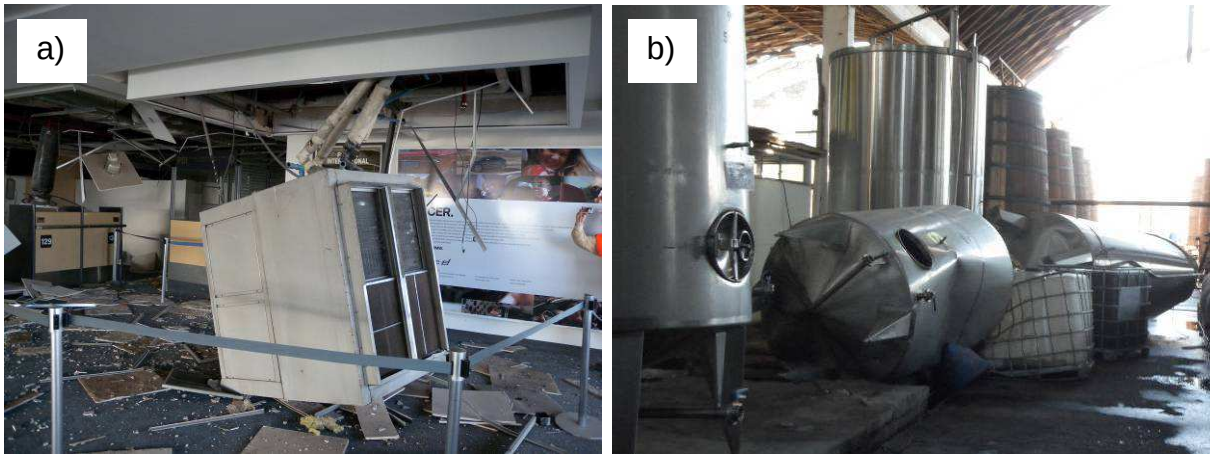

Figure 1.2 Example of earthquake damages caused by anchor failures during the 2010 Chile Earthquake: a) HVAC unit crashed through suspended ceiling (Photo by G. Mosqueda, University at Buffalo); b) Silo for liquid storage toppled (Photo by R. Leon, Georgia Tech)

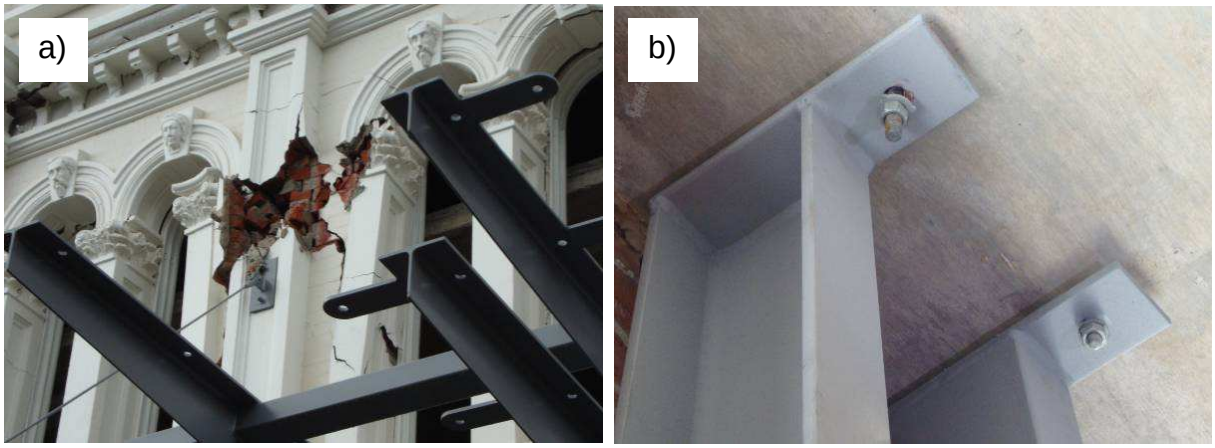

Figure 1.3 Example of earthquake damage caused by anchor failure during the 2011Christchurch Earthquake: a) Historical masonry façade nearly collapsed due to insufficiently anchorage to retrofit steel frame; b) Displaced anchors at footing of retrofit steel frame (Photos by J. Silva, Hilti North America / C. Mahrenholtz, University of Stuttgart)

Poor seismic performance moved non-structural components into the focus of the seismic research community. The response of NCS to earthquakes and their role in performance-based earthquake engineering was studied in detail in *Taghavi, S.; Miranda, E. (2003)*. It was concluded that, first, the NCS generally represent the major portion of the total building investment costs and thus represent a large potential loss. Second, damage to NCS in buildings is usually triggered at levels of

deformation much smaller than those required to initiate structural damage. Third, important economic loss can result from a temporary loss of function due to NCS failure. The particular vulnerability of NCS even for moderate earthquakes is also highlighted *Gould, N.; Griffin, M. (2003)*. For example, the 1994 Northridge Earthquake caused significant non-structural damage to a number of area hospitals due to insufficient anchorages. The hospitals remained structurally sound, but had to be closed because of unserviceability. To address the importance of the consideration of NCS in the performance based earthquake engineering, large seismic research programmes particularly in the US placed the emphasis on NCS lately (e.g. *ATC-29-1 (1998)*, *ATC-58 (2004)*). A comprehensive overview of the research on NCS is given in *Whittaker, A.; Soong, T. (2003)*.

a)

Earthquake frequency	Return period in years	Probability of exceedance
Frequent	43	50% in 30 years
Occasional	72	50% in 50 years
Rare	475	10% in 50 years
Very rare	970	5% in 50 years or 10% in 100 years
Extremely rare	2475	2% in 50 years

b)

Performance Level		Description
NEHRP Guidelines	Vision 2000	
Operational	Fully Functional	No significant damage to structural and non-structural elements
Immediate Occupancy	Operational	No significant damage to structural elements. Non-structural elements are secure and most would function.
Life Safety	Life Safe	Significant damage to structural elements. Non-structural elements are secure but may not function.
Collapse Prevention	Near Collapse	Substantial damage to structural and non-structural elements.

c)

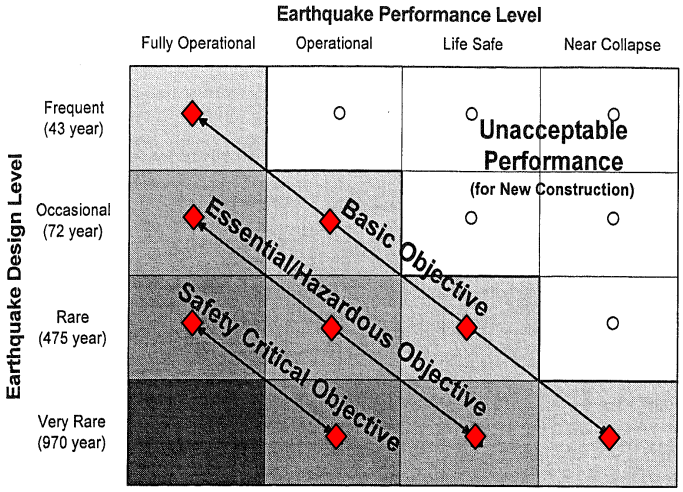

d)

Table 2-9 Building Performance Levels/Ranges

Nonstructural Performance Levels	Structural Performance Levels/Ranges					
	S-1 Immediate Occupancy	S-2 Damage Control Range	S-3 Life Safety	S-4 Limited Safety Range	S-5 Collapse Prevention	S-6 Not Considered
N-A Operational	Operational 1-A	2-A	Not recommended	Not recommended	Not recommended	Not recommended
N-B Immediate Occupancy	Immediate Occupancy 1-B	2-B	3-B	Not recommended	Not recommended	Not recommended
N-C Life Safety	1-C	2-C	Life Safety 3-C	4-C	5-C	6-C
N-D Hazards Reduced	Not recommended	2-D	3-D	4-D	5-D	6-D
N-E Not Considered	Not recommended	Not recommended	Not recommended	4-E	5-E Collapse Prevention	No rehabilitation

Figure 1.4 a) Definition of earthquake hazard levels (taken from *Ghobarah, A. (2001)*); b) Definitions of seismic performance levels according to *FEMA-273 (1997)* and *SEAOC (1995a)*; c) Performance levels after *SEAOC (1995b)*; d) Performance levels after *FEMA-273 (1997)*

The Performance Based Design (PBD) relates the earthquake hazard level (Figure 1.4a), to the desired performance levels (Figure 1.4b). The desired performance

level, e.g. damage control or collapse prevention, depends on the importance of the building. In the Vision 2000 of the Structural Engineers Association of Southern California (SEAOSC) presented in *SEAOC (1995b)*, earthquake performance levels are related to the earthquake design level in order to define performance objectives for buildings (Figure 1.4c). In the BSSC / NEHRP guidelines for the seismic rehabilitation of buildings presented in *FEMA-273 (1997)*, an instructive approach is presented which defines the building performance level in respect to the structural and non-structural performance (Figure 1.4d). It is apparent that for the first two performance levels described in Figure 1.4b, suitable anchor systems are essential to limit damage on the basic structural and non-structural systems. These aspects are substantiated in *FEMA-356 (2000)*, and discrete non-structural performance levels are given.

A list of possible damage to installations caused by anchor failure and appropriate measures to make connections earthquake resistant can be found in *Marxer, G.; Kunz, J. et al. (2003)*. The majority of the anchors on the market today are not qualified for seismic applications, however commonly used in seismic active regions. The reason for this is not only the unawareness of the designer but also the lack of conclusive seismic anchor qualification guidelines. In Europe, this deficit is recognised in the meantime and actions were taken to overcome the unsatisfying situation. The introduction of the seismic amendment for the qualification guideline ETAG 001, which draft is currently reviewed (*Proposal for ETAG 001 Seismic Amendment (2012)*), is envisaged for 2012. In the US, the qualification guideline ACI 355.2, which includes provisions for simulated seismic tests, is already in practice for the last decade, however, updated knowledge needs to be incorporated.

1.2 Context of Research on Post-installed Anchors for Seismic Applications

As indicated in Section 1.1, anchors are used to fix NCS to concrete, i.e. non-structural connections, and to join steel, concrete, or other structural elements, i.e. structural connections. Due to the flexibility, easy handling, and large field of possible applications, post-installed anchors have significant advantages against cast-in-place anchors and thus are increasingly popular among designers and contractors. Figure 1.5 illustrates common types of post-installed anchors and their applications.

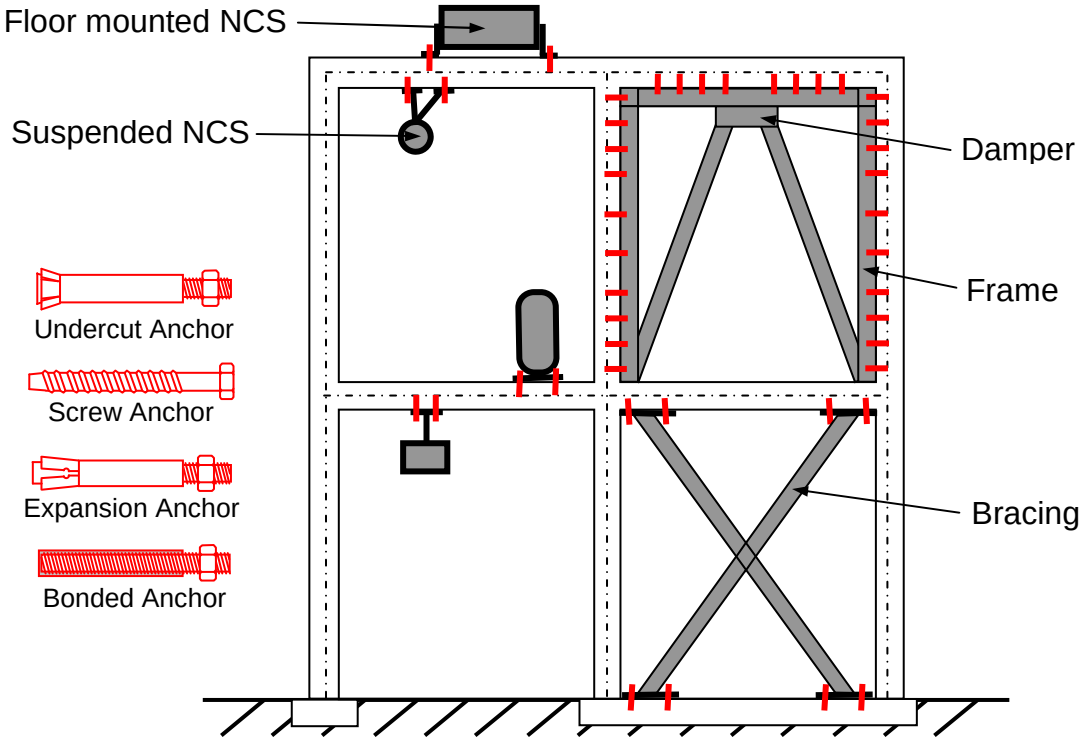

Figure 1.5 Typical anchors and structure with structural and non-structural connections (schematic)

Informal surveys indicate that the anchorage of non-structural connections represents more than half of the volume of seismic relevant applications of anchors. The connected NCS may be broadly categorized as mechanical-electrical-plumbing (MEP), architectural, or contents (*ASCE 7 (2010)*, *FEMA-356 (2000)*). Examples are components for heating, ventilating, or air conditioning (HVAC), fire suppresion system piping, as well as façades, partitions, ceilings, and racks (Figure 1.6).

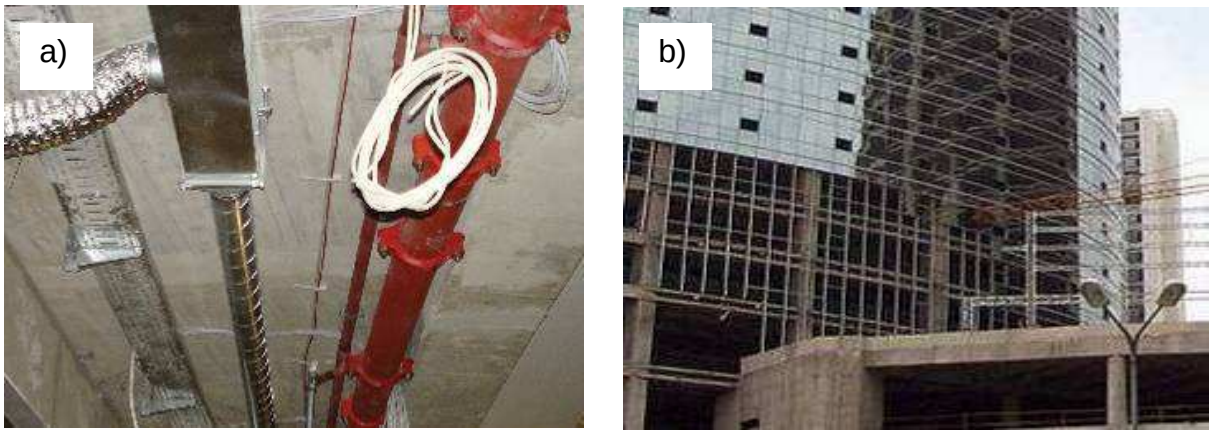

Figure 1.6 Examples of application of anchors for non-structural connections:
a) Piping installed to RC slab ceiling during construction (Courtesy C. Genesio);
b) Façade installed to partially completed RC building (Source: Wikipedia)

Anchors used for structural connections are often part of global or local strengthening measurements. Examples for global strengthening are steel bracings and shear walls, and for local strengthening steel or concrete jacketing, and restraints of fibre reinforced plastic (FRP) (Figure 1.7).

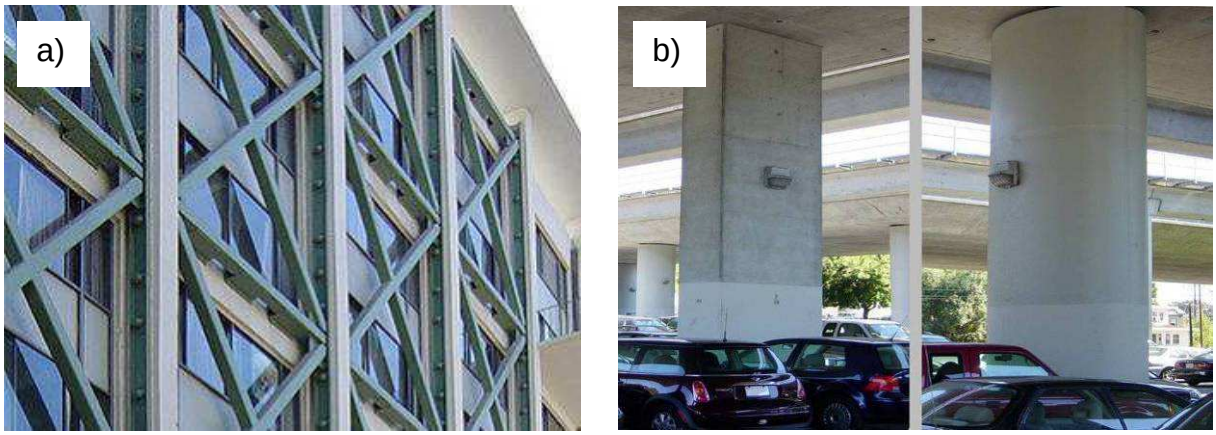

Figure 1.7 Examples of application of anchors for structural connections: a) Steel bracing fixed to main RC structure (Source: Wikipedia); b) FRP fixed to existing RC column, before (left) and after (right) jacketing (Source: Wikipedia)

Strengthening can either be for regular upgrading or for seismic retrofitting. Seismic retrofitting is further divided into precautionary retrofitting and repairing of structures which in the latter case has been already moderately damaged by an earthquake. More details of various aspects of post-installed anchor design and application for retrofit measures can be found in *CEB State of the Art Report (1996)*, a state-of-the-art report on fastenings for seismic retrofitting published by the CEB (Comite Euro-International du Beton).

Design regulations differentiate between structural and non-structural elements. The *Eurocode 8 (2006)* defines a non-structural element as an architectural, mechanical or electrical element, system and component which, whether due to lack of strength or because of the way it is connected to the structure, is not considered in the seismic design as load carrying element. In contrast, a primary seismic member, i.e. structural element, is a member considered as a part of the structural system that resists the seismic action, which is for this purpose modelled in the structural analysis and detailed accordingly. This approach is also reasonable for precast concrete (PC) elements. Depending on the design, PC elements and their connection to the adjacent structure can either be structural or non-structural. However, for other elements it is sometimes hard to decide whether they are structural or non-structural, e.g. underhung operating platforms or penthouse assemblies.

Anchor pre-qualification, however, does not distinguish between structural and non-structural connections. To date, anchors are qualified irrespective to their

application. However, the designer uses different anchor types and anchor diameters for structural and non-structural applications. Generally and simplified speaking, the typical anchor used for non-structural connections is M12 (1/2”) size while the majority of anchors used for structural connections is M20 (3/4”) and larger.

Since cracks have a significant negative influence on the anchor performance in general, it can be conservatively assumed that the anchor is always situated in a crack. The high probability that cracks intersect the anchor location is confirmed by several studies (e.g. *Eligehausen, R.; Lotze, D. et al. (1986)*; *Lotze, D. (1987)*; *Bergmeister, K. (1988)*). In case of a seismic event, the structure excited by the ground motion starts to oscillate. As the structure responds to the ground motion, it deforms depending on its ductility and general dynamic characteristics. Deformation of the structure may result in degradation of the reinforced concrete, which serves as the anchorage material. This degradation is in large part expressed through cracking in the structural elements. The cracks open and close cyclically due to the oscillating response of the structure. Therefore, a seismic event causes cycling of anchor load and crack width simultaneously. Further severe seismic conditions such as rapid loading and large maximum crack widths have to be taken into account when considering anchors for use in seismic applications (Figure 1.8).

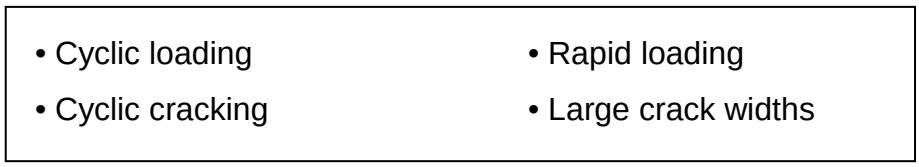

Figure 1.8 Severe conditions to be considered for anchors due to seismic actions

The structure serves as a filter which amplifies the ground acceleration a_g near the natural frequencies of the structure. By this, the wide-band ground motion embracing all frequencies in a transient or stochastic manner becomes a closer narrow-band floor motion with a more sinusoidal characteristic on the floor level response. The floor level response will vary throughout the height and location of the building. Figure 1.9 illustrates the situation for non-structural and structural connections during an earthquake.

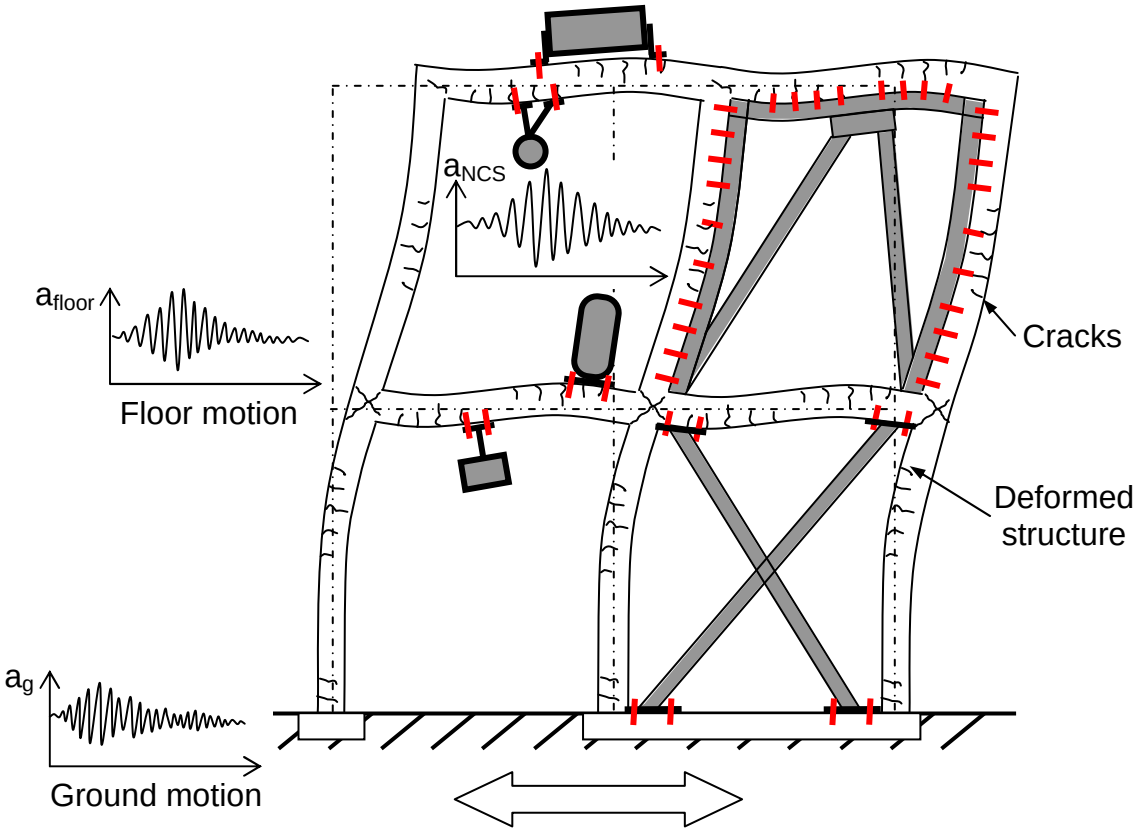

Figure 1.9 Structure response to ground motion and acceleration time histories (schematic)

In case of structural connections, the structural element connected by anchors forms an integral part of the structure and as such influences the response of the structure to the earthquake input. Deformations, imposed by the global structure either caused by strong ground motions or foundation settlement, rather than inertial forces are the main demand for these connections. The design anchor loads are the direct outcome of the structural analysis for which the anchors need to transfer reliably the loads to satisfy the equilibrium of forces at the connection. The design of structural elements is based on relevant design codes which are in Europe the *Eurocode 0 (2002)* for design loads, *Eurocode 2 (2005)* for design of concrete structures, and *Eurocode 8 (2006)* for the design of structures for earthquake resistance. Provisions for anchor design are not yet included, however, the incorporation of the anchor design code *CEN/TS 1992-4 (2009)* as part of Eurocode 2 is in progress. In the US, the relevant codes for static and seismic design are the *IBC (2009)* with the design loads specified in *ASCE 7 (2010)*, and the building code requirements stipulated in *ACI 318 (2011)*. Provisions for anchor design are included as Appendix D of ACI 318.

In case of non-structural connections, the anchor loads develop according to the inertial response of the NCS to the floor accelerations a_{floor} it is connected to. The resulting anchor response in turn feeds back the anchored NCS behaviour which is

also reflected in the design codes: Behaviour Factors q_a (Annex E in *CEN/TS 1992-4 (2009)*) and Response Modification Factors R_p (Chapter 13 in *ASCE 7 (2010)*) consider the beneficial (ductile) behaviour of a component which help to reduce the design forces, whereas Response Amplification Factors A_a (*CEN/TS 1992-4 (2009)*) and Component Amplification Factors a_p (*ASCE 7 (2010)*) consider the adverse effect of component induced amplification which increase the demand and thus the design forces. The equations given in *CEN/TS 1992-4 (2009)* and *ASCE 7 (2010)* for the maximum design loads on NCS are further a function of basically the weight of the NCS, the height of the NCS in the building, the building height, and the ground acceleration.

1.3 Objective of Research on Seismic Anchor Performance and Qualification

The preceding Sections 1.1 and Section 1.2 demonstrated the commonly underestimated personal and economic risk emanating from earthquakes also outside of seismic hotspots, outlined the importance of adequate anchor performance for damage prevention during earthquakes, and sketched the environmental conditions to which structural and non-structural connections are exposed. To address the challenge of seismically safe anchorages and to enable satisfactorily design solutions, further research on the performance and qualification of anchors under seismic applications is required.

The research presented in this thesis partly continues and extend earlier studies summarised in the Hoehler dissertation on the ‘Behavior and testing of fastenings to concrete for use in seismic applications’ (*Hoehler, M. (2006)*) which specifically identified the following open questions:

- It was concluded that high loading rates generally do not result in a reduction of load capacity. However, the loading rate sensitive friction in case of expansion anchors requires further investigations.
- Ductility is considered as an important asset in seismic design. However, it was underlined that the then existing anchor design guidelines and anchor qualification guidelines address anchor ductility inadequately. Therefore, a systematic study of anchor ductility is needed.
- The distribution of the earthquake load within an anchor group depends also on the anchor displacement particularly experienced due to seismic actions. It is pointed out that the anchor group displacement can be curbed by the attached base plate for which further research is required.

- Tests on the behaviour of anchors under crack cycling and tension load cycling were carried out only on a limited number of anchor types. The anchor size predominantly tested was M16 which is more robust against large crack widths than smaller sizes. Anchor behaviour under shear load cycling was not addressed at all. Further tests are necessary.

New aspects have been contributed since these studies. The introduction of scientifically more substantiated load and crack cycling test protocols (*Wood, R.; Hutchinson, T. et al. (2010)*; *Hutchinson, T.; Wood, R. (2010)*; *Eligehausen, R.; Hutchinson, T. et al. (2010)*) together with upgraded testing equipment made the investigation of seismic anchor behaviour under more realistic and precisely defined conditions possible.

To further characterise seismic performance of post-installed anchors, which also allows the development of qualification tests representing the loading conditions relevant for seismic applications, an extensive research programme was carried out at the Institut für Werkstoffe im Bauwesen, Universität Stuttgart (IWB). While the studies presented in *Hoehler, M. (2006)* provided fundamental background on the testing methods and behaviour of anchors under seismic conditions, the investigation of this thesis focused on the specific performance of post-installed anchors and the development of meaningful testing criteria for their pre-qualification. For this reason, the thesis starts with a comprehensive review of existing qualification guidelines in Chapter 2

- to evaluate the state of the art of anchor qualification guidelines and to identify the needs for improvements.

The above listed open questions formulated in *Hoehler, M. (2006)* regarding loading rates, available anchor ductility and anchor groups are resolved in this thesis. Further, the previous experimental tests on anchor behaviour under cyclic load and cycled cracks, carried out on an exploratory level, were enhanced to a broad range of anchor types and products, in particular for medium anchor sizes. The tests were conducted on the basis of stepwise increasing protocols proposed in *Wood, R.; Hutchinson, T. et al. (2010)* and amended by simultaneous load and crack cycling tests reported in Chapter 3 with the objective

- to further evaluate the performance of post-installed anchors under seismic conditions, to decide what should be considered for future qualification guidelines and to check the suitability of stepwise increasing protocols for anchor qualification.

Together with the results of research conducted in parallel at the University of California, San Diego (UCSD), the efforts finally led to a proposal for the seismic amendment of the European anchor qualification guideline (*Hutchinson, T.; Wood, R.*

(2010); *Eligehausen, R.; Hutchinson, T. et al. (2010)*). Chapter 4 provides the background of this proposal and presents the tests which have been carried out

- to verify the proposed protocols and assessment criteria, and to check the feasibility of the stipulated test procedures.

In the context of the above described research, some of the most advanced and technically challenging anchor tests have been conducted. To that point, however, all tests were carried out on a component level as quasi-static seismic simulation tests. The shake table tests reported in Chapter 5 allowed the investigation of the dynamic behaviour on a system level

- to understand whether the proposed seismic test protocol for anchor qualification is able to mimic the real demand on anchors during earthquakes.

This study was the first ever directly opposing anchor test data derived from component and system level tests which allowed the assessment of many behavioural aspects previously investigated on the component level. The evaluation of all investigations finally results in concluding recommendations given in Chapter 6 with the objective

- to improve seismic qualification and design guidelines for post-installed anchors.

The anchor displacement is one of the driving factors for the anchor performance, but its experimental determination is very laborious. Therefore a model estimating the accumulated anchor displacement for any given seismic demand is developed in Chapter 7

- to further aid the anchor product development and qualification by facilitating a better assessment of the anchor behaviour.

Though intensive research was carried out, some open questions remained unanswered for future generations of doctoral researchers, which are summarised in Chapter 8.

2 State of the Art of Qualification Guidelines

The aim of this thesis is to study anchor performance aspects relevant for seismic applications in order to improve the procedures for seismic anchor qualification and to make seismic application of anchors safer. In Section 1.3 some specific deficiencies in the knowledge of seismic anchor performance were identified. In this chapter, the state-of-the-art of current anchor qualification guidelines is presented and discussed in order to understand what questions need to be answered before a conclusive scheme for seismic anchor qualification can be set up. After some general introductive notes (Section 2.1), the following aspects are discussed: Loading rate (Section 2.2), anchor ductility (Section 2.3), anchor groups (Section 2.4), cyclic load (Section 2.5), cyclic crack (Section 2.6), and simultaneous cyclic load and cyclic crack (Section 2.7). Deficits are highlighted and the resulting questions are outlined. The key findings are conclusively summarised in Section 2.8.

2.1 General

Before the various aspects are discussed in detail, a brief introduction is given by means of some general remarks on the approach of anchor qualification. Since the purpose of this thesis is not to embrace all qualification guidelines available worldwide, it focuses on the situation within the US and Europe which are the two largest economic regions having highly developed qualification schemes available. It is also noted that for anchor design the design codes of many other countries refer to the US design code ACI 318 which in turn correlates to the US qualification guideline ACI 355.2. For example, the provisions given in Chapter 17 of the New Zealand design code *NZS 3101 (2006)* refers to Appendix D of ACI 318 and also explicitly requires that anchors are qualified according to ACI 355.2 for seismic applications. Other examples are the design codes *Nch433Of (1996)* in Chile or *CICHE 401 (1996)* in Taiwan.

2.1.1 Design, Technical Approval, and Qualification of Anchors

It is not the objective of this thesis to explain in depth the general procedure necessary to achieve the technical approval for an anchor product. However, it is helpful for the reader to understand the main features in this process.

To ensure that the structure and its components is fit for the assigned purpose, durable and safe, in Europe the design and construction of the whole structure or individual components have to comply with the construction law for civil constructions and construction products. In principle, the following schemes are available (similar provisions apply to the US):

- Design and construction according to a standard.
- Design and construction provided with an individual approval by the construction authority.
- Design and construction provided with a general technical approval by the construction authority.

A technical approval is only granted if no standards for the product exists or the authorities consider that a standard cannot be developed. However, any attempts to standardize anchor products failed so far due to the complexity and diversity of anchors. On the other hand, individual approvals issued for a specific project are too expensive. Therefore, the application of the vast majority of all post-installed anchors in use is based on general technical approvals.

The qualification tests required for a general technical approval are conducted by independent laboratories and engineering offices according to anchor qualification guidelines. After checking the correctness of qualification tests and evaluation reports, the responsible authority grants the technical approval. Within the technical approvals, characteristic resistances as well as minimum anchor spacing and edge distances are obtained. Design codes establish the boundary conditions to be represented in qualification tests and often refer directly or indirectly to relevant anchor qualification guidelines as a prerequisite. Anchor qualification, in turn, facilitates the proper design of anchorages. Figure 2.1 illustrates the three‒fold development of anchor qualification guideline, technical approval and anchor design guideline.

In Europe, anchor design is generally carried out according to Annex C of the *ETAG 001 (2006)* until the implementation of the *CEN/TS 1992-4 (2009)* as Part 4 of the *Eurocode 2 (2005)* is completed. In the US, anchor design is regulated since 2002 in Appendix D of the ACI 318 (*ACI 318 (2002)*), most currently revised in 2011 (*ACI 318 (2011)*). Additionally, the *CEB Design Guide (1997)* and its revision *Fib Bulletin No. 58 (2011)* are available as an international design guide.

Qualification guidelines such as the *ETAG 001 (2006)* in Europe or the *ACI 355.2 (2007)* in the US, provide detailed specifications on the required test setup. Furthermore, the guidelines establish the criteria for evaluating the test results. After checking the correctness of the anchor qualification testing and evaluation reports, the responsible authority grants the technical approval, which is the European

Technical Approval (ETA) in Europe, and the Evaluation Service Report (ESR) in the US. The first ETA was granted in 1998 based on *ETAG 001 (1997)*, and the first ESR based on *ACI 355.2 (2001)* was granted in 2004. The European, German, and US anchor qualification guidelines are briefly introduced in the following sections.

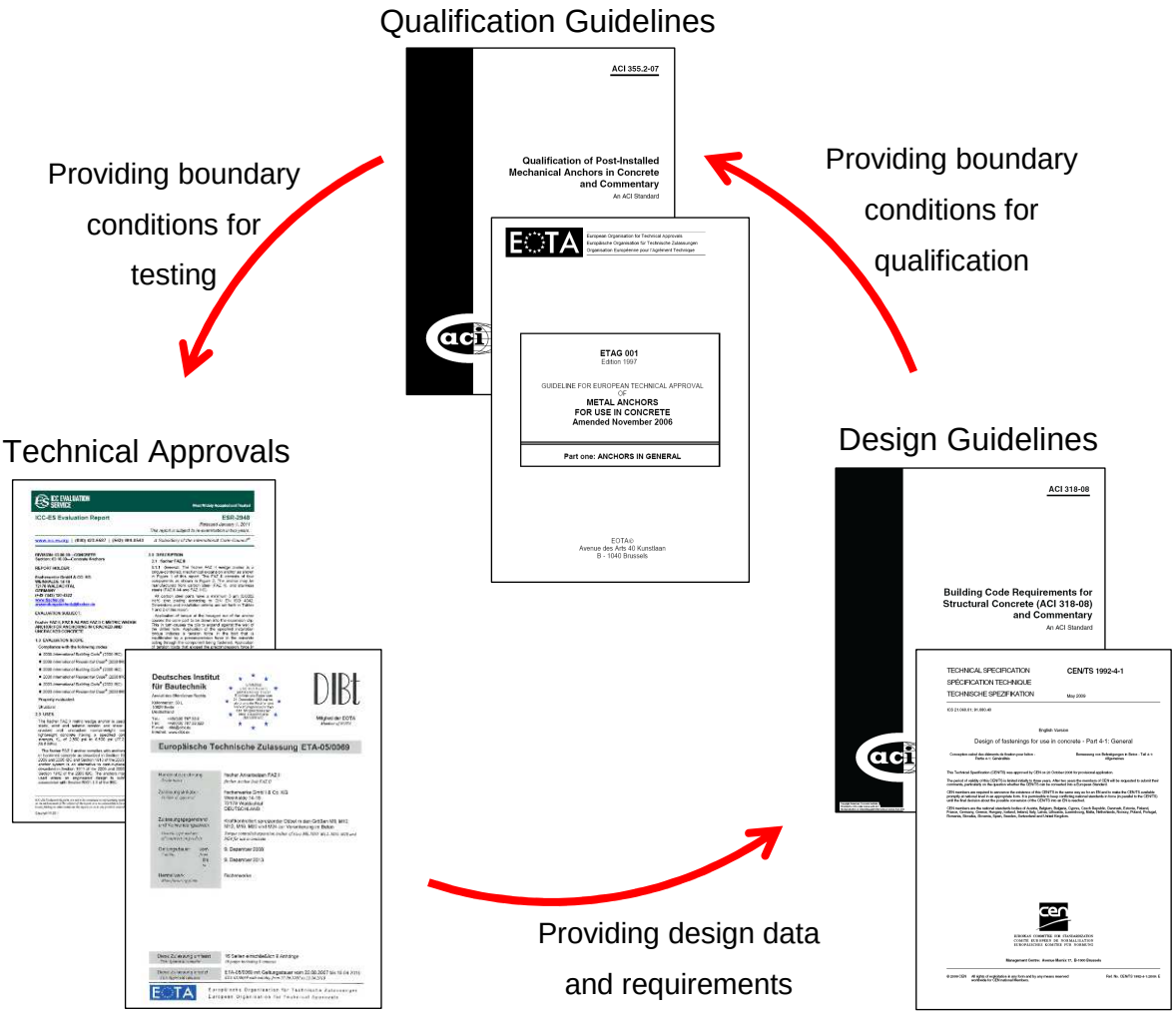

Figure 2.1 Interrelation Qualification Guideline, Technical Approval, and Design Guideline

2.1.2 European and German Anchor Qualification Guidelines

For non-seismic applications, an approval system for anchorages was introduced in Germany in 1975 on national level as a result of several fatal accidents due to anchors not fit for purpose (*Nürnberger, U. (1990)*, *Menzel, K. (1995)*). Through increasing European harmonisation of standards, it was desired that also construction products and their qualification are regulated on a European level. Consequently, European Technical Approval Guidelines (ETAG) are published by the European Organisation of Technical Approvals (EOTA). The first ETAG was

implemented in 1997 (*ETAG 001 (1997)*), dealing with the evaluation of post-installed metal anchors. This Guideline for European Technical Approval of Metal Anchors for Use in Concrete (ETAG 001) establishes the basis for assessing anchors to be used in cracked and uncracked concrete and also provides design guideline within Annex C. The application of the ETAG 001 is limited to anchors subject to static or quasi-static actions only, not addressing any seismic conditions. However, an amendment for the assessment of metal anchors under seismic actions is currently in preparation (*Proposal for ETAG 001 Seismic Amendment (2012)*). The latest revision of the ETAG 001 is the *ETAG 001 (2006)*.

In parallel, the German Guideline for fastenings in nuclear power plants and other nuclear technical facilities *DIBt KKW Leitfaden (1998)* ('NPP Guideline') defines the requirements for the use of anchors in nuclear power plants and nuclear technology installations. The NPP Guideline provides testing details and criteria for the evaluation of fastenings seeking permission in individual cases according to the regulations of the federal states of Germany. The validity of the 1998 edition was limited to undercut anchor types. The revised 2010 edition (*DIBt KKW Leitfaden (2010)*) is valid for all anchor types with an ETA for use in cracked concrete, however, a preference is explicitly placed on undercut anchors. Its test programme scheme for anchor qualification reflects extreme loading conditions such as earthquake, explosion and aircraft impact, and the resulting large crack widths. Further, additional design provisions as a supplement to Annex C of *ETAG 001 (2006)* are given. The required tests are separated three parts, namely: (A) Suitability tests to check the proper functioning under extreme conditions; (B) Tests to determine the characteristic load capacity under service condition; and (C) Tests to determine the anchor displacement under service conditions. A comprehensive explanation of this guideline can be found in *Mahrenholtz, P.; Asmus, J. et al. (2011)*.

2.1.3 US Anchor Qualification Guidelines

In 1975, the first anchor system in the US was certified code-compliant. However, the poor performance of anchors during the 1994 Northridge Earthquake revealed deficits in approvals for seismic applications and led to a temporary ban on post-installed anchors in the US and a surge in research on their seismic suitability (*Silva, J. (2001)*). The ban was revoked in 1997 and post-installed anchors were again qualified for use in seismic applications according to an adoption of either the Canadian Standard *CAN/CSA-N287.2-M91 (1991)* or the load cycling test proposed by the SEAOSC in *SEAOSC (1997)* for the time being. With the adoption of the ACI 355.2 in 2001 (*ACI 355.2 (2001)*), the first US standard for seismic anchor qualification was implemented as outlined by the ACI (American Concrete Institute). This guideline for the Qualification of Post-Installed Mechanical Anchors in Concrete

(ACI 355.2) applies to post-installed mechanical anchors intended for use in structural applications covered by the design guideline ACI 318. Seismic qualification can be acquired and is based on simulated seismic tests as cyclic tension and cyclic shear tests. Further requirements for the qualification of post-installed mechanical anchors are given in the Acceptance Criteria for Mechanical Anchors in Concrete Elements AC 193 (*AC193 (2010)*), published by the ICC-ES (International Code Council-Evaluation Service), an organisation evaluating building products. It consists mostly of the Annex 1 that summarises the amendments given for the ACI 355.2. Post-installed adhesive anchors are covered by the Acceptance Criteria for Post-Installed Adhesive Anchors in Concrete Elements AC 308 (*AC308 (2009)*) and most recently by the Acceptance Criteria for the Qualification of Post-Installed Adhesive Anchors in Concrete ACI 355.4 (*ACI 355.4 (2010)*). ACI 355.4 is in many aspects identical to ACI 355.2, and therefore both guidelines are sometimes addressed together as ACI 355 in the following. The latest revision of the ACI 355.2 is the *ACI 355.2 (2007)*.

2.1.4 Suitability and Serviceability Tests

The European qualification guideline ETAG 001 and the US qualification guideline ACI 355 were harmonised in many aspects over the past decade. These guidelines follow a similar approach to differentiate the tests according to their purpose:

- Suitability Tests (ETAG 001) and Reliability Tests (ACI 355): The purpose for these tests is to establish whether an anchor exhibits a safe and effective behaviour under ‘adverse’ conditions. If the anchor does not achieve the required strength under the prescribed ‘extreme’ conditions, the characteristic strength to be used in design is reduced.
- Admissible Service Condition Tests (ETAG 001) and Service-Condition Tests (ACI 355): These tests reflect conditions which are generally understood as (interchangeably) ‘normal’, ‘realistic’, or ‘moderate’ and serve the determination of the characteristic load capacity, i.e. characteristic resistance, as well as the minimum spacing between two anchors and minimum distance to the adjacent edge necessary to achieve the full design strength.

For easier reference, the Reliability Tests are addressed as Suitability Tests, and the Admissible Service Condition Tests / Service-Condition-Tests are addressed as Serviceability Test from this point forward. For both test types, the guidelines specify test conditions and assessment criteria. Key assessment data include the ultimate load (F_u), the displacement corresponding to half the mean ultimate load ($s(0.5F_{u,m})$), and their scatter expressed by the coefficient of variation (CV).

The test conditions and assessment criteria reflect the situation the tests are meant to simulate. If carried out in cracked concrete, suitability tests require 0.5 mm cracks. For the extreme test conditions of suitability tests, however, the allowable scatter of failure load is relatively high. In contrast, the crack width for serviceability tests is defined as 0.3 mm. The allowable scatter is lower than for suitability tests and there are additional requirements regarding the load-displacement (Ld) curve. The main test conditions and assessment criteria valid for all respective tests provided by to *ETAG 001 (2006)* and *ACI 355.2 (2007)* are summarised in Table 2.1.

Table 2.1 Main test conditions and assessment criteria according to *ETAG 001 (2006)* and *ACI 355.2 (2007)*

Test Type	Test Conditions		Assessment Criteria		
	General	Crack Width	Ld Curve	$CV(F_{u,m})$	$CV(s(0.5F_{u,m}))$
Suitability Test	Adverse/ extreme	0.5 mm (0.020 in)	steady	20 %	40 %
Serviceability Test	Normal	0.3 mm (0.012 in)	steady	15 %	25 %

2.1.5 Concrete strength classes

For testing, anchors are installed in concrete specimens (term used interchangeably with ‘concrete member’ and ‘concrete slab’). The qualification guidelines ETAG 001 and ACI 355 define two nominal compressive strength classes:

- C20/25 (ETAG 001) $f_{cc,150}$ = 25 to 35 N/mm²
  Low strength (ACI 355) f_c = 2500 to 4000 psi
- C50/60 (ETAG 001) $f_{cc,150}$ = 60 to 70 N/mm²
  High strength (ACI 355) f_c = 6500 to 8500 psi

When one coverts the compressive strengths to metric cubic strengths, the ranges given in the ACI 355 in imperial units agree fairly well with the ranges given in the ETAG 001 (Table 2.2). Consequently, results derived from tests in C20/25 and C50/60 concrete are also valid for low and high strength concrete, respectively.

Table 2.2 Concrete strength classes according to *ETAG 001 (2006)* and *ACI 355.2 (2007)*

Guideline	Concrete Class	Cube 150 x 150 x 150 mm		Cylinder Ø 150mm x 300 mm	
		Minimum	Maximum	Minimum	Maximum
ETAG 001	C20/25	25 MPa	35 MPa	20 MPa	30 MPa
	C50/60	60 MPa	70 MPa	50 MPa	60 MPa
ACI 355	Low strength	21 MPa(1)	35 MPa(1)	17 MPa	28 MPa
	High strength	58 MPa(1)	75 MPa(1)	46 MPa	60 MPa

(1) Calculated by $f_{cc,150} = 1.25 \cdot f_c$

2.1.6 Mean and Characteristic Strength

In the following, the mean and characteristic strength as defined in *ETAG 001 (2006)* and *ACI 355.2 (2007)* are given for easier reference:

- Mean ultimate strength $F_{u,m}$ is the arithmetic mean of the ultimate loads measured in individual tests within a test series:

$$F_{Ru,m} = \frac{1}{n}\sum_{i=1}^{n} F_{Ru,i} \qquad \text{Equation 2.1}$$

- Characteristic strength F_{Rk} is taken as the 5 % fractile (i.e. quantile) $F_{5\%}$ of the ultimate loads measured in a test series and calculated according to statistical procedures for a confidence level of 90 %:

$$F_{5\%} = F_{Ru,m}(1 - k \cdot CV) \qquad \text{Equation 2.2}$$

For more details regarding stochastic evaluation within the scope of structural engineering, refer to *Fischer, L. (1995)*. For anchors within current experience, a normal distribution is assumed and the k-factor is generally taken as 1.645 (for $n = \infty$). The lower bound of characteristic load can be estimated with the maximum allowable CV for serviceability tests of 15 % and for a large number of tests as:

$$F_{Rk} = F_{Ru,m}\,(1 - 1.645 \cdot 15\,\%) \approx 0.75\,F_{Ru,m} \qquad \text{Equation 2.3}$$

2.1.7 Residual capacity, α-factors, and reduction

ETAG 001 (2006), *DIBt KKW Leitfaden (2010)*, and *ACI 355.2 (2007)* stipulate for some qualification tests requirements regarding the residual capacity determined in a pullout test after the testing of the primary test parameter is completed. Primary test parameters are e.g. cyclic loads or cyclic cracks which testing is carried out for a certain anchor loading demand, e.g. F_0. The corresponding assessment criteria are given in the relevant sections of the guidelines.

DIBt KKW Leitfaden (2010) and *ACI 355.2 (2007)* evaluate the mean capacity F_m and require a certain minimum residual capacity (reqF) as a fraction or percentage of the reference capacity. In contrast, *ETAG 001 (2006)* evaluates mean and characteristic values separately and introduces the α-factor (Clause 6.1.1 (d)) which is defined as the minimum of the respective ratio of (residual) test capacity (F^t) to the corresponding reference capacity (F^r):

$$\alpha = \min \left\{ \frac{F^t_{Ru,m}}{F^r_{Ru,m}} ; \frac{F^t_{Rk}}{F^r_{Rk}} \right\} \qquad \text{Equation 2.4}$$

If certain requirements (reqF or req.α) are not met, the anchor can still be approved for a reduced strength. Depending on the type of qualification test, the strength is either reduced by the ratio of the tested capacity to the required capacity F_m / reqF for ACI 355 and α / req.α for ETAG 001, or the test series is repeated with reduced loading F_{red} and the strength is reduced by the ratio of reduced to unreduced loading (F_{red} / F_0). Further details are given in the relevant sections.

2.2 Loading Rate

Seismically induced inertia forces are explicitly considered as a source for impact loads on anchors (e.g. *CEB Bulletin d'information No. 187 (1988)*; *CEB Bulletin d'information No. 216 (1994)*). However, impact loads, i.e. rapid loading or loading at high rates, are more associated with blast loads deriving from explosions. In the following, available qualification guidelines are reviewed with respect to loading rate.

2.2.1 European and German Anchor Qualification Guidelines

To date, no European qualification guideline for anchors directly addresses loading rates. However, there are anchor products which have been shock tested to evaluate and approve their suitability according to the regulations stipulated in *BM Bau (1981)* for Germany or *BZS (1980)* for Switzerland. The regulation do not specify the source of the shock loading the anchor is intended to get qualified for, however, the required anchor performance under impact loads is also desirable for seismic loads. Shear and tension tests are carried out by means of a so-called shock table which principal setup is shown in Figure 2.2a. The anchors are installed in 1.0 mm cracks and accelerated for 10 ms. The qualification is based on the criterion that the anchor does not exceed the displacement limit of 4 mm under the defined impact load. The dynamic ultimate strength is defined by the mean dynamical strength which is calculated by means of measured load-deformation curves (Figure 2.2b,

D = dynamical strength). The loading rate is defined with respect to the desired approval class. It is interesting to note that expansion anchors are explicitly preferred against other mechanical anchor types. For additional details, refer to *Hunziker, P. (1999)*.

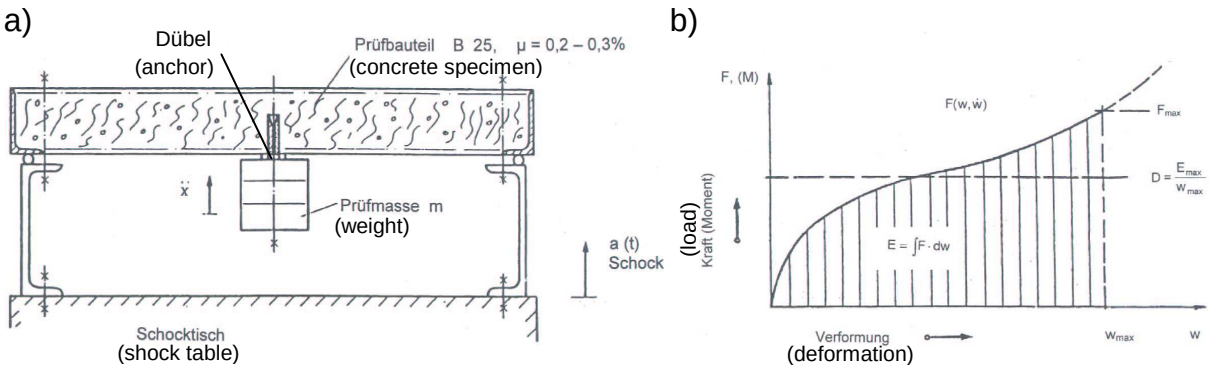

Figure 2.2 Test arrangement for anchor shock testing according to *BM Bau (1981)*: a) Test setup; b) Dynamic load-deformation curve

2.2.2 US Anchor Qualification Guidelines

Likewise in the US, no anchor qualification guideline directly addresses loading rates. However, there are several standards from the Department of Defence which deal with explosion safety for building products in case of terrorism attack, e.g. *DoD 6055.9 (2004)*.

2.2.3 Conclusions

Currently no anchor qualification guideline includes high loading rate tests for whatsoever application. However, anchor qualification for seismic loads implies that the anchor is able to resist loads at rates typical for earthquakes.

For a conclusive seismic anchor qualification scheme, the following points need to be addressed regarding loading rate:

- Is it necessary to qualify anchors for earthquake relevant loading rates?
- What loading rate is relevant for seismic application?

2.3 Anchor Ductility

Ductility plays an important role for the seismic design of structures. Its beneficial effect on the performance during an earthquake is assumed to be true also for anchors. However, a conclusive definition of anchor ductility is currently not given in any relevant design or qualification guidelines. In the following, the qualification

guidelines are reviewed with respect to anchor ductility. A comprehensive review on normative standards regarding anchor ductility can be found in *Mahrenholtz, P. (2010a)*.

2.3.1 European and German Anchor Qualification Guidelines

Clause 6.7 in Part 1 of *ETAG 001 (2006)* (identification of anchors) states that during tests on the constituent materials of the components, the elongation at rupture shall be reported. However, no assessment requirements for anchor ductility are specified. In contrast, the design guideline *CEN/TS 1992-4 (2009)* requires the rupture elongation to be at least 12 % (measured over a gauge length equal to 5 d) but does not give any details on the testing method. It may be reasonably assumed that the elongation is to be determined analogue to *ISO 6892-1 (2009)* which is a common standard for material tensile tests. If yielding of the attached element or baseplate (Figure 2.3a), or the capacity of attached element (Figure 2.3b) do not govern the failure, *CEN/TS 1992-4 (2009)* requires ductile anchor failure (Figure 2.3c), however, allows explicitly ductile failure modes other than ductile steel failure if the equivalency to ductile steel failure can be shown in the relevant European technical specification, i.e. ETA; however, no further details are given. For non-structural elements, the connection may be designed for brittle failure but increased design loads.

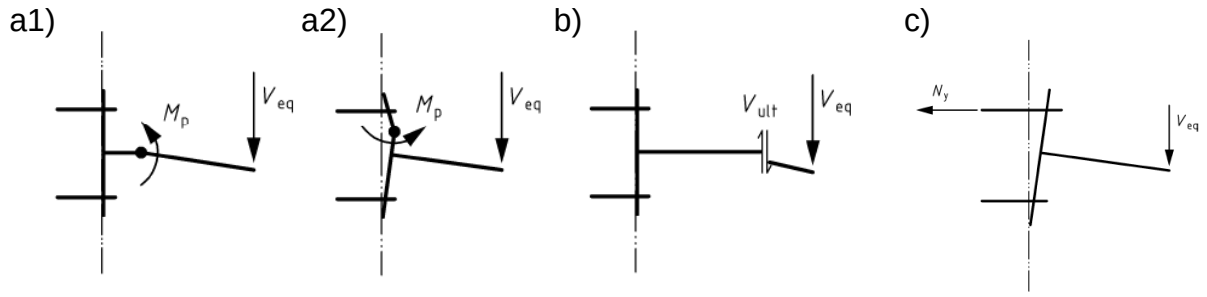

Figure 2.3 Ductile failure mechanism of anchorages considered in *CEN/TS 1992-4 (2009)* (M_p = plastic moment; V_{eq} = earthquake shear load): a1) Yielding in attached element; a2) Yielding in baseplate; b) Capacity of attached element; c) Yielding of anchor

Clause 2.1 of the former German NPP Guideline (*DIBt KKW Leitfaden (1998)*) was supplemented by the remark that safety relevant fastenings should be designed as ductile to improve the safety level by the possibility of load redistribution. The required ductility can be achieved by the anchor, the attached element or the fixture. Concrete failure should not be the critical failure mode. The revised NPP Guideline (*DIBt KKW Leitfaden (2010)*), however, does not address anchor ductility anymore.

2.3.2 US Anchor Qualification Guidelines

ACI 355.2 (2007) does not address ductility. However, provisions are given for the acceptance criteria in Annex 1 of *AC193 (2010)* which require in Clause 6.3.6 tension tests on machined coupon specimens according to *ASTM F606 (1998)* and classifies an anchor as ductile if the elongation is at least 14 % (measured over a gauge length equal to 4 d) and the reduction of area of at least 30 %. If the ductility and reduction in area cannot be determined, the anchor shall be reported as brittle in the report. It is further recommended that the material testing on machined coupons is supplemented by tests on full-size anchor specimens to identify possible deviations from the coupon tests results, as they may be caused by the forming and finishing processes of anchor production. The acceptance criterion for adhesive anchors, *AC308 (2009)*, requires also an elongation of at least 14 % and a reduction of area of at least 30 %. The requirements are in line with the design guideline *ACI 318 (2011)* which defines in Section D.1 an element with a tensile test elongation of at least 14 % and reduction in area of at least 30 % as ductile. For specifications regarding the tensile testing, it refers to the *ASTM A307 (1997)*, which, in turn, refers to *ASTM F606 (1998)*. If the anchor is not classified as ductile, the anchor shall be designed for the maximum load that can be transmitted to the anchor based on a ductile yield mechanism or by a non-yielding element. Alternatively, the anchor shall be designed for increased design loads.

2.3.3 Conclusions

The designation of whether an anchor is ductile or brittle affects several aspects of design. The most prominent aspect is the seismic design of anchoring according to CENT/TS 1992-4 and ACI 318. Both guidelines punish brittle anchor failure if it cannot be shown that either the element fixed by the anchor yields before anchor failure or the anchor is qualified as ductile. According to Clause 8.4.3(3) of *CEN/TS 1992-4 (2009)*, the seismic design resistance is taken at least 2.5 times the effect of the applied seismic actions which equals to a strength reduction factor of 0.4. Also Clause D.3.3.6 of *ACI 318 (2008)* Appendix D permits to take the design strength of the anchors as 0.4 times the regular design strength in case of brittle anchor failure: The lately revised *ACI 318 (2011)*, however, dropped the approach to apply a strength reduction factor but stipulates in Clause D.3.3.4.3(d) the application of amplification factors Ω_0 on the design load in case of brittle anchor failures which is technically the same. According to Clause R21.13.7, the Ω_0 factors given in documents such as the *ASCE 7 (2010)* and the *IBC (2009)* to account for overstrength of the seismic resisting system can be used for this purpose. Table 12.2-1 provides overstrength factors for building structures which are in the range of 2.0 to 3.0. The discussion on overstrength factors for non-structural

elements is still ongoing, however, it may be assumed that they are in the range of 1.5 and 2.5. In conclusion, it still holds that the design guidelines strongly privilege ductile anchor behaviour.

ETAG 001 (2006) does not recognize seismic actions, however, ductility is not only relevant for seismic design but it is believed to be generally beneficial in structural engineering. In particular, *ACI 318 (2011)* Clause D.4.3 promotes ductile anchorages by a beneficial reduction factor ϕ, which is given for anchors governed by strength of ductile steel given as 0.75 for tension loads and 0.65 for shear loads; and for anchors governed by strength of a brittle steel element as 0.65 for tension loads and 0.60 for shear loads. Also the plastic design of structural connections according to *CEN/TS 1992-4 (2009)* Annex B is acceptable only when the failure is governed by ductile steel failure of the anchor.

In conclusion, recent developments in the design codes provisions show an increasingly substantiated approach for the appropriate recognition of anchor ductility. In contrast and despite of the importance of anchor ductility, qualification guidelines address anchor ductility insufficiently.

For a conclusive seismic anchor qualification scheme, the following points need to be addressed regarding anchor ductility:

- What is anchor ductility, how is it defined, and what is its impact on seismic design?
- How can anchor ductility be tested and what is the requirement to be qualified as ductile?

2.4 Anchor Groups

The distribution of loads in an anchor group is influenced by the stiffness and displacements of the individual anchors. In order to avoid adverse load distribution and overloading of individual anchors, existing qualification guidelines limit the allowable scatter for monotonic pullout curves. For seismic anchor qualification, meaningful assessment criteria need to be established. In the following, the qualification guidelines are reviewed with respect to anchor groups. A comprehensive review on normative standards as well as on other literature regarding anchor groups can be found in *Mahrenholtz, P. (2008)*.

2.4.1 European and German Anchor Qualification Guidelines

Clause 3.2.1 in Part 1 of *ETAG 001 (2006)* defines an anchor group as several anchors working together. Chapter 6 in Part 1 of *ETAG 001 (2006)* provides limits on

the scatter of the load-displacement curves explicitly to prevent a significant decrease of anchor group capacity by unequal load distribution. For this purpose, the coefficient of variation (CV) of the displacement at 50 % of the mean ultimate load, $s(0.5\ F_{u,m})$ is generally limited to 40 % for suitability tests and 25 % for serviceability tests. Further, for anchors to be used in cracked and uncracked concrete, the ratio of the average secant modulus between maximum load and the origin in cracked and uncracked concrete shall not be larger than about 3. The additional limitation of the CV of the ultimate load, $F_{u,m}$, to 20 % for suitability tests and 15 % for serviceability tests, however, is not specifically related to anchor group behaviour.

Table 5.4 in Part 1 of *ETAG 001 (2006)* provides the test programme for admissible service conditions (Option 1) and lists Test No. 13 with the purpose to evaluate the spacing for characteristic tension resistance. The test is carried out on a quadruple anchor group installed in uncracked concrete and enables the determination of the spacing required for the transmission of the full characteristic concrete cone resistance of a single anchor loaded in tension, $s_{cr,N}$. Clause 5.2.2 of *ETAG 001 (2006)* Annex A specifies the fixture of the quadruple anchor group test to be rigid, i.e. non-flexible or stiff. The connection between the fixture and the load actuator shall be hinged to allow for different anchor displacement. However, according to Clause 6.2.2.3, $s_{cr,N}$ can be deemed as being equal to $3\ h_{ef}$ if the anchor falls within the current experience for concrete cone failure. Clause 2.0 of *ETAG 001 (2006)* Annex B in conjunction with Part 1 of *ETAG 001 (2006)* clarifies that the current experience is generally valid for expansion and undercut anchors. Therefore, Test No. 13 is generally not included anymore in regular qualification test programmes for expansion and undercut anchors.

Clause 1.1 of *ETAG 001 (2006)* Annex C specifies that in an anchor group only anchors of the same type, size and length shall be used. In case of an anchor group, the loads are applied to the individual anchors of the group by means of a rigid fixture (see also Clause 4.2.1). Conversely, flexible fixtures are not covered. The design methods cover anchor groups with up to 8 anchors (Figure 2.4) which configurations are basically in line with those given in *CEN/TS 1992-4 (2009)*.

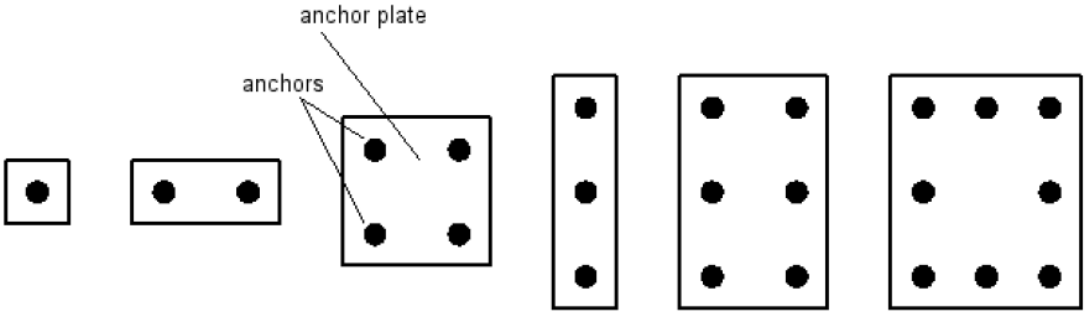

Figure 2.4 Anchorages covered by the design methods of *ETAG 001 (2006)* Annex C

The German NPP Guideline *DIBt KKW Leitfaden (2010)* does not give any additional provisions concerning anchor groups.

2.4.2 US Anchor Qualification Guidelines

ACI 355.2 (2007) Clause 2.1.2 defines an anchor group as a number of approximately equal effective embedment depth with each anchor spaced at less than three times its embedment depth. Clause 5.5.2 requires the mean anchor stiffness value $\beta = (N_{30\%} - N_{10\%}) / (\Delta_{30\%} - \Delta_{10\%})$ and its variation to be determined within one test series. In contrast to the provisions as given in the *ETAG 001 (2006)*, however, no specific limit is given. However, the requirements given in Chapter 7 (for serviceability tests) to Chapter 8 (for suitability tests) state that the CV of the ultimate load shall not exceed 15 and 20 %, respectively. This is in line with the provisions given in *ACI 355.4 (2010)*. The test programme as given in Table 4.2 does not provide any group test for the determination of the minimum spacing for full characteristic concrete cone resistance. The definition of an anchor group given in *ACI 318 (2008)* corresponds to that of *ACI 355.2 (2007)*.

2.4.3 Conclusions

The understanding of anchor groups in the qualification guidelines is directly (*ACI 355.2 (2007)*) or indirectly (*ETAG 001 (2006)*) linked to the spacing of the anchors: For an anchor spacing of $s_{cr,N} = 3\ h_{ef}$, full characteristic concrete cone resistance can be assumed. As a result, a group of anchors with each anchor spaced more than $3\ h_{ef}$ is technically not an anchor group, because according to the concrete capacity design method underlying the design provisions given in *ETAG 001 (2006)* Annex C and *ACI 318 (2011)* Appendix D, the potential concrete cones do not overlap then.

Provided that the scatter of the individual load-displacement curves is small enough, it is assumed that the load capacity of an anchor group with $s_{cr,N} \geq 3\ h_{ef}$ is not reduced if compared to single anchors. The limits given in the qualification guidelines for the stiffness and displacement at peak load, however, were developed for monotonic loading in the first place.

For a conclusive seismic anchor qualification scheme, the following points need to be addressed regarding anchor groups:

- Are the assessment criteria given in the qualification guidelines regarding limitation of scatter sufficient also for seismic loading and, if not, is any additional criteria required?
- Is the implementation of a seismic group factor necessary to capture potential reduction in load capacity?

2.5 Cyclic Loads

Cyclic loads may be caused by live loads, which are generally considered as quasi-static loads due to their slow variation in time and negligible inertial and damping forces, or earthquake loads, which are in principle designated as dynamic forces. The review on the state-of-the-art of anchor qualification guidelines is limited to Europe/Germany and the US, however, for the sake of completeness it is mentioned here that *CAN3-N289.4-M86 (1986)* and *SEAOSC (1997)* were the first published testing procedures for seismic anchor qualification and are still often cited in the literature. In the following, qualification guidelines are reviewed with respect to tests involving cyclic loads. A comprehensive review on existing normative standards for existing seismic anchor qualification can be found in Appendix B.2 of *Hoehler, M. (2006)*.

2.5.1 European and German Anchor Qualification Guidelines

One suitability test type according to *ETAG 001 (2006)* is defined to test the functioning of the anchor under repeated load. The anchor is installed in uncracked concrete and is subjected to 10^5 tension load cycles between N_{min} = min {0.25·N_{Rk} and $A_s \cdot \Delta\sigma$} and N_{max} = max {0.6·N_{Rk} and 0.8·$A_s \cdot f_{yk}$} (where N_{Rk} = characteristic monotonic strength in uncracked concrete; A_s = cross-sectional area; f_{yk} = characteristic yield strength of anchor; $\Delta\sigma$ = 120 N/mm²). The cycle frequency is defined as 6 Hz maximum. The stipulated parameters clearly reflect the intention of the test as a high cycle fatigue (HCF) test. The requirement on the anchor performance is that the residual strength measured in the pullout test after the load cycling reaches 100 % of the monotonic reference strength. If this criterion is not met, the characteristic strength is reduced as described in Section 2.1.7.

The *DIBt KKW Leitfaden (2010)* includes cyclic tension tests for suitability and service condition test series. Cyclic shear tests are carried out only as service condition tests because the aim of the suitability test series is to check the effect of extreme crack widths on the anchor performance. The crack width, however, has a relatively small influence on the shear behaviour. The number of uniform load cycles vary between 10 and 15 (maximum frequency 1 Hz), and the maximum anchor load is defined as $N_{max} = N_{Rk} / \gamma_{Mc}$ for tensile load cycling and $V_{max} = V_{Rk} / \gamma_{Ms}$ for shear load cycling where γ_{Mc} = partial safety factor for concrete failure = 1.7 and γ_{Ms} = partial safety factor for steel failure = 1.25. The crack width is generally taken as w = 1.0 mm for serviceability tests and w = 1.5 mm for suitability tests. The residual capacity is required to achieve 90 % of the mean ultimate load measured in monotonic reference tests in the same crack width. In case of failure during cycling or not meeting the requirement regarding the residual load capacity, the tests are

retaken with lower maximum load and the design strength is reduced accordingly (refer to Section 2.1.7). As a unique feature of this test type it is noted that the guideline requires that in cyclic tension tests the anchor is not only unloaded to zero load for each cycle but is also pushed back to its original position. This demands a special setup allowing for transmission of compressive loads on the anchor. In addition, precautionary measures have to be taken to avoid control problems since cyclic load tests are run load controlled and the anchor may experience slackness when pushed back.

2.5.2 US Anchor Qualification Guidelines

ACI 355.2 (2007) provides a suitability test under repeated load (HCF test). The test conditions and assessment criteria are virtually identical to those stipulated in *ETAG 001 (2006)* and are not repeated here.

As already noted in Section 2.1.3, anchor qualification for seismic actions can be acquired according to *ACI 355.2 (2007)* by passing simulated seismic tests for which the anchor is loaded in separate tension and shear load cycling tests. The same applies to *ACI 355.4 (2010)*. The term 'simulated' indicates that (dynamic) earthquake loads deriving from a transient oscillation are simulated by a (quasi-static) load regime which is applied to the anchor on a component level. The stepwise decreasing loading patterns of 140 cycles are shown in Figure 2.5. The maximum anchor loads, designated as earthquake loads, N_{eq} and V_{eq}, respectively, correspond to 50 % of the mean monotonic reference strength $N_{u,m}$ tested in 0.3 mm crack. The maximum anchor loads are reduced to $N_i = 0.75\ N_{eq}$ and $V_i = 0.75\ V_{eq}$, respectively, for the intermediate cycles and to $N_m = 0.5\ N_{eq}$ and $V_m = 0.5\ V_{eq}$, respectively, for the final cycles. Qualification is based on (1) completing all load cycles, and (2) achieving a residual capacity of at least 160 % N_{eq} and 160 % V_{eq}, respectively, i.e. 80 % of the mean monotonic reference strength. If the anchor fails to fulfill the aforementioned requirements, the tests have to be repeated with a reduced maximum anchor load and the nominal seismic strength has to be reduced linearly (refer to Section 2.1.7). It is noted that contrary to the repeated load test (HCF test) in *ETAG 001 (2006)* and *ACI 355.2 (2007)*, the simulated seismic tests are considered as serviceability tests. However, the required crack width of 0.5 mm and the assessment procedure are identical to that of static suitability tests.

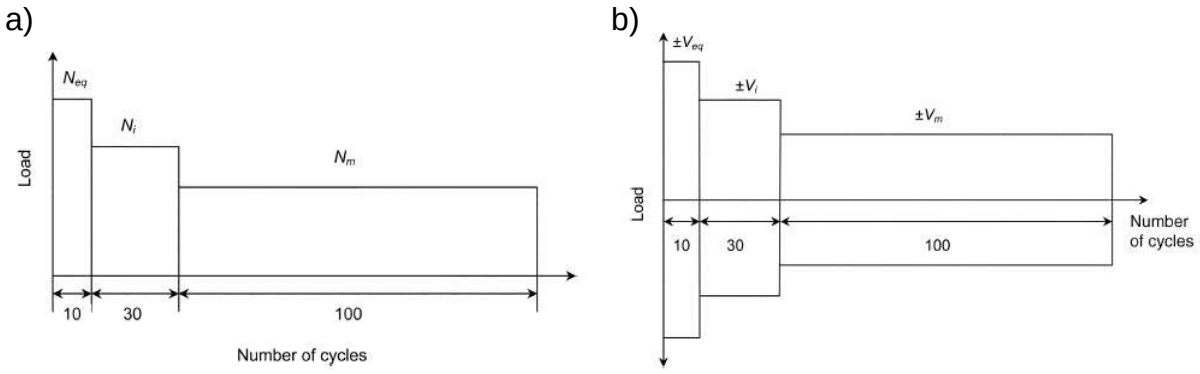

Figure 2.5 Loading pattern given in *ACI 355.2 (2007)*: a) Simulated seismic tension tests; b) Simulated seismic shear tests

2.5.3 Conclusions

Cyclic loads are a characteristic if not the most prominent feature of seismic actions. Therefore, load cycling tests will also form in future one of the main pillars of seismic anchor qualification.

The test conditions and assessment criteria compiled in Table 2.3 reflect the difference of repeated load tests (HCF test of tension loaded anchors) and cyclic load tests according to the NPP Guideline or simulated seismic tests according ACI 355. Apart from the crack widths, the cyclic (NPP Guideline) and simulated seismic (ACI 355) tests are relatively similar in view of number of cycles and maximum load level. If considering the decreasing load pattern shape of the simulated seismic tests with only 10 large strikes in the beginning and neglecting the other 130 cycles (Figure 2.5), also the number of cycles seems to be in the same magnitude. Further, the approach for the assessment criteria of minimum residual capacity expressed as a percentage of the corresponding reference test is virtually the same. However, it is noted that even small variations in critical test parameters may have a substantial impact on the anchor demands which in turn leads to different anchor performances.

Table 2.3 Overview of main test conditions and assessment criteria for qualification tests involving cyclic loads

	Test Conditions				Assessment Criteria	
	Crack Width w	Number of Cycles n	Max Anchor Load N_{max}	Frequency f	Residual Capacity	Scatter $CV(F_u)$
Repeated tension load test ETAG	0.0 mm	10^5	0.6 $N_{Rk,0.0mm}$	≤ 6 Hz	≥ 1.0 $N_{Rk,0.0mm}$ (3), ≥ 1.0 $N_{Ru,m,0.0mm}$ (3)	≤ 20 %
Repeated tension load test ACI	0.0 mm	10^5	0.6 $N_{Rk,0.0mm}$	≤ 6 Hz	≥ 1.0 $N_{Ru,m,0.0mm}$ (3)	≤ 20 %
Cyclic load tests NPP, tension	1.5 mm	15	0.6 $N_{Rk,1.5mm}$	≤ 1 Hz	≥ 0.9 $N_{Ru,m,1.5mm}$ (3)	-
Cyclic load tests NPP, shear	1.0 mm	15	0.8 $V_{Rk,1.0mm}$	≤ 1 Hz	≥ 0.9 $V_{Ru,m,1.0mm}$ (3)	≤ 10 % (1)
Simulated seismic test ACI	0.5 mm	140	0.5 $F_{Ru,m,ref}$ (2)	0.1 ÷ 2 Hz	≥ 0.8 $N_{Ru,m,ref}$ (4)	-

(1) For CV > 10 % but < 30%, characteristic shear strength reduced by 1/(1+0.03 (CV-10%))
(2) For CV = 10 %: 0.5 $N_{Ru,m,ref}$ ≤ 0.5/(1-1.645·10 %) $N_{Rk,ref}$ = 0.60 $N_{Rk,ref}$
For CV = 15 %: 0.5 $N_{Ru,m,ref}$ ≤ 0.5/(1-1.645·15 %) $N_{Rk,ref}$ = 0.67 $N_{Rk,ref}$
(3) If requirement is not fulfilled, reduce the characteristic strength
(4) If requirement is not fulfilled, repeat the test with reduced load level and reduce the strength accordingly

Contrary to fatigue loading with load cycle numbers in the range of 10^4 to 10^8 (HCF), earthquake loading is characterised by a relatively limited number of cycles. The number of significant amplitudes depends on many boundary conditions, however, it can be assumed to be in the range of 10 to 1000 at maximum (e.g. *Ammann, W. (1992)*). Therefore, repeated load tests are not an adequate substitute for seismic qualification and were never intended to replace.

The simulated seismic test according to *ACI 355.2 (2007)* provides qualification procedures developed for the specific demands of earthquake loads. Its loading protocol falls back on fundamental research reported in *Tang, J.; Deans, J. (1983)*, however, the number of cycles had been reduced because it was felt that the originally proposed 340 cycles are too many to represent seismic anchor load characteristics plausibly. In particular the very small cycles may be assumed to have virtually no effect on the residual load capacity of the installed anchor and thus lengthen the test procedure unnecessarily.

The simulated seismic tests according to *ACI 355.2 (2007)* are separated for shear and tension loads, though the anchor may be subjected to the combination of both. This approach is more practical and less expensive than combined tension and shear load tests, while generally deemed to be conservative. According to *ACI 318 (2011)*

Section D.7, anchors that are subjected to both shear and axial loads shall be designed to satisfy a linear interaction equation while for design loads less than 20 % of the design strength the full strength may be taken. This provision applies to static as well as seismic loads.

All qualification tests discussed above are carried out at quasi-static loading rates. This approach is deemed conservative because it can be generally assumed that dynamic loading rather increases the resistance i.e. material strength. The same holds for the cycling frequencies which are consequently limited to an upper value.

For a conclusive seismic anchor qualification scheme, the following points need to be addressed regarding cyclic loads:

- What number and shape of load cycles is scientifically substantiated and meaningful? What are the minimum and maximum anchor loads during load cycling? What is the crack width during load cycling and residual capacity testing?
- How do various anchor types behave under these conditions?

2.6 Cyclic Cracks

Cracking of concrete may have various causes which are described in detail e.g. in *CEB Bulletin d'information No. 158 (1984)*. The crack widths vary if located in a flexural member which state of stress changes over time. For reverse actions caused by live or earthquake loads, the effect results in cycled crack widths, abbreviated to cycled cracks or simply cyclic cracks. In the following, qualification guidelines are reviewed with respect to tests involving cyclic cracks. A comprehensive review on normative standards regarding cyclic crack tests can be found in *Mahrenholtz, C. (2010)*.

2.6.1 European and German Anchor Qualification Guidelines

One suitability test type according to *ETAG 001 (2006)* is defined to test the functioning of the anchor for crack movements. The anchor is installed in special concrete slabs and loaded until a constant tension load of $N_P = 0.75\ N_{Rk} / \gamma_{Mc}$ (with N_{Rk} = characteristic monotonic strength in cracked concrete and $\gamma_{Mc} \geq 1.5$). The crack, in which the anchor is located, is then opened and closed 1000 times between $\Delta w_1 = 0.3$ mm and $\Delta w_2 = 0.1$ mm at an approximate frequency of 0.2 Hz. The 'Δ' indicates that the crack width is measured in addition to the hairline crack width which remains after initial crack generation. The closing of the crack is generated by the restoring force in the tensioned reinforcement. With increasing numbers of cycles and wear of the crack faces, the restoring force of the reinforcement is not sufficient

to close the crack fully. Therefore, Δw_2 may increase up to 0.2 mm in the course of crack cycling, however, is not allowed to be controlled. The curved line in Figure 2.6a illustrates an example for the allowable lower crack width. The upper crack width Δw_1 must be increased if the crack difference between Δw_1 and Δw_2 further deteriorates to maintain a minimum difference of 0.1 mm. The number of crack cycles and maximum crack width shall simulate the condition deriving from frequently repeated deformations in the anchorage material caused by loading and unloading of the structure during life time, for which reason this kind of test is also sometimes addressed as service life test (SLT). In each test, the rate of increase of anchor displacements, plotted in a half-logarithmic scale should either decrease or be almost constant. Further, it is required that the displacement experienced by the anchor during cycling δ_{1000} does not exceed 2 mm after 20 crack cycles and 3 mm after 10000 crack cycles (Figure 2.6b) and that the residual strength measured in the pullout test carried out after crack cycling reaches 90 % of the monotonic reference strength. If the 3 mm criterion is not met, the test has to be repeated with a reduced permanent load N_P and the design strength of the anchor is reduced accordingly. If the criterion on the residual strength is not met, the characteristic strength is also reduced as described in Section 2.1.7.

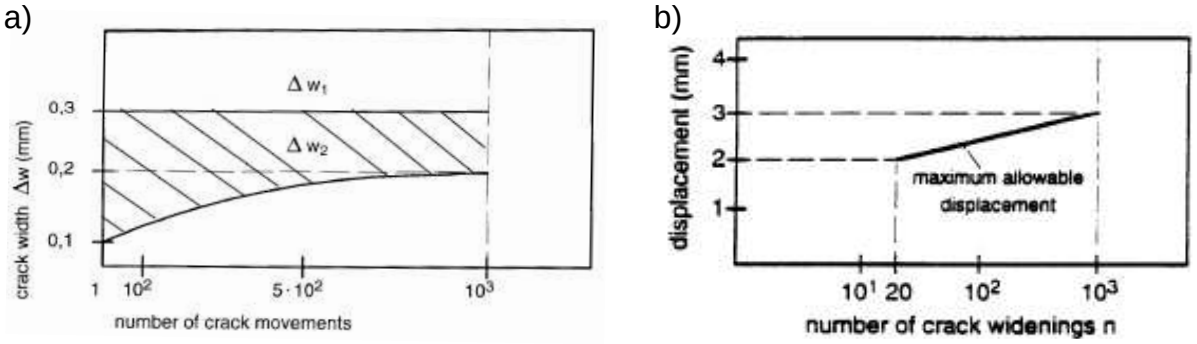

Figure 2.6 Specification for cyclic crack tests according to *ETAG 001 (2006)*: a) Variation of crack opening during the crack movement test; b) Criteria for maximum allowable anchor displacement

The *DIBt KKW Leitfaden (2010)* includes cyclic crack tests for suitability and service condition test series. The number of uniform crack cycles vary between 5 (serviceability tests) and 10 (suitability tests) at an approximate frequency of 0.2 Hz, and the permanent anchor load for crack cycling is defined as $N_P = N_{Rk} / \gamma_{Mc}$. The crack is opened to the maximum crack width of w_{max} = 1.0 mm for serviceability tests and w_{max} = 1.5 mm for suitability tests. The maximum crack width can be reduced if a detailed analysis is performed for the concrete structure in which the anchor is going to be installed. Minimum crack width is w_{max} – 0.5 mm or, for w_{max} < 1.2mm, 0.0 mm which is achieved by applying a compression force to the concrete test specimen equal to 15 % of the compressive strength of concrete specimen. The residual

capacity in the suitability test is required to achieve 90 % of the mean ultimate load measured in monotonic reference tests in the same crack width. In case of failure during cycling or not meeting the requirement regarding the residual load capacity, the tests are retaken with lower permanent load and the design strength is reduced accordingly (refer to Section 2.1.7). Additional to the assessment criteria in principle explained in Section 2.5.1, the mean displacement of the anchor is limited to 3 mm if in the structural analysis the anchor connection is assumed to be rigid. This requirement originates from the Nuclear Committee Guideline (*KTA 3205.3 (2006)*, Clause F 4.4).

2.6.2 US Anchor Qualification Guidelines

Also *ACI 355.2 (2007)* and *ACI 355.4 (2010)* provide a suitability test in cracked concrete where the crack width is cycled. It is also often addressed as crack movement test. The test conditions and assessment criteria are virtually the same as for *ETAG 001 (2006)* (Figure 2.7) and thus are not repeated here in detail. The permanent load, however, is basically calculated as $N_w = 0.3\ N_{Rk}$.

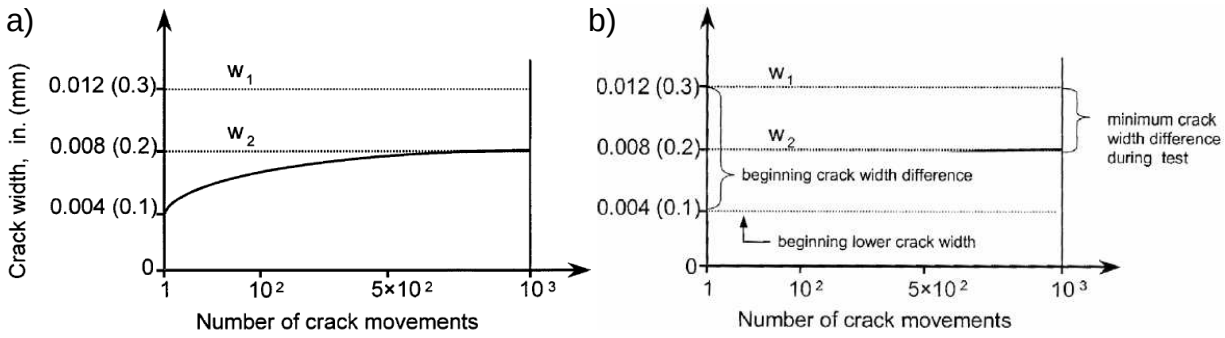

Figure 2.7 Variation of crack opening during the crack movement test: Specification according to a) *ACI 355.2 (2007)* and b) *ACI 355.4 (2010)*

2.6.3 Conclusions

Cyclic loads acting on the structure and resulting cycled cracks in the concrete elements are characteristic features of a seismic event. Cycled cracks results in accumulating anchor displacement and due to the reduced embedment depth in reduced residual capacity. Therefore, crack cycling tests demand special attention in respect to seismic anchor qualification.

The main test conditions and assessment criteria compiled in Table 2.4 reflect the difference of crack movement tests (tests of the effects of frequently repeated deformations in the anchorage material) and cyclic tests according to NPP Guideline. It is noteworthy that the provisions for the crack movement test according to ACI 355

show a significant smaller permanent anchor load level N_p, and that an assessment criterion in respect to minimum residual capacity is not stipulated.

Table 2.4 Overview of main test conditions and assessment criteria for qualification tests involving cycled cracks

	Test Condition				Assessment Criteria		
	Min Max Crack Width w	Num. of Cyc. n	Permanent Anchor Load N_P	Frequency f	Residual Capacity	Scatter CV(F_u)	Anchor Displ.
Crack movement test ETAG	0.1 mm 0.3 mm	10^3	0.5 $N_{Rk,0.3mm}$	~ 2 Hz	≥ 0.9 $N_{Rk,0.3mm}$ (2)., ≥ 0.9 $N_{Ru,m,0.3mm}$ (2)	≤ 20 %	≤ 2 mm (3) ≤ 3 mm (4)
Crack movement test ACI	0.1 mm 0.3 mm	10^3	0.3 $N_{Rk,0.3mm}$	≤ 2 Hz	-	≤ 20 %	≤ 2 mm (3) ≤ 3 mm (4)
Cyclic crack tests NPP, service.	0.0 mm (1) 1.0 mm	10	0.6 $N_{Rk,1.5mm}$	~ 0.2 Hz	≥ 0.9 $N_{Ru,m,1.5mm}$ (2)	-	≤ 2 mm (3) ≤ 3 mm (4)
Cyclic crack tests NPP, suitability	1.0 mm (1) 1.5 mm	10	0.6 $N_{Rk,1.5mm}$	~ 0.2 Hz	≥ 0.9 $N_{Ru,m,1.5mm}$ (2)	-	≤ 3 mm (5)

(1) Crack width corresponding to compression force to the concrete specimen of 0.15 $A_c.f_c$ (A_c = cross section and f_c = compressive strength of concrete specimen)
(2) If requirement is not fulfilled, reduce the characteristic strength
(3) After 20 cycles; if requirement is not fulfilled, repeat the test with reduced load level and reduce the strength accordingly
(4) After 10000 cycles; if requirement is not fulfilled, repeat the test with reduced load level and reduce the strength accordingly
(5) Only for displacement sensitive anchorages

Other than for load cycling, the *DIBt KKW Leitfaden (2010)* is the only guideline incorporating a simulated seismic test procedure to test the anchor response to crack cycling. However, crack movement tests form an integral part of anchor qualification and the compliance with their assessment criteria may be considered as a prerequisite for anchors seeking approval for seismic loads. Because of the slip the loaded anchor experiences every time when the crack opens and the resulting reduction of embedment depth and load capacity, crack movement tests are known to be very demanding qualification tests. In fact they are for some anchor types more critical than the simulated seismic test currently stipulated. However, their test parameters are not representative for earthquakes, as the number of cycles is high and the maximum crack width is small. Consequently, crack movement tests are not an adequate substitute for seismic qualification.

While cracks have a significant negative influence on the anchor performance when loaded in tension, the effect of cracks on the performance of anchors loaded in shear is comparatively small. This is also true for cycled cracks. In particular, the lateral

anchor displacement of an anchor loaded in shear does not increase when the cracks cycle. In conclusion, crack cycling matters only for tension, not for shear. It is further pointed out that currently all qualification tests involving cycled cracks require the permanent load acting on the anchor to be constant over time.

As for the qualification tests involving cyclic loads, the crack cycling is performed quasi-statically. It is generally believed that this approach is on the safe side since higher crack cycling frequencies would prevent the anchor from experiencing any slip as a reaction on the crack opening and closing while being permanently loaded.

For a conclusive seismic anchor qualification scheme, the following points need to be addressed regarding cycled cracks:

- What number and shape of crack cycles is scientifically substantiated and meaningful? What are the minimum and maximum crack widths during cycling? What is the permanent anchor load during crack cycling?
- How do various anchor types behave under these conditions?

2.7 Simultaneous Load and Crack Cycling

Anchor load and crack width may cycle simultaneously. For the needs of reasonably simplified testing procedures, however, cyclic demands are tested by separate tests for which only one parameter is cycled and the other is kept constant. This approach is deemed to be conservative and was followed by the qualification guidelines ETAG 001, NPP Guideline, and ACI 355 since the implementation of cyclic tests. In consequence, there are only qualification tests with cyclic anchor load but constant crack width (Figure 2.8b1, refer to Section 2.5), and with cyclic crack width but constant anchor load (Figure 2.8b2, refer to Section 2.6).

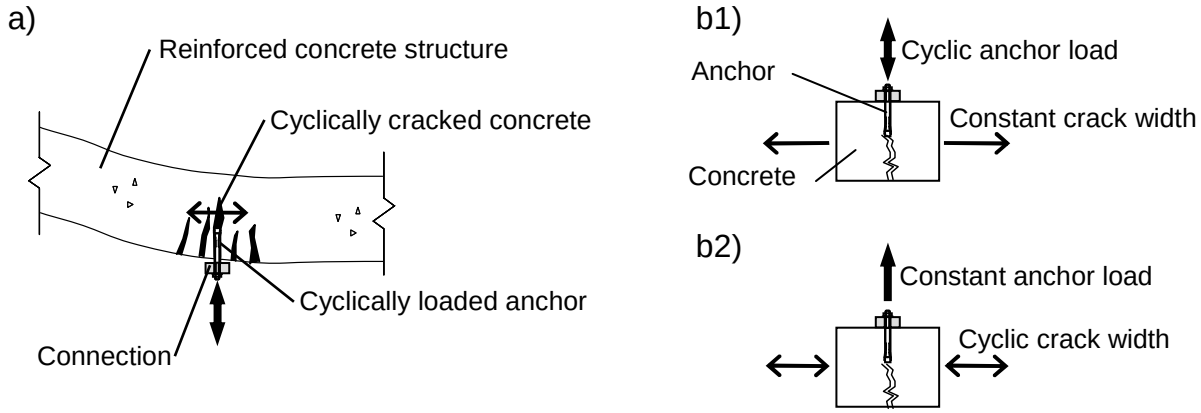

Figure 2.8 a) Simultaneous load and crack cycling in a reinforced structure responding to seismic actions; b) Experimental approach to test b1) Cyclic loads and b2) Cyclic cracks

Since post-installed anchors are in particular sensitive to cyclic cracks, it is worthwhile to study the simultaneous load and crack cycling behaviour in order to answer the following question:

- Is a permanent load acting during cyclic crack tests conservative if simultaneous load and crack cycling is considered?

2.8 Summary

After a long process, European and US qualification guidelines are harmonised to a very significant degree. The qualification test programme of *ETAG 001 (2006)*, *ACI 355.2 (2007)* and *ACI 355.4 (2010)* include repeated load tests and crack movement tests. However, repeated load tests and crack movement tests simulate loading conditions other than those prevalent during seismic actions. Repeated load tests check fatigue behaviour in tension. Crack movement tests check axial displacement behaviour of anchors during service life. The *ACI 355.2 (2007)* for anchors in the US and the *DIBt KKW Leitfaden (2010)* for anchors in nuclear power plants in Germany are currently the only anchor qualification guidelines considering seismic actions (tension and shear). The effective European anchor qualification guideline does not cover seismic actions, however, a seismic amendment is under preparation (*Proposal for ETAG 001 Seismic Amendment (2012)*) which will be presented in Chapter 4.

In case of not completing all cycles or not meeting the required residual capacity, all relevant cyclic qualification tests allow repeating the tests under lower maximum or permanent anchor load, respectively, to establish a reduced nominal strength. This procedure often results in several runs and increased costs. Future seismic anchor qualification guidelines, however, are expected not to increase the testing burden further while significantly improving the understanding of their behaviour.

Dynamic loads arising from earthquakes are located between impact loading with one strike of high intensity (shock testing, Section 2.2) and mechanical vibration with large cycle number of moderate intensity (repeated load tests, Section 2.5). High loading rate tests are necessary in order to close the gap for earthquake relevant dynamic loads.

It is noteworthy that the test conditions and assessment criteria of existing qualification guidelines are very much load rather than displacement oriented. While Displacement Based Design (DBD) is a structural design approach very much considered in last decades, the consequent consideration of seismic anchor capacity as a matter of displacement driven failure has just started. However, the tests for the determination of the anchor displacement under service condition (crack movement tests, Section 2.6) limit the anchor displacement after crack cycling to 3 mm.

Minimum and maximum anchor displacements occurring under seismic conditions are also relevant in conjunction with anchor ductility (Sections 2.3) and with anchor groups (Sections 2.4). These aspects have to be dealt with in more detail.

In summary, the preceding sections identified deficits in the qualification guidelines and outlined the resulting questions. Understanding the existing qualification guidelines can give important but not exhaustive information on possible deficiencies in anchor qualification procedures. Also earlier studies carried out on the various aspects of seismic loading and related anchor behaviour help to reveal the necessity of further investigations. This is done in the following Chapter 3 next to the presentation of the investigations on anchor performance under seismic conditions.

3 Studies at Component Level: Simulated Seismic Tests

This chapter presents the theoretical and experimental studies carried out to overcome the deficiencies identified in Chapter 2. The scope of the work presented in the following is very large. Altogether, the documentation of the studies carried out by the author comprises more than 2500 report pages. Therefore, the discussions in Chapter 3 are very focused on the relevant items. After some general remarks given in Section 3.1, each of the following sections deals with one of the aspects discussed in Chapter 2:

Sections 3.2: Loading Rate

Sections 3.3: Anchor Ductility

Sections 3.4: Anchor Groups

Sections 3.5: Cyclic Load

Sections 3.6: Cyclic Crack

Sections 3.7: Simultaneous Load and Crack Cycling

Introductorily to each section, the state of knowledge is briefly presented. Finally, Section 3.8 summarises the core statements for future seismic qualifcation procedures.

3.1 General

Some general remarks which hold for all experimental tests are discussed in the following sections.

3.1.1 Anchor types

A large variety of qualified anchor products are available, and designers, authorities and contractors can pick the most appropriate and economic anchor product for the targeted use. Detailed description of available anchor types, their specific load transfer mechanism and associated failure mode can be found in *Eligehausen, R.; Mallée, R. et al. (2006)* and other literature, and are not repeated here. It is noted the term ‘anchor’ is synonymous to the term ‘fastener’. Figure 3.1 provides an overview on the basic anchor types relevant for the presented thesis including their abbreviation used in this thesis, the associated load transfer mechanism (LTM) and

predominant failure mode (PFM) in tension. Further details are given in the relevant sections.

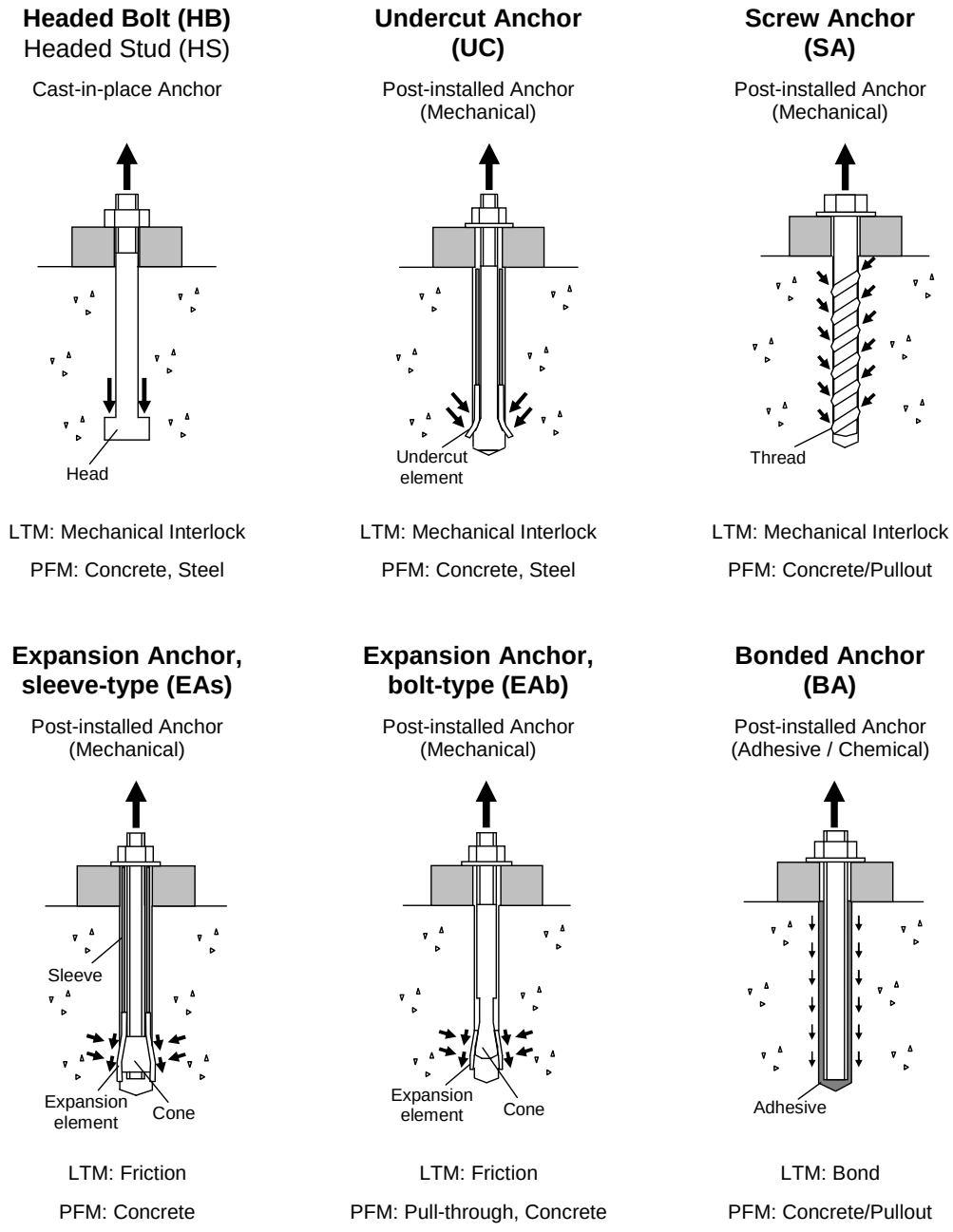

Figure 3.1 Basic anchor types, their load transfer mechanism (LTM) and associated predominant failure mode (PFM)

The investigations presented in the following sections were carried out on various anchor types and products of different manufacturers. For reasons of confidentiality, the anchor types are represented in anonymous form. If several anchor products of the same anchor type were tested, the abbreviations were amended by a numeric suffix.

It is noted that the anchors were to a great extent tested under conditions they were not qualified for. In particular, the maximum crack width of 0.8 mm (Section 3.1.5), which is substantially larger than the 0.5 mm specified in effective guidelines, pushes certain anchor types to their limits. Also, the maximum or permanent anchor loads in case of load or crack cycling tests were higher than what is required according to the current anchor qualification tests. In conclusion, any adverse load-displacement behaviour does not disqualify the tested anchors in the sense of currently effective qualification guidelines. However, the goal was to study the seismic performance of a wide range of anchor products on the market, and not to qualify the anchors from the spot for extreme seismic demands. In addition, testing anchors in larger crack widths than what they were originally qualified for was also instructive since it is a common practice to install anchors in an environment they are not necessarily suitable for.

3.1.2 Failure modes and ultimate capacity

The load capacity of anchors loaded in tension is governed by the failure mode corresponding to the smallest capacity. The following three basic failure modes and associated capacities can be determined:

- Steel failure (S): The steel capacity is given by the steel resistance of the anchor. Exceedance of the steel capacity results in rupture of the anchor (Figure 3.2a1). The ultimate steel capacity $N_{u,s}$ of an anchor with the cross section A_s and ultimate steel strength f_u is given by:

  $$N_{u,s} = A_s \cdot f_u \qquad \text{Equation 3.1}$$

  Since most anchor products are designed for maximisation of the load capacity for a given embedment depth, hardly any anchor develop the steel failure mode. However, the characteristic steel strength is generally provided in the technical approval.

- Concrete failure (C): The concrete capacity is given by the concrete resistance of the anchorage material. Exceedance of the concrete capacity results in a conical concrete breakout (Figure 3.2a2) and primarily depends on the embedment depth h_{ef} and concrete strength f_c. The ultimate concrete capacity is evaluated according to the Concrete Capacity Design (CCD Method; *Fuchs, W.; Eligehausen, R.; Breen, J. (1995)*), termed in Europe as Concrete Capacity Method (CC Method; *Fuchs, W.; Eligehausen, R. (1995)*):

  $$N_{u,c} = k \cdot \sqrt{f_c} \cdot h_{ef}^{1.5} \qquad \text{Equation 3.2}$$

  where ‘k’ is an empircally determined factor which is defined in the relevant anchor design guideline, or otherwise given in the technical approval for the calculation of the characteristic strength for uncracked or cracked concrete.

- Pullout failure (P): For this failure mode, the anchor is pulled out the drilled hole before the anchor ruptures or the concrete breaks (Figure 3.2a3). The pullout capacity depends on the anchor type. The pullout capacity of mechanical anchors can generally be determined only experimentally and is provided in the technical approval as characteristic strength for uncracked or cracked concrete. The pullout capacity of adhesive anchors depends primarily on the embedment depth h_{ef} and bond strength τ_u, and can be determined on the basis of the Uniform Bond Model (UB Model; *Cook, R.; Kunz, J. et al. (1998)*):

  $$N_{u,p} = \pi \cdot d \cdot h_{ef} \cdot \tau_u \qquad \text{Equation 3.3}$$

  where 'd' equals the diameter of the anchor. The bond strength τ_u is highly product type dependent and given in the technical approval as characteristic strength for uncracked or cracked concrete.

  For headed bolts, the pullout capacity can be calculated by empirical formulas assuming that the exceedance of the critical bearing pressure results in a pullout failure before concrete breakout occurs. According to Clause D.5.3.4 (Equation D–15) of *ACI 318 (2011)* Appendix D the nominal bearing pressure is limited to 8 times the target concrete strength f_c', which is nearly the same as 6 times the target concrete strength $f_{ck,cube}$ stipulated in Clause 6.2.4 (Equation 23.1.1a) of *CEN/TS 1992-4 (2009)* Part 4:

  $8\ f_c' = 0.8 \cdot 8\ f_{ck,cube} = 6.4\ f_{ck,cube}$ (ACI 355) Equation 3.4a

  $6\ f_{ck,cube}$ ($\approx 6.4\ f_{ck,cube}$) (ETAG 001) Equation 3.3b

Anchors with a large edge distance loaded in shear generally fail in steel failure mode:

- Steel failure: The steel capacity is limited by the steel resistance of the anchor. Exceedance of the steel capacity results in shear shearing-off of the anchor (Figure 3.2b). The ultimate steel capacity $V_{u,s}$ of an anchor loaded in shear depends in the first place on the cross section A_s and the ultimate steel strength f_u:

  $$V_{u,s} = \alpha \cdot A_s \cdot f_u \qquad \text{Equation 3.5}$$

  where 'α' is an empircally determined coefficient and mostly assumed in the range of 0.6 to 0.7 (e.g. *Eligehausen, R.; Mallée, R. et al. (2006)*, *Matsuzaki, Y.; Akiyama, T. (2008)*). The characteristic steel strength in shear is given in the technical approval.

Figure 3.2 depicts the schematic of the failure modes discussed above. Further details on the failure modes are given in the relevant sections.

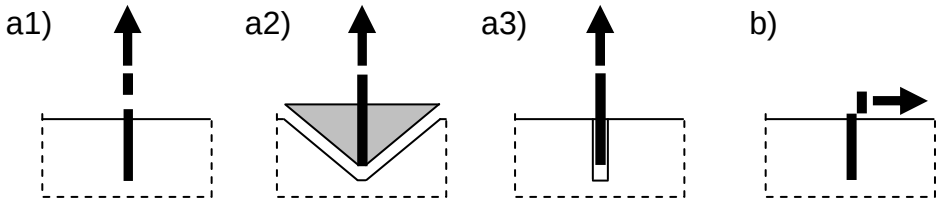

Figure 3.2 Failure modes of anchors loaded in a) Tension and b) Shear: a1) Steel failure; a2) Concrete failure; a3) Pullout failure; b) Steel failure

3.1.3 Concrete strength

For qualification tests involving cyclic load (Section 2.5) and cyclic crack (Section 2.6), the concrete specimens are specified as C20/25 (*ETAG 001 (2006)*) and low strength concrete (*ACI 355.2 (2007)*) because this concrete class (Section 2.1.5) is critical for displacements. For the same reason, most of the experimental tests within the scope of this thesis were carried out in C20/25 concrete.

3.1.4 Drill bit diameter

Every post-installed anchor is installed in a borehole. Anchor qualification guidelines as *ETAG 001 (2006)* or *ACI 355.2 (2007)* recognise three different drill bit diameters d_0, namely minimum, medium, and maximum drill bit diameter, which are to be used depending on the purpose of the specific test. The medium drill bit diameter is stipulated for repeated load tests, whereas the maximum drill bit diameter is stipulated for crack movement tests.

The difference between minimum and maximum drill bit diameter is e.g. for an M12 (anchor according to Annex A of *ETAG 001 (2006)* 0.2 mm and for a 1/2” anchor according to *ACI 355.2 (2007)* 0.008 in (≈ 0.2 mm). For all tests discussed in the following, however, it was decided to stick generally to the medium drill bit diameter. It is deemed that the adverse effect of extreme crack widths is already included in the definition of the maximum crack width of 0.8 mm for seismic applications. The use of the medium drill bit diameter also complies with the existing provisions for the simulated seismic tests according to *ACI 355.2 (2007)*.

3.1.5 Seismic crack width

The crack width is one of the driving test parameters in anchor qualification tests, which influences the test results very much. Its definition needs to be carefully considered therefore. In existing anchor qualification guidelines as *ETAG 001 (2006)* or *ACI 355.2 (2007)*, a crack width of 0.5 mm is specified for suitability tests, representing adverse conditions. Also the simulated seismic tests according to *ACI 355.2 (2007)* are considered as suitability tests and therefore fall back on this crack width. For serviceability tests, a crack width of 0.3 mm is specified for serviceability tests, representing normal conditions.

There was a lengthy debate in the past five years within the research community regarding the crack width applicable for seismic qualification tests (e.g. *Hoehler, M. (2006)*; *Nuti, C.; Santini, S. (2008)*; *Franchi, A.; Rosati, G. et al. (2009)*; *Bergmeister, K.; Rieder, A. (2009)*). The debate is still ongoing and was extended to the question how certain crack widths can be assigned to the concept of suitability and serviceability level (Section 2.1.4). However, in the meantime a crack width of 0.8 mm is generally accepted as the maximum crack width which may occur before yielding of the reinforcement just outside the plastic hinge zone. In consequence and in contrast to Table 2.1, the following crack widths were deemed relevant for seismic applications:

- 0.8 mm cracks are assumed to represent extreme condition and therefore associated with the suitability level.
- 0.5 mm cracks are considered as moderate and therefore associated with the serviceability level.

Within the scope of this thesis, the specified crack width is generally measured in addition to the hairline crack width as the crack is initialised before the installation of anchor and measurement devices. For reasons of better readability and as the denomination of the additive crack width as ‘w’ or ‘Δw‘ is inconsistent in the literature anyway, the crack width variable is taken as ‘w’ without ‘Δ‘.

3.2 Loading Rate

3.2.1 State of knowledge

As a structure responds to an earthquake, anchors located in the structure are subjected to relatively high loading rates. As known from material sciences, short term loading may influence the material properties in a positive way. Hence, an anchor subjected to high loading rates is expected to develop a load capacity that is higher than its quasi-static load capacity. Anchor behaviour under seismic relevant loading rates was also studied within the scope of the dissertation by *Hoehler, M. (2006)*. Together with the findings of a detailed review of earlier investigations (*Eibl, J.; Keintzel, E. (1989a)*; *Klingner, R.; Gross, J. et al. (1998)* and others), the author concluded that high loading rates generally do not negatively affect the ultimate load-bearing capacity of cast-in-place or post-installed anchors loaded in tension or shear. This is also in line with the findings of more recent studies on mechanical and adhesive anchors, e.g. *Rodriguez, M.; Lotze, D. et al. (2001)*; *Fujikake, K.; Nakayama, J. et al. (2003)*; *Salim, H.; Dinan, R. et al. (2005)*; *Solomos, G.; Berra, M. (2006)*. However, expansion anchors transfer the load via friction for which increasing loading rates are not necessarily beneficial. In fact, for bolt-type expansion anchors, typically failing in pull-through failure mode, the tensile capacity may be reduced (*Klingner, R.; Gross, J. et al. (1998)*; *Salim, H.; Dinan, R. et al. (2005)*). This reduction in load capacity is potentially associated with a change in failure mode from concrete failure under static loading rate to pull-through under high loading rate. In *Hoehler, M. (2006)*, only a limited number of tests on expansion anchors were carried out, and therefore further investigations were recommended to study the effects of loading rate on load transfer by friction.

Consecutively, an extensive literature review on the effect of high loading rates on friction between steel and concrete, as well as between steel and steel was carried out and reported in *Mahrenholtz, P. (2007a)*. No specific friction data are available for the special problem of a post-installed anchor under tensile loading, let alone for various loading rates. The study of basic literature in the field of friction as *Rabinowicz, E. (1965)* and *Bowden, P.; Tabor, D. (1959)* highlights that the boundary conditions actually present in the tribosystem (Figure 3.1a) play an eminent role. Friction, expressed in quantitative terms as a force that tends to oppose relative tangential displacement of two contacting bodies (Material 1 and Material 2 in Figure 3.3a), depends on innumerous parameters. Not only the materials and their properties (composition, roughness, hardness etc.) are important, but also the lubrication between these two materials (uncontrolled or factory made) and the environment (temperature, normal pressure etc.) at the interface are highly relevant. The proportional ratio of the tangential force F and the normal force N is called friction coefficient ($\mu = F / N$) which is dimensionless. It is generally distinguished

between static and kinetic friction coefficient, which again may be dependent on the velocity at which the materials are relatively displaced. Friction values found in literature generally lacks of precision because the main goal of the research undertaken in tribology is mostly to reduce the friction in order to reduce abrasive, wear, or energy consumption, rather than to define explicit friction values. This is the reason why friction coefficients are always given as range rather than as distinctive value. The typical test setup for the determination of the friction coefficient is shown in Figure 3.3b which allows the determination of friction coefficients for velocities of up to 200 mm/s.

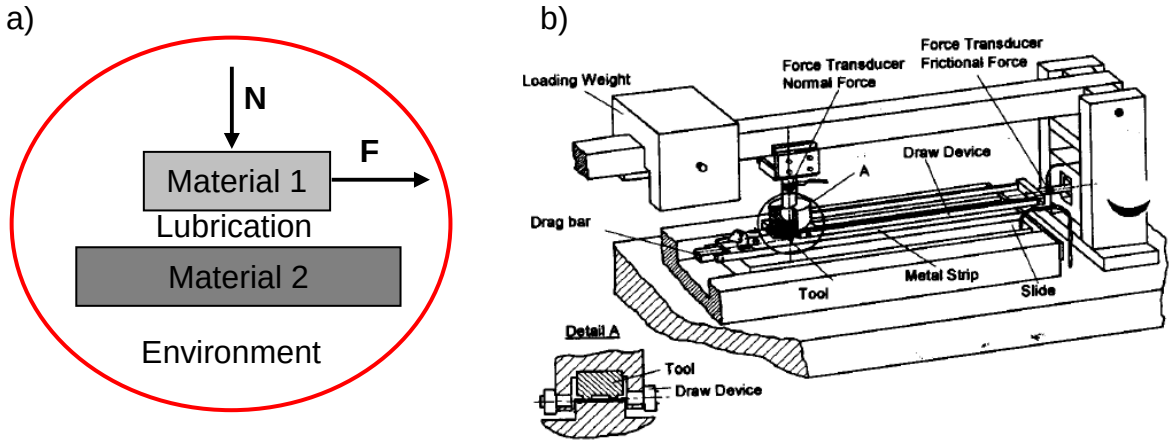

Figure 3.3 a) Tribosystem; b) Strip-draw test setup

However, it is impossible to theoretically predict exact conditions present when an anchor is pulled out at high loading rates. It is rather a singular event and cannot be compared to long lasting laboratory tests. Also in *Asmus, J. (1999)*, a dissertation on the design of tension loaded anchors for concrete splitting, the determination of the friction present in expansion anchors is judged as a difficult task. *Czichos, H.; Habig, K.-H. (1992)* are quoted who state that the actual frictional behaviour cannot be determined theoretically, but only experimentally. Accordingly, the literature review *(Mahrenholtz, P. (2007a))* concluded that experimental tests on installed anchors need to be carried out if light is to be shed on the question whether the load bearing behaviour of expansion anchors may be negatively influenced by high loading rates.

3.2.2 Pullout tests with various loading rates

The load transfer mechansim of expansion anchors depends on friction which is created by pulling the cone at the anchor head into the expansion elements which then press against the concrete. By doing so, actually two friction properties are relevant:

- External friction between expansion elements and borehole wall
- Internal friction between expansion elements and anchor cone

For the proper functioning of expansion anchors it is essential that they exhibit a sufficient follow-up expansion. This is only possible if the external friction is higher than the internal friction. It is unknown, how the external and internal friction are influenced by a high loading rate as in the case of a seismic event. If the ratio of internal to external friction deteriorates, the anchor load capacity may be reduced. Therefore, previous research (Section 3.2.1) identified expansion anchors as critical. In consequence of this, experimental tests on installed expansion anchors were carried out. Tests were limited to torque-controlled anchors since displacement-controlled anchors are generally not suitable for seismic applications. The complete test programme is reported in *Mahrenholtz, P. (2007b)*; further background information can also be found in *Mahrenholtz, P. (2011a)*.

3.2.2.1 Definition of loading rates

The rate at which a non-structural connection is loaded during an earthquake depends on the frequency the non-structural element is oscillating and may be approximated as one quarter of the period (Figure 3.4a). According to *AC156 (2007)*, frequencies between 1.3 and 8.3 Hz are deemed to generate peak spectral accelerations for NCS testing. This parametrical space expanded to 10 Hz also represents the majority of NCS fundamental periods T according to a wide-spread survey reported in *Watkins, D.; Chui, L. et al. (2009)* (Figure 3.4b). Taking frequency limits of 1 Hz (T = 1 sec, i.e. flexible NCS) and 10 Hz (T = 0.1 sec, i.e. stiff NCS) as the boundary values, one obtains rise times of 0.25 to 0.025 sec. It may be reasonably assumed that the rise times for structural connections correspond to the lower value valid for stiff NCS which period is close to the fundamental period of the structure.

a) b)

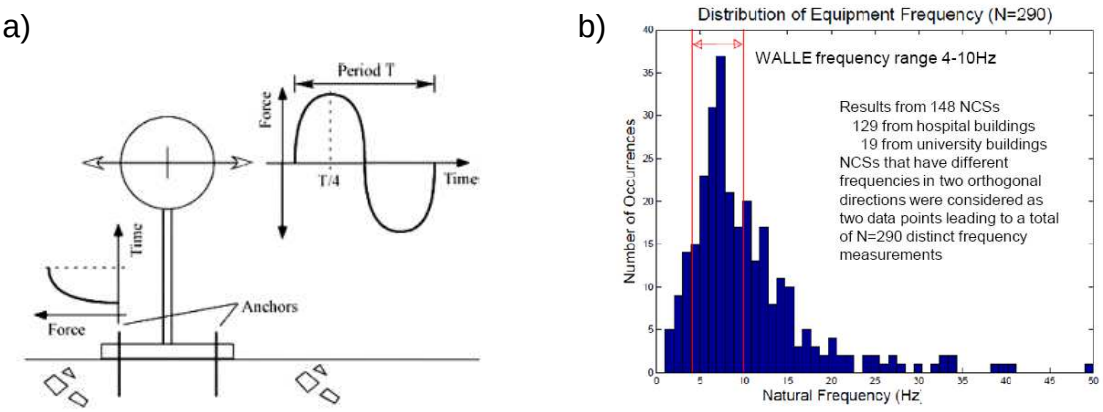

Figure 3.4 a) Anchor loading during cycling of NCS (*Hoehler, M. (2006)*; b) Distribution of eigenfrequencies of hospital and university building NCS (*Watkins, D.; Chui, L. et al. (2009)*)

Depending on the ultimate load, which in turn is a result of anchor type, size, embedment etc., the rise time [s], however, correspond to different loading rates [kN/s] and displacement rates [mm/s]. The higher the ultimate load, the more rapidly the anchor is loaded for a given rise time. The loading rate can also be expressed as a strain rate [ε/s] for which the strain at ultimate load is related to the strain length. However, this approach is problematic in respect to the definition of the strain length, and only useful for anchors failing in steel.

In absence of any better definition, quasi-static and earthquake relevant loading rates are assumed as follows:

- Quasi-static loading rate: < 0.5 kN/s
- Lower bound of earthquake relevant loading rate: 20 kN/s
- Upper bound of earthquake relevant loading rate: 1000 kN/s

3.2.2.2 Definition of failure modes

Failure modes are a decisive factor when investigating anchor performance under high loading rates. It is therefore necessary to have a common understanding on the various failure modes. Expansion anchors loaded in tension exhibit the following failure modes: Steel failure (Figure 3.5a), splitting failure (only in case of thin concrete slabs or anchor installation close to an edge, Figure 3.5b), concrete failure (Figure 3.5c), and pullout failure (Figure 3.6a).

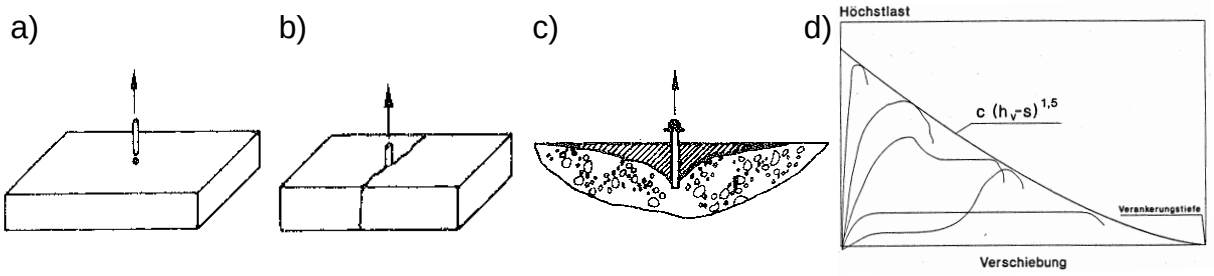

Figure 3.5: Tension failure modes (*Eligehausen, R.; Mallée, R. et al. (2006)*): a) Steel failure; b) Concrete failure; c) Splitting; d) Limitation of anchor capacity in case of concrete failure (*Furche, J. (1994)*)

Ultimate steel strength of the anchor forms the upper limit of the load capacity which is in practice never reached by expansion anchors. For the assumption of compliance with the minimum edge distance given in the technical approval, splitting can be excluded for qualified anchors. Therefore, the following discussion is limited on concrete and pullout failure.

Depending on the embedment depth, crack width, and size of the expansion element, expansion anchors fail either in concrete or pull-out fashion. In case of concrete failure, the anchor is able to transfer all load to the concrete by friction. An increase in crack width is compensated by follow-up expansion. When the ultimate concrete strength is reached, cracks propagate through the concrete starting from the tip of the anchor, and finally a cone-shaped concrete breakout develops. The ultimate capacity depends primarily on the remaining embedment depth at the moment of failure (Figure 3.5d). However, if the anchor is not able to transfer the load necessary to activate full concrete strength, the anchor is pulled out before concrete failure occurs. Often the still attached expansion sleeve causes on its way to the concrete surface a secondary concrete breakout (abbreviated by ‘Cs’) in the close vicinity of the anchor, sometimes of considerable size (see also Figure 3.6c and d).

Since the behaviour and ultimate resistance of an anchor pulled out cannot be predicted, pull-out is not an approved failure mode according to the qualification guidelines and thus does not occur for qualified anchors, provided that the crack width is not larger than the crack width the anchor is qualified for.

If the expansion elements of the anchor remain in the borehole, the corresponding failure mode is called pull-through (abbreviated by ‘Pt’). This sub-failure mode is unique to expansion anchors and typical for bolt-type expansion anchors which expansion elements are small. To distinguish the Pt failure from the pull-out failure with expansion elements still attached to the anchor bolt, the later one is indexed as ‘Po’. An anchor, which cone was completely driven through the expansion elements, proved its functionality and therefore the Pt is an approved failure mode (Figure 3.6b). Other than for concrete failure, the ultimate capacity of anchors failing in this

mode principially depends not on the embedment depth but on the geometry of the anchor bolt and expansion elements. The maximum possible displacement is defined by the length of the expansion element.

It is noted here that the differentiation of Po and Pt is not consistent in the literature. According to *Mayer, B. (1990)*, the expansion elements do not necessarily remain in the borehole in case of a Pt failure. If the expansion element is not expanded (Figure 3.6c), the failure mode was designated as Po, however, if the expansion element is driven around the expansion cone and shows a bulb like shape (Figure 3.6d), the failure mode was designated as Pt because the expansion cone was properly pulled into the expansion elements and thus a satisfying functioning of the anchor was assumed.

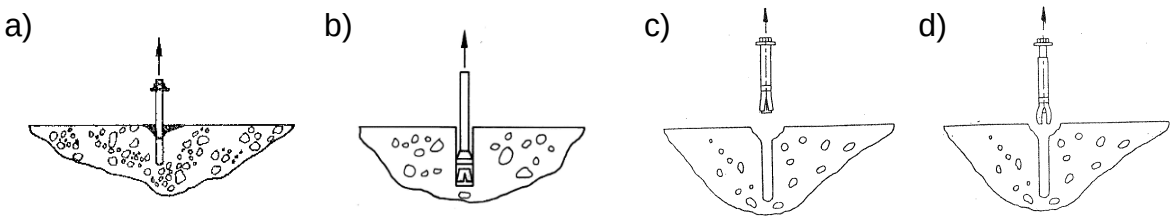

Figure 3.6 Pull-out failure modes: a) Po and b) Pt according to *Eligehausen, R.; Mallée, R. et al. (2006)*; c) Po and d) Pt according to *Mayer, B. (1990)*

3.2.2.3 Test setup and testing procedure

Due to the limited amount of expansion anchors tested in the scope of *Hoehler, M. (2006)*, a test programme comprising torque-controlled expansion anchors of various manufacturers and make was conducted. One sleeve-type expansion anchor (EAs1: see Figure 3.1d) and three bolt-type expansion anchors (EAb1', EAb2, EAb3: see Figure 3.1e) were tested. Among these anchors, also anchors which were believed to be sensitive to variations in friction conditions were explicitly selected. All anchors were size M12 and tested in $w = 0.8$ mm. Anchor EAb1' was installed with an increased embedment depth to ensure consistent pull-through failure, and was also tested in $w = 0.5$ mm to investigate the effect of crack width. The outline of the test programme is also depicted in Table 3.1.

All tests were carried out in normal weight concrete C20/25 with a mean tested concrete cube compressive strength between $f_{cc,150} = 28.5$ and 32.9 MPa. The slabs were produced according to the state of the art after *DIN 1045 (2001)* and *DIN 1048 (1991)* and designed to allow for the generation and control of static cracks by means of wedges driven into sleeves placed in preformed holes in the slab (Figure 3.7a). Checking the crack formation in the borehole using a borescope clearly showed that drilling the hole prior to crack formation is essential in order to guarantee that the crack runs through the hole over the entire depth. After crack formation and removing

of the wedges, the anchor was installed unmodified according to the installation manual of the manufacturer. Full installation torque was released after the elapse of 10 min to half to make good for the relaxation which occur over time in reality. After the installation of the crack width transducers, the wedges are sequentially hammered into the sleeves until the desired crack width is reached.

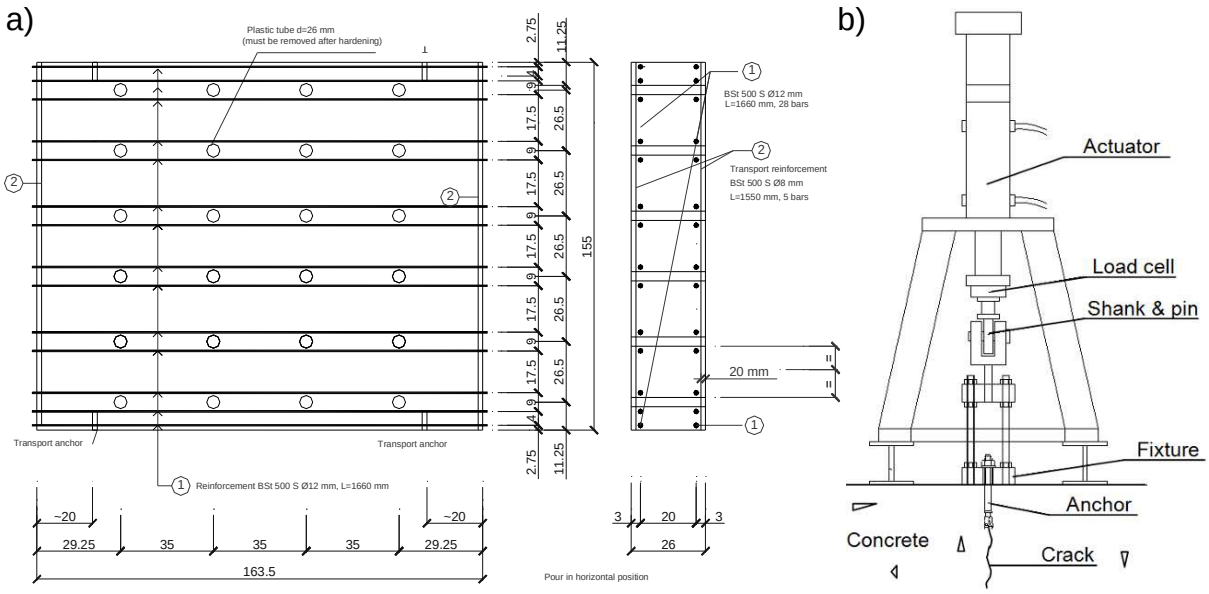

Figure 3.7 a) Drawing of wedge-split concrete slab; b) Schematic loading setup

Next, a 50 kN servo-hydraulic actuator was placed overhead the anchor and supported such that an unconfined concrete cone breakout could occur (Figure 3.7b). All tests were run displacement controlled. For quasi-static tests, ultimate load was reached within 1 to 3 min. In combination with the 65 ℓ/min servo-valve, the 50 kN servo-hydraulic actuator was agile enough to push the cylinder to rates of up to 30,000 mm/s for high loading rate tests. The tension load applied to the anchor, the anchor displacement, and the crack width were measured and recorded at a sampling rate of 5 Hz for quasi-static, and 1000 Hz for high loading rate tests. Figure 3.8 shows pictures of the test setup. Further details are given in *Mahrenholtz, P. (2007b)*.

3.2.2.4 Experimental results and discussion

Table 3.1 provides the test conditions and key test results. The test programme included more tests which however are not important in the context of the following discussion and therefore not reported herein.

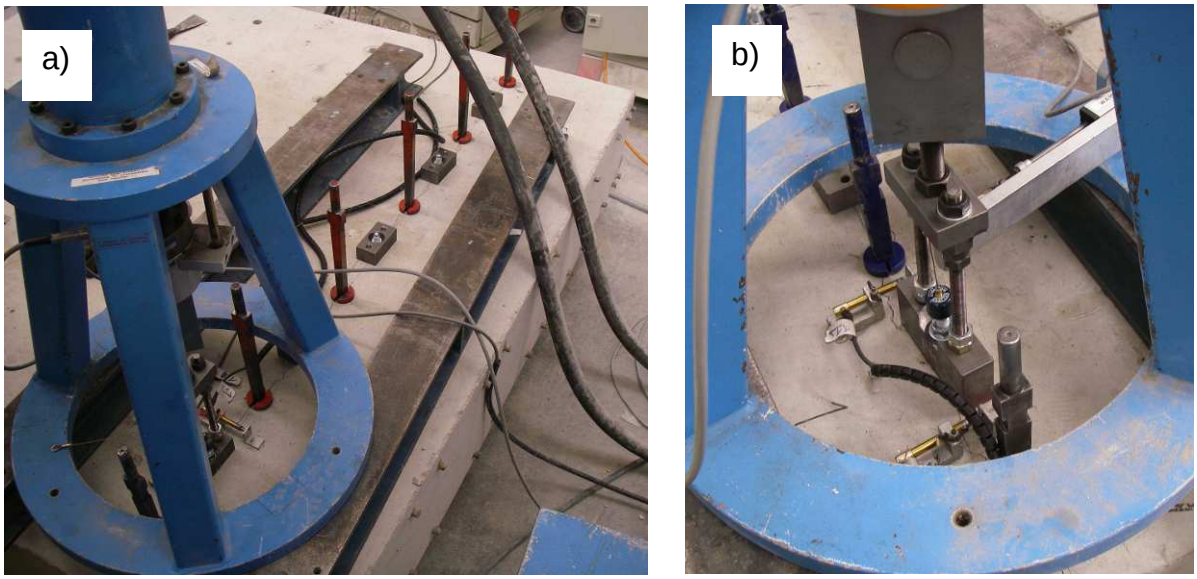

Figure 3.8 a) Actuator resting on wedge-split concrete slab; b) Close-up of installed anchor, fixture, anchor displacement and crack width transducers

Table 3.1 Test conditions and key test results of pullout tests with various loading rates

Anchor Type, Anchor Size, Emb. Depth	Crack Width w	Mean Rise Time	Num. of Tests	PFM	$N_{u,m}$, kN	CV, %	Load Rate, kN/s	$s(N_u)_m$, mm	CV, %	Disp. Rate, mm/s
EAb1'; M12; 85 mm	0.5 mm	153 sec	5	Pt	24.56	4.4	0.16	13.19	22.9	0.09
		0.51 sec	5	Pt	29.08	9.6	57.0	14.29	13.2	28.0
		0.06 sec	5	Pt	27.75	16.0	463	16.17	23.7	270
EAb1'; M12 90 mm	0.8 mm	149 sec	2	Pt	23.21	0.2	0.16	14.10	40.9	0.09
		0.58 sec	3	Pt	25.99	4.8	44.8	17.20	21.1	29.7
		0.05 sec	3	Pt	23.02	18.5	460	17.99	38.6	359
EAb2; M12; 68 mm	0.8 mm	119 sec	5	Pt	12.37	9.1	0.11	11.25	16.8	0.09
		0.58 sec	5	Pt	16.77	10.4	28.9	9.68	35.1	16.7
		0.03 sec	5	Pt	17.58	12.4	586	8.64	36.4	288
EAb3; M12; 68 mm	0.8 mm	182 sec	5	Pt	19.72	7.6	0.11	13.77	30.3	0.08
		0.42 sec	5	Pt	21.31	11.3	50.7	12.34	30.8	29.4
		0.04 sec	5	Pt	19.74	8.3	494	14.86	25.6	372
EAs1; M12; 80 mm	0.8 mm	88 sec	5	C	32.47	5.8	0.37	7.75	33.0	0.09
		0.59 sec	5	C	37.78	7.5	64.0	6.68	28.8	11.3
		0.05 sec	5	C	41.47	6.3	829	9.52	9.9	190

For the sleeve-type expansion anchor concrete breakout occurred (Figure 3.9a). As expected, this failure mode resulted in increasing load capacity ($N_{u,m}$) for increasing loading rates. A transition from concrete failure mode to pull-through or pull-out failure mode could not be observed. Bolt-type expansion anchors predominantly

failed in pull-through failure mode, sometimes in pull-out failure mode with attached expansion element due to the crack width too large for bolt-type expansion anchors of that size (Figure 3.9b). An increased loading rate did not result in a statistically significant decrease in capacity. The trend to higher loads for increased loading rates is clearly visible. The results indicate that crack width is more significant than loading rate for these anchors. The displacement capacities ($s(N_u)_m$) versus the loading rate do not show a clear trend.

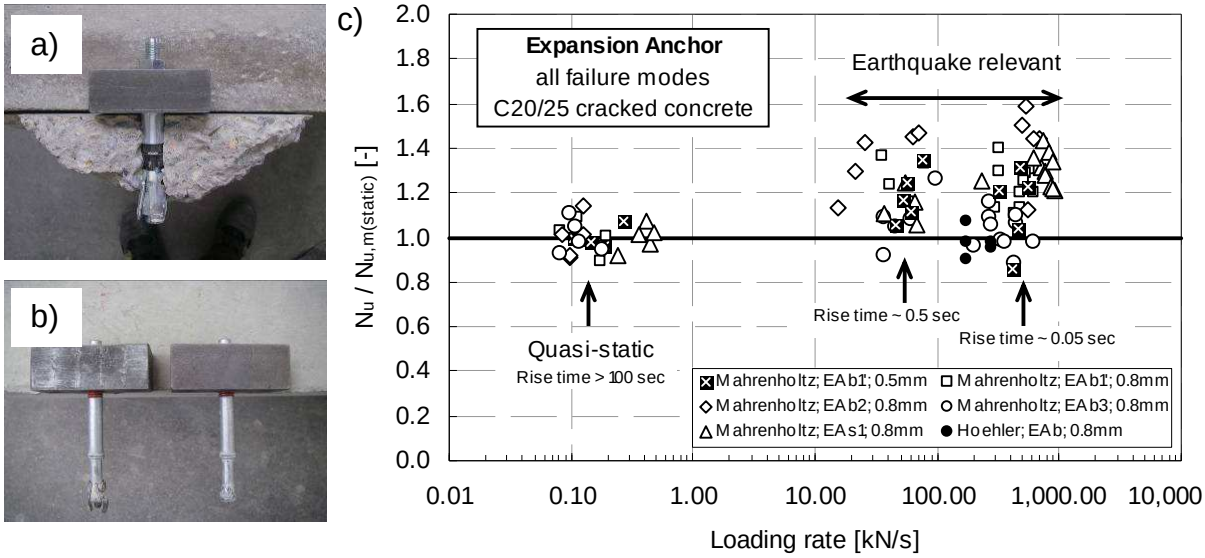

Figure 3.9 a) Sleeve-type expansion anchor (C); b) Bolt-type expansion anchor (Po on the left and Pt on the right); c) Influence of loading rate on expansion anchors (all failure modes)

In conclusion, the pullout tests carried out within the scope of *Hoehler, M. (2006)* and *Mahrenholtz, P. (2007b)* on expansion anchors confirmed the general trend of increasing capacities for increasing loading rates also for expansion anchors (Figure 3.9c). The occasional occurrence in reduction of load capacities in older test programmes (Section 3.2.1) could not be observed. Due to a very limited availability of older documentation, a definite evaluation is not possible, however, it is noted that all along the incident of reduced load capacity was rare and it is questionable whether the negative influence of rapid loading is reproducible, the more so as the technology of expansion anchors has significantly improved over the past decades. In response to more stringent approval criteria more attention was paid to a balanced frictional behaviour.

Although the results showed that increasing loading rates generally cause an increase in load capacity, increased ultimate anchor loads may also hypothetically indicate the increase of (internal) frictional resistance and, in consequence, the deterioration of the ratio of internal and external friction. For that reason, additional tests were carried out under controlled conditions, which allowed the separate

investigation of the effect of loading rate on the internal friction and on the external friction. These investigations are presented in the following Section 3.2.3.

3.2.3 Additional testing on anchor friction mechanisms

The goal of the investigations was to better understand the load transfer mechanisms of expansion anchors and their effects on the anchor performance. The experimental tests carried out to evaluate the influence of loading rate on the coefficients of friction are briefly presented and discussed in the following. The internal friction was investigated by means of modified FEP II tests, the external friction was investigated by means indentation tests. Both test series are reported in detail in *Mahrenholtz, P. (2011a)*; further background infromation can also be found in *Mahrenholtz, P. (2012)*.

3.2.3.1 Modified FEP II tests

The FEP II test setup was developed in *Mayer, B. (1990)* to investigate the splitting forces of expansion anchors. Therefore anchors were installed in between two concrete prisms and pulled out by a manually controlled actuator (Figure 3.10a). Figure 3.10b) shows an exemplary load-displacement curve measured for a constant expansion force.

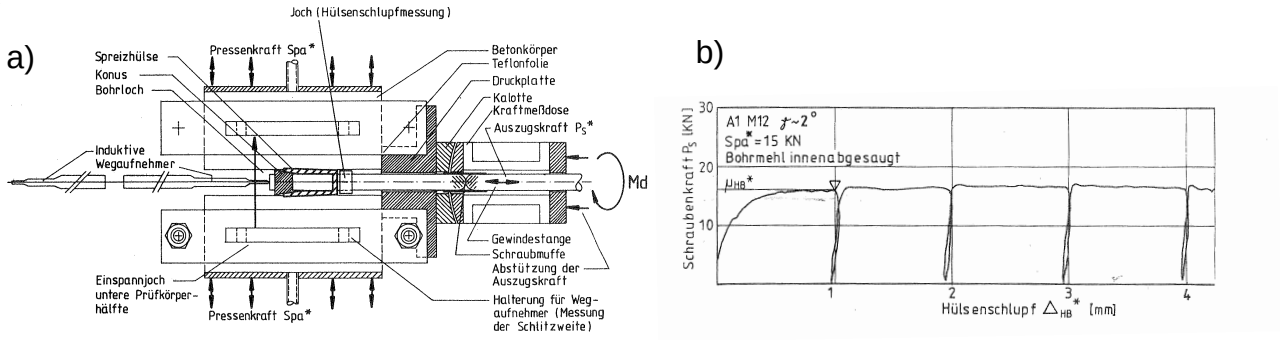

Figure 3.10 a) FEP II test setup (*Mayer, B. (1990)*); b) Anchor load (denoted P_s) over anchor displacement (denoted Δ_{HB}) for a given expansion force (denoted Spa)

The anchor load N generates via the anchor cone and expansion elements a force perpendicular to the anchor axis, the expansion force F_{exp} (Figure 3.11a). The ratio of N and F_{exp} is the tangent of the so-called angle of friction (δ^*), which in turn equals to the coefficient of friction μ^*, where δ^* and μ^* are theoretical values related to a friction plane perpendicular to the axial force N:

$$N / (F_{exp}) = \tan \delta^* = \mu^* \qquad \text{Equation 3.6}$$

In anchor technology, μ* is also called pull-out resistance and the ratio of F_{exp} and N describes the transmission of anchor load to expansion force (k):

$$F_{exp} / N = k \qquad \text{Equation 3.7}$$

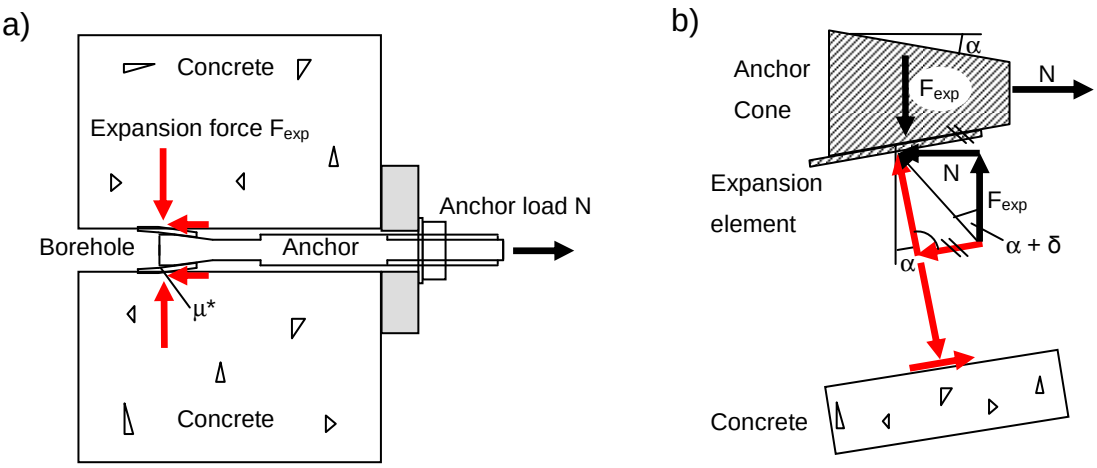

Figure 3.11 a) Forces acting on an installed anchor; b) Simplified mechanical model

In the following, the equilibrium of forces is considered for the inclined external friction plane of an installed anchor (Figure 3.11b - compare to Figure 3.3a) to determine the coefficient of friction μ acting between the borehole wall and the expansion elements. The expansion force equals to the splitting force integrated over the circumference of the expansion element. The external angle of friction δ_e equals μ with respect to the inclined friction plane, and the relation of anchor force and expansion force is after *Mayer, B. (1990)* given by:

$$N / F_{exp} = \pi \cdot \tan(\alpha+\delta_e) \qquad \text{Equation 3.8}$$

Equation 3.6 inserted in Equation 3.8 and equalised with Equation 3.7 yields Equation 3.9:

$$k = 1 / (\pi \cdot \tan(\alpha + \delta_e)) = 1 / \mu^* \qquad \text{Equation 3.9}$$

After trigonometric conversion of Equation 3.9, an equation for the coefficient of friction μ based on μ* and α can be given:

$$\leftrightarrow \tan(\alpha + \delta_e) = 1 / (k \cdot \pi)$$

$$\leftrightarrow \frac{\tan\alpha + \tan\delta_e}{1 - \tan\alpha \cdot \tan\delta_e} = 1 / (k \cdot \pi)$$

$$\leftrightarrow k \cdot \pi \cdot \tan\alpha + k \cdot \pi \cdot \tan\delta_e = 1 - \tan\alpha \cdot \tan\delta_e$$

$$\leftrightarrow 0 = -1 + \tan\alpha \cdot \tan\delta_e + k \cdot \pi \cdot \tan\alpha + k \cdot \pi \cdot \tan\delta_e$$

$$\rightarrow 0 = -1 + \tan\alpha \cdot \mu + k \cdot \pi \cdot \tan\alpha + k \cdot \pi \cdot \mu \qquad (\text{with } \tan\delta_e = \mu)$$

$\rightarrow 0 = -1 + \tan\alpha \cdot \mu + (1 / \mu^*) \cdot \pi \cdot \tan\alpha + (1 / \mu^*) \cdot \pi \cdot \mu_e$ (with $k = 1 / \mu^*$)

$$\rightarrow \mu = \frac{\mu^* - \pi \cdot \tan\alpha}{\pi + \mu^* \cdot \tan\alpha}$$ Equation 3.10

Equation 3.10 together with Equation 3.6 allows the determination of the coefficient of friction μ based on α, N and F_{exp}.

The test setup as shown in Figure 3.12 required some substantial changes in order to facilitate high loading rate tests. For this purpose, the test specimen, consisting of the anchor and two concrete cubes, was positioned opposite to a 50 kN servo controlled actuator. The two concrete cubes were fixed by two braces. The lower brace was bolted to the strong floor. The upper brace was hold down by means of a traverse and four threaded rods. A load cell was placed in between the upper brace and the traverse. The actuator with the load cell was mounted horizontally on a steel abutment which in turn was bolted to a strong floor.

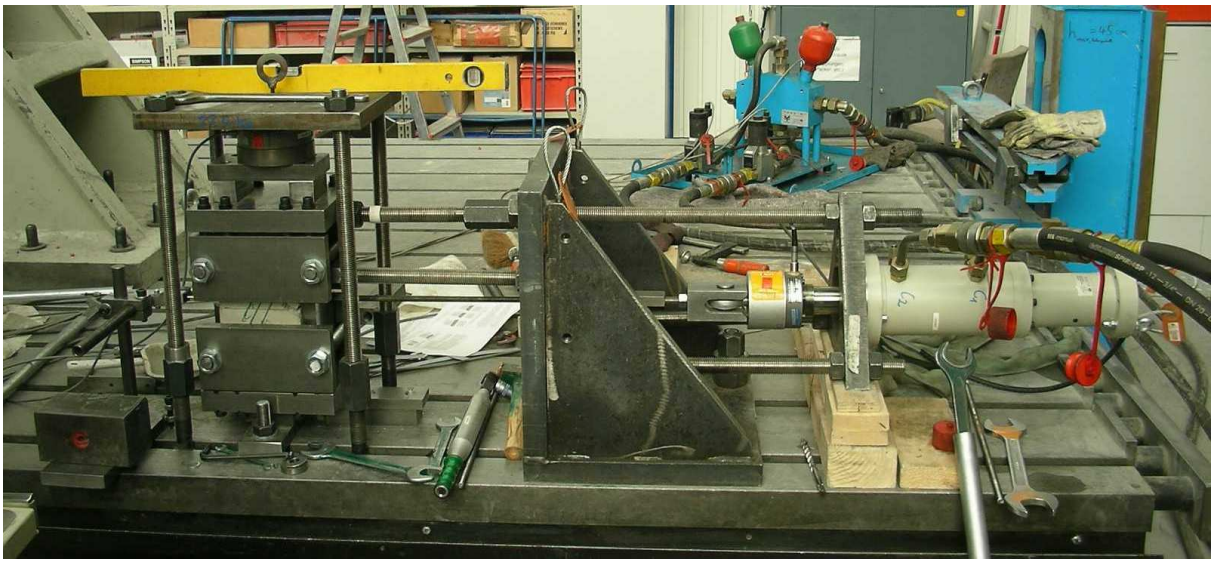

Figure 3.12 Modified FEP II test setup

To ensure that the anchor displacement is generated between expansion elements and concrete (and not between cone and expansion elements), the expansion elements had to be fixed to the anchor cone. For this, the concrete cubes were clamped together, a hole was bored and the anchor was installed by applying full installation torque. Next, the anchor was recovered and the expanded expansion elements were tack welded to the anchor cone. Finally, the anchor and the two concrete cubes were reassembled such that the expansion elements rested exactly in the indentation marks they have been created in the concrete before (Figure 3.13a).

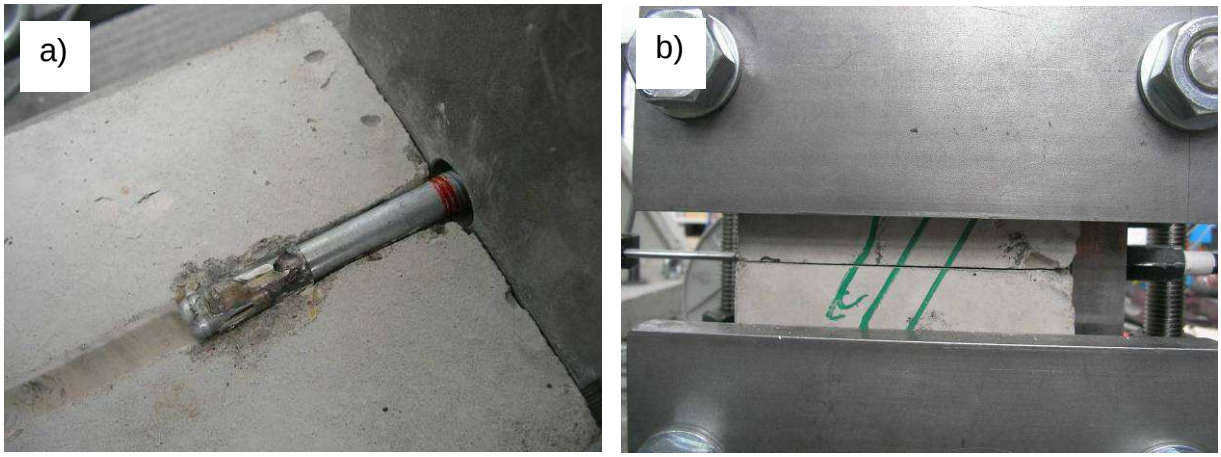

Figure 3.13 a) Embedding of the anchor with fixed expansion elements; b) Aligning the concrete cubes between upper and lower brace

The borehole was drilled through the entire concrete cubes to enable the displacement measurement by a transducer at the unloaded end. By tightening the nuts of the four threaded rods, a preload on the anchor sandwiched between the concrete prisms was applied. Adjusting the nuts allowed keeping a uniform and constant gap between the two concrete prisms (Figure 3.13b).

Then, the anchor was pulled out. The anchor load, the expansion force and the anchor displacement were measured. Contrary to the tests described in *Mayer, B. (1990)*, where the expansion force was held constant (Figure 3.10b), the test setup allowed the expansion force to vary over anchor displacement (Figure 3.14a). The variability in the expansion force does not have an influence on μ^* since μ^* is expressed as the ratio of N and F_{exp} (Equation 3.6). The scaling of the curve to a constant expansion force of 15 kN (Figure 3.14b) and comparison to former results (Figure 3.10b) verified the capability of the modified FEP II test setup. In Figure 3.14b, also the calculated external friction coefficient is plotted versus the displacement. For constant expansion force, it is approximately constant over the pullout test.

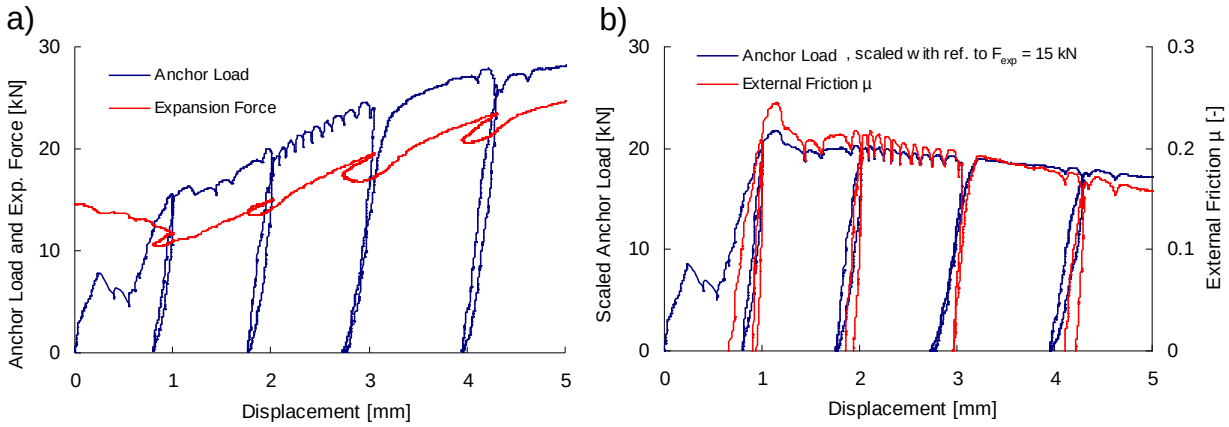

Figure 3.14 a) Measured anchor load and expansion force versus anchor displacement; b) Curve scaled with reference to the expansion force

In this manner the external friction was determined for the bolt-type expansion anchor EAb1' (α = 11°) and the sleeve-type expansion anchor EAs1 (α = 13°) under quasi-static and high loading rates. To investigate the influence of concrete strength, concrete cubes made of C20/25 and C50/60 were used for the EAb1' anchor. Another test parameter was the preload acting as a preset expansion force on the anchor. Table 3.2 comprises the test parameters and the key results for the external friction. The friction coefficient was taken as the maximum within the first 3 mm anchor displacement. This complies with the procedure applied in *Mayer, B. (1990)*.

Table 3.2 Test parameters and key results for external friction

Anchor Type, Angle of Cone	Concrete Strength Class	Preload, kN	Loading Rate	Num. of Tests	Range of Coefficient of External Friction
EAs1; α=13°	C20/25	5	quasi-static	3	0.17 ÷ 0.37
			high	3	0.28 ÷ 0.45
EAb1'; α=11°	C20/25	5	quasi-static	3	0.30 ÷ 0.40
			high	3	0.22 ÷ 0.46
EAb1'; α=11°	C20/25	15	quasi-static	5	0.16 ÷ 0.32
			high	5	0.12 ÷ 0.38
EAb1'; α=11°	C50/60	15	quasi-static	5	0.23 ÷ 0.33
			high	5	0.16 ÷ 0.37

The scatter in the determined coefficient of friction is large which was already observed by *Mayer, B. (1990)* where the results were not more consistent. The range of the coefficient is for high loading rate tests even larger than for quasi-static loading rate tests. For increasing expansion force, the friction coefficient is getting lower by

trend, what it should not be in theory. However, this complies with the test results presented in *Mayer, B. (1990)*. The influence of the concrete strength on the coefficient of friction is not significant. In contrast, in *Mayer, B. (1990)* lower values were evaluated for higher concrete strengths. However, the number of tests carried out for a specific boundary condition was small.

In conclusion, any potential trend in the influence of loading rate on the external friction coefficient is overcast by the large scatter. It has to be assumed that there is no significant change in the external friction for high loading rates.

3.2.3.2 Indentation tests

In *Lehmann, R. (1992)* the theoretical calculation of the pull-out load of mechanical anchors is shown and verified. The approach for this calculation falls back on indentation tests carried out by *Lieberum, K.-H. (1989)* to establish a relation of indentation and resulting compressive force. For these tests, a dice was pressed into a concrete filled cylinder and the three-dimensional stress was measured. Figure 3.15a depicts the idealised stress σ as a function of the indentation e for various concrete strengths.

a) b)

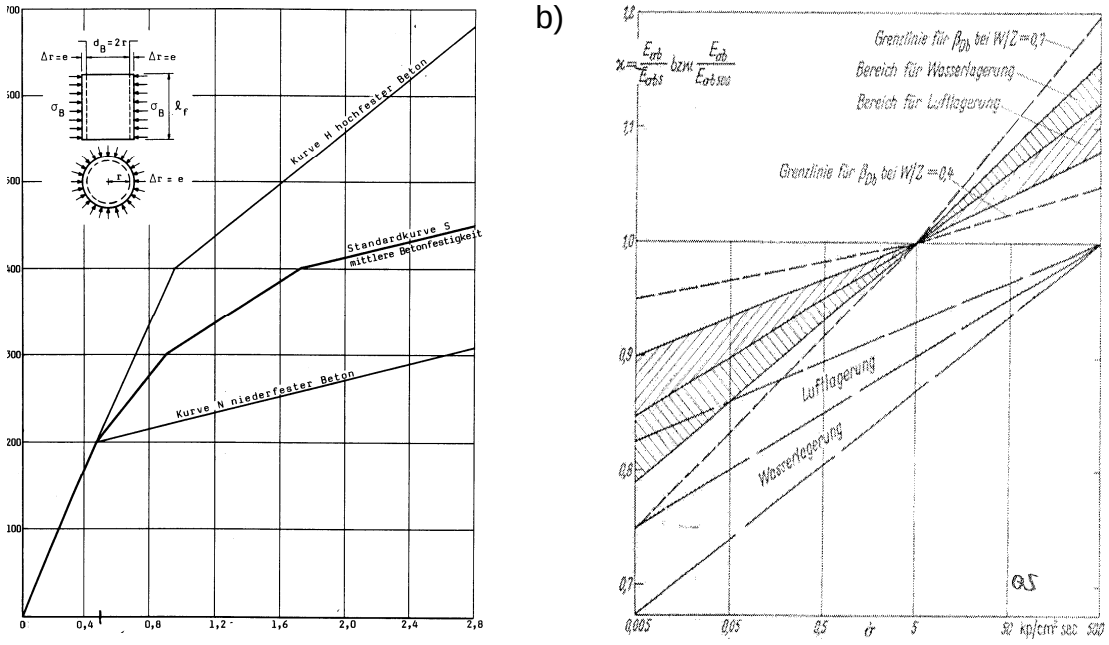

Figure 3.15 a) Idealised stress-indentation curves (*Lieberum, K.-H. (1989)*);
b) Stress-rate dependent E-modulus (*Wesche, K.; Krause, K. (1972)*)

If an expansion anchor functions properly, the anchor bolt is pulled through the expansion elements which then indent the concrete due to the cone angle. The balance of forces in Figure 3.11b applies but the sliding plane is for this case

between the cone and expansion element. The resulting compressive force acting on the concrete at that moment equals to the expansion force F_{exp}. Since the amount of anchor load which can be transferred to the concrete via friction depends on F_{exp}, the actual indentation stress is critical for the magnitude of the ultimate anchor load. For the following discussion, it is sufficiently accurate to assume that the stress is proportional to the indentation. Likewise, also the stress rate is proportional to the indentation rate.

The angle of friction δ_i equals the internal friction related to the friction plane formed by expansion elements and anchor cone and is after *Mayer, B. (1990)* given by:

$$F_{exp} = N / \tan(\alpha + \delta_i) \qquad \text{Equation 3.11}$$

$$\leftrightarrow N_0 / F_{exp0} = \tan(\alpha + \delta_i)$$

$$\leftrightarrow \arctan(N_0 / F_{exp0}) = \alpha + \delta_i$$

$$\leftrightarrow \delta_i = \arctan(N_0 / F_{exp0}) - \alpha$$

Comparing N and F_{exp} measured in two test series with quasi-static loading rate (index 0) and high loading rate (index 1) allows the evaluation of the influence of the loading rate on δ_i:

$$\rightarrow \frac{\delta_{i1}}{\delta_{i0}} = \frac{\arctan(N_1 / F_{exp1}) - \alpha}{\arctan(N_0 / F_{exp0}) - \alpha} \qquad \text{Equation 3.12}$$

This equation can be further transformed that it is based on the ratio of anchor load (N_1 / N_0) and ratio of expansion force (F_{exp1} / F_{exp0}):

$$\rightarrow \frac{\delta_{i1}}{\delta_{i0}} = \frac{\arctan[(N_1 / N_0)(N_0 / ((F_{exp1} / F_{exp0}) \cdot F_{exp0}))] - \alpha}{\arctan(N_0 / F_{exp0}) - \alpha}$$

$$\leftrightarrow \frac{\delta_{i1}}{\delta_{i0}} = \frac{\arctan[(N_1 / N_0)(N_0 / F_{exp0}) / (F_{exp1} / F_{exp0})] - \alpha}{\arctan(N_0 / F_{exp0}) - \alpha}$$

F_{exp0} / N_0 is the ratio of transmission k (Equation 3.7) which was investigated in detail for various mechanical anchors in *Asmus, J. (1999)*. For the EAs1 and EAb1' anchor, k can be assumed as 1.2 and 1.3, respectively. It is accurate enough to assume a value of 1.25 in the following:

$$\rightarrow \frac{\delta_{i1}}{\delta_{i0}} = \frac{\arctan[1/1.25 \cdot (N_1 / N_0) / (F_{exp1} / F_{exp0})] - \alpha}{\arctan(1/1.25) - \alpha} \qquad \text{Equation 3.13}$$

At ultimate load and maximum indentation of the expansion elements, the cone is forced into the expansion elements by about 20 mm. That means that the rate of indentation is about 1/10 of the displacement rate of the anchor. The anchor displacement rates as reported in Table 3.1 are in the range of 0.1 mm/s for

quasi-static loading rates and 300 mm/s for high loading rates. This equals an indentation rate of 0.01 mm/s and 30 mm/s, respectively, and a factor of 3000.

As for most materials, the E-modulus of concrete also increases for short-time loading or increased loading rate. In *Wesche, K.; Krause, K. (1972)* a relation of loading rate and E-modulus can be found. The diagram in Figure 3.15b depicts the stress-rate dependent E-modulus normalised with reference to the E-modulus at $\sigma = 5$ N/mm²/s as a function of stress rate $\dot{\sigma}$. With a maximum stress rate of 500 N/mm²/s, the diagram covers only an increase in stress rate by the factor 100. The substantially higher increase in stress rate and the punctuated load application typical for when anchors are pulled out at earthquake relevant loading rates, however, suggests a much more pronounced increase in the E-modulus. Therefore, tests were carried out for which a dice was pressed into concrete cubes by means of a 250 kN servo controlled actuator (Figure 3.16a).

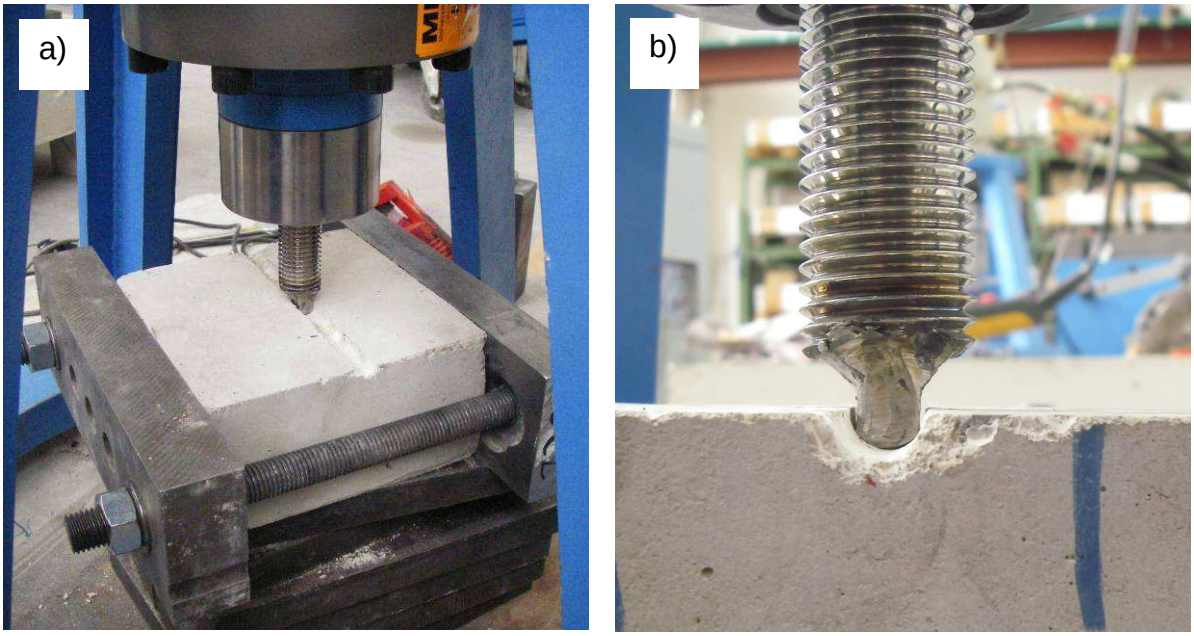

Figure 3.16 a) Indentation test setup; b) Close up of the dice and concrete groove

Two different dices were machined so that they replicate radius and length of the bolt-type and sleeve-type expansion anchors. The concrete cubes were prepared as for the modified FEP II tests by drilling a hole right into the joint of two clamped together concrete cubes. One cube was then fixed by a steel bracket to the strong floor and the dice was first lowered into the groove until it just touched concrete (Figure 3.16b). The dice was then pressed into the concrete quasi-statically by 1.0 mm to simulate the indentation of the expansion element during anchor installation.

Then the anchor was loaded to failure at quasi-static and high loading rates. The load and the displacement of the dice were measured. For high loading rates, i.e. displacement rates of ~ 30 mm/s, the measured resistance to indentation was significantly increased (Figure 3.17a). For the problem given, the indentation from 1.0 to 2.0 mm is critical since this indentation represents the indentation of the expansion anchor after installation due to follow-up expansion when the anchor is pulled out. By normalising the respective increase in resistance to indentation between 1.0 and 2.0 mm with reference to that for the quasi-static tests, the percentage increase in resistance (and thus expansion force) due to higher loading rates can be estimated to 50 %.

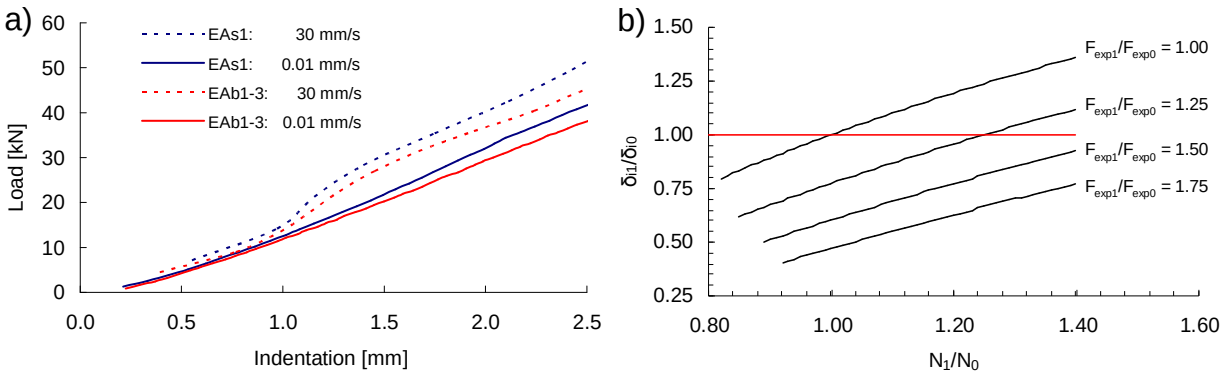

Figure 3.17 a) Average load-indentation curves; b) Friction ratio versus anchor load ratio

The array of curves in Figure 3.17b is the graphical representation of Equation 3.9 and allows determining the change in the internal angle of friction (δ_{i1} / δ_{i0}) based on expansion forces evaluated by indentation tests.

The compressive force measured over indentation increased by approximately 50 % for high loading rates if compared to quasi-static loading rates. Therefore, also F_{exp} may be assumed to increase by 50 % for high loading rates. With reference to Figure 3.9b, the increase in anchor load due to high loading rates may be tentatively assumed as 25 % on average. With $F_{exp1} / F_{exp0} = 1.50$ and $N_1 / N_0 = 1.25$, the diagram in Figure 3.17b reads 0.82 for $\delta_{i1} / \delta_{i0}$ which equals a reduction in internal friction of 18 %. The result reveals that the increase in expansion force rather than the hypothetical increase in friction is the reason for increased anchor loads under high loading rates. Table 3.1 comprises the test parameters and key results regarding the internal friction.

Table 3.3 Test parameter and key results for internal friction

Anchor Type; Outer Diam. of Exp. Elements	Concrete Strength Class	Radius/ Length of Dice, mm	Loading rate	Num. of Tests	Normalised Increase in Compressive Force	Normalised Coefficient of Internal Friction
EAs1; 18 mm	C20/25	9/200	quasi-static	5	-	-
			high	6	1.53	~ 0.80
EAb1'; 12 mm	C20/25	6/150	quasi-static	5	-	-
			high	6	1.47	~ 0.84

The deduction of the load rate dependent coefficient of internal friction based on measured anchor loads and expansion forces is very theoretical. However, the investigations pointed out that high loading rates have in general a beneficial effect because of the increase in indentation resistance: For a constant internal angle of friction ($\delta_1/\delta_0 = 1.00$), the anchor load increases for high loading rates (Figure 3.17b). This creates a safety margin for the case of decreasing internal friction which results in decreasing anchor loads.

3.2.4 Conclusions

Considerable number of experimental tests on installed anchors has shown that the mean capacity of anchors tested under high loading rate is generally greater than that observed under static loading. This is true independent of the failure mode and type of anchor. In *Hoehler, M.; Mahrenholtz, P. et al. (2011)* it was concluded that a reduction in load capacity under earthquake relevant loading rates can be excluded in practice. However, it was unknown whether this behaviour is accompanied by a potentially adverse change in the ratio of internal and external friction. For this reason, further investigations on expansion anchors were carried out to deepen the understanding of the external and internal frictional behaviour.

The modified FEP II test setup allowed determining the pull-out resistance of fully expanded anchors. The deduced coefficients of external friction show a large scatter overcasting any high loading rate effect. It was not possible to establish a relation between friction and loading rate that was distinguishable from the general scatter in the test data. Therefore, the external friction has to be assumed as relatively constant for variable loading rates. To investigate the internal friction, indentation tests on concrete specimens were carried out determining the influence of the loading rate on the concrete resistance when an anchor cone is pulled through the expansion elements. It turned out that the internal friction decreases with increasing loading rate which ensures a proper functioning of the expansion anchor for all loading rates. The reason for increased anchor load capacities despite of reduced frictional resistance is

the beneficial effect of increased loading rates on the indentation resistance of the concrete. Increasing expansion forces permit that the anchor load capacity under high loading rates is not reduced in comparison to the capacity under quasi-static loading.

Based on these findings, it is concluded that in general high loading rates do not have a negative influence on the load capacity factor of expansion anchors. In consequence, the earlier established conclusion that high loading rate tests are not necessary for seismic anchor qualification holds also for expansion anchors, irrespective of the failure mode.

3.3 Anchor Ductility

3.3.1 State of knowledge

Anchor ductility was till very recently not a subject for systematic experimental tests or for systematic theoretical consideration. The available literature on testing and assessment of anchor ductility is very limited. However, approval authorities and anchor manufacturers in Europe and the US have worked to achieve more clarity and consistency in the manner in which the classification of anchor ductility is made. The results of experimental tests investigating current procedures for assessing the ductility of anchor products is presented in *Hoehler, M.; Silva, J. et al. (2011)*. Existing ductility definitions in material sciences and earthquake engineering and their applicability on anchor technology, as well as exploratory tensile tests on anchor specimens are discussed in *Mahrenholtz, P. (2010a)*. In the following, literature addressing directly anchor ductility is shortly summarised.

In *Rieder, A. (2002)* the deformation capacity of installed undercut and expansion anchors under static shear loading is investigated to assess their potential seismic performance. The manufacturing process and the sleeve were found to play a major role in influencing the steel failure load and ductility. Due to the lack of a pronounced yield point in the load-displacement curve, the yield load was defined as $F = F_{Rk,s} / (\gamma_F \cdot \gamma_{Ms})$, where $F_{Rk,s}$ = characteristic resistance for steel failure, γ_F = partial load safety factor, and γ_{Ms} = partial material safety factor for steel failure (Figure 3.18a). This approach is commonly used in structural engineering when estimating the maximum possible load level for the serviceability limit state for which linear behaviour is generally assumed. Also in *Hegger, J.; Döinghaus, P. et al. (2003)* it is used for the idealisation of load-displacement curves of headed bolts loaded in shear. In this case, the yield load corresponds to the maximum allowable load level at serviceability limit state. Depending on the applied partial safety factors, the yield load corresponds to ~ 50 or 60 % of the ultimate load capacity (Figure 3.18b). This definition identifies the beginning of inelasticity; however, the actual load-

displacement curve is too steep at this point to recognise it as the onset of plastic behaviour. Therefore, the ideal plastic plateau is found by extrapolating the initial stiffness to the maximum load level (Figure 3.18b and Figure 3.25a).

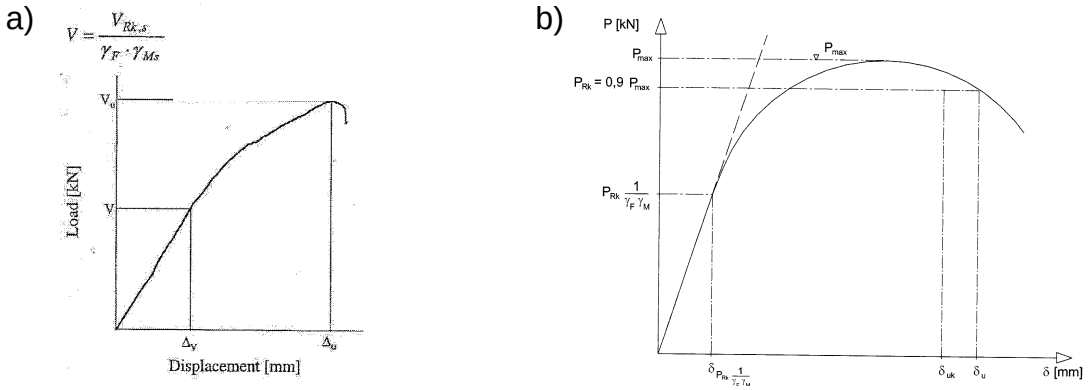

Figure 3.18 Approach for estimating linearity up to the maximum possible load level for the serviceability limit state: a) *Rieder, A. (2002)*; b) *Hegger, J.; Döinghaus, P. et al. (2003)*

In *Silva, J.; Eligehausen, R. et al. (2006)* it is pointed out that there is practically no hysteretic energy dissipation during tension load cycling. Furthermore, the concept of bolt elongation as a measure of tension anchor ductility has meaning in one direction of load only since compression forces are generally transferred directly to the concrete from the fixture or base plate. For shear loading, the reference to (axial) bolt elongation has little meaning. Further it is concluded that the relationship of local and global ductility as described in *Paulay, T.; Priestley, N. (1992)* requires very high local ductility factors for moderate global ductility demands, and that deformation capacity is required in particular for anchor groups (Figure 3.19a) as it was addressed in *Klingner, R. (1993)*. The fact of pinched and narrow looped hysteresis resulting in limited energy dissipation was also pointed out in *Hoehler, M. (2006)* for tension load cycling and in *Genesio, G. (2007)* for shear load cycling.

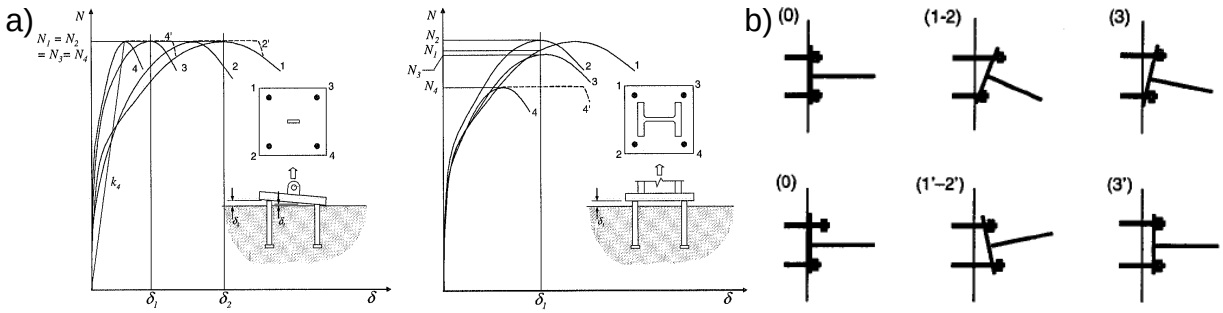

Figure 3.19 a) Ductility demand in case of anchor groups (*Silva, J.; Eligehausen, R. et al. (2006)*); b) Failure mechanism of a typical anchor connection (*Nuti, C.; Santini, S. (2008)*)

The work presented in *Nuti, C.; Santini, S. (2008)* aims to clarify the understanding of the fundamental principles of seismic anchor behaviour. It is argued that the yielding of the anchor itself results in a non-ductile mechanism. Its behaviour is governed by sliding of yielded anchors at zero force as soon as the steel yielding has been reached during load cycling. In other words, anchor ductility means an irreversible deformation that leads to lifting of fixture and pounding effects. In that case, no energy dissipation occurs and the mechanism (Figure 3.19b) cannot be assumed as ductile.

In conclusion, there is limited literature on anchor behaviour available which falls back on the term ductility. If general load-displacement characteristics of different anchor types were considered in earlier studies (e.g. *Cook, R.; Collins, D. et al. (1992)*), the emphasis was clearly placed on the load bearing behaviour rather than on the displacement capacities. Anchor ductility is not clearly defined yet, let alone quantified. A systematic and basic approach is therefore required to shed light on this issue.

3.3.2 Background

In structural design, ductile failure modes are generally considered as desirable because of their beneficial effects on the behaviour prior to failure. In particular for seismic design, ductility is important in order to overcome the extreme demands on the elements in view of load and displacement capacities. This fundamental idea is also transferred to anchor design. Their load-displacement behaviour ranges from very brittle to moderate or pronounced ductile. However, before anchor ductility can be evaluated and quantified, it is necessary to understand what ductility means and what its behavioural objectives are. In the following sections, the meaning of the term ductility is discussed for material sciences, earthquake engineering, and anchor technology.

3.3.2.1 Ductility in material sciences

In material science, ductility is mostly understood as the percentage elongation with reference to the original length of a specimen tested in tensile tests, e.g. according to *ISO 6892-1 (2009)* or *ASTM F606 (1998)*. Tensile tests reveal the properties of the pure material. The plastic behaviour and thus material ductility is generated by dislocations of the atoms. Ductile materials such as most steels, exhibit a linear stress-strain relationship up to a the yield point at which material strain changes from elastic to plastic deformation, causing it to deform permanently. As deformation continues, the stress increases due to strain hardening until it reaches the ultimate strength. Until this point, the strain is almost equal over the whole length of the

specimen. Beyond this point necking of the specimen occurs and eventually the specimen ruptures (Figure 3.20a).

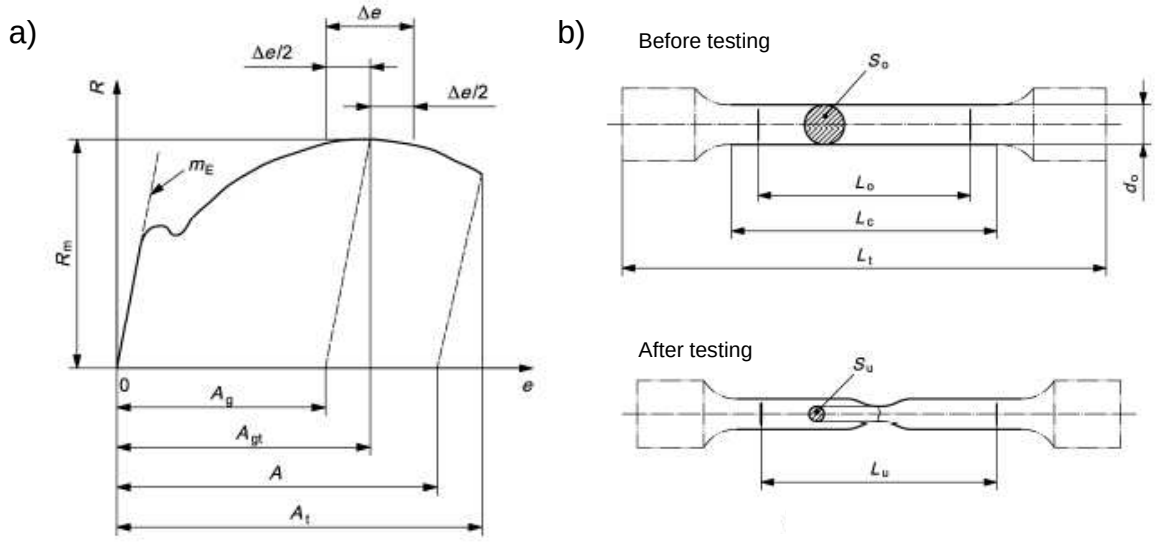

Figure 3.20 a) Tensile testing according to *ISO 6892-1 (2009)*: a) Stress-strain diagram with A_g = strain before necking and A = strain after rupture; b) Specimen before and after testing with L_o = Original reference length before testing and L_u = reference length after testing

The reduction in area can be measured and given unambiguously as a percentage value. For the determination of the percentage elongation, i.e. plastic strain, the two halves of the ruptured specimen are joined (Figure 3.20b) and the measured absolute elongation is then related to a reference length. The definition of the reference length is crucial since it directly affects the percentage result. The provisions given in *ISO 6892-1 (2009)* fall back on the so-called proportional specimen which original reference length is fixed in proportion to the square root of the original cross section area by $L_o = 5.65 \cdot (S_o)^{0.5}$. The compliance with this proportion ensures that the calculated strain of different specimen dimensions and cross sections are comparable. For round specimen, the formula yields $L_o = 5\ d_o$. In case of non-proportional specimen length, the elongation value needs to be converted for which *ISO 6892-1 (2009)* refers to *ISO 2566-1 (1999)*. An elongation value derived from a test with $L_o = 4$ d has to be divided by the factor 1.094. Thus an elongation requirement of 14 % for a 4 d specimen as given in *ACI 318 (2011)* is equivalent to a requirement for a 5 d specimen of 14 / 1.094 = 12.8 %. This comes pretty close to the provision in *CEN/TS 1992-4 (2009)* of 12 %.

3.3.2.2 Ductility in seismic engineering

The goal of designing an earthquake safe structure is to have “tolerance with respect to inevitable crudeness of predicting earthquake imposed displacements” (Paulay in *Reitherman, R. (2006)*) for which ductility is a very important property. The term is generally used to describe the ability of a structure or its components to offer resistance in the inelastic deformation response parameters of the structure such as displacement, rotation or curvature, and is defined as the ratio of maximum to yield deformation $\mu = \Delta_m / \Delta_y$ (Figure 3.21).

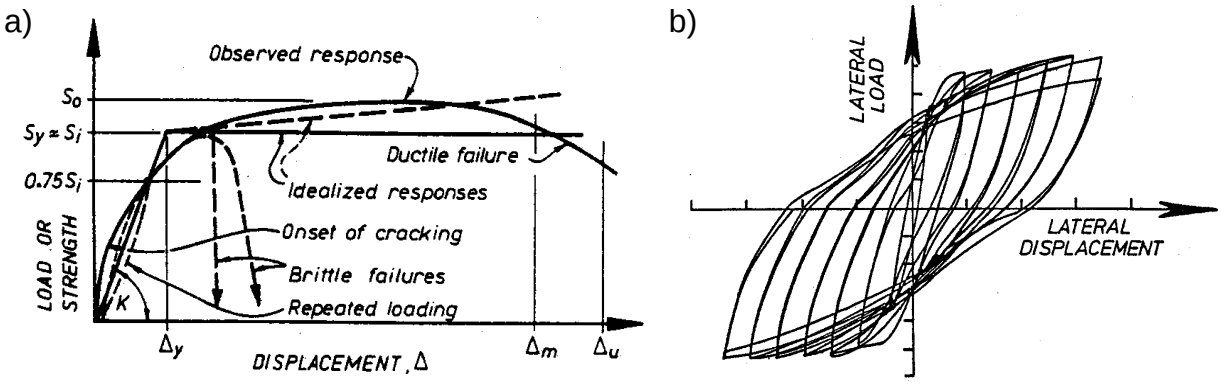

Figure 3.21 Load-displacement behaviour of reinforced concrete members: a) Idealisation of load-displacement curve (*Paulay, T.; Priestley, N. (1992)*; b) Typical measured hysteresis loop (*Park, R. (1989)*)

The ductility factor is often illustrated by monotonic load-displacement curves (Figure 3.21a). However, and most important for seismic design, a ductile element is also able to undergo cyclic deformations in the inelastic domain without a substantial reduction in strength. During the hysteretic deformation, the element dissipates energy (Figure 3.21b).

3.3.2.3 Ductility in anchor technology

In anchor technology, ductile behaviour is associated with similar capacities. Ductile failure modes are considered as desirable (e.g. *Silva, J. (2001)*, *Gurbuz, T.; Ilki, A. (2011)*. The reasons for this are as follows:

- Large absolute deformation (Figure 3.22a): This is understood as critical for deformation controlled failure modes and enables load redistribution within anchor groups or between anchors at different supports.
- Large relative deformation (Figure 3.22b): This parameter describes an early activation of full strength for a given maximum deformation. An early activation

of the full strength is also critical for anchor groups because large absolute displacement alone does not guarantee a favourable load distribution.

- Robustness (Figure 3.22c): A robust anchor shows a load-displacement behaviour which is soft at peak load and prolonged in the post-peak range. Final failure is indicated by large displacements.
- Resistance to cycling (Figure 3.22d): While the first three behavioural objectives apply to both static and seismic load cases, the ability to resist several load cycles beyond yield is a critical feature for seismic applications.

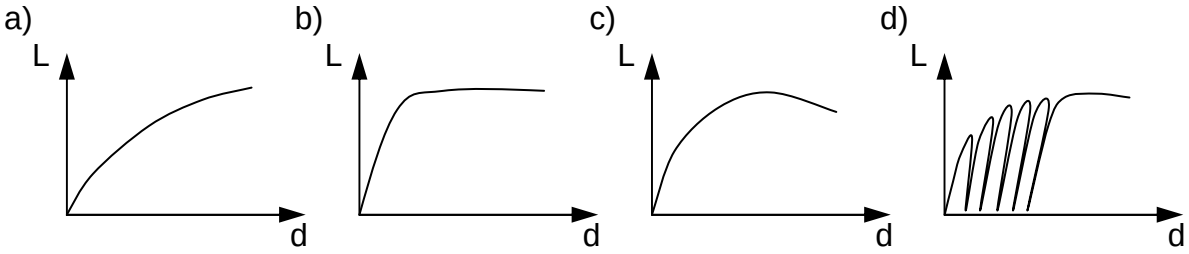

Figure 3.22 Schematic illustration of the objectives on the load (L) – displacement (d) behaviour of anchors: a) Large absolute deformation capacity; b) Large relative deformation capacity; c) Robustness; d) Resistance to cycling

Notwithstanding the lack of a conclusive definition or quantification of anchor ductility, the designation of whether an anchor is ductile or brittle affects several aspects of anchor design. As noted by *Hoehler, M.; Silva, J. et al. (2011)*, the anchor has to be classified as ductile for the following cases:

- Plastic design approach of structural connections according to *CEN/TS 1992-4 (2009)* Annex B. The plastic analysis is acceptable only when the failure is governed by ductile steel failure of the anchor.
- Partial safety factors ϕ as given in of *ACI 318 (2011)* Appendix D which are sensitive with reference to the ductility classification of the anchor.
- Seismic design of anchoring according to Clause 8.4.3(3) of *CEN/TS 1992-4 (2009)* or Clause D.3.3.6 of *ACI 318 (2008)* Appendix D: Both guidelines require the seismic design of the anchorage using an overstrength factor of 2.5 if it cannot be shown that either the element fixed by the anchor yields before anchor failure or the anchorage fails in steel and the anchor is qualified as ductile. The latest revision *ACI 318 (2011)*, however, dropped this factor, see also Section 2.3.3.

Section 2.3 concluded that to date anchor ductility is tested by material tensile tests (Section 3.3.2.1). However, it is evident that in reality the behaviour of an installed anchor system differs in many cases significantly from what the material test result may suggest. As demonstrated in *Hoehler, M.; Silva, J. et al. (2011)* the threaded rod

of an adhesive anchor system certainly yields ductile load-deformation characteristics in a material tension test, however, when being bonded to the concrete, the threaded rod cannot generate any substantial deformation because the available free strain length is very small. On the other hand, many mechanical anchor types experience considerable overall movement when the installed system is loaded, resulting in displacements capacities larger than indicated by the material test (*Mahrenholtz, P. (2010a)*).

This leads to the conclusion that anchor ductility should be tested on the installed system rather than by a material test alone. Basis of the evaluation is then the load-displacement behaviour of the anchor. The definition of anchor ductility based on load-displacement curves will be more general than a definition based on steel strain alone and may also allow for failure modes other than steel failure to be classified as ductile. For this goal, potential anchor ductility parameters were developed (Section 3.3.3) and applied to a database of several hundred experimental tests (Section 3.3.4).

3.3.3 Development of anchor ductility parameters

The quantification of anchor ductility requires a discussion of which ductility parameters are suitable to characterise the load-displacement behaviour best in due consideration of the behavioural objectives and how they can be determined by means of characteristic points on the load-displacement curves. The following sections are a brief extract from extensive investigations reported in *Mahrenholtz, P. (2011b)*.

3.3.3.1 Behavioural objectives and deformation parameters

In the following, the four behavioural objectives, namely (i) Large absolute deformation, (ii) Large relative deformation, (iii) Robustness, and (iv) Resistance to cycling as described in Section 3.3.2.3 are characterised by means of deformation parameters which are extracted from load-displacement curves.

Absolute deformation describes the ability of the anchor to develop displacement capacity. Relative deformation can be interpreted as a ductility factor μ which relates in seismic design the maximum to yield deformation. The idea of yield and maximum deformation implies that the load-displacement curve flattens (or softens) after the point of yield. Thus, the behavioural objective of robustness is checked by the relative deformation: A certain relative deformation ensures a corresponding plateau length and thus robustness. Further, a high resistance to cycling can generally be assumed for post-installed anchors. This is in particular true for tension loads for

which a large number of load cycles at load levels below peak and/or considerable number of load cycles near ultimate load can be performed without failure, irrespectively of the failure mode (Figure 3.23).

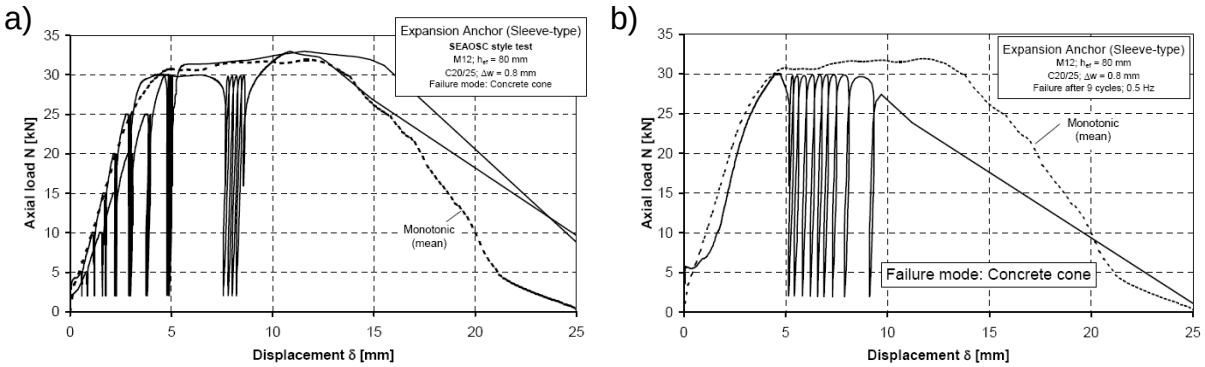

Figure 3.23 Examples of tension load cycling tests on anchors (*Hoehler, M. (2006)*): a) Large number of load cycles after *SEAOSC (1997)*; b) Load cycling near ultimate load

As mentioned earlier, energy dissipation, which is generally sought for applications in seismic engineering, is nearly non-existent because axially loaded anchors primarily transfer tension loads only. Compression loads are directly transferred by the fixture to the concrete. This behaviour results in stiff, closely spaced loading and unloading branches typical for cyclic loading of anchors. This is also true for cyclic shear loading for which the anchor can only take up load when in direct contact with the concrete but not at the beginning of the reverse stroke (Figure 3.24). Energy dissipation is therefore not a suitable parameter to quantify anchor ductility.

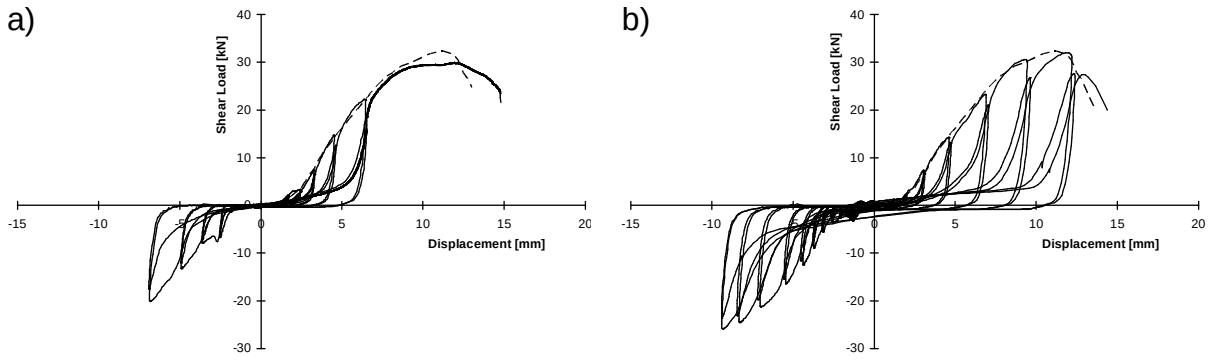

Figure 3.24 Examples of shear load cycling tests on anchors (*Mahrenholtz, P.; Eligehausen, R. et al. (2011)*): a) Displacement controlled load cycling after *FEMA-461 (2007)*; b) Continued load cycling to failure

In conclusion, investigations on potential anchor ductility parameters should focus on the aspects of the following displacement parameters of the installed anchor:

- Absolute deformation
- Relative deformation

Due to the strong association of ductility with seismic applications – as all above mentioned behavioural objectives also apply to seismic design – it may appear reasonable to determine anchor ductility by means of cyclic tests. However, extensive experience in anchor testing has verified that the scatter band of cyclic load-displacement curves follow the mean of corresponding monotonic tests (Figure 3.23 and Figure 3.24), provided that the anchor does not fail prematurely due to low cycle fatigue. For anchor qualification, however, this has no effect since the anchor is required to sustain all cycles of a given qualification protocol (e.g. *ACI 355.2 (2007)*).

Therefore, the evaluation of the deformation characteristics can be carried out by means of monotonic load-displacement curves. To investigate potential system ductility parameters and to check their suitability, existing load-displacement curves from qualification tests are evaluated in the following.

3.3.3.2 Characteristic points and potential ductility parameters

The determination of quantitative ductility parameters requires the definition of characteristic points that describe the load-displacement of a loaded anchor. In *Hoehler, M. (2006)* it is suggested that the displacement at 80 % of the ultimate load on the ascending and descending branches of the load-displacement curves should be recorded for qualification tests. The aim of this was to gain additional information about the deformation capacity. This general approach is refined and substantiated in the following.

As discussed above, two critical deformation values need to be derived from the load-displacement curves: (i) Absolute deformation, and (ii) Relative deformation. The absolute deformation is equivalent to the maximum deformation capacity. By relating that capacity to the yield deformation, the relative deformation capacity is determined. In conclusion, the following two characteristic points on the load-displacement curve need to be defined:

- Yield deformation Δ_y
- Maximum deformation Δ_m

In seismic engineering, the load-displacement curve is often idealised as a bilinear ideal elasto-perfectly plastic system that allows the direct extraction of the ductility factor μ based on the yield and maximum deformation. When the load-displacement curve does not have a well defined yield point, it is often defined by an idealised curve balancing the areas between actual and idealised curve. Structures generally have some capacity beyond peak and it is reasonable to recognize at least parts of

this post-peak capacity. The definition of yield and maximum deformation is always somewhat subjective and innumerous alternative approaches of various complexities can be found in literature. Some examples are shown in Figure 3.25.

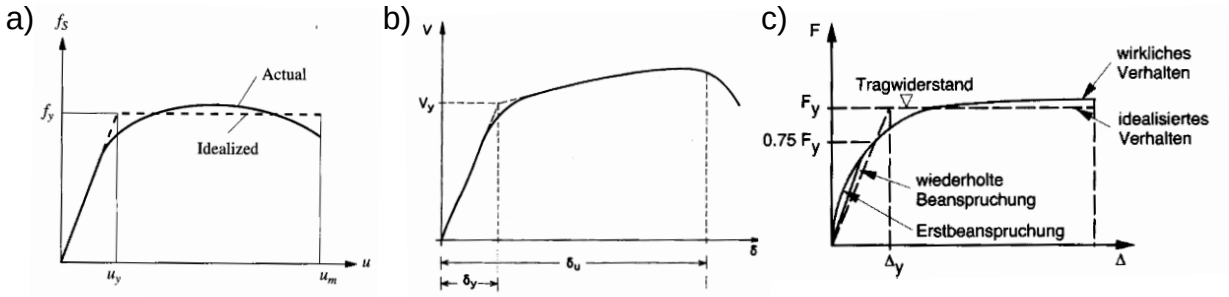

Figure 3.25 Examples for idealisation of load-displacement curves: a) Elasto-perfectly plastic idealisation (*Chopra, A. (2007)*); b) Elasto-plastic idealisation (*Penelis, G.; Kappos, A. (1997)*); c) Elasto-plastic idealisation for non-linear initial stiffness (*Paulay, T.; Bachmann, H. et al. (1990)*)

Also in *Priestley, N.; Calvi, G. et al. (2007)* it is pointed out that there is no consensus within the research community as to the appropriate definition of yield and ultimate displacement. With the wide choice of definitions (Figure 3.26a), there are problems when realistic modelling is required for the straightforward concept of ductility capacity and demand, and its relation to the reduction factor (*ATC-24 (1992)*, *ATC-40 (1996)*).

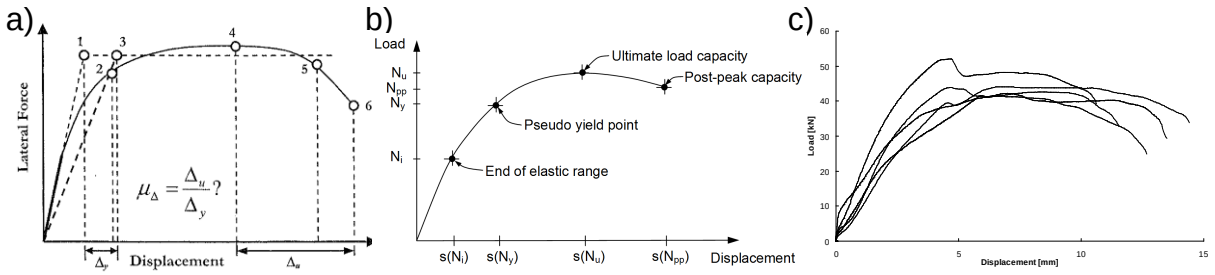

Figure 3.26: a) Possible definition of deformation capacity according to *Priestley, N.; Calvi, G. et al. (2007)*; b) Schematic of anchor load-displacement curve and key characteristic points and c) Example of qualification test series (*Mahrenholtz, P.; Eligehausen, R. et al. (2011)*)

Further, for anchor ductility, the identification of the yield and maximum deformation is critical, yet even more difficult. Other than in case of tensile tests on steel specimens, however, a clear stiffness variation after the elastic range is not visible and a pseudo yield point needs to be found. Figure 3.26b depicts schematically the load-displacement curve of an anchor loaded in tension and the key characteristic points which are:

- End of elastic range
- Pseudo yield point
- Ultimate load capacity
- Post-peak capacity

The following discussion is based on tensile load-displacement curves, however, the discussion is principally also applicable to anchors loaded in shear.

The study on potential definitions of the characteristic points checked several approaches which are reported in detail in *Mahrenholtz, P. (2011b)*. The approach of area balancing is not practical when evaluating a vast quantity of anchor load-displacement curves. Anchor test series consist typically of 5 repeats which load-displacement curves may show significant scatter in particular for displacement values (Figure 3.26c). It was aimed to find a solution which would allow the use of data assessment software and which at best is in line with the assessment criteria of existing anchor qualification guidelines.

As for laterally loaded structural elements, the range of truly elastic behaviour is very short, if existent at all. For this reason, the end of the elastic range may be identified by definition. E.g. *ETAG 001 (2006)* approximates the initial, i.e. elastic, stiffness to a load level half of the mean ultimate load 0.5 $N_{u,m}$, which corresponding displacement is an important assessment criterion (Section 2.4.1). However, since the end of the elastic range marks the beginning of the inelasticity, it may be interpreted as the pseudo yield point. Another possible approach for the definition of the pseudo yield point would be an algorithm analogue to the reduced tangent stiffness approach given in *ETAG 001 (2006)*-Part 5, which was also adopted in *ACI 355.4 (2010)*, for the determination of the load at loss of adhesion $N_{u,adh}$ in case of bonded anchors (Figure 3.27a). However, the data evaluation (Section 3.3.4) resulted in large scatter within a test series and turned out to be impracticable. The approach to find the yield displacement by means of the secant stiffness at 75 % of the peak load, as it is common practice for reinforced concrete elements in seismic engineering (Figure 3.21a, Figure 3.25c), and its simple application has clear advantages.

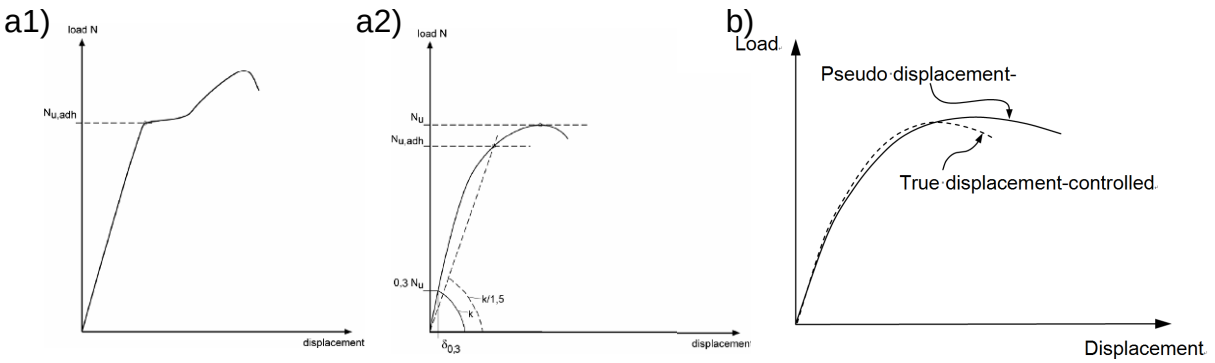

Figure 3.27: a) Determination of the load at loss of adhesion according to *ETAG 001 (2006)*-Part 5: a1) Significant change of stiffness; a2) Load at reduced secant stiffness; b) Effect of true and pseudo displacement controlled tests

Also the maximum available deformation is estimated in seismic engineering by various assumptions. Considerable portion of the inelastic region is generated beyond the peak of the load-displacement curve. However, the allowable loss in post-peak strength needs to be limited. In seismic engineering, a reduction in load of 20 % is generally considered as acceptable (*Park, R. (1989)*). The post-peak branch of load-displacement curves is particularly affected by the control mode of the testing actuator. True displacement controlled tests are run by means of a servo-hydraulic actuator and guarantee a constant displacement rate during the test. In contrast, pseudo displacement controlled hydraulic actuators typically used for monotonic anchor qualification tests results in increased loading rates at peak load. Consequently, for anchors failing in steel, concrete, or bond, the load and deformation capacities may be overestimated (*Mahrenholtz, P. (2011c)*, Figure 3.27b). For this reason and since the scatter within a test series gets increasingly massive down the descending branch, it is reasonable to define the post-peak strength for anchors at a higher load level. The deformation at 85 % of the ultimate load seems to be reasonable.

In conclusion, the following can be stated for the characteristic deformations of anchor load-displacement curves: The identification of the yield deformation is essential for calculating the relative deformation capacity. However, the definition of the yield point is generally problematic and the quantification of the yield deformation is difficult. In contrast, the peak point is easy to find and its scatter is reasonably low. As a conservative approach, the corresponding deformation can be taken as the maximum deformation. When the post-peak strength is taken into account, the data needs to be carefully checked concerning a possible overestimation of the deformation capacity due to pseudo displacement controlled test methods.

3.3.4 Evaluation of data base

The preceding section identified absolute and relative deformation as the most meaningful anchor ductility parameters, for which determination the yield and the maximum deformation have to be extracted from load-displacement curves. To quantify these parameters, a database of several hundred experimental tests on diverse anchor types was developed and evaluated. The data base falls back on qualification test performed on anchors of various makes and manufacturers at the IWB. Test data were d assessed with reference to anchor type, anchor size, concrete strength, crack width, and type of loading. The complete evaluation of the data base is available in *Mahrenholtz, P. (2011b)*.

3.3.4.1 Characteristics of load-displacement curves and anchor types

For the data base, all anchor test reports written at the IWB dating back to the year 2001 were screened in view of their general usability. 507 test series including 19 different products which came from 10 different manufacturers based in Europe and the US were identified as suitable. For further processing, they were classified according to their type (bonded, expansion, screw, and undercut anchor), their size (metric range M6 to M36, imperial range 1/4” to 1 1/4”), the concrete strength (low (C20/25) and high (C50/60)) and the crack width the anchors were installed in (0.0 mm to 1.5 mm), the load direction (tension, shear, and load at an inclined angle) and type (monotonic and cyclic). Next, the relevant load-displacement (x,y) data were extracted from the reports (Figure 3.28a), for which the diagrams of older reports had to be digitalised first, and then processed by a professional assessment software for anchor test data. The characteristic points of all test repeats were calculated first individually (Figure 3.28b) and then taken as the arithmetic mean (Figure 3.28c). The horizontal and vertical bars represent the fluctuation of the data.

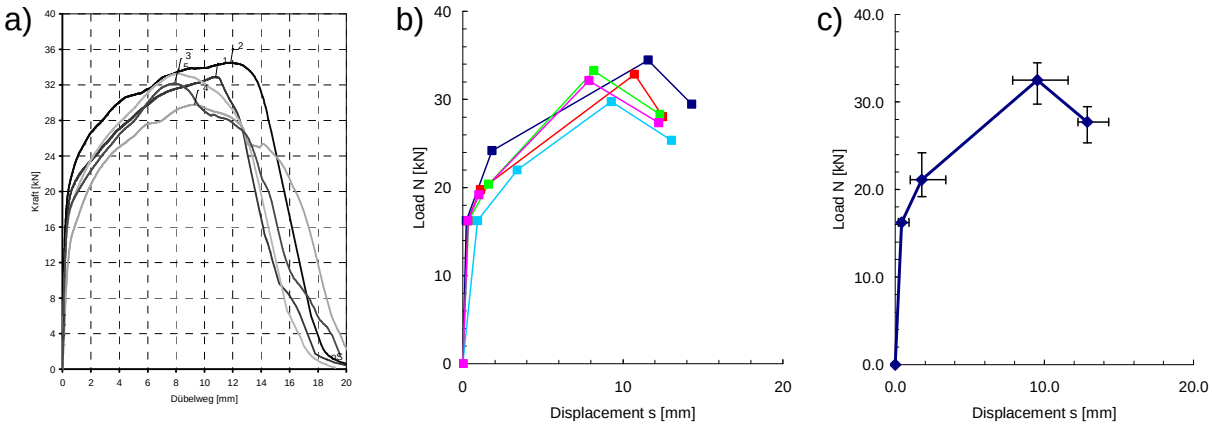

Figure 3.28 Exemplary procedure of data base evaluation: a) Original data; b) Polygon intersecting characteristic points; c) Arithmetic mean of all test repeats

Before evaluating the data base in detail, it is instructive to know the general difference in the load-displacement behaviour of the main anchor types. Figure 3.29 shows tensile load-displacement curves derived from monotonic tension tests on different post-installed anchor types. The load-displacement curves were calculated as an average value of relevant tests of the data base. Data sets for anchors with a diameter of d = 12 mm, tested in low strength (C20/25) cracked concrete (w = 0.3 mm) with an effective embedment depth h_{ef} of 75 to 90 mm were extracted.

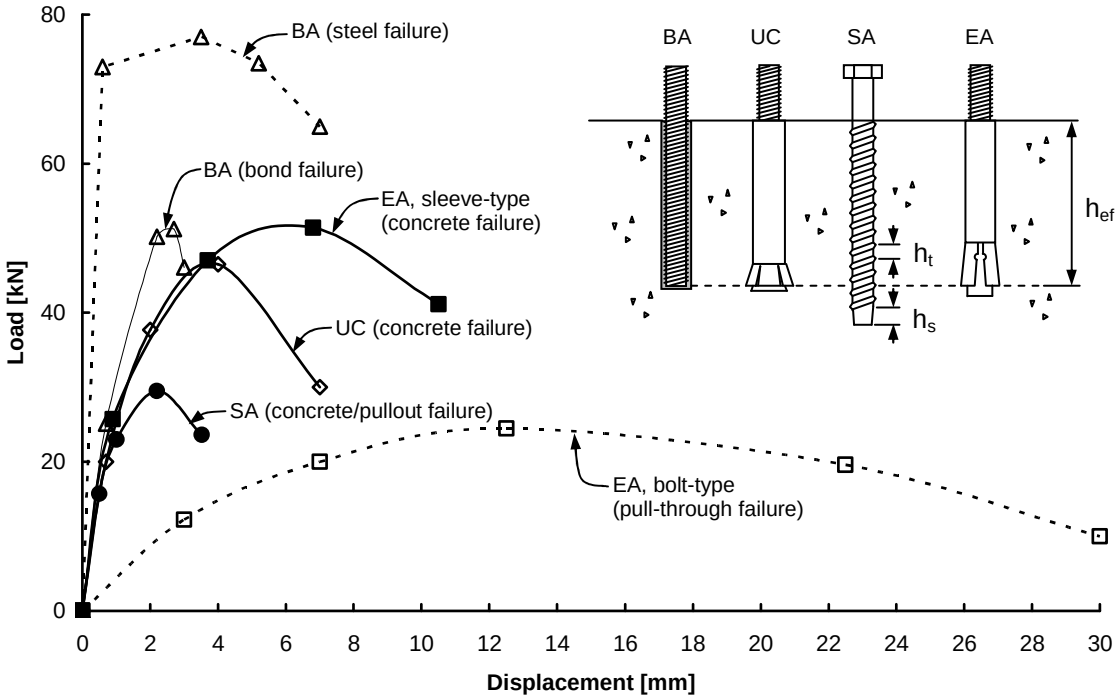

Figure 3.29 Average tension load-displacement curve for anchors d = 12mm: Bond anchor (BA), undercut anchor (UC), screw anchor (SA), and expansion anchor (EA)

For bonded anchors, Figure 3.29 depicts the average load-displacement curve of anchors with a 12 mm steel element. The tension load is transferred over the entire depth h_{ef} by mechanical interlock from the steel element into the adhesive mortar and by bond and micro interlock (due to the geometric imperfection of the drilled hole) from the mortar into the concrete. When installed with an embedment depth of 6 d, the anchor fails in a bond failure mode. When set deep enough, steel failure with a steep elastic ascending branch and a pronounced inelastic load plateau occurs. The steel failure mode is basically a pure material test as indicated by the dashed line in Figure 3.29. The load plateau, however, is relatively short because of the small free strain length of the installed anchor.

For screw anchors, Figure 3.29 depicts the average load-displacement curve of anchors with a nominal diameter of 12 mm. The effective embedment depth h_{ef} can be estimated as $h_{ef} = 0.85\ (h_{nom} - 0.5\ h_t - h_s)$ (refer to *CUAP Concrete Screw (2003)*, *Küenzlen, J. (2005)*, and *AC193 (2010)* Clause 8.7). The load is transferred by mechanical interlock into the concrete. The ultimate capacity is reached when the concrete consoles are sheared off, resulting in a combined pullout/concrete failure mode with a shallow cone. The average load-displacement curve of undercut anchors inidicates a pure concrete failure. Undercut anchors function by mechanical interlock which is created by an undercut element at the anchor base which depth

equals h_{ef}. The concentrated load transfer at the anchor base allows a deep concrete cone to develop. Load and displacement capacities are larger than for a screw anchor with the same embedment depth.

For expansion anchors, Figure 3.29 depicts the average load-displacement curve of anchors M12 (1/2”). This anchor type transfers the load by friction between anchor body and expansion element, and expansion element and concrete. Sleeve-type expansion anchors fail predominantly by concrete breakout and h_{ef} equals the depth of maximum expansion of the expansion elements. During loading, the anchor is pulled further into its expansion element (follow-up expansion). Therefore, the anchor experiences larger displacement than an undercut anchor with the same embedment depth. Bolt-type expansion anchors may also fail by being pulled through the expansion element, in particular in case of thin expansion elements and increased crack widths. This failure mode shows the characteristic bell-shaped curve as indicated by the dashed line. In fact, the failure mode may vary even within one test series of several repeats on exact the same anchor product, size and embedment.

The qualitative conclusion is that post-installed anchors of various type but same embedment depth display a very different load-displacement behaviour. Typically, bonded, screw, and undercut anchors, which do not have sufficient free strain length, have only limited displacement capacities in tension. In contrary, expansion anchors exhibit substantial displacements before failure, especially in case of a pull-through failure mode. All anchor load-displacement curves in common is the very short elastic range, and the lack of a distinctive yield point and plateau.

3.3.4.2 Tension deformation capacities and percentage elongation criteria

Depending on size, concrete strength etc. but also on the actual embedment depth, every anchor yields different displacements, resulting in a certain data base fragmentation. Assessment of the data base showed that the influence of concrete strength on the displacement parameters is small. Therefore, the displacement data derived from anchors tested in various concrete strengths (low and high) were merged. Since cyclic load-displacement curves are not critical in respect to ductility parameters (Section 3.3.3.1), but their evaluation is demanding, cyclic load-displacement curves are not further considered here. The results of tension load data assessment are presented for absolute deformation first, then for relative deformation.

As a conservative approach (Section 3.3.3.2), the absolute deformation and thus maximum deformation Δ_m is taken as the displacement at ultimate load $s(N_u)$. Table 3.4 depicts the range of the data base evaluation for bond (vinyl and epoxy), screw, and torque-controlled expansion anchors for common sizes. Displacement-controlled

expansion anchors are generally not appropriate for seismic applications because of unfavourable performance in cracked concrete and are therefore not taken into consideration. For undercut anchors, there are too few test data available to give meaningful results of evaluation, however, the values of $s(N_u)$ for undercut anchors may be assumed to be in the upper bound of the range for screw anchors. Virtually all anchors incorporated in the table failed in a mode other than steel.

Table 3.4 Range of absolute displacement at ultimate load $s(N_u)$ in [mm] for various anchor types and sizes

Anchor Type	Crack Width	M10 (3/8")	M12 (1/2")	M16 (5/8")	M20 (3/4")	M24 (1")
Bonded	0.0 mm	0.7 ÷ 2.6	0.8 ÷ 3.0	0.8 ÷ 3.4	1.1 ÷ 1.2	1.3 ÷ 4.0
Anchor	0.3 mm	1.1 ÷ 1.4	1.4 ÷ 3.8	1.1 ÷ 4.3	4.6 ÷ 4.8	1.4 ÷ 5.0
	0.5 mm	1.0 ÷ 1.4	–	1.3 ÷ 1.6	–	1.4 ÷ 1.6
	Combined	0.7 ÷ 3.5	0.8 ÷ 3.8	0.8 ÷ 4.3	1.1 ÷ 4.7	1.3 ÷ 5.0
	Median	1.7	2.3	2.6	2.9	3.2
Screw	0.0 mm	1.0 ÷ 2.1	1.6 ÷ 1.8	1.4 ÷ 3.4	2.8 ÷ 3.3	–
Anchor	0.3 mm	1.0 ÷ 2.3	1.0 ÷ 3.1	2.4 ÷ 3.3	3.0 ÷ 3.2	–
	0.5 mm	1.4 ÷ 2.6	1.9 ÷ 3.1	2.3 ÷ 3.8	2.2 ÷ 4.5	–
	Combined	1.0 ÷ 2.6	1.0 ÷ 3.1	1.4 ÷ 3.8	2.2 ÷ 4.5	–
	Median	1.8	2.1	2.6	3.4	–
Expansion	0.0 mm	3.7 ÷ 7.5	4.1 ÷ 9.5	5.4 ÷ 12.6	6.4 ÷ 10.9	9.0 ÷ 9.4
Anchor	0.3 mm	3.9 ÷ 9.5	4.0 ÷ 10.7	3.7 ÷ 11.6	7.9 ÷ 9.8	10.1 ÷ 12.7
	0.5 mm	4.3 ÷ 8.5	4.2 ÷ 9.0	4.1 ÷ 10.4	8.4 ÷ 12.9	–
	Combined	3.7 ÷ 18.5	4.0 ÷ 10.7	4.1 ÷ 12.6	6.4 ÷ 12.9	9.4 ÷ 12.7
	Median	6.1	7.4	8.4	9.7	11.1

As already indicated before, expansion anchors yield at much larger displacements than the other anchor types. Larger anchor diameters are generally accompanied by larger embedment depths and develop larger displacements. By dividing the absolute displacement $s(N_u)$ with the effective embedment depth h_{ef}, a percentage displacement is determined with reference to the embedment depth (Table 3.5).

Table 3.5 Range of percentage displacement at ultimate load $s(N_u)/h_{ef}$ in [%] for various anchor types and sizes

Anchor Type	Crack Width	M10 (3/8")	M12 (1/2")	M16 (5/8")	M20 (3/4")	M24 (1")
Bonded	0.0 mm	0.9 ÷ 3.3	0.8 ÷ 3.1	0.6 ÷ 2.7	0.7 ÷ 0.8	0.7 ÷ 2.1
Anchor	0.3 mm	1.4 ÷ 4.4	1.5 ÷ 4.0	0.9 ÷ 3.4	2.8 ÷ 3.0	0.7 ÷ 2.6
	0.5 mm	1.3 ÷ 1.8	–	1.3 ÷ 1.6	–	0.7 ÷ 0.9
	Combined	0.9 ÷ 4.4	0.8 ÷ 4.0	0.6 ÷ 3.0	0.7 ÷ 2.9	0.7 ÷ 2.3
	Median	1.7	2.3	2.6	2.9	3.2
Screw	0.0 mm	1.6 ÷ 3.6	2.2 ÷ 2.6	1.3 ÷ 4.1	2.3 ÷ 2.7	–
Anchor	0.3 mm	1.5 ÷ 4.0	1.3 ÷ 4.8	2.9 ÷ 4.0	2.4 ÷ 2.6	–
	0.5 mm	2.3 ÷ 4.5	2.5 ÷ 4.8	2.1 ÷ 4.6	1.8 ÷ 3.7	–
	Combined	1.6 ÷ 4.5	1.3 ÷ 4.8	1.3 ÷ 4.6	1.8 ÷ 3.7	–
	Median	1.8	2.1	2.6	3.4	–
Expansion	0.0 mm	5.7 ÷ 9.1	5.1 ÷ 12.9	5.4 ÷ 12.6	5.1 ÷ 8.7	6.0 ÷ 6.3
Anchor	0.3 mm	6.0 ÷ 13.8	5.0 ÷ 11.4	3.7 ÷ 11.6	6.3 ÷ 7.8	6.7 ÷ 8.5
	0.5 mm	6.6 ÷ 12.1	5.3 ÷ 11.3	4.1 ÷ 10.4	6.7 ÷ 10.3	–
	Combined	5.7 ÷ 13.8	5.0 ÷ 13.4	4.1 ÷ 12.6	5.1 ÷ 11.8	6.3 ÷ 8.5
	Median	6.1	7.4	8.4	9.7	11.1

The scatter of the displacement at ultimate load within a test series is relatively small. The coefficients of variation (CV) within a test series is less than 25 % for $s(N_u)$ (*Mahrenholtz, P. (2011b)*). For a specific anchor product, anchor displacements generally increase with increasing crack widths for otherwise constant boundary conditions (Section 3.4.5.2). However, the wide range of the displacement data caused by large scatter between different anchor products overcast this effect and makes the data less significant with respect to the influence of the crack width. Sensitivity studies have shown that the significance of the results cannot be increased by differentiating the failure mode, which is in line with other anchor test data analyses (*Cattaneo, S. (2007)*).

The following discussion of ductility parameters is not to quantify exact displacement capacities but rather to indicate trends for various anchor types in order to identify potential approaches for the definition of anchor ductility. Therefore, the data are further consolidated by combining the displacement data for all crack widths (0.0, 0.3, and 0.5 mm). In Figure 3.30a the median of the displacements at ultimate load is plotted as a function of anchor size, in Figure 3.30b the median of the percentage displacements. Parameter is the type of anchor. It becomes evident that the medians of the percentage displacements seem to be relatively constant for variable anchor sizes.

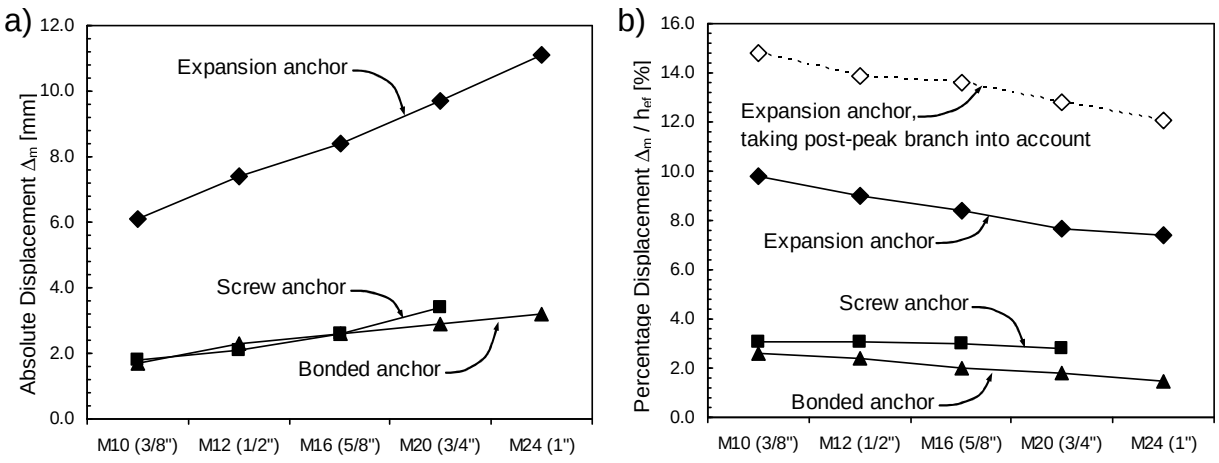

Figure 3.30 Displacement capacity versus anchor size:
a) Absolute displacement $s(N_u)$ in [mm]; b) Percentage displacement $s(N_u)/h_{ef}$ in [%]

The findings suggest the following analogy: If an anchor failing in any mode yields a percentage displacement that is as large as the percentage elongation of an anchor tested in a material tensile test with a gauge length equal to the embedment depth, it shall be considered as providing equivalent ductility (Figure 3.31a). The required percentage elongation for an anchor to be classified as ductile is according to *CEN/TS 1992-4 (2009)* 12 % (L_o = 5 d) and *ACI 318 (2011)* 14 % (L_o = 4 d), respectively. Figure 3.30b shows that bonded and screw anchors are far from meeting this requirement, however, expansion anchors are potentially close to it. By taking the post-peak branch into account, which is in particular reasonable for expansion anchors failing in a pull-through failure mode, the maximum available displacement is increased (Figure 3.30b).

As implemented in *Mahrenholtz, P.; Eligehausen, R. et al. (2011)*, the required percentage needs to be adjusted for anchor embedment depths different to the proportional length, e.g. by multiplying it by the conversion factor 2 $(S_o^{0.5} / L)^{0.4}$ given in *ISO 2566-1 (1999)*. S_o is the cross section area, taken as $\pi \cdot d^2 / 4$ for an anchor, and L the gauge length, taken as the embedment depth h_{ef} of the anchor. The diagram in Figure 3.31b depicts the absolute displacement required to get classified as ductile for given h_{ef}.

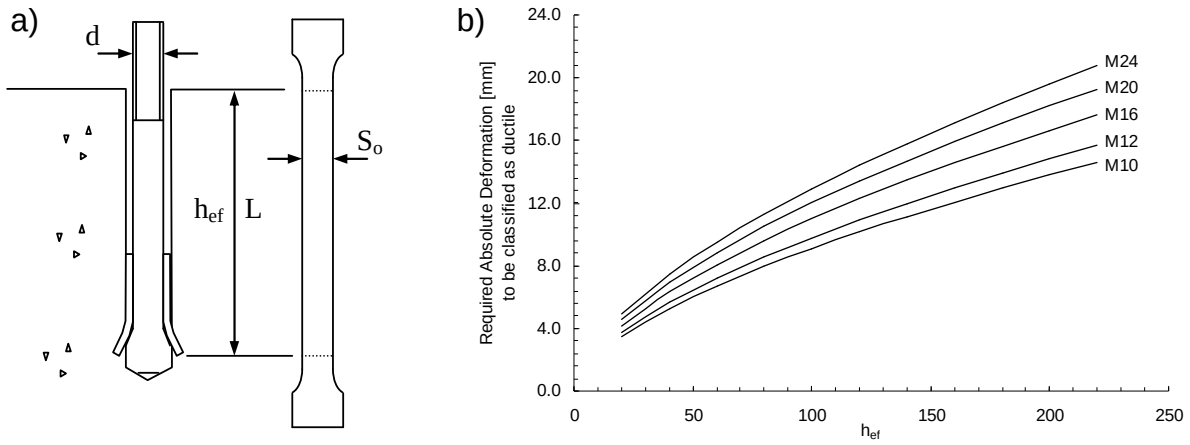

Figure 3.31 a) Illustration of the analogy of percentage displacement for a test on an installed anchor and the percentage elongation for a corresponding material tensile test; b) Required absolute deformation to be classified as ductile

As discussed, the quantification of the relative deformation for anchor load-displacement curves is problematic. For load-displacement curves of individual anchors, the elasto-perfectly plastic system can vary significantly from the actually measured load-displacement curve and the CV for yield displacements $s(N_y)$ within a test series is high (Figure 3.26c). For the following discussion, the averaged curves from Figure 3.29 are taken and their yield and maximum deformations extracted (Figure 3.32). Since the magnitude of available local ductility is not affected very much by the idealisation rule and is small in any case, the 75 % rule was applied for the determination of yield deformation Δ_y. The maximum deformation was taken as the displacement at ultimate load. Though irrelevant for the determination of deformation parameters, it is noted here that this procedure results in the conventional bi-linear idealization of the load-displacement curves.

Analysing the relative deformation by calculating the ratio of maximum deformation Δ_m to yield deformation Δ_y, results in different magnitudes depending on the anchor types. For bonded anchors, the ratio may be assumed to be just above 1.0, for screw anchors less than 2.0, for expansion anchors also in the order of 2.0. Apparently, expansion anchors do not benefit from their displacement capacities because of the soft ascending branch that leads also to large yield deformations. Even by taking the maximum deformation as the post-peak deformation at 85 % of the ultimate load ($s(N_{pp})$), the ratio of Δ_m to Δ_y may be increased only to 2.5.

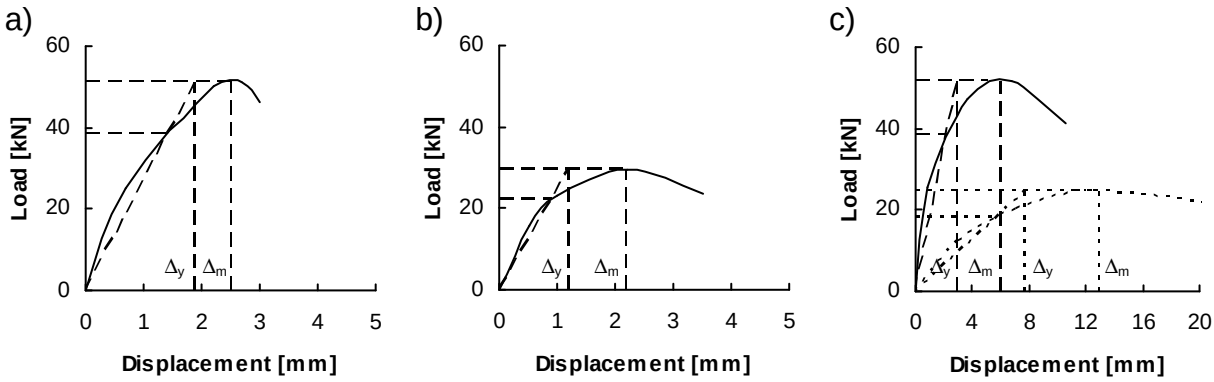

Figure 3.32 Average load-displacement curves and extracted values for Δ_y and Δ_m: a) Bonded anchor; b) Screw anchor; c) Expansion anchor, dashed line for pull-through failure

3.3.4.3 Shear deformation capacities and shear/tension interaction

There are not enough shear test data available to give a meaningful parametrical space for shear deformation capacities of post-installed anchors. However, in the following anchor shear ductility is briefly discussed and key conclusions are drawn.

In contrast to anchors loaded in tension, anchors away from edges loaded in shear fail under normal conditions always in steel. However, substantial material ductility is not generated by shear deformation because the cross section area of anchors is simply too small. Due to the offset of the acting shear anchor load to the resulting supporting forces, a bending moment and thus bending ductility develops, resulting in system shear ductility. Fixture lifting due to axial load, as well as lateral concrete compaction and concrete spalling increase the available system ductility further. Because of the concrete stress reducing influence, anchors with sleeves (refer to Figure 3.1) show increased ultimate load and displacement capacities if compared to an anchor of same size but without sleeve.

The methods presented in Section 3.3.4.1 for load-displacement curve characterisations to evaluate deformation capacities also apply to shear tests. The envelope of the cyclic load-displacement curve follows the monotonic mean curve, provided that the anchor does not tend to low cycle fatigue (LCF) for which the envelope of the cyclic load-displacement curve may divert from the monotonic curve and premature failure is likely. However, for anchor qualification it is required to sustain all cycles of a given qualification protocol (e.g. *ACI 355.2 (2007)* or *DIBt KKW Leitfaden (2010)*), if necessary by reducing the strength (refer to Section 2.5.2). The deformation capacities can be extracted from the corresponding backbone curve of that cyclic test for which the anchor has completed all cycles.

Variable boundary conditions are the reason for large variations in the deformation data of different test series. Because the boundary conditions have a paramount impact on the test result, they need to be defined in detail. Qualification tests are carried out with a downholder which prevent the anchor from lifting off. The more rigid this device is guided perpendicular to the shear plane, the higher is the load capacity but the lower the deformation capacity. While this approach is unsafe for the determined strength, it is conservative for the deformation capacities.

The analysis of available test data showed that in general the maximum displacement increases with increasing size and is in the range of 5 to 30 mm for anchor sizes M10 to M20, which is for most cases more than the corresponding anchor would yield under tension load. Interaction of tensile and shear ductility is always on the safe side since any axial loading increases system shear ductility.

3.3.5 Conclusions

In the preceding sections it was shown that absolute and relative deformation capacities are the driving anchor ductility parameters which cover all relevant behavioural objectives. Large absolute deformations are desirable for static and seismic applications. In this context, however, it is noted that contrary to structural design which rely very much on displacement capacities (DBD and PBD), the requirements of existing anchor design guidelines are strictly force oriented. Predicting deformation demand for structural or non-structural connections and correlating this to anchor response characteristic is beyond the capabilities of current design concepts (*Silva, J. (2007)*). One problem is the scatter of the deformations in the post-elastic range which result in widely spread characteristic minimum and maximum displacements (*Mahrenholtz, P. (2011b)*). In consequence, the question of how much ductility or deformation capacity is actually required is not addressed in this thesis and depends further on the design situation which first of all needs to be identified as force or deformation controlled.

The current classification of anchor ductility given in *AC193 (2010)* and *AC308 (2009)* are founded in the material science and needs to be transferred to the installed anchor system. The requirement concerning the reduction in area is not meaningful since it is physically not needed. For the required elongation it is proposed to define the ratio of absolute deformation capacity to the effective embedment depth as the available percentage elongation. This approach is more substantiated and allows classifying anchor ductility based on monotonic load-displacement curves, irrespective of the failure mode. The approach is compatible with the existing provisions given in the design guidelines *ACI 318 (2011)* and *CEN/TS 1992-4 (2009)* (Section 3.3.2.3). The evaluation of a data base of several hundred experimental tests confirmed that absolute deformation is a good parameter

to characterise the deformation behaviour of various anchor types. Contrary to any other anchor type and for all embedment depths, expansion anchors may exhibit ultimate displacements in the magnitude similar to an anchor which fails in steel with a free strain length equal to the embedment depth. Therefore, expansion anchors could comply with the requirements on the percentage elongation to get classified as ductile. However, it is noted that the load-displacement behaviour of anchors not failing in steel depends on the anchorage material, i.e. concrete, leading to larger scatter and less defined response, and may be less robust to tension cycling near ultimate load. Further research is therefore required to reach sound conclusions.

The definition of the yield deformation is essential for the calculation of the relative deformation capacity. Due to the lack of a pronounced yield point, however, the definition of the (pseudo) yield deformation is problematic. The relative deformation derived from the evaluation of the data base is for all anchor types small. Depending on the definition of yield and maximum displacement, the relative deformation capacity may be in the magnitude of 1.0 to 2.0, potentially above if the post-peak deformation is taken into account in case of pull-through failure.

The discussion of the data base evaluation with regard to seismic design requires distinguishing between structural and non-structural connections. In case of non-structural connections, anchor loads develop according to the inertial response of the NCS to the floor accelerations it is connected to. The resulting anchor behaviour in turn feeds back the anchored NCS behaviour and therefore the ductility of the anchorage is one of the characterising parameters of the NCS. Ductile behaviour of the NCS allows reduction of the seismic design loads obtained by linear elastic analysis according to *ASCE 7 (2010)* Chapter 13 or *CEN/TS 1992-4 (2009)* Annex E. If the NCS does not show beneficial ductile behaviour ($q_a = 1.0$), one might want to assign a reduction factor to the anchorage itself. For $\mu = \Delta_m / \Delta_y = 2.0$, the behaviour factor can be theoretically calculated to $q_a = 2.0$ for NCS oscillating in the long period domain or 1.73 for NCS oscillating in the medium period domain (principle of equivalent displacement or equivalent energy, *Newmark, N.; Hall, W. (1982)*). In light of the load transfer characteristics of post-installed anchors resulting in extremely pinched hysteresis, however, it is arguable whether the principles developed to recognize the beneficial effect of ductility also apply on anchors connecting NCS to the structure. In case of structural connections, the anchor forms an integral part of the structure and as such influences the structural response to the earthquake input. Deformations imposed by the global structure are the main demand for these connections. Predicting the exact deformation demand for connections is difficult, however, while interpreting anchor ductility as local ductility, the ductility factor $\mu = \Delta_m / \Delta_y$ in the range of 1.0 to 2.0 or 2.5 is not large in any case. Local ductility generally has to be considerably larger than the required global ductility (*Paulay, T.; Priestley, N. (1992)*, *Bachmann, H. (1995)* etc.). The interaction

of local and global ductility is not discussed in more detail here, however, the small magnitude of the calculated ductility indicates that at least for seismic design, the available relative deformation capacity of anchors can only play a minor role. Further research, however, is necessary to understand local anchor ductility and its impact on the global ductility.

Notwithstanding the outcome of the data base analysis, anchor deformation during seismic events can be disadvantageous in some aspects. Increasing anchor displacement may lead to the pounding or hammering effect (*Nuti, C.; Santini, S. (2008)*, *Smith, J.; Dowell, R. (2008)*, *Rieder, A. (2009)*), and to a potential increase in NCS amplification due to the elongation of the period as described in *Smith, J.; Dowell, R. (2008)* for loading in tension and in *Rieder, A. (2009)* for loading in shear.

Despite of its importance, shear anchor ductility is currently not addressed in any code. For shear loads, the data base is not enough populated to draw significant conclusions. More test data are needed for the investigation of the shear ductility, for which the boundary conditions of the test setup have to be defined in detail. Further, the effects of filling the clearance hole as it is common practice for seismic applications and recommended by design guidelines, e.g. in Clause 8.2.7 of *CEN/TS 1992-4 (2009)*, but not for qualification testing need to be carefully investigated. For anchors of common size and embedment depth failing in steel when loaded in shear, the shear deformation capacity is generally not less than the tension deformation capacity of the respective anchor and therefore not critical.

In conclusion, a new approach is presented which is based on the equivalent percentage elongation of the anchor. The percentage elongation equals the ratio of absolute deformation capacity to the effective embedment depth. An anchor should be qualified as ductile if the equivalent percentage elongation meets the current requirement on the percentage elongation of 12 % (for 5 d) (Figure 3.31b). The proposed criterion is more general and substantiated than the definition given in current codes.

3.4 Anchor Groups

3.4.1 State of knowledge

While there is lot of experimental and numerical test data on single anchors and therefore their behaviour is quite well understood, there are relatively few tests reported in literature on anchor groups. This is especially true if the connection is exposed to cyclic loads or cyclic cracks as under seismic excitation. A detailed literature review on anchor group testing is given in *Mahrenholtz, P. (2008)*. In the following, the most relevant literature is shortly summarised for tension loaded

anchor groups which was the research focus within the scope of this thesis for reasons explained later.

In *Mayer, B.; Eligehausen, R. (1983)* the influence of different load-displacement behaviours of the individual anchors on the ultimate load of anchor groups is theoretically investigated. The calculation of the ultimate load is based on idealised load-displacement curves of a torque-controlled expansion anchor for cracked and uncracked concrete (Figure 3.33a1). 2-anchor and 4-anchor groups with large and small spacing, loaded monotonically in tension were considered. Rotational-unrestrained and rotational-restrained base plates as well as all possible crack cases were included. Further, a potential variation in the load-displacement behaviour of that anchor located in the crack was taken into account (Figure 3.33a2). The ultimate load was determined graphically allowing for condition of equilibrium and the compatibility. The crack case was identified as the major influencing factor on the ultimate group load, irrespectively of the anchor spacing. For the 2-anchor and 4-anchor groups it was concluded that in most crack cases the ultimate load of an anchor group is at least n-times the capacity of a single anchor in crack. The only exception is the crack case with 3 anchors located in a crack for a 4-anchor group. This crack case ends up with an ultimate load that is 15 % lower than 4-times capacity of a single anchor in crack.

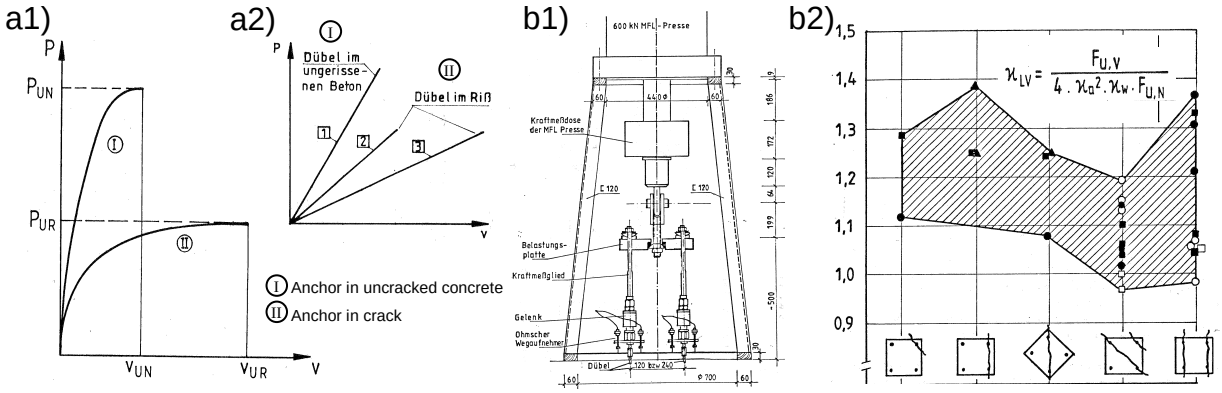

Figure 3.33: a) Theoretical investigations in *Mayer, B.; Eligehausen, R. (1983)*: a1) Assumed Ld curves; a2) Variation in Ld curves for anchors located in cracks; b) Experimental investigations in *Mayer, B.; Eligehausen, R. (1984)*: b1) Load setup; b2) Reduction factor κ_{LV}

The theory was validated by experimental tests as reported in *Mayer, B.; Eligehausen, R. (1984)*. 2-anchor and 4-anchor groups were installed in cracked concrete ($w \approx 0.35$ mm) and loaded monotonically to failure by a displacement controlled actuator. The base plate used is assumed as relatively stiff; and the connection between the loading device and the base plate was hinged (Figure 3.33b1). The investigations included all crack cases and the anchor spacing was taken as 1.5 or 3 times of the embedment depth. The failure mode was a concrete

cone breakout in all cases. Interestingly, the reduction in ultimate load is smaller than the theoretical consideration suggested. It was assumed that the reason of this is a (pseudo-) ductility of the anchors, manifested in a continuously post-peak branch of the load-displacement curve. All together, the experimental tests verified the theoretical considerations. The reduction factor κ_{LV}, reflecting the reduction due to scatter of the load-displacement curves, was generally larger than 1 (Figure 3.33b2). Slightly lower values for a 4-anchor group with 3 or 4 anchors located in a crack was deemed as secondary since it is not very likely in practice.

In *Lotze, D. (1986)* and *Lotze, D. (1993)* the behaviour of anchor groups under load cycling was investigated. A method for the calculation of maximum loads and load amplitudes of the individual anchors was developed for rotational-unrestrained and rotational-restrained base plates (Figure 3.34a and b) and applied to various crack cases. It was shown that in the course of the load alternation, the load was distributed towards the stiffer anchors. As expected, the displacement is larger for anchors located in cracked concrete than for those located in uncracked concrete; whereas the stiffness of the unloading branch is about the same for anchors located in cracked and uncracked concrete. These investigations highlighted the beneficial effect of load redistribution for a rotational-restrained anchor plate. On the other hand, uneven load distribution also results in different load amplitudes during cycling. However, it is noted that the herein described effects of load cycling, though generally valid, are only critical for large number of load cycles. The theoretical and experimental investigations targeted on the group effects of load cycling on high cycle fatigue (HCF).

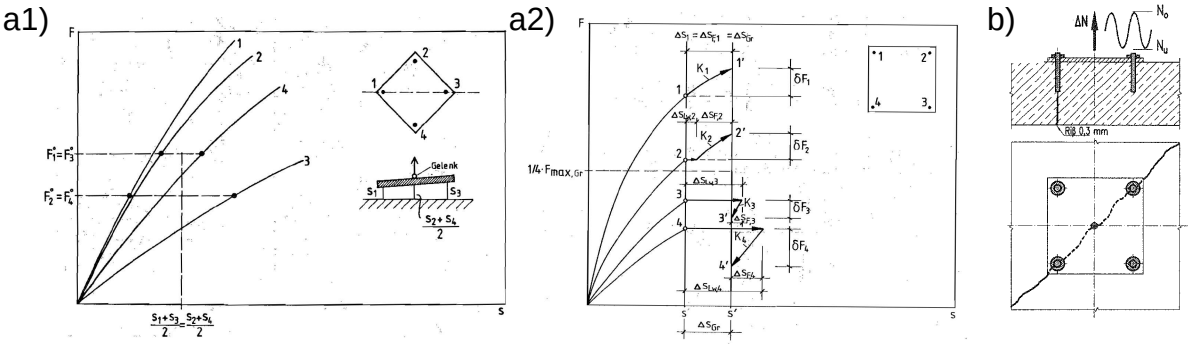

Figure 3.34: a) Load bearing behaviour of anchor groups (*Lotze, D. (1993)*): a1) Rotational-unrestrained anchor group; a2) Rotational-restrained anchor group and theoretical load redistribution; b) Test setup in *Block, K.; Dreier, F. (2002)*

The so-called interactive approach already introduced for single anchors in *Block, K.; Dreier, F. (1998)* was picked up again in *Block, K.; Dreier, F. (2002)* and extended to anchor groups. The fatigue behaviour and load redistribution was investigated by means of 4-anchor groups subjected to up to 3 million load cycles. 2 diagonally opposing anchors were installed in a crack (Figure 3.34c). With reference to *Lotze,*

D. (1993), this configuration has been identified as the most critical in view of load redistribution effects. The theoretical results found in *Lotze, D. (1993)* were confirmed experimentally. Since the considered crack case is point symmetric, the type of connection between loading device and base plate (rotational-unrestrained or rotational-restrained) did not matter. In fact, the configuration with 2 parallel anchors in a crack yielded similar load distributions in *Lotze, D. (1993)*, so the advantages associated with the insensitivity towards the base plate configuration might have been the decisive argument to test the group with 2 diagonal anchors in a test.

In *Okelo, R. (1996)*, the influence of the scatter of load-displacement curves was investigated. Therefore, innumerous numerical tests on quadruple anchor groups were carried out. The base plate was assumed to have infinite bending stiffness. Two different cases for the displacement of the base plate were considered: Translation and rotation (rotational-unrestrained) and translation only (rotational-restrained). The following crack cases were employed: All anchors are located in uncracked concrete; all anchors are located in cracked concrete and 3 out of 4 anchors are located in cracked concrete. The incremental loading followed monotonic tensile load-displacement curves. The calculations yielded that the bearing capacity of 4-anchor groups decreases with increasing scatter of the load-displacement curves. The report concluded that the limitations on the coefficient of variation of the displacement at 0.5 F_u and at F_u to 25 % and 15 %, respectively, might not be appropriate for anchor groups which anchors are located in uncracked and cracked concrete. Though this report highlights the influence of scatter on the ultimate group capacity, it is not very explanatory regarding the actual group behaviour.

In conclusion, there is only little literature on anchor group behaviour available, however, all of them have in common the consideration of the following features which will be discussed in Section 3.4.2: (i) The differentiation of base plate configuration with rotational-unrestrained and rotational-restrained base plates as the borderline cases; (ii) The importance of cracks on the group performance; (iii) The influence of the crack pattern on the load distribution and associated effects as fatigue load range, load redistribution etc.; (iv) The spacing of the individual anchors is only considered when it comes to ultimate load capacities. Further it is noted that all investigations were limited on 2- and 4-anchor groups. However, none of the reported experimental tests were carried out with a base plate which is connected rotationally rigid to the loading device. Moreover, there is no study on anchor groups under constant axial load and with some of the anchors installed in a cycled crack. Crack cycling and associated large axial anchor displacement, however, certainly have a big impact on anchor group behaviour, in particular in case of rotationally rigid base plates, and therefore needs to be investigated.

3.4.2 Theoretical background

Connections between steel and concrete employ either single anchors or anchor groups consisting of several anchors. Though there is no statistical data available, it may be reasonably assumed that most of the structural connections involve multiple anchors due to the large forces to be transferred. In contrast, the extensive survey on NCS as reported in *Watkins, D.; Chui, L. et al. (2009)* concluded that the majority of non-structural connections are carried out as more or less widely spaced single anchor points. It is noted that with reference to the CC Method, anchor groups are associated with a number of anchors spaced at less than three times its embedment depth, however, anchor groups are also understood as several anchors working together and thus allowing load distribution what also applies to NCS fixed by widely spaced single anchors. In the following, the key parameters describing anchor groups are briefly discussed.

3.4.2.1 Base plate configuration

All anchors of an anchor group share a base plate which allows for load distribution among the anchors. If the individual anchors do not experience any other constraints, the load acting on a rotation-unrestrained anchor group is distributed equally among the individual anchors and, if the stiffness of the individual anchors differs, the base plate rotates. In contrast, a stiff connection of a rotation-restrained anchor group requires all anchors to follow the same displacement but the load is distributed among the individual anchors according to their stiffness. The resulting eccentricity creates a bending moment (Figure 3.35a).

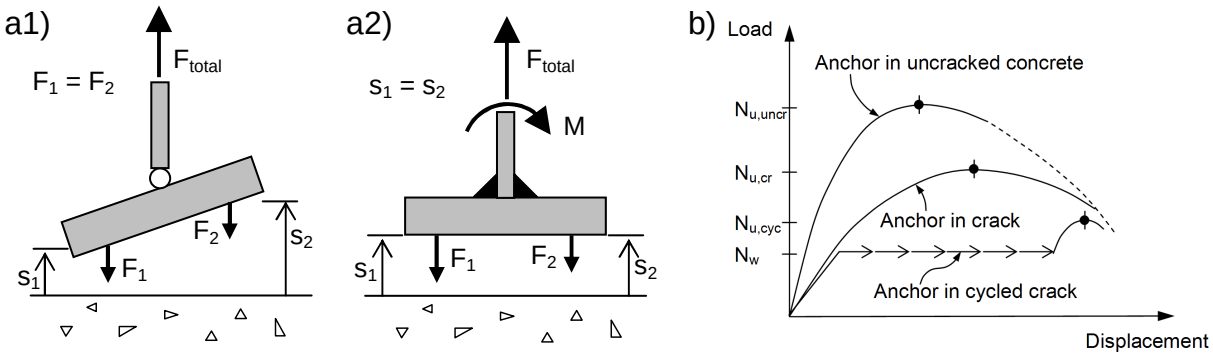

Figure 3.35: a) Base plate configuration: a1) Rotational-unrestrained anchor group; a2) Rotational-restrained anchor group; b) Load-displacement curves of individual anchors (schematic)

3.4.2.2 Static and cyclic cracks

One or more anchors of an anchor group may be located in a crack. The tensile stiffness of anchors located in uncracked concrete and in cracks is different. In

addition, the scatter in stiffness of anchors located in cracks may be substantial. Depending on the base plate configuration, the asymmetry in stiffness results in rotation of the base plate and / or uneven load distribution. For cyclic cracks associated with seismic actions, the stiffness of the affected anchor changes over time and the anchor tends to slip. This in turn results in further base plate rotation and load redistribution. The load capacity can either increase or decrease in relation to the sum of the individual anchor capacities. This effect is the driving factor for the overall behaviour and performance of anchor groups under seismic applications. It occurs only if the anchor group is loaded permanently in axial direction. The effect of cracks and crack cycling on individual anchors loaded in tension is illustrated by the curves in Figure 3.35b. More detailed background on anchor behaviour in cycled cracks can be found in Section 3.6.

For anchor groups loaded in shear, the effect of scatter is generally associated with unevern load distribution due to variable stiffness mainly caused by more or less pronounced spalling of the concrete and variable annular gap between anchor and base plate. However, the investigations presented in this thesis focused on anchor group loaded in tension, but not in shear.

3.4.2.3 Cyclic and permanent loads

The effect of seismic load cycling on the tensile anchor performance is generally low (Section 3.5.3). In particular the increased displacement the anchor experiences during the limited number of cycles is relatively small. In conclusion, load redistribution effects as in case of cyclic loads are not an issue. What matters, is the magnitude of the permanent load during crack cycling (N_w in Figure 3.35b).

3.4.2.4 Crack cases

The load-displacement behaviour of anchor groups highly depends on the actual crack pattern the individual anchors are located in. One or several anchors may be located in a crack. Anchor groups with more than 4 anchors were not subject of the investigations, however, they are deemed to be not critical since the load distribution is increasingly smeared with an increase in number of anchors. Their load-displacement behaviour would be equivalent or better than for 2- and 4-anchor groups, which are the most common patterns. Figure 3.36a shows all possible crack cases. The crack cases of all anchors located in uncracked concrete and all anchors located in cracks are trivial and thus not shown here.

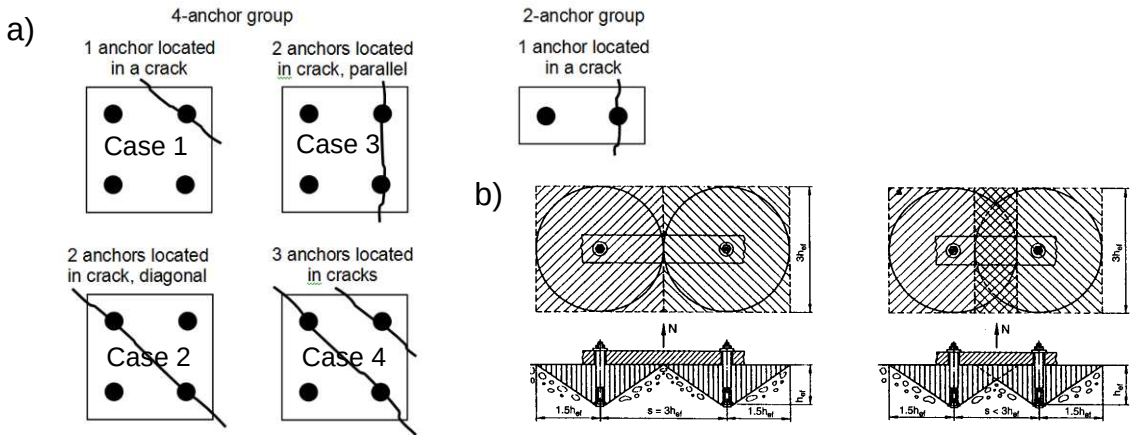

Figure 3.36: a) Possible crack cases for 4- and 2- anchor groups; b) Large (left) and small (right) anchor spacing (*Eligehausen, R.; Mallée, R. et al. (2006)*)

3.4.2.5 Anchor spacing

The CC Method, underlying the relevant anchor design guidelines, implies that if the spacing is less than $3\,h_{ef}$, the individual failure cones interfere and the failure capacity is reduced. Therefore, anchor groups are often distinguished as anchor groups with small and large anchor spacing (Figure 3.36b). However, overlapping failure surfaces matter only for the ultimate load, provided that adjacent anchors fail in concrete and reach their ultimate capacity at the same time, and is just then considered by the CC Method. The general applicability of the statements made in the preceding sections irrespective of the anchor spacing is not affected by this. In particular the initial load-displacement behaviour prior to ultimate failure is independent of the anchor spacing.

3.4.2.6 Reduction factors

For anchor located in a region of a concrete member where cracking is expected, which is generally the case in particular for seismic applications, the anchor design load shall be reduced according to Clause 5.2.2.4 of *ETAG 001 (2006)* Annex C and Clause D.5.2.6 of *ACI 318 (2011)* Appendix D by the factor ψ_w of 10.1 / 7.2 ≈ 0.7 and 1 / 1.4 ≈ 0.7, respectively. An additional reduction in the design load may be introduced by the technical approval reporting a seismic design strength which is lower than the static design strength, e.g. due to reduced performance in case of load cycling tests or the more demanding crack cycling tests (refer to Section 2.5 and 2.6).

In light of this, the group performance is assessed best by comparing the ultimate group load ($N_{u,group}$) with the corresponding ultimate load of a single anchor. For static applications, $N_{u,group}$ is compared with n-times the capacity in cracked concrete ($N_{u,cr}$). For the seismic case, however, it makes more sense to compare the group capacity

to the capacity of a single anchor under cyclic condition, i.e. in a cyclic crack ($N_{u,cyc}$). In this case, the reduction factor can be taken as $N_{u,group}$ / (n · $N_{u,cyc}$).

Numerical tests (Section 3.4.3) and experimental tests (Section 3.4.4) were carried out to determine the group factor which account for any reduction that arise from the group configuration (Section 3.4.5). The knowledge on the load redistribution effects gained by the tests was implemented in a group model which allows simulating the behaviour of statically indeterminate anchor groups (Section 3.4.6).

3.4.3 Re-evaluation of numerical tests

In the following, results of numerical investigations on the behaviour of anchor groups with 4 anchors under static and cycled crack conditions presented in *Periskic, G. (2009)* are discussed. The influence of the anchor type (bolt-type expansion anchor and headed stud, representing various load transfer mechanisms and range of stiffness typical for anchors), the crack condition (static and cyclic cracks), the base plate configuration (rotational-unrestrained and rotational-restrained), the number of anchors located in a crack (crack case 1 to 4 in Figure 3.36a) on the anchor group capacity was investigated. Further, the effect of the scatter in the load-displacement curves was investigated.

3.4.3.1 FE model and simulations

The FE model was basically a rigid base plate with 4 springs (N_1, N_2, N_3, N_4, Figure 3.37a), whose characteristics were described by load-displacement curves. For the simulation, the FE algorithm just followed the input load-displacement curves derived from experimental tests on single anchors tested under different concrete conditions, i.e. uncracked, cracked and cyclically cracked (termed as seismic crack in *Periskic, G. (2009)*) concrete (Figure 3.37b).

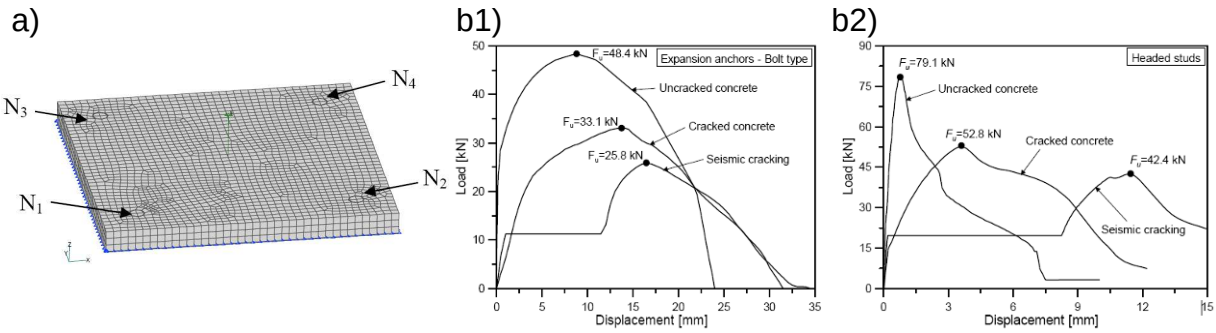

Figure 3.37: a) FE model; b) Input load-displacement curves for numerical investigations: b1) Headed bolt; b2) Expansion anchor (*Periskic, G. (2009)*)

First, a basic investigation was run for each anchor, each crack case, both configurations (rotational-unrestrained and rotational-restrained), and static and cycled cracks. In the second step, the influence of scatter in the load-displacement curves for static and cyclic cracks was investigated for the critical crack cases 3 and 4. The output data in the *Periskic, G. (2009)* report are mainly given by diagrams of the simulated load-displacement curve of the group. For this thesis, those data were re-evaluated and compiled to tables as given in Appendix B: Numerical Group Test.

The scatter in the load-displacement curves for anchors installed in static cracks was expressed by input load-displacement curves modified according to the maximum allowable CV as given in *ETAG 001 (2006)* and *ACI 355.2 (2007)* for suitability tests (refer to Section 2.4.1). Accordingly, the ultimate load was increased and decreased by ± 20 %, and the ratio of the secant stiffness ($k_s = N_u / s(N_u)$) for uncracked and cracked condition (k_{ucr} / k_{cr}) was increased and decreased by ± 40 % (Figure 3.38a). The output curves for a specific crack case were calculated by combining the load-displacement curve of the anchor located in uncracked concrete with all modified curves for the anchor located in the crack, where for all anchors in uncracked concrete the same curve was used. Figure 3.38b shows an example of output curves normalised with reference to the ultimate capacity of a single anchor tested in cracked concrete ($F_u / F_{u,all\ cracked}$, i.e. $N_{u,group} / (4 \cdot N_{u,cr})$). The results are compiled in the first column of Table B.1 in Appendix B.

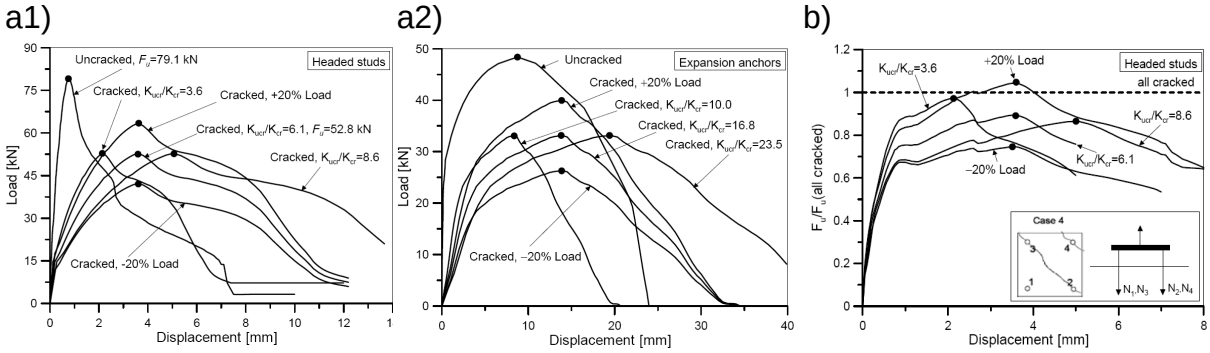

Figure 3.38: a) Modified input load-displacement curves (investigation of scatter for static cracks): a1) Headed stud; a2) Expansion anchor; b) Normalised output curve (*Periskic, G. (2009)*, example: Headed stud, crack case 4, rotational-restrained base plate, same input load-displacement curves for anchors in cracks).

For the scatter in the load-displacement curves for anchors located in cyclic cracks representing seismic conditions, several modified curves were generated such that the displacement at the maximum residual load capacity were arbitrarily varied (Figure 3.39a). For the anchors in the crack, either the same or different curves were used. Since all preceding simulation results identified the rotational-unrestrained configuration as the critical configuration case, the simulations under the third step

were carried out for the rotational-unrestrained configuration only. Figure 3.39b shows an example of output curves normalised with reference to the ultimate capacity of a single anchor tested in a cycled crack (F_u / $F_{u,all\ seismic\ crack}$, i.e. $N_{u,group}$ / (4 · $N_{u,cyc}$)). The results are compiled in the second and third column of Table B.1 in Appendix B.

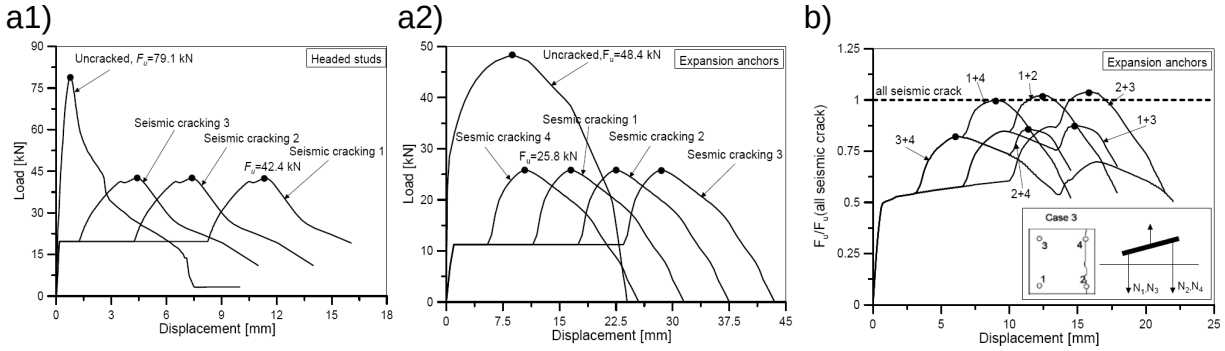

Figure 3.39: a) Modified input load-displacement curves (investigation of scatter for cyclic cracks): a1) Headed stud; a2) Expansion anchor; b) Normalised output curve (*Periskic, G. (2009)*example: Expansion anchor, crack case 3, rotational-unrestrained base plate, different input load-displacement curves for anchors in cracks).

The study concludes that for the applied scatter the reduction of the 4-anchor group capacity relative to 4-times the capacity of a single anchor is up to 15 % in case of static cracks and 20 % in case of cycled cracks. The main factors influencing the anchor group capacity were identified as: (i) Number of anchors in a crack with crack case 4 being the worst, crack case 3 the second but worst case. (ii) Scatter of the individual anchors located in cracked concrete.

3.4.3.2 Detailed assessment of assumptions and results

The detailed assessment of the procedure applied to the numerical tests showed that the implemented variation in the input load-displacement curves to simulate the scatter is rather large. For the investigations on the static cracks, the ratio of secant stiffness of the anchor in uncracked and cracked concrete (Figure 3.38a) exceeds the allowable ratio of 3 for post-installed anchors according to *ETAG 001 (2006)*. More importantly, for the investigations on the cyclic cracks, the absolute displacement and its spread (Figure 3.39a) were substantially larger than actually measured in experimental crack cycling tests. The load-displacement curve for anchors in cycled cracks is supposed not to exceed the monotonic envelope too much (refer to Section 3.2.3). Also, for test series reported in *Mahrenholtz, C. (2009)*, the ratio of maximum and minimum displacement after crack cycling was in the range of 2.0 to 2.5 for expansion anchors, and much less for undercut anchors having similar load-displacement behaviour to headed studs. While the extreme variation in

the input load-displacement curves was helpful to indicate trends and to identify the critical cases, it resulted in reductions of the group capacity which may be deemed as unrealistic and over-conservative. For this reason, the test results based on curve 1 for the headed studs (Figure 3.39a1) and on curve 3 for the expansion anchor (Figure 3.39a2) are omitted for further evaluation.

Further, crack case 4 (three out of 4 anchors are located in a crack, Figure 3.36a) was deemed as unlikely in *Periskic, G. (2009)* which can be substantiated by considering the average spacing of adjacent cracks. According to *Bergmeister, K. (1988)*, among the various approaches for the calculation of crack width and spacing, the formula after *Martin, H.; Schießl, P. et al. (1980)* yields the most realistic results. For a seismic crack width of 0.8 mm and a steel stress equal to the yield stress, the average spacing s_{ave} of adjacent cracks can be estimated as s_{ave} = 375 mm. Due to the diagonal crack pattern of crack case 4 (refer to Figure 3.36a), the corresponding anchor spacing is further increased to $s = \sqrt{2}\ s_{ave}$ = 530 mm. Conclusively, the general assumption made regarding the low probability of crack case 4 can be supported.

Disregarding crack case 4, the basic investigation for the static case always results in reduction factors $F_u / F_{u,all\ cracked} = N_{u,group} / (4 \cdot N_{u,cr})$ greater than 0.97 (Table B.1 in Appendix B), what is virtually 1.0. Because of the adverse effects of variations in the load-displacement curves, the investigation of the influence of scatter results necessarily in smaller factors. The critical, i.e. minimum factors are comprised in Table 3.6. The reduction factors for the cyclic crack are given as $F_u / F_{u,all\ cracked}$ and $F_u / F_{u,all\ seismic\ crack} = N_{u,group} / (4 \cdot N_{u,cyc})$, for which the results for crack case 4 were excluded. For crack case 3, the diagram in Figure 3.40 depicts the reduction factor $F_u / F_{u,all\ seismic\ crack}$ versus the ratio of minimum displacement (u_1) and maximum displacement (u_2) at ultimate load of the individual anchors located in cycled cracks u_2 / u_1. The data points derived from unrealistic load-displacement curves are crossed out. The reduction of the anchor group capacity decreases with increasing ratio u_2 / u_1 by trend. The ratio u_2 / u_1 is a degree for the scatter. Taking u_1 as the lower 5 % fractile and u_2 as the upper 95 % fractile (refer to Equation 2.1), a CV of 30 % corresponds to the allowable spread of maximum and minimum anchor displacement of $u_2 / u_1 = (1 + 1.645 \cdot 0.30) / (1 - 1.645 \cdot 0.30) \approx 3$, and a CV of 20 % to $u_2 / u_1 \approx 2$.

Table 3.6 Critical reduction factors derived from investigations on the influence of scatter extracted from *Periskic, G. (2009)*

Crack Type	Base Plate(2)		Headed Stud	Exp. Anchor
Static crack	RU	$F_u/F_{u,all\ cracked}$	0.88	0.84
	RR	$F_u/F_{u,all\ cracked}$	0.93	1.10
Cyclic crack(1)	RU	$F_u/F_{u,all\ cracked}$	0.77	0.68
		$F_u/F_{u,all\ seismic\ cr.}$	0.96	0.87

(1) Crack case 3 only, crack case 4 excluded
(2) Base plate configuration: RU: Rotational-unrestrained; RR: Rotational-restrained

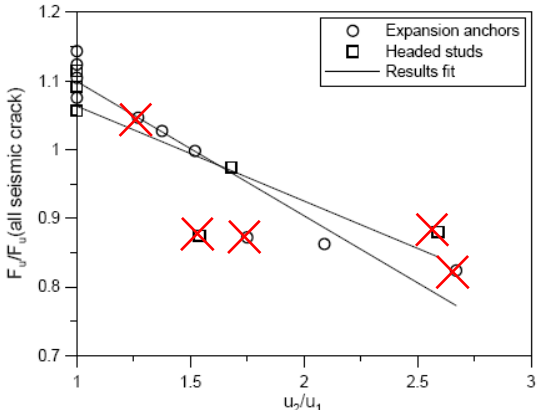

Figure 3.40: Reduction versus u_2/u_1 (after *Periskic, G. (2009)*(1))

(1) Crack case 3, data points derived from unrealistic load-displacement curves are crossed out

It is important to note that the reduction factors for static cracks given in Table 3.6 are primarily the result of the input load-displacement curves with decreased ultimate loads. Contrary, variations in the displacements at ultimate load capacities do not have a substantial negative influence on the reduction factor (refer also to Figure 3.38b and Table B.1 in Appendix B). In conclusion, determined reduction factors down to 0.80 are caused by the maximum allowable scatter of 20 % as stipulated for the ultimate load in *ETAG 001 (2006)* and *ACI 355.2 (2007)*. Also *Periskic, G. (2009)* concludes that the static group capacity primarily depends on the degree of strength reduction assigned to the individual anchors. In argumentum e contrario, the results confirmed for the case of static cracks that the group load capacity may be assumed to be at least n-times the ultimate load of an anchor installed in a static crack provided that the anchor meets the criteria given in the qualification guidelines for the CV and thus is qualified.

In contrast, the reduction factors for cyclic cracks have to be taken fully into account. In consequence, factors smaller than 1.00 mean a reduction in capacity if compared to a single anchor in a crack and need to be followed up when considering a group factor for seismic applications (Section 3.4.5).

In conclusion, the key take-aways of the numerical tests and their re-evaluation are:

- One main influencing factor on the group capacity is the number of anchors in a crack. Crack case 3, i.e. 2 parallel anchors are located in a crack, is deemed to be the critical case under realistic conditions. This approach is in line with earlier studies (refer to Section 3.4.1).
- The other important influencing factor on the group capacity is the scatter in the load-displacement curves of the individual anchors located in a crack. Any scatter in the load-displacement behaviour of the anchor installed in uncracked

concrete is not considered. This approach is in line with earlier studies (refer to Section 3.4.1).

- For the FE calculation based on static cracks, the scatter is expressed by variations in ultimate load and corresponding anchor displacement. Calculated reductions in group capacity, however, are not only caused by the group behaviour and have partly to be attributed to the reduction of the load capacity of the individual anchor. Taking this into account, the group behaviour in response to scatter did not result in a reduction of anchor group capacity smaller than 100 % of a single anchor installed in static crack, provided the allowable CV given in the qualification guidelines are not exceeded.
- For seismic applications, the FE calculation based on cyclic cracks is relevant. With reference to the results for the static case, tests with variation in (residual) load proved to be unnecessary also for the seismic case. Instead, the scatter in load-displacement curves for cyclic cracks is primarily expressed by the variation in the displacement during crack cycling. For realistic range of displacements, the group capacity was never smaller than 87 % of a single anchor installed in cyclic crack.

The numerical tests delivered sound results for the basic investigation and in general for the investigation of the influence of scatter on the group capacity. However, the FE model was not capable to capture the load redistribution effects of rotational-restrained anchor groups. However, this configuration allows the anchor located in uncracked concrete to support the anchors located in the crack for which the displacement is substantially reduced if compared to a single anchor in a crack and therefore was further investigated by experimentally tests.

3.4.4 Experimental tests on anchor groups

To better understand the load bearing behaviour of anchor groups, and to close gaps in knowledge of earlier investigations (Section 3.4.1 and 3.4.3), experimental tests on anchor groups were carried out. As shown before, crack cycling under permanent group load is the key parameter having the strongest impact on group performance. Therefore, the anchors within a group were either installed in uncracked concrete or in a crack which was cycled later. The primary research objectives were the load redistribution and anchor displacement during cycling, and the potential reduction in the residual load capacity. In particular, the tests simulating rotationally rigid base plates required a sophisticated test setup including several hydraulic actuators which are operated by a capable servo control system.

3.4.4.1 Parametrical background

For 4-anchor groups, earlier investigations identified the crack case with 3 anchors located in a crack (crack case 4 in Figure 3.36a) as being the most critical one. However, this crack case is deemed to be irrelevant in practice for reasons pointed out in Section 3.4.3.2. Therefore, the experimental tests focused on the critical crack cases with 2 anchors in a crack. Provided that the stiffness of all anchors located in uncracked concrete and all anchors located in a crack, respectively, is the same, the number of relevant base plate configurations can be substantially reduced (Figure 3.41): Due to the point symmetry of the crack case with 2 diagonally opposed anchors in a crack (crack case 2 in Figure 3.36a), there is no rotation of the base plate at all and the rotational-unrestrained base plate behaves like a rotational-restrained base plate. In consequence, the 4-anchor group of both configurations can be replaced by a rotational-restrained 2-anchor group. For the crack case with 2 parallelly located anchors in a crack, (crack case 3 in Figure 3.36a), the axis of symmetry runs perpendicular to the crack across the base plate and the 4-anchor group can be replaced by the corresponding 2-anchor group for rotational-unrestrained and rotational-restrained base plates.

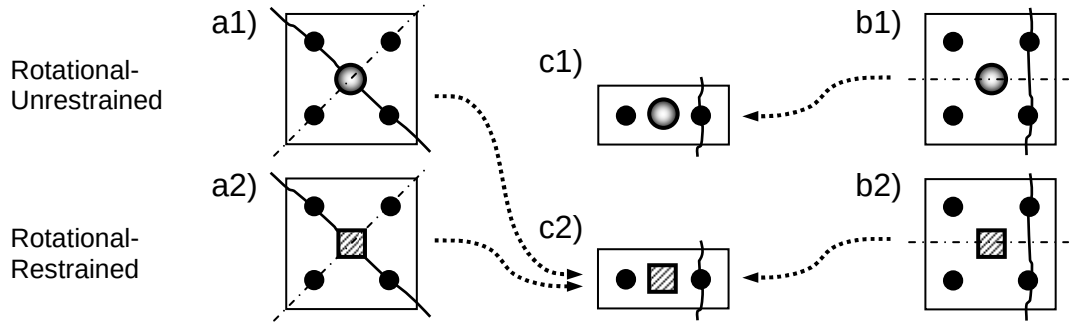

Figure 3.41: Symmetry effect on anchor group configuration: a) 4-anchor group, diagonal; b) 4-anchor group, parallel; c) 2-anchor group

In conclusion, the behaviour of the 2- and 4-anchor group, rotational-unrestrained and rotational-restrained, can be investigated by just two base plate configurations:

- 2-anchor group rotational-unrestrained
- 2-anchor group rotational-restrained

It is interesting to note, that the exemplary calculations of the ultimate group load in *Lotze, D. (1986)*, based on discrete load-displacement curves and theoretical considerations on rotation-unrestrained and rotation-restrained anchor groups, allows the same conclusion. However, some experimental tests were carried out on rotational-unrestrained 4-anchor group (Figure 3.41b1) to compare the results with those of the rotational-unrestrained 2-anchor group (Figure 3.41c1).

3.4.4.2 Test setup and testing procedure

Based on the above considerations, a test programme on 2- and 4-anchor groups and correlated reference tests was conducted. In order to cover the complete range of behavioural response of post-installed anchors to load and crack conditions (refer also to Figure 3.29), 3 types of anchors were tested. One bolt-type expansion anchor (EAb1', M12: see Figure 1.5e, soft behaviour), one undercut anchor (UC1, M10: see Figure 1.5b, stiff behaviour but with displacement capacity), and one screw anchor (SA1, ∅16: see Figure 1.5c, stiff behaviour). The crack width of static cracks and the maximum crack width of cyclic cracks was w = 0.8 mm. The outline of the test programme is also apparent in Table 3.7.

All tests were carried out in normal weight concrete C20/25 with a mean tested concrete cube compressive strength between $f_{cc,150}$ = 28.5 and 32.9 MPa. The slabs were produced according to the state of the art after *DIN 1045 (2001)* and *DIN 1048 (1991)*. This extended version of the special concrete slab designed for crack cycling tests, which is introduced in Section 3.6.2.2 in more detail, was large enough to accommodate the anchor group and the test setup (Figure 3.42).

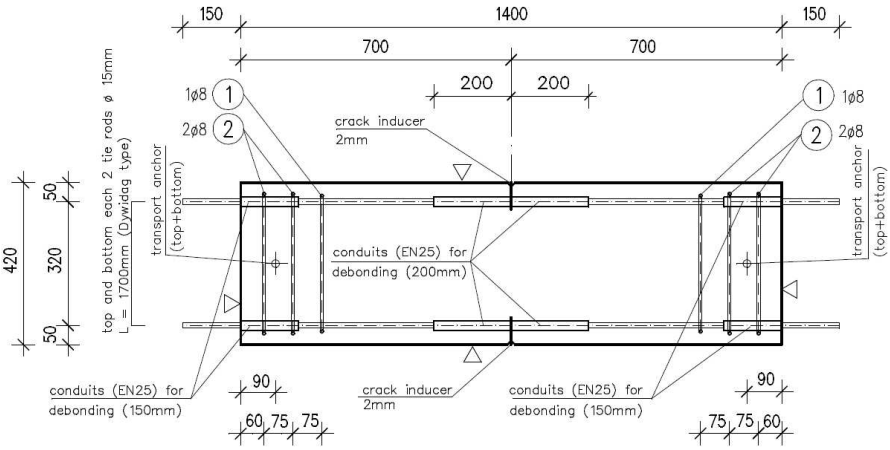

Figure 3.42 Drawing of special concrete slab

To avoid any influence of the specimen design and dimensions, reference tests on single anchors were also carried out in the same type of concrete specimen. The slab was mounted horizontally in between an abutment and an actuator. Four high strength tie rods running longitudinally through the member were connected to the abutment and 630 kN actuator. The application of an adequate force formed a crack which was initialised at the centre of the member by means of a sheet metal crack inducer. After initial crack formation, the anchors were installed unmodified according to the installation manual of the manufacturer. Where required, full installation torque was released after the elapse of 10 min to 50 % to model the relaxation which occurs over time in reality. The loading device for the anchor load was placed overhead the

anchors and supported such that an unconfined concrete cone breakout could occur. A set of displacement transducers was installed to measure the displacements of the individual anchors; and another set to measure and control the crack width. Further details are given in *Mahrenholtz, P. (2010b)*.

This test setup allows loading the specimen in compression or in tension. By doing so, the crack is closed or opened. To distinguish the actuator load generated to open and close the cracks better from the actuator load on the anchor, the actuator load on the concrete specimen is addressed as force from this point on.

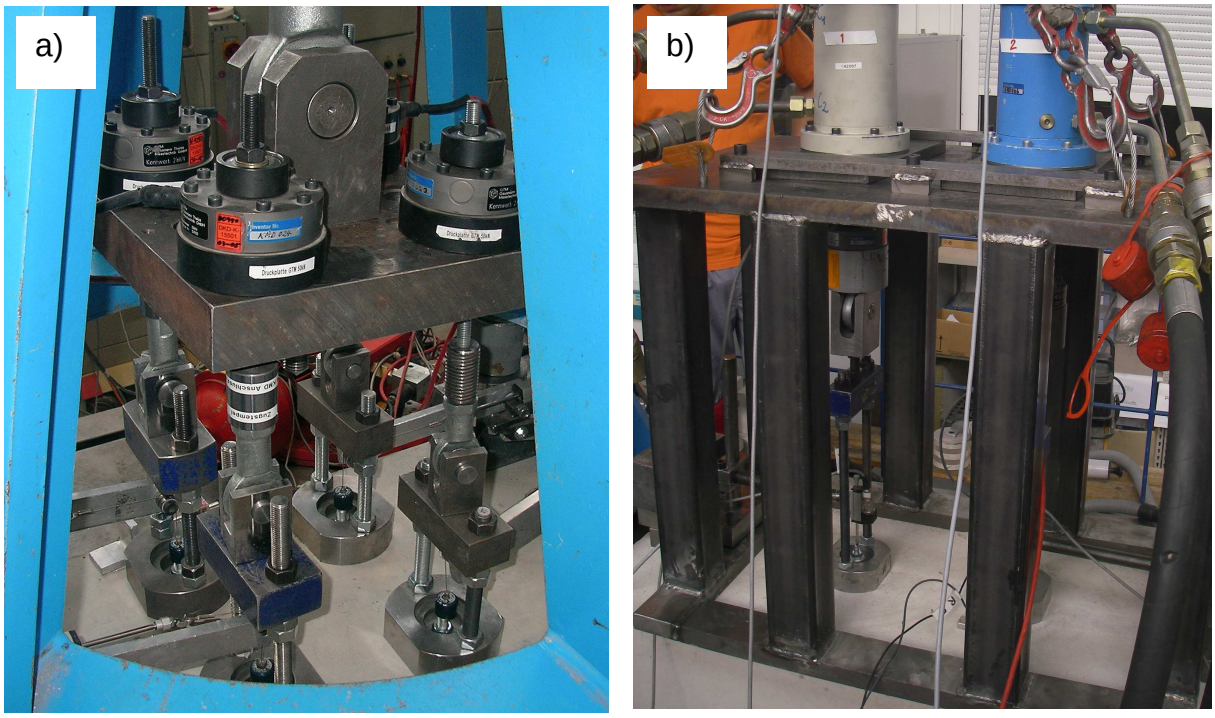

Figure 3.43 Close-up of test setup for a) Rotational-unrestrained configuration (4-anchor group); b) Rotational-restrained configuration (2-anchor group)

For the tests on rotational-unrestrained anchor groups, a 250 kN servo controlled actuator was used as loading device. Every loading rod of the 2- and 4-anchor group was hinged to ensure fully unrestrained conditions (Figure 3.43a). The test setup is, in principle, identical to the one used for crack cycling tests (Section 3.6.2.2). Originally it was planned to also run the tests on rotational-restrained groups by means of a single actuator for anchor loading. However, exploratory tests showed that this is not feasible: A base plate directly connected to the actuator simply does not provide sufficient stiffness and, moreover, caused potential damages of the actuator due to load eccentricities. Therefore, a multiple actuator loading and servo control setup was developed. It enabled the separate loading of two anchors according to defined boundary conditions. For the simulation of a rotation-restrained base plate, two 50 kN servo controlled actuators loaded the anchors separately (Figure 3.43b) and were controlled such that the magnitude of the individual anchor

displacements was identical at all times while the individual anchor loads varied (Figure 3.44a). These group tests were, to the author's knowledge, the first of its kind. The required control accuracy was within the range less than 1 kN and 10 µm. Further details are provided in *Mahrenholtz, P. (2011d)*.

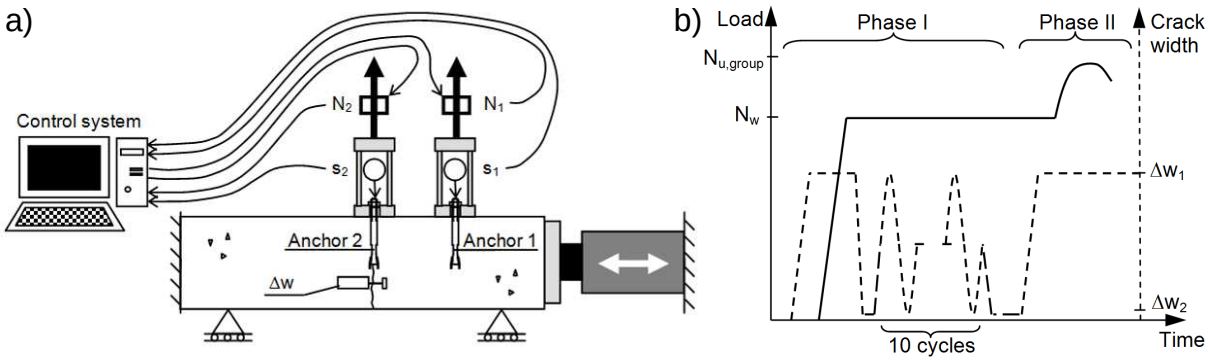

Figure 3.44 a) Schematic of multi-axes control system used for rotational-restrained tests; b) Loading pattern of of test Phases I and II

10 crack cycles between $w_1 = 0.8$ mm and $w_2 \approx 0.0$ mm were specified, with w_2 defined as the crack width at a compression force equivalent to 10 % of the concrete compression strength. The load level N_w during crack cycling was chosen as n times 40 % of the mean reference load capacity of a single anchor determined by monotonic pullout test in a static crack ($N_{u,m,cr}$) with n equal to the number of anchors in the group. This percentage approximates the load the anchorage would be loaded in reality (Section 3.6.2.1). This yields a permanent load level of $N_w = n \cdot 0.4 \cdot N_{u,m,cr}$. The test conditions are based on the test procedure developed as representative seismic crack cycling protocol in *Hoehler, M. (2006)*. Reference is also made to Section 3.6.1. Figure 3.44b shows the two test phases. Phase I begins with the expanding of the concrete member until the crack is opened by $w_1 = 0.8$ mm. Then the anchor group is initially loaded up to the defined load level N_w. This level is kept constant during crack cycling. In the following Phase II, the anchor group is loaded displacement controlled to failure to determine the residual group load capacity $N_{u,group}$. The tension loads applied to the anchors, the anchor displacements, and the crack width were measured and recorded at a sampling rate of 10 Hz.

3.4.4.3 Experimental results and discussion

For reference, tests on single anchors were carried out. Table 3.7 shows the test conditions and key test results. The ultimate load capacity in cracked concrete was used to calculate the load level by which the anchor is permanently loaded during crack cycling of the cycled crack test with $N_w = 0.4\ N_{u,m,cr}$.

Table 3.7 Test conditions and key test results of reference tests

Anchor Type; Emb. Depth	w, mm	Cr. T.(1)	N_w, kN	No. of Tests	PFM	$s_{cyc,m}$, mm	CV, %	$\frac{s_{cyc,max}}{s_{cyc,min}}$	$N_{u,m}$, kN	CV, %
UC1; 90 mm	0.0	uncr	-	1	S	-	-	-	48.9	-
	0.8	cr	-	3	S	-	-	-	45.5	7.5
	0.0/0.8	cyc	18.2	3	S	6.0	7.4	1.1	48.5	0.7
60 mm	0.0	uncr	-	3	C	-	-	-	44.9	11.2
	0.8	cr	-	3	C	-	-	-	33.2	3.6
	0.0/0.8	cyc	13.3	3	C	4.2	28.8	1.8	30.7	21.6
SA1; 105 mm	0.0	uncr	-	2	Po/C	-	-	-	43.3	8.3
	0.8	cr	-	3	Po/C	-	-	-	18.9	18.7
	0.0/0.8	cyc	7.6	3	Po/C	5.1(2)	-	-(2)	12.7(2)	-
EAb1'; 70 mm	0.0	uncr	-	4	C	-	-	-	33.4	4.8
	0.8	cr	-	4	Pt	-	-	-	23.9	17.0
	0.0/0.8	cyc	9.6	4	Pt	22.8	12.0	1.3	10.8	30.1

(1) Crack type: uncr = uncracked concrete; cr = cracked; cyc = cycled crack
(2) 2 out of 3 test repeats did not complete all crack cycles

For the bolt-type expansion anchor installed in uncracked concrete, concrete failure occurred, and pull-through failure occurred if installed in a crack. Accordingly, the anchor displacements in particular after crack cycling (s_{cyc}) are large, and the residual ultimate load capacity $N_{u,m}$ is reduced. In general, the residual capacity in case of pull-through failure mode is not sensitive to the actual embedment depth, however, at the end of crack cycling the anchor resistance is nearly gone because of excessive anchor displacement, whereas for the undercut anchor s_{cyc} is relatively small, yet showing considerable displacement capacities at $N_{u,m}$. The anchor was installed at two different embedment depths to gain either concrete or steel failure for all crack conditions. Its behaviour is very stable in case of steel failure. In case of concrete failure, the anchor shows decreasing load capacities if tested in a crack or cycled crack. In contrast, the screw anchor shows a very brittle behaviour which is very sensitive towards cracking. The anchor fails in a mixed pull-out/concrete failure. The displacement capacity is small and the majority of the test repeats did not complete all crack cycles.

The group test programme comprised 30 tests in total. The basic test conditions and key test results of those tests relevant for the scope of this thesis can be taken from Table 3.8. The group displacement after crack cycling $s_{cyc,group}$ and the ultimate group capacity $N_{u,m,group}$ are given as the average of all test repeats.

Table 3.8 Test conditions and key test results of group tests

Anchor Type; Emb. Depth	n	Base Plate(1)	N_w, kN	No. of Tests	PFM	$s_{cyc,group}$ mm	CV, %	$N_{u,m,group}$ kN	CV, %
UC1; 90 mm	2	RR	36.4	3	S	0.9	10.0	91.6	3.7
60 mm	2	RR	26.6	3	C	1.2	9.3	58.5	6.1
SA1; 105 mm	2	RR	15.2	3	Po/C	0.1	100.0	61.9	8.2
EAb1'; 70 mm	2	RR	19.2	3	Pt	0.9	10.5	51.7	1.9
	2	RU	19.2	4	Pt	6.0	10.5	45.8	11.2
	4	RU	38.4	4	Pt	5.12	11.3	77.9	1.4

(1) Base plate configuration: RR = Rotational-restrained; RU = Rotational-unrestrained

The following discussion is limited to the key findings. For a detailed evaluation of the in many aspects interesting group test results, reference is made to *Mahrenholtz, P. (2010b)*. The report includes more test series which were found to be irrelevant for the scope of this thesis. Diagrams of actually measured load-displacement curves can be found in Section 3.4.6.

The fundamental performance of anchor groups depends on the load-displacement beviour of the individual anchors. The overall behaviour of anchor groups follows two different principles for rotational-unrestrained and rotational-restrained base plate configurations (Figure 3.45).

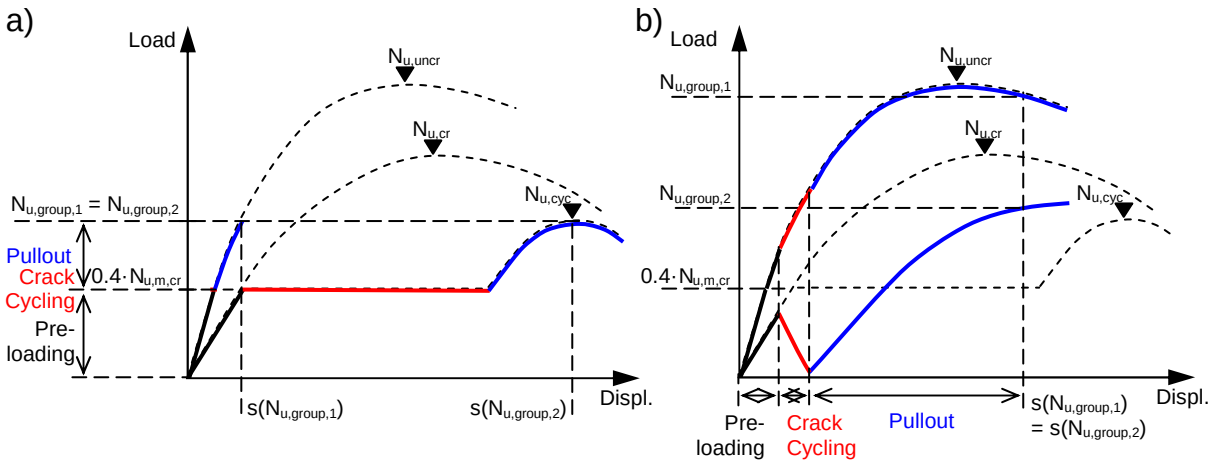

Figure 3.45 Schematic load-displacement curves of anchors; dashed lines indicate behaviour of single anchors (→ ultimate anchor loads $N_{u,uncr}$, $N_{u,cr}$, and $N_{u,cyc}$); solid lines indicate behaviour of individual anchors within a 2-anchor group (→ individual anchor loads $N_{u,group,1}$ and $N_{u,group,2}$ at ultimate group load): a) Rotational-unrestrained group; b) Rotational-restrained group

In case of rotation-unrestrained anchor groups, the load-displacement curves of the anchors follow ideally the corresponding load-displacement curves of single anchors (Figure 3.45a): The load-displacement curve of the anchor located in uncracked

concrete follows the monotonic mean curve of the reference tests in uncracked concrete. The load-displacement curve of the anchor located in the crack basically follows the monotonic mean curve of the reference tests in a cycled crack.

In case of rotation-restrained anchor groups, the load-displacement curve of the anchor located in the crack is significantly altered due to the restraint of this statically indeterminate system (Figure 3.45b): During crack cycling, the slip of the anchor located in the crack is hindered. In consequence, this anchor looses part of its stiffness and a redistribution of the load from the anchor installed in the cycled crack to the anchor installed in uncracked concrete takes place. The load-displacement curve of the anchor located in uncracked concrete follows the monotonic mean curve of the reference tests in uncracked concrete; the load-displacement curve of the anchor located in the crack describes a decrease that is of same size but opposite to the increase in the load-displacement curve of the anchor located in uncracked concrete.

In the subsequent pullout test, the anchor located in the crack gains load again and its load-displacement curve approaches the mean curve of the reference tests in cracked concrete. Depending on the reduction in embedment depth experienced during crack cycling, the residual load capacity may be smaller than the ultimate capacity of a single anchor in a crack, but is always larger than the ultimate capacity of a single anchor in a cycled crack.

This load-displacement behaviour is reflected in the test results. The diagram in Figure 3.46a depicts the absolute displacement after crack cycling for the tested single anchors and anchor groups. Figure 3.46b depicts the residual group load capacity normalised with reference to the single anchor capacity in a crack and in a cycled crack.

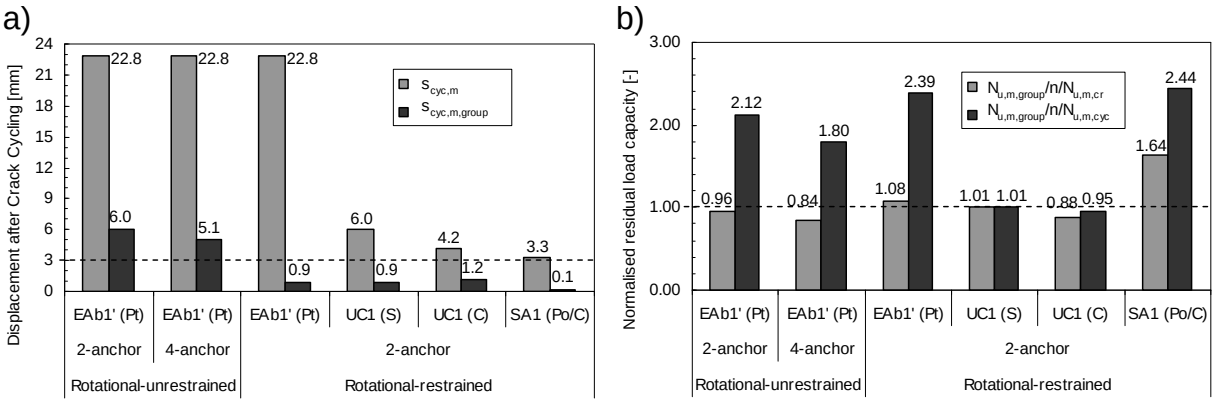

Figure 3.46 a) Absolute anchor displacement after crack cycling for reference tests on single anchors ($s_{cyc,m}$) and group tests at centre of base plate ($s_{cyc,m,group}$); b) Residual load capacity normalised with reference to the capacity of a single anchor in a crack ($N_{u,group}/n/N_{u,m,cr}$) and in a cycled crack ($N_{u,group}/n/N_{u,m,cyc}$)

For rotational-unrestrained anchor groups, the crack cycling results in a rotation of the base plate. In case of a 2-anchor group, the system is statically determinate and both anchors behave as an independent single anchor. The residual group corresponds to the average of the anchor capacity in uncracked concrete and of that in the cycled crack, and in consequence is always larger than the capacity of an anchor installed in a cycled crack. In case of a 4-anchor group, the scatter in the load-displacement behaviour of the anchor installed in uncracked concrete and of the anchor installed in a crack, respectively, results in a rotation of the base plate around the secondary axis. Due to the statical indeterminacy of the 4-anchor group, the variable displacements of the individual anchors introduce a constraint within the group. Accordingly, the displacements are reduced if compared to the 2-anchor group. When the anchor located in the crack fails, the secondary failure of the anchor in uncracked concrete is inevitable. In conclusion, the load-displacement behaviour for rotational-unrestrained groups is governed by the anchor located in the cycled crack.

For rotational-restrained anchor groups, the base plate does not rotate; instead, load redistribution takes place during crack cycling. Since the displacement deriving from load cycling on an anchor installed in uncracked concrete is small for a small number of load cycles, the overall displacement of the anchor group is substantially reduced in comparison to a single anchor installed in a cycled crack. The residual group load capacity depends mainly on the displacement capacity of the anchor installed in uncracked concrete, which is loaded in the first place due to its larger stiffness. In conclusion, the load-displacement behaviour for rotational-restrained groups is governed by the anchor located in uncracked concrete.

3.4.5 Anchor group factor

Current anchor design guidelines do not provide any so-called group factor. However, there is a seismic strength reduction factor given in Clause D.3.3.4.4 of *ACI 318 (2011)* Appendix D and Clause 8.4.2 of *CEN/TS 1992-4 (2009)* as $\alpha_{eq} = 0.75$ for all failure mode other than steel. This factor is often referred to as ‘seismic factor’ and is intended to provide additional conservatism for seismic design cases. To the best of the author’s knowledge, it has only limited theoretical or empirical basis. It was introduced before substantial seismic research on anchors was performed to account for:

- Adverse load redistribution in anchor groups due to cyclic actions including the effects of large scatter in the anchor displacement. However, this is inconsistent with applying the factor to single anchors.
- Wide cracks present during earthquakes, reducing the anchor capacity.

- Other potential effects during a seismic event like high cycling frequencies and loading rates.

For the introduction of a group factor and corresponding references to the qualification guidelines it is meaningful to split the general seismic factor into separate factors accounting for the individual influencing factors. In the following, above listed aspects are discussed in reverse order by wrapping up the findings of the previous sections to draw conclusions for seismic reduction factors.

3.4.5.1 Seismic factor for other potential effects

The aspect of potentially adverse high loading rate effects was dealt with in detail in Section 3.2 which concluded that high loading rates do not yield a reduction in the load capacity of post-installed anchors.

The effect of high load and crack cycling frequencies on the performance of undercut anchors was subject of a research programme which outcome is presented in *Mahrenholtz, C.; Eligehausen, R. et al. (2010)*. It was found that the capacity tend to increase for increasing high cycling frequencies what may be assigned to the beneficial effects of short term actions. Though other anchor types than undercut anchors were not tested, it may be reasonably argued that earthquake relevant cycling frequencies in general have no significant negative effect on the load capacity of post installed anchors.

Since there are no other unknown effects which could be thought of, the aspect of potential effects other than wide cracks and group effects can be omitted.

3.4.5.2 Seismic crack width factor

This aspect accounts for the current qualification guideline provision of testing anchors in 0.5 mm cracks maximum (*ACI 355.2 (2007)*), what is substantially less than the wide cracks associated with the structural response to earthquakes (Section 3.1.5). Future seismic anchor qualification will account for wide cracks by conducting simulated seismic tests in 0.8 mm cracks (*Proposal for ETAG 001 Seismic Amendment (2012)*). If the determined seismic load capacity is not meeting the required percentage of the static load capacity, the seismic design strength will be reduced accordingly and the failure will be deemed as pullout (Section 4.4.5). Therefore, only the pullout capacity is measured by the qualification test. For concrete cone failure, a reduction factor is required to allow for strength reduction in 0.5 mm cracks when determing the concrete capacity according to the CC Method which is valid for 0.3 mm cracks.

A comprehensive study on the effect of crack widths on anchor behaviour can be found in *Eligehausen, R.; Balogh, T. (1995)*. For the extensive investigation presented therein, a large data base of anchor tests carried out in the late 1980s and early 1990s was analysed for which the ultimate load was plotted over the crack width separately for undercut and expansion anchors as well as headed bolts. In *Eligehausen, R.; Mallée, R. et al. (2006)* the diagrams were reproduced and supplemented by diagrams of further studies presented in *Mészároš, J. (2002)* for bonded anchors and in *Küenzlen, J. (2005)* for screw anchors. As a seismic crack width factor, the ratio of the ultimate load capacity for 0.5 and 0.3 mm cracks can be defined. Depending on the anchor type, $N_{u,m}(w = 0.5\ mm) / N_{u,m}(w = 0.3\ mm)$ can be determined to 0.95 for undercut anchors, 0.85 for screw anchors, 0.92 for expansion anchors, and 0.80 for bonded anchors.

The tentatively proposed seismic crack width reduction factor for wide cracks of 0.8 to be applied in addition to the design factor for cracked concrete (refer to Section 3.4.2.6), would multiplicate to a total reduction of $0.7 \cdot 0.8 \approx 0.55$ compared to the load capacity in uncracked concrete.

It is noted, however, that the load capacities of monotonic tests on anchors installed in 0.5 and 0.8 mm cracks carried out within the scope of this thesis (Section 3.5 and 3.6), consistently yielded smaller reduction factors than the diagrams in *Eligehausen, R.; Mallée, R. et al. (2006)* suggest for these crack widths. This is in particular true for screw anchors which small thread undercut is sensitive towards wide cracks. Also in *Watkins, D.; Hutchinson, T. (2011)* tests are reported which result in lower reduction factors. Further research is required.

3.4.5.3 Seismic group factor

First it is pointed out that a group factor is in principle valid irrespective of the anchor spacing because during the crack cycling (Phase I) the spacing does not have any effect, and when it comes to the residual load capacity (Phase II), the effect of spacing in case of overlapping concrete cones is considered by the CC Method. Spacings smaller than $3\ h_{ef}$ result in a uniform reduction of the full concrete capacity for all anchors within a regular group, and also the design load and thus N_w is reduced accordingly. In conclusion, all load parameters are scaled down and the results of the investigations on the group behaviour generally holds also for groups with spacings smaller than $3\ h_{ef}$.

According to the current guidelines, for anchor groups under static conditions, all anchors are assumed to be located in a crack unless it is demonstrated that the concrete remains uncracked (Section 2.4). For anchor qualification according to *ETAG 001 (2006)* adverse group effects are excluded by limiting the allowable

scatter in the load-displacement curves within the test series. For the static case, numerical investigations presented in Section 3.4.3 in particular on the effect of scatter in monotonic load-displacement curves confirmed the validity of the provisions.

Effects due to seismic actions have not been considered in any qualification guideline so far. *ETAG 001 (2006)* does not consider any seismic applications, and *ACI 355.2 (2007)* does not recognise scatter limitation with respect to group behaviour. For this reason, numerical tests based on seismic relevant load-displacement curves were carried out to verify whether the current design concept according to *CEN/TS 1992-4 (2009)* and *ACI 318 (2011)* based on the provisions given in the qualification guidelines are sufficiently conservative. While the tests delivered meaningful results for rotational-unrestrained anchor groups, they failed to simulate rotational-restrained groups because the simplifying approach disregarded any load redistribution effects (Section 3.4.3).

The experimental tests carried out thereupon to overcome the lack of understanding had therefore a strong emphasis on the rotational-restrained configuration (Section 3.4.4). The test results for various types of post-installed anchors for rotational-unrestrained and rotational-restrained base plate configurations have shown that the reduction of the group capacity was for the anchors tested never smaller than 0.84 (Figure 3.46b) if compared to the capacity of a single anchor. The experimental tests have also shown that anchor group behaviour for rotational-unrestrained configurations is governed by the anchor located in the (cycled) crack, and for rotational-restrained configurations by the anchor located in uncracked concrete. Since the variation in the load-displacement curves is only significant for anchors installed in a crack (refer to Section 3.4.1 and 3.4.3.2), the influence of the scatter is irrelevant for rotational-restrained anchor groups. For the rotational-unrestrained anchor groups, in turn, the results gained by the numerical tests are valuable. Taking the effect of scatter in account, the minimum reduction factor can be taken as 0.87 provided that the CV of the displacement after crack cycling does not exceed 30 %.

Conclusively, the numerical and experimental test results of the investigations carried out so far suggest, for anchor groups loaded in tension, a preliminary seismic group factor of 0.85 to be applied on the seismic design strength given in the technical approval (refer also to Section 3.4.2.6). For concrete failure, the seismic crack width factor (Section 3.4.5.2) needs to be applied in addition. Further research is required for anchor groups loaded in shear. Preliminary studies presented in *Mahrenholtz, P.; Eligehausen, R. (2012)* suggests that depending on the dimension of the annular gap (refer also to Section 3.3.5) the factor strength reduction factor is in the range between 0.6 and 0.8.

3.4.6 Group model allowing for load redistribution effects

Since the group capacity depends on the specific load-displacement behaviour of the anchor in uncracked concrete and in cracks (Figure 3.45), a parametrical study including more anchor products could verify the general applicability of the proposed group factor. In particular, the possible overloading of the anchor located in uncracked concrete, which in the worst case have to bear the total group load alone, needs to be investigated. Experimental group tests are very laborious and costly. Moreover, due to practical limitations only 2-anchor groups can be experimentally tested in the rotation-restrained configuration. For these reasons, numerical tests are desirable. However, the effect of the load redistribution on the load-displacement curves needs to be taken into account. In the following section a group model is presented which is capable to reflect the redistribution of anchor loads and reduction of anchor displacements due to rotational-restrained configuration.

Figure 3.47a depicts the individual anchor load portions of the group load during Phase I of the experimental tests on 2-anchor groups for various anchor types. The load-displacement curve of the anchor located in uncracked concrete approaches the total group load, while the load of the anchor located in the crack decreases towards zero. Figure 3.47b depicts for the same anchors the cumulative absolute group displacement.

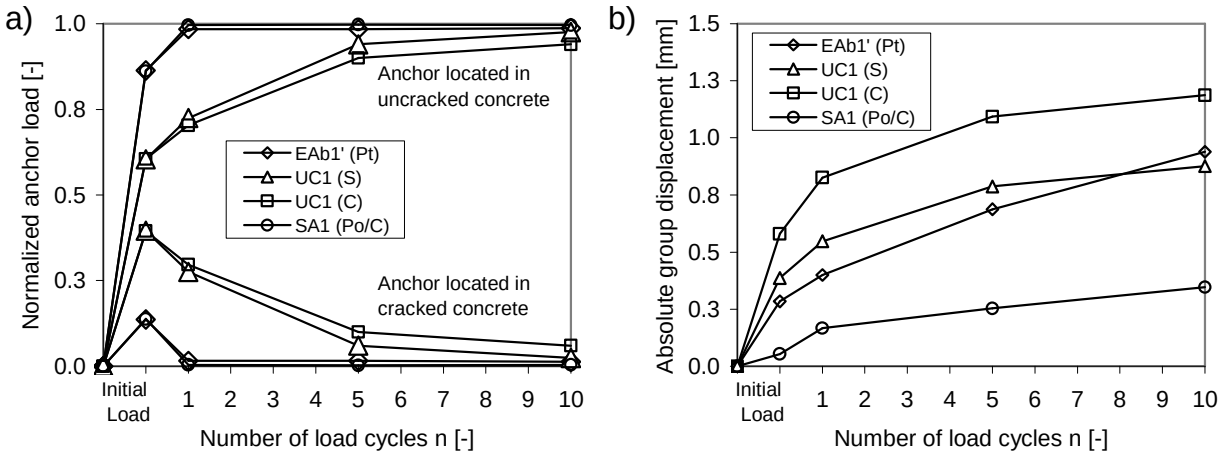

Figure 3.47 a) Individual anchor loads normalised with reference to the group load; b) Cumulated absolute group displacement for various ancor types

The rate of redistribution depends on the anchor type. The larger the difference in stiffness of the individual anchors is, the larger are the effects of load redistribution. In the following, an analytical model describing the load redistribution behaviour is presented and verified.

3.4.6.1 Analytical approach

The diagrams in Figure 3.48 show the measured load-displacement curves for two exemplary group tests on expansion and undercut anchors. It is clearly visible that the crack cycling induces load cycling in both anchors. Every time the crack is compressed, the anchor in the crack (Anchor 2) regains its stiffness and picks up load. The anchor in uncracked concrete (Anchor 1) is unloaded by the same degree. When the crack opens again, the anchor in the crack loses its stiffness and dismisses part of the load that has to be taken up by the anchor in uncracked concrete. This behaviour recurs 10 times. Ultimately, the anchor is pulled out in the residual capacity test.

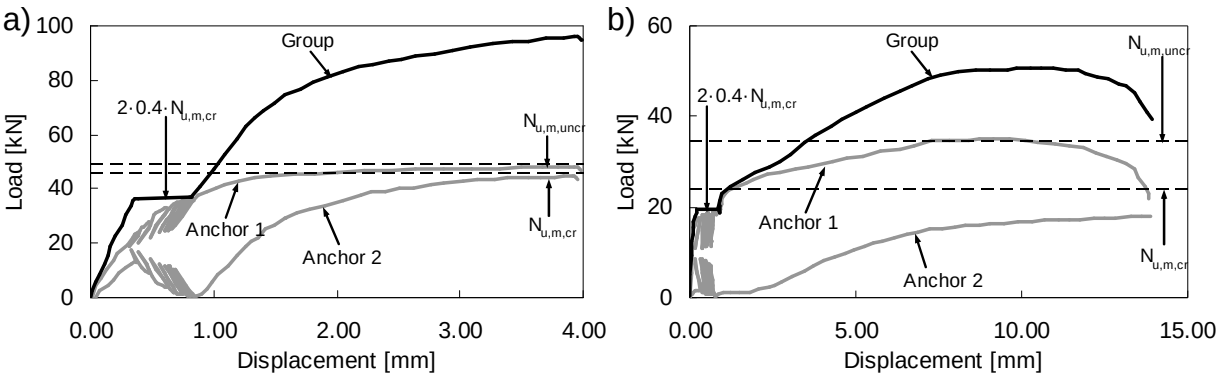

Figure 3.48 Example for load-displacement curve for a) Expansion anchor; b) Undercut anchor

The goal was to find a model which is able to simulate this behaviour. The simulation of the load-displacement curves in Phase II is relatively straightforward: The anchor in uncracked concrete follows the monotonic curve of a single anchor in uncracked concrete. The anchor in the crack follows the shifted monotonic curve of a single anchor in cracked concrete. The incorporation of the redistribution effects in an analytical model is quite challenging since the stiffness of both anchors interacts and alters in the course of crack cycling. Thus no static load-displacement curve can be assigned to the anchors.

The model presented in the following is based on the analytical model developed in *Lotze, D. (1993)* to calculate maximum anchor loads and load amplitudes of groups under continuously repeated load. A brief discussion of the method can be found in *Mahrenholtz, P.; Eligehausen, R. (2010)*. This model was adapted and expanded to the conditions as they are present for anchor groups located in cyclically cracked concrete areas. For this purpose, the effects of crack cycling were incorporated and the extended model was then implemented in a spreadsheet calculation which allowed the generation of load-displacement curves.

The load redistribution and group displacement is calculated for each crack cycling incrementally. The load increment $\Delta N_{gr,n}$ is given as:

$$\Delta N_{gr,n} = \frac{\Delta s_{cr,diff,n}}{1/k_{uncr} + 1/k_{cr}} \qquad \text{Equation 3.14}$$

Where $\Delta s_{cr,diff,n}$ Displacement per crack cycle of a single anchor installed in a crack;

k_{uncr} Stiffness of a single anchor installed in uncracked concrete when it is loaded;

k_{cr} Stiffness of a single anchor installed in cracked concrete when it is unloaded.

For this approach it is assumed that the free displacement $\Delta s_{cr,diff,n}$ of a single anchor is fully incompatible in a statically indeterminate system and leads to the load redistribution (Figure 3.49a).

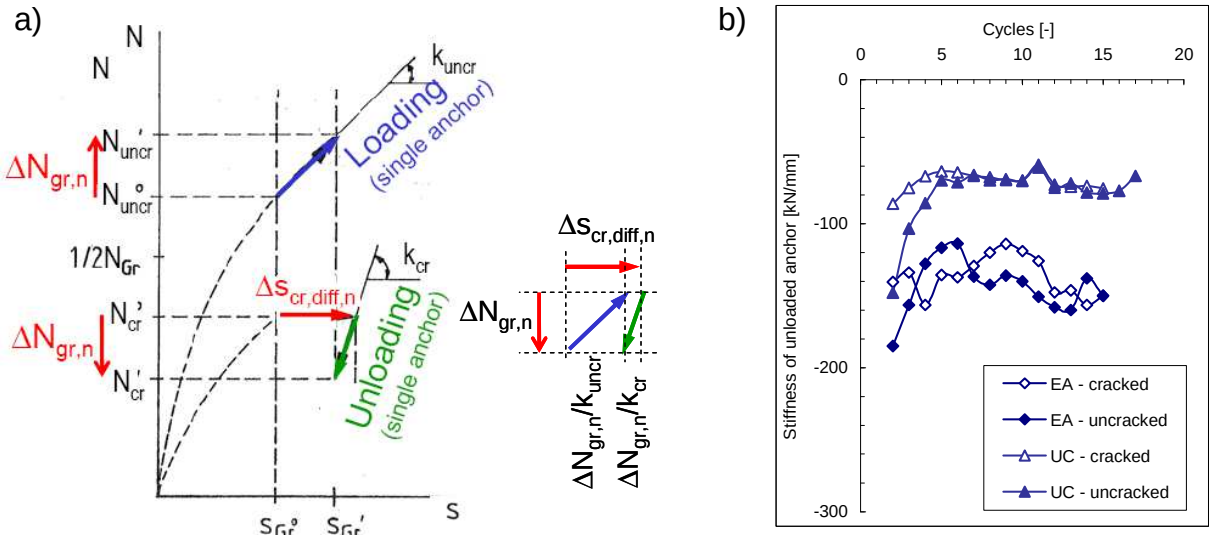

Figure 3.49 a) Distribution of load increment after *Lotze, D. (1993)* and resulting anchor displacement per cycle n_i; b) Stiffness of unloaded anchors over load cycles

In addition, the anchor group experiences displacements because of the load cycling effect and the total displacement increment $\Delta s_{gr,n}$ can be given as:

$$\Delta s_{gr,n} = \Delta N_{gr,n} \cdot k_{uncr} + \Delta s_{uncr,diff,n} \qquad \text{Equation 3.15}$$

Where $\Delta s_{uncr,diff,n}$ Displacement per load cycle of a single anchor installed in uncracked concrete.

For the simulation, the parameters need to be determined by tests on single anchors installed in uncracked concrete ($\Delta s_{uncr,diff,n}$ and k_{uncr}) or in a crack ($\Delta s_{cr,diff,n}$ and k_{cr}). For the examples presented herein, $\Delta s_{cr,diff,n}$ was extracted from the cyclic crack and

k_{uncr} from the monotonic reference tests listed in Table 3.7. It is useful to express the monotonic load-displacement curve in uncracked concrete, which is the governing parameter for the simulated group load-displacement curves, as a polynomial function of load (f(N)). The tangential stiffness equals then its first derivative ($k_{uncr} = f'(N)$). For the determination of $\Delta s_{uncr,diff,n}$ and k_{cr}, another test series was carried out. It is sufficiently accurate to assume the stiffness of the unloaded anchor to be constant over cycles and load level (Figure 3.49b).

3.4.6.2 Simulation of load-displacement curves

Based on the displacement values gained by single anchor tests, the crack cycling induced load redistribution and displacement of an anchor group can be calculated incrementally per cycle as $\Delta N_{gr,n}$ and $\Delta s_{gr,n}$ according to Equation 3.14 and Equation 3.15. The capability of this model to simulate various load-displacement behaviours of anchor groups was verified for both the expansion and undercut anchor types which cover the range of stiffness ratio typical for post-installed anchors. For the expansion anchor, the diagram in Figure 3.50a depicts the load-displacement curves as derived from the simulation. The computation is shown in Figure B.1 in Appendix B. Opposed to the recorded test data of an exemplary test (Figure 3.50b, which is a windowed cutout of Figure 3.48a), the load-displacement curves show a good correlation in both, redistribution of the load and displacement.

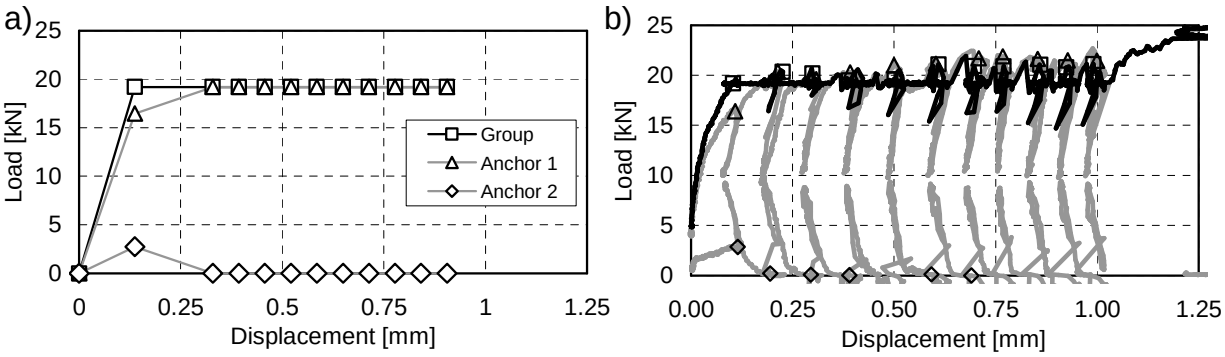

Figure 3.50 Load re-distribution during crack cycling for expansion anchor:
a) Simulation; b) Experimental test data

The same applies to the undercut anchor, which simulated load-displacement curves are depicted in the diagram in Figure 3.51a. The load-displacement curves, which computation is shown in Figure B.2 in Appendix B, match well with the recorded test data (Figure 3.51b, which is a windowed cutout of Figure 3.48b).

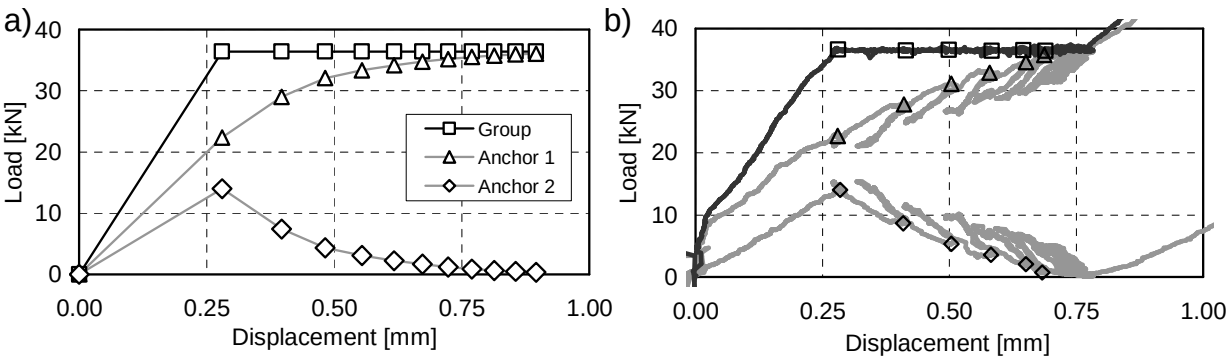

Figure 3.51 Load re-distribution during crack cycling for undercut anchor: a) Simulation; b) Experimental test data

3.4.7 Conclusions

Anchors located in cracks lose a part of their inherent stiffness and, in comparison to anchors in uncracked concrete, slip more when being loaded. For anchor groups, the load is distributed among the anchors according to their individual stiffness. In case of a seismic event, the cracks open and close several times. This leads to increasing anchor displacements and a redistribution of the load within the group. The supporting character of a shared base plate has a beneficial effect on the overall displacement behaviour and residual capacity. The degree of load redistribution and resulting limitation of anchor displacement primarily depends on the actual base plate configuration and crack pattern.

For the experimental tests carried out within the scope of the research on anchor groups under seismic application, the test setup was explicitly designed to mimic ideally rotational-unrestrained and rotational-restrained base plate configurations. Various anchor types were tested under defined boundary conditions. The residual capacity was in all cases larger than n-times the capacity of a single anchor in a cycled crack, however, showed a reduction of up to 15 % if compared to a single anchor in a crack. It was shown that the load redistribution within the anchor group during earthquakes is possible irrespective of the failure mode. The stronger anchors support the weaker anchors (social behaviour). The resulting beneficial effect of reduced overall group displacement in case of rotation-restrained anchor groups, however, leads on the other hand to unused strength of the weaker anchor.

Based on numerical test results, which have been re-evaluated for the purpose of this thesis, the influence of the seismically caused scatter on the residual load capacity was investigated. Depending on the variation in the anchor displacement after crack cycling and for a CV of 30 %, the group capacity may be as low as 85 % of the corresponding capacity of a single anchor in a cycled crack. To take this adverse group effect into account, it is proposed to apply a seismic group factor of 0.85 to the seismic design strength given in the technical approval. To take the effect

of 0.8 mm wide cracks on the concrete capacity into account, the design strength should be further reduced by the tentatively proposed reduction strength factor for wide cracks of 0.8. In return, the seismic strength reduction factor of 0.75 as given in the *ACI 318 (2011)* Clause D.3.3.4.4 and *CEN/TS 1992-4 (2009)*, which is currently accounting for wide cracks and group effects (*Mallée, R.; Fuchs, W. et al. (2012)*) for all concrete related failures, should be dropped. However, these factors are preliminary and further research is desirable since only a limited number of anchor products were tested so far. The limitation of the allowable scatter in the anchor displacement after crack cycling to a maximum CV of 30 % needs to be incorporated in the qualification guidelines.

The deepened understanding in particular of the load-displacement behaviour of rotational-restrained anchor groups enabled the development of an analytical model. Based on load-displacement curves gained in reference tests on single anchors, this model simulates the group effects on load redistribution and displacement behaviour. It helps avoiding costly group tests and allows parametrical studies on the general validity of the proposed reduction factors. The general applicability of the model was shown for 2-anchor groups. It is capable to qualitatively and quantitatively replicate measured group load-displacement curves. An extension to rotational-unrestrained and rotational-restrained 4-anchor groups based on the approaches presented in *Lotze, D. (1993)* is possible. The principle investigational approach for this task is described in *Mahrenholtz, P. (2010c)*.

3.5 Cyclic Load

3.5.1 State of knowledge

Anchor behaviour for load cycling was studied within the scope of the dissertation *Hoehler, M. (2006)*. Various load protocols were used, for which exemplary load-displacement curves are given in Figure 3.23 and Figure 3.52. A detailed literature review was also performed and therefore only the most crucial aspects are highlighted in the following.

For anchors loaded in tension, a high resistance to cycling can generally be assumed for post-installed anchors (*Eibl, J.; Keintzel, E. (1989b)*; *Hoehler, M. (2006)* and others). This is also true for tension loads for which a large number of load cycles at load levels below peak (Figure 3.52a) or considerable number of load cycles near ultimate load (Figure 3.23b) can be performed without failure, irrespectively of the failure mode (*Hoehler, M. (2006)*). Further, tension cycling well below the peak monotonic capacity does not significantly influence the ultimate load and corresponding displacement upon subsequent monotonic loading for residual capacity testing.

In *Hoehler, M. (2006)*, two kinds of increasing load protocols were used: Tension load protocol with 30 cycles (increasing load regime which last 10 cycles were chosen with respect to the study on the number of deformation cycles at near ultimate anchor capacity, see Section 3.6.1), or the protocol as proposed in *SEAOSC (1997)* was taken. The comparison of these two test series (Figure 3.52a and Figure 3.23a) with respect to anchor displacement and residual capacity displyed that the influence of the load cycling pattern is very small. This indicates that tension load cycling has generally little effect on the anchor performance provided that the load level or number of cycles is not too high.

Tension load cycling tests reported in *Weigler, H.; Lieberum, K. H. (1984)* indicated that the sequence of the load steps is not significant. In conclusion, decreasing load protocol as for the simulated seismic tests according to ACI 355 (Figure 3.52b) yield the same displacement after cycling and residual load capacity as a test protocol of same amplitudes but in a reverse, i.e. increasing load pattern.

The investigation on the effect of load cycling frequency also presented in *Hoehler, M. (2006)* concluded for expansion and screw anchors that increasing the frequency from 0.5 to 5 Hz did not negatively affect the residual anchor strength, but led to a reduction in the anchor displacement during cycling. This is basically in line with the results reported for undercut anchors in *Mahrenholtz, C.; Eligehausen, R. et al. (2010)*. If anchor displacement during cycling is considered as negative, which is generally the case, one can conclude for all anchor types and failure modes that low cycling frequencies are on the safe side.

The effect of crack width on the capacity is for cyclic tests in tension principally the same as for monotonic tests (*Eligehausen, R.; Mallée, R. et al. (2006)*). In general, the tests have shown that the backbone curve of the cyclic load-displacement path follows the monotonic mean curve of a corresponding reference test series.

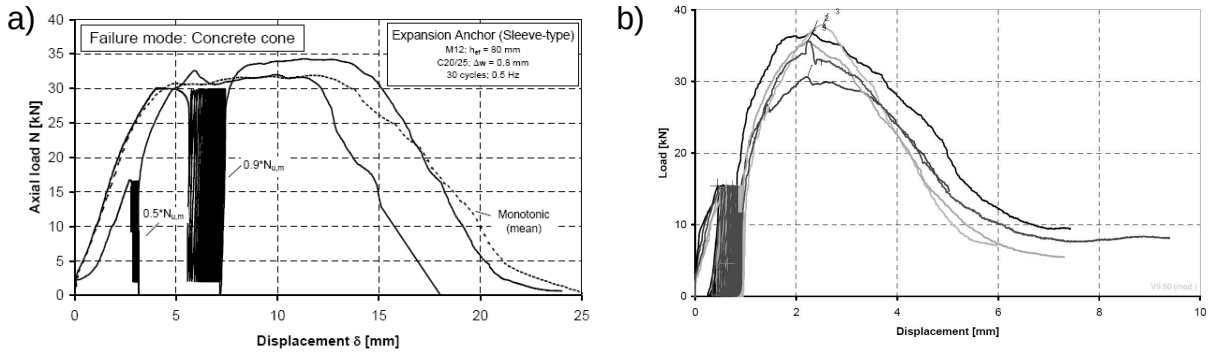

Figure 3.52: Examples for cyclic tension load tests: a) 30 cycles at 50 % and 90 % $N_{u,m,ref}$ (*Hoehler, M. (2006)*); b) ACI 355.2 simulated seismic test with 140 cycles (*Mahrenholtz, P. (2011b)*)

For shear load cycling, however, the picture is not that uniform. In *Vintzeleou, E.; Eligehausen, R. (1981)* displacement controlled tests with target displacement equal 75 % of the displacement corresponding to the ultimate monotonic load were performed. It was found that the cyclic load-displacement curve generally followed the monotonic load-displacement curve and that shear cycling had no significant influence on the shear capacity and corresponding displacement (Figure 3.53a). The same conclusion was drawn in *Kim, S.-Y.; Yu, C.-S. et al. (2004)* for load controlled tests with target loads equal to 12.5 % of the mean ultimate capacity. In contrast, *Klingner, R.; Mendonca, J. et al. (1982)* carried out shear load cycling tests with stepwise increasing load protocols and concluded that generally the cyclic loading path did not follow the monotonic mean envelope, the cyclic load capacity is smaller than the monotonic load capacity, and the deformation corresponding to the ultimate shear load increases with increasing number of cycles.

The different results are caused by the different demand in respect to load level and cycle number the anchor is subjected to. Cyclic shear performance of anchors is governed by its sensitivity to low cycle fatigue (LCF). If LCF occurs during shear load cycling, the strength may be substantially reduced and should be assumed to be less than 40 % of the monotonic shear strength according to *Eligehausen, R.; Mallée, R. et al. (2006)*. *Guillet, T. (2011)* concludes that the shear load level has to be limited to 30 to 50 % of the static mean reference capacity to reach a seismically relevant number of cycles. In contrast to alternating shear cycling, however, pulsating shear cycling is not as demanding for anchors and achieved strengths are substantially higher (*Usami, S.; Abe, U. et al. (1981)*).

Other than for cyclic tension load, the sequence of the shear load steps has a significant effect on the result because the anchor system is highly non-linear: Due to the irreversible deformation in the concrete (compaction, spalling off), which is accumulating during load cycling, the load and thus stress amplitude does not directly relate to the anchor displacement. This behaviour is called the “memory effect“ in *Rieder, A. (2009)*. In consequence, the load pattern has a direct impact on the anchor displacement behaviour during cycling which, in turn, affects the LCF strength and the residual capacity. This is in contrast to purely steel related problems (e.g. *Malhotra, P.; Senseny, P. et al. (2003)*) based on general cumulative damage models (*Miner, M. (1945)*).

The decreasing load protocol as for the simulated seismic tests according to ACI 355 (Figure 3.53b) certainly results in performance characteristics other than a test protocol of same amplitudes but in a reverse, i.e. increasing load pattern would yield. In fact, long-time experience has shown that anchors not failing during the first 10 large amplitude cycles will not experience LCF during the rest of the cycles.

Anchors away from edges loaded in shear generally experience steel failure. Therefore one may assume that for increased shear load cycling frequencies, the residual load capacities may increase and the corresponding anchor displacement may decrease. However, a statistically significant change in the load capacity or a reduction of the displacement could not be inferred in *Mahrenholtz, C.; Eligehausen, R. et al. (2010)* for the frequency range 0.1 to 5 Hz.

The effect of cracking on the capacity is for cyclic tests principally the same as for monotonic tests. Capacity and displacement wise, shear cycling parallel to the crack, and not perpendicular to the crack, is crucial (e.g. *Kim, S.-Y.; Yu, C.-S. et al. (2004)*, *Eligehausen, R.; Mallée, R. et al. (2006)*, *Guillet, T. (2011)*).

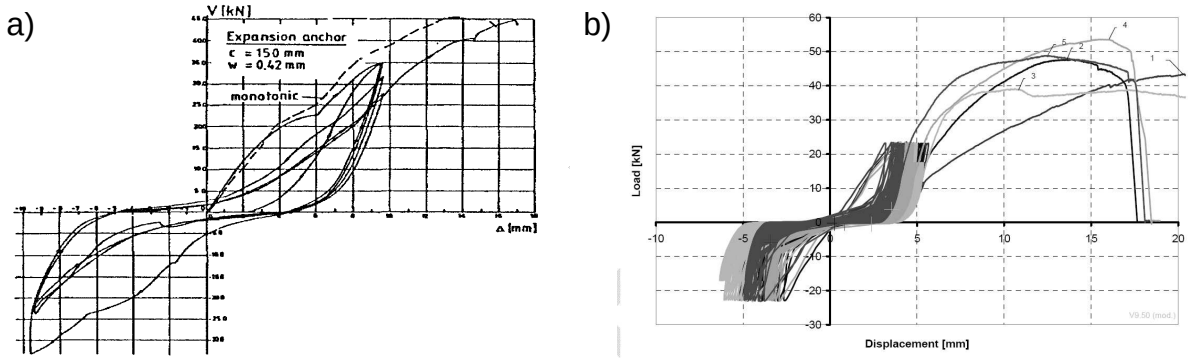

Figure 3.53: Examples for cyclic shear load tests: a) Load cycling at 70 % s($V_{u,m,ref}$) (*Vintzeleou, E.; Eligehausen, R. (1981)*); b) ACI 355.2 simulated seismic test (*Mahrenholtz, P. (2011b)*)

For both, tension and shear load cycling, the additional value of the small amplitude load cycles required by the ACI 355 simulated seismic tests is only limited. It is difficult to relate them to the monotonic load-displacement curve and the low amplitude cycles are to a great extent hidden by the large amplitude cycles (Figure 3.52b and Figure 3.53b). Further, as pointed out in *Silva, J. (2001)*, stepwise increasing load pattern is preferable for anchor qualification because the stiffness response of the anchor can be determined throughout the entire loading range.

3.5.2 Load cycling tests

The chapter on cyclic load tests in *Hoehler, M. (2006)* concludes with the recommendation of a stepwise increasing load protocol for seismic anchor qualification. The suggested protocol of 35 cycles comes close to that provided in *SEAOSC (1997)* for which some tension load cycling tests have been carried out. Shear load cycling tests with stepwise increasing load protocol, however, was never carried out so far. Further research resulted in an extensive load cycling test programme reported in detail in *Mahrenholtz, P. (2009)* which is discussed in the following. The primary objective of the tests was to investigate the performance of

different anchor types installed in a static crack and subjected to either cyclic tensile or cyclic shear loads. It was aimed to generate cyclic load-displacement curves for all key failure modes and to demonstrate the efficiency of the stepwise increasing load cycling protocol.

3.5.2.1 Load protocol, target anchor load and permanent crack width

The technical background of the load protocol used for the load cycling tests discussed in the following is beyond the scope of this thesis. However, detailed non-linear numerical simulations of representative reinforced structures carried out at the UCSD 2007/2008 (*Wood, R.; Hutchinson, T. et al. (2010)*) resulted in methodological protocols which are more scientifically substantiated than any other protocols used for cyclic tests on anchors previously. After subjecting a suite of 7 building of variables heights to 21 earthquakes, the floor level accelerations were used as input for four elastic single-degree-of-freedom oscillators of 5 to 20 Hz representing the response of attached non-structural components. Using rainflow counting on the oscillator responses and re-arranging with respect to their amplitudes, averaging, and normalization, a stepwise increasing load cycling protocol of 71 cycles resulted (Figure 3.54a). The cycles of the lowest amplitude, however, were assumed to have negligible impact on the test result and were removed. Figure 3.54b shows the symmetric and reverse load cycles for shear load cycling tests with 36 cycles. For tension load cycling tests, only positive excursions of the protocol were used.

a)

Step	N
0.1	35
0.20	11
0.30	7
0.40	4
0.50	4
0.60	3
0.70	2
0.80	2
0.90	2
1.00	1
SUM	71

- Cycle Count for 10% Cutoff of Max: 71
- Impose a Cutoff of 20% of Max
  - Cycle count reduces to 36

b)

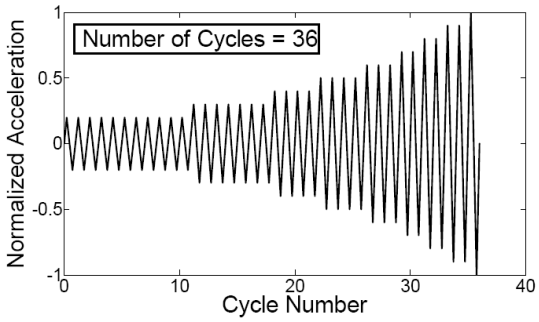

Figure 3.54: a) Normalised load cycling protocol proposed in *Wood, R.; Hutchinson, T. et al. (2010)*; b) Load cycling protocol after cutoff of first load step

For clarity it is noted here that this load cycling protocol slightly differs from the protocol used for the seismic amendment of qualification guidelines presented in Chapter 4. The reasons are discussed in Section 4.1.

The target load is taken as the 5 % fractile of the mean ultimate load of monotonic tests in a static crack. In conclusion, an anchor loaded cyclically is expected to reach

a residual load capacity which is equal to the ultimate load of at least 95 % of that of the anchors tested monotonically. Otherwise, the cyclic, i.e. seismic capacity has to be reduced. Based on a broad experience, the coefficient of variation (CV) can be estimated as 15 % for anchors loaded in tension and failing in concrete. This is also the maximum acceptable CV according to ETAG 001. For anchors loaded in shear, steel is the predominant failure mode and the CV was estimated as ~ 6 %. Equation 2.2 yields 5 % fractiles and thus target loads corresponding to 75 % of the mean ultimate tensile capacity for tension load cycling tests ($N_{max} = 0.75\ N_{u,m,cr}$) and 90 % for shear load cycling tests ($V_{max} = 0.90\ V_{u,m,cr}$). The mean ultimate capacities were derived from monotonic reference tests in cracked concrete.

The crack width during load cycling and during the monotonic pullout test was constant. For tension tests, all anchors were installed in w = 0.5 mm cracks which is the relevant crack width for simulated seismic tension and shear tests according to ACI 355. Some anchors were additionally tested in w = 0.8 mm cracks representing adverse seismic conditions (refer to Section 3.1.5). Since it is well known that the actual crack width has only a small impact on the behaviour of the anchor when loaded in shear, only one crack width was specified for shear tests. All anchors were installed in w = 0.8 mm cracks and loaded parallel to the crack.

3.5.2.2 Test setup and testing procedure

The test programme comprised mechanical and adhesive anchors of various manufacturers and make. In total, 123 tests were carried out on 7 different anchor types: One undercut anchor (UC1 (M10): Figure 3.1b), one screw anchor (SA1 (∅16): Figure 3.1c, tested only in shear), two sleeve-type expansion anchors (EAs1 (M12), EAs2 (5/6”): Figure 3.1d), one bolt-type expansion anchor (EAb1 (1/2”): Figure 3.1e), and two bonded anchors (BA1, BA2 (both with threaded rod M12): Figure 3.1f), were tested. All tests were performed on single anchors with large anchor spacing and edge distances. The outline of the test programme is also shown in Table 3.9.

As anchorage material, normal weight concrete C20/25 with a mean tested concrete cube compressive strength between $f_{cc,150} = 28.7$ and 31.8 MPa were used. The slabs were produced according to the state of the art after *DIN 1045 (2001)* and *DIN 1048 (1991)* and were of same type as those used for pullout tests with various loading rate. The cracks were opened to the designated 0.5 or 0.8 mm. For further details on slab design and crack formation refer to Section 3.2.2.3.

The test setup used for tension tests is in principle identical to that introduced in Section 3.2.2.3 but with a 250 kN servo-hydraulic actuator which was supported by two aluminium beams (Figure 3.55a). Mechanical anchors were tested under

unconfined conditions with a clear distance between the beams of 4 h_{ef}. Adhesive anchors were tested under confined condition to ensure bond failure. For this configuration, a smooth sheet of PTFE and a steel plate with a clearance hole equal to ~ 2.0 d_0 were placed around the anchor on which the beams rested (Figure 3.55b).

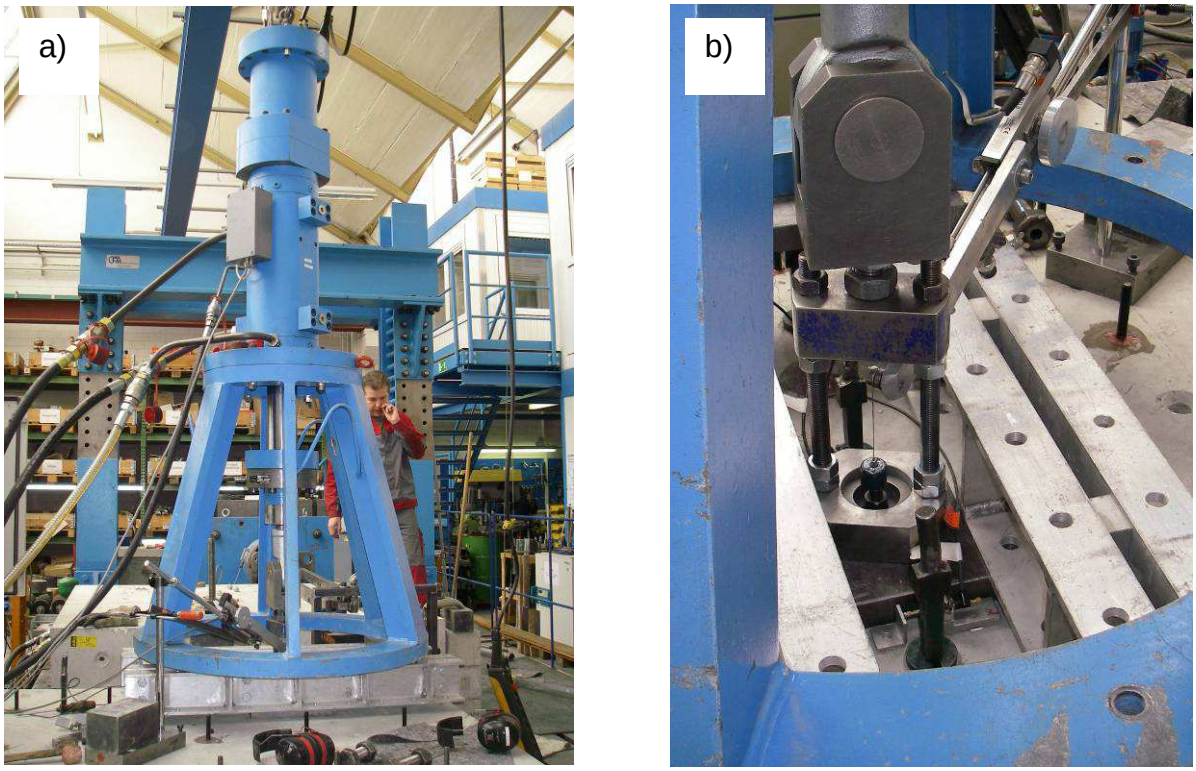

Figure 3.55 a) Actuator resting on wedge-split concrete slab; b) Close-up of installed anchor, confining steel plate, and anchor displacement and crack width transducers

For the tests in shear, a 630 kN servo-hydraulic actuator was used. The concrete slab was braced against the strong floor and a frontal supports acted as horizontal bearing. The anchor was loaded by a special shear load device which was mechanically held down to avoid uplifting of the anchor during testing. In the shear load device, bushings made of hardened steel of appropriate size were fixed, providing a clearance gap of 2 mm. In order to minimize friction, a smooth sheet of PTFE was placed between the concrete member and the shear load device.

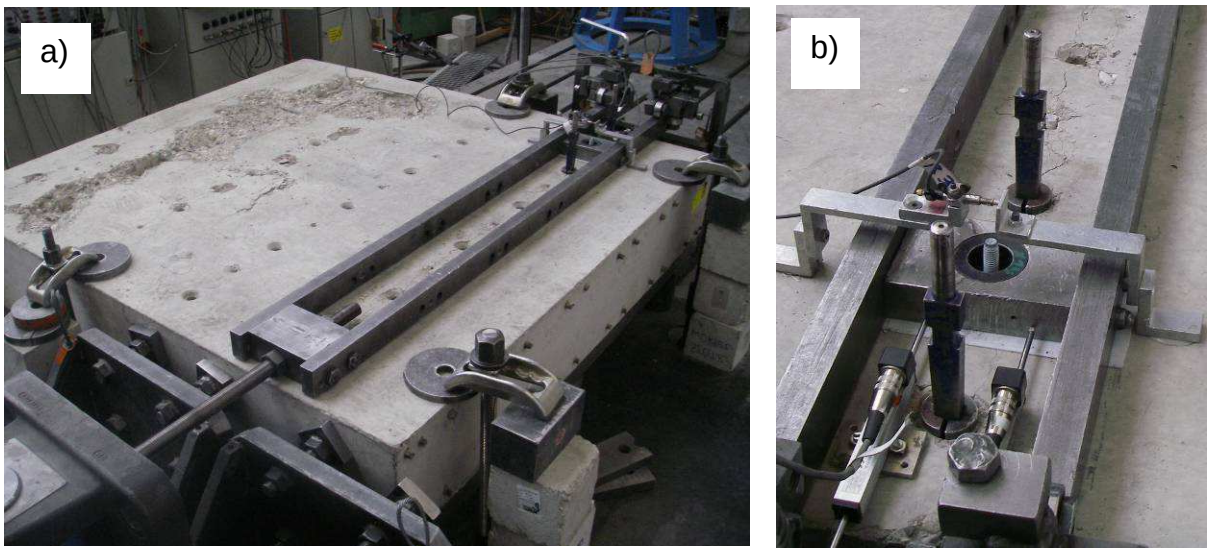

Figure 3.56 a) Loading device resting on wedge-split concrete slab and mechanically held down by a guiding frame (left) and the actuator (right); b) Close-up of installed anchor, fixture with brushing, and anchor displacement and crack width transducers

The cyclic tests were run load controlled at quasi-static frequencies of about 0.1 to 0.2 Hz. The servo control program consisted of sinusoidal load cycles. Figure 3.57 shows the load protocols normalised with reference to the monotonic mean capacities. For tension load cycling, the anchor was not completely unloaded to avoid conflicts of the servo control due to slackness between fixture and concrete surface caused by the displaced anchor. 0.1 kN was taken as the lower load level instead. For the same reason, the shear load cycles were split into two half sinus cycles with interconnecting displacement controlled ramps (Section 4.2.3). Here, the slackness of the clearance hole inevitably causes difficulties in the servo control.

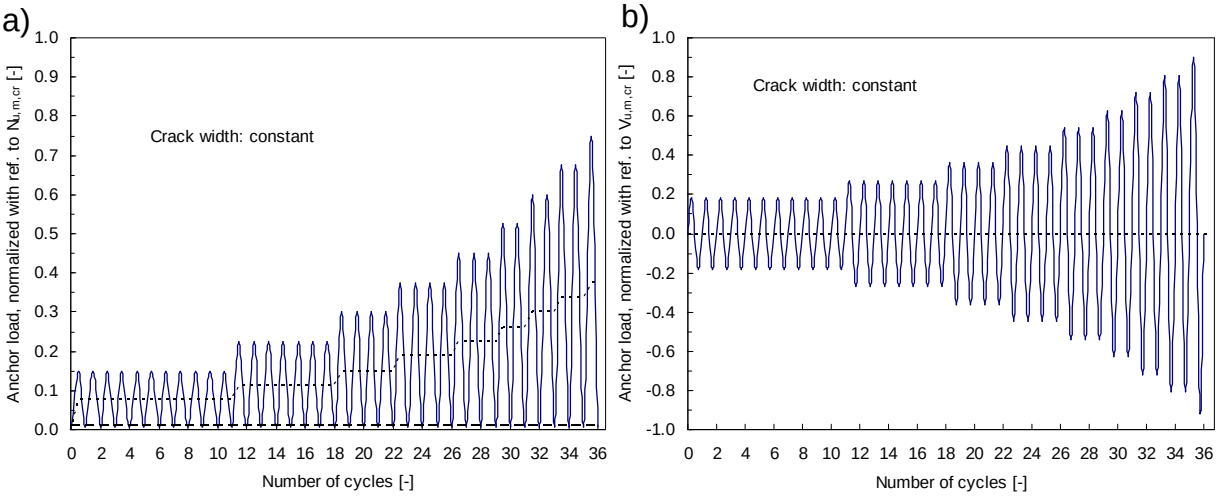

Figure 3.57 Load protocol: a) Tension load cycling tests; b) Shear load cycling tests

After completion of the load cycles, the anchors were unloaded and then loaded displacement controlled to failure to determine the residual capacity. The ultimate load was reached as for monotonic tests within 1 to 3 min. The anchor load, the anchor displacement, and the crack width were measured and recorded at a sampling rate of 5 Hz. Further details are given in *Mahrenholtz, P. (2009)*.

3.5.2.3 Experimental results and discussion

First the tension load tests are discussed. The plots and pictures in Figure 3.58 to Figure 3.61 show the load-displacement and failure behaviour of the tested anchors. For reasons of confidentiality, the exemplary pictures of the anchors are partly blackened. UC1, EAs1, EAb1, and BA1 were taken as representative for their type. The general behaviour of EAs2 and BA2 was similar to that of EAs1 and BA1, respectively. The plots are only shown for the tests in 0.5 mm cracks, the leading crack width in the test programme, to enable best comparability among the anchor types. Plots of tests in 0.8 mm cracks are not shown, however, the overall load cycling behaviour was consistent for both crack widths.

The load-displacement curves of the tension cycling tests on the undercut anchor UC1 followed the corresponding monotonic mean curve (Figure 3.58a). All anchors failed in concrete (Figure 3.58b).

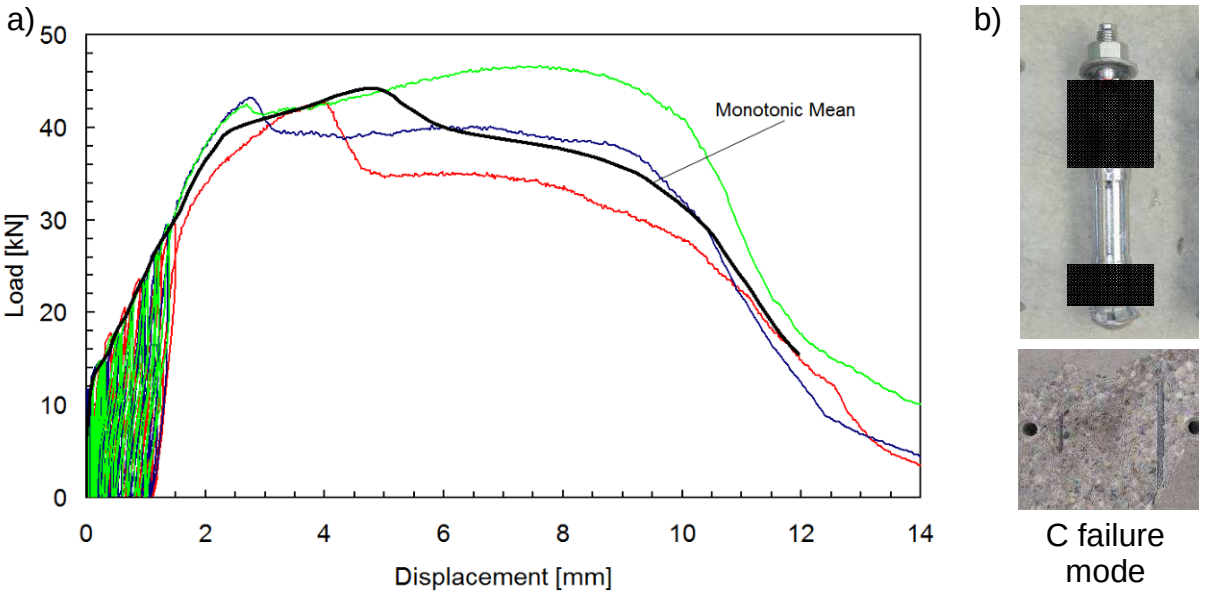

Figure 3.58 UC1 anchor tested in tension (0.5 mm): a) Cyclic load-displacement curves and monotonic mean curve; b) Picture of anchor and concrete after failure

Also the load-displacement curves of the tension cycling tests on the sleeve-type expansion anchors followed the corresponding monotonic mean curves (Figure 3.59a). Both, EAs1 and EAs2, failed in concrete (Figure 3.59b).

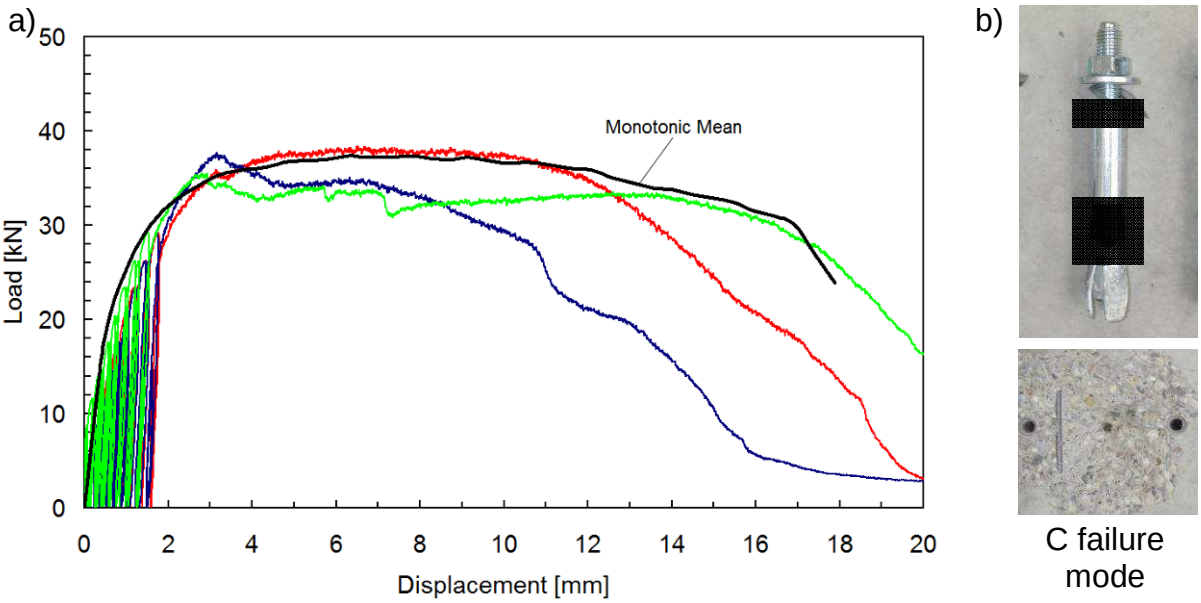

Figure 3.59 EAs1 anchor tested in tension (0.5 mm): a) Cyclic load-displacement curves and monotonic mean curve; b) Picture of anchor and concrete after failure

The load-displacement curves of the tension cycling tests on the bolt-type expansion anchor EAb1 were not as perfectly enveloped by the monotonic mean curve, however, still fair enough (Figure 3.60a). The anchors predominantly failed in pull-through mode (Figure 3.60b).

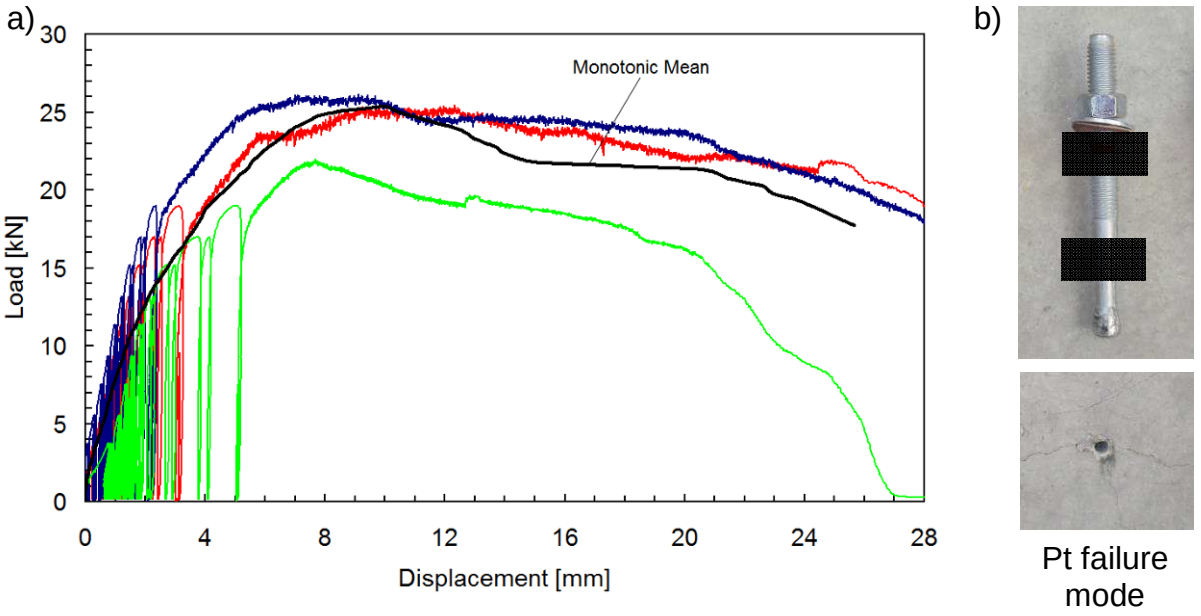

Figure 3.60 EAb1 anchor tested in tension (0.5 mm): a) Cyclic load-displacement curves and monotonic mean curve; b) Picture of anchor and concrete after failure

The load-displacement curves of the tension cycling tests on the bonded anchors followed the corresponding monotonic mean curves (Figure 3.61a). Both, BA1 and

BA2, failed in bond as the threaded rod was pulled out the borehole (Figure 3.61b). The mortar remained partly in the borehole.

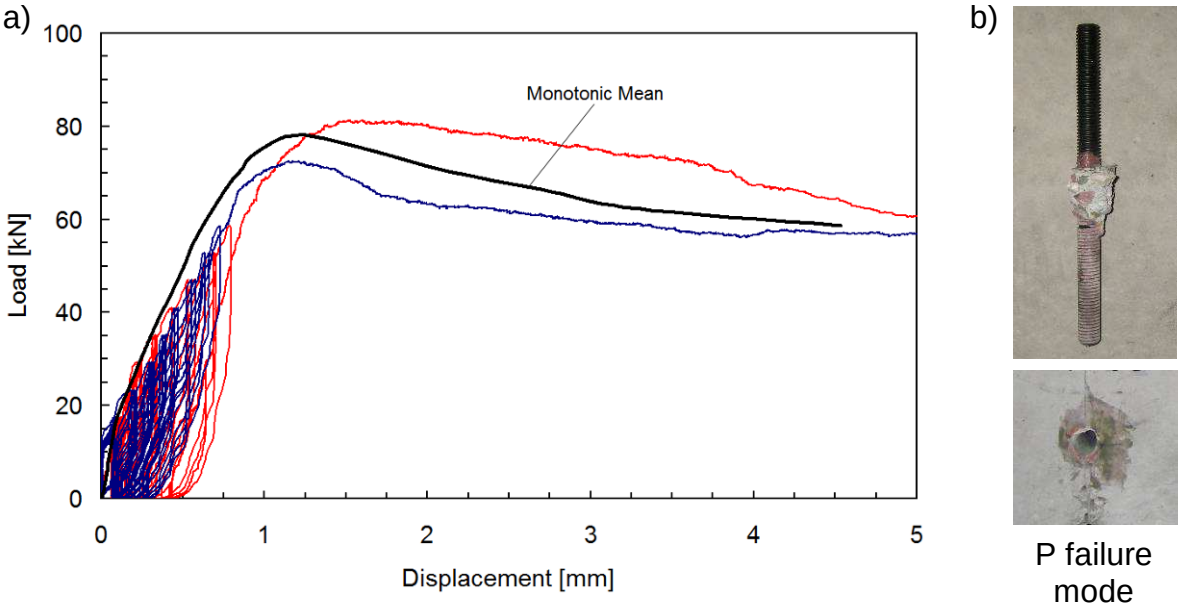

Figure 3.61 BA1 anchor tested in tension (0.5 mm): a) Cyclic load-displacement curves and monotonic mean curve; b) Picture of anchor and concrete after failure

Table 3.9 provides the test conditions and key test results of all anchor types tested in cyclic tension. The test programme included more tests which however are not important in the context of the following discussion and therefore not reported herein.

Table 3.9 Test conditions and key test results of tension load cycling tests

Anchor Type, Anchor Size, Emb. Depth	Crack Width w	Load. Type (1)	Num. of Tests	PFM	$N_{u,m}$, kN	CV, %	$\frac{N_{u,cyclic,m}}{N_{u,cr,m}}$	$s(N_u)_m$, mm	CV, %	$\frac{s(N_{u,cyclic})_m}{s(N_{u,cr})_m}$
UC1; M10; 90 mm	0.5 mm	m	3	C	39.4	11.0		3.90	67.2	
		c	3	C	44.5	4.8	1.13	4.78	53.1	1.23
	0.8 mm	m	3	C	34.2	5.7		1.64	11.8	
		c	3	C	36.7	19.6	1.07	3.92	49.0	1.71
EAs1; M12; 80 mm	0.5 mm	m	3	C	38.9	15.3		6.54	62.6	
		c	3	C	37.2	3.9	0.96	4.16	49.1	0.64
EAs2; 5/6"; 85 mm	0.5 mm	m	3	C	23.4	7.4		8.29	4.5	
		c	3	C	26.4	2.5	1.13	6.14	40.1	0.74
EAb1; 1/2"; 83 mm	0.5 mm	m	3	Pt	25.2	6.6		7.94	13.0	
		c	3	Pt	24.6	9.4	0.98	9.70	25.0	1.22
	0.8 mm	m	3	Pt	21.8	7.3		10.98	10.1	
		c	3	Pt	23.5	2.7	1.08	13.52	7.5	1.23
BA1; M12 treaded rod; 96 mm	0.5 mm	m	3	P	78.2	8.1		1.21	29.5	
		c	2	P	76.4	6.1	0.98	1.37	16.1	1.13
	0.8 mm	m	3	P	62.6	10.3		1.87	32.5	
		c	3	P	67.4	15.4	1.08	1.71	30.2	0.92
BA2; M12 thr. rod; 96 mm	0.5 mm	m	3	P	44.2	16.6		0.83	21.8	
		c	2	P	46.2	1.4	1.05	0.61	39.5	0.74

(1) Loading Type: m = monotonic; c = cyclic

Generally it can be said that the residual load capacities after tension load cycling were equal or higher compared to the respective monotonic capacity. Ratios of $N_{u,cyclic,m}$ / $N_{u,cr,m}$ smaller than 1.00 can be assigned to scatter. The CV was for several test series high also due to the small number of test repeats.

The test results indicate that load cycling had even positive influence on the performance of mechanical anchors. The residual load capacities of the undercut anchor UC1 and expansion anchors EAs1, EAs2, and EAb1 were generally higher compared to the corresponding monotonic capacity. This effect was already observed in earlier studies (*Kim, S.-Y.; Yu, C.-S. et al. (2004)*, *Ghobarah, A.; Aziz, T. (2004)*, *Hoehler, M. (2006)*) and is assigned to the setting of the expansion mechanism or compaction of the concrete near the anchor head. Also the adhesive anchors showed a stable behaviour, as the bonded anchors BA1 and BA2 completed all load cycles.

The effect of load cycling on the anchor displacement is not consistent and the displacement is subject to large scatter with a maximum CV of 67 %. The determination of the displacement is always difficult because of the unsteadiness of the curves. However, it is noted that the displacement after tension load cycling is small and ranges from less than 1 mm for bonded anchors to 5 mm at maximum for expansion anchors failing in pull-through.

Tests in 0.8 mm cracks always resulted in significantly reduced ultimate load capacities and increased anchor displacements if compared to the results of the tests in 0.5 mm cracks. The difference was up to 20 % and more. This is true for monotonic as well as for cyclic tests. It is noteworthy, however, that the response of anchors tested in 0.8 mm cracks to load cycling was as stable as that of anchors tested in 0.5 mm cracks.

In contrast, the actual crack width generally does not affect the behaviour of anchors loaded in shear, provided cracking is not excessive. This was the reason why the test programme only included 0.8 mm for the shear load tests which are discussed in the following. The plots and pictures in Figure 3.62 to Figure 3.66 show the load-displacement and failure behaviour of the anchors tested in 0.8 mm cracks. Next to UC1, EAs1, EAb1, and BA1, also the screw anchor SA1 was tested in shear.

The load-displacement curves of the shear cycling tests on the undercut anchor UC1 with the sleeve in the shear plane were clearly below the corresponding monotonic mean curve (Figure 3.62a). All anchors failed during cycling in steel (Figure 3.62b). First the sleeve surrounding the bolt broke (compare to Figure 3.1b), then, one or several cycles later, the anchor bolt.

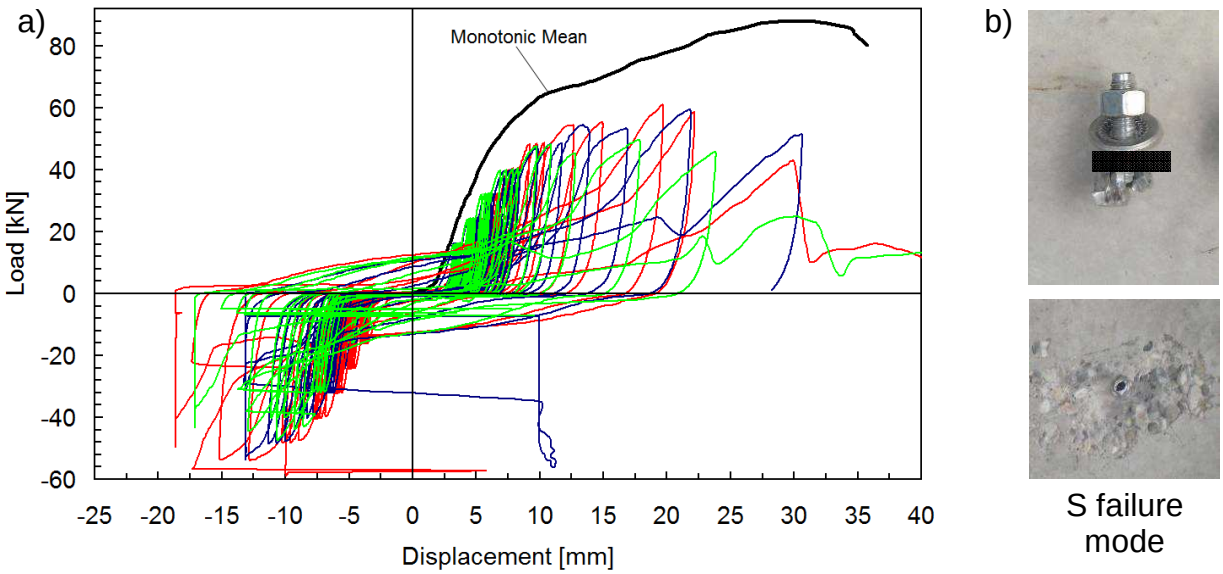

Figure 3.62 UC1 anchor tested in shear (0.8 mm): a) Cyclic load-displacement curves and monotonic mean curve; b) Picture of anchor and concrete after failure

The load-displacement curves of the shear cycling tests on the screw anchor SA1 followed the corresponding monotonic mean curve (Figure 3.63a). All anchors failed in steel (Figure 3.63b) after completion of all cycles when being tested to failure. The resistance to cycling is quite remarkable in that screw anchors are generally known to be brittle due to the hardening process during manufacturing.

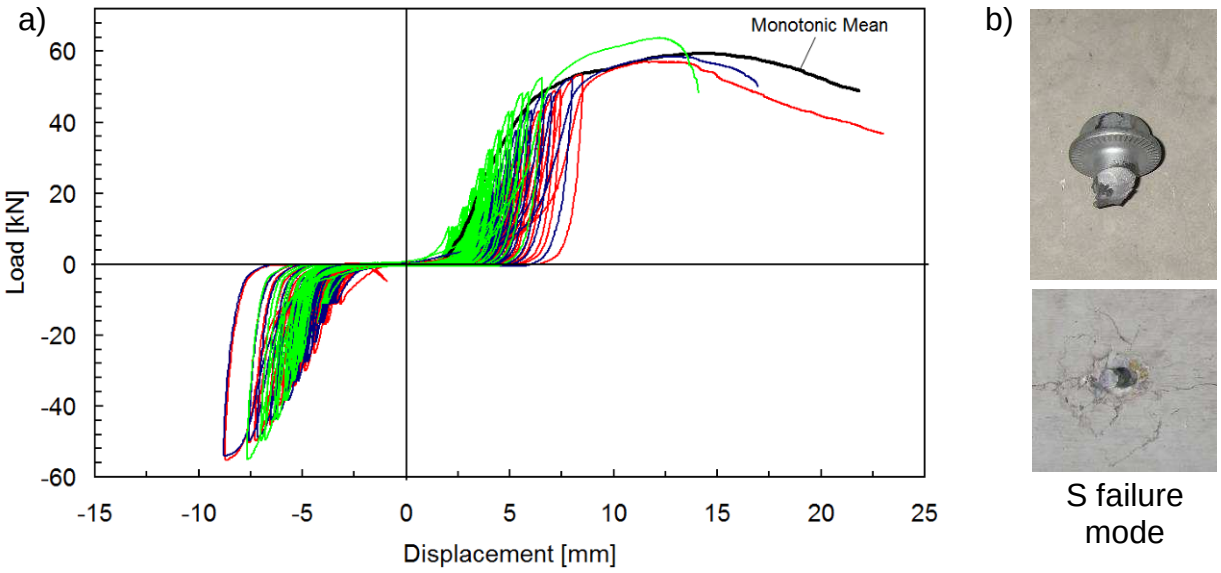

Figure 3.63 SA1 anchor tested in shear (0.8 mm): a) Cyclic load-displacement curves and monotonic mean curve; b) Picture of anchor and concrete after failure

The concrete spalling around the screw anchor is very limited and much less than that for the undercut anchor. The observation that anchors with a sleeve generally display more concrete spalling than anchors without a sleeve is confirmed by the other tests on expansion and bonded anchors.

As for the undercut anchor, the load-displacement curves of the shear cycling tests on the sleeve-type expansion anchor EAs1 were clearly below the corresponding monotonic mean curve (Figure 3.64a). All anchors failed in steel during cycling (Figure 3.64b). Anchor bolt and sleeve, which upper edge were installed flush with the fixture (compare to Figure 3.1d), broke at the point where the fixture is sliding on the concrete.

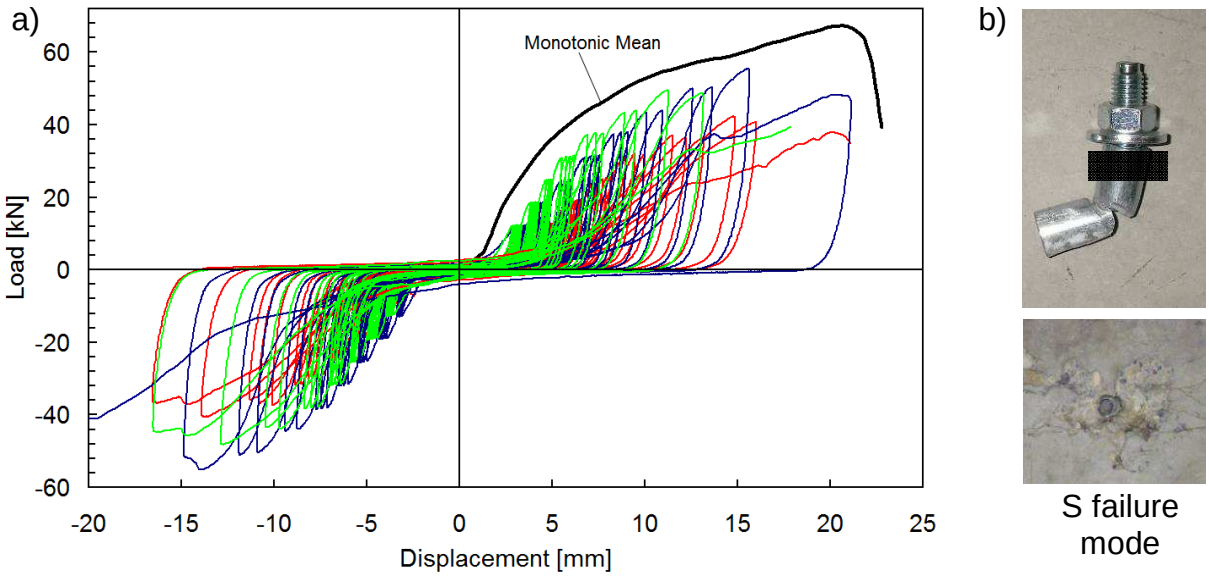

Figure 3.64 EAs1 anchor tested in shear (0.8 mm): a) Cyclic load-displacement curves and monotonic mean curve; b) Picture of anchor and concrete after failure

The load-displacement curves of the shear cycling tests on the bolt-type expansion anchor EAb1 followed again the corresponding monotonic mean curve (Figure 3.65a). All anchors failed in steel (Figure 3.65b) after completion of all cycles when being loaded to failure.

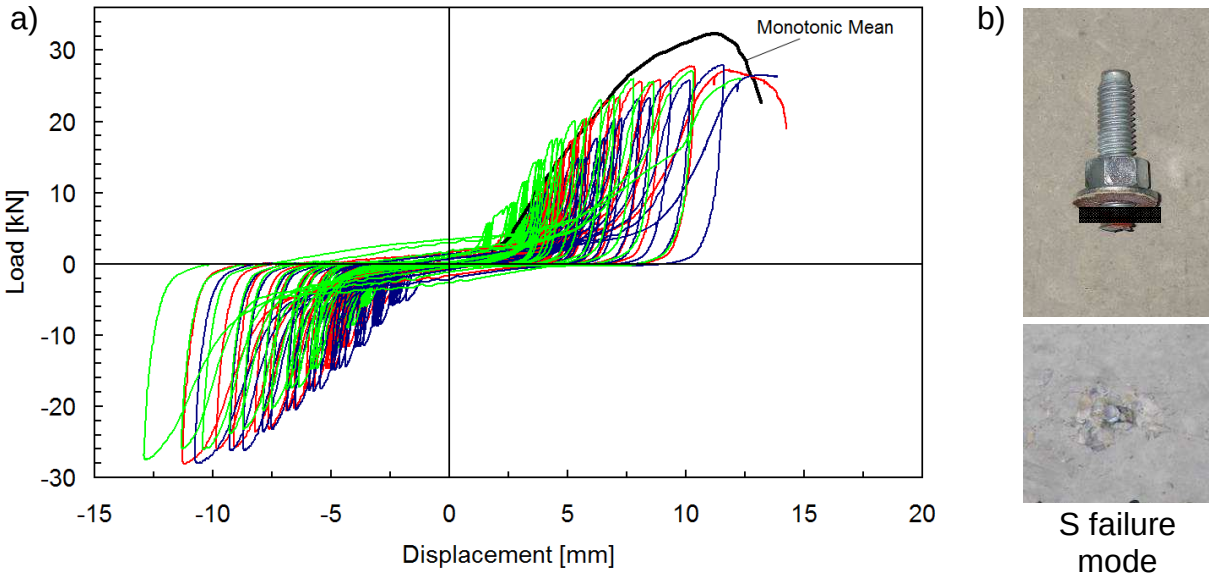

Figure 3.65 EAb1 anchor tested in shear (0.8 mm): a) Cyclic load-displacement curves and monotonic mean curve; b) Picture of anchor and concrete after failure

Also the load-displacement curves of the shear cycling tests on the bonded anchor BA1 followed the corresponding monotonic mean curve (Figure 3.66a). All anchors

failed in steel (Figure 3.66b) after completion of all cycles when being tested to failure.

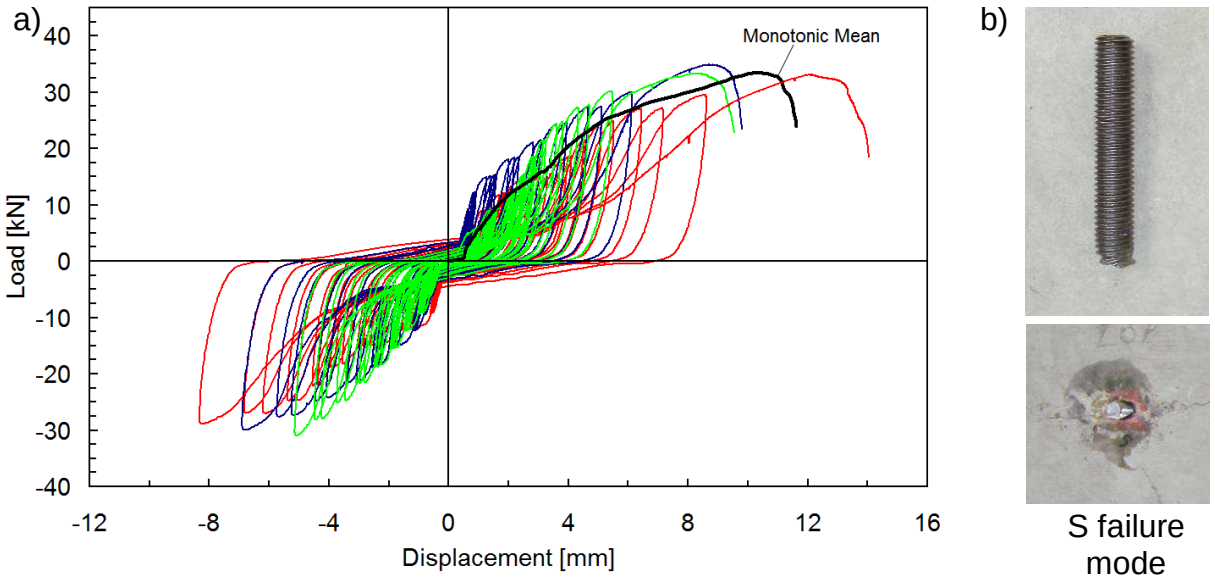

Figure 3.66 BA1 anchor tested in shear (0.8 mm): a) Cyclic load-displacement curves and monotonic mean curve; b) Picture of anchor and concrete after failure

Table 3.10 provides the test conditions and key test results of all anchor types tested in cyclic shear. The test programme included more tests which however are not important in the context of the following discussion and therefore not reported herein.

Table 3.10 Test conditions and key test results of shear load cycling tests

Anchor Type, Anchor Size, Emb. Depth	Crack Width w	Load. Type (1)	Num. of Tests	PFM	$V_{u,m}$, kN	CV, %	$\frac{V_{u,cyclic,m}}{V_{u,cr,m}}$	$s(V_u)_m$, mm	CV, %	$\frac{s(V_{u,cyclic})_m}{s(V_{u,cr})_m}$
UC1; M10; 90mm	0.8 mm	m	3	S	89.2	4.7		31.18	25.2	
		c	3	S	56.7(2)	10.9	0.64	19.71	10.1	0.63
SA1; ∅16; 105mm	0.8 mm	m	3	S	59.7	6.2		14.36	8.0	
		c	3	S	60.1	5.9	1.01	12.06	3.0	0.84
EAs1; M10; 80mm	0.8 mm	m	3	S	68.1	6.9		21.12	11.1	
		c	3	S	49.0(2)	13.4	0.72	13.83	16.5	0.66
EAb1; 1/2"; 83mm	0.8 mm	m	3	S	32.4	4.6		11.21	10.5	
		c	3	S	26.7(3)	2.3	0.82	12.37	5.9	1.10
BA1; M12 thr. rod; 96mm	0.8 mm	m	3	S	33.4	5.7		10.31	22.1	
		c	3	S	33.8	2.9	1.01	9.69	21.6	0.94

(1) Loading Type: m = monotonic; c = cyclic
(2) LCF during cycling; V_u taken as maximum achieved load
(3) No LCF during cycling but residual load V_u smaller than target load V_{max}

The performance of the anchors loaded in shear is governed by LCF. In principle, the anchors can be distinguished according to their make: The load path of anchors without sleeves (SA1, BA1, and EAb1) followed that of the monotonic mean and the anchors completed all cycles. In contrast, the load path of anchors with sleeves (UC1, EAs1) deviated soon from that of the monotonic mean and the anchors experienced LCF prior to completion of load cycles. In these cases, the ultimate load was reduced by approximately 30 % if compared to the ultimate load of the corresponding monotonic test series. This observation might initially surprise since anchors with sleeves are generally assumed to be particularly appropriate for shear loads. However, the stiff sleeve is more loaded than the bolt which is having play in the sleeve. Consequently, the sleeve is subject to higher load amplitudes and therefore more prone to LCF. Moreover, the high monotonic capacity of these anchor types results in large target anchor loads (V_{max} = 0.90 $V_{u,m,cr}$). In consequence, an anchor with sleeve is relatively higher stressed during load cycling than an anchor without sleeve. Also the residual load capacity of the EAb1 anchor was reduced and was even smaller than the achieved maximum load at the end of load cycling. This points out that every cyclic capacity lower than the static capacity may be actually interpreted as LCF.

Compared to cyclic tension tests, the scatter was relatively low in case of cyclic shear tests. The CV was generally below 6 %. Larger CV can be assigned to excessive concrete breakout which was observed for cyclic tests on anchor types with sleeves (see Figure 3.62 and Figure 3.64b).

The anchor displacements generated during shear load cycling is relatively large in comparison to that of cyclic tension tests. The displacements at ultimate failure were in the range of 10 to 30 mm. In case of LCF, the displacements were accordingly smaller.

3.5.2.4 Evaluation of seismic strength and strength reduction factor

The fundamental assessment criterion of a minimum required residual capacity with reference to the monotonic capacity is stipulated for various qualification tests involving load and crack cycling (Sections 2.5 and 2.6). For simulated seismic tests according to ACI 355, the minimum required residual capacity equals 80 % of the monotonic capacity in a crack (0.8 $F_{u,cr,m}$, Section 2.5.2). This criterion ensures that after cyclic actions the anchor still provides sufficient residual load capacity. If it is not met, the reported strength is reduced as described in Section 2.1.7. This procedure is ultimately also the background of the reduction factors $\alpha_{V,seis}$ given in technical approvals (ESR) based on the ACI 355. However, the reduction procedure requires test repeats with maximum anchor load which is reduced until the residual capacity is meeting the requirement.

The same conceptual approach can be used when evaluating the performance of anchors tested by stepwise increasing load protocols. Figure 3.67 illustrates the assessment criteria for the evaluation of seismic tension and shear strengths based on minimum required residual capacities

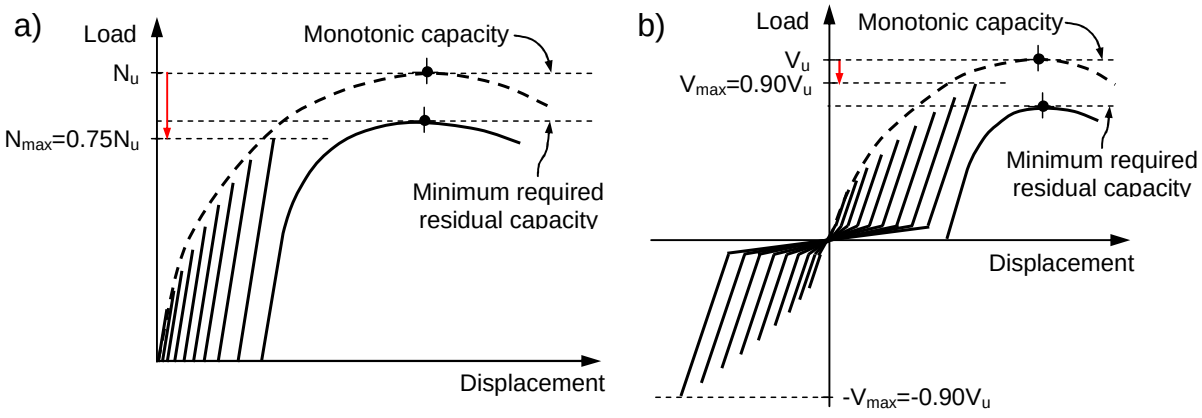

Figure 3.67 Illustration of conceptual approach for evaluation of seismic strength a) Tension test and b) Shear test

It is interesting to know whether the proposed stepwise increasing protocols yield seismic strengths which are similar to those gained by existing qualification guidelines. The tested UC1, EAs1, and EAb1 anchors hold a valid seismic approval according to ACI 355, and the BA1 anchor according to AC 308. The approvals of some of these anchors provide reduction factors for seismic shear. Reduction factors

for seismic tension are not to be expected as also existing seismic qualification tests are not critical in tension. However, a detailed analysis in this respect is problematic due to reasons of confidentiality and because the ratio of reduced maximum load to unreduced maximum load is not necessarily identical to the reduction factor. Moreover, the tests on UC1 and EAs1, resulting in LCF, were not repeated and which residual capacities meeting the requirement are therefore not available for further evaluation.

Nevertheless, a general statement regarding the ultimate loads determined in the tests (Table 3.9 and Table 3.10) in comparison to the nominal strengths given in the relevant ESR may be allowed:

All anchors tested in tension and 0.5 mm cracks yielded mean ultimate loads which are above the nominal strengths given in the corresponding ESR. More importantly, however, are the characteristic strengths determined as the 5 % fractile (Section 2.1.6) because the nominal strengths given in the ESR as design information are to be understood as characteristic strengths. It turned out that the calculated characteristic strengths are sometimes lower than the nominal strengths given in the ESR, however, this is partly owed to the large CV. All anchors tested in tension and 0.8 mm cracks yielded mostly mean ultimate loads which are substantially smaller than the nominal strengths given in the ESR. The reason for this, however, is not any specific load cycling protocol but in the first place the increased crack width. Reference is also made to Section 3.4.5.2. It is noted that all anchors tested in tension fulfill the requirement in that the mean residual capacity was for all anchors at least 0.8 $N_{u,cr,m}$.

Anchors tested in shear (0.8 mm cracks) yielded ultimate loads depending on their LCF behaviour. The ultimate loads were either largely lower (UC1 and EAs1), moderately lower (EAb1), or not lower (BA1) than 0.8 $V_{u,cr,m}$. It is noteworthy, that the corresponding ESR provides seismic reduction factors $\alpha_{V,seis}$ for UC1 and EAs1 but not for EAb1. This is an indication that UC1 and EAs1 anchors also suffer LCF when tested according to simulated seismic tests provisions given in ACI 355. However, the ultimate loads determined by stepwise increasing load protocol were reduced if compared to the nominal strengths given in the ESR. In conclusion, the tested stepwise increasing shear load protocol is apparently more demanding than the existing protocol given in ACI 355 (Figure 2.5) basically due to the different target loads (0.5 $V_{u,cr,m}$ versus 0.9 $V_{u,cr,m}$) and potentially results in smaller seismic reduction factors.

3.5.2.5 Displacement controlled tests and tests with continued cycles

Some of the cyclic tests reported in *Mahrenholtz, P. (2009)* were conducted on the UC1 and EAb1 anchor type according to the testing protocol given in *FEMA-461 (2007)*. This guideline is published by the Federal Emergency Management Agency (FEMA) for determining the seismic performance characteristics of structural and nonstructural components by displacement controlled fragility tests. The aim of the exploratory tests discussed in the following was to check the general applicability or benefits of displacement controlled tests which are potentially handier than load controlled tests. In particular the displacement controlled crossing of the zero loading in case of cyclic shear tests is favourable. Further, displacement oriented test protocols would better reflect the loading conditions in case of displacement controlled failures.

The loading history is provided as relative displacement amplitudes defined as $a_{i+1} = 1.4\ a_i$ (Figure 3.68a). The number of cycles and loading steps is not explicitly given, however, the exploratory tests stuck to the generally recommended scheme of 10 steps with 2 cycles each. Figure 3.68b shows the normalised protocol with a maximum amplitude of $a_i / a_n = \Delta_m = 1.0$.

a)

n	13	12	11	10	9	8	7	6	5	4	3	2	1
a_i/a_n	0.018	0.025	0.035	0.048	0.068	0.095	0.133	0.186	0.260	0.364	0.510	0.714	1.000

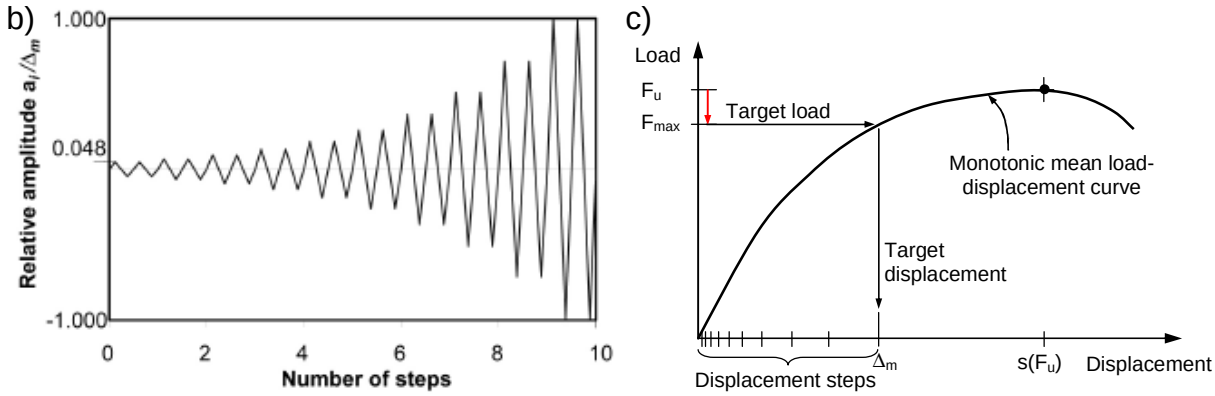

Figure 3.68 a) Relative amplitudes and b) Normalised protocol provided in *FEMA-461 (2007)*; c) Illustration of conceptual approach for development of displacement steps

The target displacement (Δ_m) after completion of the 20 cycles was taken as the mean displacement at the target load defined for the load controlled tests. The individual displacement steps can then be calculated (Figure 3.68c). The protocols normalised with reference to the displacement of the monotonic load capacity correspond to those given in Figure 3.57. The displacement control signal was that of the actuator.

A detailed evaluation of the tests is beyond the scope of this thesis, however, the discussion of some key findings is instructive for further development of loading protocols. Figure 3.69 compares exemplary load-displacement curves derived from load controlled and displacement controlled tests on the same anchor. Both curves follow basically the same envelope and achieve virtually the same ultimate residual capacity. In contrast to load controlled tests with increasing displacements within a load step, displacement controlled tests show decreasing loads within a displacement step. In consequence, displacement controlled tests result in less accumulating displacements and, in particular for shear loading, less demand in view of LCF.

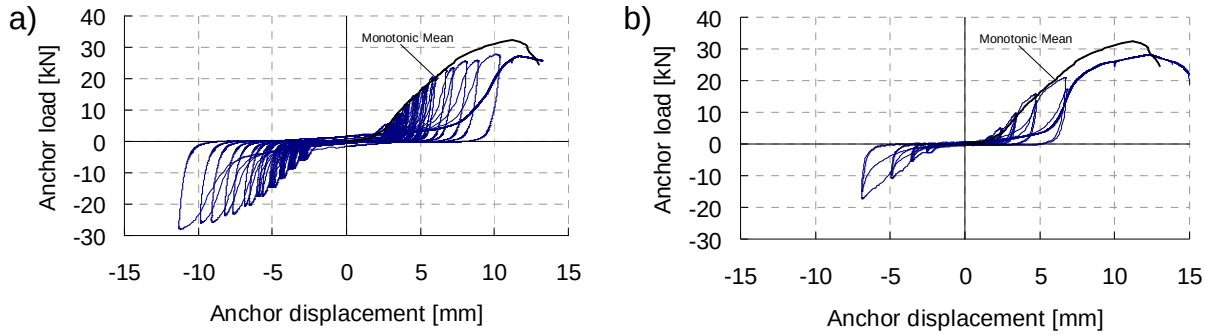

Figure 3.69 Comparison of load-displacement curves (exemplary shear tests): a) Load controlled cyclic test; b) Displacement controlled cyclic test

Characteristic features of load controlled and displacement controlled tests become visible when analysing the time histories. Figure 3.70 and Figure 3.71 show windowed time-histories for anchor load and displacement side-by side to visualize the effect of the different control modes. For cyclic tension, the anchor load show load cycles in case of load controlled test (Figure 3.70a). Since anchors remain in the displaced position, displacement controlled tests do not show any clear displacement cycles (Figure 3.70b).

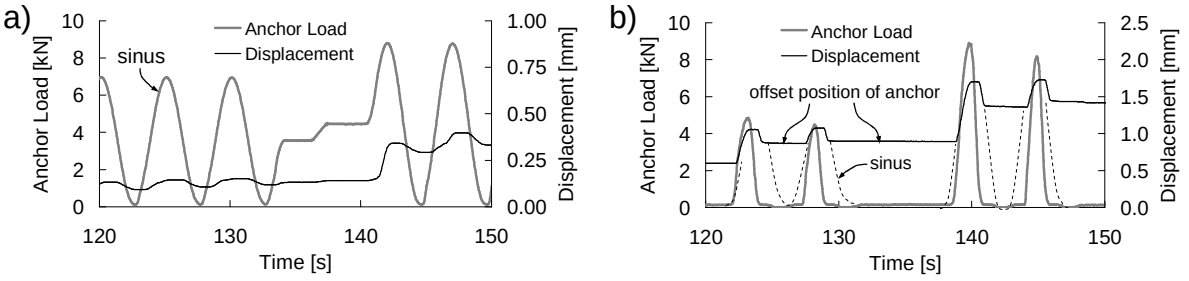

Figure 3.70 Windowed anchor load and displacement time-histories (tension tests): a) Load controlled cyclic test (sinus); b) Displacement controlled cyclic test (sinus)

For cyclic shear, the load-displacement curves reveal the effect of the intermediate ramps used for the zero load crossing in case of load controlled test, resulting in an

odd load time history. Further, the time-consuming crossing of the clearance gap around the anchor is reflected by long periods of zero loading (Figure 3.71a). In case of displacement controlled cyclic shear tests, the displacement show full cycles. The clearance gap has to be crossed as well, however, this can be done at a higher rate because the servo control is more stable due to the lack of the transition from ramp to half sinus (Figure 3.71b).

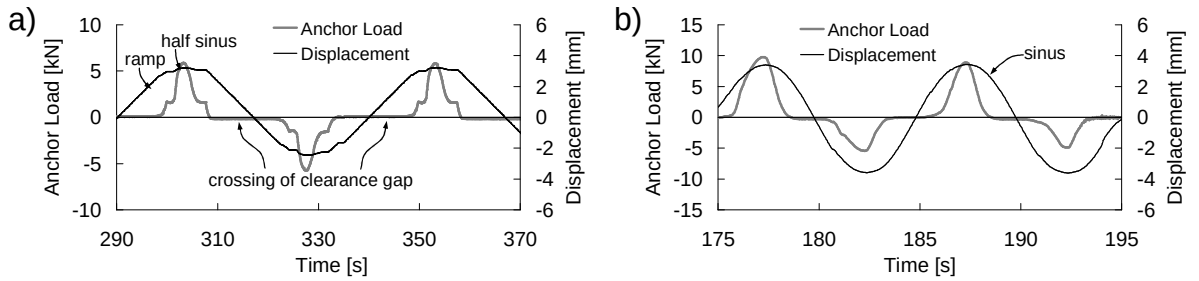

Figure 3.71 Windowed anchor load and displacement time-histories (shear tests): a) Load controlled cyclic test (half sinus / ramp); b) Displacement controlled cyclic test (sinus)

The disadvantage of displacement controlled cyclic shear test is that a large portion of the target displacement is consumed by the clearance gap between the anchor and the bushing. In consequence, the anchor is less loaded if compared to load controlled tests (Figure 3.69b). Moreover, misalignment may lead to asymmetric load-displacement curves (Figure 3.72a).

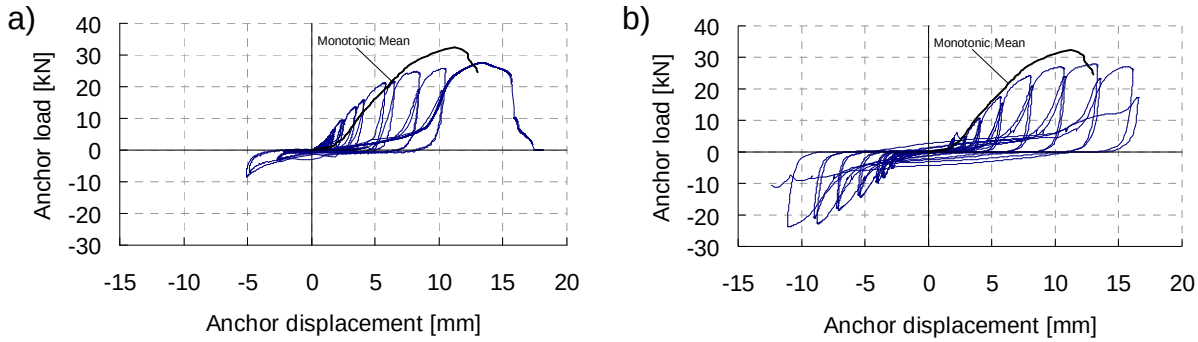

Figure 3.72 a) Example for asymmetric load-displacement curve due to misalignment; b) Example for load-displacement curve of tests with continued cyles

One goal of stepwise increasing load protocols was to enable the evaluation of stiffness, strength and deformation throughout the entire loading range (*Silva, J. (2001)*). In ultimate consequence, the load cycling has to be continued till failure to cover also near ultimate load behaviour. Another benefit of continued load cycling is that defining a load or displacemnent target as a fraction of the monotonic capacity is not required. This approach was checked out by an exploratory cyclic shear test series on the EAb1 anchor for which the protocol given in Figure 3.68b was

prolonged beyond the target displacement till failure. The displacement increments after the achievement of the original target displacement were chosen according to the recommendations given in *FEMA-461 (2007)* as 30 % of the target displacement.

The envelope of the exemplary cyclic load-displacement curve with continued cycles shown in Figure 3.72b coincides well with the envelopes derived from the other load controlled and displacement controlled tests shown in Figure 3.69. Because the portion up to the target displacement bases on the same displacement cycle regime, any deviation would be of random nature. The anchor in Figure 3.72b finally failed in steel due to LCF. Since the LCF occurred after the peak load, the ultimate load capacity is equivalent to that determined in the other load controlled and displacement controlled tests.

In summary, the following can be stated:

- The envelopes of load-displacement curves from load controlled cyclic tests, as well as displacement controlled cyclic tests and displacement controlled cyclic tests with continued cycles are identical. Provided that no LCF occurs before peak load, both control modes yield approximately the same residual load capacities and corresponding displacements.
- However, if the anchor is loaded beyond the linear-elastic range and the anchor strength is prone to fatigue phenomena, as potentially every anchor loaded in shear is, the envelope of cyclic load-displacement curves may be lower than the monotonic mean curve, documenting increasing degradation.
- For displacement controlled tension tests, the anchor is not subjected to full loading cycles. For displacement controlled shear tests, the clearance gap has a fundamental impact on the test result.
- For the conceptual approach presented in this section, displacement controlled tests can be deemed to be less demanding than load controlled tests. This is in particular true for LCF prone anchors loaded in shear.

3.5.3 Conclusions

The experimental tests on a variety of anchors yielded load-displacement curves for every type of anchor and associated typical failure mode. In general, the results for mechanical anchors loaded cyclically in tension verified the observations made earlier. Cyclic shear tests and displacement controlled tests yielded a number of unprecedented results. The test programme also included two adhesive anchors which were the first ever tested by a stepwise increasing load cycling protocol.

For tension load cycling, the testing verified that the scatter band of cyclic load-displacement curves follow the mean of corresponding monotonic tests within

acceptable limits. For the given load regime of the relatively small number of cycles, tensile load cycling on anchors does not yield large anchor displacements. This verifies the assumptions made for group tests (Section 3.4.2.3) for which the displacements accumulating during tensile load cycling were deemed of secondary importance if compared to those accumulating during crack cycling.

For shear cycling tests, the envelope of the cyclic load-displacement curves followed in principle the load-displacement curve of the monotonic mean. However, depending on the relative stress level the envelope may be lower than the monotonic mean. This is particularly observed for anchors which fail during cycling due to LCF or are close to doing so. This highlights the fact that the performance is ultimately dependent on the specified load protocol. For anchor qualification, however, the anchor load has to be reduced to a level which enables the completion of all cycles. In consequence, the assumption made for ductility parameters (Section 3.3.2.3) that the envelope of cyclic load-displacement curves follows the monotonic mean also holds for qualified anchors loaded in shear. The reduction relative to the monotonic capacity is more likely for anchors with sleeves owing to their larger monotonic capacities and uneven share of the applied shear between sleeve and bolt.

The results showed that in principle every anchor type is suitable for seismic application with respect to load cycling, just as hysteresis during cycling is non-existent irrespective of the anchor type and failure mode. It is noted that also the bonded anchors installed in a static crack, despite their probably disadvantaged load transfer mechanism, exhibited good resistance to tensile load cycling which is assumed to be generated by mechanical interlock due to imperfections in the borehole.

The effect of crack width on the ultimate tension capacity was clearly visible. Tests in larger cracks consistently resulted in reduced load capacities. The reduction for tests in 0.8 mm cracks was about 20 % for all anchors if compared with the capacity in 0.5 mm cracks. All tests showed relatively large scatter in particular for displacements. The CV is increases by trend for large crack widths and cyclic actions.

The evaluation of the seismic strengths showed that for the tested stepwise increasing tension load protocol no reduced seismic capacities have to be expected if compared to the seismic strengths given in technical approvals based on ACI 355 or AC 308, provided that the crack width is specified to 0.5 mm as hitherto. For tests in 0.8 mm cracks, however, the monotonic and cyclic capacities are fundamentally reduced due to the increased crack width. For the stepwise increasing shear load protocol tested on LCF prone anchors, seismic capacities have to be expected which are lower than the (reduced) seismic shear strength given in technical approvals based on ACI 355 due to the substantially higher target shear load level.

The exploratory tension and shear tests conducted on anchors loaded displacement controlled with or without continued cycles displayed in general anchor behaviour similar to load controlled loading protocol. Displacement controlled tests allow shortening the testing time, however, they do not provide additional information and are in some respect inadequate. Therefore load controlled tests are the preferred choice for anchor qualification testing. The test results did not indicate that the stepwise increasing load protocol would allow a differentiation of robust and non-robust anchors though.

The detailed evaluation of the results also pointed out that for a sound assessment the repeat of the tests is necessary in case of premature failure or residual capacities lower than the minimum required capacity. For this case, however, the feature of the stepwise increasing load protocol allows at least a better estimation of the potential anchor capacity than the stepwise decreasing and coarser load protocol stipulated in ACI 355. The goal should be to activate every possibility to reduce the testing burden in any other extent. For example, it should be checked whether small cycles may be truncated to speed up testing. The main aim shall be how to test an anchor for variable level of demand without increasing the number of required test runs too much. These aspects will be dealt with in Chapter 4.

3.6 Cyclic Crack

3.6.1 State of knowledge

Anchor behaviour under crack cycling was one of the main focuses of the dissertation *Hoehler, M. (2006)*, which also included a literature review. The number of available literature on cycled crack tests, however, is relatively limited if compared to that available on cyclic load tests.

Based on the analysis of studies on the number of deformation cycles in structures during earthquakes (*Malhotra, P. (2002)*, *Dutta, A.; Mander, J. (2001)*, *Kunnath, S.; Chai, Y.-H. (2004)*) 10 uniform-amplitude crack cycles were taken as representative for crack cycling tests in *Hoehler, M. (2006)* (Figure 3.73a). Further, empirical equations suggested by *Oh, B.-H.; Kang, Y.-J. (1987)*, *Martin, H.; Schießl, P. et al. (1980)*, *Gergely, P.; Lutz, L. (1968)*, and *prEN 1992-1 (2002)* (Eurocode 2) for the prediction of the crack width in reinforced structures yielded a maximum crack width of 0.8 mm outside of zones of plastic deformation. The permanent load acting on the anchor axially during crack cycling N_w was tentatively taken as $0.4\ N_{u,cr,m}$. It was confirmed that according to *Rehm, G.; Lehmann, R. (1982)* a progressive increase of anchor displacement during crack cycling indicates imminent failure. In *Seghezzi, H. (1985)*, it is found that the performance of an anchor installed in cycled cracks

depends on the number of cycles, the maximum crack width and the ratio of minimum to maximum crack width during cycling.

To the knowledge of the author of this thesis, all cycled crack tests carried out ever showed constant maximum crack widths and constant axial anchor loads. For example, the crack pattern used for the cycled crack tests reported in *Hoehler, M. (2006)* showed 10 cycles with constant maximum crack widths of 0.8 mm (Figure 3.73a). Therefore, statements regarding the effect of various shaped crack patterns and sequence cannot be made.

The tests on the effect of crack cycling frequency presented in *Hoehler, M. (2006)* indicated that an increase of the frequency from 0.01 to 0.2 Hz did not significantly affect the anchor displacement behaviour. A more comprehensive study presented in *Mahrenholtz, C.; Eligehausen, R. et al. (2010)* for the frequency range of 0.005 to 5 Hz supported this finding.

Compression forces on the anchor present during crack closure negatively affect the anchor performance. The higher the compression force applied to the concrete test specimen, the more the concrete around the anchor is damaged and the higher is the anchor displacement experienced when the crack opens again. However, compression forces are difficult to create by standard test equipment, for which reason qualification guidelines as the *DIBt KKW Leitfaden (1998)* do not require full crack closure and increase the maximum crack width instead. The investigations in *Hoehler, M. (2006)* of the influence of compression forces during crack closure and maximum crack opening widths on the test results yielded that further increase of the compression force beyond the concrete pressure of 0.10 or 0.15 $f_{cc,150}$ over the gross cross section area does not lead to further crack closure. Further increased forces would also not affect anchor load-displacement behaviour because the compression force would be transferred through the surrounding concrete material. The tested anchors were size M16. For anchors with larger diameter, the limiting compression force beyond which the anchor behaviour is not influenced might increase. Regarding the crack opening width, it was concluded that in case of absence of full crack closure, the missing negative effect cannot be compensated by additional crack opening width.

Due to the mechanical interlock, headed bolts and undercut anchors generally show a robust behaviour in cycled cracks. However, anchors possessing an insufficient bearing area may be pulled out after a small number of cycles (*Eligehausen, R.; Mallée, R. et al. (2006)*). In particular, insufficient undercut due to improper installation may deteriorate the performance. Provided that the anchor is large enough and is installed correctly, undercut anchors shows a predictable behaviour even under extreme conditions (*Mahrenholtz, P.; Asmus, J. et al. (2011)*) (Figure 3.73b).

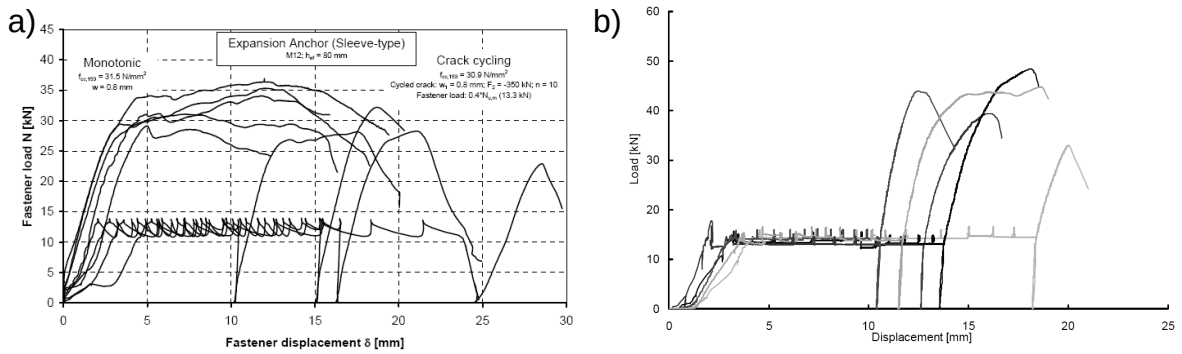

Figure 3.73: Examples for cycled crack tests: a) Cycled crack test on expansion anchor (sleeve-type) with 10 cycles and a constant load at 40 % $N_{u,m,ref}$ (*Hoehler, M. (2006)*); b) Cyclic crack test on undercut anchor according to NPP guideline with 10 cycles and a constant load at N_{Rk} / γ_{Mc} (taken from *Mahrenholtz, P. (2011b)*)

Anchor performance is largely expressed by the anchor displacement behaviour during crack cycling. The permanent axial anchor load during cycling results in anchor displacements typical for cycled crack tests (see Figure 3.73). If the maximum crack width and the axial load are constant over time, the displacement increment is also nearly constant. Tests involving increasing maximum crack widths and probably increased axial anchor load, could provide additional information of the anchor response to various crack widths and anchor load levels.

3.6.2 Crack cycling tests

The relatively simple crack protocol used in *Hoehler, M. (2006)* allowed using simple actuators to open the cracks in the multi position concrete slab and to permanently load the anchors. The lack of precise control of crack width and anchor load resulted in a measured deviation from the target values of up to 20 %. However, the improved testing equipment developed ever since (*Mahrenholtz, C.; Silva, J. et al. (2012)*) made complex crack cycling tests with stepwise increasing crack protocol and precise anchor load control possible. In *Mahrenholtz, C. (2009)* an extensive crack cycling test programme is reported which is discussed in the following. The primary objective of the tests was to investigate the performance of different anchor types installed in cyclic cracks and subjected to permanent anchor load. It was aimed to generate cyclic load-displacement curves for all key failure modes and to demonstrate the feasibility of complex crack cycling protocol involving stepwise increasing crack widths.

3.6.2.1 Crack protocol, target crack width, and permanent anchor load

Based on the same non-linear analysis of reinforced structures introduced in Section 3.5.2.1, *Wood, R.; Hutchinson, T. et al. (2010)* also developed stepwise increasing protocols to represent earthquake induced concrete crack cycling on anchors. The protocol was developed using rainflow counting of the curvature histories extracted from non-linear history analyses of a suite of building models, as described in Section 3.5.2.1. For a linear-elastic region, as such for outside of the plastic hinge zone, curvature values can be linearly related to crack widths using previously studied equations, i.e: *Oh, B.-H.; Kang, Y.-J. (1987)*, *Martin, H.; Schießl, P. et al. (1980)*, *Gergely, P.; Lutz, L. (1968)*, and *prEN 1992-1 (2002)* (Eurocode 2). The cycle count resulted, after normalization, re-arranging with respect to their amplitudes, and averaging, in a stepwise increasing crack cycling protocol of 32 cycles (Figure 3.74a). With reference to Section 3.5.2.1, the target crack width was taken as w_{max} = 0.5 or 0.8 mm. This leads to crack protocols with absolute crack width values as shown in Figure 3.74b.

a)

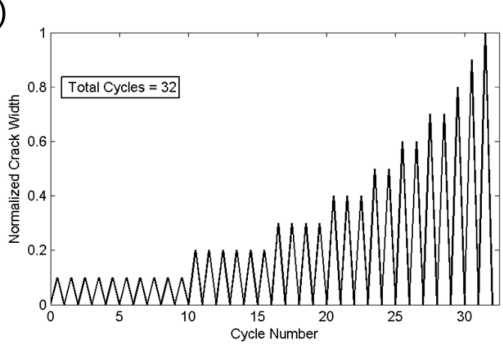

b)

Step	Count	Crack width [mm] for individual step	
		Δw_{max} = 0.5mm	Δw_{max} = 0.8mm
0.1	10	0.05	0.08
0.2	6	0.10	0.16
0.3	4	0.15	0.24
0.4	3	0.20	0.32
0.5	2	0.25	0.40
0.6	2	0.30	0.48
0.7	2	0.35	0.56
0.8	1	0.40	0.64
0.9	1	0.45	0.72
1.0	1	0.50	0.80
SUM	32		

Figure 3.74: a) Normalised crack cycling protocol proposed in *Wood, R.; Hutchinson, T. et al. (2010)*; b) Crack cycling protocol for target crack widths w_{max} = 0.5 and w_{max} = 0.8 mm

For clarity it is noted here that this load cycling protocol slightly differs from the protocol used for the seismic amendment of qualification guidelines presented in Chapter 4. The reasons are discussed in Section 4.1.

As in *Hoehler, M. (2006)*, N_w was defined as 40 % of the ultimate capacity in cracked concrete (0.4 $N_{u,m,cr}$) for which the mean ultimate capacities were determined by monotonic reference tests in cracked concrete. This permanent load level is not scientifically justified yet, but one could argue the following approach: The permanent load N_w is supposed to represent the load for which the anchor will be designed according to its assigned capacity. While the seismic capacity is still unknown at the time of seismic qualification testing, N_w is taken as a certain fraction of its monotonic capacity $N_{u,m,cr}$. The magnitude of this fraction is basically derived from the safety concept of modern codes with partial safety factors. Therefore, the safety concept of the load and resistance factor design (LRFD) is briefly introduced in the following for

the European codes which is in principle equivalent to the approach of modern US codes.

Figure 3.75 illustrates the relationship of load and resistance. The y-coordinate represents the frequency of occurrence and the x-coordinate the considered value, which is here the force acting on the anchor.

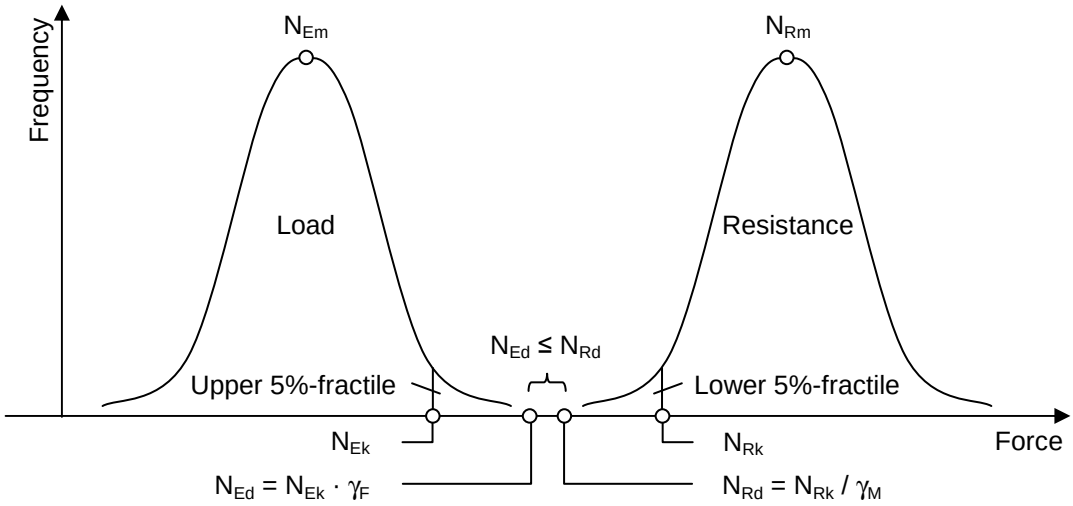

Figure 3.75: General probabilistic consideration of load and resistance as a frequency distribution

The underlying requirement is that the design load N_{Ed} is always smaller or equal to the design resistance N_{Rd}:

$$N_{Ed} \leq N_{Rd} \qquad \text{Equation 3.16}$$

The design load is derived by multiplying the characteristic load N_{Ek} by the safety factor γ_F. The design resistance is derived by dividing the characteristic resistance N_{Rk} by the safety factor γ_M. Thus, Equation 3.12 can be expressed as:

$$N_{Ed} = N_{Ek} \cdot \gamma_F \leq N_{Rk} / \gamma_M = N_{Rd} \qquad \text{Equation 3.17}$$

With the load safety factor for earthquake load cases (governing load case) of $\gamma_F = 1.0$ and the material safety factor for concrete (applicable for concrete cone and pull-out / pull-through failure modes) of $\gamma_M = 1.5$, Equation 3.13 can be rewritten as:

$$N_{Ed} \leq N_{Rk} / 1.5 \qquad \text{Equation 3.18}$$

For anchor qualification tests, the mean resistance N_{Rm} is taken as the mean ultimate load determined by a test series $N_{u,m}$. With the assumption for the characteristic load equals 0.75 $N_{u,cr,m}$ (Section 2.1.6) Equation 3.14 yields:

$$N_{Ed} \leq 0.75\ N_{u,cr,m} / 1.5 = 0.5\ N_{u,cr,m} \qquad \text{Equation 3.19}$$

The best design, i.e. most economic but safe design, uses the full capacity ($N_{Ed} = N_{Rd}$). For the considered case, N_{Ed} represents the maximum allowable load

which corresponds to the adverse (characteristic) loading condition ($N_{Ed} = N_{Ek}$). However, in reality it is unlikely that the maximum possible anchor load act permanently. For this reason, the permanent anchor load should be reduced to achieve a more realistic, i.e. relatively normal load level. This aspect was dealt with in more detail by investigations carried out later as presented in Section 3.7.2.4. Tentatively, the effect of non-permanently acting anchor load was estimated by a factor of 0.8 and the permanent load was taken as N_w:

$$N_w = 0.8 \cdot N_{Ed} = 0.8 \cdot 0.5\, N_{u,cr,m} = 0.4\, N_{u,cr,m} \qquad \text{Equation 3.20}$$

It is interesting to note that a probabilistic study discussed in *Sharma, A.; Mahrenholtz, C. et al. (2010)* supports the 0.8 factor.

3.6.2.2 Test setup and testing procedure

The test programme comprised mechanical and adhesive anchors of various manufacturers and make. More than 100 tests were carried out on 9 different anchor types: One undercut anchor (UC1 (M10): Figure 3.1b, one screw anchor (SA1 (∅16): Figure 3.1c), one sleeve-type expansion anchor (EAs1 (M12): Figure 3.1d), two bolt-type expansion anchors (EAb1 (1/2”) and EAb4 (1/2”): Figure 3.1e), and three bonded anchors (BA1, BA2, BA3 (all with threaded rod M12): Figure 3.1f), were tested. All tests were performed on single anchors with large anchor spacing and edge distances. The outline of the test programme is also apparent in Table 3.9.

As anchorage material, normal weight concrete C20/25 with a mean tested concrete cube compressive strength between $f_{cc,150} = 26.7$ and 31.8 MPa were used. The slabs were produced according to the state of the art after *DIN 1045 (2001)* and *DIN 1048 (1991)*. For monotonic reference tests, the same type of wedge-split slab was used as introduced in Section 3.2.2.3. Also the measures taken to ensure unconfined conditions for mechanical anchors and confined conditions for adhesive anchors were the same.

For the crack cycling tests, special concrete test specimens as shown in Figure 3.76 were used. Four high strength tie rods ran lengthwise through the specimen and protruded at both ends. Two thin metal sheets were embedded in the centre at both sides to aid the crack formation. The tie rods were debonded at both sides of these crack inducers, to enable large cracks.

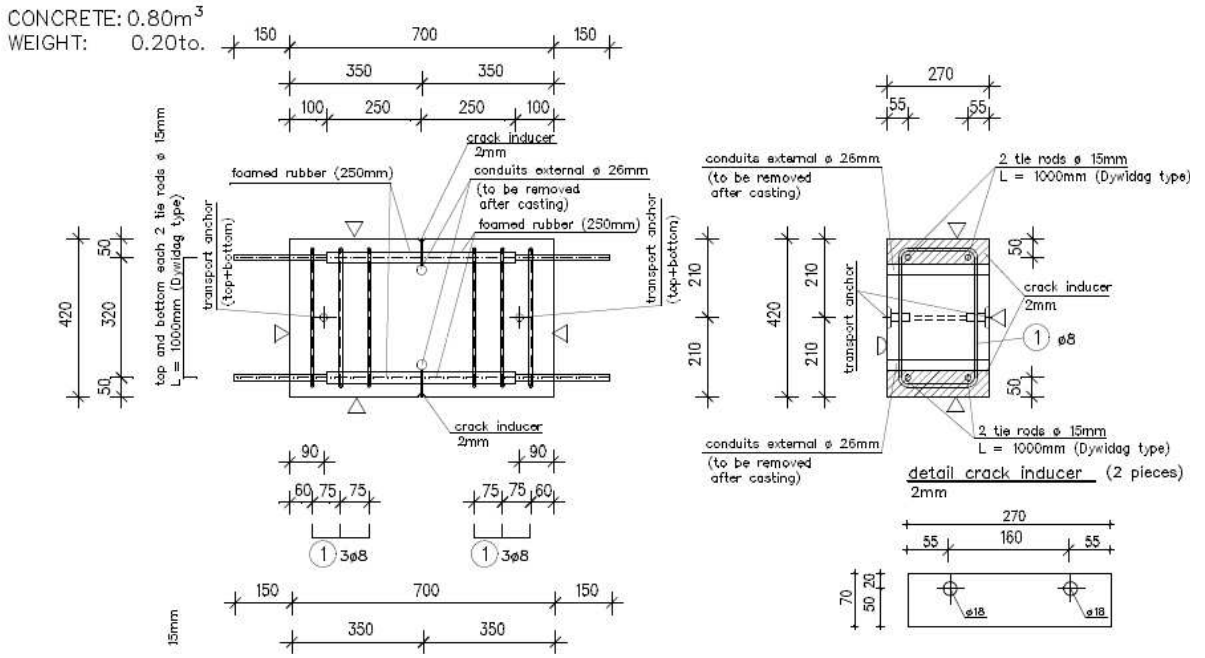

Figure 3.76 Special concrete test specimens used for cycled crack tests

The special concrete test specimen were originally developed for high crack cycling frequency tests described in *Mahrenholtz, C.; Eligehausen, R. et al. (2010)* and allowed to test one anchor at a time in virgin specimens. Together with the improved test setup, very accurate test results were achieved.

As a reasonable compromise of accuracy and economy, each specimen was used on both sides with one anchor location at the centre of the specimen on top and bottom side. Pilot holes were drilled first to ensure that the crack transects both anchor locations later. A hair crack was generated by hammering wedges into sleeves placed in two prefabricated holes. After splitting the concrete crossways, the wedges were removed. The anchor was installed according to the installation manual of the manufacturer for which the pilot hole was reamed prior to each installation. Then the specimen was mounted on the testing rig by connecting the high strength rods to the abutment on one side and to the 630 kN servo-hydraulic actuator on the other side. Next, the 50 kN servo-hydraulic actuator for the anchor load was placed on top and connected to the anchor (Figure 3.77a). Finally, the instrumentation to measure the tension load applied to the anchor, the anchor displacement and the crack width were installed (Figure 3.77b).

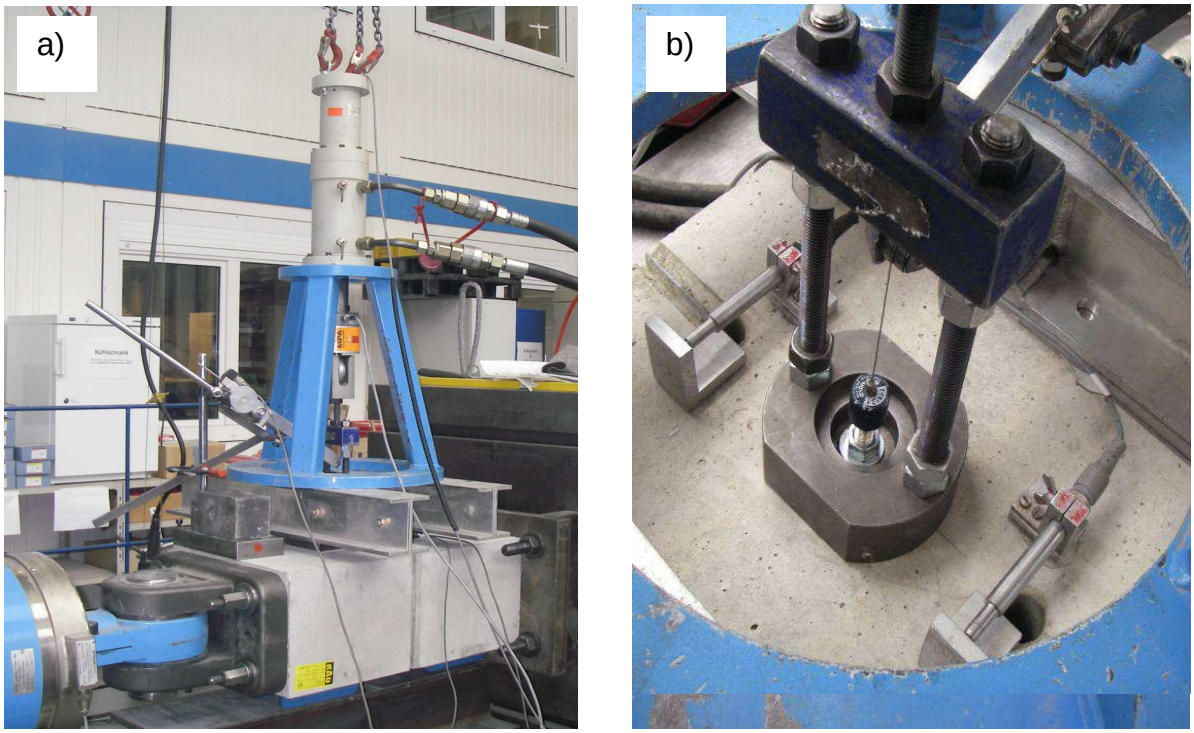

Figure 3.77 a) 50 kN actuator resting on special concrete specimen which is mounted between 630 kN actuator and abutment; b) Close-up of installed anchor, and anchor displacement and crack width transducers

The measured crack width was not only monitored and recorded but also formed the input signal for the control system of the actuator force applied to the concrete test specimen. This enabled the complex crack cycle protocol shown in Figure 3.78a normalised with reference to the crack width. Full crack closure was assumed for a concrete pressure equal to 0.10 $f_{cc,150}$ over the gross cross section area. The crack protocol was executed by crack width controlled ramps at quasi-static rates. The anchor load was controlled by a second control system and kept constant at $N_w = 0.4\ N_{u,cr,m}$ during crack cycling (Figure 3.78b). After completion of the crack cycles, the anchors were unloaded and the concrete specimen relaxed. Prior to the succeeding pullout test, the 630 kN actuator opened the crack to the specified maximum crack width first and then remained in the load-control mode. This mode is believed to represent crack width conditions which are comparable to that created by the restoring forces of reinforcement as for wedge-split slabs. The servo control is discussed in Section 4.2.3 in more detail.

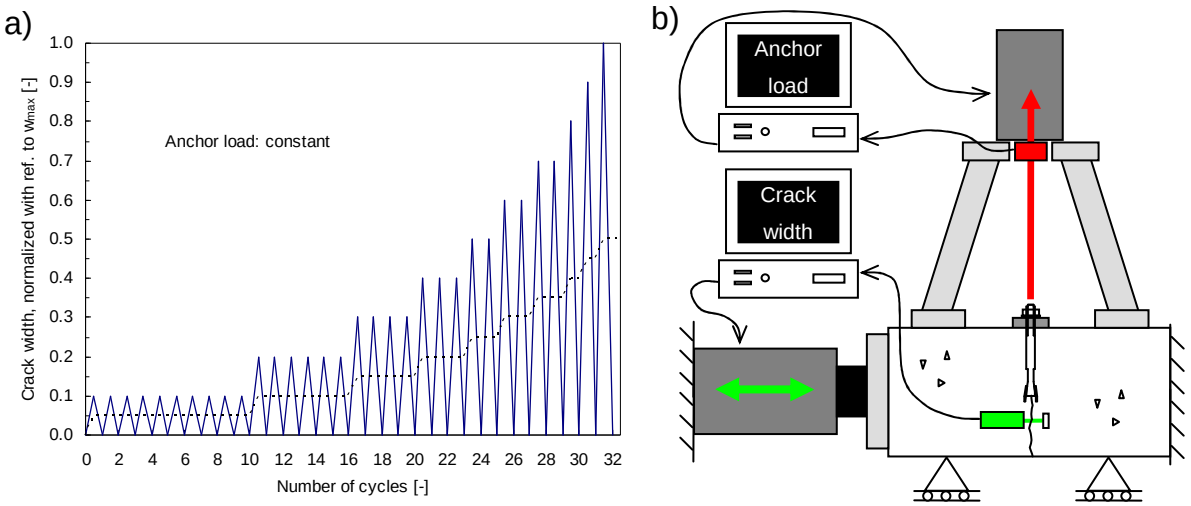

Figure 3.78: a) Crack protocol; b) Schematic of instrumentation and servo control

Then the anchors were pulled out displacement controlled to determine the residual capacity. The ultimate load was reached as for monotonic tests within 1 to 3 min. Further details are given in *Mahrenholtz, C. (2009)*.

3.6.2.3 Experimental results and discussion

Figure 3.79 to Figure 3.83 show the load-displacement and failure behaviour of the tested anchors. Again, for reasons of confidentiality, the exemplary pictures of the anchors are partly blackened. UC1, EAs1, EAb1, and BA1 were taken as representative for their type. The general behaviour of EAb2 and BA2/BA3 was similar to that of EAb1 and BA1, respectively. The plots are only shown for the tests with w_{max} = 0.8 mm cracks, the leading crack width in the test programme, to enable best comparability among the anchor types. Plots of tests with w_{max} = 0.5 mm cracks are not shown, however, the larger crack width is critical for crack cycling tests anyway.

The load-displacement curves of the crack cycling tests on the undercut anchor UC1 showed relatively small displacements during crack cycling (Figure 3.79a). The failure loads were higher and the corresponding displacements larger than for monotonic loading. All anchors failed in concrete after completion of all cycles when being tested to failure (Figure 3.79b).

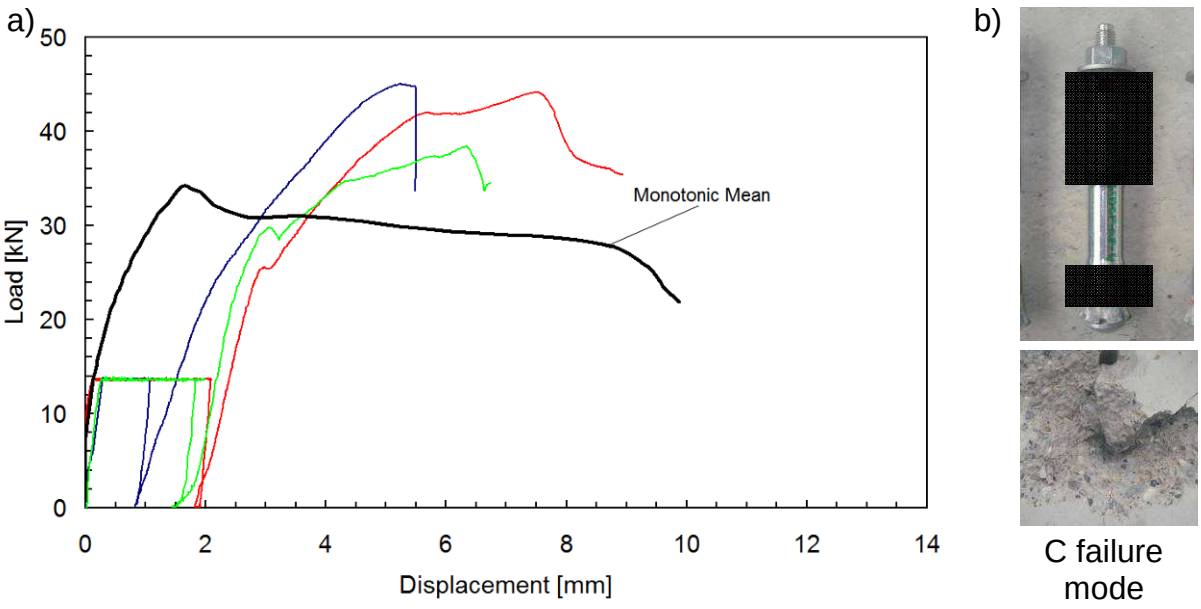

Figure 3.79 UC1 anchor tested in cycled crack (0.8 mm): a) Cyclic load-displacement curves and monotonic mean curve; b) Picture of anchor and concrete after failure

Also the load-displacement curves of the crack cycling tests on the screw anchor SA1 showed relatively small displacements during cycling and some anchors came close to the corresponding monotonic mean curve during the pullout test (Figure 3.80a). One anchor showed a significantly reduced failure load compared to the monotonic mean capacity. All anchors failed in pull-out/concrete failure mode (Figure 3.80b).

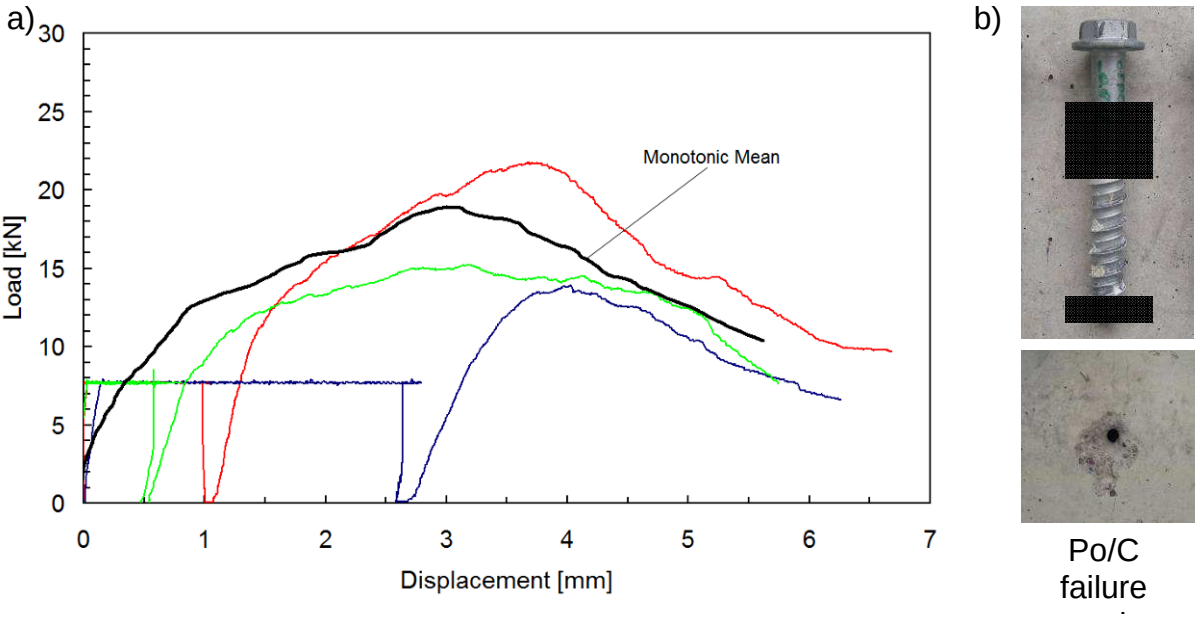

Figure 3.80 SA1 anchor tested in cycled crack (0.8 mm): a) Cyclic load-displacement curves and monotonic mean curve; b) Picture of anchor and concrete after failure

The load-displacement curves of the crack cycling tests on the sleeve-type expansion anchor EAs1 showed displacements during cycling which were larger than the displacement at peak load during monotonic loading (Figure 3.81a). All anchors failed in concrete (Figure 3.81 b).

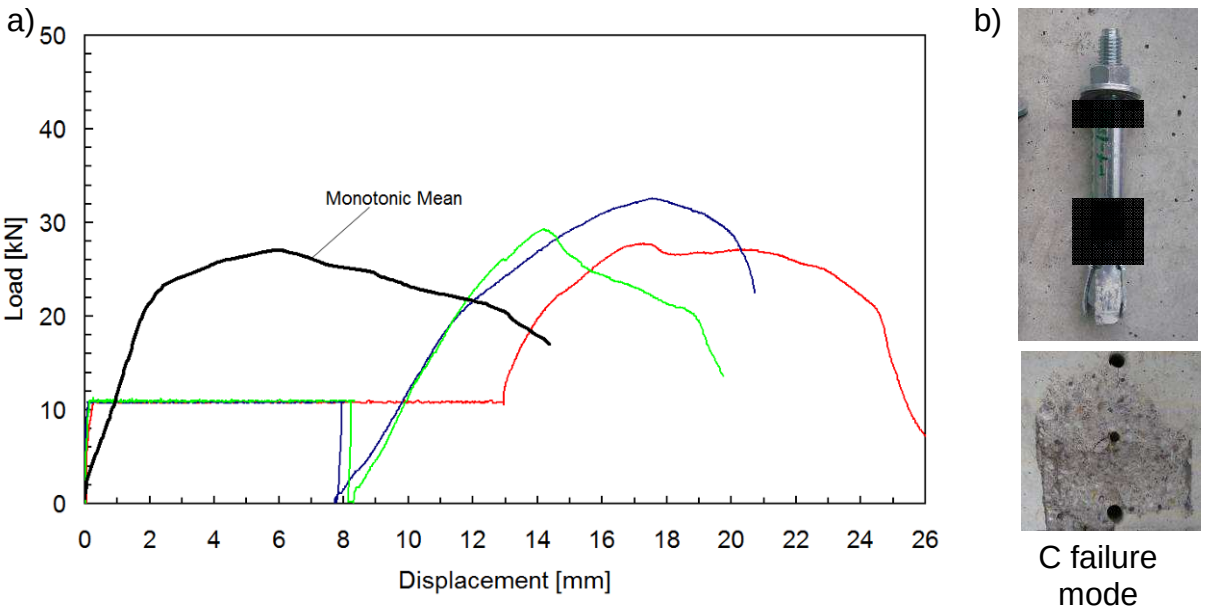

Figure 3.81 EAs1 anchor tested in cycled crack (0.8 mm): a) Cyclic load-displacement curves and monotonic mean curve; b) Picture of anchor and concrete after failure

The load-displacement curves of the crack cycling tests on the bolt-type expansion anchors showed large displacements during cycling and reduced failure loads compared to the monotonic mean capacity (Figure 3.82a). Both, EAb1 and EAb4 predominantly failed in pull-through mode after completion of all cycles while being tested to failure (Figure 3.82b).

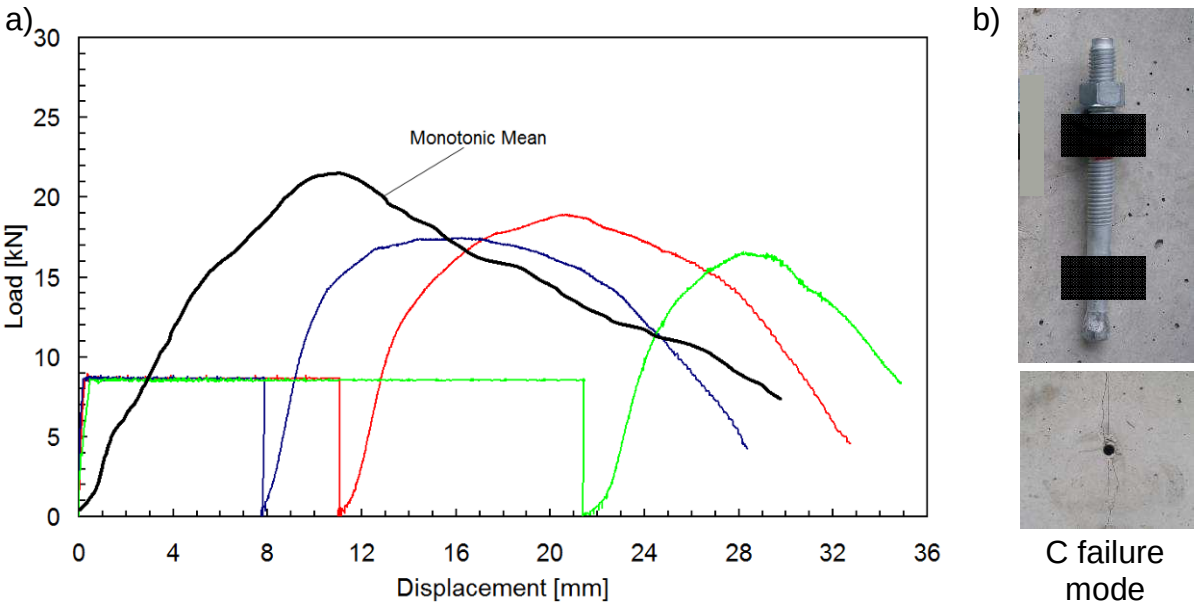

Figure 3.82 EAb1 anchor tested in cycled crack (0.8 mm): a) Cyclic load-displacement curves and monotonic mean curve; b) Picture of anchor and concrete after failure

The displacements of the bonded anchors during crack cycling were so large that some anchors did not complete all crack cycles (Figure 3.83a). All anchors of BA1, BA2, and BA3 type failed in bond as the threaded rod was pulled out the borehole (Figure 3.83b). The mortar remained partly in the borehole.

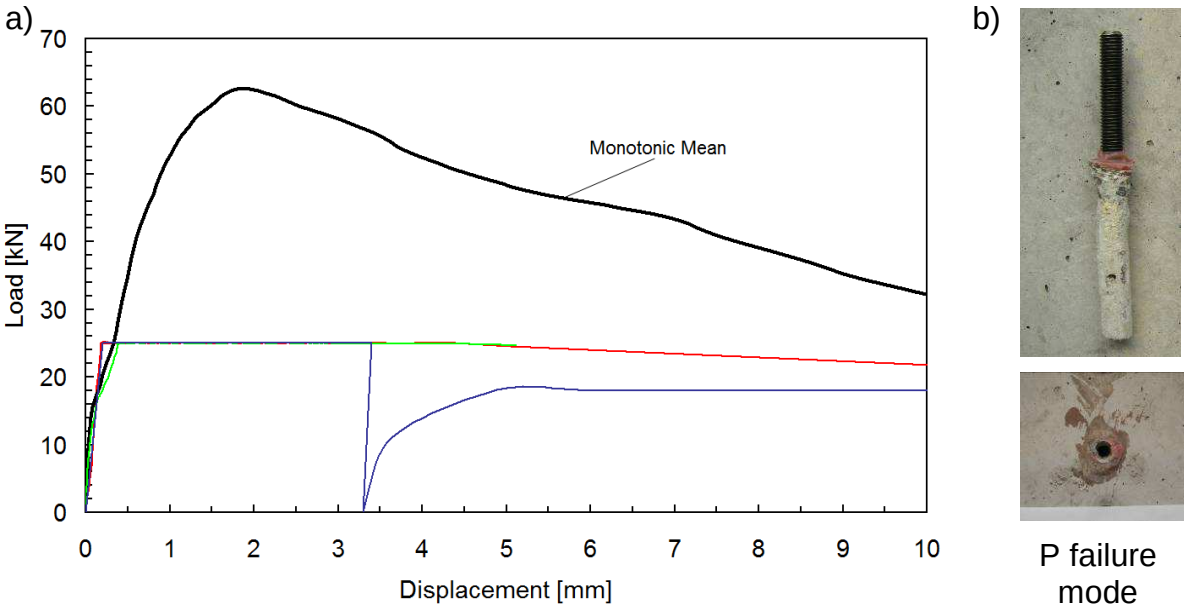

Figure 3.83 BA1 anchor tested in cycled crack (0.8 mm): a) Cyclic load-displacement curves and monotonic mean curve (displacement data repeat no.3 not recorded); b) Picture of anchor and concrete after failure

Table 3.9 provides the test conditions and key test results of all anchor types tested in cyclic crack. The test programme included more tests which however are not important in the context of the following discussion and therefore not reported herein.

Table 3.11 Test conditions and key test results of crack cycling tests

Anchor Type, Anchor Size, Emb. Depth	Crack Width w	Crack. Type (1)	Num. of Tests	PFM	$N_{u,m}$, kN	CV, %	$\frac{N_{u,cyclic,m}}{N_{u,cr,m}}$	$s(N_u)_m$, mm	CV, %	$\frac{s(N_{u,cyclic})_m}{s(N_{u,cr})_m}$
UC1; M10; 90 mm	0.8 mm	m	3	C	34.2	5.7		1.64	11.8	
		c	3	C	42.6	8.5	1.25	6.35	17.6	3.87
SA1; ∅16 105 mm	0.5 mm	m	3	Po/C	34.3	4.7		2.69	35.4	
		c	3	Po/C	19.5	4.1	0.57	4.01	9.7	1.49
	0.8 mm	m	3	Po/C	19.2	33.0		3.07	9.2	
		c	3	Po/C	17.0	24.8	0.88	3.63	11.4	1.18
EAs1; M12; 80 mm	0.5 mm	m	3	C	38.9	15.3		6.54	62.6	
		c	3	C	37.9	7.8	0.97	9.76	23.5	1.49
	0.8 mm	m	3	C	27.5	7.6		6.12	61.7	
		c	3	C	29.9	8.2	1.09	16.28	11.4	2.66
EAb1; 1/2"; 83 mm	0.5 mm	m	3	Pt	25.2	6.6		7.94	13.0	
		c	3	Pt	23.8	23.9	0.94	15.57	17.1	1.96
	0.8 mm	m	3	Pt	21.8	7.3		10.98	10.1	
		c	3	Pt	18.5	4.9	0.85	20.31	25.4	1.85
EAb4; 1/2"; 86 mm	0.8 mm	m	3	Pt	16.3	3.2		10.61	16.3	
		c	3	Pt	13.6	15.8	0.84	17.03	25.7	1.61
BA1; M12 threaded rod; 96 mm	0.5 mm	m	3	P	78.2	8.1		1.21	29.5	
		c	2	P	35.0 (2)	12.5	0.45	3.00 (2)	6.3	2.51
	0.8 mm	m	3	P	62.6	10.3		1.67	32.5	
		c	2	P	18.5 (2)	-	0.38	5.30 (2)	-	2.20
BA2; M12 thr. rod; 96 mm	0.8 mm	m	3	P	41.4	14.2		0.97	24.3	
		c	2	P	27.8	32.6	0.68	2.98	5.5	3.06
BA3; M12 thr. rod; 96 mm	0.8 mm	m	3	P	29.4	8.0		1.14	13.9	
		c	2	P	17.8	14.5	0.60	1.85	47.0	1.63

(1) Cracking Type: m = monotonic; c = cyclic
(2) Residual load capacity and corresponding displacement of repeats which completed all cycles

The results clearly indicate that crack cycling had a significant impact on the performance of post-installed anchors. All cyclic curves show the characteristic

horizontal plateau which illustrates the accumulating anchor displacement during crack cycling under constant anchor load. This displacement had the following effects on the residual capacities depending on anchor type and associated failure mode:

For the tested embedment depth, the undercut anchor UC1 and sleeve-type expansion anchor EAs1 failed in concrete. Therefore, the residual capacity is expected to be reduced if compared with the monotonic load capacity. The degree of reduction depends on the displacement accumulated during crack cycling. The applicability of the approach for the ultimate capacity of headed bolts described in *Furche, J. (1994)* (Figure 3.5d in Section 3.2.2.2) on the load-displacement behaviour of post-installed anchors installed in cycled cracks was shown in *Hoehler, M. (2006)* (Figure 3.84a1). For both anchors, UC1 and EAs1, however, the measured residual capacity outranged the monotonic capacity and the load-displacement curves transected the monotonic mean curve. Similar observations were made for some tests reported in *Hoehler, M. (2006)*. The most likely explanation for this misalignment is that the different types of concrete test specimens used for monotonic and cyclic crack tests influenced the test results.

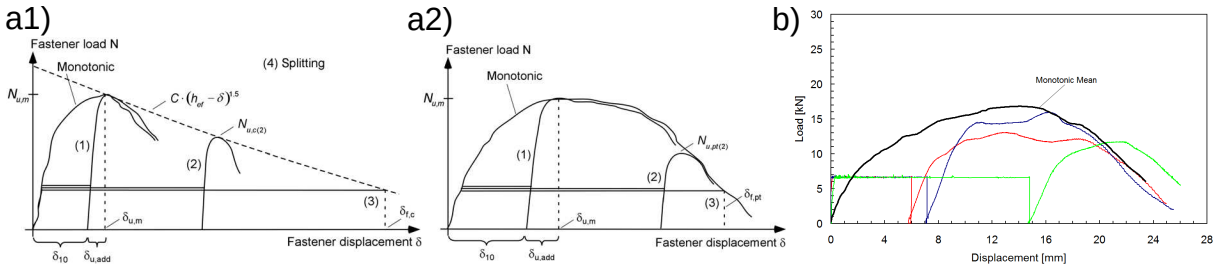

Figure 3.84 a) Load-displacement behaviour after *Hoehler, M. (2006)*: a1) Concrete failure; a2) Pull-through failure; b) Cyclic load-displacement curves and monotonic mean curve of EAb4 anchor tested in cycled crack (0.8 mm)

In contrast, the load-displacement behaviour of bolt-type expansion anchors in cycled crack is bounded by the monotonic mean curve as described in *Hoehler, M. (2006)* (Figure 3.84a2). Provided that the expansion elements do not slip, the maximum possible displacement after installation and crack cycling corresponds to the remaining length of the expansion element (Section 3.2.2.2). This behaviour can be observed for EAb1 anchor, but is more prominent for the EAb4 anchor which cyclic load-displacement curves were enveloped by the descending branch of the monotonic mean curve (Figure 3.84b).

The mixed pull-out/concrete failure mode of screw anchors prevents a simple description of the load-displacement behaviour. The measured load-displacement curves of the SA1 anchor showed large scatter, however, the mean residual capacity is approximately the same as the monotonic capacity in case of the tests with a maximum crack width of 0.8 mm, which is in line with the findings in *Hoehler, M.*

(2006). The comparison with the test results for a maximum crack width of 0.5 mm shows, however, that the influence of the crack width on the ultimate load capacities and CV is for the screw anchor much more pronounced than for the undercut and expansion anchors. The reduction of the monotonic capacity in 0.8 mm cracks was nearly 45 % if compared to the capacity in 0.5 mm cracks.

The impact of crack cycling on the performance of the bonded anchors BA1, BA2, and BA3 was even more severe. For both maximum crack widths, 0.5 and 0.8 mm, one out of two test repeats did not complete all crack cycles. The calculated average residual capacity after crack cycling of 40 % of the monotonic capacity or less is only half the truth. Excessive scatter and the possibility of premature failure make the behaviour of this anchor unpredictable if loaded with $N_w = 0.4\ N_{u,cr,m}$ during crack cycling.

Irrespective to the anchor type, crack cycling results in large overall anchor displacements $s(N_u)$ with a prominent portion accumulated during crack cycling (s_{cyc}). The load-displacement curves of the repeats within a test series dispersed very much during crack cycling, which resulted in large CV in the anchor displacements, in particular of course for bonded anchors. However, in case the bonded anchor completed all crack cycles, the displacement was very small.

3.6.2.4 Detailed evaluation of anchor displacement behaviour

The preceding section highlighted that the displacement behaviour of the anchor is of paramount importance for the seismic anchor performance. Figure 3.85a illustrates the load-displacement curve of an anchor during the crack cycling test. The horizontal plateau represents the anchor displacement during crack cycling. The actual behaviour becomes clearer when analysing the time histories of the anchor load, the crack width and the anchor displacement (Figure 3.85b). For the test conducted within the scope the test programme presented in this section of the thesis, the anchor was first loaded by N_w, resulting in the initial displacement s_i. During the crack cycling, the anchor displacement accumulated to s_{cyc} which is measured as the displacement after unloading of the anchor. The windowed diagram in Figure 3.85c demonstrates the typical anchor response to crack cycling for which the anchor is displaced when the crack is opened and hold in place when the crack is closed. This behaviour was in that clarity never observed before. Older test setup always showed unwanted load cycling for each crack cycle (Figure 3.73a) which veils the pure response of the anchor to crack cycling.

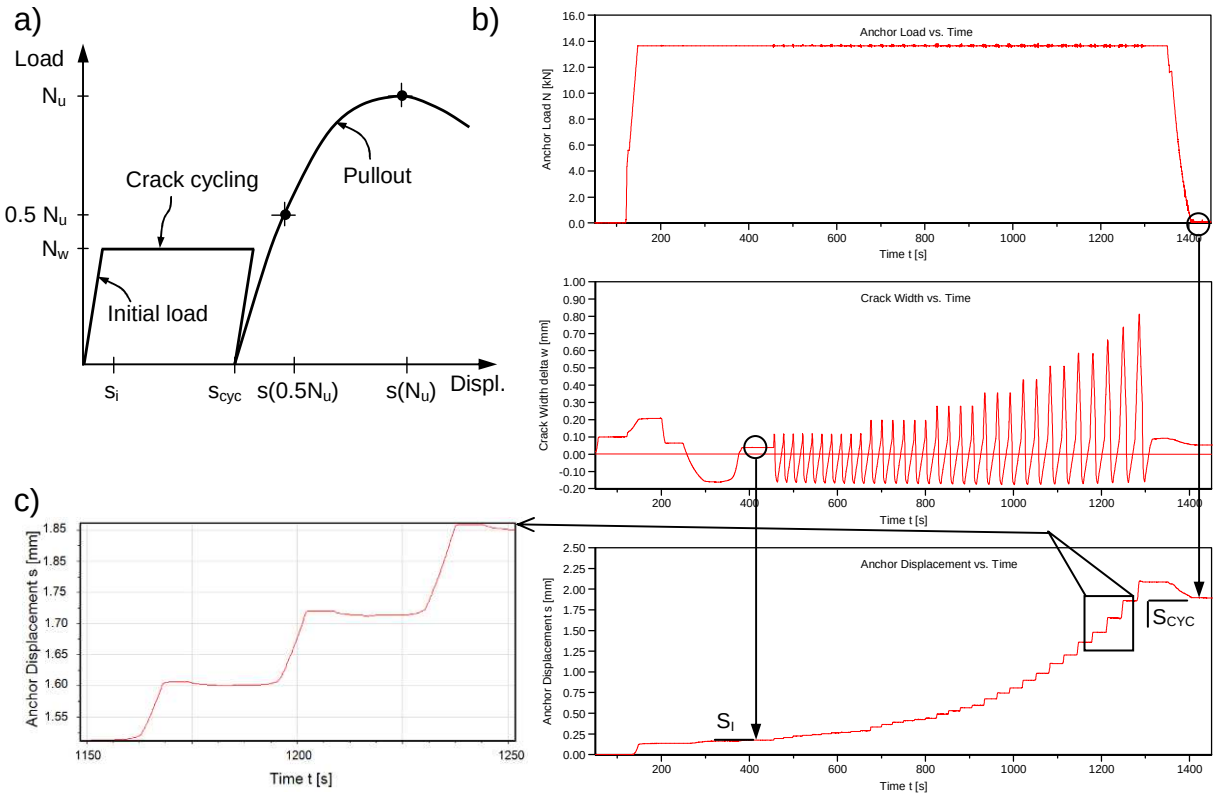

Figure 3.85 Displacement behaviour of anchor: a) Load-displacement curve with test phases; b) Exemplary time histories for anchor load, crack width, and anchor displacement (top to bottom); c) Windowed displacement time history

Anchor displacement during crack cycling results in reduced embedment depth and ultimately in reduced residual load capacity. This behaviour is the reason why crack cycling tests are generally more critical than tension load cycling tests, and why in the extreme case bonded anchors can cope well with load cycling but not with crack cycling.

The diagram in Figure 3.86 depicts the absolute anchor displacement of the anchors as a function of the number of crack cycles for tests with w_{max} = 0.5 mm and w_{max} = 0.8 mm for which the displacements at the maximum crack opening of cycle 1, 16, 27 and 32 have been extracted. The initial displacement (s_i) was zeroed out.

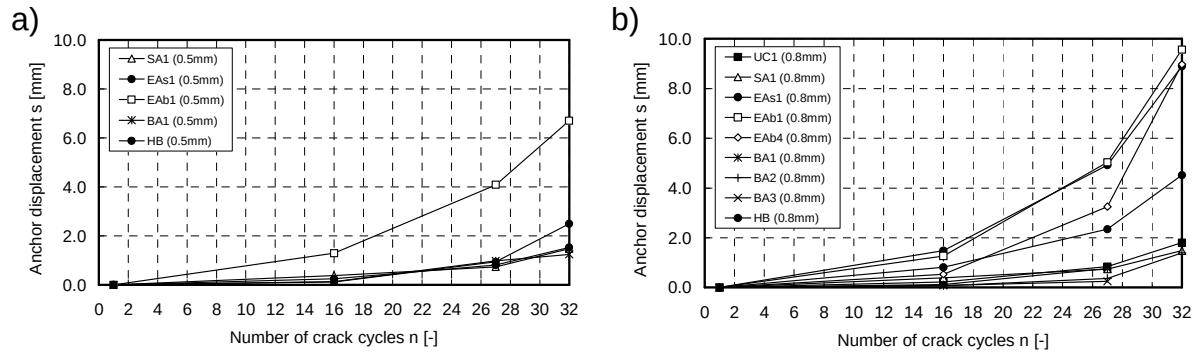

Figure 3.86 Displacement of the anchors during crack cycling: a) 0.5 mm target crack width; b) 0.8 mm target crack width

The development of the anchor displacement in the course of crack cycling is similar for both target crack widths. The displacement during crack cycling is for all anchors progressively increasing when plotted in a linear scale. This behaviour is plausible since the crack width is increasing stepwise, and was also observed in comparison tests carried out on headed bolts ('HB' in Figure 3.86). The effect is even more pronounced if plotted in a half-logarithmic scale, however, opposes the philosophy for the assessment of cycled crack tests as provided in current qualification guidelines for service life tests (*ETAG 001 (2006)* and *ACI 355.2 (2007)*, Section 2.6.1 and 2.6.2) and in *Hoehler, M. (2006)*. The assessment criteria herein stipulate that only degressively or linearly increasing displacements plotted in a half-logarithmic scale and linear scale, respectively, guarantee an acceptable anchor performance. It is beyond the scope of this thesis to discuss the background of this assessment criterion in detail, however, it is obvious that the assessment criterion is not meaningful for stepwise increasing test protocols.

The other requirement stipulated for service life tests as well as in the NPP Guideline (*DIBt KKW Leitfaden (2010)*, Section 2.6.1) limits the allowable displacement after crack cycling to 3.0 mm if in the structural analysis the anchor connection is assumed to be rigid for which case too large displacements are incompatible. If this criterion is not met, the test has to be repeated with a lower permanent load and the reported strength is reduced as described in Section 2.1.7. Figure 3.86 demonstrates that this is inevitable in case of bolt-type expansion anchors, but with reference to the premature failure (Figure 3.83a) also for bonded anchors. However, the displacement criterion may also be for some types of undercut anchor anchors critical (*Mahrenholtz, P.; Asmus, J. et al. (2011)*).

It is important to note the behavioural objectives regarding anchor displacement are different for the cyclic phase and the phase when the anchor is loaded after cycling. Anchor displacement during seismic actions, primarily caused by crack cycling, is generally not desired. The reason for this is not only the incompatibility of the displacements which is particularly important on serviceability demand level. As

mentioned before, anchor displacement during crack cycling also results in reduced embedment depth which consumes part of the available displacement capacity. In contrast, large deformation capacities associated with the displacements at ultimate residual load may be desired. In fact, the residual behavioural objectives in respect to strength, stiffness, but also ductility, are in principle the same as those for monotonically loaded anchors: To this end, qualification guidelines should limit the allowable reduction in residual capacity (as it is generally the case for serviceability tests, refer to Sections 2.5 and 2.6), limit the allowable CV for the displacements at half the load capacity ($s(0.5N_u)$), to avoid unfavourable load distributions, refer to Section 2.4), and apply the same ductility requirements on the deformation capacity at failure (refer to Section 2.3). The evaluation of $s(0.5N_u)$ requires that the anchor is unloaded before it is pulled out for the residual strength test.

3.6.2.5 Tests with increased number of crack cycles

Some crack cycling tests reported in *Mahrenholtz, C. (2009)* were conducted on the UC1 and EAb1 anchor type with increased number of crack cycles. The aim of these tests was to develop an approach which reflects the differentiation of various seismic demand levels better than a mere adaption of the crack width. If the original protocol with a target crack width of $w_{max} = 0.5$ mm is understood to represent moderate seismic conditions, protocols representing extreme seismic conditions should not only have a target crack width increased to $w_{max} = 0.8$ mm but also an increased number of cycles.

To this end, two times the standard deviation of the individual amplitudes given in *Wood, R.; Hutchinson, T. et al. (2010)* were added to the same. The reasoning of this approach is beyond the scope of this thesis, however, it results in additional 9 cycles (Figure 3.87).

Amplitude		1	2	3	4	5	6	7	8	9	10	Total
Average no.of cycles	} *	8.2	4.5	3.2	2.5	1.9	1.6	1.3	1.3	0.6	1.1	
Standard deviation		2.5	1.3	0.9	0.7	0.7	0.6	0.5	0.4	0.2	0.1	
Original protocol		10	6	4	3	2	2	2	1	1	1	32
Protocol with increased no.of cycles		13	6	5	4	4	3	2	2	1	1	41

Figure 3.87 Determination of the crack cycling protocol with increased number of cycles compared to the original protocol on *Wood, R.; Hutchinson, T. et al. (2010)* (marked by }*)

The key finding was that despite the increase in number of cycles by 28 %, the change in the residual load capacity and anchor displacements was nearly always insignificant if compared to the tests with the original protocol. The only possible reason for this is that most of the additional cycles were added to the low amplitude

cycles whose contribution to the anchor displacement during cycling and consequently to the reduction of load capacity is relatively low. Nevertheless, the attempt to come up with a more consistent approach for the differentiation of various seismic demand levels was very instructive for the further development of test protocols for seismic anchor qualification.

In summary, the following can be stated:

- The impact of the cycles near the target crack width on the test result is relatively high if not disproportionate high. Therefore, this portion of the crack cycle regime requires most attention when synthesising crack cycling protocols.
- The consistent differentiation of various seismic demand levels requires the consideration of cycle regime by varying not only the target crack width but also the number of cycles.

3.6.3 Conclusions

The experimental tests on a variety of anchors using an increasing crack cycle protocol were the first of its kind. Load-displacement curves and associated typical failure modes were generated for every type of anchor. The results verified that the demanding crack cycling tests are often critical for the seismic performance of anchors. While mechanical anchors generally coped with the crack cycling but yielded more or less large displacements, adhesive anchors yielded small displacements but were prone to early failure during crack cycling if loaded with $N_w = 0.4\ N_{u,cr,m}$.

The improved test setup and special concrete test specimen allow testing of complex test protocols with high accuracy. *Hoehler, M. (2006)* suggested that a drop of the anchor load of more than 5 % over several cycles during crack cycling should be restricted in qualification tests. However, with the further development of test specimen and setup, the accurate permanent load is not a problem anymore. The new test setup is capable to compress the concrete specimen to the required 10 % of the concrete compressive strength over the cross section area of the test specimen. Therefore, substitute tests with increased maximum crack as stipulated in *DIBt KKW Leitfaden (1998)* to mimic the effects of full crack closure are not needed. Systematic scatter in the test result can now be reduced and the attention is on the natural scatter. However, high demands are put on instrumentation.

It can be generally assumed that residual load capacities after crack cycling are substantially decreased if compared to the corresponding monotonic capacity. Every crack cycle results in anchor displacement and therefore in reduction of embedment depth, which often is so large that the monotonic capacity is not reached during the

pullout test (refer to Figure 3.84). Failure is inevitable at the moment when the capacity corresponding to the actual embedment depth equals the permanent anchor load (C failure mode) or the length of the expansion elements is consumed (Pt failure mode). Bolt-type expansion anchors develop large displacements in particular for extreme crack widths for which the expansion elements are simply too thin. Screw anchors (Po/C failure mode) experience relatively small displacements during crack cycling, however, with increasing crack widths the undercut of the thread is nearly exhausted and the behaviour gets increasingly instable. Bonded anchors appear generally incapable to withstand crack cycling even for relatively moderate maximum crack widths of 0.5 mm if loaded with $N_w = 0.4\ N_{u,cr,m}$. For lower constant tension loads, the behaviour might be acceptable. More research is required and the use of bonded expansion anchors is an option which should be tested.

In conclusion, for tension loading, cyclic cracks are more critical than cyclic loads. All tests showed large scatter in particular for displacements. The CV generally increases for large crack widths and cyclic actions. This should be accounted for in the assessment criteria of future seismic qualification guidelines.

The unreasonably large cyclic capacity of the tested undercut anchor can most likely be assigned to the use of different concrete test specimen types for monotonic and cyclic tests. Different geometry and crack width behaviour of wedge-split slabs and special concrete specimens affect the test results of the pullout test in particular for large loads. To reduce the systematic scatter it is recommended that monotonic and cyclic tests are carried out in the same concrete specimen type.

The assessment criteria that displacements are only acceptable if degressively or linearly increasing as stipulated in current qualification guidelines for service life tests proved to be inadequate for stepwise increasing crack cycling protocols. However, displacement during cyclic action is generally not desired, and therefore an assessment criterion limiting the displacement as in the provided in the NPP Guideline is meaningful. This does not alter the behavioural objectives defined in view of ductility.

The exploratory tests conducted on anchors with increased number of crack cycles pointed out that testing of the anchor performance for different level of demand requires a variation not only of the target crack width but also of the number of cycles. This finding corresponds to the respective conclusions made for cyclic load tests and will be dealt with in Chapter 4.

3.7 Simultaneous Load and Crack Cycling

3.7.1 State of knowledge

To the knowledge of the author, tests on anchors involving simultaneous load and crack cycling protocols have never been carried out before. This testing approach is commonly avoided due to its complexity and requires in particular a servo control system which is capable to control two actuators at a time: One actuator for anchor loading, the other actuator for the crack width control.

3.7.2 Simultaneous load and crack cycling tests

Seismic actions cause cycling of anchor load and crack width simultaneously (refer to Figure 1.9 in Section 1.2). As discussed in Section 2.7, it is common to investigate the effects of cyclic loads and cyclic cracks separately. This approach is conservative and results in load cycling tests (Section 3.5.2), and crack cycling tests (Section 3.6.2). However, the approach of a constant and permanently acting load for crack cycling tests (Section 3.6.2.1) is probably over-conservative and justifies a detailed study on the influence of simultaneous load and crack cycling with different phase lags and frequencies. Therefore, it is instructive to investigate the principal behaviour under simultaneous load and crack cycling in order to study the effect of simultaneous load and crack cycling and to determine the influence of their phasing on the anchor displacement behaviour. The improved test setup introduced in Section 3.6.2.2 together with a multi axes servo control system introduced in Section 3.4.4.2 made simultaneous load and crack cycling tests possible. Therefore, a study was conducted which is reported in *Mahrenholtz, P.; Mahrenholtz, C. (2010)* and discussed in the following.

3.7.2.1 Load and crack protocols

The crack protocol used for the simultaneous load and crack cycling tests consists of uniform cycles. In principle, the different anchor displacement behaviour can be investigated for any number and amplitude of cycles. However, the embedment and thus the load capacity is reduced by the accumulated anchor displacement, resulting in increasingly non-linear anchor behaviour. In order to yield more significant and clear results, the number and amplitude of load and crack cycles were limited to 10 cycles and therefore the crack protocol is identical to that one used for the anchor group tests (Section 3.4.4.2). The frequency ratio of load and crack cycling yields the number of load cycles.

Figure 3.88 shows the tested time histories of anchor load and crack width, each normalised to the maximum anchor load and crack width, respectively. The crack

cycling test with a constant load is described by the load and crack time history shown in Figure 3.88a. If load cycling is taken into account, one may consider two extreme phasing situations. Conservatively, the load and crack cycling could be in-phase, meaning the crack opens and reaches its peak simultaneously with the load demand on the anchor (Figure 3.88b). In contrast, the load and crack cycling could be out-of-phase, resulting in peak anchor load when the crack is closed (Figure 3.88c). The reality is likely to be somewhere between these two extreme conditions and load and crack cycling frequencies differ (Figure 3.88d).

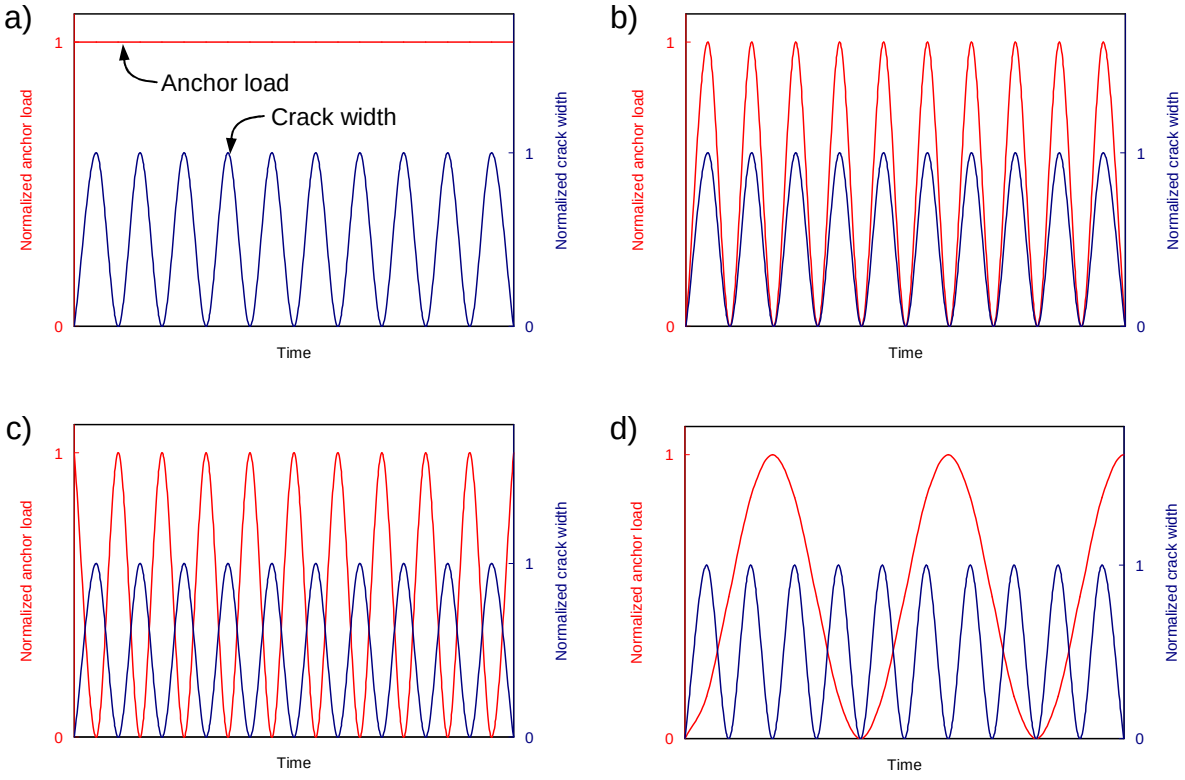

Figure 3.88 Time histories: a) Cyclic crack and constant load; b) Cyclic crack and cyclic load, in-phase; c) Cyclic crack and cyclic load, out-of-phase; d) Cyclic crack and cyclic load, different frequencies

3.7.2.2 Test setup and testing procedure

To investigate the effect of the protocols given in Figure 3.88 on the anchor displacement behaviour, a test programme comprising four test series were conducted. The tests were carried out by means of cast-in-place anchors (Figure 3.1a) which show less scatter than post-installed anchors. Any effect of anchor load and crack width phasing determined for cast-in-place anchors holds also for post-installed anchors, but the use of headed bolt ensured that the significance of the different anchor displacements is not affected by too large variation within the test series. The outline of the test programme is also apparent in Table 3.12.

The used headed bolt is a commercially available anchor product made of a mild steel (S235). Shaft and pressure-forged head are without surface treatment. This product was slightly modified to serve the needs of the test setup and procedure. The upper 50 mm of the shaft was cut with M20 threads and the head was machined to reduce the diameter from 32 mm to 26.5 mm. The embedment depth was 100 mm. A photograph of the modified headed bolt is shown in Figure 3.89a. The head modification resulted in a bearing area of A_{brg} = 268 mm². The bolts were not loaded to failure since only the displacement during crack cycling was of interest for these tests. However, if loaded to failure, a concrete cone breakout is the typical failure mode of a headed bolt.

As anchorage material, normal weight concrete C20/25 with a mean tested concrete cube compressive strength between $f_{cc,150}$ = 32.7 and 33.2 MPa were used. The concrete specimen were similar to the special concrete test specimen used for crack cycling tests (Section 3.6.2.2) which however were delivered with already cast-in headed bolts. Geometry and reinforcement details are given in Figure 3.89b.

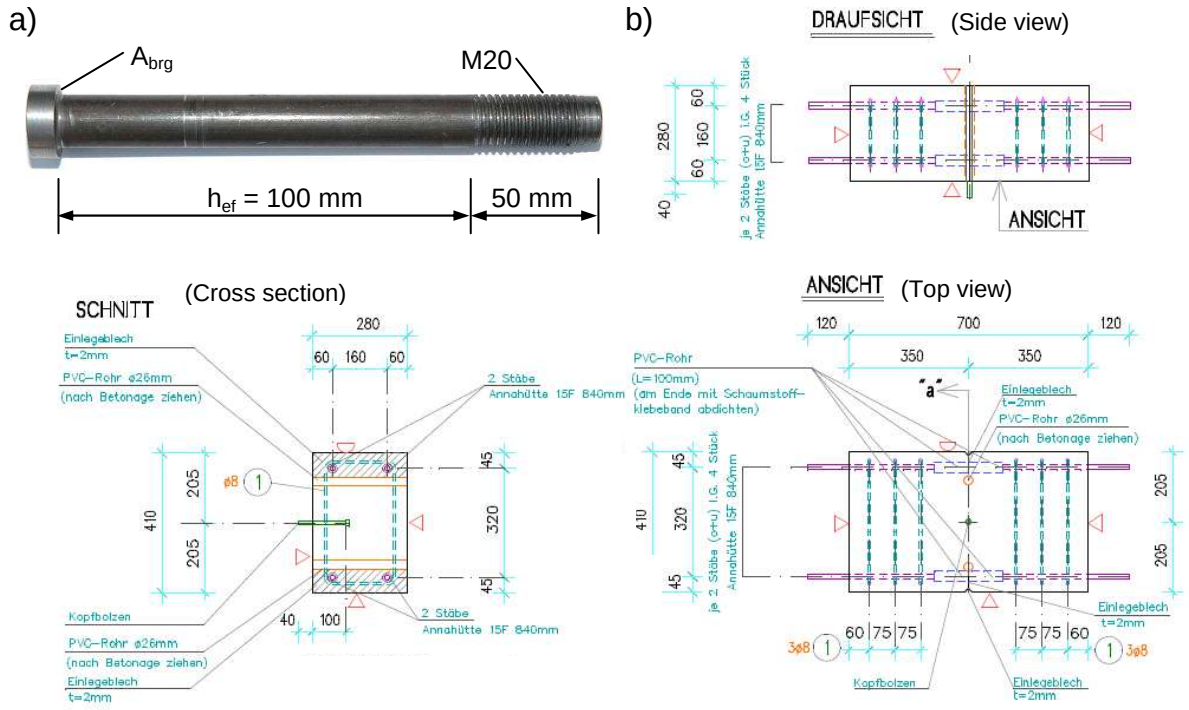

Figure 3.89 a) Photograph of modified headed bolt; b) Special concrete test specimens with cast-in headed bolt used for simultaneous load and crack cycling tests

For the evaluation of the influence of phasing, the actual definition of maximum anchor load and crack width is not crucial, however, should show reasonable magnitudes. The maximum crack width was defined as w_{max} = 0.5 mm. The maximum tension load was defined with reference to the maximum allowable design

load level (Section 3.1.2). Assuming a strength reduction factor of $\phi = 0.65$ and bearing area of 268 mm², the maximum load level was determined (Equation 3.4):
$N_{max} = 8 \cdot A_{brg} \cdot f_c' \cdot \phi = 8 \cdot 268\ mm^2 \cdot 20\ N/mm^2 \cdot 0.65 \cdot 10^3 = 27.8\ kN$

The test setup used for simultaneous load and crack cycling tests was basically the same as that used for crack cycling tests but with the multi-axes servo control system introduced in Section 3.4.4.2. First, a hair crack was generated by hammering wedges into sleeves placed in two prefabricated holes and thus splitting the concrete crossways. Then the specimen was mounted on the testing rig by connecting the high strength rods to the abutment on one side and to the 630 kN servo-hydraulic actuator on the other side. Next, the 250 kN servo-hydraulic actuator for the anchor load was placed on top and connected to the anchor (Figure 3.90a). Regarding the instrumentation, certain improvements were introduced as proposed in *Mahrenholtz, C.; Silva, J. et al. (2012)*: The anchor displacement was measured by a transducer which was fixed to a light frame bridging the crack and the concrete deformation zone with the sensor head directly touching the top of the anchor (Figure 3.90b). To achieve an accurate control of the crack width, two transducers were installed on each side of the concrete test specimen, with the centroid of the four points coinciding with the effective embedment depth (Figure 3.90c).

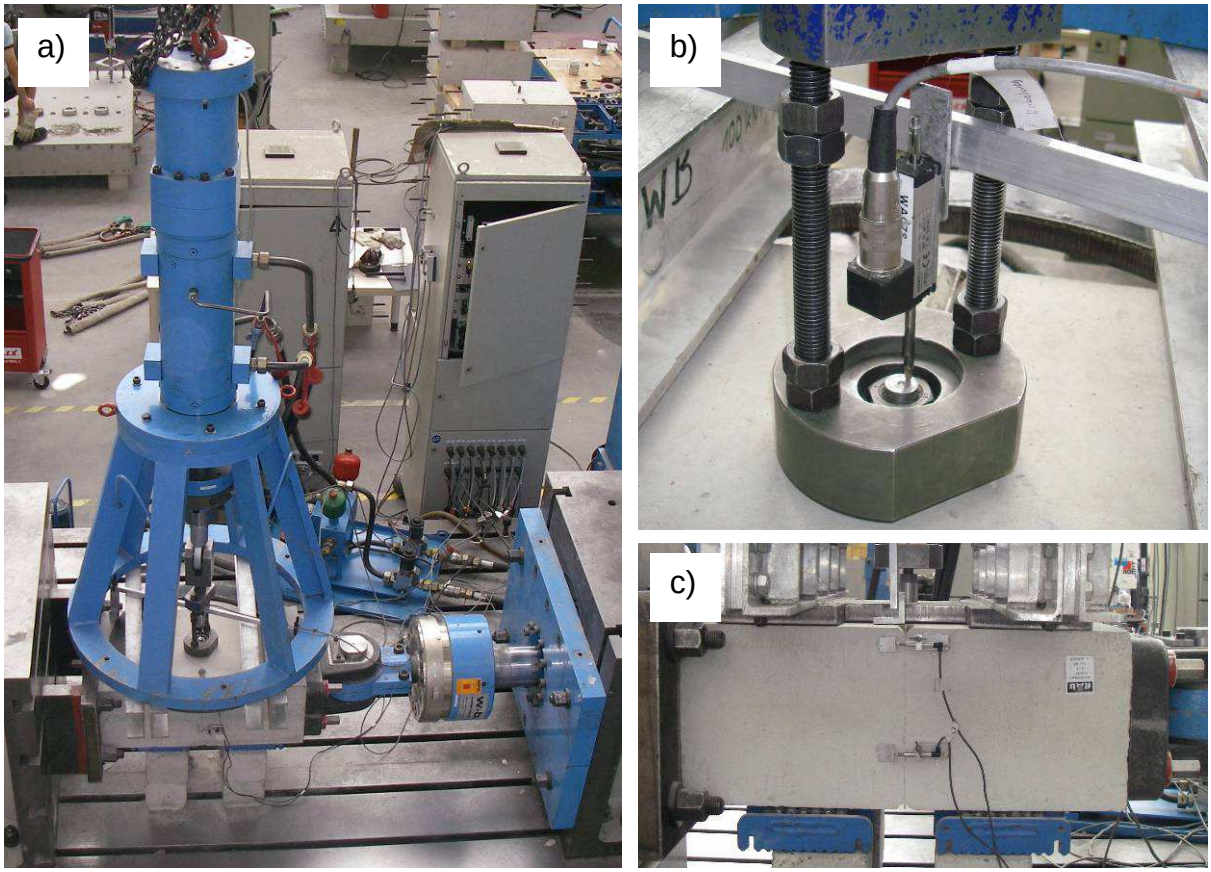

Figure 3.90 Test setup: a) Overview; b) Detail of transducer measuring anchor displacement; c) Detail of transducers measuring crack width

The data were monitored and recorded by a data acquisition system with 10 Hz. The configuration of the multi-axes servo control system was capable to average the readings of the four transducers measuring the crack width and, together with the reading of the actuator loading the headed bolt, to control the 250 kN and 630 kN actuator simultaneously (Figure 3.92a). This allowed synchronisation of anchor load and crack width according to the programmed time histories.

Since the tests are run at quasi-static loading rates, the actual shape of the load or crack time histories (Figure 3.88) is irrelevant. The servo control program consisted of ramps with intermittent breaks for a stable servo control which allowed synchronising load and crack cycles. The ramp target for the crack opening was the maximum crack width of 0.5 mm, and for the crack closing a force target of 300 kN which equals a concrete compression force of 10 % of the concrete strength over the gross cross section area and is deemed to represent full crack closure. The ramp target for the anchor loading was the maximum load level of 27.8 kN, and for the unloading 0.1 kN which was just above zero tension load to avoid conflicts of the servo control due to missing response. The change from one control mode to the other was executed at near zero actuator force. The test series with loading at a

frequency other than the crack cycling frequency (Figure 3.88d) was the most complex protocol. Since 4 crack cycles fell on 1 load cycle, the load cycle had to be cut into 4 quarter cycles. As for the other phasing tests, the load was kept constant during the compression of concrete. An example of measured crack width and load time histories as well as the corresponding control program parameters are given in Figure 3.91.

a)

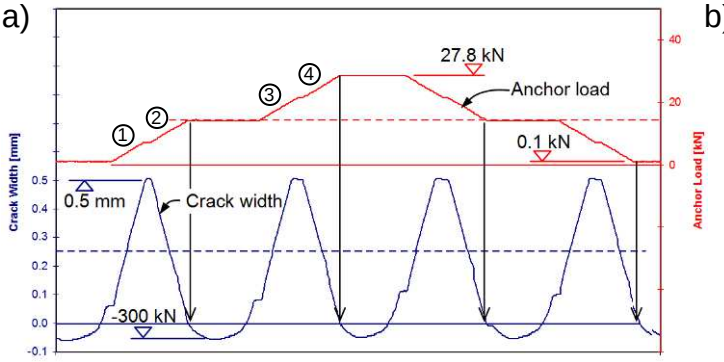

b)

Function	Actuator Anchor Load		Actuator Crack Width	
	Control	Rate/Value	Control	Rate/Value
Ramp①	load	2.78 kN/min	crack	0.2 mm/min
Target	load	6.95 kN	crack	0.5 mm
Break	load	-	crack	-
Ramp②	load	2.78 kN/min	crack	-0.2 mm/min
Target	load	13.90 kN	crack	0.0 mm
Compression	load	-	load	300 kN/min
	-	13.90 kN	load	-300 kN
Ramp③	load	2.78 kN/min	load	0.2 mm/min
Target	load	20.85 kN	load	0.5 mm
Break	load	-	crack	-
Ramp④	load	2.78 kN/min	load	-0.2 mm/min
Target	load	27.80 kN	load	0.0 mm
Compression	load	-	load	300 kN/min
	-	13.90 kN	load	-300 kN

Figure 3.91 a) Windowed time history of synchronised anchor load and crack width (example taken from test series with different cycle frequencies); b) Excerpt of corresponding control program

3.7.2.3 Experimental results and discussion

The diagram in Figure 3.92b depicts an exemplary set of time histories for anchor load, anchor displacement, and crack width, which illustrates the general anchor behaviour during crack cycling. For this test, the anchor load was kept constant while the crack opened and closed 10 times.

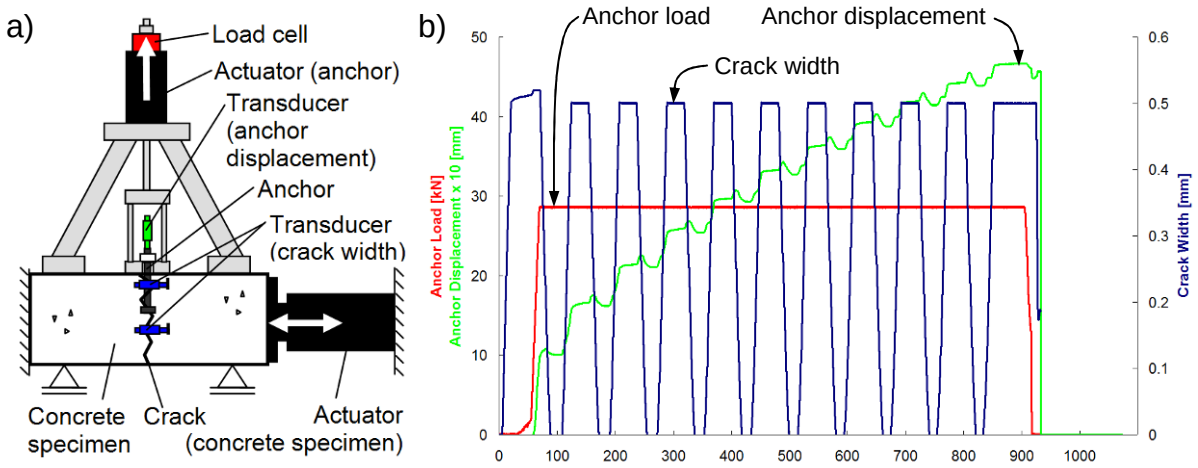

Figure 3.92 a) Setup for simultaneous control of anchor load and crack width; b) Time history of measured anchor load, anchor displacement, and crack width (example taken from test series with constant anchor load)

The headed bolt accumulates displacements for each crack cycle. The displacement during temporarily constant crack width is negligible. When the crack is closed, the anchor is slightly pushed back into the concrete. If unloaded, the anchor experiences no displacement, irrespective of the actual crack width. The influence of the actual load level on the anchor displacement is discussed in the following section.

Figure 3.93 shows exemplary load-displacement curves of each test series depicted in Figure 3.88. Apparently, simultaneous load cycling and its phasing to the crack cycling have a strong impact on the displacement behaviour.

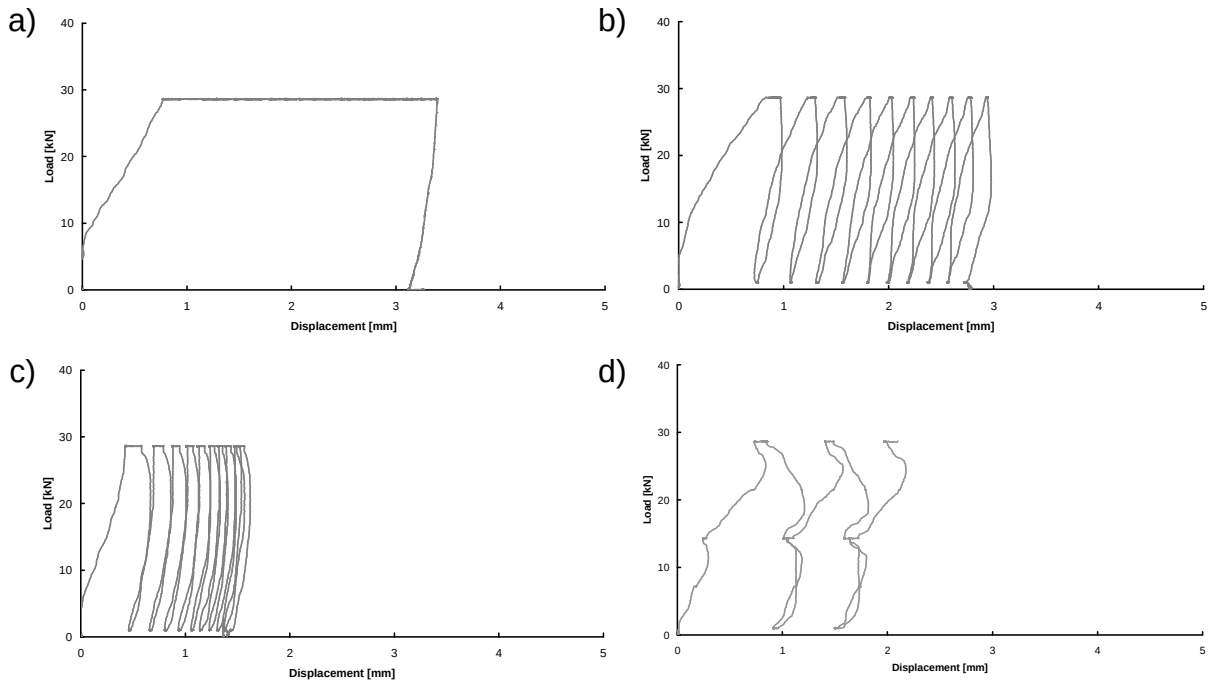

Figure 3.93 Load-displacement curves: a) Cyclic crack and constant load; b) Cyclic crack and cyclic load, in-phase; c) Cyclic crack and cyclic load, out-of-phase; d) Cyclic crack and cyclic load, different frequencies

Figure 3.93a depicts the load-displacement curve of the test with constant anchor load which time histories are shown in Figure 3.92b. Due to the constant load level, the increments in anchor displacement for the individual crack cycles are not visible. Figure 3.93b shows clearly the effect of load cycling on the load-displacement curve. Compared with the constant load test, the displacements are reduced by about 20 %. This effect is more pronounced when load and crack cycling is out-of-phase as shown in Figure 3.93c because large crack width meets low anchor load and vice versa. The restoring action of crack closure results in a decrease of displacement though the load is at its maximum. The unsteadiness in the load-displacement curve in Figure 3.93d reflects the irregular coincidence of load and crack cycles for different frequencies. In conclusion, for a given load level, crack cycling tests are in any case less demanding if the load is simultaneously cycled. The test conditions and key results of all test series are given in Table 3.12.

Table 3.12 Test conditions and key test results of simultaneous load and crack cycling tests

Test series	Crack Width Time History	Anchor Load Time History	Ratio of Frequency	Phasing	Num. of Tests	Anchor Displ. s_{cyc}, mm	CV, %	$\frac{s_{cyc,i}}{s_{cyc,constant}}$
HB constant	10 cycles	constant	1	-	3	3.76	26.7	1.00
HB in-phase	10 cycles	10 cycles	1	0°	3	2.97	4.0	0.79
HB out-of-phase	10 cycles	10 cycles	1	90°	2	1.49	2.4	0.40
HB different frequencies	10 cycles	2.5 cycles	1/4	-	1	2.17	-	0.57

The scatter of the test results was generally very low. Accordingly, the calculated CV are low despite the limited number of test repeats. The extreme CV determined for the test series with constant anchor load is the result of one outlier. The positive effect of simultaneous load and crack cycling can clearly be seen. If compared to constant loading, the anchor displacements are reduced to 80 % in case of in-phase load cycling and to 40 % in case of out-of-phase load cycling. The displacement in case of different frequency is in between the two extreme phasing situations.

3.7.2.4 Phasing as an approach to define the realistic load level

The diagram in Figure 3.94a depicts the average anchor displacements over the crack cycle number for each test series. All curves show a steady increase in anchor displacement. Except for the test with different load and crack cycling frequencies, which result reflects the irregular loading, the displacement increments over cycles are relative constant. The variation in steepness is caused by different demands arising from different phasing, or in other terms, different correlation of anchor load and crack width (Figure 3.94b). In conclusion, anchor displacement is a measurement for the degree of loading.

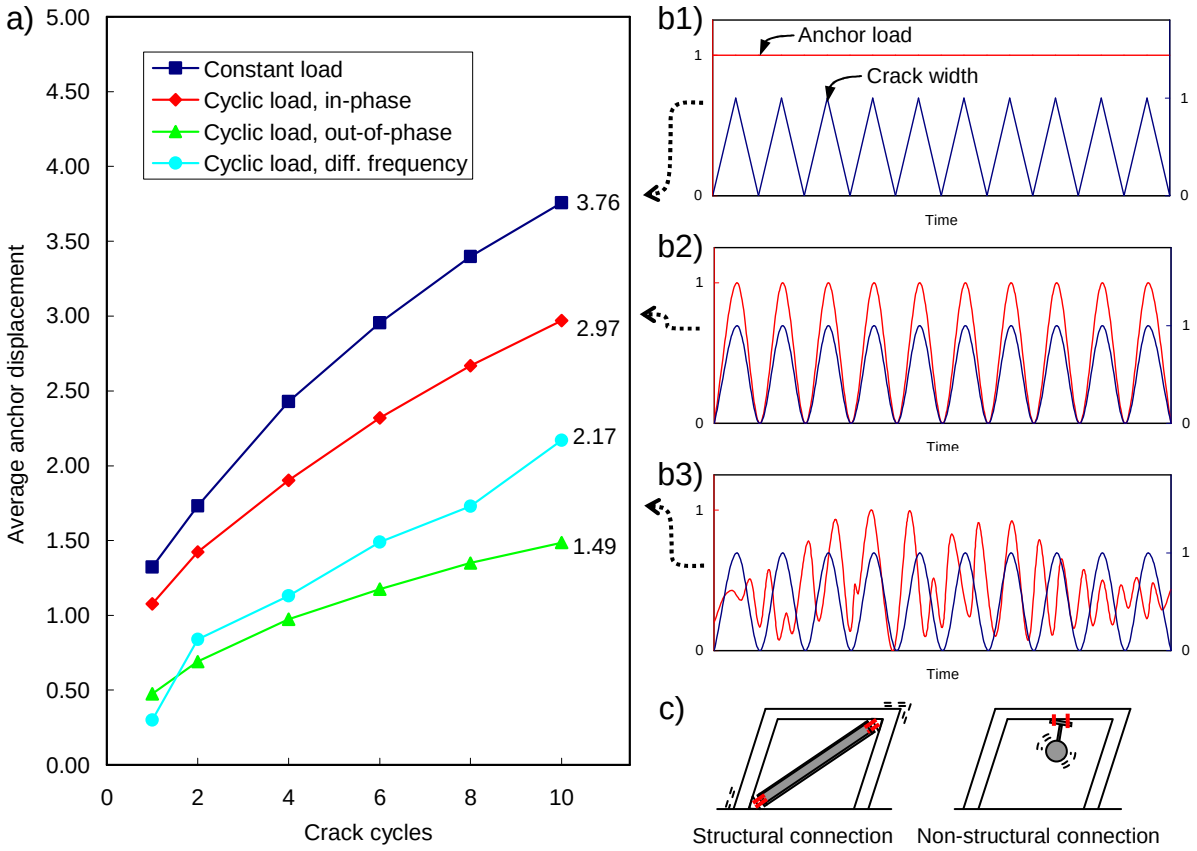

Figure 3.94 a) Average anchor displacement over crack cycle, normalised with reference to the test series with constant loading; b) Phasing or correlation of anchor load and crack width for different time histories; c) Schematic for structural and non-structural connection (concrete curvature and cracks not shown)

The approach to simulate the seismic demand on the anchor during crack cycling by a permanently acting and constant anchor load (Figure 3.94b1) is conservative. Taking this anchor load as the maximum allowable load, i.e. the design load N_{Ed} (Section 3.6.2.1), is probably over-conservative. Anchors installed in structural elements which are exposed to cyclic actions and which concrete therefore shows cycled cracks, are necessarily also loaded cyclically. Provided that the anchors are correctly designed for the demands of the design earthquake, the anchors are loaded at maximum to N_{Ed} but in a cyclic manner. The phasing of load and crack cycling depends on whether the anchor is part of a structural or non-structural connection:

- For structural connections, provided that the structure did not lose too much of its integrity, the load and crack cycling induced by the same cyclic actions are in-phase. In this case, maximum anchor load meets maximum crack width (Figure 3.94b2). Due to the reduced demand the displacement is reduced to about 80 % if compared to the case with constant loading as shown in Section 3.7.2.3.

- For non-structural connections, however, load and crack cycling are not in-phase because the fundamental periods of the structure and the non-structural element are most likely different and out-of-phase (Figure 3.94b3). The seismic loading condition may be assumed to be something in between the out-of-phase loading and loading at different frequencies, which reduces the demand and anchor displacement further. The correlation between maximum anchor load and maximum crack width is much lower. This effect will be dealt with in detail in Section 5.3.2. In view of seismic demands and particularly associated anchor displacements, non-structural applications may be considered as less critical than structural applications of anchors.

In conclusion and with reference to Section 3.6.2.1, constant loading represents the maximum allowable load which corresponds to the adverse loading condition: $N_w = 0.5\ N_{u,cr,m}$. For a more realistic demand, however, the anchor load does not act permanently on that high level. Since crack cycling tests with constant anchor loads are preferred due to easier handling, a reduction of the permanent anchor load level to compensate for the beneficial effect of phasing is desirable. Taking structural connection as the critical design case, and assuming a linear influence of anchor load and crack width on the anchor displacement (Section 3.7.2.5), a reduction of the permanent anchor load to 80 % of the original value would replicate a more realistic demand: $N_w = 0.8 \cdot (0.5\ N_{u,cr,m}) = 0.4\ N_{u,cr,m}$.

3.7.2.5 Displacement as a function of accumulated damage potential

It is obvious that the anchor displacement increases with increasing maximum anchor load N_{max} and increasing maximum crack width w_{max} (refer also to Section 3.6.2.4). As discussed in the previous section, however, the incremental axial displacement Δs during crack cycling also depends on the correlation α of anchor load and crack width which is determined by the phasing and frequency of load and crack cycling:

$$\Delta s = f(N_{max}, w_{max}, \alpha) \qquad \text{Equation 3.21}$$

The high precision achieved for the in-phase and out-of-phase tests as well as for the tests with different frequencies allows the development of an analytical model which describes the relative displacement behaviour of anchors for various load and crack cycling scenarios. This model assumes that the accumulated anchor displacement can be interpreted as accumulated damage potential (ADP) defined by the anchor load N and crack width w. Assuming a linear influence of anchor load and crack width, the ADP can be expressed as an integral:

$$ADP = \int (N \cdot w) \qquad \text{Equation 3.22}$$

To compare the ADP qualitatively for the various protocols and corresponding correlations tested, it is necessary to integrate the load and crack width over the crack cycle n (Figure 3.95a).

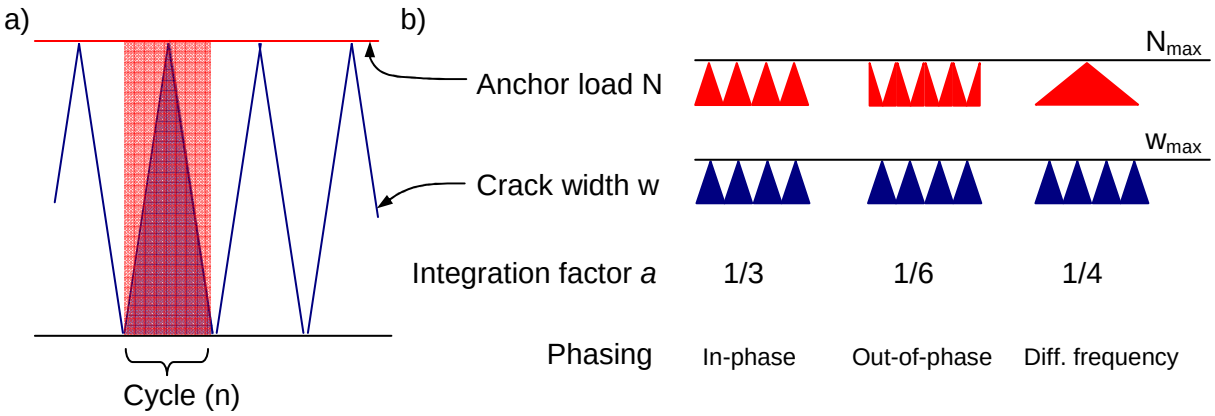

Figure 3.95 a) Illustration of damage potential for a constant anchor load and cycling crack width; b) Integration factor *a*

For the simple linear load and crack cycles with constant maximum anchor load and maximum crack width considered herein, integration factors *a* can be found in the literature for various areas (Figure 3.95b) which simplify the integral to:

$$ADP_n = \Sigma_n (a \cdot N_{max} \cdot w_{max}) \qquad \text{Equation 3.23}$$

The effect of simultaneous anchor load and crack width on the ADP and thus on the resulting displacement becomes obvious when the measured displacement given in Figure 3.94a are compared to the ratios of the specific ADP which can be expressed as the integration factors *a* given in Figure 3.95a. Table 3.13 provides the measured displacements and the ratio of ADP normalised with reference to the in-phase cycling:

Table 3.13 Measured displacements and ratio of ADP, normalised with reference to in-phase cycling

(Normalised)	In-phase	Out-of-phase	Different frequencies
Measured displacement	1.00	0.51	0.73
Ratio of ADP	1.00	0.50	0.75

These figures show a good agreement and therefore support the approach to understand anchor displacement during crack cycling as a function of accumulated damage potential. Since the anchor displacement behaviour is independent of the individual loading rates or cycling frequencies (for a given ratio of load and crack

cycling frequency), observations made for quasi-static rates are also transferable to real-time events.

3.7.3 Conclusions

The effect of simultaneous load and crack cycling and different phasing on the anchor performance was investigated by means of experimental tests. Therefore headed bolts were tested by various load and crack protocols. The use of a multi-axes servo control system, together with improved test setup and instrumentation, enabled precise evaluation of the anchor displacement behaviour.

The crack protocol consisted of 10 uniform cycles. The load was either kept constant or cycled. Load and crack cycling were either in-phase or out-of-phase, or at a different frequency. The displacement is significantly reduced if not only the crack is cycled but also the permanent load. The measured ratio of the displacements if compared to the displacement under constant load is for in-phase loading, out-of-phase loading, and loading at different frequency $1 : 0.8 : 0.4 : 0.6$. It is noted, however, that the results are based on a relatively small number of tests.

Applying a permanent anchor load, which is constant over crack cycling and corresponds to the maximum possible design load, is probably over-conservative for qualification tests. The beneficial effect of phasing suggests a reduction of the permanent anchor load applied during crack cycling. The seismic loading condition for structural anchors may be assumed to correspond to the in-phase loading. The seismic loading condition for non-structural anchorages may be assumed to be in between the out-of-phase loading and loading at different frequency. Taking the in-phase loading as the critical case in respect to anchor displacement, the permanent anchor load during the crack cycling test may be reduced to 80 % of the maximum possible design load to replicate a more realistic demand.

For the qualification of anchors which are used in non-structural applications, the permanent anchor load applied during crack cycling may be further reduced. However, a differentiation of anchors qualified for cases in structural and non-structural applications might be not desired due to the following reasons: (i) The number of tests for anchor qualification will increase and become more costly; (ii) The definition of structural and non-structural connections is probably not always clear and a false assumption may lead to erroneous design.

The anchor displacement experienced during crack cycling can be interpreted as the result of accumulated damage potential which is defined by the anchor load, the crack width and their correlation. It is noteworthy that the displacements measured for in-phase loading, out-of-phase loading and loading at different frequency yields the same ratios as the ratios of the corresponding accumulated damage potentials.

The cyclic anchor load and crack width was programmed as ramps. For quasi-static tests and constant load, the actual shape of the crack width or load histories does not matter. However, in case of simultaneous load and crack cycling, the cumulative damage is a result of load and crack correlation and therefore depends on the actual gradient of the load and crack width cycle. Additional tests should be carried out to investigate the effect of sinusoidal shaped load curve in order to compare the displacements with those derived from triangular shaped load curve.

3.8 Summary

The following findings of the investigations on the component level are critical with respect to seismic tests for the qualification of post-installed anchors.

Seismic qualification does not require:

- High loading rate tests because the effects of high loading rate can be conservatively neglected.
- Particular tests on anchor ductility for seismic applications. It is noted however, that anchor ductility should be evaluated from the results of anchor qualification tests in any case. The classification of anchors allows complying with assumptions made in design codes for ductile design.
- Tests on anchor groups to verify the applicability of effective design concepts. Provided that the scatter in anchor displacement during crack cycling is limited, possible negative effects on the load capacity can be considered by a seismic group factor.
- Technically feasible but extremely challenging simultaneous load and crack cycling tests. The beneficial effect of simultaneous load and crack cycling can be accounted for by an adequate permanent anchor load during crack cycling.

Seismic qualification requires:

- Reference tension and shear tests in cracks with w = 0.8 mm.
- Simulated seismic tension load cycling tests.
- Simulated seismic shear load cycling tests.
- Simulated seismic crack cycling tests.

Seismic qualification tests should reflect:

- Stepwise increasing loading protocols which are anchor load controlled in case of load cycling protocols and crack width controlled in case of crack cycling protocols.

- Test conditions like crack width as well as number and magnitude of cycles which are associated with serviceability level and suitability level.
- Test conditions which retain a realistic level of demand in view anchor load and crack width correlation.
- Procedures which reduces the testing burden to a minimum and boundary conditions as simple and clear as possible to speed up testing and to ensure reproducible results.

Further recommendations for anchor qualification guidelines and design codes are given in Chapter 6.

The following Chapter 4 introduces a proposal for a seismic amendment of anchor qualification guideline which pays respect to the above bullet-point list.

4 Seismic Amendment of Qualification Guidelines

In the course of the investigations presented in Chapter 3, it became apparent that seismic qualification of post-installed anchors has to be evaluated by tension load cycling, shear load cycling and crack cycling tests, as well as by reference tests under monotonic tension and shear load. As discussed in Chapter 2, current anchor qualification guidelines cover the adverse conditions of seismic actions inadequately (*ACI 355.2 (2007)*) or not at all (*ETAG 001 (2006)*). In this chapter, the investigations carried out to come up with a meaningful seismic amendment are presented and discussed. First, the test conditions for testing serviceability and suitability demand levels in separate and unified protocols are developed in Section 4.1. Next, the equivalence of testing both demand levels by separate or unified test protocols is verified by experimental tests in Section 4.2. Complementary to the test conditions defined for the cyclic test protocols, meaningful assessment criteria are outlined in Section 4.4. The verified test protocols together with the essence of the research conducted on seismic anchor qualification in past years finally results in a proposal for the seismic amendment of qualification guidelines which is briefly presented in Section 4.3.

4.1 Development of Test Conditions

The load and crack cycling tests discussed in Sections 3.5 and 3.6 provided valuable information on the behaviour of anchors under simulated seismic test conditions. The test programmes included tests with maximum crack widths of 0.5 mm and 0.8 mm, representing serviceability and suitability level demands (Section 2.1.4 and Section 3.1.5). However, in the course of detailed test data evaluation it became clear that not only the maximum crack width but also the number of cycles should reflect the different conditions of two demand levels. Increased number of cycles has a fundamental impact on the test results (Section 3.5.2.5 and Section 3.6.2.5). Further, corresponding to the approach to run load cycling tests on the serviceability level with a moderate crack width, i.e. 0.5 mm, the crack cycling tests on the serviceability level should be carried out at moderate anchor load levels. The results of the simultaneous load and crack cycling tests discussed in Section 3.7 support this approach. In conclusion, separate tests should reflect the following test conditions:

- Serviceability level tests: Moderate number of cycles n_{cyc}. Moderate crack width w and moderate maximum anchor load N_{max} (or V_{max}) for load cycling

tests, as well as moderate permanent load N_w and moderate maximum crack width w_{max} for crack cycling tests. Moderate crack width w during the residual capacity test.

- Suitability level tests: Extreme number of cycles n_{cyc}. Large crack width w and higher maximum anchor load N_{max} (or V_{max}) for load cycling tests, as well as high permanent load N_w and large maximum crack width w_{max} for crack cycling tests. Large crack width w during the residual capacity test.

Seismic tests are one of the most laborious and expensive test types and therefore running two sets of simulated seismic tests means a large testing burden for laboratories and manufacturer seeking approval for an anchor product. Moreover, the tests probably have to be repeated to finally meet all assessment requirements or to optimize utilization of the anchor. This is all the more true in that the demand in particular on the suitability level is higher than for existing simulated seismic tests according to ACI 355. Therefore it is very desirable to reduce the number of required tests. The most effective approach is to unify the two protocols testing serviceability and suitability level demand in one protocol. To achieve this target it is important to realize the main assessment objectives, refer also to Clause 4.1.1.1 of *ETAG 001 (2006)*:

- Serviceability level tests are in the first place relevant for displacement criteria. Compare to repeated load tests (Section 2.5) and service life tests (Section 2.6). According to Clause 4.1.1.1 (2) of *ETAG 001 (2006)*, the anchor shall provide an adequate resistance to displacements in the serviceability limit state (SLS).
- Suitability level tests are critical for the determination of the residual capacity which is in principle always smaller after cycling on suitability level demand than after cycling on serviceability level demand. According to Clause 4.1.1.1 (1) of *ETAG 001 (2006)*, the anchor shall provide an adequate resistance to failure in the ultimate limit state (ULS).

The development of previously mentioned test conditions and the generation of unified protocols meeting the required assessment objectives is shown in the following.

4.1.1 Development of separate P50 and P90 Protocols

Based on the non-linear analysis of buildings briefly introduced in Sections 3.5.2.1 and 3.6.2.1, the cycle counts of the stepwise increasing load and crack cycling protocols were re-evaluated at the UCSD in 2010 for additional statistical levels (*Wood, R.; Hutchinson, T. et al. (2010)*). In particular for suitability level demand, the cycle count data were evaluated as characteristic values, i.e. 95 % fractile. Moreover, to represent more conservatively the number of cycles contributing to bins of maximum anchor load or crack width the protocol methodology was further substantiated and the protocols modified accordingly. The study presented in *Hutchinson, T.; Wood, R. (2010)* resulted in two modified sets of load and crack cycling protocols:

- P50 Protocols, taken as the arithmetic mean of the cycle count data (50 %) and therefore replicating serviceability level demand.
- P90 Protocols, taken as 95 % fractile (with a 90 % confidence interval) of the cycle count data and therefore replicating suitability level demand.

Exemplary for crack cycling protocols, Figure 4.1 shows the approach of different cycle counts for serviceability and suitability level demands.

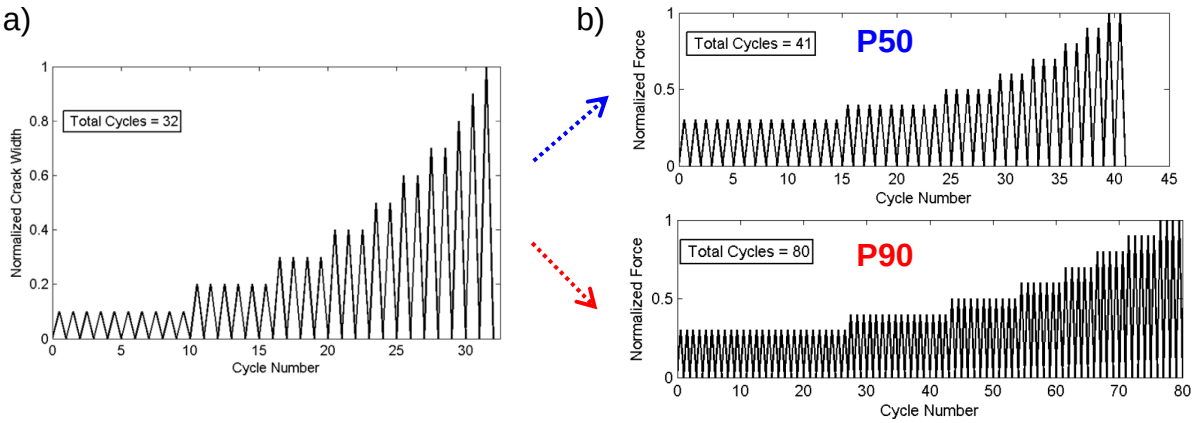

Figure 4.1 Approach for development of separate P50 and P90 Protocols (exemplary for crack cycling): a) Original protocol (*Wood, R.; Hutchinson, T. et al. (2010)*); b) Separated P50 and P90 protocols (*Hutchinson, T.; Wood, R. (2010)*)

All protocols are arranged in steadily increasing 10 % steps. The normalised protocols are given in Figure 4.2.

a)

Load Cycling	Number of Cycles	
Normalized	P50	P90
Anchor Load	Serviceability	Suitability
0.1	50	84
0.2	27	48
0.3	15	27
0.4	9	16
0.5	5	11
0.6	3	7
0.7	3	5
0.8	2	5
0.9	2	5
1.0	2	4
SUM	118	212

b)

Crack Cycling	Number of Cycles	
Normalized	P50	P90
Crack Width	Serviceability	Suitability
0.1	10	17
0.2	7	12
0.3	5	8
0.4	4	6
0.5	3	5
0.6	3	5
0.7	2	4
0.8	2	3
0.9	2	3
1.0	2	3
SUM	40	66

Figure 4.2 P50 and P90 Protocols: a) Load cycling tests; b) Crack cycling tests

4.1.2 Development of crack width and anchor load parameter

Test protocols are incomplete without the definition of the crack width and anchor load parameter: For load cycling test, the target anchor load N_{max} and V_{max} as well as the static crack width w, and for crack cycling test, the target crack width w_{max} and the permanent anchor load N_w need to be defined for the serviceability and suitability level:

- The crack width parameter w and w_{max} are defined as 0.5 mm for serviceability level tests and 0.8 mm for suitability level tests (Section 3.1.5).
- The anchor load parameter N_{max}, V_{max} and N_w are defined as a fraction of the monotonic capacities $N_{u,cr,m}$ and $V_{u,cr,m}$. The deduction of the anchor load parameters for the suitability level and their reduction for the serviceability level is discussed in the following.

In Section 3.5.2.1 it was explained that the target load is taken as the 5 % fractile of $N_{u,cr,m}$ and $V_{u,cr,m}$. For tension load cycling, the maximum acceptable CV of 15 % according to ETAG 001 yields a target load of $N_{max} = 0.75\ N_{u,m,cr}$ (Section 2.1.6) which has to be reached if unreduced seismic capacity is desired. For shear load cycling and associated steel failure, the CV was assumed to be ~ 6 %. However, the cyclic shear test results showed larger CV of about 10 % due to the non-linear influence of concrete on the failure behaviour. In consequence, the target load was reduced to $V_{max} = 0.85\ V_{u,m,cr}$ (Section 2.1.6) for the following tests. These loads, $0.75\ N_{u,m,cr}$ and $0.85\ V_{u,m,cr}$, are the ultimate capacity, representative for suitability level demand (ULS). For serviceability level demand (SLS), these loads have to be reduced to the level the anchor is designed for. Taking $0.75\ N_{u,m,cr}$ and $0.85\ V_{u,m,cr}$ as the ultimate demand (corresponding to $F_{5\%} = F_{Rk}$, Section 2.1.6), the serviceability level demand can be estimated with a partial load safety factor $\gamma_F = 1.35$ and a partial material safety factor $\gamma_M = 1.5$ to $F_{Rd} = F_{Rk} / (\gamma_F \cdot \gamma_M) = F_{Rk} / (1.35 \cdot 1.5) = 0.5\ F_{Rk}$. In

other words, for serviceability level tests, the target loads N_{max} and V_{max} may be reduced by 50 %.

In Section 3.6.2.2 the maximum allowable design load acting on the anchor during crack cycling was derived from the consideration of the LRFD approach and defined as 0.5 $N_{u,cr,m}$. This yields a permanent load for crack cycling test on suitability level of N_w = 0.5 $N_{u,cr,m}$. In Section 3.7.2.4 it was discussed that for a more realistic demand, the permanent anchor load should be reduced. With the assumption that the in-phase loading is critical, the permanent load for the crack cycling tests on serviceability level may be reduced to 80 % of the original value.

Figure 4.3 compiles the crack width and anchor load parameters for all test types. It is noted that due to the low relevance of the crack width on the results of shear load cycling tests, the crack width is taken on the safe side as 0.8 mm throughout the test.

a1)

Tension Cycling	Serviceability	Suitability
Static crack width [mm]	0.5	0.8
Target load [$N_{max}/N_{u,cr,m}$]	0.5·0.75=0.375	0.75

a2)

Shear Cycling	Serviceability	Suitability
Static crack width [mm]	0.8	0.8
Target load [$V_{max}/V_{u,cr,m}$]	0.5·0.85=0.425	0.85

b)

Crack Cycling	Serviceability	Suitability
Target crack width [mm]	0.5	0.8
Permanent load [$N_w/N_{u,cr,m}$]	0.8·0.5=0.4	0.5

Load Cycling Tests:
- Cyclic load to $\mathbf{F_{max}}$
- Constant crack **w**

Crack Cycling Tests:
- Cyclic crack to $\mathbf{w_{max}}$
- Constant load $\mathbf{N_w}$

Figure 4.3 Crack width and anchor load: a) Load cycling tests – a1) tension, a2) shear; b) Crack cycling tests

4.1.3 Development of Unified Protocols and Simple Unified Protocols

The aim of unifying the protocols is to perform only one test and extract all the information required for the assessment at serviceability and suitability level by the following procedure: (i) Perform the test on serviceability level demand and extract the anchor displacement after completing the cycles at serviceability level. (ii) Continue the test on suitability level demand, extract the anchor displacement after completing all cycles and test the residual load capacity under suitability condition. Reducing the number of cycles in the low amplitude bins would further simplify and speed up the test run. To study the feasibility of this approach, two sets of protocols were developed (*Eligehausen, R.; Hutchinson, T. et al. (2010)*):

- Unified Protocols, which unify the demands of serviceability and suitability level demand as described above.
- Simple Unified Protocols, which simplify the protocol to a constant cycle count per step under the assumption that the reduction of low level cycles does not have a significant effect on the test results.

The Unified Protocol cannot be generated by a mere sequential coupling of the P50 and P90 Protocols, in which case the tested anchor would have experienced more demand in the end than required for evaluating the anchor performance at suitability level. Rather the demand put on the anchor after completing the cycles for the serviceability level has to be taken into account when the cycles are completed for the suitability level. This procedure requires the reorganising of cycles which is discussed exemplarily for crack cycling protocols in the following (Figure 4.4).

The comparison of the P50 Protocol and the P90 Protocol (Figure 4.4a) with the corresponding target crack widths w_{max} of 0.5 and 0.8 mm (Figure 4.3b), respectively, on an absolute scale (Figure 4.4b), demonstrates the necessity of a rebinning of the P50 and P90 cycles determined for serviceability and suitability level demand (Section 4.1.1). The target crack widths given in mm suggest rebinning into joined bins of 0.1 mm steps. Therefore, the formerly normalised P50 and P90 Protocols show 5 bins ranging from 0.1 to 0.5 mm and 8 bins ranging from 0.1 to 0.8 mm, respectively (Figure 4.4c). The suitability level bins show larger numbers of cycles than the serviceability level bins. Moreover, the permanent anchor load level N_w during the serviceability level portion of the test is 0.4 $N_{u,cr,m}$, whereas testing on suitability level requires raising of the permanent load level to 0.5 $N_{u,cr,m}$ (Figure 4.3b). Therefore, if the numbers of cycles in the low level bins are reduced to comply with the demands for the serviceability level, the Unified Protocol has to compensate for the damage due to missing cycles and lower permanent anchor load level. The relocation of the cycles is conducted based on the assumption that the accumulated damage potential (ADP, Section 3.7.2.5) is approximately linear to anchor load and crack width. However, a total relocation of the cycle difference accumulating in the serviceability portion of the test would result in extreme large numbers of cycles for the remaining suitability portion of the test and the stepwise increasing crack cycling protocol would lose its steadiness character towards the end. Therefore, under the premise of the linear damage potential rule, a balance of the serviceability and suitability portion of the test is sought (Figure 4.4d).

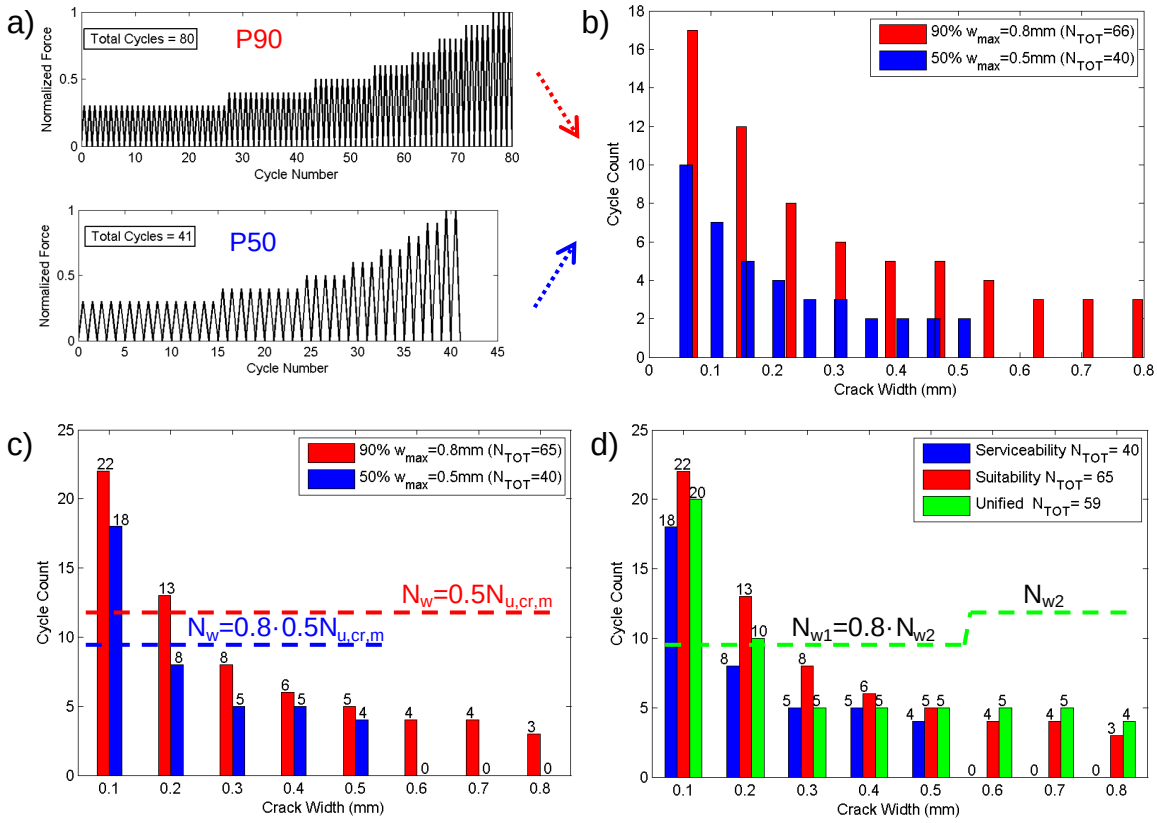

Figure 4.4 Approach for development of Unified Protocols (exemplary for crack cycling): a) Normalised P50 and P90 Protocols (*Hutchinson, T.; Wood, R. (2010)*); b) P50 and P90 Protocols as a function of absolute crack widths; c) P50 and P90 Protocols after rebinning; d) P50 and P90 Protocols unified in one protocol after compensation [Fig. b) to d) after *Eligehausen, R.; Hutchinson, T. et al. (2010)*]

The resulting Unified Protocol reduces the two test procedures into one test but allows extracting assessment data for both, serviceability and suitability level demand (Figure 4.5a). For the Simple Unified Protocol, the Unified Protocol is simplified to a constant cycle count per step. For this approach it is assumed that the reduction of small cycles has no significant influence on the results, either because their effect is too small or the missing accumulated damage is made good for in the following large cycles. The benefits would be a simpler protocol and a reduction in testing time. Therefore, the cycle counts at the beginning of the protocol, which are small in amplitude but high in number, are levelled to the cycle counts further down the protocol (Figure 4.5b).

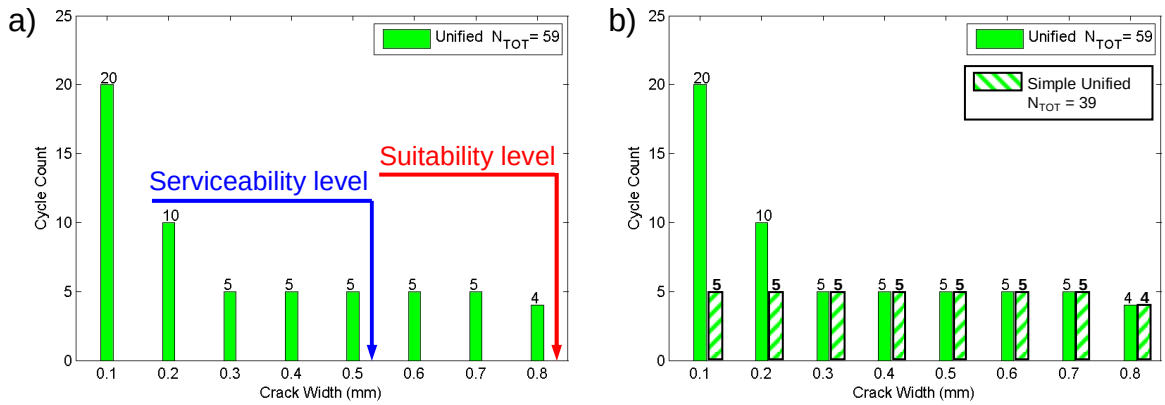

Figure 4.5 Unified and Simple Unified Protocols (exemplary for crack cycling): a) Unified Protocol (*Eligehausen, R.; Hutchinson, T. et al. (2010)*); b) Unified and Simple Unified Protocol opposed

For load cycling protocols, the approach is in principle the same. However, the target anchor loads N_{max} and V_{max} given as a normalised fraction of $N_{u,cr,m}$ and $V_{u,cr,m}$ (Figure 4.3a), respectively, allow for direct rebinning of the cycles into 10 % bins. The transition from serviceability to suitability levels takes place after reaching 50 % of the target anchor load. For tension cycling tests, the transition is accompanied with an increase of the static crack width from 0.5 to 0.8 mm (Figure 4.3a1). Due to the negligible impact of crack width on the test results for shear load cycling tests, the variation of the static crack width is omitted and the whole test is run with the larger crack width of 0.8 mm (Figure 4.3a2). Since a reasonable number of cycles was desired for the Unified Protocol, the cycles of the lowest amplitude were assumed to have virtually no impact on the test results and were truncated therefore, refer also to Section 3.5.2.1.

Figure 4.6 depicts the Unified and Simple Unified Protocols. The normalised load cycling protocols are arranged in steadily increasing 10 % steps. The crack cycling protocols are given in [mm], however, their bins could also be normalised to 8 steps 12.5 % wide.

a)

Load Cycling Anchor Load normalized	Number of Cycles	
	Unified	Simple Unified
0.1	-	-
0.2	25	5
0.3	15	5
0.4	5	5
0.5	5	5
0.6	5	5
0.7	5	5
0.8	5	5
0.9	5	5
1.0	5	5
SUM	75	45

b)

Crack Cycling Crack Width in mm	Number of Cycles	
	Unified	Simple Unified
0.1	20	5
0.2	10	5
0.3	5	5
0.4	5	5
0.5	5	5
0.6	5	5
0.7	5	5
0.8	4	4
SUM	59	39

0.8mm absolute crack width corresponds to 100% normalised crack width

Figure 4.6 Unified and Simple Unified Protocols: a) Load cycling tests; b) Crack cycling tests

4.2 Verification Tests

The test programme discussed in this section is reported in detail in *Mahrenholtz, P. (2010d)*. The aim of the experimental tests was:

- To verify that Unified Protocols can replicate serviceability and suitability level demand and therefore can replace P50 and P90 Protocols.
- To determine whether the Unified Protocols can be replaced by Simple Unified Protocols.
- To evaluate the general practicability of the Unified and Simple Unified Protocols.

Earlier experimental tests (Section 3.5 and 3.6) have shown that tension load cycling is generally not critical for anchors which is in contrast to shear load cycling tests showing pronounced LCF behaviour and crack cycling tests resulting in large axial displacements. Therefore, tension load cycling tests were not included in the verification test programme.

4.2.1 Test protocols, target anchor load and permanent crack width

The P50 and P90 Protocols and the Unified and Simple Unified Protocols are tabulated in Figure 4.2 and Figure 4.6, respectively. Figure 4.7 depicts the load and crack time histories for the load cycling and crack cycling tests, exemplary for the Unified Protocols, the most complex test protocols.

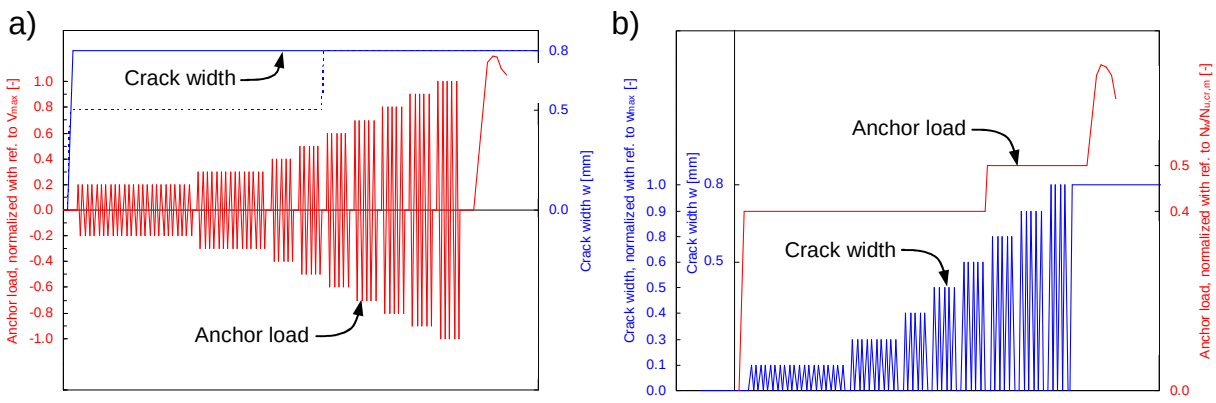

Figure 4.7 Unified Protocols: a) Shear cycling tests; b) Crack cycling test:

The monotonic reference capacities $N_{u,cr,m}$ and $V_{u,cr,m}$, which are required for the determination of V_{max} and N_w, were taken from the cyclic tests discussed in Section 3.5, Table 3.9 and Table 3.10.

Target load for shear cycling tests: UC1 loaded in shear failed in steel at the ultimate capacity of $V_{u,cr,m}$ = 89.2 kN, yielding a target load of V_{max} = 0.85 · 89.2 = 75.8 kN for the suitability level, which is reduced to 0.5 · 75.8 = 37.9 kN for tests on serviceability level. EAb1 loaded in shear failed in steel at the ultimate capacity of $V_{u,cr,m}$ = 32.4 kN, yielding a target load of V_{max} = 0.85 · 32.4 = 27.5 kN for the suitability level, which is reduced to 0.5 · 27.5 = 13.8 kN for tests on serviceability level.

Permanent load for crack cycling tests: EAb1 loaded in tension was pulled through at the ultimate capacity of $N_{u,cr,m}$ = 21.8 kN, yielding a permanent load of N_w = 0.5 · 21.8 = 10.9 kN for the suitability level, which is reduced to N_w = 0.4 · 21.8 = 8.7 kN for tests on serviceability level. For the test on HB1, no data for monotonic capacities were available and the mean capacity was calculated based on the assumption that the characteristic strength equals 75 % of the mean strength (Section 2.1.6) and with reference to *CEN/TS 1992-4 (2009)* (Section 3.1.2) to $N_{u,cr,rm} = N_{Rk,p} / 0.75 = 6\ A_h\ f_{ck,cube} / 0.75 = 8 \cdot 268\ mm^2 \cdot 33.2\ N/mm^2 \cdot 10^{-3} / 0.75$ = 71.4 kN. The permanent load can then be determined to N_w = 0.5 · 71.4 = 35.7 kN for the suitability level, which is reduced to N_w = 0.4 · 71.4 = 28.6 kN for tests on serviceability level.

4.2.2 Test setup and testing procedure

The full set of test protocols (P50, P90, Unified and Simple Unified Protocol) were evaluated by tests on UC1 anchor (Figure 3.1b) for load cycling and by tests on HB1 (Figure 3.1a) for crack cycling protocols. The reason to use the HB1 anchor was to benchmark displacement criteria for future tests on post-installed anchors. To evaluate the general practicability of the Unified and Simple Unified Protocols further,

additional load cycling tests and crack cycling tests were carried out on the EAb1 anchor. Several tests had to be repeated because of premature failure during cycling. In total, some 70 tests were conducted. The outline of the test programme is also apparent in Table 4.1.

As anchorage material, normal weight concrete C20/25 with a mean tested concrete tested cube compressive strength between $f_{cc,150}$ = 32.7 and 33.7 MPa were used. The concrete specimens were identical to the wedge-split slabs used for cyclic load tests (Section 3.5.2.2) and the special concrete specimens used for simultaneous load and crack cycling tests (Section 3.7.2.2), respectively. The special concrete specimens for testing of post-installed anchors were used on both sides for which one pilot hole was drilled in the center of each side prior to initial cracking. Just before installation of the anchor, the pilot hole was reamed to the required diameter. The specimens for testing headed bolts were delivered with already cast-in anchors and used on one side only. However, to guide the cracking in the axis of the anchor, a pilot hole was also drilled on the opposite side of the slab.

The test setup and procedure, as well as anchor installation and crack formation is basically the same as described in the relevant sections before and therefore is not repeated here in detail. The finally proposed procedures for seismic testing are summarised in Section 4.3.2. As an improvement to previous shear tests, however, the slab was mounted on rollers which enabled an accelerated repositioning of the slab for the next test position (Figure 4.8a). Regarding the crack width measurement for crack cycling tests, it is noted that two electronic displacement transducers were installed on either side of the anchor close to the fixture (Figure 4.8b). The measurement accuracy was therefore reduced if compared to the four point measurement introduced for the simultaneous load and crack cycling tests in Section 3.7.2.2. In particular the bending moment introduced into the concrete specimen by the actuator support during anchor loading results in increased crack widths measured at the top of the specimen if compared with the bottom of the specimen. However, for the seismic amendment of qualification guidelines, a simpler test setup was preferred. Further details are given in *Mahrenholtz, P. (2010d)*.

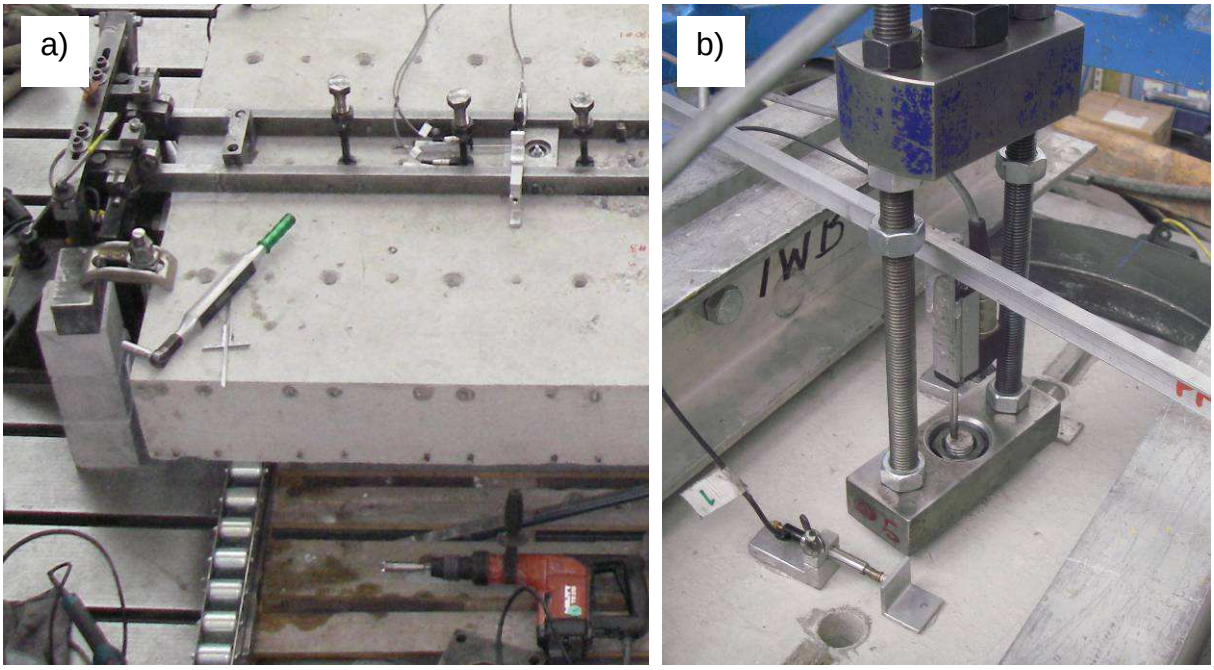

Figure 4.8 a) Bird's eye view on test setup mounted on rollers for shear cycling tests; b) Detail of crack width instrumentation for crack cycling test

4.2.3 Influence of servo controlling on test results

The servo hydraulic system is the main component of the test equipment used for simulated seismic tests as discussed in previous sections. However, there are alternatives for conducting load or crack cycling tests. The crack movement can be generated by simple hydraulic actuators either as a set of two counteracting actuators or by single action actuators in combination with external prestressing of the concrete specimen. The permanent load can be applied by means of spring discs or air pressure. Sequential hammering of wedges can create stepwise increasing crack widths in wedge-split concrete slabs. Also repeated load tests can be performed by simple actuators, particularly for the limited number of cycles in case of simulated seismic tests.

However, servo hydraulic systems outclass any other method in terms of flexibility, handiness, reproducibility, and accuracy. The propagation of servo hydraulic systems for anchor qualification testing will increase in future. Therefore it is important to understand the servo control methods and their influence on the test results. In the following, some critical aspects are briefly discussed.

4.2.3.1 Load cycling tests

Cyclic loads in the context of seismic actions are commonly understood as a sinusoidal loading. Therefore, ACI 355 stipulates sinus load cycles for simulated

seismic tests. The servo control executes each sinus load controlled with defined load amplitudes. To avoid uncontrolled slip during load reversal (Section 3.5.2.2), however, ACI 355 allows to approximate the sinus cycles by two half sinus cycles with interconnecting displacement controlled ramps (Figure 4.9a).

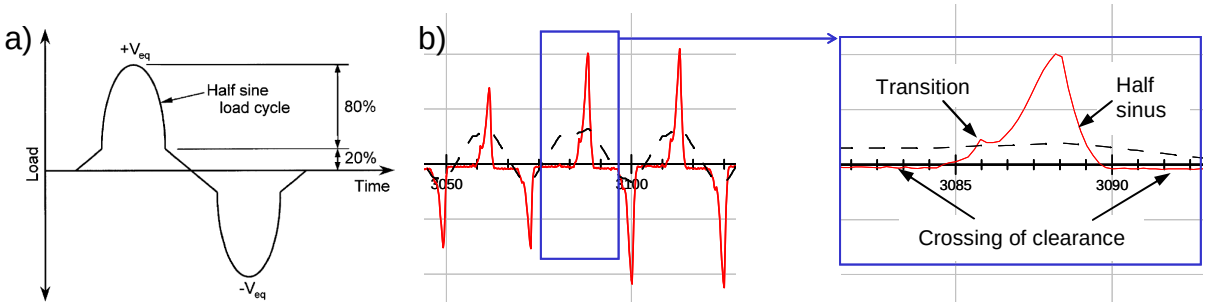

Figure 4.9 a) Permitted approximation of alternating seismic shear cycle after *ACI 355.2 (2007)*; b) Windowed load history of exemplary test and close-up

The transition from the ramp to the half sinus wave at 20 % of the load amplitude is demanding for the servo control system. In particular for small initial amplitudes as stipulated for the Unified Protocols, the point of transition and the actual amplitude maximum are extremely close together. The servo control system staggers and hardly keeps on track (Figure 4.10a). For large cycle amplitudes near ultimate load at the end of the Unified Protocols, the servo control system struggles with the load control mode when the the system becomes increasingly inelastic and therefore easily loses control (Figure 4.10b).

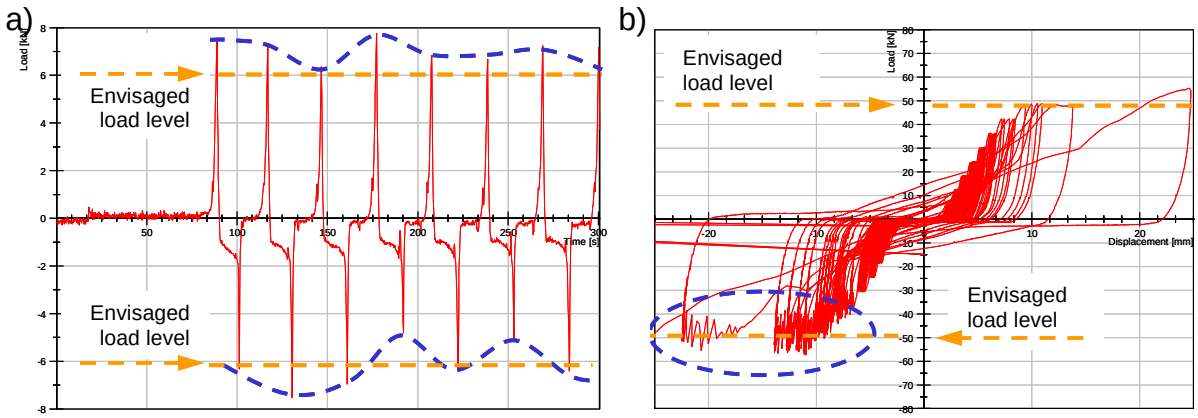

Figure 4.10 a) Over- and undershooting for very low load amplitudes (load-time history); b) Lost of servo control in the inelastic range of the anchor (load-displacement curve)

To prevent overshooting and to reduce the risk of uncontrolled slip, small displacement rates are required for the interconnecting ramps. This, in turn, increases the testing time for which the ramps are decisive because the clearance of the annular gap is crossed during this phase. Figure 4.9b shows the windowed load

history measured for an exemplary test. The horizontal sections represent the time required for crossing of the clearance. It can also be clearly seen that the load curve does not simulate an ideal sinusoidal shape and instead is described by a series of spikes, similar to a direct delta function.

In conclusion, the load control mode and sinus approximation proposed in ACI 355 is extremely demanding for stepwise increasing seismic shear protocols but despite the efforts, the goal of generating nearly sinusoidal load histories is not achieved. Since the load is cycled at quasi-static loading rates, the actual shape of the load curve over time does not matter. These aspects together with the problems encountered for the shear cycling tests on the UC1 anchor strongly suggest a modification of the procedure. To this end, a simplified loading scheme based solely on displacement controlled ramps with load targets was developed (Figure 4.11a) and successfully tested on the EAb1 anchor. This approach enabled a faster test run and experienced no servo control problems at all. The load histories were actually smoother than those of the former half sinus approximation. The loading scheme is also applicable to tension load cycling tests for which the target loads are N_{max} and N_{min}.

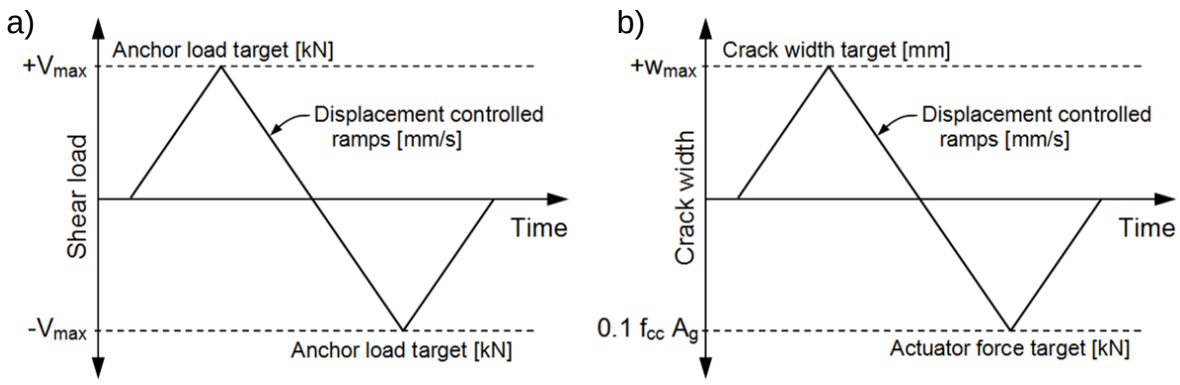

Figure 4.11 Simplified servo control schema: a) Shear load cycling; b) Crack width cycling

4.2.3.2 Crack cycling tests

Other than for seismic load cycling tests, there is currently no procedure for seismic crack cycling tests given in any anchor qualification guideline. However, intuitively a sinusoidal crack width function was considered in the style of the simulated seismic tests according to ACI 355. The zero load crossing of the actuator in load control mode is unproblematic in crack cycling tests since the cycling actuator is connected to the specimen without any slackness. However, the maximum crack width specified in mm requires a crack width controlled sinus function, whereas the minimum crack width is defined as the compression force corresponding to 10 % of the compressive strength of the concrete section ($0.10\ f_{cc,150}\ A_g$). Furthermore, the crack width cycling is not synchronous with the actuator force cycling (Figure 4.12a). In consequence,

the sinus cycles require splitting into two differently controlled half sinus and an interconnecting ramp to transit from one half sinus to the other (Figure 4.12b).

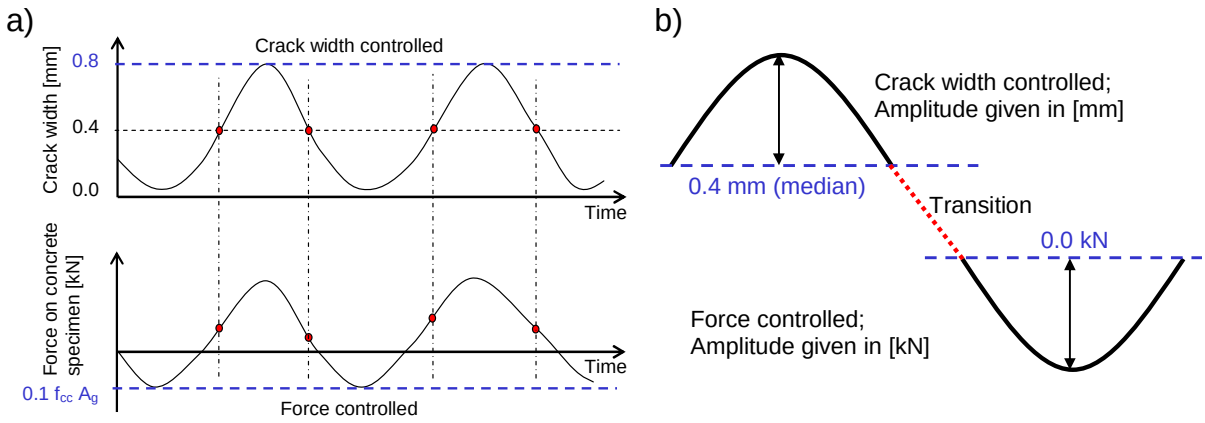

Figure 4.12 a) Schematic history of the crack width and the load on the concrete slab over time; b) Illustration of the principle for approximation of crack width cycling

This approach is very complex and demanding for the servo control and programmer. To meet the crack width target, small und therefore time consuming crack cycling frequencies are required. The crack width histories of exploratory tests, however, were way off the sinusoidal shape. Therefore, a simplified servo control scheme based on displacement controlled ramps was also developed for crack cycling tests (Figure 4.11b). With crack width targets for the crack opening and actuator compression force targets for the crack closure, the tests on the EAb1 and HB1 anchor showed satisfactory crack width histories.

4.2.3.3 Pullout tests

For the pullout tests conducted after the crack cycling tests discussed in Section 4.2.4.2, the crack was first opened to the specified target crack width. Then the actuator was kept force controlled to approximate the condition present for the corresponding monotonic tests in static cracks. The effect of the servo control settings during the pullout test on the test results is briefly discussed in the following.

When the anchor is loaded to failure to determine the residual load capacity, the crack is forced open due to wedging effects. This behaviour is much less pronounced for shear loading than for tension loading. However, in particular for expansion and undercut anchors loaded in tension, the wedging effect caused by the conical shape of the anchor head is substantial.

For tension loading and a given anchor product, the degree of crack opening due to wedging primarily depends on the type of concrete specimen. In case of wedge-split

slabs, the crack opening depends on the response of the tensioned reinforcement in the slab (Figure 4.13a1). In case of special concrete specimens, the specimen remains connected to the actuator after cycling and the crack opening depends on the control mode of the actuator during the pullout of the anchor: If the actuator force on the specimen is controlled by the crack width, the actuator counteracts the expansion force of the anchor to keep the crack width constant (Figure 4.13a2). Alternatively, the actuator force on the specimen can be kept constant during the pullout to approximate the situation present in wedge-split test (Figure 4.13a3). In this case, however, the opening is not limited and can be considerable (Figure 4.13b).

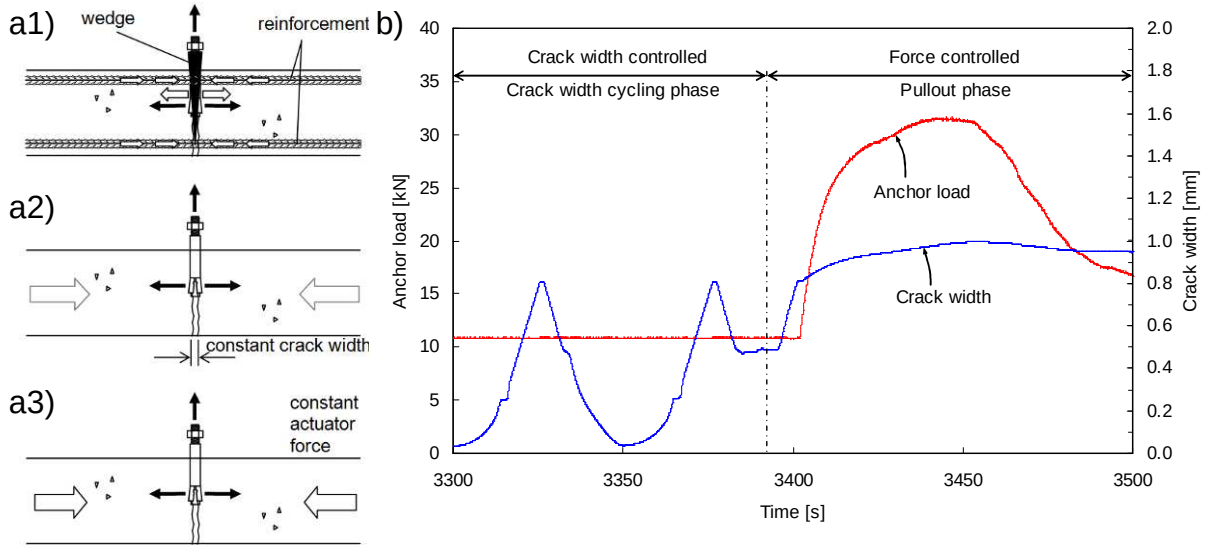

Figure 4.13 a) Crack opening mechanisms during pullout test; b) Example anchor load and crack width time history illustrating crack opening in case of force controlled actuator during pullout of anchor

The evaluation of the test data gained in the crack cycling test programme discussed in Section 3.6.2 yielded that on average, the crack opens approximately 0.1 mm in case of wedge-split concrete slabs, and 0.4 mm in case of force controlled special concrete specimens. The larger crack opening is caused by the low reinforcement ratio (0.65 %) and large debonded length (250 mm = 16.5 d) in the special concrete specimens.

Variable crack widths have a strong impact on the test results and influence the outcome of the test data assessment for which monotonic and residual load capacities potentially gained in different test specimens are opposed (Section 4.4). To ensure reproducible test results, either the crack width needs to be controlled or the test specimen has to be specified in detail. It may be assumed that for reinforcing ratios $\geq$ 1 % and debonding length $\leq$ 3 d the additional crack opening due to wedging is limited to about 0.1 mm.

It is noted, however, that crack width control is not applicable for the service life tests according to ACI 355 and ETAG 001 (Section 2.6.1 and Section 2.6.2) which crack cycling is realistically generated by the restoring force of the reinforcement *Mahrenholtz, C.; Silva, J. et al. (2012)*. Consequently, the crack width during the residual capacity tests is also controlled by the tensioned reinforcement as illustrated in Figure 4.13a. Reference is made to *Mahrenholtz, C.; Silva, J. et al. (2012)*.

4.2.4 Experimental results and discussion

As the aim of the verification tests was to verify the Unified and Simple Unified Protocol, only test results relevant in this respect are presented in the following. In particular, the aspects of anchor performance are not assessed in detail.

Testing started with the most demanding protocol to avoid unnecessary failed attempts in that premature failure is more likely for the most demanding protocol than for any other protocol. Therefore, the test series on the UC1 and HB1 anchors started with the P90 Protocol and the test series on the EAb1 anchors with the Unified Protocol.

4.2.4.1 Load cycling tests

All UC1 and EAb1 anchors failed in steel. LCF occurred for both anchor products during cycling and the target load had to be reduced twice. After reduction to 64 % and 72 % of the original values for UC1 and EAb1, respectively, all cycles were completed and the residual capacity corresponded to 102 % and 94 % of the monotonic capacity, respectively. Table 4.1 provides the test conditions and key test results of the relevant load cycling tests.

Table 4.1 Test conditions and key test results of verification tests (load cycling)

Anchor Type, Anchor Size, Emb. Depth	Proto. Type (1)	Num. of Cycles	Crack Width w	Target Load $V_{max}/V_{u,cr,m}$	$s_{cyc,m}$, mm	CV, %	$V_{u,m}$, kN	CV, %
UC1; M10; 90 mm	P90	212	0.8 mm	0.85	Failure in cycle 201			
		1st reduction		0.8·0.85	Failure in cycle 204			
		2nd reduction		0.8·0.8·0.85	9.95	13.3	93.0	11.7
	P50	118	0.8 mm	0.5·(0.8·0.8·0.85)	4.90	4.2	91.9	9.8
	Uni	75	0.8 mm	0.8·0.8·0.85	12.34	20.9	91.4	18.9
			0.8 mm	0.5·(0.8·0.8·0.85)	5.10	6.6	Service. level	
	SUni	45	0.8 mm	0.8·0.8·0.85	13.41	6.7	88.4	6.5
			0.8 mm	0.5·(0.8·0.8·0.85)	5.13	22.3	Service. level	
EAb1; 1/2"; 83 mm	Uni	75	0.8 mm	0.85	Failure in cycle 69			
		1st reduction		0.8·0.85	Failure in cycle 70			
		2nd reduction		0.9·0.8·0.85	6.31	9.9	30.6	4.7
			0.8 mm	0.5·(0.9·0.8·0.85)	3.66	9.3	Service. level	
	SUni	45	0.8 mm	0.9·0.8·0.85	6.32	20.6	32.0	3.9
			0.8 mm	0.5·(0.9·0.8·0.85)	3.87	12.8	Service. level	

(1) Protocol Type: Uni = Unified Protocol; SUni = Simple Unified Protocol

Exemplary for the tests on the UC1 anchor, the load-displacement curves are shown for the following protocols: P50 and P90 Protocol in Figure 4.14; Unified and Simple Unified Protocol in Figure 4.15. In addition, example load-time and displacement-time histories are shown in Figure 4.16.

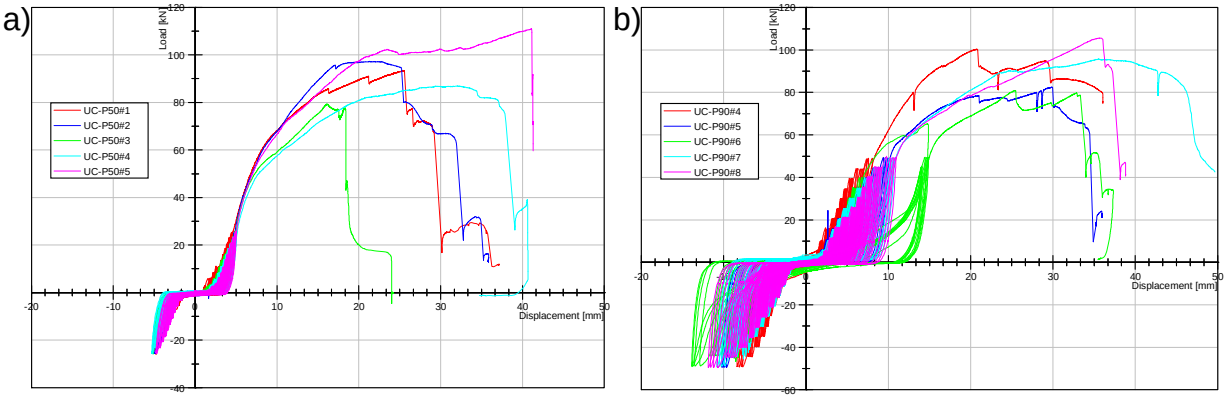

Figure 4.14 Load-displacement curves of load cycling tests on UC1: a) P50 Protocol (w = 0.8 mm; V_{max} = 24.3 kN); b) P90 Protocol (w = 0.8 mm; V_{max} = 48.1 kN)

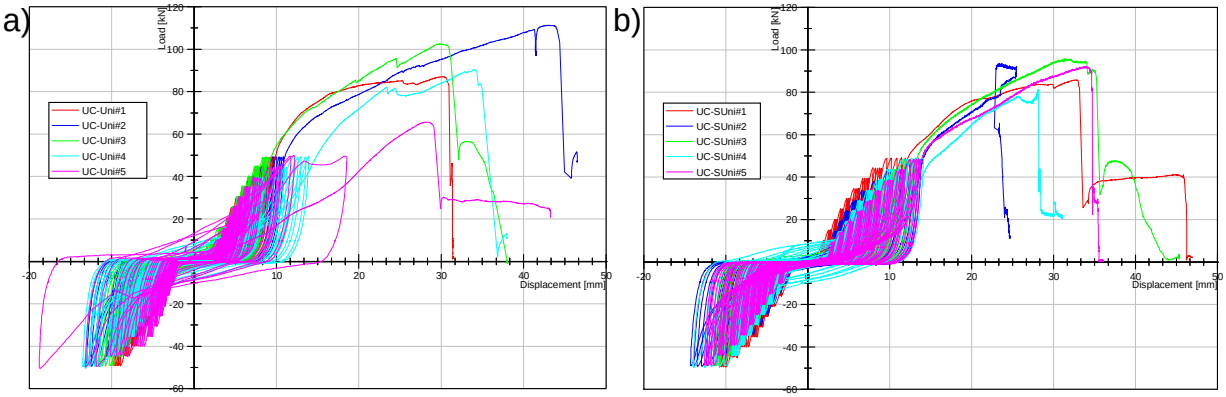

Figure 4.15 Load-displacement curves of load cycling tests on UC1 (w = 0.8 mm; V_{max} = 48.1 kN): a) Unified Protocol; b) Simple Unified Protocol

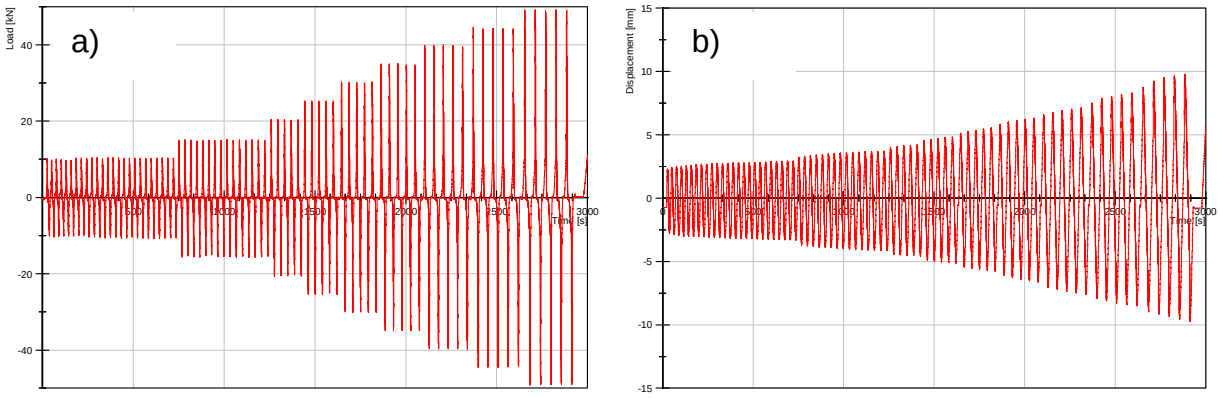

Figure 4.16 Example time histories of Unified Protocol test on UC1: a) Load; b) Displacement

For a better comparison of the effect of the protocol types on the test results, Table 4.2 compares the relevant data for the UC1 and EAb1 anchor. The respective mean ultimate load $V_{u,m}$ measured for the P90, Unified, and Simple Unified Protocol can be deemed as statistically equivalent. The same applies to the mean displacement $s_{cyc,m}$ measured after completion of all cycles on serviceability level (for the P50, Unified,

and Simple Unified Protocol) and measured after completion of all cycles on suitability level (for the P90, Unified, and Simple Unified Protocol). The scatter is reasonably small for s_{cyc} and V_u. The high CV for the Unified Protocol test series on the EAb1 anchor is caused by one outlier which apparently nearly experienced LCF during cycling. This confirms that the behaviour of anchors loaded in shear is robust if LCF is excluded by sufficient reduction of the load level. The mean displacements at serviceability level are about 5.0 mm for the UC1 and 3.7 mm for the EAb1 anchor.

Table 4.2 Comparison of selected test results (load cycling)

Anchor Type	Protocol Type(1)	Displacement $s_{cyc,m}$ on Serviceability Level	Displacement $s_{cyc,m}$ on Suitability Level	Residual Capacity $V_{u,m}$
UC1	P50	4.90 mm	-	91.9 kN
	P90	-	9.95 mm	93.0 kN
	Uni	5.10 mm	12.34 mm	91.4 kN
	SUni	5.13 mm	13.41 mm	88.4 kN
EAb1	Uni	3.66 mm	6.31 mm	30.6 kN
	SUni	3.87 mm	6.32 mm	32.0 kN

(1) Protocol Type: Uni = Unified Protocol; SUni = Simple Unified Protocol

Plotting the displacement over the anchor load level of the tests on the UC1 anchor (Figure 4.17) allows analysing the displacement behaviour for various load cycling protocols. The averaged displacement increase per cycle (Figure 4.17a) spread and do not show a uniform correlation. In contrast, the averaged displacements experienced for each load step shows a good correlation of absolute displacement and load level (Figure 4.17b). For all load protocols, the anchor displacement depends on the load level, rather than on the number of cycles. In other terms, the cyclic load paths follow the monotonic curve irrespective of the actual load cycle regime, provided that no LCF occurs. This finding complies with the observations earlier made on stepwise increasing load protocols.

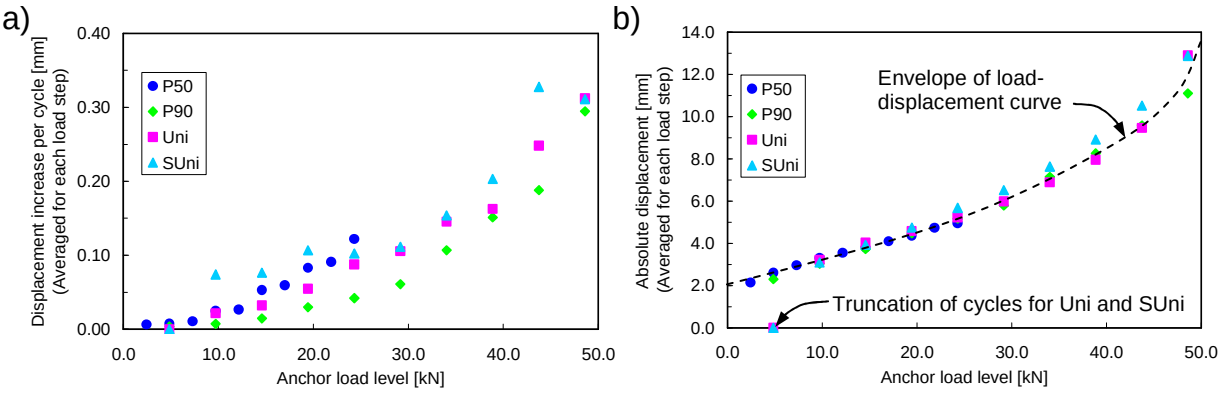

Figure 4.17 Displacement versus anchor load level (averaged for each load step): a) Displacement increase per cycle; b) Absolute displacement

Figure 4.17b illustrates the increasing non-linearity in the anchor response. Further, it is demonstrated that the truncation of the cycles of the lowest amplitude for the Unified and Simple Unified Protocol had no effect on the anchor displacement. Moreover, the reduction in number of cycles for the second and third but lowest amplitudes of the Simple Unified Protocol did not have any effect either.

4.2.4.2 Crack cycling tests

All EAb1 anchors failed in pull-through mode. In the first test series failure occurred during crack cycling and the permanent load was reduced to 87.5 % for which all test repeats completed all cycles. The residual load corresponded to 111 % of the monotonic capacity. The HB1 anchors completed all cycles at first go and failed in concrete. The residual load corresponded to 88 % of the calculated monotonic capacity. Table 4.3 provides the test conditions and key test results of the relevant load cycling tests.

Table 4.3 Test conditions and key test results of verification tests (crack cycling)

Anchor Type, Anchor Size, Emb. Depth	Proto. Type (1)	Num. of Cycles	Crack Width w_{max}	Num. of Tests	Permanent Load $N_w/N_{u,cr,m}$	$s_{cyc,m}$, mm	CV, %	$N_{u,m}$, kN	CV, %
EAb1; 1/2"; 83 mm	Uni	59	0.8 mm	1	0.5	Failure in cycle 57			
		1st reduction		5	0.875·0.5	23.18	22.5	24.3	26.7
			0.5 mm	-	0.875·0.4	8.52	9.1	Service. level	
	SUni	39	0.8 mm	5	0.875·0.5	26.47	12.4	17.0	16.7
			0.5 mm	-	0.875·0.4	8.84	9.6	Service. level	
HB1; M20; 100 mm	P90	66	0.8 mm	4	$0.5 \cdot 8 \cdot A_h \cdot f_c$	5.90	6.6	59.9	13.7
	P50	40	0.5 mm	4	$0.4 \cdot 8 \cdot A_h \cdot f_c$	2.74	10.8	71.8	5.0
	Uni	59	0.8 mm	4	$0.5 \cdot 8 \cdot A_h \cdot f_c$	6.87	8.8	62.8	17.4
			0.5 mm	-	$0.4 \cdot 8 \cdot A_h \cdot f_c$	2.87	7.4	Service. level	
	SUni	39	0.8 mm	4	$0.5 \cdot 8 \cdot A_h \cdot f_c$	6.48	18.1	54.0	20.5
			0.5 mm	-	$0.4 \cdot 8 \cdot A_h \cdot f_c$	2.92	23.7	Service. level	

(1) Protocol Type: Uni = Unified Protocol; SUni = Simple Unified Protocol

Exemplary for the tests on the HB1 anchor, the load-displacement curves are shown for the following protocols: P50 and P90 Protocol in Figure 4.18; Unified and Simple Unified Protocol in Figure 4.19. In addition, example crack-time and displacement-time histories are shown in Figure 4.20.

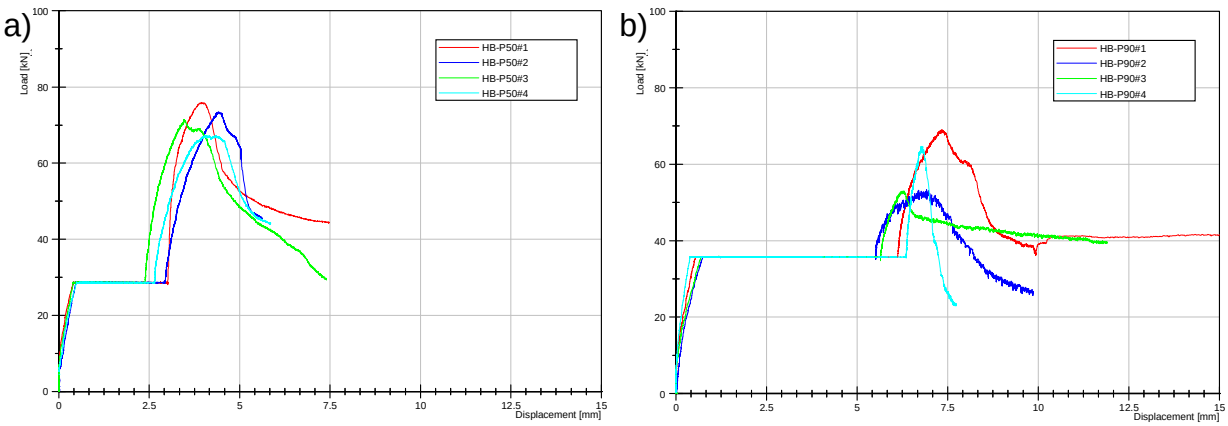

Figure 4.18 Load-displacement curves of load cycling tests on HB1: a) P50 Protocol (w_{max} = 0.5 mm; N_w = 28.6 kN); b) P90 Protocol (w_{max} = 0.8 mm; N_w = 35.7 kN)

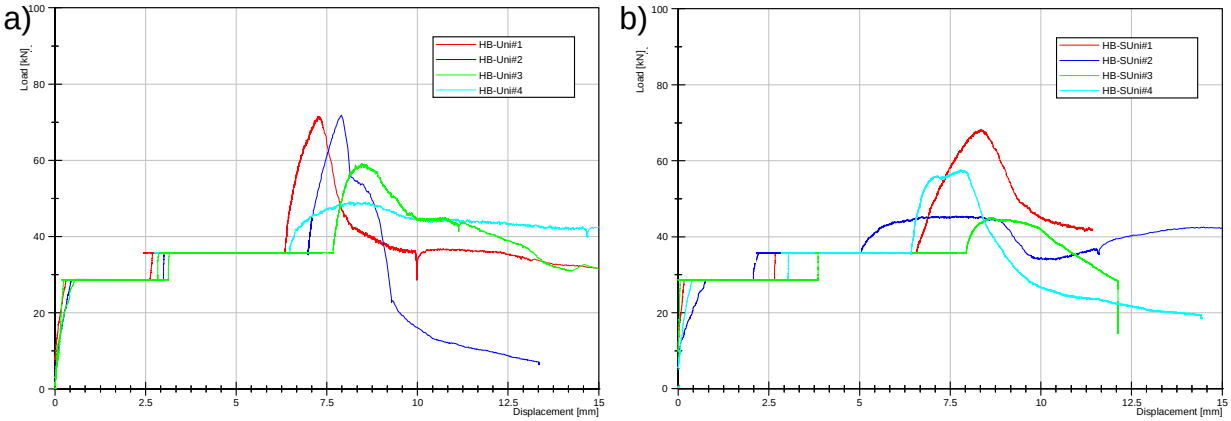

Figure 4.19 Load-displacement curves of load cycling tests on HB1 (w_{max} = 0.8 mm; N_{w1} = 28.6 kN; N_{w2} = 35.7 kN): a) Unified Protocol; b) Simple Unified Protocol

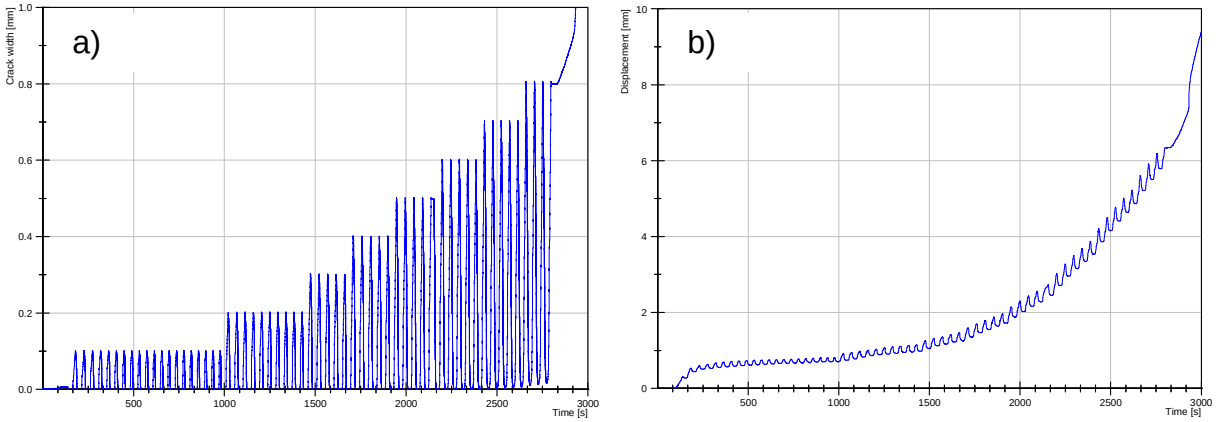

Figure 4.20 Example time histories of Unified Protocol test on HB1: a) Crack; b) Displacement

For a better comparison of the effect of the protocol types on the results, Table 4.4 compares the relevant data for the EAb1 and HB1 anchor. The respective mean ultimate load $N_{u,m}$ measured for the P90, Unified, and Simple Unified Protocol show large variations. For the HB1 anchor, the P50 Protocol yields the highest capacity due to the smallest reduction in anchor displacement after completion of the crack

cycles. The P90 and Unified Protocol yield similar capacities. It is noteworthy that for both anchors, EAb1 and HB1, the ultimate load after the Simple Unified Protocol is substantially lower than for the Unified Protocol. However, the test series showed extreme scatter in particular at suitability level and therefore confirmed observations made in earlier studies on anchor behaviour under crack cycling, though the high CV for the Simple Unified Protocol tests on the HB1 anchor was unexpected and cannot be conclusively reasoned. However, the displacements $s_{cyc,m}$ at serviceability level measured for the P50, Unified, and Simple Unified Protocol match considerably well, whereas the mean displacements after completion of all cycles on suitability differ. The mean displacement at serviceability level is about 5.0 mm for the EAb1 anchor, and 2.9 mm for the HB1 anchor.

Table 4.4 Comparison of selected test results (crack cycling)

Anchor Type	Protocol Type(1)	Displacement $s_{cyc,m}$ on Serviceability Level	Displacement $s_{cyc,m}$ on Suitability Level	Residual Capacity $N_{u,m}$
EAb1	Uni	8.52 mm	23.18 mm	24.3 kN
	SUni	8.84 mm	26.47 mm	17.0 kN
HB1	P50	2.74 mm	-	71.8 kN
	P90	-	5.90 mm	59.9 kN
	Uni	2.87 mm	6.87 mm	62.8 kN
	SUni	2.92 mm	6.48 mm	54.0 kN

(1) Protocol Type: Uni = Unified Protocol; SUni = Simple Unified Protocol

Plotting the displacement over the crack width level of the tests on the HB1 anchor (Figure 4.21) allows for analysing the displacement behaviour for various crack cycling protocols. Contrary to the shear load cycling tests (Figure 4.17), the averaged displacement increase per cycle is a function of the cycling parameter (Figure 4.21a) and the proportionality of anchor displacement and crack width level for the different permanent load levels is clearly visible in spite of the scatter.

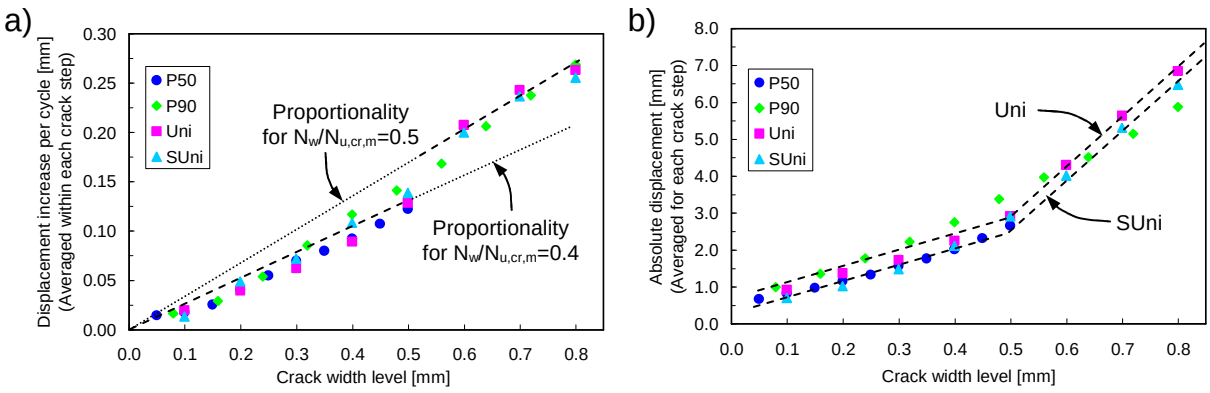

Figure 4.21 Displacement versus crack width level (averaged for each load step): a) Displacement increase per cycle; b) Absolute displacement

In consequence, the assumption of linear damage made for the reorganisation of cycles when generating the Unified Protocols (Section 4.1.3) is reasonable. The anchor displacement accumulates over crack cycles and the reduced number of cycles in the beginning of the Simple Unified Protocol is conveyed till the end of crack cycling (Figure 4.21b). However, due to the small crack widths in the beginning, the absolute difference in displacement is very small ($\Delta s_{cyc} \approx 0.5$ mm).

4.2.5 Conclusions

Differentiating serviceability and suitability demand level for anchor test protocols is a progressive approach for testing seismic anchor performance. Together with the crack width and anchor load test parameters associated with the respective demand levels, the developed P50 and P90 Protocols allow the consistent evaluation of anchor performance under serviceability and suitability test conditions. However, the high testing burden resulting from this approach suggests unifying the separate protocols to one Unified Protocol which then might be further simplified to the Simple Unified Protocol. To verify the equivalence of the P50, P90, Unified Protocol and Simple Unified Protocol, a dedicated test programme was carried out.

In respect to the potential introduction of the test protocols in the seismic amendment of qualification guidelines, the testing procedures were further refined. In particular the formerly propagated sinusoidal loading and its approximation was thoroughly studied. It was shown that the complex and time consuming sinus or half sinus load cycling is not accurate for simulating the desired sinusoidal loading character. Therefore for future qualification tests, it is proposed to reproduce load cycling and crack cycling by simple but practical displacement controlled ramps. Further, the need to specify the test specimen and control the crack width during the residual load capacity test under supposedly static crack conditions is highlighted.

The shear load cycling tests revealed that the shear displacement behaviour is primarily governed by the load level. For all test protocols, the anchor displacement followed the same path. This behaviour corresponds to the load cycling tests presented in Section 3.5 for which the cyclic load-displacement curves generally followed the monotonic curve. Therefore, neither the truncation of the smallest amplitude cycles for the Unified and Simple Unified Protocol, nor the further reduction of the low amplitude cycles for the Simple Unified Protocol had a significant effect on the test result, provided that LCF is excluded. The target load reduction required to pass all cycles without LCF showed that an anchor, which did not complete all cycles in the first run, may also fail if the target load has been reduced to the load level successfully passed before, and therefore underlined the requirement that all test repeats have to develop the resistance to complete the cycling.

Conclusively, all shear cycling protocols yielded statistically equivalent displacement data and residual load capacities. It may be reasonably assumed that tension load cycling tests would yield similar results in that load-displacement curves of anchors loaded in tension also follow the monotonic curve, irrespective of the actual cycle regime. Therefore the equivalence of the separate and unified protocols was successfully verified for load cycling in general.

The crack cycling tests showed that the axial displacement depends on the crack width level, but also on the permanent load and number of cycles which is in line with the accumulating anchor displacement behaviour described in Section 3.6 for crack cycling tests. The linear damage rule as proposed in Section 3.7 was confirmed and therefore the basic assumption made for reorganising of crack cycles was proved valid. As every crack cycle counts, the reduction of the low amplitude cycles in case of the Simple Unified Protocol affected the test result. However, since the initial crack width amplitudes are small, the difference in anchor displacement may be deemed as insignificant.

Conclusively, the results showed an acceptable correlation of test data for all crack cycling protocols and therefore successfully demonstrated the applicability of unified protocols. The tests on the headed bolt resulted in a serviceability displacement of just less than 3 mm and form the baseline reference for future qualification tests on post-installed anchors which are assumed to behave as a headed bolt at best.

In summary, the Unified Protocols for load cycling and crack cycling represent an adequate testing approach for the seismic amendment of qualification guidelines. Suitable assessment criteria which allow a meaningful evaluation of the test data are developed in the following section.

4.3 Proposal for Seismic Amendment of Qualification Guidelines

The verified Unified Protocols form the key elements of a proposal for the seismic amendment of qualification guidelines which is introduced in the following. This proposal recognises all relevant aspects of the research presented in previous sections. It basically corresponds to the draft of the European Guideline for the technical approval of metal anchors under seismic actions (*Proposal for ETAG 001 Seismic Amendment (2012)*). This document is compiled within the EOTA Working Group ‘Metal Anchors’ and is the outcome of specific discussions to which also research results of other universities and institutions unnamed in this thesis contributed. It is beyond the scope of this thesis to present the document of the Working Group in all aspects; also to avoid collision with the ongoing process. Aim of the following discussion is to outline the principle concept of the Seismic Amendment of the European Guideline, to highlight critical aspects, and to point out some

modifications made in the proposal if compared to the test protocols and procedures described in Section 4.2.

4.3.1 Introduction and background

The basic idea of the proposed seismic amendment is to provide detailed information on the additional tests which are required to qualify anchors for seismic applications including test conditions and assessment criteria, as well as additional design provisions. A precondition for the seismic qualification is the qualification for static applications in cracked concrete.

The test conditions stipulated for the Unified Protocols given in Section 4.1 are very demanding and in particular for the suitability level more adverse than the test conditions given in existing guidelines for tests involving load or crack cycling (Sections 3.5.2.4 and 3.6.2.4). On the other hand, the hazard level is variable and not the same for all earthquake prone areas. To reflect the different demands probably put on the anchor, a grading of the required seismic performance is reasonable. To this end, the proposed seismic amendment recognizes two anchor seismic performance categories (ASPC) which are in the following named ASPC1 and ASPC2. ASPC1 is the performance category required for lower seismic demands, and ASPC2 that required for higher seismic demands. The allocation to one or the other demand level is planned to be conducted according to the seismicity of the site and importance of the building.

The seismicity is defined by the ground acceleration a_g which is according to *Eurocode 8 (2006)* given by the reference peak ground acceleration (a_{gr}) and the soil factor (S) as $a_g = a_{gr} \cdot S$. For details, Eurocode 8 refers to the relevant National Annexes, e.g. *Eurocode 8 / NA (2009)* for Germany. The peak ground acceleration a_{gr} equals 0.0 to 0.8 m/s² depending on the seismic zone (0 – 3, Figure 4.22a). The soil factor S is based on the soil class (A – E) and deep geology class (R, T, S, Figure 4.22b). The importance of the building is evaluated with respect to the impact on life safety or public security (Section 1.1, Figure 1.4b) and is assigned to one of the importance classes (I – IV).

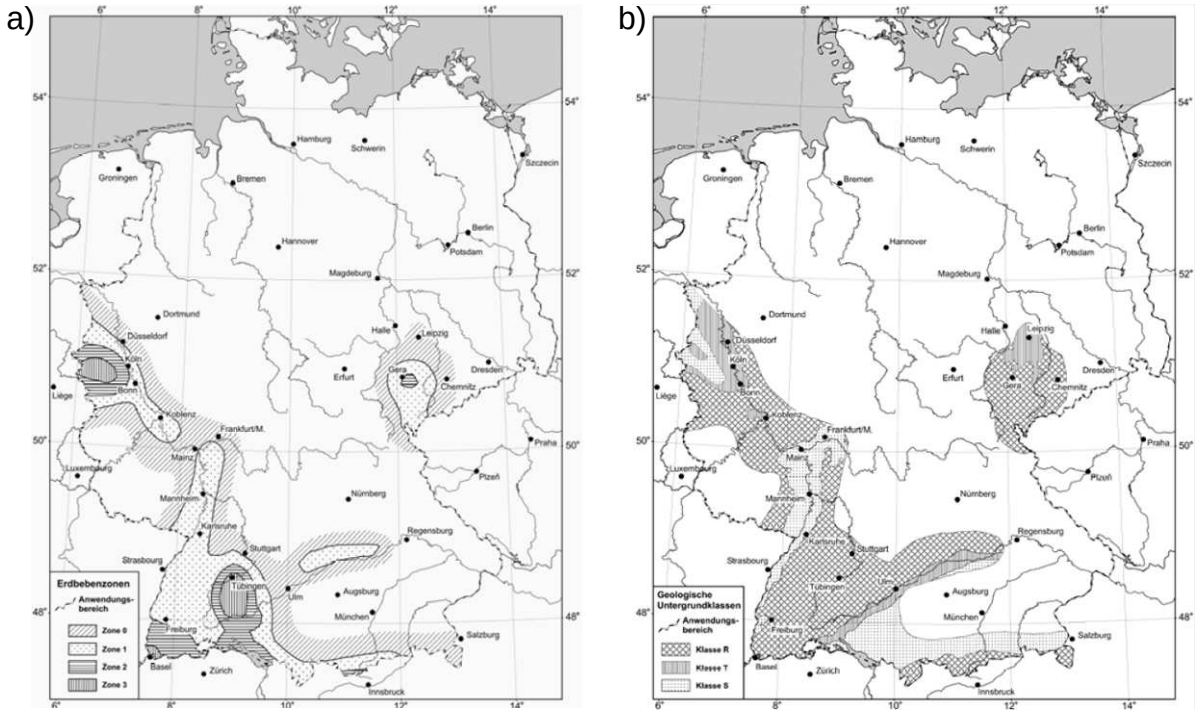

Figure 4.22 *Eurocode 8 / NA (2009)*: a) Seismic risk map for determing the peak ground acceleration a_{gr}; b) Deep geology map for determing the soil factor S

The qualification of anchors for regions of low / moderate seismic activity or relatively unimportant buildings (ASPC1) may be carried out by means of less stringent qualification tests, e.g. ACI 355, and is not further discussed here. The qualification tests on anchors for high seismic demands (ASPC2) is planned to be conducted according to the Unified Protocols as outlined in the following section.

4.3.2 Testing and assessing of anchors for high seismic demands

As indicated in the previous section, the envisaged test protocols of cyclic tests required for high seismic demands (ASPC2) are in principle identical to the Unified Protocols discussed in Section 4.1. The cyclic tests together with the reference tests make up the basic test programme as outlined in Table 4.5. The assessment criteria are subject to discussions, however, will be similar to those proposed in Section 4.4. The test conditions will mostly reflect those developed in the course of the research presented in this thesis.

Table 4.5 Outline of the basic test programme for seismic anchor qualification

Test No.	Purpose	Cyclic Phase		Monotonic Phase
		Crack Width	Anchor Load	Crack Width
ASPC2.1	Seismic reference tension test → $N_{u,cr,m}$	-	-	0.8 mm
ASPC2.2	Seismic reference shear test → $V_{u,cr,m}$	-	-	0.8 mm
ASPC2.3	Tension load cycling test	0.5, 0.8 mm	0.0 ÷ 0.75 $N_{u,cr,m}$	0.8 mm
ASPC2.4	Shear load cycling test	0.8 mm	0.0 ÷ 0.85 $V_{u,cr,m}$	0.8 mm
ASPC2.5	Crack cycling test	0.0 ÷ 0.8 mm	0.4, 0.5 $N_{u,cr,m}$	0.8 mm

Above listed tests are carried out in C20/25 concrete (Section 3.1.3). However, reference tests in high strength concrete have shown that additional ASPC2.1 tests in C50/60 concrete are meaningful and are therefore included in the test program stipulated in the *Proposal for ETAG 001 Seismic Amendment (2012)*. All tests are performed at quasi-static loading rates and cycling frequencies. All anchor holes are drilled using the medium drill bit diameters d_0 (Section 3.1.4).

The seismic reference tests in tension and shear yields the monotonic capacities $N_{u,cr,m}$ and $V_{u,cr,m}$, respectively, which are required to determine the anchor load and crack width parameters for the load and crack cycling tests. Possibly, $N_{u,cr,m}$ and $V_{u,cr,m}$ have to be normalised to account for the actual material strengths. In case of steel failure, normalisation is conducted linearly with reference to the ultimate steel strengths f_u. In case of concrete failure or concrete related failure, normalisation is conducted with reference to the square root of the concrete strengths f_c. In case of bond failure, normalisation is conducted with reference to the ratio of the concrete strengths f_c to the power of n which is the normalization factor according to Part 5 of *ETAG 001 (2006)*.

The *Proposal for ETAG 001 Seismic Amendment (2012)* provides further requirements regarding the test setup. In particular, the concrete specimens are described in detail. The key features of the cyclic tests together with some remarks on the procedures are compiled in the following sections.

4.3.2.1 Tension load cycling tests

The proposed procedure is generally identical to the procedure presented in Section 3.5.2.2 and consists mainly of the following steps: (1) Install the anchor in the hairline crack. (2) Open the crack to w = 0.5 mm. (3) Subject the anchor to triangular cyclic tension load of stepwise increasing amplitudes up to $0.5 \cdot 0.75 \cdot N_{u,cr,m}$.

(4) Open the crack to w = 0.8 mm. (5) Subject the anchor to triangular cyclic tension load of stepwise increasing amplitudes up to $0.75 \cdot N_{u,cr,m}$. (6) Unload the anchor. (7) Load the anchor in tension to failure. The schematic procedure is illustrated best as anchor load time history which is given together with the tension anchor load amplitudes in Figure 4.23.

a)

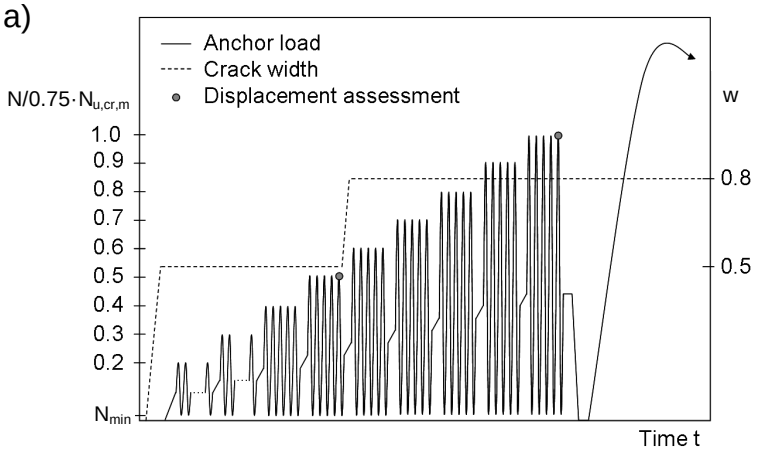

b)

No. of cycles	Anchor Load [N/0.75·$N_{u,cr,m}$]	Crack width [mm]
25	0.2	0.5
15	0.3	0.5
5	0.4	0.5
5	0.5	0.5
5	0.6	0.8
5	0.7	0.8
5	0.8	0.8
5	0.9	0.8
5	1.0	0.8
75	Total	

Figure 4.23 Tension load cycling tests: a) Time history after *Proposal for ETAG 001 Seismic Amendment (2011)*; b) Anchor load amplitudes and corresponding crack width

The following remarks are given for tests in tension:

- For tension tests (monotonic and cyclic), anchors are generally loaded under unconfined conditions, allowing a full concrete cone to develop in case of mechanical anchors. This is achieved by unsupported concrete within a radius of $2\ h_{ef}$ around the anchor location. For adhesive anchors, bond failure is desired for which the embedment depth has to be chosen accordingly. For most embedment depths, however, either steel failure (large embedment depth) or concrete failure (small embedment depth) is critical. In this case, adhesive anchors have to be tested under confined conditions (Sections 3.5.2.2 and 3.6.2.2) and a medium embedment depth is recommended (Section 3.3.4.1).
- The minimum load during cycling N_{min} should be taken slightly greater than zero to avoid servo control problems (Section 3.5.2.2), however, limits for N_{min} are helpful to avoid undermining the intention of the test. Simulated seismic tests according to ACI 355 are commonly run with $N_{min} = 200$ N but not exceeding 2 % of N_{max}.
- For tension load cycling tests, each cycle starts and ends at mid level. Transition from one load level step to the next is done from mid level to mid level. To enable the evaluation of residual displacement parameter, however,

it is necessary to unload the anchor after cycling and prior to final pullout test (Section 3.5.2.5).

4.3.2.2 Shear load cycling tests

The proposed procedure is generally identical to the procedure presented in Section 3.5.2.2 and consists mainly of the following steps: (1) Install the anchor in the hairline crack. (2) Open the crack to w = 0.8 mm. (3) Subject the anchor to triangular cyclic shear load of stepwise increasing amplitudes up to $0.85 \cdot N_{u,cr,m}$. (4) Load the anchor in shear to failure. The schematic procedure is illustrated best as anchor load time history which is given together with the shear load amplitudes in Figure 4.24.

a)

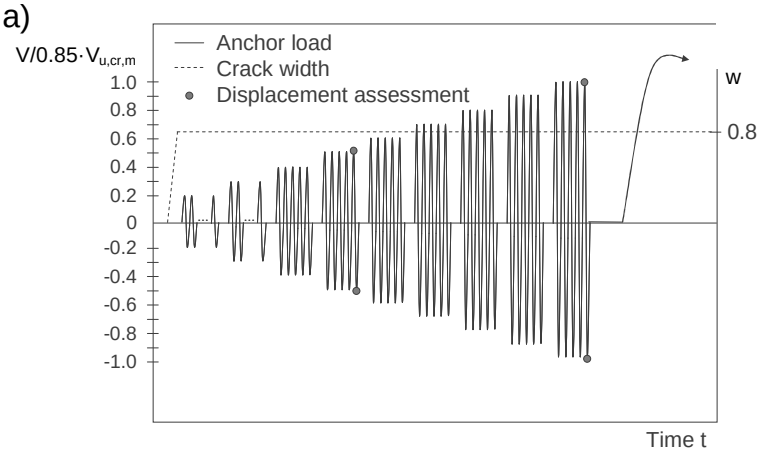

b)

No. of cycles	Anchor Load [V/0.85·$V_{u,cr,m}$]	Crack width [mm]
25	0.2	0.8
15	0.3	0.8
5	0.4	0.8
5	0.5	0.8
5	0.6	0.8
5	0.7	0.8
5	0.8	0.8
5	0.9	0.8
5	1.0	0.8
75	Total	

Figure 4.24 Shear load cycling tests: a) Time history after *Proposal for ETAG 001 Seismic Amendment (2011)*; b) Anchor load amplitudes and corresponding crack width

The following remarks are given for tests in shear:

- For shear testing, the monotonic tests may be omitted if the results of exisiting test series in uncracked concrete are taken for reference. For shear loads the effect of cracks is low (Section 3.5.2.1). Moreover, taking potentially larger monotonic reference capacities makes the testing conditions and assessment criteria for the shear cycling more adverse. Therefore this approach is conservative.
- Each cycle starts and ends at mid level, i.e. zero displacement. Displacements are considered as positive in the direction of $+V_{max}$. The pullout test is performed in positive direction.

4.3.2.3 Crack cycling tests

The proposed procedure is generally identical to the procedure presented in Section 3.6.2.2 and consists mainly of the following steps: (1) Install the anchor in the hairline crack. (2) Load the anchor to $0.8 \cdot 0.5 \cdot N_{u,cr,m}$. (3) Subject the anchor to triangular cyclic crack width of stepwise increasing amplitudes up to w = 0.5 mm. (4) Load the anchor to $0.5 \cdot N_{u,cr,m}$. (5) Subject the anchor to cyclic crack width of stepwise increasing amplitudes up to w = 0.8 mm. (6) Unload the anchor. (7) Open the crack to w = 0.8 mm. (8) Load the anchor in tension to failure. The schematic procedure is illustrated best as anchor load time history which given together with the tension anchor load amplitudes in Figure 4.25.

a)

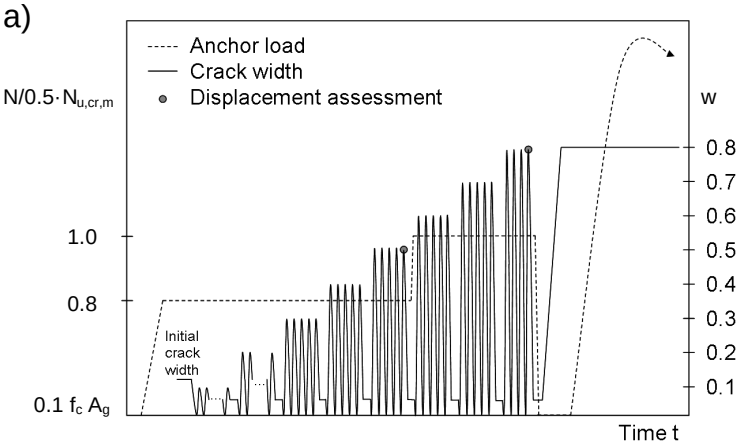

b)

No. of cycles	Crack width [mm]	Anchor Load [N/0.5·$N_{u,cr,m}$]
20	0.1	0.8
10	0.2	0.8
5	0.3	0.8
5	0.4	0.8
5	0.5	0.8
5	0.6	1.0
5	0.7	1.0
4	0.8	1.0
59	Total	

Figure 4.25 Crack cycling test: a) Time history after *Proposal for ETAG 001 Seismic Amendment (2011)*; b) Crack width amplitudes and corresponding tension load

The following remarks are given for tests in cycled cracks:

- Some guidelines recommend for service life tests (Section 2.6) to establish a constant relationship between the loading of the concrete specimen and the width of the thereby opened crack by applying several load cycles on the concrete test specimen (crack training). However, the presented crack cycling tests are basically controlled by the crack width and do not require this procedure (Section 3.6.2.2).
- Full crack closure (w = 0.0 mm) is assumed for 0.10 $f_{cc,150}$ over the gross cross section area.
- The load is applied first, and then the crack is opened. For the small initial crack width, however, a reversed order is believed to have no effect on the test results. During the initial load application the crack is slightly forced open due to wedging effects of the anchor and may even exceed the first crack width step of 0.1 mm. This is, however, for the programming of the servo control not a problem. Each cycle starts and ends at relaxation of the concrete

specimen and crack movement in the direction of crack closure. Transition from one crack width step to the next is done while the concrete specimen is relaxed. After cycling and prior to the final pullout test, the crack is opened to 0.8 mm.

- If the crack width is measured by electronic displacement transducers installed on either side of anchor (Section 4.2.2), the difference between the crack width measured on the top (w_{top}) and bottom (w_{bottom}) of the concrete specimen have to be limited to an acceptable ratio. Calculations have shown that a ratio of $w_{bottom} / w_{top} \geq 0.9$ can be assumed for a concrete specimen depth of $h \geq 2\ h_{ef}$ and a reinforcement ratio of $A_s \geq 0.01\ A_c$.

4.3.3 Reporting of design information

The technical approvals (ETA, Section 2.1.1), provide information on the intended use, the installation, and the design. The following design information should be reported in ETA for anchors qualified for seismic applications.

- Structural and non-structural connections: Since the qualification is applicable to structural and non-structural connections despite different anchor demands and behaviour, the design of both types of connections is covered by an ETA (Section 3.7.2.4).
- Concrete and cracks: The concrete is generally assumed to be cracked. However, the qualification applies only to anchors installed outside of plastic hinge zones for which the maximum crack width may be assumed as 0.8 mm (Section 3.1.5).
- Displacement: Generally, the strength is assumed to be the most relevant design parameter which is also critical for the choice of a certain anchor product. However, in particular for seismic applications with associated large displacements and displacement controlled failures (Section 3.3.5), displacement data may actually be critical. Therefore, the anchor displacement occurring during cyclic actions has to be evaluated in detail and should be reported in the ETA accordingly. Approved anchor strengths are principally understood as the lower 5 % fractile of the mean strength in that this is the lower end of capacity. In contrast, for displacement design small or large displacements may be critical depending on the design situation (Section 3.3.5). In consequence, minimum and maximum characteristic displacements at serviceability level and suitability level are required to be reported in the ETA. For tension load cycling tests, displacements should be reported for minimum and maximum tension load (Figure 4.23). For shear load cycling tests, displacements should be reported for minimum and maximum

shear load (Figure 4.24). For crack cycling tests, displacements should be reported for maximum crack width (Figure 4.25).

4.4 Development of Assessment Criteria

Testing and reporting the performance of anchors is only one part of the qualification programme. The other part is the evaluation of the anchor behaviour. To this end, critical parameters are evaluated and compared to assessment criteria given in the qualification guidelines. If these criteria are not met, the anchor is either not qualified (fail-pass tests, also termed No go / Go tests) or the strength the anchor is approved for is reduced if compared to the full strength. But even if an anchor did not comply with a fail-pass criterion, the test can generally be repeated with reduced demands and the approved strength is reduced in return (Section 2.1.7).

Specific limits on allowable anchor displacements, strength reductions, coefficients of variation (CV) etc. are always arguable and to some extent subjective. For the *Proposal for ETAG 001 Seismic Amendment (2012)*, the assessment criteria are discussed within the EOTA Working Group 'Metal Anchors'. Due to ongoing discussions and due to the sensitiveness of the test data in respect to product confidentiality, the presentation of a detailed assessment is not desired in this thesis. Moreover, the assessment of the test results presented in the previous section is of little interest since the tested post-installed anchors were not developed for the extreme conditions that they were actually exposed to. However, it is instructive to discuss potential assessment criteria as they can be reasoned by the results of the research carried out within the scope of this thesis. It is noted that the assessment criteria and reduction factors slightly differ from those given in the *Proposal for ETAG 001 Seismic Amendment (2012)*.

4.4.1 Minimum monotonic capacity in seismic reference tests

Reference tests in extreme crack widths of 0.8 mm are required to determine the monotonic capacities $N_{u,cr,m}$ and $V_{u,cr,m}$ which, in turn, are decisive for target and permanent loads for load and crack cycling tests, respectively. For clarity, these tests are called seismic reference tests in the following. Since the decrease in load capacity due to extreme cracks is a critical performance criterion of anchors used for seismic applications, the allowable reduction should be limited for anchors seeking seismic qualification to ensure robustness of the anchor towards extreme cracks. For this reason, the monotonic load capacity $F_{u,cr,m}$ determined in seismic reference tests is compared with the monotonic load capacity determined in the reference tests which can be taken from the ETA for non-seismic applications.

The load-bearing behaviour of anchors loaded in tension is in particular sensitive to the crack width. For many anchors tested within the scope of this thesis, the capacity in 0.8 mm cracks was as low as 70 % of the capacity in 0.5 mm cracks (Section 3.4.5.2). For anchors engineered for adverse seismic conditions, a less pronounced decrease in load capacity is realistic and the criterion is proposed as $N_{u,cr,m} / N_{u,cr,m(0.5mm)} > req.\alpha = 0.80$.

This criterion could also be applied to the shear capacity $V_{u,cr,m}$ which is then compared with the monotonic load capacity in 0.3 mm cracks $V_{u,cr,m(0.3mm)}$. However, anchors loaded in shear are not sensitive to crack widths and seismic reference tests in shear are not necessarily required anyway. Therefore, this criterion may not be required for the evaluation of shear capacities.

In case the proposed criterion is not fulfilled and with reference to the deduction of the permanent anchor load for crack cycling tests in Section 4.1.2, the permanent load during crack cycling should be reduced by the factor $\alpha_{mon} = N_{u,cr,m} / N_{u,cr,m(0.5mm)}$.

4.4.2 Uncontrolled slip during pullout

Anchor should show a good load response which is expressed by steadily increasing load-displacement curves. If anchors at low load levels experience significant displacements without increase in load, the behaviour is considered as uncontrolled slip. Extreme crack widths make uncontrolled slip behaviour more likely. According to Clause 6.1.1 (a) of *ETAG 001 (2006)*, a reduction in load or a plateau in the curve caused by uncontrolled slip of the anchor is not acceptable up to a load of $N_1 = 0.7\ N_u$ (Figure 4.26a). The same criterion should apply to monotonic load-displacement curves of seismic reference tests (Section 4.4.1) and the pullout tests carried out after load or crack cycling to determine the residual capacity (Section 4.4.5). In principle, this criterion could also be applied to tests in shear, though it may be assumed as uncritical.

If the criterion is not met, Clause 6.1.2.2.1 (b) of *ETAG 001 (2006)* requires the reduction of the characteristic strength corresponding to $\alpha_{slp} = \min(N_1 / N_u) / 0.7$ with $\min(N_1 / N_u)$ equal to the lowest ratio of all tests within a series. This requirement should also be applied to seismic tests.

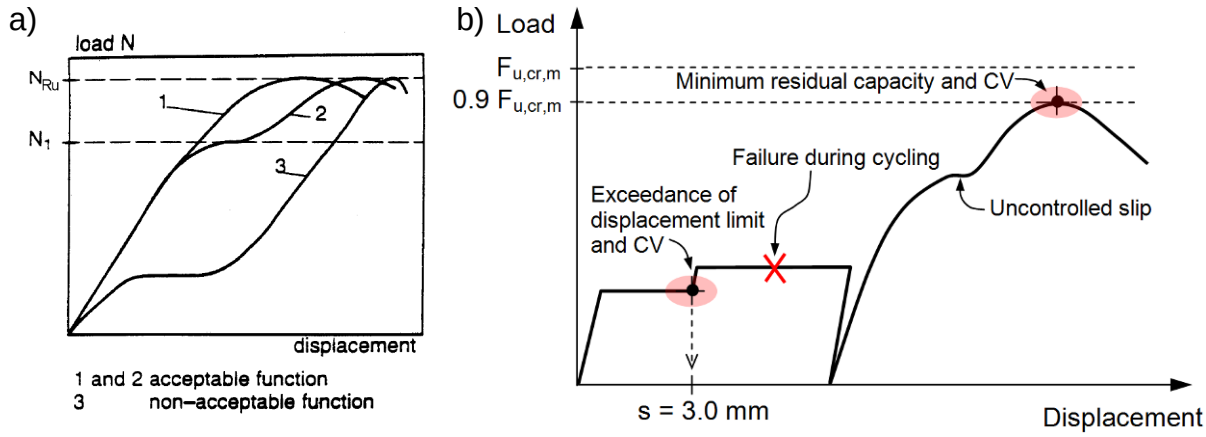

Figure 4.26 a) Uncontrolled slip (*ETAG 001 (2006)*); b) Illustration of assessment criteria yielding reduction factors (example for crack cycling)

4.4.3 Failure during cycling

If the anchor cannot cope with the demands during cycling, the anchor fails before completing all cycles. Analogue to the repeated load tests and service life tests according to ETAG 001 as well as for reasons discussed in Section 3.5.3 and Section 4.2.5, tests with anchor failure before completing all cycles are not acceptable.

Since the cycle regime and crack width are given, the premature failure is understood as the result of the anchor load level which was chosen too high. In conclusion, premature failure requires repeating the tests with reduced target load F_{max} or permanent load N_w to iteratively determine sustainable load levels. Consequently, the approved seismic strength is then reduced by $\alpha_{cyc,N} = \{N_{max,red} / N_{max}; N_{w,red} / N_w\}$ for tension loading and $\alpha_{cyc,V} = V_{max,red} / V_{max}$ for shear loading.

4.4.4 Exceeding of displacement limit during cycling

The anchor displacements accumulated during load or crack cycling may be excessive by the end of cycling and therefore challenge the structural integrity of the connection. For this reason, the displacement during cycling needs to be limited. Clause 6.1.1.2 (a) of *ETAG 001 (2006)* limits the axial displacement measured in service life tests to 3 mm (Section 2.6.1). Also for seismic tests, similar provisions should be effective. It is not very much agreed on whether a shear displacement limit is required at all. However, a strong argument for the same limit on shear displacement as on axial displacement is that for the design of the connected element it does not matter whether the displacement is generated in axial or shear

direction of the anchor. This applies to both, structural and non-structural connections.

Also according to *DIBt KKW Leitfaden (2010)* the displacement during load or crack cycling must not exceed 3 mm in any direction if a rigid connection is assumed for the design. The mean displacement of the headed bolt at serviceability level of just below 3 mm (Section 4.2.3.2) encourages this limit since for the qualification of post-installed anchors no stricter requirements should apply than a comparable headed bolt can meet. Therefore and in absence of any better definition, the 3 mm mean displacement ($s_{cyc,m}$) limit should be specified as assessment criteria for axial and shear displacements during load cycling and crack cycling tests on serviceability level. It is noted, however, that allowable design displacements always depend on the specific design situation.

If the limit is exceeded, the tests could be repeated at lower anchor load levels to reduce the displacement during cycling. The approved seismic strength is then reduced by $\alpha_{dis,N} = \min \{N_{max,red} / N_{max};\ N_{w,red} / N_w\}$ for tension loading and $\alpha_{dis,V} = V_{max,red} / V_{max}$ for shear loading.

For the sake of clarity it is repeated here that despite of the limit on anchor displacements during cycling, large deformation capacities might be desired at ultimate limit state because of the associated ductile behaviour (Section 3.3.5 and Section 3.6.2.4). However, an assessment criterion for minimum anchor displacements is not required for the seismic qualification of anchors (Section 3.8).

4.4.5 Minimum residual capacity after load or crack cycling

After completing the load or crack cycles, the residual capacity has to be determined by a monotonic pullout test in order to evaluate whether the anchor is capable to carry the assigned load. Clause 5.2.1 of *ETAG 001 (2006)* requires for repeated load tests or service life tests a minimum residual capacity of 90 % of the corresponding monotonic reference capacity (Section 2.5.1 and Section 2.6.1). Also for seismic tests, a minimum residual capacity ensures that the anchor is capable to carry the assigned load even after an earthquake. For simulated seismic tests, *ACI 355.2 (2007)* requires that the residual capacity is at least 80 % of the monotonic capacity in a crack $F_{u,cr,m}$ (Section 3.5.2.4). However, since the target load F_{max} for tests based on the Unified Protocol is close to $0.80 \cdot F_{u,cr,m}$ (tension load cycling tests, Section 4.3.2.1) or even above of $0.80 \cdot F_{u,cr,m}$ (shear load cycling tests, Section 4.3.2.2), the criterion should rather fall back on the requirement stipulated in ETAG 001 and the criterion is proposed as $F_{u,res} / F_{u,cr,m} > req.\alpha = 0.90$.

If this requirement is not met, the strength is reduced in accordance to the provisions given in ETAG 001 for the ultimate loads in suitability tests by $\alpha_{res,N} = N_{u,res} / N_{u,cr,m}$

for tension load cycling tests and $\alpha_{res,V} = V_{u,res} / V_{max}$ for shear load cycling tests. For clarity, it is noted that the simulated seismic tests according to ACI 355 requires a repeat of the tests at reduced load levels in case the criterion is not met. For the residual load capacity after crack cycling, the same requirement as for tension load cycling tests should apply. The reduction factor $\alpha_{res,N}$ is then the minimum of the values resulting from tension load cycling test and crack cycling test.

4.4.6 Coefficient of variation

The coefficient of variation (CV) is the parameter quantifying scatter. Large scatter in the test results is an indicator for unreliable and unstable load-displacement behaviour of anchors. Further, a large CV reduces the characteristic strength (Section 2.1.6) and makes the statistical evaluation less significant. In conclusion, limitations on the CV are important assessment criteria. ETAG 001 stipulates criteria for the CV of the ultimate load F_u and of the displacement at 0.5 $F_{u,m}$. The criteria are applied to the reference tests as well as to repeated load tests and service life tests. The limit on the CV for the displacement at 0.5 $F_{u,m}$ is mostly owed to the requirements of equal load distributions within anchor groups (Section 2.4.1).

The limits should apply to the ultimate load determined in seismic reference tests (Section 4.4.1) and to residual load capacity tests after load or crack cycling (Section 4.4.5), for which the anchor has to be unloaded after completion of the cycles as shown in Figure 4.26b. Both test types are suitability level tests in 0.8 mm cracks, for which Clause 6.1.1.1 (b) and (c) of *ETAG 001 (2006)* limits the CV of the ultimate load F_u and the displacement at 0.5 $F_{u,m}$ to 20 and 40 %, respectively. Though these requirements on the CV are hard to be met after the anchor was tested in 0.8 mm cracks in particular after load or crack cycling, they should be consistently applied to seismic qualification tests.

If the limit is not met in case of a cyclic test, the test could be repeated at lower target load level F_{max} or permanent load level N_w which generally yields reduced CV. The strength the anchor is approved for is then reduced by $\alpha_{CV} = F_{max,red} / F_{max}$ for load cycling tests and $\alpha_{CV} = N_{w,red} / N_w$ for crack cycling tests. Alternatively, one may want to allow a certain exceedance of that limit and introduces a regulation in accordance with Clause 6.1.2.2.2 in Part 5 of *ETAG 001 (2006)* which stipulates a safety factor for CV between 20 and 30 % as $\gamma_3 = 1 + (CV[\%] - 20) \cdot 0.03$. This is of particular importance for the monotonic tests which cannot be repeated at lower anchor load levels.

In addition, the CV for the displacement during crack cycling should be limited to ensure that the seismic group factor (Section 3.4.5.3) is sufficiently conservative. For

a seismic group factor of 0.85, the CV has to be limited to 30 % (Section 3.4.5.3). This holds for displacements at serviceability and suitability level.

4.4.7 Combination of reduction factors

As presented in the previous sections, not meeting the stipulated requirements results either in disqualification (requirements on residual capacity for monotonic tests, Section 4.4.1), reduction factors (requirements for load and crack cycling tests, Figure 4.26b) or in increased safety factor γ_3 (requirement on CV of the ultimate loads, Section 4.4.6). It is important to note the difference in the reduction factors and how several reduction factors are combined for the evaluation of the results of load and crack cycling tests.

The following reduction factors are considered:

- Uncontrolled slip → α_{slp} (Section 4.4.2)
- Failure during load or crack cycling → α_{cyc} (Section 4.4.3)
- Exceedance of displacement limit during load or crack cycling → α_{dis} (Section 4.4.4)
- Minimum residual load capacity after load or crack cycling → α_{res} (Section 4.4.5)

These criteria can be categorised as follows: Uncontrolled slip and residual load results in reduction factors based on the achieved strength, whereas failure during cycling and exceedance of the displacement limit requires a repeat of the test at reduced load levels and results in reduction factors based on the reduced load levels. The reduction factors within a category should be merged before their minima are multiplied:

$$\alpha_{total,N} = \min\{\alpha_{slp}; \alpha_{res,N}\} \cdot \min\{\alpha_{cyc,N}; \alpha_{dis;N}\}$$

$$\alpha_{total,V} = \alpha_{res,V} \cdot \min\{\alpha_{cyc,V}; \alpha_{dis,V}\}$$

It is noted that other than provided in ETAG 001, the α-factors should not consider individual tests but the mean capacities. This is in line with the provisions given in ACI 355 and the NPP Guideline and avoids reductions which would be unreasonable large for the extreme event of an earthquake.

4.5 Summary

After comprehensive experimental and numerical investigations presented in Chapter 3, the development of testing conditions focused on load cycling and crack cycling tests which were identified as critical previously. Based on further statistical

evaluations carried out at the UCSD, the protocol methodology was refined. The result was a set of load cycling and crack cycling protocols reflecting serviceability and suitability demand levels.

Together with crack width and anchor load levels taken as representative for serviceability and suitability demand, P50 and P90 Protocols were defined which allowed testing of the seismic anchor performance at serviceability and suitability demand level, respectively. In a second step, the separate P50 and P90 Protocols were combined in one Unified Protocol replicating both demand levels. The goal was to test seismic anchor performance at serviceability and suitability level in one test yet meeting the requirements on both demand level and therefore allowing the extraction of the relevant assessment data.

The equivalence of the separate and unified protocols was experimentally verified by comparative tests on various anchor types. The tests also confirmed earlier findings on anchor behaviour under load cycling and crack cycling. The repeatedly required reduction of the target load backs up the requirement that for a sound assessment all test repeats have to complete the cycling without failure. The truncation of the lowest amplitude cycles for the load cycling protocol had no effect on the test results but reduced the testing time substantially. The crack cycling tests on the headed bolt yielded on the serviceability level anchor displacements near 3 mm and supports this limit as a benchmark for the performance evaluation of post-installed anchors.

In addition, the possibility to aid testing by simplified protocols was evaluated. Therefore, Simple Unified Protocols with reduced number of low amplitude cycles were tested. Though the difference in test results deriving from this kind of small cycle cut-off is virtually non-existent in case of load cycling or insignificant in case of crack cycling, the practical benefit of this approach is very limited. Therefore and since there is no scientific justification for the reduced number of cycles, the simplified protocols are not recommended for the seismic amendment of qualification guidelines. In contrast, the proposed approximation of sinusoidal cycling by triangular ramps is clearly an improvement for servo controlled seismic testing of anchors which also shortens the testing time.

Meaningful assessment criteria were established on the basis of current anchor qualification guidelines and with reference to conclusions of the investigations presented in Chapter 3. Possible limits for anchor displacements, reduction of residual strengths, and the corresponding coefficients of variation were proposed.

The verified protocols unifying serviceability and suitability level demands are proposed for the seismic amendment of qualification guidelines. The load cycling and crack cycling tests will form the core of the guideline amendment which general approach was briefly introduced. Finally the testing procedures for the tension load

cycling, shear load cycling, and crack load cycling tests were outlined and critical aspects highlighted.

5 Studies at System Level: Shake Table Tests

The experimental investigations presented in Chapter 3 and Chapter 4 were carried out on component level by means of simulated seismic tests on anchors. To investigate the seismic performance under real earthquake conditions, the anchor has to be tested on system level. Therefore, shake table tests were conducted on anchors connecting a suspended model NCS to cyclically cracked concrete. For the studies discussed in the following, the anchored system was subjected to floor acceleration and corresponding cracking histories of real earthquakes. After a brief introduction on the background and experimental approach of the tests in Section 5.1, the test setup and procedure is explained in Section 5.2. The test programme consisted of several test suites which are discussed in Section 5.3. The main targets of the tests were the investigation of the correlation of anchor load and crack width, the verification whether the anchor displacements occurring during shaking are in line with those measured for the proposed seismic qualification tests, and the investigation of the ultimate seismic performance. Section 5.4 summarises the observations and conclusions from the testing.

5.1 Introduction

Shake table tests and their technical background are complex. The following introduction helps to understand the underlying experimental approach of the conducted test programme. The complete test report is available in *Mahrenholtz, P.; Hutchinson, T.; Eligehausen, R. (2012)*.

5.1.1 System level tests on a shake table

The investigations presented in the previous chapters contribute to the increasing knowledge on seismic anchor behaviour gained over the past years. All these studies, however, considered the behaviour of the isolated anchor only. For these component level tests, the demands originating from seismic actions are introduced by load and crack protocols (Figure 5.1a) which simulate the environment the anchor is exposed to if installed in a real structure as part of a system (Figure 5.1b). However, the validation is yet missing whether the test conditions and assessment criteria developed in Sections 4.1 and 4.4 for the proposed seismic qualification tests are able to replicate the demands a real earthquake and stipulate meaningful requirements.

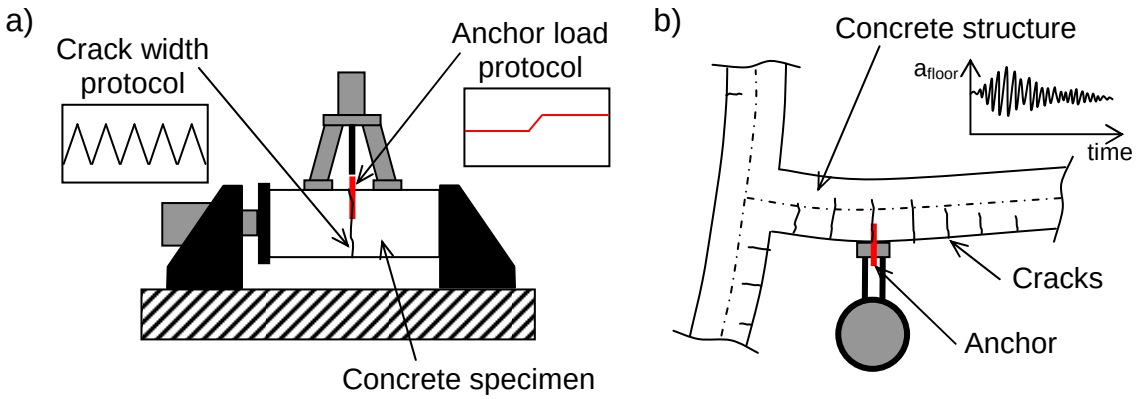

Figure 5.1 Schematic of a) Component level test; b) System level test

To date, there are only few studies on the system level performance of anchors available. In *Hoehler, M.; Silva, J. et al. (2007)*, the performance of anchors connecting pipe systems to a 7-storey building, which was tested in a full-scale shake table test programme, are described. The primary target of the tests was to investigate the anchor loads during a diverse range of input ground motions. In *Rieder, A. (2009)*, a weight was anchored horizontally to an uncracked concrete block and excited tri-axially by real earthquake input motions. The single anchor were loaded dominantly in shear and failed by excessive axial and shear deformations resulting in anchor bending and concrete crushing. It is noted, however, that the setup of the investigated connection did not replicate any specific design situation. For shake table tests presented in *Watkins, D.; Hutchinson, T. (2011)*, a model NCS was anchored on top of a cracked concrete slab and subjected to axial acceleration. This study is referred to in more detail in Section 5.2.

In contrast, shake table tests focussing on the seismic performance of the NCS are common practice in academic and corporate research programmes (Section 1.1). For these tests, however, the anchorage of the NCS is generally overdesigned, preventing any significant deformations and connection failures.

5.1.2 Testing of anchored NCS on a building segment

Non-structural connections are in several aspects more interesting than structural connections. In case of structural connections, the anchor is loaded by deformations of the global structure. The anchor behaviour does not influence the response of the connected structural element. In contrast, anchors for non-structural connections are loaded according to the inertial response of the NCS to the floor accelerations which, in turn, feeds back the anchored NCS behaviour (Section 1.2). This behaviour has the following consequences:

- Since oscillation of concrete structure and NCS are not in phase, the correlation of maximum anchor load and maximum crack width in the concrete is transient and hardly predictable.
- The axial anchor displacement accumulating during the shaking is the result of specific NCS acceleration and concrete cracking time histories, but is also influenced by the anchor performance in response to the demand.
- Ultimate capacity and failure mechanism of non-structural connections are not just determined by the load and displacement characteristics of the anchor, but also by the system performance of the anchored NCS.

This complex interaction can only be investigated by system level tests based either on a full-scale model building or a building segment. For testing on a full-scale model building, the NCS is anchored to a real concrete structure and tested for specified ground accelerations (i.e. Ground Motion (GM)) on a shake table (Figure 5.2a). This approach, however, is impractical in particular if the anchor performance is investigated for the specific demands present in multi-storey buildings. An economic option is to test the anchor performance using a building segment, for which the test setup has to mimic the acceleration and crack behaviour at that particular location (Figure 5.2b).

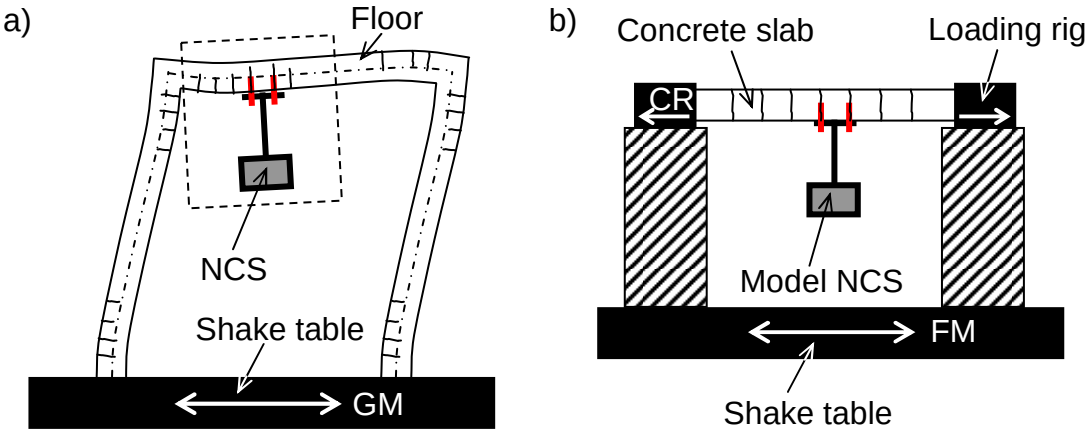

Figure 5.2 Schematic of test setups for testing anchored components: a) Full-scale model building; b) Segment of the structure

This approach was chosen for shake table tests with floor mounted NCS reported in *Watkins, D.; Hutchinson, T. (2011)*. The time histories for the cracking in the concrete slab (Crack Record (CR)) as well as for the acceleration of the concrete slab that the NCS was attached to (Floor Motion (FM)), based on the non-linear analysis presented in *Wood, R.; Hutchinson, T. et al. (2010)*.

For tension dominated anchor design situations, however, on-floor installations are in many aspects less critical than suspended installations for which the anchors are permanently loaded by gravity loads and the system does not get re-centered during

the earthquake as it is the case for floor mounted NCS. Therefore, the behaviour of anchors connecting suspended NCS to concrete under combined acceleration and cracking demand was investigated by shake table tests which are described in the following sections.

5.2 Experimental Procedure

The experimental procedure of the shake table tests on anchors connecting suspended NCS is a further development of procedures presented in *Watkins, D.; Hutchinson, T. (2011)*. The experimental procedure of shake table tests and the elaborate infrastructure to conduct them is very extensive and therefore only described to an extent which allows understanding the determination of the test parameters and the discussion of the results.

5.2.1 Input motions and time histories

5.2.1.1 Context of acceleration, curvature, anchor loads and crack widths

Acceleration and curvature time histories simulate the response of the floor segment to a specific earthquake excitation and depend on the layout and design of the structure and the storey of the building actually considered (Section 5.2.1.2). The model NCS, representing typical non-structural components and systems, is anchored to the concrete slab which in turn is mounted in the elevated loading rig on the shake table (Section 5.2.2). During shaking, the anchor load develops according to the response of the anchored NCS to the acceleration time history and the evolving load transfer mechanism, and in parallel, the cracks are opened and closed according to the given curvature time history. By scaling the input time histories, the maximum anchor load and crack width can be controlled (Section 5.2.3.2).

5.2.1.2 Selection of ground motions and floor motions

The shake table input motions were developed from extensive non-linear building simulations which are reported in *Wood, R.; Hutchinson, T. et al. (2010)*. The simulation was conducted for representative reinforced concrete frame structures with 2, 4, 8, 12, and 20 storeys which were subjected to 21 ground motion time histories (Figure 5.3a) selected from the *PEER Database (2010)*. These were scaled to the specified design spectrum by the geometric mean method which minimizes the sum of the squares error between the design spectral acceleration and the spectral acceleration ordinate of the selected records. The resulting spectra using scaled records and the target design spectrum are shown in Figure 5.3b.

a)

Event	Date	Location
Baja California	Jul 2, 1987	Mexicali, Mexico
Cape Mendocino	Apr 25, 1992	Cape Mendocino, CA, USA
Cape Mendocino	Apr 25, 1992	Cape Mendocino, CA, USA
Chi Chi	Sep 25, 1999	Taichung City, Taiwan
Friuli	Nov 12, 1999	Fruili, Italy
Gazli	May 17, 1976	Gazli, USSR
Irpina	Nov 23, 1980	Irpina, Italy
Kobe	Jan 16, 1995	Kobe, Japan
Kobe	Jan 16, 1995	Nishi-Akashi, Japan
Landers	Jun 28, 1992	Lucerne, CA, USA
Loma Prieta	Oct 18, 1989	San Jose, CA, USA
Loma Prieta	Oct 18, 1989	Saratoga, CA, USA
Morgan Hill	Apr 24, 1984	Morgan Hill, CA, USA
Nahanni	Dec 23, 1985	Nahanni, Canada
Northridge	Jan 17, 1994	Castaic, CA, USA
Northridge	Jan 17, 1994	Los Angeles, CA, USA
San Fernando	Feb 9, 1971	Castaic, CA, USA
San Salvador	Oct 10, 1986	San Salvador, El Salvador
Superstition	Nov 24, 1987	Superstition Mtn, CA, USA
Tabas	Jun 28, 1991	Tabas, Iran
Victoria	Jun 9, 1980	Mexicali, Mexico

b)

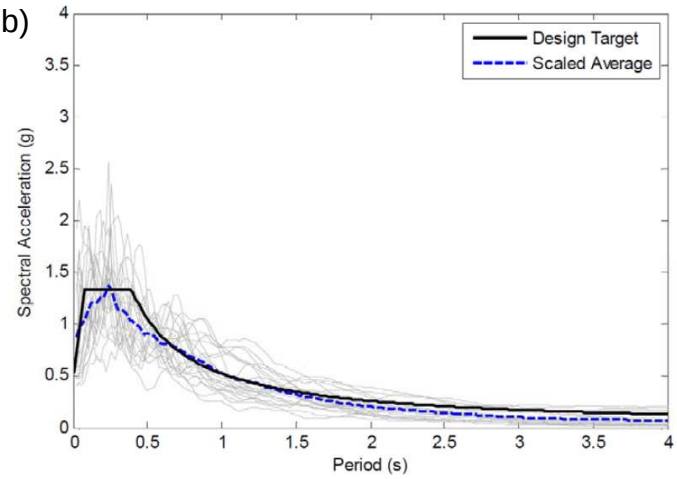

Figure 5.3 Ground motions in *Wood, R.; Hutchinson, T. et al. (2010)*: a) Details of ground motions selected from *PEER Database (2010)*; b) Design spectrum target and pseudo spectral acceleration for scaled ground motions, elastic 5 % damped

In *Wood, R.; Hutchinson, T. et al. (2010)*, 966 acceleration time histories and corresponding curvature time histories were generated. For the test programme discussed in the following, 11 floor motions were selected. The goal of the selection process was to obtain a random sampling of motions with a wide variety of characteristics in terms of magnitude, earthquake, distance, frequency content, and effective duration.

The selected FM are from the GM of the Nishi-Akashi Earthquake (‘kobe’) which has narrow band frequency and long predominant period characteristics, the Northridge Earthquake (‘north’) which has narrow band frequency and short predominant period characteristics, and Superstition Earthquake (‘super’) which frequency characteristics is relatively broad. Figure 5.4 provides details of the selected floor motions, their peak floor acceleration (PFA) and spectral accelerations (Sa) at characteristic periods, as well as underlying building details (building height given in number of storeys and considered floor) and associated building periods for the first four modes (T1 to T4).

Floor Motion	Earthquake	Peak Floor Acceleration (PFA) [g]	Spectral acceleration (Sa) at 0.10sec/10Hz [g]	Spectral acceleration (Sa) at 0.25sec/4Hz [g]	Building Height	Floor	First Mode T1 [s]	Second Mode T2 [s]	Third Mode T3 [s]	Fourth Mode T4 [s]
FM02	kobe	0.950	1.17	7.28	2st	1	0.24	0.06	-	-
FM03	north	1.371	2.85	13.83	2st	1				
FM05	super	0.592	1.23	1.54	4st	1	0.47	0.13	0.07	0.04
FM08	north	0.786	3.99	1.71	4st	2				
FM12	kobe	0.450	0.67	2.71	8st	5	0.89	0.29	0.15	0.10
FM13	super	0.564	1.34	2.52	12st	2	1.33	0.45	0.24	0.16
FM14	super	0.596	1.18	1.57	12st	5				
FM16	kobe	0.401	0.73	1.13	12st	10				
FM18	kobe	0.450	0.61	1.95	20st	4	2.07	0.71	0.39	0.26
FM19	super	0.460	0.65	1.45	20st	9				
FM20	super	0.475	0.61	0.76	20st	18				

Figure 5.4 Details of selected floor motions and underlying building details

The spectral acceleration of the floor motions shows one or several peaks. The analysis of the curvature history by Fast Fourier Transformations (FFT) identifies the frequency content of cracking. Since the crack width cycling is a direct result of the structural deformation, the peak cracking content generally aligns with the first or second mode of building vibration and is therefore relatively constant for floor motions of same building heights (Figure 5.4).

Since the acceleration expressed by the FM as well as the crack width cycling expressed by the CR derive from the response of the structure to the ground motion input, both cyclic actions are closely related to the building period. This becomes obvious when opposing the periods of the first and second spectral acceleration peak of all tested FM to the period of peak cracking content of corresponding CR (Figure 5.5a). In many cases, the peak in cracking content coincides with the first or second FM peak (Figure 5.5b).

a)

Floor Motion	Period at First Peak [s]	Period at Second Peak [s]	Crack Record	Period at Peak [s]
FM02	0.25	0.45	CR02	0.25
FM03	0.24	0.07	CR03	0.25
FM05	0.50	0.13	CR05	0.47
FM08	0.13	0.43	CR08	0.44
FM12	0.95	0.25	CR12	0.92
FM13	0.48	0.27	CR13	1.38
FM14	0.43	0.22	CR14	1.39
FM16	0.50	0.23	CR16	0.48
FM18	0.43	0.26	CR18	2.28
FM19	0.70	0.38	CR19	2.09
FM20	0.74	0.42	CR20	0.74

b)

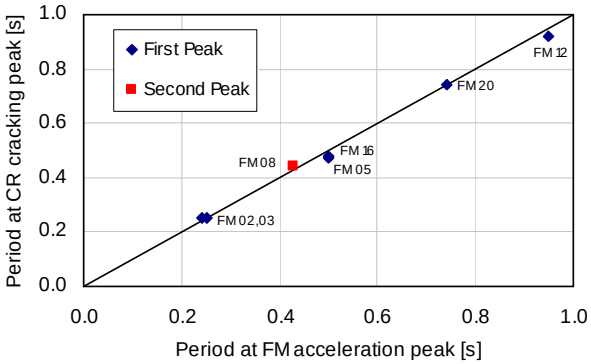

Figure 5.5 Compilation of periods at FM acceleration and CR cracking peak

Correlation Tests (Section 5.3.2) and Displacement Tests (Section 5.3.3) were run for all floor motions, whereas FM02 was the dedicated reference floor motion taken for the Failure Tests (Section 5.3.4). Its large spectral acceleration at the period of the used model NCS (T_{NCS}) guaranteed that anchor tension failure could be achieved without exhausting the limits of the shake table. The spectral acceleration of the floor motion FM02, as well as the normalised time histories of all selected floor motions and corresponding curvatures are given in Figure 5.6.

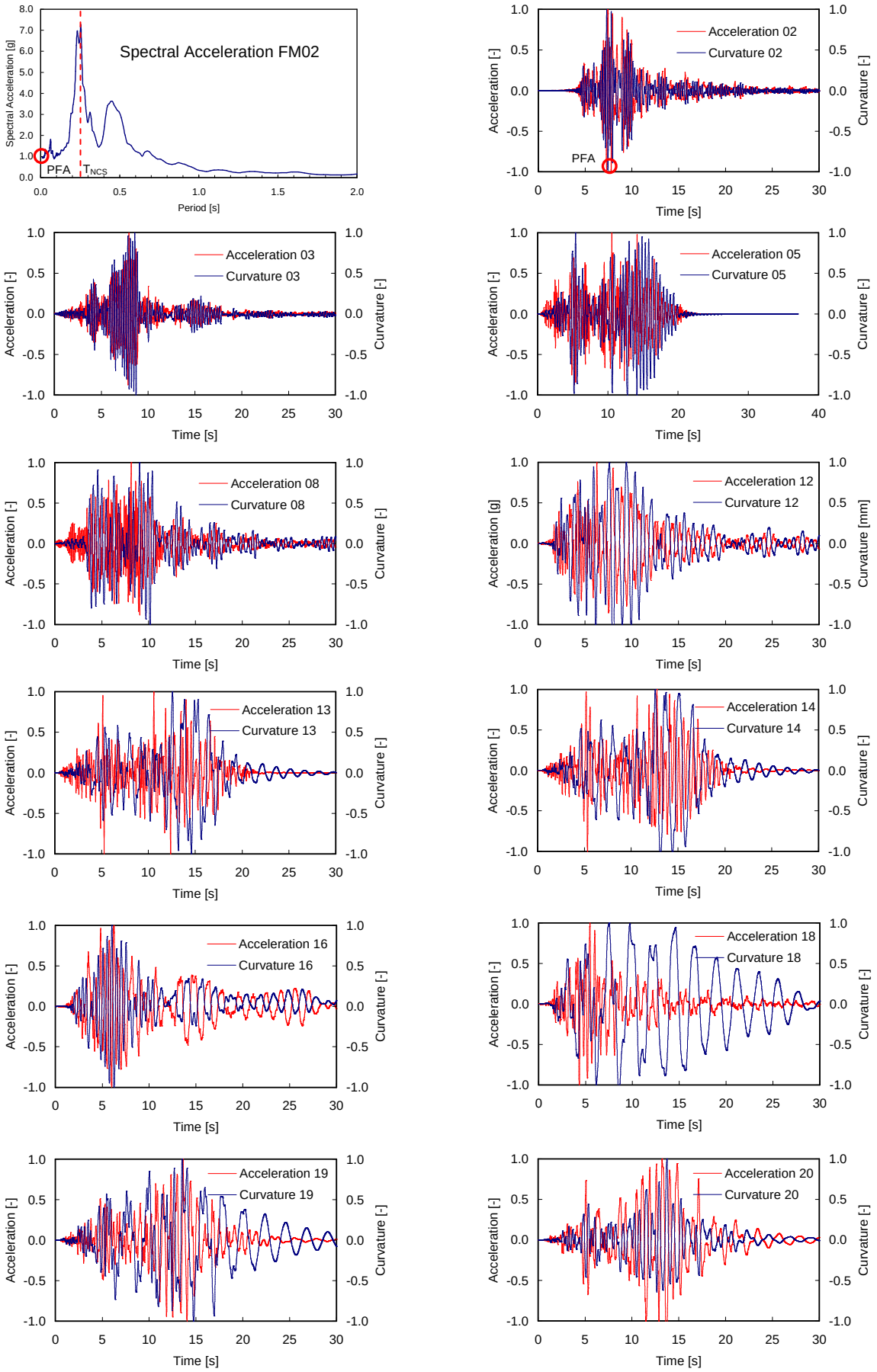

Figure 5.6 Sa(FM02) and normalised floor acceleration and curvature time histories

5.2.2 Test setup and testing procedure

5.2.2.1 Test equipment

The main components of the test setup were the shake table, the elevated frame, the loading rig, the concrete slab and the model NCS (Figure 5.7). The total weight of the elevated test setup sums up to approximately 8750 kg. The centre of gravity is approximately 700 mm above shake table floor. The single axis shake table 3050 x 4875 mm is operated by one actuator with a nominal capacity of 445 kN (at 5.5 g) allowing a maximal acceleration of the unloaded table of 10 g. The peak velocity is 900 mm/s, the maximum displacement ± 140 mm. The table is controlled by an accelerometer installed underneath the table.

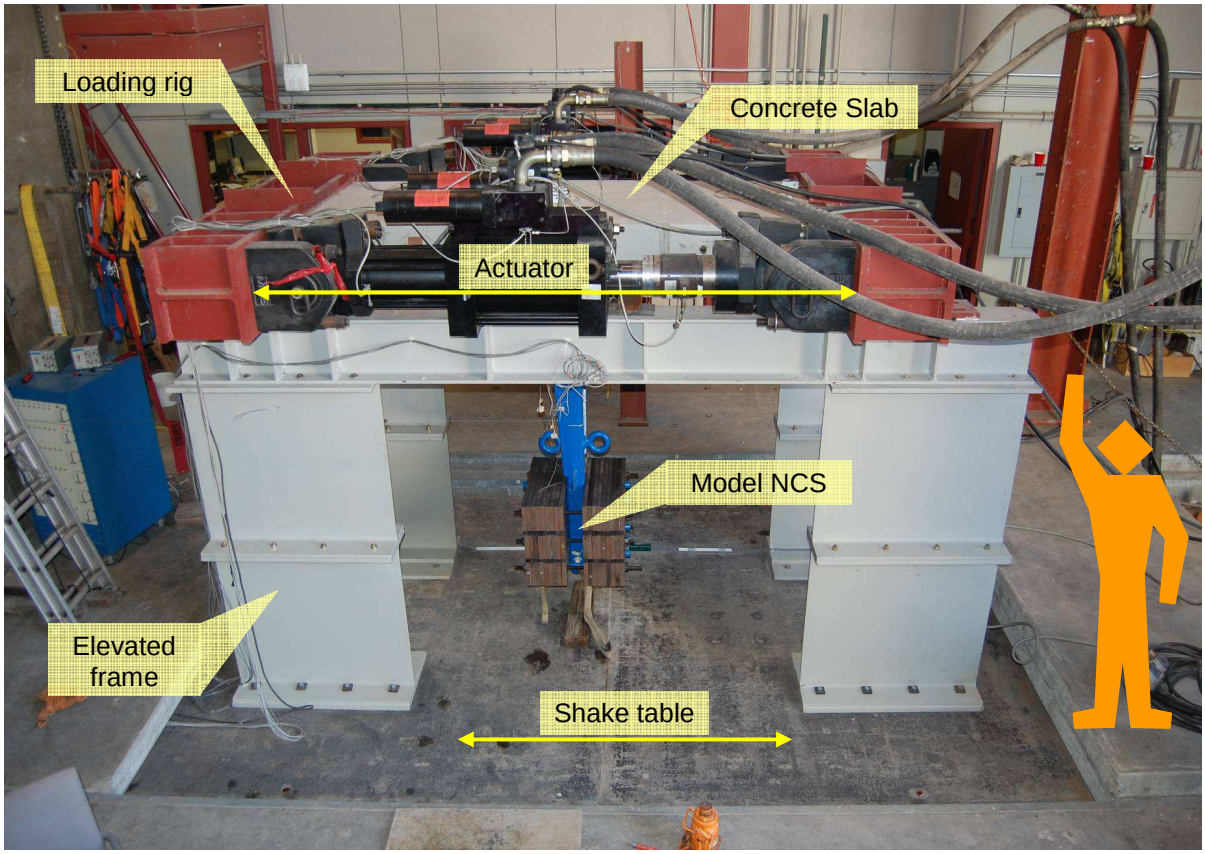

Figure 5.7 Overview of test setup with the main components

The elevated frame consisted mainly of assembled steel sections (piers) which form together with the longitudinal beams of the loading rig a stiff frame. The conceptual design is based on the assumption of allowable maximum accelerations of 4 g in longitudinal direction, i.e. direction of the shaking, and 2 g in transversal direction to account for out of plane modes. The structural analysis included the lateral bracing and bolts.

A modal analysis was run to analyse possible shaking modes for which the commercial software SAP2000© was used. Figure 5.8a shows the detailed finite element (FE) model of the elevation including bracings, the loading rig, the concrete slab, and the model NCS. The key output of the modal analysis was the determination of the eigenfrequencies of the elevated test setup. 12 modes were identified. Mode 4 (19.1 Hz) showed the lowest frequency involving the elevated frame, which suggests that the frame is sufficiently stiff and no major response problems have to be expected during the shaking.

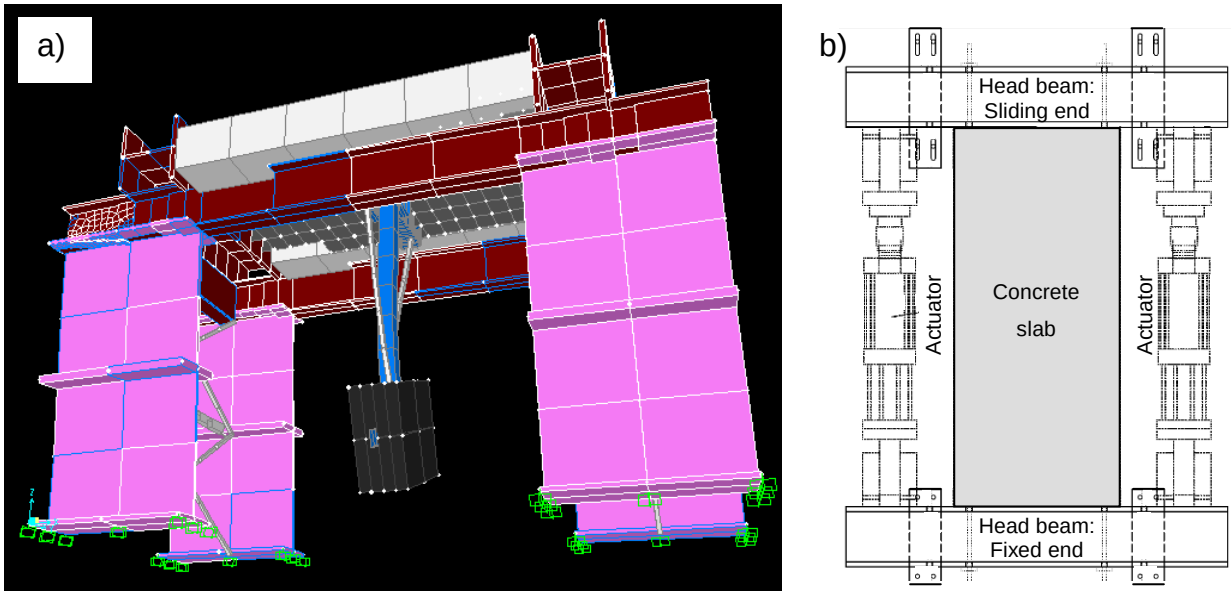

Figure 5.8 a) Rendering of FE model for Mode 4; b) Top view of loading rig

The loading rig (Figure 5.8b) was used nearly unchanged from the test setup developed for the shake table tests on anchors connecting floor mounted NCS and reported in *Watkins, D.; Hutchinson, T. (2011)* in detail. The loading rig consists basically of two steel beams, to which the concrete slab is attached to, coupled with a pair of servo hydraulic actuators (735 kN) used to open and close the cracks in the slab dynamically. The head beams are mounted on two longitudinal beams, which are bolted to the piers. One head beam is permanently fixed, the other rests on sliding panels allowing a free movement in longitudinal direction.

Also the model NCS was originally manufactured for the tests with the on-floor configuration. Its design parameters bases on evaluations of the *OSHPD Database (2009)* and observations made in an extensive survey on NCS reported in *Watkins, D.; Chui, L. et al. (2009)* which indicated that a considerable percentage of NCS shows periods in the range of 0.10 to 0.25 seconds (Figure 3.4b). The model NCS is basically a rack made of hollow sections and four footings which are fixed to the concrete slab by means of the post-installed anchors. Varying the number of attached weight plates allows tuning its fundamental period given by

$T = 1 / f = 2 \cdot \pi \cdot (m / k)^{0.5}$ with m = mass and k = stiffness, and influencing the gravity and inertial loading transferred to the anchors. Two configurations were used during testing: Light (8 weight plates, 3.8 kN in total) and heavy configuration (56 weight plates, 11.3 kN in total), with natural periods of vibration of 0.10 and 0.25 seconds, respectively. Figure 5.9a shows a photograph of the light NCS anchored overhead to the soffit of the concrete slab which is supported by rollers resting on the longitudinal beams. Each concrete slab provided 3 test locations with 2 cracks each, which defined the locations of the anchors. The drawing in Figure 5.9b depicts the heavy NCS and the concrete slab with indicated test positions. The 4 anchors were numbered and labelled unambiguously according their geographic direction. Anchor 1 and 3 made up the south anchor pair; Anchor 2 and 4 the north anchor pair.

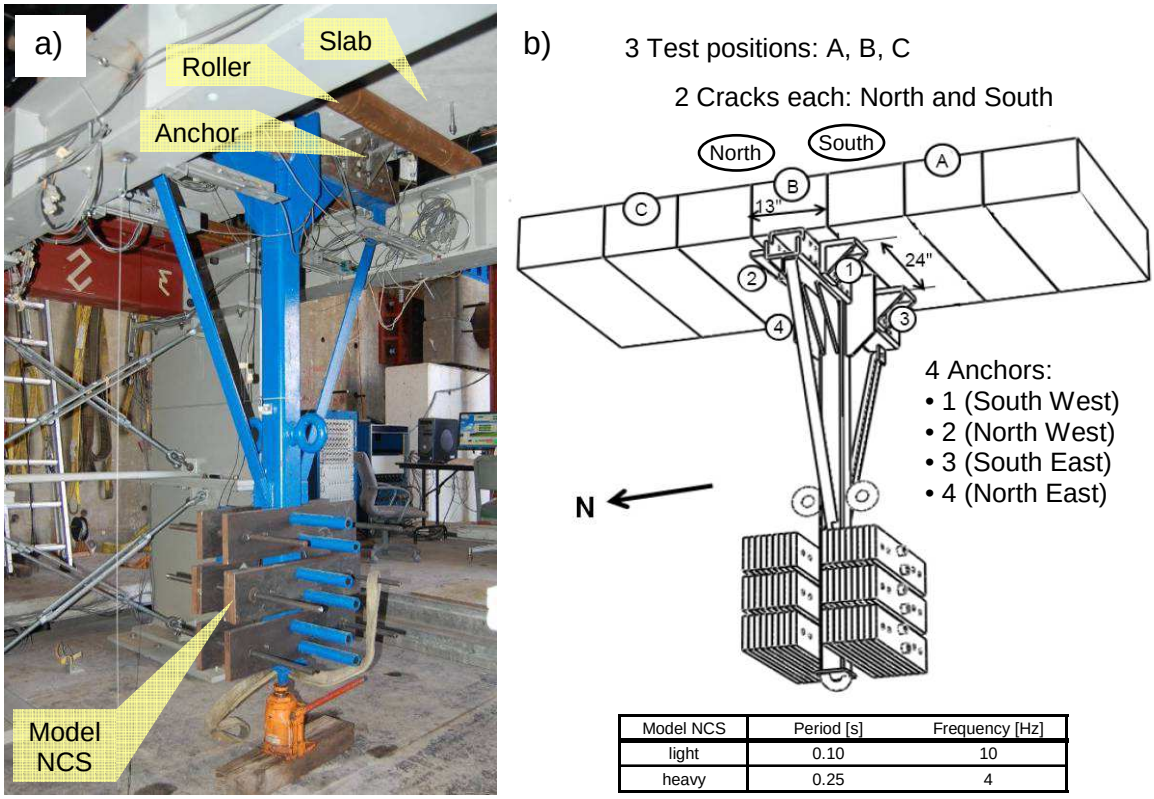

Model NCS	Period [s]	Frequency [Hz]
light	0.10	10
heavy	0.25	4

Figure 5.9 a) Photograph of test setup; b) Drawing of model NCS and concrete slab

5.2.2.2 Anchors and concrete specimens

Two types of post-installed anchors were tested: One undercut anchor (UC1 (M10)): Figure 5.10a1), representing an anchor of moderate displacement capacity and high load capacity, which is relative insensitive to large cracks, and one bolt-type expansion anchor (EAb1 (1/2”): Figure 5.10a2), representing an anchor of large displacement capacity and moderate load capacity, which is relative sensitive to large cracks. To enable multiple test runs (Section 5.2.2.4), the upper portion of the

sleeve of the UC1 anchors was cut off. This allowed the anchor to move out of the borehole without contacting the footing of the installed model NCS.

The anchor were installed with embedment depths equal to those for the load cycling and crack cycling tests discussed in Sections 3.5, 3.6, and 4.2, i.e. 90 mm for UC1 and 83 mm for EAb1. This allowed the direct comparison of component level and system level test results.

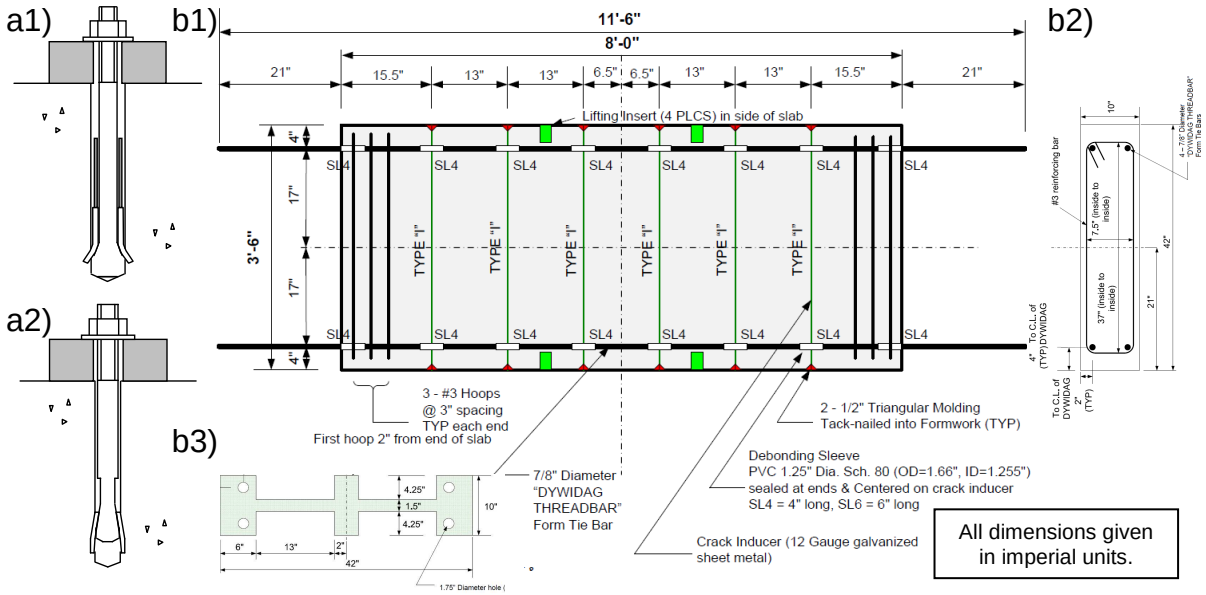

Figure 5.10 a) Tested anchor types: a1) Undercut anchor UC1 with modified sleeve, a2) Expansion anchor Eab1; b) Concrete slab used for tests: b1) Horizontal section, b2) Cross section; b3) Crack inducer

The used reinforced concrete slabs 2438 x 1067 x 254 mm were made of low strength concrete with a mean concrete compressive strength between $f_{cc,150}$ = 29.6 and 37.1 MPa. The slabs were designed to produce a 330 mm crack spacing (Figure 5.10b1). The longitudinal reinforcement of the slabs consisted of four 7/8" nominal diameter high strength reinforcing bars. Three #3 reinforcing hoops were placed at the ends of the slab to provide confinement (Figure 5.10b2). Six 3 mm thick stainless steel sheet metal crack inducers at each crack position were installed to aid the initial crack formation. 109 mm deep voids provided space for the concrete and anchors to be installed therein (Figure 5.10b3). For better crack generation, the longitudinal reinforcement was debonded around the envisaged crack positions by 100 mm long PVC tubes.

To ensure that the crack runs through the borehole over the entire depth, the holes were drilled prior to crack initialisation (Section 3.2.2.3). To guide the crack further, series of 1/4 in. pilot holes were pre-drilled into the slab. All anchor boreholes were visually inspected using a borescope. All cracks found to be satisfactorily generated, confirming the adequacy of the applied method.

5.2.2.3 Instrumentation and data acquisition

The instrumentation for the tests consisted of 84 channels in total (Figure 5.11a) to record accelerations (18), displacements (17), loads (4), and strains (2). Load measurement devices were load washer (LW) type which are installed like a washer between the footing of the model NCS and the nut of the anchor (*Hoehler, M.; Dowell, R. et al. (2011)*). Displacement measurement devices were either string pot type (SP) or linear potentiometer type (LP, Disp for anchor displacements, Wcr for crack widths). The key measurements were the anchor loads (LW1 to LW4), anchor displacements (Disp1 to Disp4), and the crack widths adjacent to the anchor locations (Wcr1 to Wcr4). Figure 5.11b shows exemplary the instrumentation for the northeast anchor.

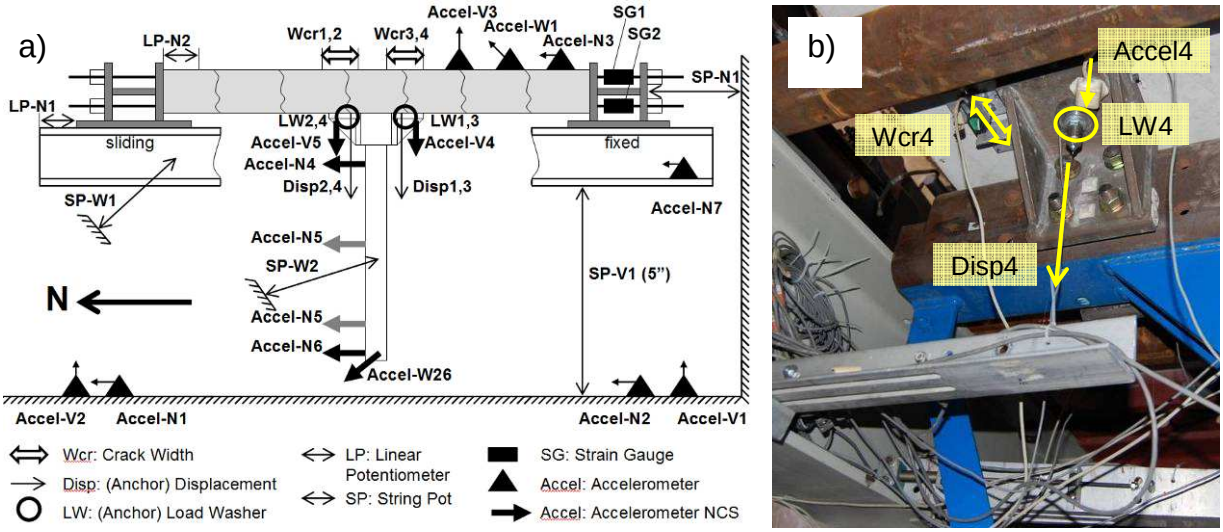

Figure 5.11 a) Schematic of instrumentation of shake table, elevated loading rig, and model NCS; b) Detail of instrumentation at the vicinity of an anchor

The measured data were transferred via an amplifier and conditioner to the data acquisition (DAQ) computer. The DAQ software program creates a binary file which is then transformed to a text file for further data processing. For evaluating the measurements in respect to the achieved maximum anchor loads and crack widths, the data were initially processed by a matlab© code. For filtering, baseline correction, and the calculation of spectral accelerations, the program SeismoSignal© was used with a 3rd order Butterworth bandpass filter and cutoff frequencies of 0.1 to 25 Hz.

5.2.2.4 Multiple test run procedure

The principle procedure for each test run was: (i) Tighten the model NCS with the installed anchors; (ii) Install the instrumentation and start DAQ system; (iii) Run the

test; (iv) Stop DAQ, save data file, carry out preliminary data evaluation; (v) Resume testing by jacking the model NCS back into position and restart with (i).

This efficient procedure allowed running multiple tests at one test position. For Correlation and Displacement Tests, the test run were continued until the minimum embedment depth was achieved. Since for these tests the anchors were not loaded near their ultimate capacity, the behaviour was not affected by this reduced embedment depth. For Failure Tests, however, one test position was used to load the anchors incrementally to failure.

5.2.3 Targets and scaling

5.2.3.1 Targets for anchor load and crack width

The target anchor load N_{target} is the targeted maximum load N_{max} in the anchor during a specific test run. Basically, two target anchor load levels were defined:

- 50 % of the mean monotonic load capacity in cracked concrete $N_{u,cr,m}$, representing the load level typical in design practice.
- 100 % of the design seismic strength $N_{5\%} / \gamma_M$, representing the highest load level the anchor could be designed for.

$N_{u,cr,m}$ was determined by reference tests in 0.8 mm cracks carried out within the scope of the tests reported in *Watkins, D.; Hutchinson, T. (2011)*. $N_{5\%}$ is the characteristic strength which was determined as 5 % fractile of the resistance evaluated for the proposed seismic qualification tests (Section 4.2). The material safety factor γ_M is given in Clause 4.4.3 of *CEN/TS 1992-4 (2009)* for all failure modes other than steel as 1.5 ($= \gamma_{Mp} = \gamma_{Mc} = \gamma_c \cdot \gamma_2 = 1.5 \cdot 1.0$) and corresponds approximately to the reciprocal of the strength reduction factor ϕ given in Clause D.4.1 of *ACI 318 (2011)ACI 318 (2008)* for failure governed by concrete breakout and pullout strength as 0.65 ($\approx 1 / 1.5$).

The target crack width is the maximum crack width w_{max} that is reached during the test. Two target crack widths were defined:

- 0.5 mm, representing serviceability level crack widths.
- 0.8 mm, representing suitability level crack widths.

The vast majority of tests were run with all 4 anchors located in a crack. To investigate the influence of reduced number of anchors in a crack on the performance, however, some tests were run with only 2 anchors located in a crack

5.2.3.2 Scaling of time histories

The acceleration time histories represent the FM which are introduced via the shake table to the concrete segment and accelerate the anchored NCS. The curvature time histories form the basis for CR which control the actuators of the loading rig to generate the crack width histories (Figure 5.2b). The processing and scaling of the acceleration and curvature time histories are explained in the following.

The discrete floor motions given in Figure 5.4 with their specific and absolute acceleration characteristics is not identical to the acceleration of the model NCS necessary to create the targeted maximum anchor load. Therefore, the original acceleration time history needs to be scaled. Provided that the NCS oscillates with a constant period and the load transfer system is known, the required scale factor α_{req} could be determined for any given spectral acceleration Sa(T) and target anchor load N_{target} to $\alpha_{req} = a_{req} / Sa(T)$. Assuming a simplified load transfer system (Figure 5.12a), a_{req} can be estimated for the equilibrium of forces at the moment of maximum acceleration.

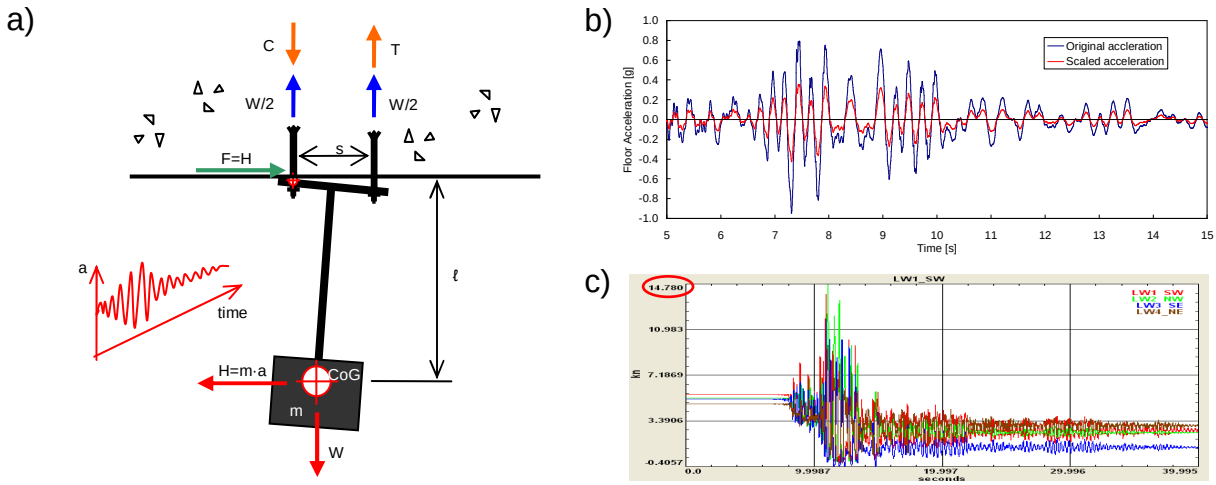

Figure 5.12 Scaling of FM: a) Simplified load transfer model for estimation of anchor load to acceleration factor (one anchor represents an anchor pair); b) Original and scaled acceleration time history (FM02); c) Example measured anchor load histories

The anchor pair opposite the deflected mass is loaded by the dead load corresponding approximately to half of the NCS weight (W / 2) and the earthquake load corresponding to the inertia induced tension load (T):

$$N_{target} = D + E \qquad \text{Equation 5.1}$$

where $D = ½ \cdot W / 2$ (D = Dead load acting on one anchor)

$E = ½ \cdot T$ (E = Earthquake load acting on one anchor)

With $T = H \cdot \ell / s$, $H = m \cdot a_{req}$, and $m = W / g$, Equation 5.1 yields:

$$\rightarrow N_{target} = W / 4 + (W \cdot a_{req} \cdot \ell) / (2 \cdot g \cdot s)$$

$$\leftrightarrow a_{req} = 2 \cdot (N_{target} \; D)s / \ell / (W / g) \qquad \text{Equation 5.2}$$

The acceleration time histories multiplied by the determined scale factor generates the desired acceleration time history (Figure 5.12b) out of which a command file for the shake table is generated. After the test run, the measured maximum anchor load was evaluated (Figure 5.12c) and the scale factor modified if required.

To create the target crack width time histories, the positive range of the normalised curvature time histories are multiplied by the target maximum crack width. Next, the crack width time histories are transformed into actuator commands for which a relationship between the actuator force and crack width is established by a tri-linear approximation (Figure 5.13a). This relationship allows calculating the actuator command for the positive range. The negative range of the normalised curvature time histories are scaled with reference to a compression force equal to 10 % of the compressive strength over the cross section area of the test specimen for which full crack closure is assumed (Section 3.6.1). By combining positive and negative range, the crack record (CR) is created. For the control of the actuators loading the concrete slab, an actuator command file is generated consisting of actuator force values given in lbf for 0.05 second time steps (Figure 5.13b). After each test, the measured crack width time histories was checked against the target crack width time history (Figure 5.13c) and the scale factor modified if required.

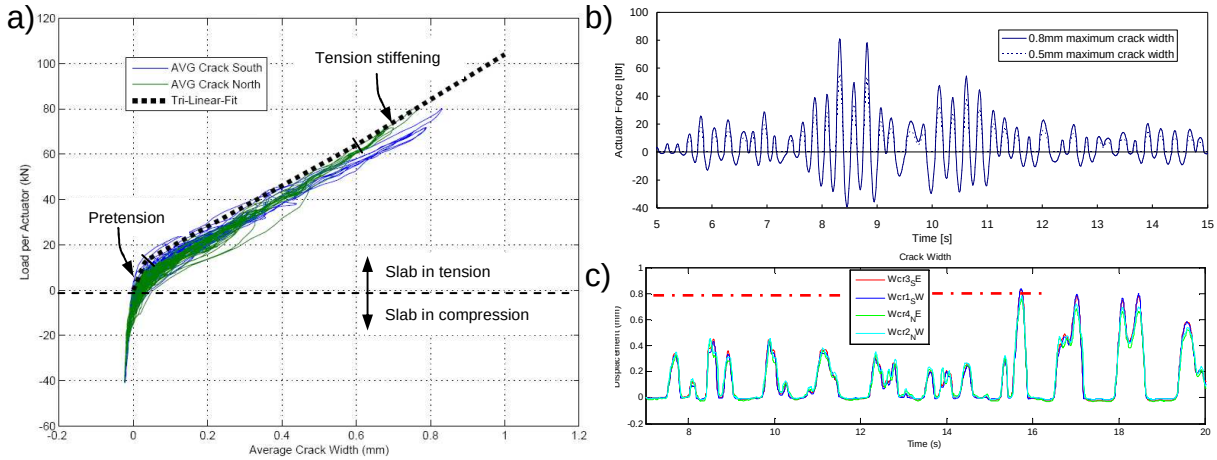

Figure 5.13 Scaling of CR: a) Measured actuator force versus crack width and tri-linear approximation; b) Actuator force time history for maximum crack width of 0.5 and 0.8 mm (CR02); c) Exemplary measured crack width histories (windowed)

5.2.4 Test programme

5.2.4.1 Test types and associated key test parameters

The general objective of the shake table tests was to study the performance of anchors connecting suspended NCS to concrete under real seismic conditions. The test programme consisted of several test suites serving the investigation of particular points of interest. The test types, their specific test objectives and the associated key test parameters are listed in the following:

- Correlation Tests: The primary test objective of the Correlation Tests was to investigate the coincidence of anchor load and crack width amplitude and draw conclusions regarding the realistic anchor load demand for crack cycling tests. The tests enlarge the correlation statistics already implemented in *Watkins, D.; Hutchinson, T. (2011)* for floor mounted NCS and allowed investigations on the effect of combined gravity and inertia loads.

  For consistency with the earlier correlation tests, all tests were conducted on the UC1 anchor with the same target anchor load of 0.5 $N_{u,m,cr}$ = 13.5 kN and crack width of 0.8 mm. Testing heavy and light configuration of the model NCS allowed studying the effect on the amplification and correlation. The deep installation of the modified UC1 anchor, together with the relative low maximum anchor load enabled to run scores of tests at one test location.

- Displacement Tests: The primary test objective of the Displacement Tests was to verify whether the dynamic shake table tests yield results that are in line with the results of the qualification test protocols proposed for the seismic amendment of qualification guidelines in Section 4.2. In the first place this is done by comparing the accumulated displacement of a fully utilised anchor after shaking with the displacement during crack cycling of a seismic qualification test.

  To investigate the impact of anchor type and crack width variation on the anchor load and displacement characteristics, tests were carried out on the UC1 and EAb1 anchor with maximum crack widths of 0.5 and 0.8 mm. Only the heavy model NCS was able to provide sufficient gravity and inertial loads required for the targeted high anchor loads. The FM time histories were scaled to load the anchors to the full seismic design strength. For the EAb1 anchor providing a mean capacity of $N_{u,m}$ = 24.3 kN with CV = 17.5 % (Table 4.3), the characteristic strength was determined to 16.6 kN after normalisation with reference to the actual concrete strength. For the UC1 anchor, no crack cycling tests according to the proposed seismic qualification tests were available. Instead, the test results gained in earlier crack cycling tests (Table 3.11) were taken and interpreted. With the displacement after crack cycling

extrapolated on basis of the ADP approach (Section 5.3.3.2), the hypothetical embedment depth remaining after a crack cycle regime as proposed for seismic qualification tests was estimated and the corresponding mean residual strength calculated to $N_{u,m}$ = 40.7 kN. With CV = 8.5 % and after normalisation with reference to the actual concrete strength, the characteristic strength was determined to 37.0 kN.

- Failure Tests: The primary goal of the Failure Tests was to investigate the failure mechanism and system performance of the anchor. It was aimed to validate that anchor and system fail simultaneously when the load capacity of an anchor is reached, rather than the system benefits from the gravity induced re-centering as it is the case for on-floor installations.

  For the given shake table capacity, only the heavy model NCS was able to break the anchorage. Testing of UC1 and EAb1 with different load-displacement characteristics allows investigating the impact of anchor type variation on the failure mechanism. The anchored NCS was tested by several test runs with incrementally increased peak input acceleration (PIA). For this incremental dynamic analysis (IDA), no target load is to be specified. Instead, the scale factor is increased after each test run until the anchorage finally fails. As the ultimate failure capacity is clearly associated with the maximum possible crack width, all tests were run with a target crack width of 0.8 mm.

Further test aspects included group behaviour for various number of anchors in crack, the effect of anchor ductility, and high loading rates.

5.2.4.2 Test matrix

The complete test programme and key test parameters are compiled in the test matrix given in Figure 5.14.

Test Suite	Test Characterization	Anchor Type	Embedm. Depth	Target Anchor Load	Model NCS Type	Target Crack Width	No. of Anchor in Crack	No. of Tests
-	Pretests, Sinewave	-	-	-	-	-	-	4
-	Whitenoise, Shakedown w/o NCS	-	-	-	-	-	-	3
-	Whitenoise, Shakedown w/ NCS	-	-	-	heavy & light	-	0	5
-	Crack width callibration	-	-	-	-	0.5 & 0.8mm	-	6
Suite1	Correlation Tests UC1	UC1	variable	0.5 $N_{u,cr,m}$ = 13.5kN	heavy & light	0.8mm	4	52
Suite2	Verification Tests UC1, moderate crack width	UC1	variable	$N_{5\%}$ / γ_M = 37.0kN	heavy	0.5mm	4	11
Suite3	extreme crack width					0.8mm	4	11
Suite4							2	11
Suite5	Verification Tests EAb1, moderate crack width	EAb1	variable	$N_{5\%}$ / γ_M = 16.6kN	heavy	0.5mm	4	11
Suite6	extreme crack width					0.8mm	4	11
Suite7	Failure Test UC1	UC1	90mm (3.54")	40,70,100,130% PIA	heavy	0.8mm	4	4
Suite8	Failure Test EAb1	EAb1	83mm (3.25")	20,40,60% PIA	heavy	0.8mm	4	3

Figure 5.14 Test matrix: Test programme and key test parameters

5.3 Test Results and Discussion

To validate the test setup and the fidelity of its components, an elaborate test programme was carried out before the actual testing on the anchored NCS started (Figure 5.14). After extensive calibration of the shake table and actuators, the divergence between target and achieved test parameters were within the expected tolerances. Figure 5.15 shows exemplary the target acceleration response spectra for FM02 and the acceleration response spectra measured on table and slab for shakedown tests with the heavy and light model NCS.

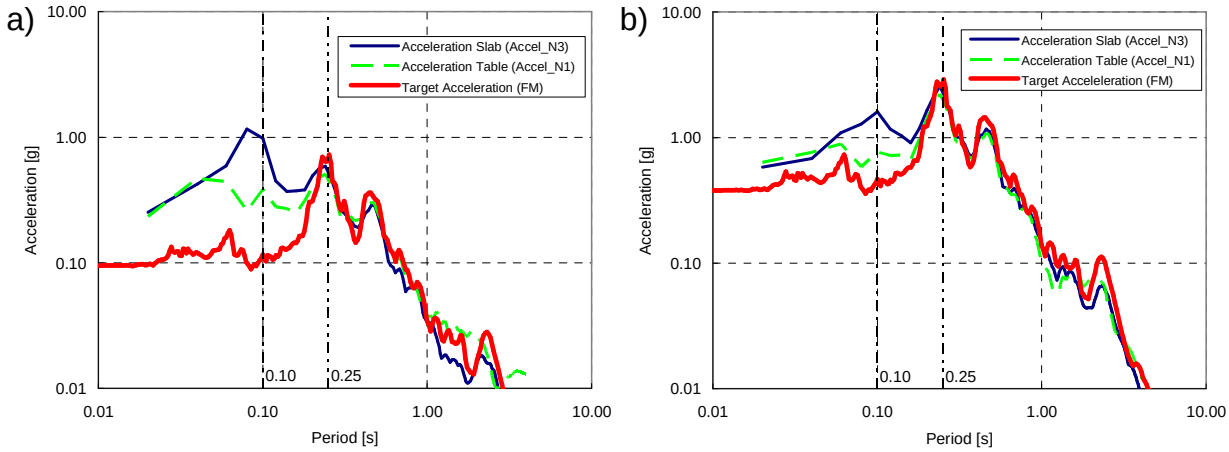

Figure 5.15 Acceleration response spectra of given floor motion (target) and measured acceleration on table and slab level (double) logarithm scale (example: FM02): a) 10% scaling, heavy model NCS; b) 40% scaling, light model NCS

The robustness of the test setup was confirmed during testing by test repeats which yielded nearly the same measurements, even if several test runs were carried out in between the repeats. In conclusion, the assumption of the feasibility of multiple test runs at one test location (Section 5.2.2.4) proved to be valid.

5.3.1 General behaviour

Before the key test results of the particular test types are discussed in Section 5.3.2 to 5.3.4, the general anchor behaviour during the shake table test is described by means of a test employing UC1 anchors and the heavy model NCS as an example. Target anchor load was 13.5 kN and target crack width 0.8 mm.

5.3.1.1 Anchor load, crack width, and anchor displacement

Figure 5.16 shows representative time histories of the anchor load, the crack width, and the anchor displacement, which are discussed in more detail in the following.

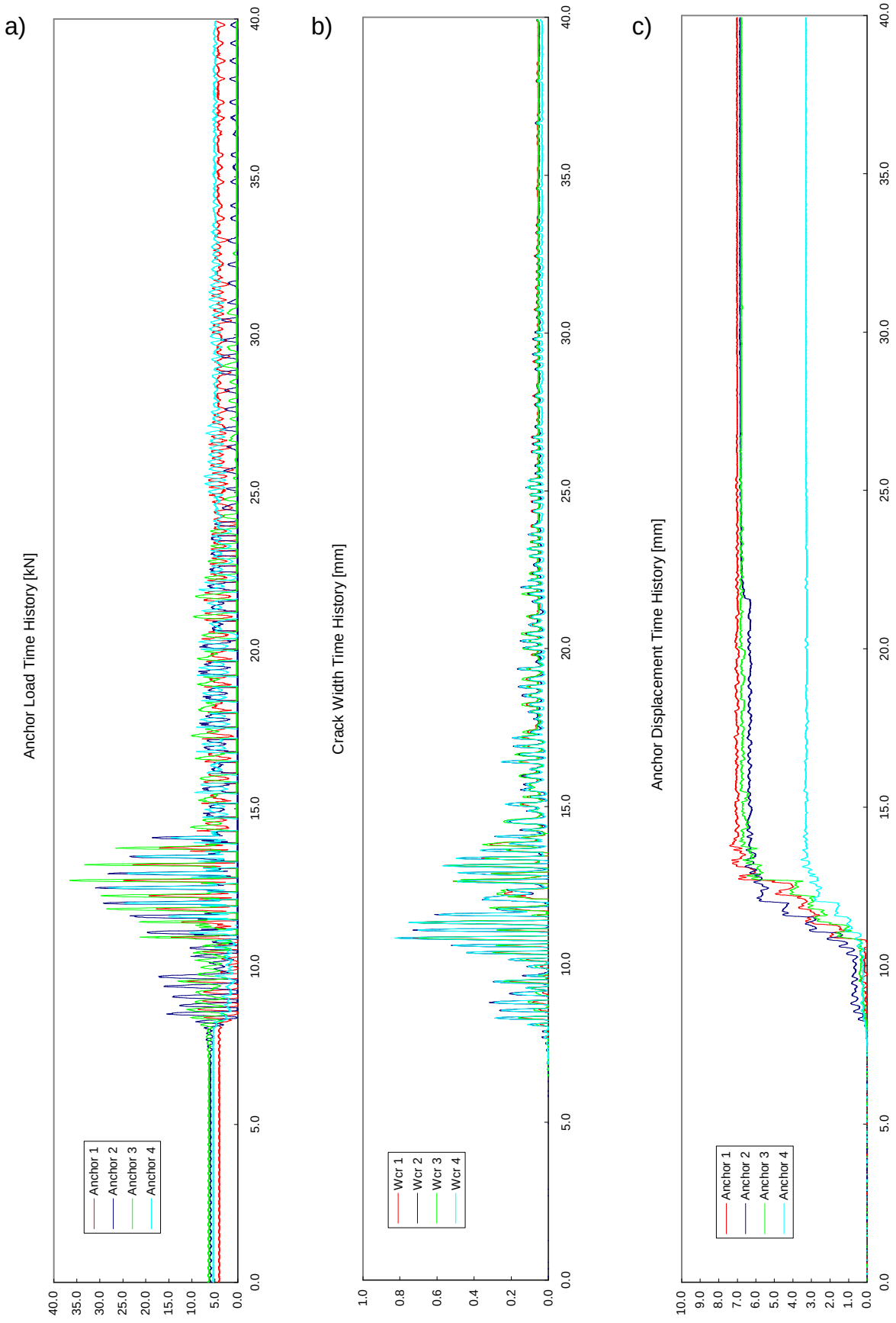
a)
Anchor Load Time History [kN]
Anchor 1
Anchor 2
Anchor 3
Anchor 4
b)
Crack Width Time History [mm]
Wcr 1
Wcr 2
Wcr 3
Wcr 4
c)
Anchor Displacement Time History [mm]
Anchor 1
Anchor 2
Anchor 3
Anchor 4

Figure 5.16 Time histories of measured primary test data (example: FM02 40 %, UC1, heavy model NCS): a) Anchor load; b) Crack width; c) Anchor displacement

The anchor loads show a pronounced cyclic behaviour (Figure 5.16a). Strong tensile loading magnitudes are followed by phases of complete unloading. Figure 5.17 is the same anchor load time history as Figure 5.16a but windowed for the medium section during which the anchors are highly loaded. The two anchor pairs (north and south) are loaded alternately. Though the magnitudes of the individual anchor loads differ to a certain degree, the two anchors of a pair are principally loaded at the same time and approximately achieve the target load. The intermediate small magnitudes load cycles are discussed in more detail in Section 5.3.1.3.

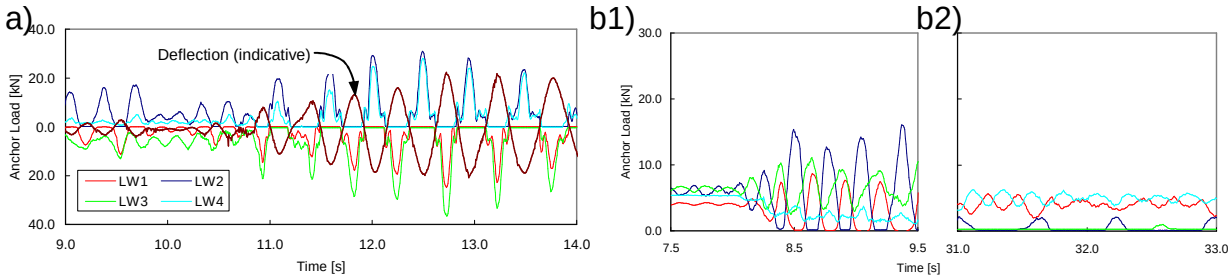

Figure 5.17 Windowed load time histories (example: FM02 40 %, UC1, heavy model NCS): a) Anchor load; b1) Extinction of preload at the beginning of shaking; b2) Fading out of swinging actions after shaking

Figure 5.17b1 windows the section at the beginning of the motion. The preload of 5 kN reflects the gravity load of the model NCS acting on the anchors. In addition, the anchors are to a certain degree prestressed. This preload vanishes within the first few strokes. In the initial phase of shaking, the anchors are not completely unloaded after each impulse. However, with increasing inertial loading the offset of the minimum anchor load to complete unloading (0 kN) disappears. Figure 5.17b2

windows the section at the end of the motion. At this moment, the concrete slab already came to a complete halt and the swinging action on the anchors is fading out.

The crack width histories at the four points of measurement next to the anchors generally show a good agreement and the target crack width is approximately achieved (Figure 5.18a). For smaller crack widths and more complex crack width target curves with intermediate maxima, there is some discrepancy between the crack width measured for the north anchor pair and south anchor pair. Since the influence of smaller crack widths on the anchor behaviour is limited, however, the difference is tolerable.

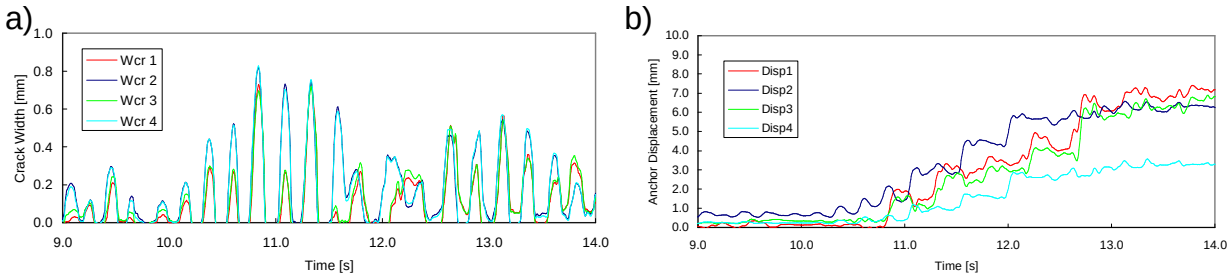

Figure 5.18 Windowed load time histories (example: FM02 40 %, UC1, heavy model NCS): a) Crack width (CR02 with 0.8 mm target crack width; b) Anchor displacement

The displacements of the individual anchor differ due to natural scatter (Figure 5.18b). The interrelationship of anchor load, crack width and resulting anchor displacement is discussed in more detail in Section 5.3.3.

5.3.1.2 Acceleration and period shift

Measured acceleration data can be evaluated best by response spectra which allow comparing the input acceleration measured on floor level, i.e. concrete slab, and the output acceleration measured at the centre of gravity of the model NCS (Figure 5.19a). Provided that the system of the anchored NCS remains perfectly elastic, the peak spectral acceleration of the NCS would occur at its original natural period, irrespective of the specific input acceleration on floor level. However, due to increasing anchor displacements, the connection gets sloppy and the period of the anchored NCS elongates. Though the original natural period of the heavy model NCS used for this test was 0.25 seconds, the peak spectral acceleration was at about 0.45 seconds. This corresponds to a period shift of 0.2 seconds. Since the underlying floor motion FM02 (compare also to Sa(FM02) given in Figure 5.6) is having its peak close to 0.25 seconds, the NCS eludes the maximum amplification by the elongation shift down the descending branch of the floor acceleration spectrum This behaviour was also observed for tests on floor mounted model NCS (*Watkins, D.; Hutchinson, T. (2011)*).

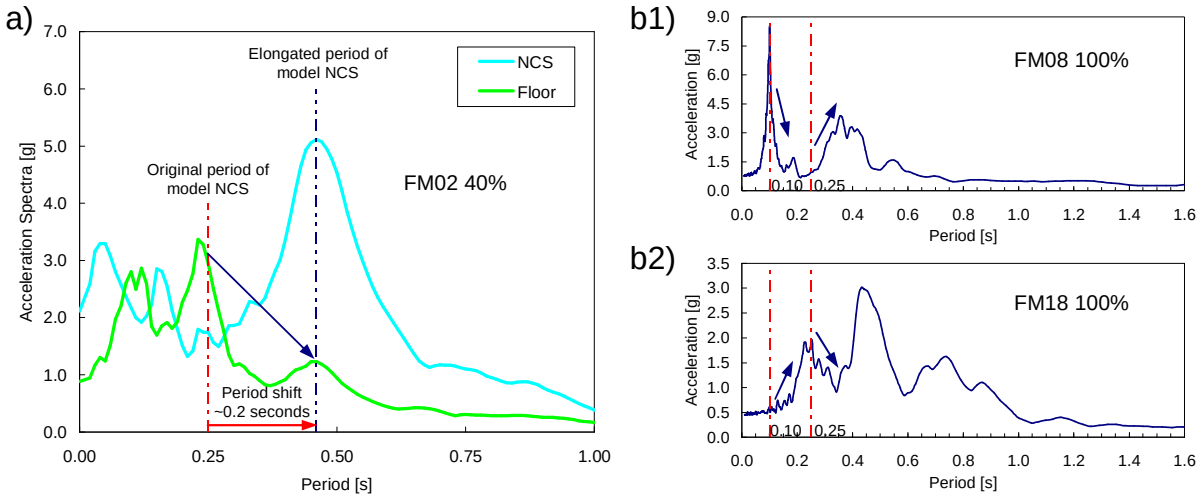

Figure 5.19 a) Response spectra based on measured floor and NCS accelerations (example: FM02 40 %, UC1, heavy model NCS); b) Spectral acceleration of unscaled input floor motions: b1) FM08; b2) FM18

It is important to note that the NCS period generally elongate in response to any FM, however, the resulting amplification depends on the specific fundamental NCS period and spectral acceleration of the input motion. This is exemplary shown in Figure 5.19b: The shift to longer periods during shaking has different results for the light model NCS (T = 0.10 seconds) and heavy model NCS (T = 0.25 seconds). In case of FM08, the amplification decreases for the light, but increases for the heavy model NCS, whereas in case of FM18 it is vice versa. Therefore, no general statement can be made whether the effect of period shift is beneficial or adverse.

5.3.1.3 Load transfer mechanism

The load history in Figure 5.20a is the same as in Figure 5.17a but further windowed. The opposite plotting of the north and south anchor pair loads together with the corresponding deflection (Figure 5.20b), allows understanding how the load is transferred during the phase of strong motions. The inertial loads generated due to the induced floor acceleration and the lever action (Figure 5.12a) result in a deflection of the model NCS and alternating loading of the north and south anchor pair (earthquake load). In addition, the anchors are loaded by the permanent gravity load (dead load). The following distinct load transfer phases can be identified and opposed to the deflected model NCS (Figure 5.20c, north is left hand side).

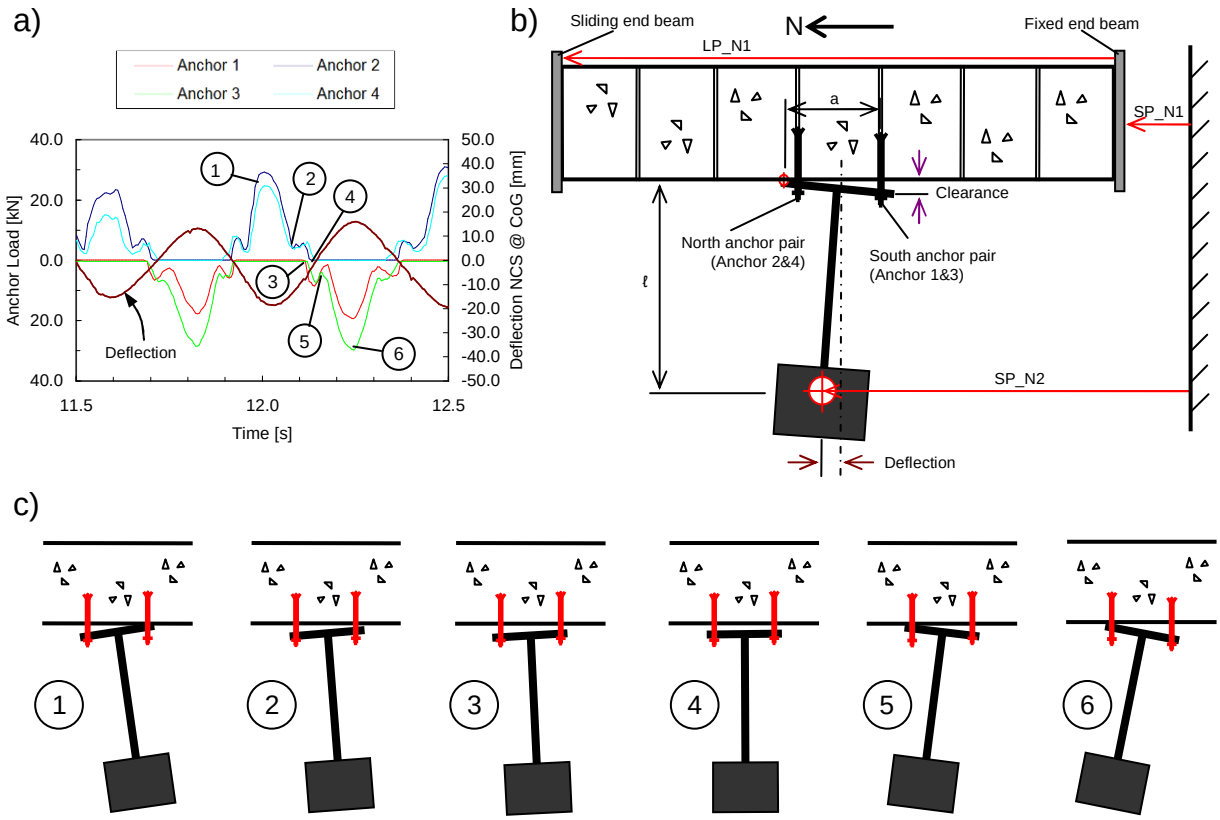

Figure 5.20 Load transfer mechanism: a) Anchor load time histories and deflection; b) Measured displacement and calculated deflection; c) Load transfer phases

(1) At the moment of largest deflection, the load on the north anchor pair reaches its peak. The footing touches the concrete on the opposite side and transfers compressive load. The anchor load is a reaction of the prying action derived from the supporting of the horizontally accelerated NCS by the concrete. (2) When the NCS swings back, the north anchor pair is gradually unloaded and finally, at the point of intermediate minimum anchor load, the opposite footing loses contact to the concrete. The NCS is now resting only on the north anchor pair and behaves like a pendulum. (3) On its way down, the vertical load component increases and makes the north anchor pair picking up tensile load again till the opposite footing touches the south anchor pair. The NCS is not leveled yet, so apparently the south pair anchor are less displaced than the north pair anchors. (4) With further swinging and increasing load on the south anchor pair, the displacement of the south anchor pair increases. The NCS is leveled and then deflected to the north side. At the same time the north anchor pair is completely unloaded. (5) The NCS is a pendulum again and with ongoing rotation the vertical load component decreases. In consequence, the tensile load of the south pair anchors decreases till the opposite footing touches the concrete. (6) At this point the prying action is effective and the load on the south pair anchor increase till it reaches its maximum at maximum deflection.

In conclusion, the load transfer mechanism is dominated by the earthquake load; the much smaller dead load plays only a minor role. This is also reflected by the alternating loading over time showing no permanent load level (Figure 5.17a and Figure 5.20a). The increased anchor displacement results in an impact loading of the anchors when the footing hits the anchor.

5.3.1.4 Cracking and NCS oscillation

The predominant period of cracking $T_{p,cr}$ characterise the crack width cycling in the slab and correspond to the peak cracking period content depicted in Figure 5.5. The oscillatory behaviour of the NCS is identified best by the deflection of the NCS (Figure 5.20b). The corresponding time history in Figure 5.21 shows after a phase of transient oscillation, a relatively constant oscillation during the phase of strong motions. The corresponding period is also reflected in the peak of the NCS response spectra (Figure 5.19a) and is defined as the predominant period of NCS oscillation $T_{p,NCS}$. Its magnitude depends on the fundamental period of the model NCS and the floor motion characteristics. Maximum anchor loads are achieved at the maxima and minima of deflection (Figure 5.17a), illustrating that the period of NCS oscillation is in principle identical with the period of anchor load cycling.

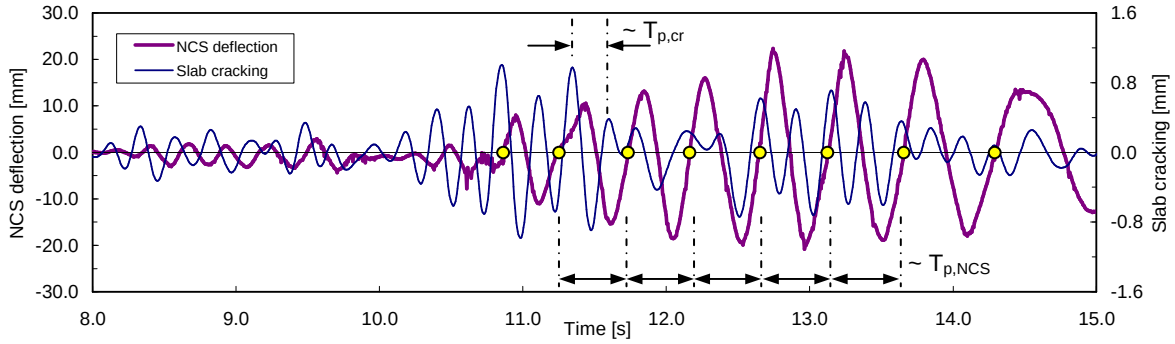

Figure 5.21 Windowed time histories of slab cracking and calculated NCS deflection

For relatively constant periods $T_{p,cr}$ and $T_{p,NCS}$, their ratio is also constant. For the particular example shown in Figure 5.21, the period of NCS oscillation is approximately twice the period of cracking. This aspect is discussed in more detail in the relevant sections.

5.3.1.5 Conclusions

For the critical frequency domain, the test setup is capable to sufficiently replicate the floor motions and crack records targeted for the slab, i.e. floor level. Its robustness guarantees repeatable test results. The chosen testing procedure proved feasible.

The shake table tests delivered unprecedented test data to evaluate the behaviour of anchored NCS in suspended configuration.

The time histories of anchor load, crack width, and anchor displacement helped to understand the load transfer mechanism of suspended NCS. Anchor loading in this configuration is dominated by earthquake loads which overcome the dead load and cause alternate loading of opposite anchors. The predominant periods of cracking $T_{p,cr}$ and NCS oscillation $T_{p,NCS}$ characterise the crack width and anchor load cycling, respectively.

The anchor displacement results inevitably in a period elongation of the NCS and confirmed the observations made on floor mounted NCS. However, whether the period shift helps to reduce the anchor load or results in amplified accelerations and increased anchor loads depends on the specific floor motion.

5.3.2 Correlation tests

The primary aim of the Correlation Tests was to investigate the coincidence of anchor load and crack width amplitude for the critical design case of a suspended NCS. Correlation describes a relation of two statistical variables (here: anchor load and crack width) between which, however, a causal relationship does not necessarily exist. The findings on the statistical distribution of the anchor load over crack width during seismic events (Figure 5.22a) allow drawing conclusions on the average load level if interpreted as the corresponding permanent load applied during crack cycling of the proposed seismic qualification test (Section 4.2.1, Figure 5.22b).

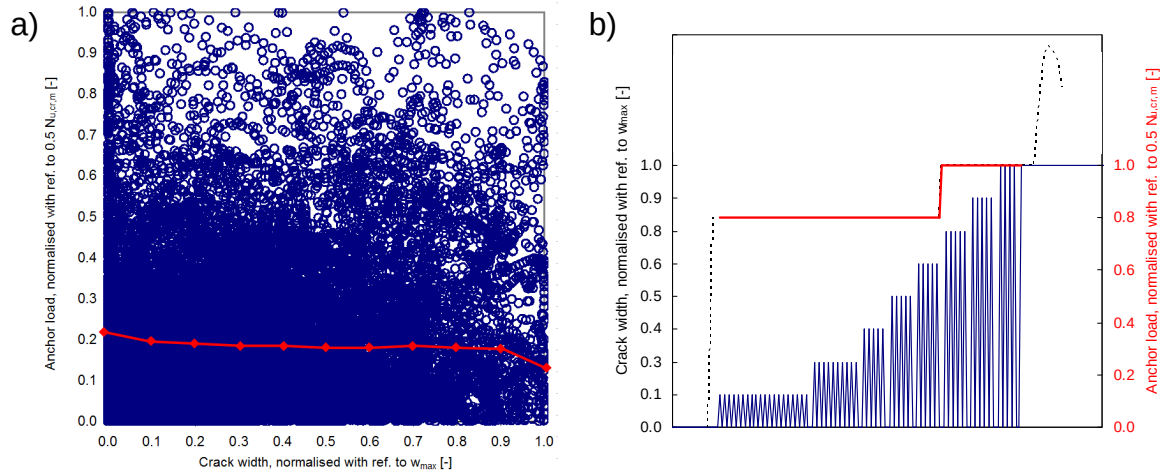

Figure 5.22 a) Statistical correlation of anchor load and crack width; b) Permanent anchor load and crack width cycling of simulated seismic test

For the Correlation Tests, only the UC1 anchor was used, and a maximum anchor load of $N_{target} = 0.5\ N_{u,cr,m} = 13.5$ kN and a maximum crack width of $w_{max} = 0.8$ mm

were targeted. To achieve the target anchor load, generally several test repeats with modified scale factors (Section 5.2.3.2) were required. Finally, both parameters were achieved with an adequate accuracy and just slightly over- or undershot the targets.

5.3.2.1 Correlation of anchor load and crack width during shaking

The Correlation Tests were conducted to collect statistical data on the correlation of anchor load and crack width (N-w correlation) which are representative for suspended NCS. The evaluation methodology is illustrated exemplary in Figure 5.23. During each test run, anchor load and crack width data are sampled for all four anchors at a rate of 200 Hz (Figure 5.23a). For further statistical evaluation, the data pairs measured at the four anchor locations are combined (Figure 5.23b, target value area is shaded). Binning the data with reference to the crack width allowed calculating the mean and one standard variation of the anchor load which then represents the complete data of the normalised N-w correlation. It is noted that due to small data population in the outmost crack width bins, the corresponding mean value is sometimes not representative.

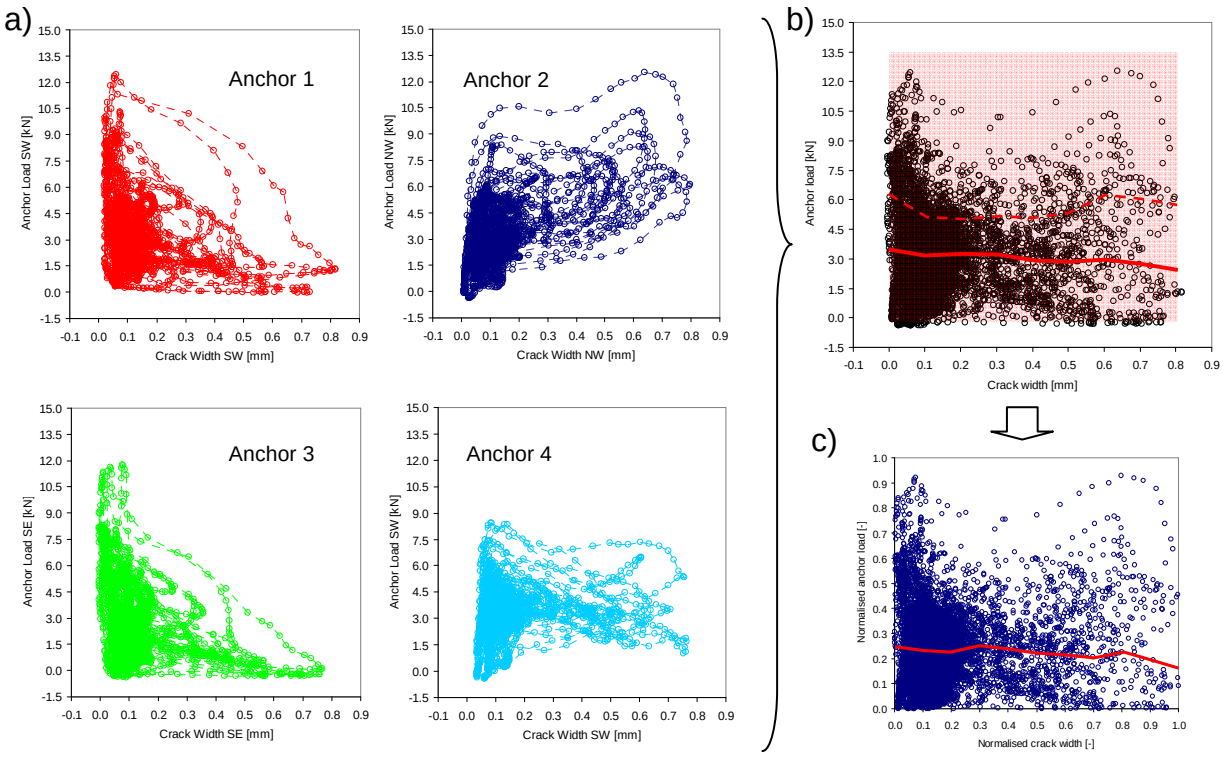

Figure 5.23 Measured anchor load versus crack width (example: FM03 21 %): a) Statistic for Anchor 1 to 4; b) Combined for Anchor 1 to 4, mean and one standard deviation of anchor load; c) Normalised with reference to N_{target} and w_{max}, mean anchor load

The aim to evaluate the N-w correlation in respect to the average load level during seismically induced shaking and cracking of the concrete, requires the normalisation of the test data (Figure 5.23c). If the normalisation is carried out with reference to $N_{target} = 0.5\ N_{u,cr,m}$, the correlation factor α can be interpreted as the reduction factor to be applied to the permanent load level in order to derive realistic demand level during crack cycling (Figure 5.22, Section 4.1.2).

5.3.2.2 Average anchor load level and effect of predominant periods

The diagrams in Figure 5.24 plot the mean (μ) and one standard deviation ($\mu + \sigma$) of the anchor loads measured for all floor motions versus the normalised crack width. The anchor loads are normalised with reference to $0.5\ N_{u,cr,m}$. Figure 5.24a depicts the data for the tests on the heavy model NCS, Figure 5.24b those on the light model NCS.

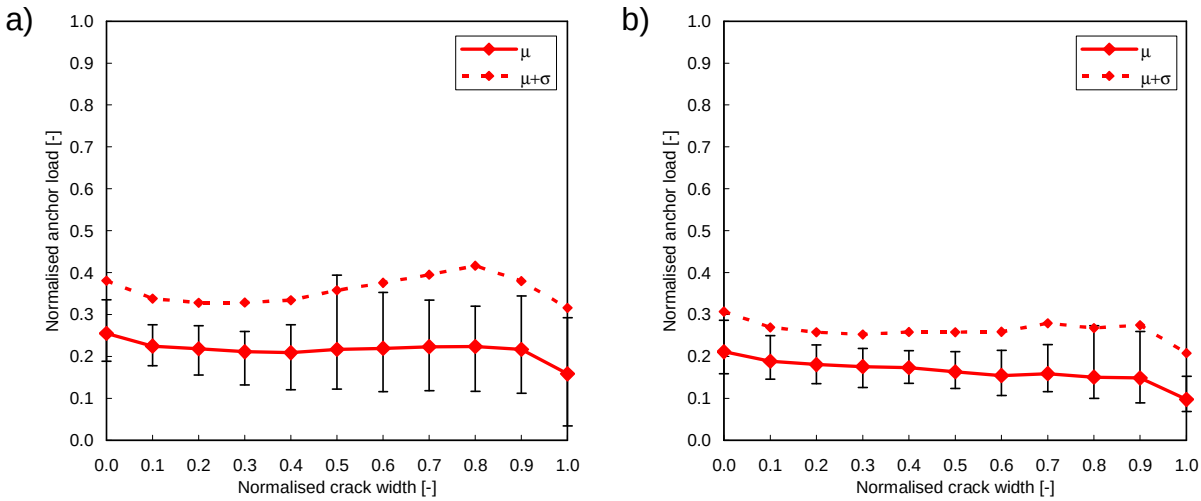

Figure 5.24 Mean anchor loads, normalised with reference to $0.5\ N_{u,cr,m}$, as mean (μ, solid line) and one standard deviation ($\mu + \sigma$, dashed line), and the fluctuation measured for the floor motions: a) Heavy model NCS, b) Light model NCS

The normalised anchor load over crack width is relatively constant. Table 5.1 provides the predominant periods of cracking $T_{p,cr}$ and NCS oscillation $T_{p,NCS}$, their ratio and the normalised average anchor load level N_{ave} / ($0.5\ N_{u,cr,m}$).

Table 5.1 Predominant periods of cracking and anchor loading, their ratio and the corresponding average anchor load level for the Correlation Tests

Floor motion	Heavy Model NCS				Light Model NCS			
	$T_{p,cr}$, s	$T_{p,NCS}$, s	$\frac{T_{p,cr}}{T_{p,NCS}}$	$\frac{N_{ave}}{0.5N_{u,cr,m}}$	$T_{p,cr}$, s	$T_{p,NCS}$, s	$\frac{T_{p,cr}}{T_{p,NCS}}$	$\frac{N_{ave}}{0.5N_{u,cr,m}}$
FM02	0.25	0.45	0.56	0.25	0.25	0.14	1.79	0.18
FM03	0.25	0.26	0.96	0.20	0.25	0.24	1.04	0.20
FM05	0.47	0.50	0.94	0.24	0.47	0.15	3.13	0.14
FM08	0.44	0.40	1.10	0.18	0.44	0.14	3.14	0.15
FM12	0.92	0.93	0.99	0.23	0.92	0.24	3.83	0.13
FM13	1.38	0.35	3.94	0.28	1.38	0.17	8.12	0.17
FM14	1.39	0.47	2.96	0.22	1.39	0.21	6.62	0.17
FM16	0.48	0.49	0.98	0.20	0.48	0.49	0.98	0.15
FM18	2.28	0.45	5.07	0.13	2.28	0.44	5.18	0.16
FM19	2.04	0.74	2.76	0.21	2.04	0.70	2.91	0.19
FM20	0.74	0.74	1.00	0.23	0.74	0.75	0.99	0.18
Mean [-]				0.22				0.17
CV [%]				18.2				13.1

The ratio of periods ($T_{p,cr}$ / $T_{p,NCS}$) varies substantially, however, the deviation in the average anchor load level calculated for various NCS periods and floor motions is relatively small with the corresponding CV at about 15 %.

5.3.2.3 Correlation factor

Since the anchor load level is nearly independent of the crack width, the normalised average anchor load level N_{ave} can be taken as the correlation factor α. Though not part of the correlation study, the analysis of the Displacement Tests (Section 5.3.3) with respect to the N-w correlation enhances the correlation statistic and is instructive for general conclusions. Table 5.2 compiles for various shake table tests the correlation factor as the average of all 11 tested FM.

Table 5.2 Mean, coefficient of variation, and mean plus one standard deviation of correlation factors determined for various shake table tests

	Correlation Test Suites $N_{target} = 0.5\ N_{u,cr,m}$		Displacement Test Suites $N_{target} = N_{5\%} / \gamma_M$				
	UC1, w_{max} = 0.8mm		UC1, Heavy NCS			EAb1, Heavy NCS	
	Heavy NCS	Light NCS	w_{max} = 0.5mm	w_{max} = 0.8mm	w_{max} = 0.8mm[1]	w_{max} = 0.5mm	w_{max} = 0.8mm
μ	0.22	0.17	0.22	0.22	0.22	0.21	0.21
CV	18.2 %	13.1 %	17.8 %	16.2 %	19.7 %	15.9 %	12.0 %
$\mu+\sigma$	0.29	0.22	0.28	0.34	0.29	0.26	0.25

(1) 2 anchors in crack, 4 anchors in crack for all other tests

The correlation factor is virtually identical for all test suites using the heavy model NCS. Only the tests on the light model NCS yield a smaller correlation factor.

5.3.2.4 Conclusions

The correlation in terms of normalised anchor load over crack width is relatively constant. The Correlation Tests on the heavy model NCS yield an average anchor load level of $N_{ave} = 0.22 \cdot (0.5\ N_{u,cr,m})$ and the Correlation Tests on the light model NCS yield $N_{ave} = 0.17 \cdot (0.5\ N_{u,cr,m})$. This corresponds to a correlation factor of about $\alpha = 0.2$. Taking one standard deviation into account, the factor is increased by about 50 %.

The average anchor load level is relatively low, however, due to the gravity loads, higher than for tests on floor mounted NCS (*Watkins, D.; Hutchinson, T. (2011)*) which yielded correlation factors of about $\alpha = 0.1$. In conclusion, to replicate realistic demand levels, the permanent load level during crack cycling may be reduced to $0.2 \cdot (0.5\ N_{u,cr,m})$ when simulating seismic actions on non-structural connections. This observation could be recognised in the proposed seismic qualification tests by further reducing the reduction factor of 0.8 applied to the permanent load during the serviceability portion of the test, provided that the anchor qualification is limited to non-structural connections only.

The comparative study on correlation factors determined for the N-w data of Displacement Tests clearly showed that the correlation factor is independent of the maximum anchor load and crack width during shaking, as well as the number of anchors in a crack, but primarily depends on the fundamental period of the NCS. These findings support a correlation factor of $\alpha = 0.2$.

5.3.3 Displacement tests

The primary aim of the Displacement Tests was to verify whether the dynamic shake table tests yield anchor displacement results which are in line with the displacement results of the qualification test protocols proposed for the seismic amendment of qualification guideline (Section 4.2). Figure 5.25 illustrates this approach by comparing the anchor displacement accumulated during a shake table tests and a seismic qualification test.

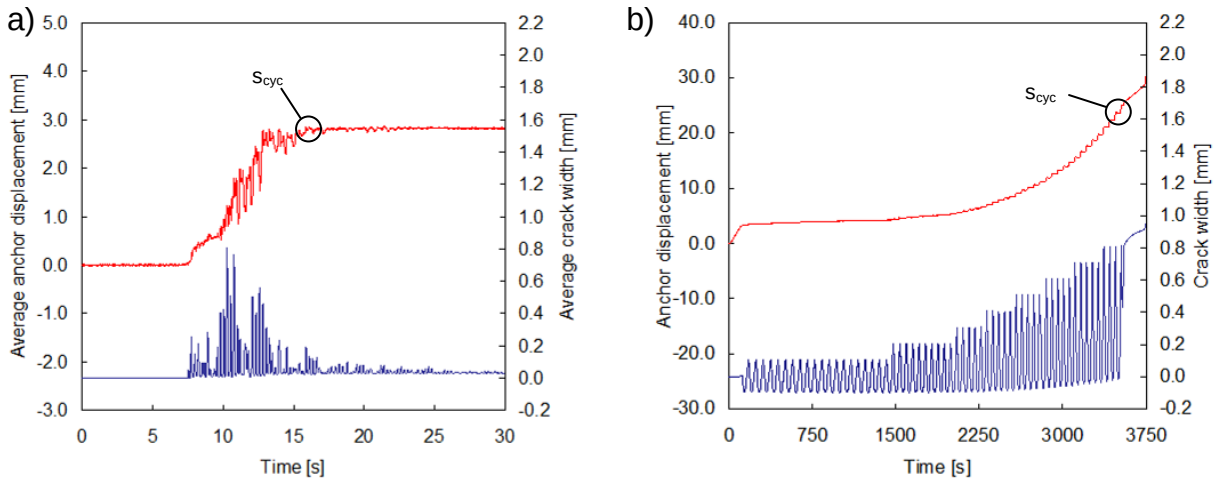

Figure 5.25 Measured anchor displacement and crack width time histories (examples taken from tests on EAb1 anchor): a) System level test; b) Component level test

All Displacement Tests were run on the heavy model NCS. The selected floor motions (Section 5.2.1.2) were scaled (Section 5.2.3.2) to achieve maximum anchor loads approximately equal to the seismic design strength $N_{5\%} / \gamma_M$. of 24 kN for the UC1 anchor and 11 kN for the EAb1 anchor. The scale factors were kept constant for all tests on the particular anchor type.

5.3.3.1 Anchor displacements accumulated during shaking

During shaking, the anchor displacements accumulate according to the seismic demand articulated in the anchor load and crack width time histories (Figure 5.26a) which in turn depend on the characteristics of the FM and CR. The increase in anchor displacement is highest when high anchor loads meet large crack widths. In contrary, if the anchor is loaded but the crack is closed or, vice versa, if the crack is opened but the anchor is not loaded, there is virtually no increase in anchor displacement.

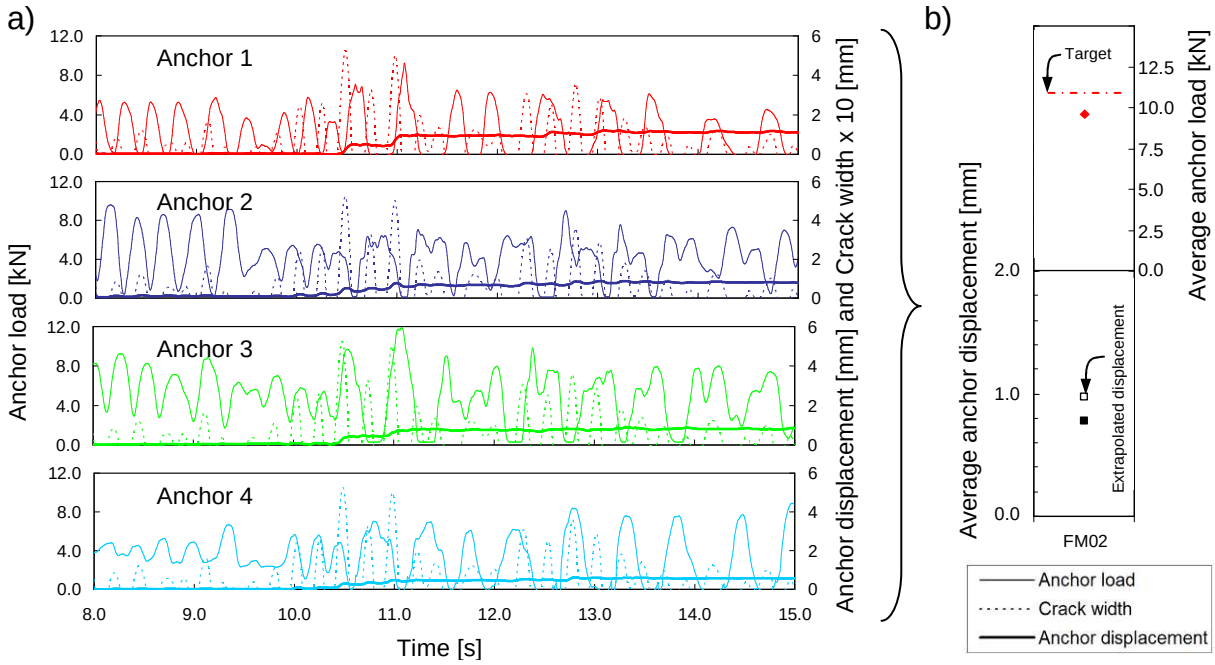

Figure 5.26 Measured and extrapolated anchor displacement (example: FM02 15 %): a) Combined time histories of anchor loads, anchor displacements and crack widths; b) Calculation of the extrapolated average anchor displacement

As the crack width time history is not affected by any response actions of the NCS, the targeted maximum crack width is generally achieved with a high degree of accuracy (Section 5.3.1.1). However, though the individual scale factors required for achieving the targeted anchor loads were estimated on the basis of earlier Correlation Test results, the anchor load over- and undershot the targets. Contrary to the Correlation Tests with associated minimal displacements, however, the relative large anchor displacements occurring during the Displacement Tests prohibited frequent test retakes. The available embedment reduction and limited number of test position would have been consumed up quickly. Instead, the average anchor displacement was extrapolated (Figure 5.26b) assuming an approximately linear relationship between anchor load and displacement (Section 3.7.2.5).

5.3.3.2 Average anchor displacements and effect of predominant periods

The diagram in Figure 5.27a depicts the extrapolated average anchor displacement for all tested FM. The displacements are smaller for 0.5 than for 0.8 mm maximum crack widths, and smaller for the stiffer UC1 than for the EAb1 anchor. For the tests on the UC1 anchor with just 2 anchors in crack, the average anchor displacement decreased by approximately 40 % on average, though the maximum anchor loads increased by 10 % on average.

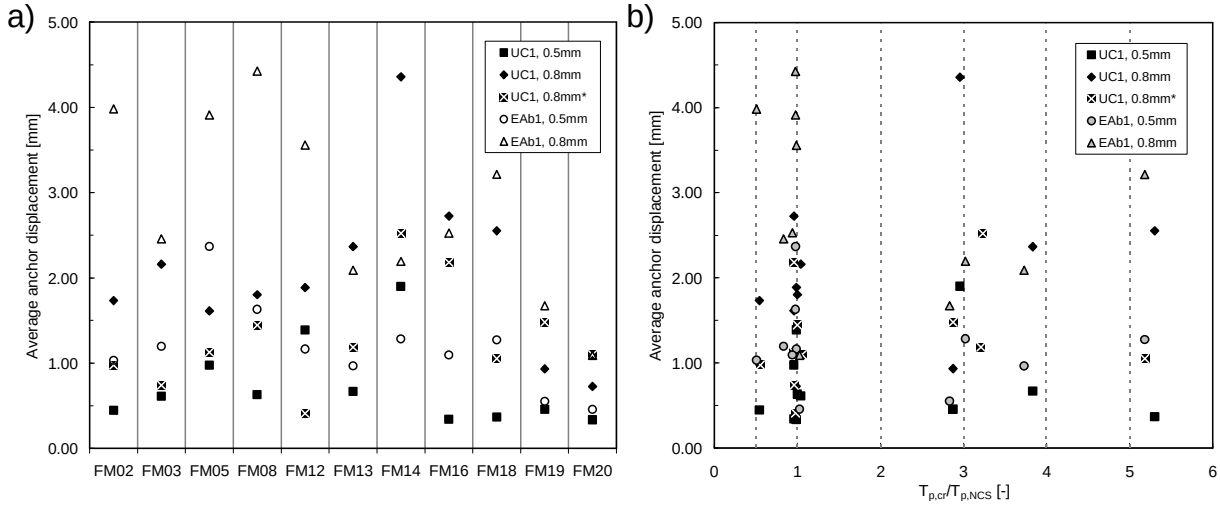

Figure 5.27 Average anchor displacement (test suite with 2 anchors in crack marked by *): a) Values versus FM; b) Values versus $T_{p,cr}$ / $T_{p,NCS}$

Table 5.3 provides the ratio of predominant period of loading $T_{p,NCS}$, the ratio of predominant periods $T_{p,cr}$ / $T_{p,NCS}$ and the displacement after shaking s_{cyc}. The values of $T_{p,NCS}$ and $T_{p,cr}$ were derived as those for Table 5.1.

Table 5.3 Predominant periods of cracking and anchor loading, their ratio and the resulting average weighted anchor displacement for the Displacement Tests

Floor motion	UC1 Anchor				EAb1 Anchor			
	$T_{p,NCS}$, s	$\frac{T_{p,cr}}{T_{p,NCS}}$	s_{cyc} (w_{max}=0.5mm), mm	s_{cyc} (w_{max}=0.8mm), mm	$T_{p,NCS}$, s	$\frac{T_{p,cr}}{T_{p,NCS}}$	s_{cyc} (w_{max}=0.5mm), mm	s_{cyc} (w_{max}=0.8mm), mm
FM02	0.46	0.54	0.45	1.73	0.49	0.51	1.03	3.98
FM03	0.24	1.04	0.61	2.16	0.30	0.83	1.20	2.46
FM05	0.49	0.96	0.98	1.61	0.48	0.98	2.37	3.91
FM08	0.44	1.00	0.63	1.80	0.45	0.98	1.63	4.43
FM12	0.93	0.99	1.39	1.89	0.93	0.99	1.16	3.56
FM13	0.36	3.83	0.67	2.37	0.37	3.72	0.97	2.09
FM14	0.47	2.96	1.90	4.36	0.46	3.02	1.28	2.19
FM16	0.50	0.96	0.34	2.72	0.41	1.17	1.09	2.53
FM18	0.43	5.30	0.37	2.55	0.44	5.18	1.27	3.22
FM19	0.71	2.87	0.46	0.93	0.72	2.83	0.55	1.67
FM20	0.75	0.99	0.33	1.00	0.72	1.04	0.46	1.09
Mean [mm]			0.74	2.10			1.18	2.83
CV [%]			47.5	44.8			43.3	37.5

The predominant periods of cracking $T_{p,cr}$ are identical to and the predominant periods of NCS acceleration $T_{p,NCS}$ are approximately the same as those determined for the Correlation Tests on the heavy model NCS given in Table 5.4. In conclusion, also the ratios of periods $T_{p,cr} / T_{p,NCS}$ are approximately the same as for the Correlation Tests and apparently cluster around 1.0 and its integral multiples. However, a relation between $T_{p,cr} / T_{p,NCS}$ and the magnitude of anchor displacement cannot be inferred (Figure 5.27b), though the specific characteristics of the floor motion seem to have a significant influence on the anchor displacement which CV is in the order of 40 %.

5.3.3.3 Comparison of component and system level displacements

Before comparing the component and system level displacements, it is interesting to know whether there is a relation between the demand deriving from the floor motion and the resulting anchor displacement. Therefore, the input motion data are evaluated based on the accumulated damage potential (ADP) approach formulated in Equation 3.22 [$ADP = \int (N \cdot w)$]. It is assumed that the anchor load N is the result of the floor acceleration arising from the FM, and the crack width is the result of the floor curvature history defined by the CR:

$$ADP_t = \int_{t1}^{t2} \left|FM(t)\right| \cdot CR(t)^{+} \cdot dt \qquad \text{Equation 5.3}$$

FM(t) and CR(t) are the normalised time histories as shown in Figure 5.5. Since the displacement of the anchor during crack closure can be neglected for design load levels, only the positive range of the CR is considered (Figure 5.28a). In contrast, the acceleration creates anchor loads in both directions of the motion and therefore the FM is taken as the absolute value. Since the anchor is loaded to its design strength at maximum, it is further reasonable to assume that all anchor displacement is generated by slip during crack cycling and not due inelastic load levels.

Figure 5.28b depicts the values for ADP_t for all floor motions tested. The diagram further shows the average anchor displacement s_{cyc} as presented in Table 5.3 for the tests with $w_{max} = 0.5$ mm. It can be seen that by trend, the accumulated anchor displacements develop according to the ADP_t of the underlying floor motion. For better visualisation, the ADP_t values as well as the anchor displacements of the respective anchor type and crack width are interconnected.

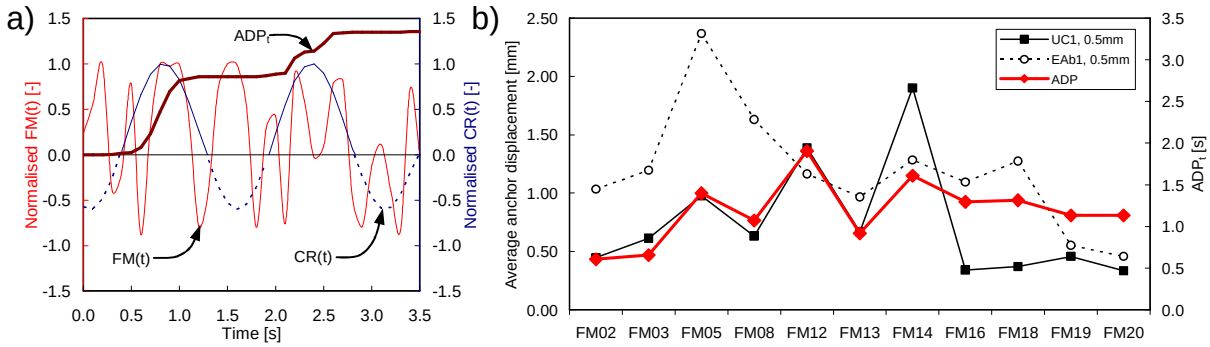

Figure 5.28 Accumulated damage potential: a) Integration of FM and CR over time (schematic); b) Measured anchor displacement and ADP_t for the tested floor motions

Due to the specific load transfer system (Figure 5.20) the acceleration time history is not identical with the anchor load time history. However, the approach shows that there is a relation between the demand arising from the input motions and the resulting anchor displacements, though the lines in Figure 5.28b are not perfectly congruent. It is noted that the test data depicted in Figure 5.28b represents only one test and that in particular the anchor displacement due to crack width cycling is subject to large scatter (Section 3.6.2.3).

Table 5.5 compiles the mean, the CV, and the mean plus one standard deviation of the anchor displacements measured for all floor motions, and compares them to the corresponding displacement after crack cycling measured for the tests which were carried out according to the proposed seismic qualification tests (Section 4.2.1).

Table 5.5 Mean, coefficient of variation, and mean plus one standard deviation of anchor displacements measured for system and component level tests

Anchor type and max. crack width	s_{cyc} System Level Tests			s_{cyc} Component Level Tests		
UC1, Heavy NCS	$N_{max} = N_{5\%} = 24$kN			$N_{max} = 0.5N_{u,m,cr} = 17.1$kN		
	μ, mm	CV, %	μ+σ, mm	μ, mm	CV, %	μ+σ, mm
w_{max} = 0.5mm (serviceability level)	0.7	47.5	1.8	~ 2.0(2)	~ 17.1(2)	~ 2.6(2)
w_{max} = 0.8mm (suitability level)	2.1	44.8	3.6	~ 4.5(2)	~ 27.4(2)	~ 6.4(2)
w_{max} = 0.8mm(1) (suitability level)	1.3	46.3	1.9	-	-	-
EAb1, Heavy NCS	$N_{max} = N_{5\%} = 11$kN			$N_{max} = 0.5N_{u,m,cr} = 10.9$kN		
	μ, mm	CV, %	μ+σ, mm	μ, mm	CV, %	μ+σ, mm
w_{max} = 0.5mm (serviceability level)	1.2	43.3	1.7	8.5	9.1	9.3
w_{max} = 0.8mm (suitability level)	2.8	37.5	3.9	23.2	22.5	28.4

(1) 2 anchors in crack, 4 anchors in crack for all other tests
(2) Values extrapolated on basis of the ADP approach

As discussed in Section 5.2.4.1, no performance data were available for the UC1 anchor tested according to the proposed seismic qualification test. However, comparing the load and crack demand of the proposed seismic qualification test with that of earlier crack cycling tests (Figure 5.29a) allows estimating the displacement. By means of Equation 3.23 [$ADP_n = \Sigma_n (a \cdot N_{max} \cdot w_{max})$; N normalised with reference to 0.5 $N_{u,m,cr}$; w normalised with reference to w = 0.8 mm], the ADP of the proposed seismic qualification test is 4.95 after 45 cycles (serviceability level) and 11.01 after 59 cycles (suitability level), whereas the test protocol of the earlier crack cycling tests yielded an ADP of 4.32 after 32 cycles and a displacement of s_{cyc} = 1.75 mm (Figure 5.30a). In conclusion, the displacement after crack cycling can be estimated to 1.75 · 4.95 / 4.32 = 2.0 mm (serviceability level) and 1.75 · 11.01 / 4.32 = 4.5 mm (suitability level).

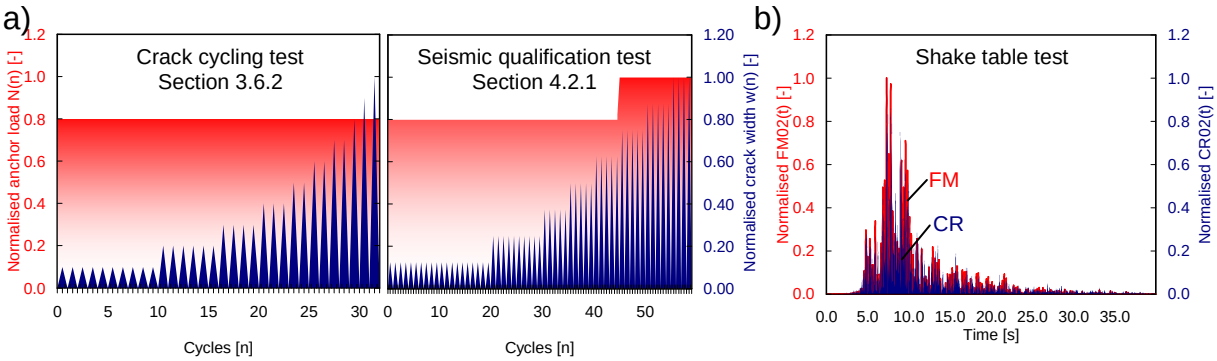

Figure 5.29 Load and crack demand: a) Test protocol of component level tests; b) FM and CR histories of system level test (example: FM02)

The anchor displacements experienced during shaking of system level tests are much smaller than those during crack cycling of component level tests (Table 5.5). This is conclusive since the anchor load level during the shake table tests was relatively low. In order to compare the load and crack demand of the component and system level tests, the accumulated damage potential has to be normalised. For the component level tests, the ADP_n was determined by integrating over the number of cycle n. Normalisation with reference to n yields 11.01 / 59 = 0.19 on suitability level and 4.95 / 45 = 0.11 on serviceability level. In contrast, for the system level tests, the ADP_t was determined by integrating floor motion and crack records (Figure 5.29b) over time t (Equation 5.3). Normalisation with reference to t yields 0.065 (suitability level) and 0.040 (serviceability level) on average for all tested 11 floor motions (Figure 5.30b). In conclusion, the seismic qualification test is approximately three times (0.19 / 0.065 ~ 0.11 / 0.04 ~ 3) as demanding as the shake table test, provided that same maximum anchor load and crack width are tested.

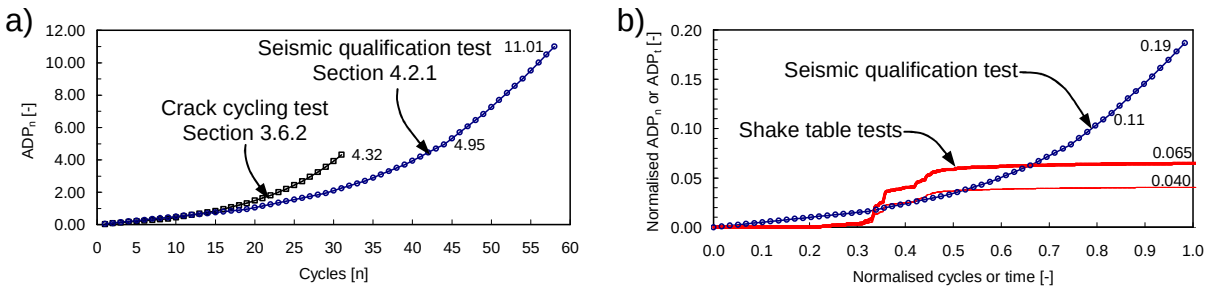

Figure 5.30 Accumulated damage potential: a) ADP_n for component level tests; b) Normalised ADP_n of seismic qualification test and normalised ADP_t as average of the 11 floor motions tested

After weighing the mean plus one standard variation displacements $s_{cyc}(\mu + \sigma)$ determined for crack cycling on the serviceability level (Table 5.5), the magnitude comes quite close to the corresponding displacements measured at the end of shaking: 2.6 mm · 24 kN / (3 · 17.1 kN) = 1.2 mm ≈ 1.8 mm for the UC1 anchor and 9.3 mm · 11 kN / (3 · 10.9 kN) = 3.1 mm ≈ 1.7 mm for the EAb1 anchor.

5.3.3.4 Conclusions

Anchor displacement accumulates during shaking and is the result of anchor load and crack width. For the same degree of strength utilisation, the anchor displacement depends primarily on the anchor type and the maximum crack width. Though the maximum anchor load increases for a given peak input motion, the anchor displacement is substantially reduced if not all anchors are located in a crack. The influence of the floor motion characteristics on the anchor displacement is significant but scatters.

It was demonstrated that the relative seismic demand, which is largely expressed by the accumulating anchor displacement, can be estimated by integrated input motions according to the ADP approach. Normalisation of the ADP enables comparing the load and crack demand of component and system level tests.

The anchor displacements measured in shake table tests on fully utilised anchors are much smaller than those determined in proposed seismic qualification tests. If however the load and crack demand is taken into account and the results are extrapolated accordingly, the anchor displacements are of about the same magnitude. Since the residual load capacity primarily depends on the remaining embedment depth after load and crack cycling, one may assume that also the residual load capacities are comparable. In conclusion, the shake table tests yield results that are in line with the results of the seismic qualification tests.

5.3.4 Failure tests

The primary aim of the Failure Tests was to investigate the failure mechanism and ultimate seismic capacity. The IDA approach allowed several test runs on the anchored model NCS before it finally failed. The final failure was targeted for the third or fourth test run. All Failure Tests were captured by three video cameras. Two were pointing at the model NCS footings, another camera took the big picture of the shaking slab and NCS from the side. Test videos containing the three camera shots and synchronised test data plots were produced. The shown data included the table acceleration and displacement, the averaged crack width for the north and south anchor pairs, as well as the loads and displacements of all anchors (Figure 5.31).

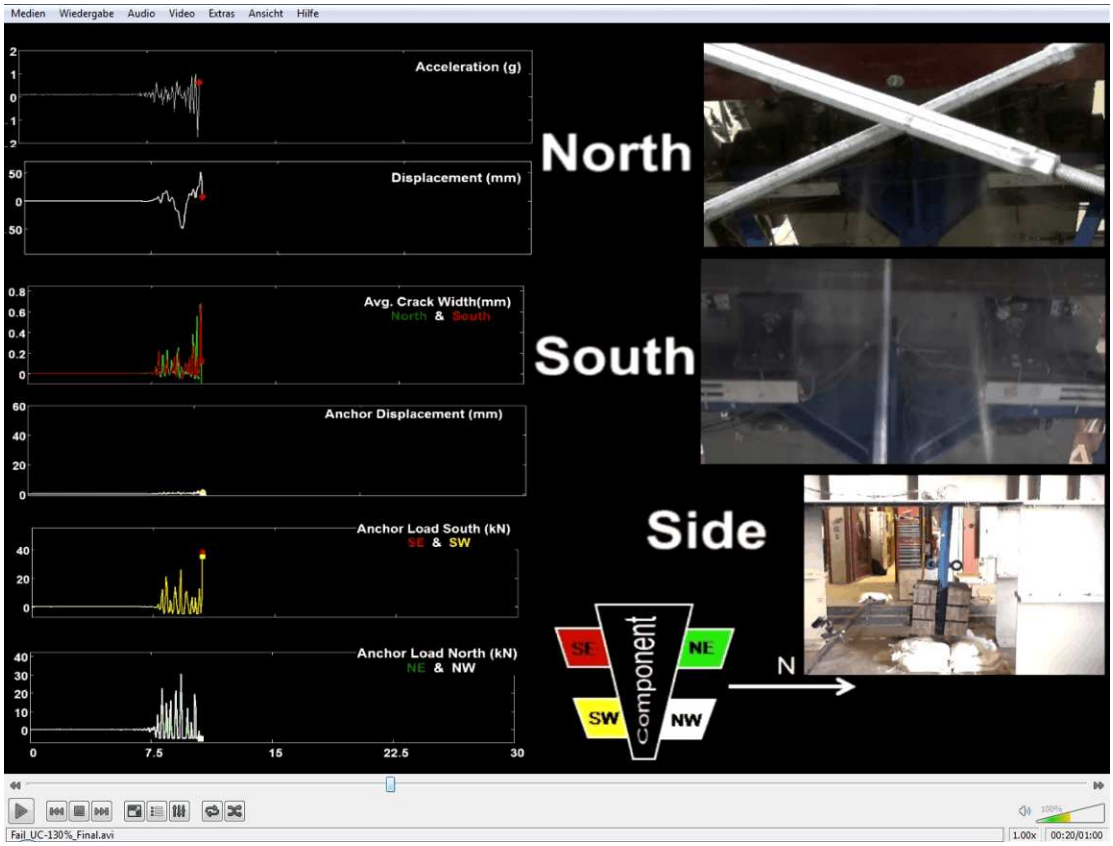

Figure 5.31 Screenshot of a video compiling synchronised test data and videos

For all Failure Tests, the heavy model NCS was tested using FM02 and CR02 with w_{max} = 0.8 mm. One series was carried out on the UC1 anchor, another one on the EAb1 anchor. The original embedment depths were identical to those used for the component level tests. After each test run without failure, the anchors were re-tightened. The permanent displacement the anchor already experienced at that stage was deemed to be negligible. Further details are presented in *Mahrenholtz, P.; Hutchinson, T.; Eligehausen, R. et al. (2012)*.

5.3.4.1 Load-displacement behaviour and partial failure

The UC1 anchor represents an anchor type failing in a quasi brittle concrete mode. The anchors were installed with an original embedment depth of 90 mm. After test runs with scale factors of 40, 70 and 100 %, the north anchor pair (Anchor 2 and 4) broke almost simultaneously after 10.68 seconds during the test run with a scale factor of 130 % (Figure 5.32).

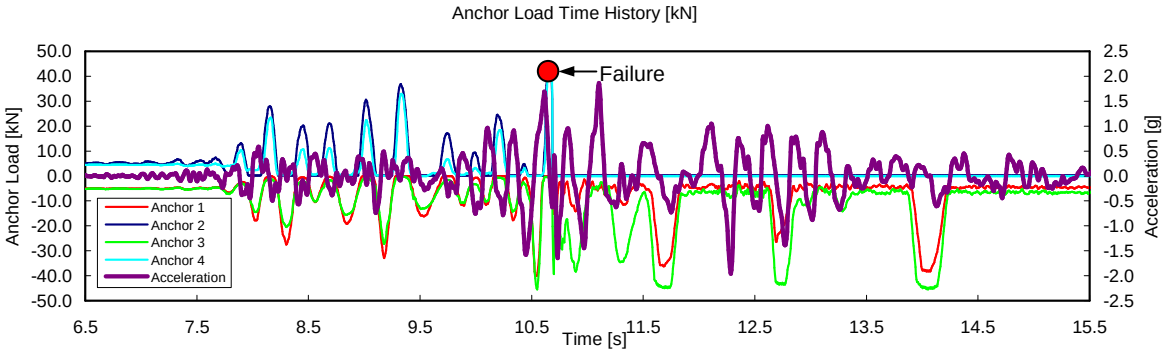

Figure 5.32 Anchor load and acceleration time histories for Failure tests on UC1 (FM02 130%); moment of partial failure marked by red dot

The load-displacement curves are given for all four anchors in Figure 5.33. Since no reference test were carried out within the shake table test programme, the monotonic mean curves were extracted from *Watkins, D.; Hutchinson, T. (2011)* and adjusted for the actual embedment depth.

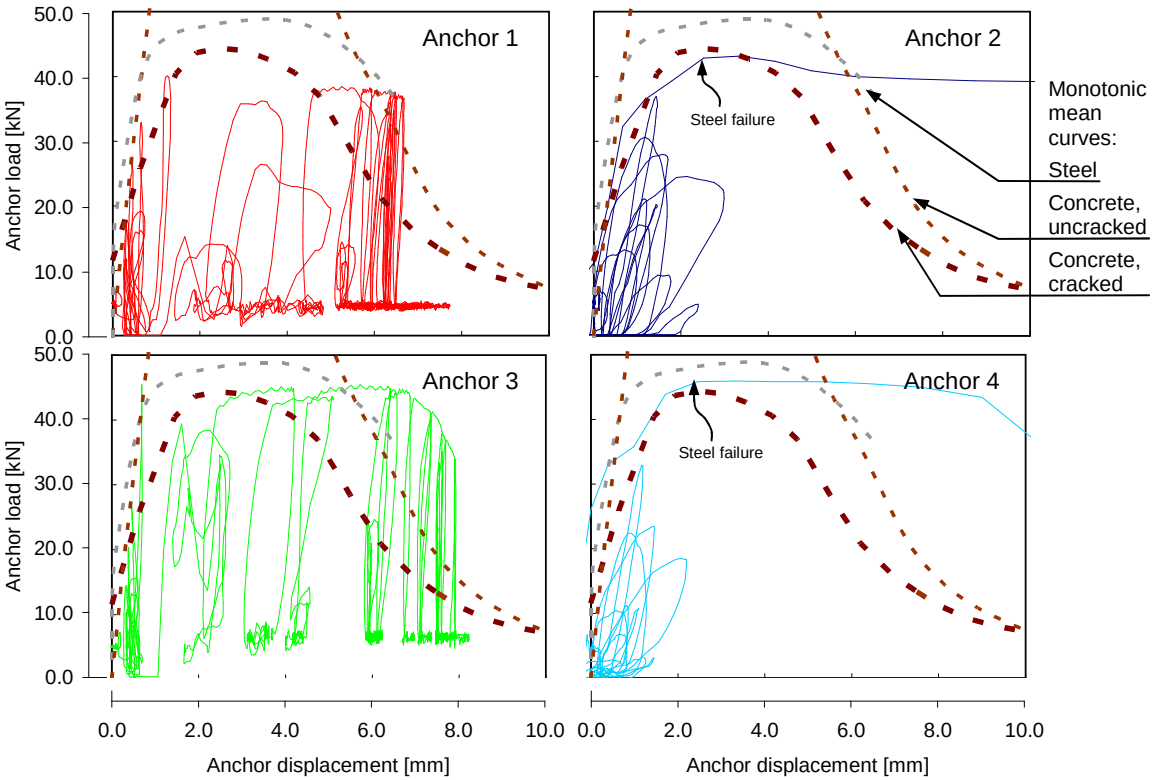

Figure 5.33 Load-displacement curves of Failure Test on UC1 (FM02 130%)

The curves frequently exceeded the monotonic mean envelope for cracked concrete due to crack closure. At the moment of failure, the crack width was 0.15 mm. Steel failure load in Anchor 2 and 4 was significantly lower than the steel capacity of the anchor bolt of 48.9 kN, probably because of LCF induced by bending of the bolt in the tight footing during strong NCS deflections. Anchor 1 and 3 were heavily loaded at the moment of failure of Anchor 2 and 4, however, made it through the floor motion. The load-displacement curves show large displacement capacities which significantly went beyond what was expected for the cracked concrete monotonic envelop. This indicates that also these anchors were at the onset of steel failure. The failure occurred before the peak acceleration was reached. After failure of Anchor 2 and 4, the installed model NCS behaved like an ideal pendulum with a period of $T = 2 \cdot \pi \cdot (\ell / g)^{0.5} = 2 \cdot \pi \cdot (1.397 / 9.81)^{0.5} = 2.37$ seconds.

Figure 5.34 shows pictures taken after failure and removal of the model NCS. The concrete remained intact (Figure 5.34a). The bolts ruptured about 10 mm below the nuts (Figure 5.34b).

Figure 5.34 a) Failure photograph of the 130 % test run on the UC1 anchor;
b) Photograph of ruptured bolts

The EAb1 anchor represents an anchor type with substantial displacement capacity due to the pseudo ductile pull-through failure mode. The anchors were installed with an original embedment depth of 83 mm. After test runs with scale factors of 20 and 40 %, Anchor 2 failed after 14.97 seconds during the test run with a scale factor of 60 %. (Figure 5.35). Anchor 4 (also north anchor pair) was clearly beyond its peak capacity.

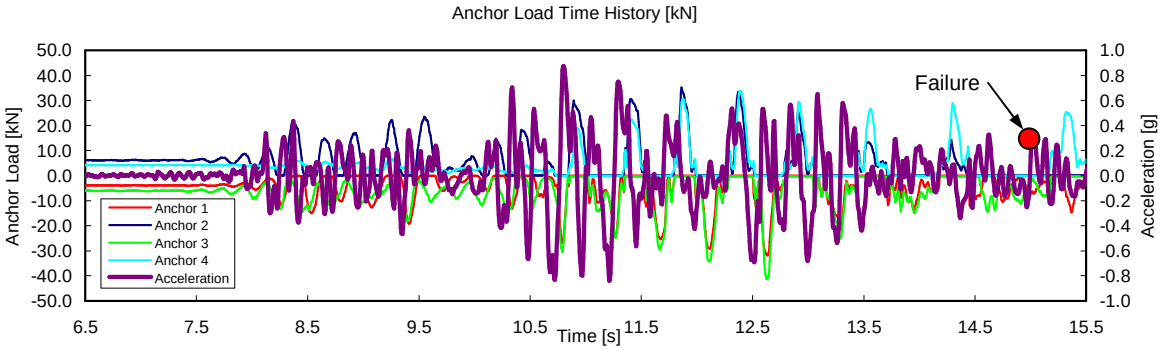

Figure 5.35 Anchor load and acceleration time histories for Failure Test on EAb1 (FM02 60%); moment of partial failure marked by red dot

The load-displacement curves are given for all four anchors in Figure 5.36. Again, the monotonic mean curves in the following load-displacement diagrams were extracted from *Watkins, D.; Hutchinson, T. (2011)*.

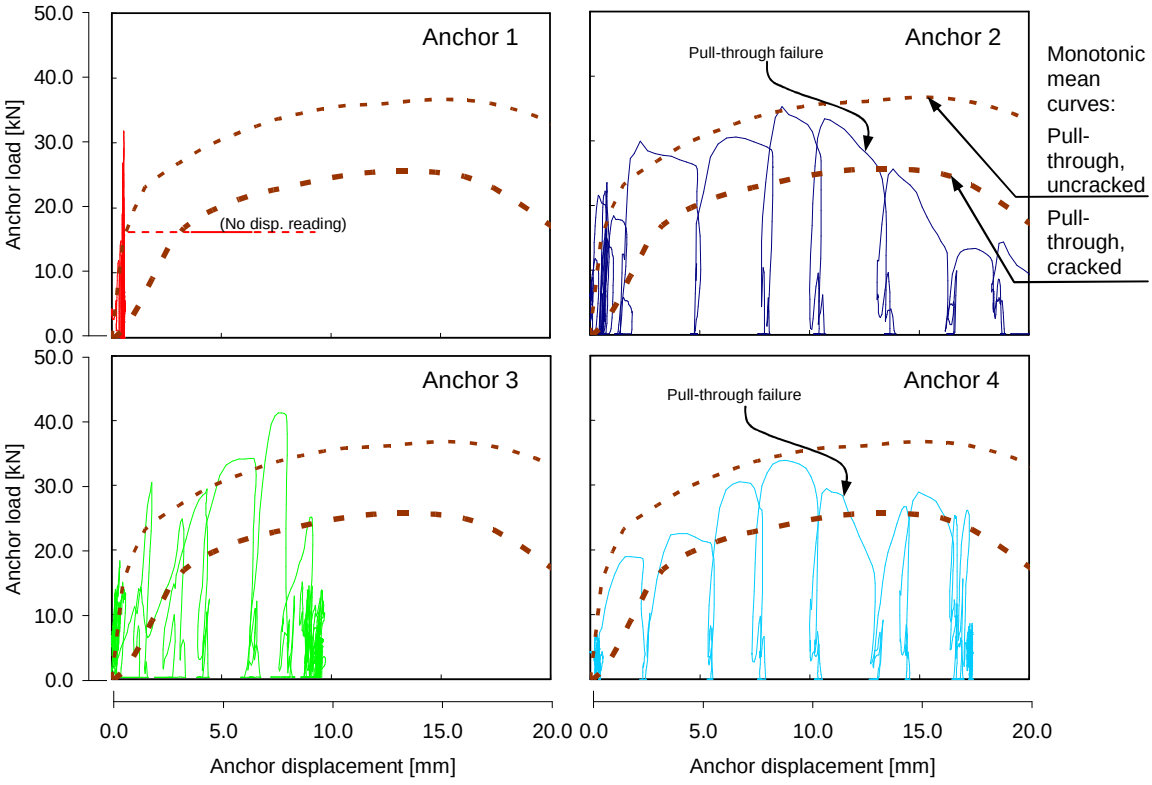

Figure 5.36 Load-displacement curves of Failure Test on EAb1 (FM02 60%)

The curves frequently exceeded the monotonic mean envelope for cracked concrete, and there were also brief excursions above the envelope for uncracked concrete due to crack closure. At the moment of failure, the crack width was 0.15 mm. The displacement of Anchor 2 and 4 was substantially larger than that of Anchor 3. Prior to failure, Anchor 2 was decreasingly loaded and Anchor 4 was taking over a steadily increasing share of the north anchor pair load. This soft transition of the load avoided an abrupt overload of Anchor 4 at the moment of final failure. The failure occurred when the peak acceleration was just reached. The model NCS anchored by only three anchors turned into an asymmetric system and showed an out of plane vibration mode.

Figure 5.37 shows pictures taken after failure and removal of the model NCSThe concrete remained intact (Figure 5.37a). The expansion clip of the pulled through bolt was left in the borehole (Figure 5.37b).

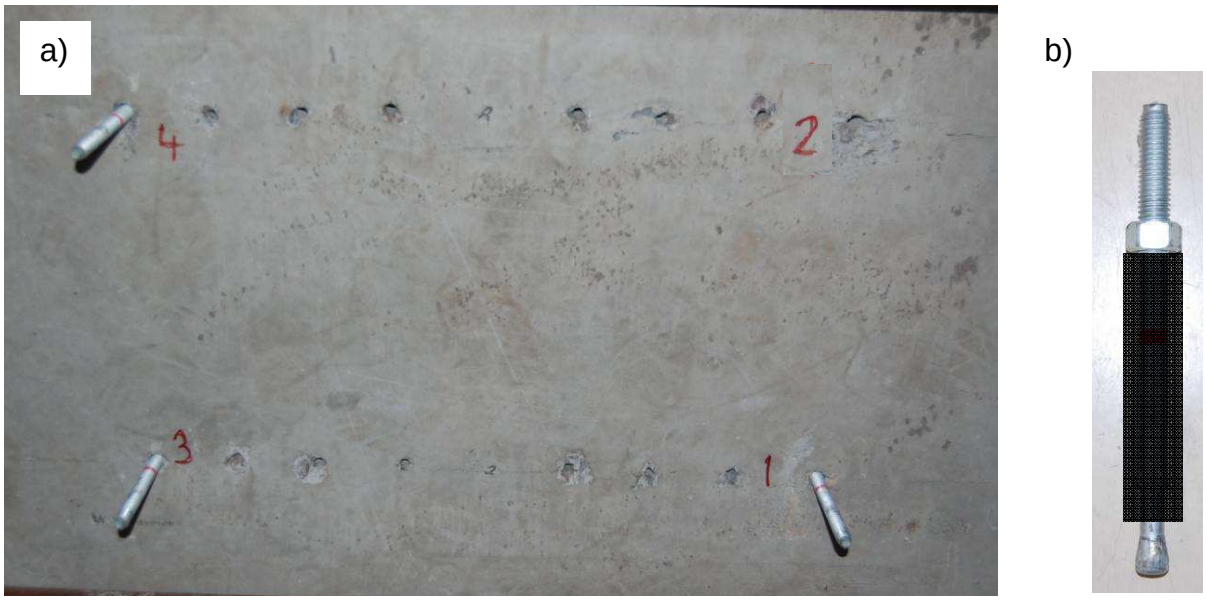

Figure 5.37 a) Failure photograph of the 60 % test run on the EAb1 anchor
b) Photograph of pulled through bolt

5.3.4.2 Seismic anchor strength and system performance

Anchor strength is the main anchor performance parameter current design methodology falls back on. The tests carried out according to the test protocols of proposed seismic qualification tests yielded seismic anchor capacities which were introduced in Section 5.2.4.1 as the nominal seismic strength $N_{5\%}$ (characteristic strength taken as the 5 % fractile). The ultimate loads measured for shake table tests allow determining the seismic capacity of the anchor in the installed situation. For the individual maximum, i.e. ultimate anchor loads during the final Failure Tests $N_{max,i}$,

the corresponding characteristic capacity N_k (characteristic strength taken as the 5 % fractile) can be calculated based on the mean ultimate loads and corresponding CV (Section 2.1.6). Table 5.6 summarises the relevant test data.

Table 5.6 Comparison of key test results of component level and system level tests

	UC1			EAb1		
Component Level Test	$N_{u,cr,m}$, kN	$s(N_{u,cr,m})$, mm	$w(N_{u,cr,m})$, mm	$N_{u,i}$, kN	$s(N_{u,i})$, mm	$w(N_{u,i})$, mm
Anchor (3 nos.)	40.7(1)	5.0(1)	0.80	24.3	7.61	0.80
$N_{5\%}$, kN	37.0			16.6		
System Level Test	$N_{max,i}$, kN	$s(N_{max,i})$, mm	$w(N_{max,i})$, mm	$N_{u,i}$, kN	$s(N_{u,i})$, mm	$w(N_{u,i})$, mm
Anchor 1 (SW)	40.1	1.19	0.10	31.8	0.48	0.10
Anchor 2 (NW)	43.1	2.49	0.16	35.3	8.48	0.19
Anchor 3 (SE)	45.5	5.60	0.10	41.2	7.46	0.05
Anchor 4 (NE)	45.9	2.52	0.16	33.9	8.55	0.10
Mean	43.7	2.95	0.13	35.5	6.25	0.11
CV, %	6.1			11.4		
N_k, kN	39.3			28.8		
N_k / $N_{5\%}$	1.06			1.74		

(1) Values extrapolated on basis of the ADP approach

The ratio of the characteristic strengths N_k / $N_{5\%}$ compares the system to the component level capacity. Values near 1 represent a good consistence of the seismic strength assigned to the anchor on basis of qualification tests and the seismic strength determined by shake table tests. For the UC1 anchor, the shake table tests yielded capacities which were marginally higher (6 %) than the seismic strengths based on qualification tests. For the EAb1 anchor, the shake table tests yielded capacities which were significantly higher (74 %) than the seismic strengths anticipated by the qualification tests. The reason for this is that the crack was only opened to $w \approx 0.12$ mm compared to $w_{max} = 0.80$ mm at the moment of ultimate anchor load. This also applies to the Failure Test on the UC1 anchor; however, the effect was not visible because the concrete capacity for the partly closed crack exceeded the steel capacity.

The results of the Failure Test series are also useful to characterise the system performance. Analysis of the spectral response as well as of load time histories confirmed for both anchor types and all tests an elongated NCS period as already observed in Correlation and Displacement Tests. The spectral acceleration of the model NCS Sa(NCS) shows its peak at 0.45 seconds and the amplification increases

with increasing amplitude scales α of the input motion. This holds for all test runs but for the α = 130% test run on the UC1 anchor type which resulted in anchor failure early during the test run.

Figure 5.38a plots the maximum anchor load N_{max} as the average of all 4 anchors to various acceleration parameters. The percentage scales used in the tests are given at the bottom line of the diagram. It can be seen that the spectral accelerations on slab level Sa(floor) at 0.45 seconds are proportional to the corresponding amplitude scales, therefore identifying Sa(floor) at the elongated NCS period as the driving floor acceleration parameter. The maximum anchor load N_{max} develops approximately in proportion to the peak NCS acceleration (PNA) which is in line with the load transfer mechanism (Figure 5.12 and Equation 5.2). However, N_{max} is not proportional to the scale factor because of non-linearity of the system which is discussed in the following.

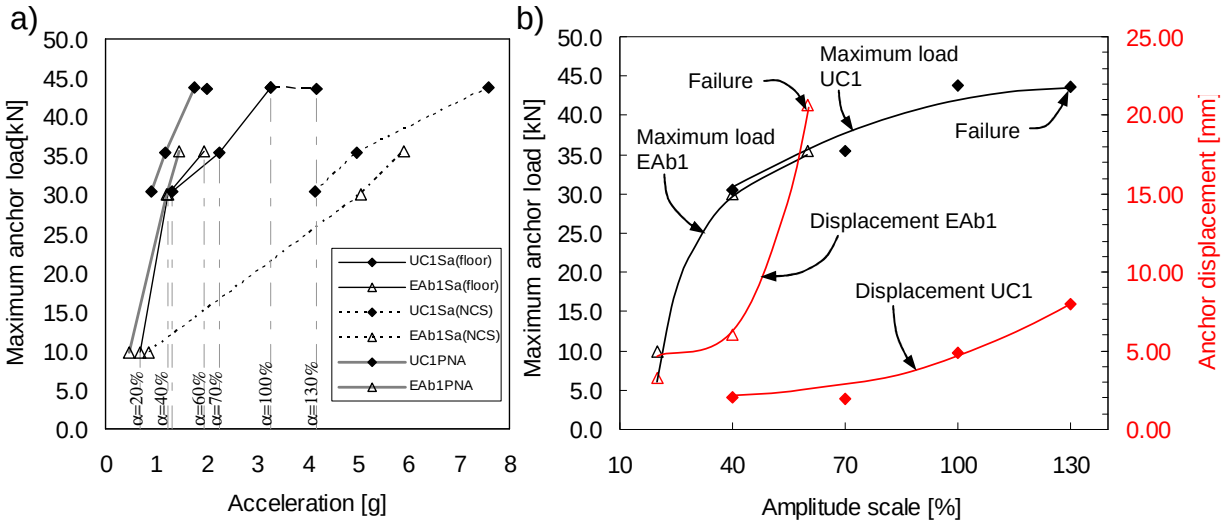

Figure 5.38 a) Maximum anchor load versus spectral accelerations Sa(Floor) and Sa(NCS) at 0.45 seconds and peak NCS acceleration (PNA); b) Maximum anchor load and accumulated anchor displacement versus amplitude scale

Figure 5.38b plots maximum anchor load and accumulated anchor displacement as the average of all 4 anchors. The anchor displacements increase progressively with increasing scales, whereas the maximum anchor loads also increase but degressively. The non-linearity of the system response helps to reduce the seismic demand for increasing scales. This observation may mislead to the conclusion that soft load-displacement behaviour supports the reduction of peak loads. For a given scale factor, however, the anchor displacements for the UC1 and EAb1 anchors are very different, but the maximum anchor load is not. Apparently, different load-displacement characteristics of various anchor types do not influence the earthquake driven oscillating behaviour. Equal NCS periods for both anchor types tested in this study (T = 0.45 seconds) support this conclusion.

For constant periods but increasing maximum anchor loads, the loading rate increases. For the considered Failure Tests, the loading rate ranges from 100 kN/s (EAb1, 20 %) to 420 kN/s (UC1, 130 %). Since the anchor loads showed pronounced impact actions, it may be assumed that the achieved loading rates are at the upper limit of what may be observed in shake table tests on anchored NCS.

5.3.4.3 Conclusions

Partial anchor failure does not lead inevitably to a complete system failure though the kinematic changes and the remaining anchors have to cope with high reactive loads. It is important to note, however, that the ultimate capacity of the remaining anchors was nearly exhausted and the complete system failure was impending. Compared to the situation of floor mounted NCS, the situation of suspended NCS is generally more critical.

The Failure Tests yielded ultimate seismic strengths which are larger than those determined in tests according to the proposed seismic amendment of qualification guidelines. The main reason for this is that the maximum anchor load does not coincide with the maximum crack width in the shake table tests. In conclusion, the qualification tests yielded seismic load capacities which are conservative at least if compared to shake table tests on NCS.

Detailed analysis of accelerations and maximum anchor loads revealed that the maximum anchor load is proportional to the peak NCS acceleration, and the amplitude scale to the spectral acceleration of the floor at the elongated NCS period. However, due to non-linearity of the system, the maximum anchor load is not proportional to the amplitude scale, i.e. seismic demand, but increases degressively. This effect is independent of anchor types and associated load-displacement characteristics.

Though (pseudo) ductile anchor behaviour does not have beneficial effects for the considered case, anchor displacement allows the NCS to elongate its period. It is important to note, however, that a period elongation may also result in an increase in amplification, depending on the floor motion characteristics (Section 5.3.1.2)

With increasing anchor loads but constant period, the loading rates increases for increasing floor accelerations. The rise times and loading rates measured for the Failure Test series are well in line with the loading rates taken as a basis for experimental investigations on earthquake relevant loading rates between 20 and 1000 kN/s conducted under the scope of this thesis (Section 3.2.2.1).

5.4 Summary

The shake table tests on anchored NCS in suspended configuration were the first of its kind and delivered valuable data for investigating the anchor behaviour when subjected to real earthquake acceleration time histories and corresponding crack demand. Though gravity loads acting on the connection, the pendulum like load transfer system is earthquake load dominated and loads the anchors alternatingly by high load impulses. In view of load and displacement demands, this configuration is more critical than the configuration of floor mounted NCS.

Anchor load normalisation with reference of $0.5\ N_{u,m,cr}$ allows interpretation of the statistically representative average anchor load level as correlation factors α by which the permanent load level during crack cycling tests may be multiplied to derive realistic demand levels for seismic qualification tests. The correlation is nearly constant for all floor motions and anchor types and relatively low, but higher than for floor mounted NCS. The results derived from the tested heavy NCS may be assumed as crucial in respect to average anchor load level. Therefore, the statistically representative anchor load level can be conservatively estimated by $0.2 \cdot 0.5\ N_{u,m,cr}$.

Due to the relatively low average anchor load level, the shake table tests yield anchor displacements which are much smaller than those measured for the proposed seismic qualification tests. For a fully utilised anchor, the mean plus one standard variation equals 1.0 mm on the serviceability level. In case of reduced number of anchors in a crack, the anchor displacement is further decreased. However, the anchor displacements measured for the suspended component tests are in a magnitude which could hypothetically be expected for qualification tests with reduced permanent anchor load levels. In this respect, the shake table test results verify the seismic demands stipulated in the proposal of the seismic amendment (*Proposal for ETAG 001 Seismic Amendment (2012)*).

The impact of various floor motions on the test results is significant, however, the difference is small with respect to the prevalent scatter. Anchor displacement allows the NCS to elongate its period to the next integral multiples of the building period. Therefore, the predominant cracking period, i.e. crack width period as well as the predominant floor motion period, both closely related to the building period, coincide with the (elongated) NCS period, i.e. anchor loading period. The non-linearity of the system helps to reduce the load demand on the anchors, irrespective of the anchor type and associated load-displacement characteristics. It is noted, however, that the magnitude period elongation and system non-linearity is neither the result of nor is it influenced by the anchor ductility.

The maximum anchor load increases proportionally with increasing peak NCS acceleration, and degressively with the amplitude scale. It was demonstrated that partial failure does not necessarily lead to complete system failure. For constant NCS

periods, the loading rates increases with increasing amplitude. The determined loading rates confirmed the assumed range of earthquake relevant loading rates.

During shaking, the cracked concrete capacity is often exceeded because of partial crack closure due to the low correlation of maximum anchor load and crack width. The low correlation also results in relatively small anchor displacements. In consequence, the seismic strengths determined on basis of the shake table tests results are greater than those determined in qualification tests according to the proposed seismic amendment which therefore may be deemed as conservative for anchors used for non-structural connections.

6 Recommendations for Design Codes and Qualification Guidelines

In Chapter 4, testing procedures, test conditions and assessment criteria for seismic qualification tests on post-installed anchors were developed and discussed. The tension load cycling, shear load cycling, and crack cycling tests form an integral part of a proposed seismic amendment of the European ETAG 001 qualification guideline (*Proposal for ETAG 001 Seismic Amendment (2012)*). The amendment is scientifically substantiated and provides a high level of earthquake safety. The introduction of the ASPC2 test standard could supersede the highly specialised application of the NPP Guideline in Germany. The presented research was conducted also with regard to the situation in the US. Therefore, an adoption of the proposed seismic amendment for a revision of the ACI 355 anchor qualification guideline is conceivable. The revenue of the presented research on the seismic performance of anchors, however, is not restricted to the proposed seismic qualification tests. Moreover, findings made in component level tests (Chapter 3) and system level tests (Chapter 5) yield further recommendations for design codes and qualification guidelines which are described in the following sections.

6.1 General

The presence of cracks in the concrete and their widths are critical for the anchor performance. Therefore, in order to conduct qualification testing of anchors for use in cracked concrete, the generation of the crack in the target location is very important. It is critical such that the crack passes through the anchor location over the entire depth. In previous chapters, it was repeatedly highlighted that drilling of the anchor hole prior to crack initialisation ensures best results. Qualification guidelines should require a verification of a full depth crack by a borescope inspection.

Furthermore it is strongly recommended that identical concrete specimen types are used throughout the test programme. In particular this applies for the cyclic tests and their corresponding monotonic reference tests. Different geometry and reinforcement layout in the concrete specimens introduce an unnecessary and systematic scatter which may jeopardise the high demands on accuracy seismic qualification test procedures require.

6.2 High Loading Rate

It was shown that the general assumption of the beneficial effects of high loading rates holds irrespective of the anchor type. Additionally dynamic tests on anchors have shown that the load capacity also increases for high load or high crack cycling frequencies of 1 to 5 Hz (*Mahrenholtz, P.; Mahrenholtz, C. et al. (2012)*). Consequently, it is conservative to neglect these effects in anchor design and qualification and tests at high loading or cycling rates are not required for qualification.

6.3 Anchor Ductility

Testing of anchor ductility is deemed unnecessary for seismic anchor qualification. Since the classification of an anchor as brittle or ductile effects the anchor design in general, however, it is recommended to incorporate tests on anchor ductility in qualification guidelines. Moreover, anchor displacements are critical in case of displacement controlled problems in particular for seismic applications and deformation based design. In this respect, future technical approvals should provide additional anchor displacement data, i.e. the minimum and maximum characteristic displacements during cyclic actions and the ultimate (residual) displacement capacity. The specific anchor displacement demands need to be evaluated and compared to displacement capacities, independent of the classification of an anchor as ductile or not. Large anchor displacements are not necessarily beneficial for the behaviour of anchored NCS. Moreover, the residual displacement for moderate and more frequently occurring earthquakes is generally desired to be small. Consequently, the universal promotion of ductile anchor behaviour in seismic design irrespective of any specific demands should be reconsidered. In this context, the one‑sided punishment of brittle anchorages as stipulated by the overstrength design approach for brittle anchorages in *CEN/TS 1992-4 (2009)* and *ACI 318 (2011)* should be revised and harmonised.

The filling of clearance holes as currently recommended in *CEN/TS 1992-4 (2009)* and widely exercised for seismic applications of anchors loaded in shear, has certainly a positive effect on the reliability of attributed displacement behaviour. Further, closure of the annular gap prevents gap induced amplification. Therefore, filling the clearance hole can be conservatively neglected in anchor qualification test, however, should be more explicitely addressed in *CEN/TS 1992-4 (2009)* and *ACI 318 (2011)*.

Apart from seismic aspects of anchor ductility, anchor qualification guidelines should generally stipulate anchor ductility tests on the basis of the proposed equivalent percentage elongation criteria. Failure modes other than steel should be allowed to

be classified as ductile if they generate comparable anchor displacements. The requirements for the plastic design approach of structural connections according to *CEN/TS 1992-4 (2009)* Annex B as well as the partial safety factors as given in *ACI 318 (2011)* Appendix D should be revised accordingly.

6.4 Anchor Groups

The CC Method and UB Model (Section 3.1.2) have been adopted by relevant design codes as *ETAG 001 (2006)*, *ACI 318 (2008)* and *ACI 349 (2006)*, and proved valid ever since. The design equations given in *ETAG 001 (2006)* Annex C are also applicable for anchor groups provided that the used anchors fall within current experience which are according to Annex B Clause 2.0 all expansion and undercut anchors. Group design of bonded anchors is covered in *EOTA TR 029 (2010)*. However, group design of screw anchors is yet to be regulated, but will follow the same approach for overlapping concrete cones and influencing areas as stipulated for the CC Method and UB Model, respectively. In conclusion, tests for the determination of the critical spacing s_{cr} required for the transmission of the full anchor strength are no longer considered as s_{cr} is generally assumed to be 3 h_{ef}. However, if the group behaviour is desired to be evaluated, the test conditions in *ETAG 001 (2006)* need to be defined in more detail, e.g. as rotational-restrained configuration.

The introduction of the seismic group factor of 0.85 allows to drop the seismic strength reduction factor of 0.75 as currently stipulated in the design codes *ACI 318 (2011)* and *CEN/TS 1992-4 (2009)*. The strength reduction factor was originally meant to cover several effects, which are either ruled out or, as the effect of extreme crack widths of 0.8 mm, can be taken into account in the design by a seismic crack width factor of ~ 0.9 to reduce the strength of a single anchor for concrete cone failure.

6.5 Cyclic Load

The proposed seismic amendment for qualification guidelines includes tension and shear load cycling tests as described in Section 4.3.2.1 and Section 4.3.2.2, where also detailed recommendations for the testing procedures are given.

Boundary conditions of shear qualification tests require further specification to achieve reproducible test results. In particular the hold down mechanism has a strong impact on the test results, however, is currently not defined in the guidelines yet. Other influencing but undefined factors include the height of the fixture and the filling of the annular gap. For increased fixture heights or if the gap is filled, an additional bending moment is introduced at the anchor head. Since the seismic

performance in shear is governed by LCF, qualification testing with large fixture heights or filled gaps yields conservative results.

6.6 Cyclic Crack

The proposed seismic amendment for qualification guidelines includes crack cycling tests as described in Section 4.3.2.3, where also detailed recommendations for the testing procedure are given.

The anchor displacements during crack cycling are critical for the evaluation of qualification tests and consequently should be measured accurately. Anchor displacements in the range of 100 μm require direct measurement on the free end of the anchor. If the measurement devices are installed next to the anchor, the anchor load induced bending of the concrete test specimen may lead to a significant undershooting of the crack width at the point of anchorage. Therefore, it is recommended to mount the measurement devices on each side of the concrete test specimen at the level of the theoretical embedment depth. Further improvement in measurement accuracy can be achieved by the four point method.

7 Reference-Test Based Model for Cyclic Anchor Displacement

Large axial displacement accumulated during crack cycling with a permanently acting load is a critical performance aspect of post-installed anchors. For anchors seeking seismic qualification, the crack cycling test is the most demanding test type which likely causes a reduction in the approved seismic tensile strength to meet the allowable displacement criterion. On the other hand, crack cycling tests offer the largest potential for product optimisation. However, the required technical equipment together with time consuming procedures make crack cycling tests a decisive cost factor in anchor qualification test programmes. Moreover, when a test is halted due to a premature failure, additional tests with iteratively reduced anchor loads are required. Consequently, a model that is able to predict the anchor displacement during crack cycling on basis of monotonic reference test data is beneficial. In Section 7.1 the analytical background of a model developed in Section 7.2 is presented. Its capability is shown in Section 7.3 by exemplary calculations, which results are concluded in Section 7.4.

7.1 Analytical Background

The effect of cracks and crack cycling on anchor displacement is the central theme of this thesis. The stiffness of anchors located in cracks is reduced as compared to the stiffness of anchors located in uncracked concrete (Section 3.4.2.2). As a result, the anchor displacement increases for decreased stiffness. In the case of crack cycling, the accumulated displacement is a result of slip during crack opening (Section 3.6.2.4). For constant anchor load and maximum crack width, the displacement increment is approximately constant (Figure 7.1a). As the permanent anchor load and crack opening width increase, the anchor slip increases (Figure 7.1b). For discrete phasings (Figure 7.1c), the relative effect of anchor load cycling can be taken into account by integrating anchor load and crack width over the cycles, leading to the ADP approach which basically assumes an approximate linear influence of anchor load and crack width on the anchor slip (Section 3.7.2.5).

The proposed seismic qualification tests with variable permanent load level (Figure 7.1d) demonstrated that the accumulated anchor displacement is proportional to anchor load level and crack opening width (Section 4.3.2.3). The relative load and crack demand acting on the anchor can be expressed for various test protocols by the ADP approach, which could also be extended to transient anchor load and crack

width time histories (Figure 7.1e). To compare the displacement results of various load and crack demands, the time histories have to be normalised (Section 5.3.3.3).

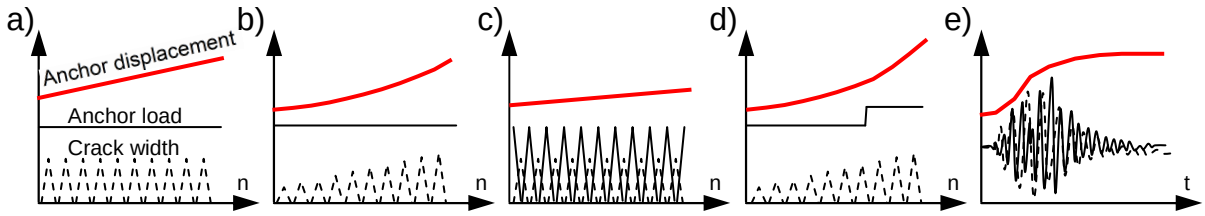

Figure 7.1 Effect of variable anchor load and crack width (schematic): a) Crack cycle protocol with constant load; b) Stepwise increasing crack cycle protocol with constant load; c) Protocol for simultaneous load and crack cycling; d) Stepwise increasing crack cycle protocol with variable load; e) Anchor load and crack width time histories

The anchor displacement can be calculated provided that the fundamental response of the anchor to a given anchor load and crack width opening is known. However, the experimental determination of a single anchor displacement increment Δs_{cyc} for a particular anchor load and crack width opening is disproportionately elaborate because a full test setup for crack cycling tests is required.

The general idea for the model developed is to estimate the anchor displacement during crack cycling based on test data of monotonic pullout test. The aim is not to calculate exact displacements, which is nearly impossible due to scatter within crack cycling tests, but to provide a simplistic tool to predict the trend. Herein the incentive is the avoidance of unnecessary and costly premature failures during seismic qualification tests.

7.2 Development of Model

Figure 7.2 depicts schematic load-displacement curves for tests on an anchor installed in uncracked concrete, in a static crack, and in a cycled crack. The effect of static cracks on the anchor performance was extensively investigated over past decades also in quantifiable terms, e.g. strength reduction factor ψ_w (Figure 7.2a). Despite the direct influence of anchor displacement on the remaining embedment depth and residual capacity, the effect of crack cycling on the increase in anchor displacement from the initial displacement, s_i, to the displacement after crack cycling, s_{cyc}, is not quantified to date.

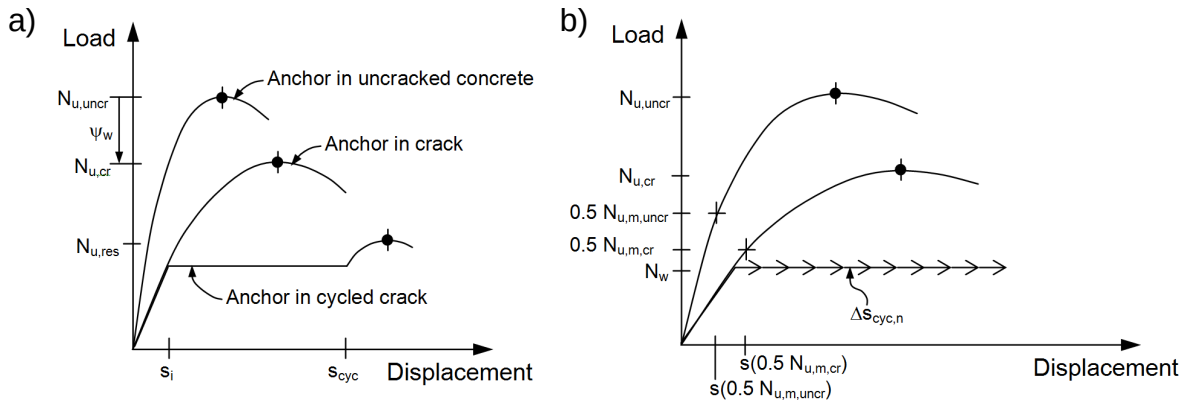

Figure 7.2 Schematic load-displacement curves for tests on an anchor installed in uncracked concrete, in a static crack, and in a cycled crack: a) Key performance parameter; b) Displacement at 50 % $N_{u,m}$ and displacement increment $\Delta s_{cyc,n}$

The experimental data of earlier tests is studied in the following to find an approximate interrelation of characteristic displacement data $s(0.5\ N_{u,m,uncr})$, $s(0.5\ N_{u,m,cr})$, and $\Delta s_{cyc,n}$ (Figure 7.2b) which serves as a basis for the calculation of the displacement increments.

7.2.1 Characteristic displacement data

The group test programme reported in *Mahrenholtz, P. (2010b)* included reference tests on single anchors installed in uncracked concrete, static crack, and cycled cracks (Section 3.4.4). The static crack width and crack opening width were 0.8 mm. The characteristic displacement data are compiled in Table 7.1 for further analysis.

Table 7.1 Characteristic displacement data of reference tests on anchors installed in uncracked concrete, in static crack, and in cycled cracks

Anchor Type	$s(0.5N_{u,m,uncr})_m$ (1), mm	$s(0.5N_{u,m,cr})_m$ (2), mm	Δs (3), mm	$\Delta s_{cyc,n,m}$ (4),(5) mm	$\frac{\Delta s}{\Delta s_{cyc,n}}$
UC1	0.75	1.14	1.14-0.75=0.39	(4.22-0.58)/10=0.36	1.08
SA1	0.20	0.66	0.66-0.20=0.46	(5.10-0.53)/10=0.45	1.03
EAb1’	0.08	2.33	2.33-0.08=2.23	(22.81-1.86)/10=2.09	1.07

(1) Tests in uncracked concrete
(2) Tests in static cracks (w = 0.8 mm)
(3) $\Delta s = s(0.5N_{u,m,uncr})_m - s(0.5N_{u,m,cr})_m$
(4) Tests in cycled cracks: n = 10; $N_w = 0.4\ N_{u,m,ct}$; $w_1 = 0.8$ mm; $w_2 = 0.0$ mm;
(5) $\Delta s_{cyc,n} = (s_{cyc} - s_i) / n$; $s_i = s(0.4N_{u,m,cr})_m \approx (0.4 / 0.5) \cdot s(0.5N_{u,m,cr})_m$

The data reveal that the difference in the displacement at 50 % $N_{u,m}$ for tests in uncracked and cracked concrete, Δs, is approximately equal to the displacement

increment, $\Delta s_{cyc,n}$, which an anchor experiences every crack cycle. This is conclusive because for load levels in the elastic range, the difference in displacement for an anchor installed in uncracked concrete to an anchor installed in a crack of the width w corresponds to the displacement increment of a permanently loaded anchor due to opening the crack from full crack closure to w (Section 4.3.2.3). This principle is also valid for tests conducted in 0.5 mm cracks, assuming a linear influence of the crack width on the displacement.

7.2.2 Calculation of displacement increment

Based on this hypothesis, the reference displacement increment $\Delta s_{cyc,n}^*$ is calculated for the reference tests carried out for the crack cycling tests presented in Section 3.6.2 and Section 4.2.3.2. Since reference tests on anchors installed in uncracked concrete were not carried out, the values for $s(0.5N_{u,m,uncr})$ are calculated by means of specific displacement ratios $s(0.5N_{u,m,cr}) / s(0.5N_{u,m,uncr})$ taken from the data base reported in *Mahrenholtz, P. (2011b)* (Table 7.2).

Table 7.2 Calculation of displacement increment for one crack cycle with

Anchor Type	$s(0.5N_{u,m,cr})^{(1)}$, mm	$cal.\left(\frac{s(0.5N_{u,m,cr})}{s(0.5N_{u,m,uncr})}\right)^{(2)}$	$cal.s(0.5N_{u,m,uncr})$, mm	$cal.\Delta s_{cyc,n}^*$, mm
UC1	0.38	1.5	0.35/1.5=0.25	0.38-0.25=0.13
SA1	0.70	1.5	0.70/1.5=0.47	0.70-0.47=0.23
EAb1	2.01	3.0	2.01/3.0=0.67	2.01-0.67=1.34

(1) Tests in static cracks (w = 0.5 mm)
(2) Values calculated by data base for anchor tests in uncracked concrete and in 0.5 mm cracks

For the crack closing width w_2 = 0.0 mm, the displacement increment $\Delta s_{cyc,n}$ can be calculated for any given anchor load and crack width by:

$$cal.\Delta s_{cyc,n} = cal.\Delta s_{cyc,n}^* \cdot \left(\frac{N_{w,n}}{N_w^*} \cdot \frac{w_{1,n}}{w_1^*}\right) \qquad \text{Equation 7.1}$$

Where $N_{w,n}$ Permanent anchor load for the crack cycle n

N_w^* Permanent anchor load for which $\Delta s_{cyc,n}^*$ was determined

$w_{1,n}$ Crack opening width for the crack cycle n

w_1^* Crack opening width for which $\Delta s_{cyc,n}^*$ was determined

7.3 Example Calculations

The hypotheses are verified by predicting the displacements during crack cycling for exemplary experimental tests reported in *Mahrenholtz, P. (2009)* and *Mahrenholtz, P. (2010d)*. The calculations presented in this section benchmark the practical applicability of the proposed model.

7.3.1 Application to Simulated Seismic Tests

Figure 7.3 and Figure 7.4 depict load-displacement curves measured for crack cycling tests discussed in Section 3.6.2 and Section 4.2.3.2. The displacement increments calculated by Equation 7.1 are indicated by hollow dots.

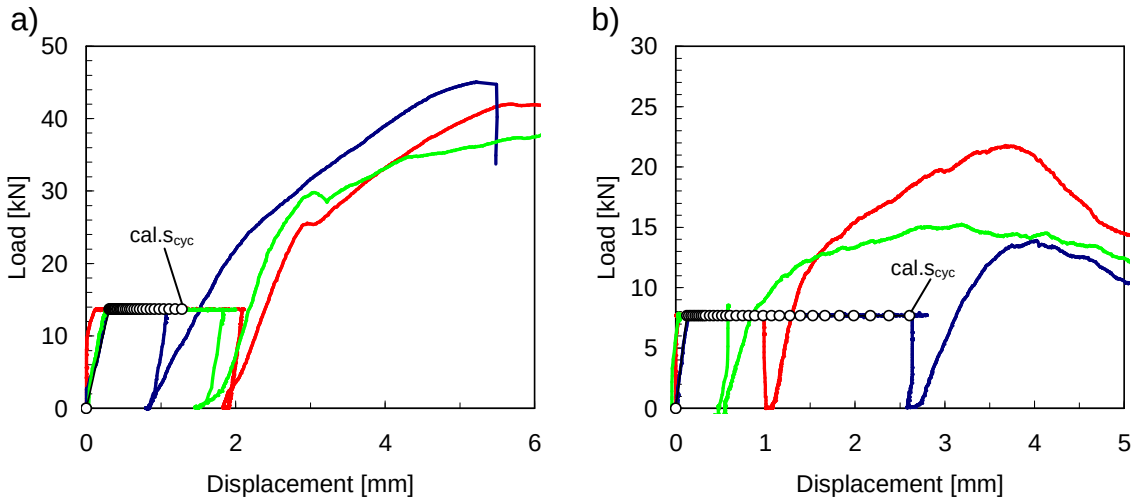

Figure 7.3 Measured Ld curves and calculated anchor displacement: Stepwise increasing crack cycle protocol with constant load: a) UC1 anchor and b) SA1 anchor

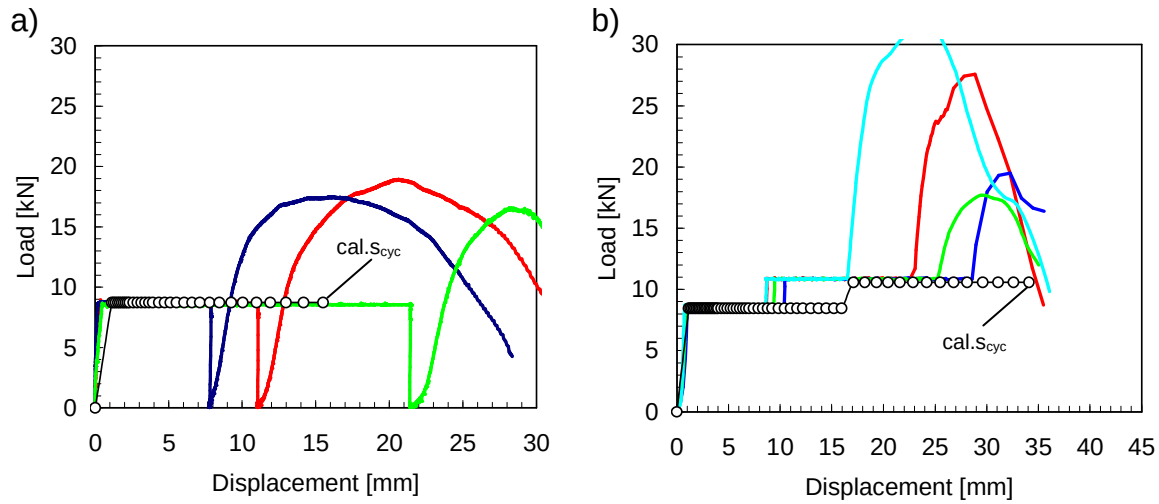

Figure 7.4 Measured Ld curves and calculated anchor displacement for tests on EAb1 anchor: a) Stepwise increasing crack cycle protocol with constant load; b) Stepwise increasing crack cycle protocol with variable permanent load

The results for the stepwise increasing crack cycle protocol (n = 32; Figure 7.3 and Figure 7.4a) show satisfactory agreement of calculated and experimental displacement s_{cyc}. In case of the seismic qualification tests (n = 59; Figure 7.4b) the model clearly overestimates the experimental displacement measured at serviceability and suitability levels. However, the divergence in the measured load-displacement curves indicates that the anchor behaviour is not stable.

7.4 Conclusion

Based on the findings of the comprehensive research presented in this thesis, a model was developed to enable an approximate prediction of the anchor displacements during crack cycling given only displacement data of simple reference tests. Exemplary calculations are performed on the data and the comparison of load-displacement data between experimental results and the model predictions demonstrated a positive result. It is noted that a mismatch between experimental and analytical data for more complex test protocols may be related to the extreme scatter typical of crack cycling tests.

The proposed model is a useful tool to estimate displacements, but it would not replace experimental tests. Further reference tests on single anchors are required to substantiate and refine this approach. The test programme should comprise tests in uncracked concrete, in static cracks, and in cycled cracks employing identical test specimens.

8 Summary and Open Questions

The previous chapters investigated systematically the performance and qualification of post-installed anchors for seismic applications. Existing anchor qualification guidelines were analysed and deficits in the understanding of anchor behaviour were identified. For the comprehensive research programme conducted to overcome these deficits, an experimental approach supplemented by analytical models was chosen. The conducted research directly addressed the lack of understanding in the relevant aspects, namely: loading rate, anchor ductility, anchor groups, cyclic loads and cracks, and simultaneous load and crack cycling. The studies herein contributed to the proposal for the seismic amendment of the anchor qualification guideline, which refined test protocols were evaluated by additional experimental testing. The component level results were then compared to the system level results, where post-installed anchors were tested in cyclically cracked concrete on a shake table. In the following, the key findings of the individual aspects are summarised (Section 8.1) and open questions outlined (Section 8.2).

8.1 Summary

Experimental test data confirmed that the preclusion of high loading rate tests for seismic qualification also apply to expansion anchors. Detailed studies have shown that due to dynamically increased concrete strengths, tests at earthquake relevant loading rates also result for anchors failing in pull-through mode in increased load capacities despite a decreased friction between the anchor cone and expansion elements. Therefore, any high loading rate test is deemed to be unnecessary for seismic anchor qualification.

Detailed studies on anchor deformation characteristics, in particular with respect to seismic applications, resulted in a meaningful understanding of anchor ductility. Evaluation of a data base of compiled test data of a large range of anchor products enabled the quantification of anchor displacement capacities. A new definition is proposed based on the percentage displacement and would allow for other failure modes than just steel failure to be classified as ductile. This is provided that the percentage displacement is as large as the percentage elongation of the anchor tested in a material tensile test with a gauge length equal to the embedment depth. Current provisions given in qualification and design guidelines should be modified accordingly, irrespective of whether the intended use of the anchor is seismic or static.

A sophisticated test setup with multi-axes servo control system was developed which allows testing of rotational-unrestrained and rotational-restrained anchor groups under defined conditions. Based on the experimental results and the re-evaluation of numerical simulations, the seismic group factor was determined to 0.85 provided that the CV of the displacement after crack cycling of the individual anchor is not larger than 30 %. A group model is developed which realistically considers the load redistribution caused by crack cycling and induced load cycling. This model allows for simulating the axial displacement behaviour during crack cycling which largely defines the anchor performance and constitutes a good basis for further numerical simulations. Properly embedded in a numerical routine, this model could certainly become a valuable tool to avoid costly group tests.

Extensive experimental load and crack cycling tests on on a broad variety of anchor types and failure modes increased substantially the understanding of cyclic anchor behaviour. In particular the test setup for crack cycling tests was improved, allowing tests of high precision and complexity. The magnitude of the permanent anchor load was reasoned. The tests proved the beneficial applicability of stepwise increasing test protocols developed at the University of California, San Diego, and delivered valuable input for further refinement of the test protocols for final implementation in the seismic amendment or revision of anchor qualification guidelines. The test results highlighted the paramount impact of crack widths on the anchor behaviour for tension load and crack cycling tests. Low cycle fatigue makes shear load cycling tests critical for the seismic performance of anchors loaded in shear. Large accumulated axial anchor displacements during crack cycling tests are critical for the performance of anchors loaded in tension.

Simultaneous load and crack cycling tests carried out within the scope of this thesis were the first of its kind and delivered new insights regarding the influence of phasing and frequency on the anchor displacement behaviour and corresponding performance. The results justify a reduction factor of 0.8 for the permanent load during the serviceability level of crack cycling tests, retaining a realistic anchor load level. Furthermore, it was shown that the anchor displacement collected over load and crack cycles can be described by accumulated damage potentials which take the correlation of anchor load and crack width into account.

All investigations on the component level resulted in a set of load cycling protocols and crack cycling protocol, which are carried out anchor load controlled and crack width controlled, respetively. Exploratory tests verified the general approach to test serviceability and suitability demand level by one unified test protocol. Herein the stipulated test conditions were validated, reasonable assessment criteria postulated, and concluding testing procedures proposed.

Shake table tests delivered valuable information on the seismic performance and failure mechanisms of anchors connecting suspended components to concrete. The suspended configuration were tested with a model NCS with a representative periods and can be deemed as the critical case for non-structural connections. For the considered configuration, the shake table tests verified that the proposed seismic qualification tests sufficiently replicate the characteristic demands of a real earthquake. The tests showed that for anchors used to fasten non-structural elements, earthquake motions generally result in a low correlation of anchor load and crack width. Accordingly, the anchor displacements are relatively small if compared to simulated seismic tests carried out for anchor qualification. This indicates that the permanent anchor load in qualification tests could be substantially reduced, if the anchor application is limited to non-structural connections. Moreover, findings on loading rates, anchor ductility, and anchor group behaviour observed on a component level were confirmed.

In addition to the proposed seismic qualification tests, the knowledge agglomerated during the investigations presented in this thesis finally resulted in a number of recommendations for anchor design codes and qualification guidelines. Further, a model was developed to reasonably predict the displacement of post-installed anchors subjected to load and crack cycling. This model utilizes known data from monotonic load-displacement curves and allows estimating the anchor displacement and therefore the sustainable load for a given anchor load and crack width demand. Inplementation of this model can greatly reduced the number of costly and labour intensive simulated seismic tests, while accelerating pretesting phase.

8.2 Open Questions

The presented research reduced the gap in knowledge as identified in the opening sections. Additional issues arose during extensive testing and were dealt with in the course of progressing investigations. However, some questions could not be answered completely.

Ideally, further research is necessary to understand local anchor ductility and its impact on the global ductility in case of structural connections. Numerical simulations similar to those carried out previously on non-structural connections (*Smith, J.; Dowell, R. (2008)*) could help to address this problem. Regarding the ductility parameter, more experimental test data would help to back up the conclusions for anchors loaded in shear while defining realistic and reproducible boundary conditions in the test.

Additional group tests along with other anchor types and products would help to further substantiate the proposed seismic group factor. For tension loads, it is recommended to conduct numerical tests which are based on the presented load

redistribution model, as described in *Mahrenholtz, P. (2010c)*. For anchor groups loaded in shear, effects related to crack cycling and the associated scatter are not relevant for the load distribution. However, other performance affecting factors such as variable clearances should be investigated. In this context, the question of filling the annular gap as recommended but not explicitly required in some design guidelines should be addressed more vigorously.

The cyclic load tests showed that in principle every anchor type is not sensitive to this type of loading, while the behaviour during crack cycling depends significantly on the anchor type. However, the seismic shear capacity is governed by low cycle fatigue which in turn depends on the anchor design and used material. Additional research is required to identify the driving parameters for the anchor performance in cyclic shear and to foster the development of suitable anchor systems. The seismic capacity in axial direction is governed by the displacement behaviour of the anchor during crack cycling. Due to the unfavourable load transfer mechanism, bonded anchors did not cope well with cycled cracks. It is evident that for use in seismic applications, the generally promising adhesive technology can only be successfully qualified as bonded expansion anchors which should be investigated by crack cycling tests.

Theoretical considerations identified structural connections as the critical design case in that, contrary to non-structural connections, load and crack cycling is potentially in phase. Non-linear structural analysis or experimental tests could confirm this hypothesis. Furthermore, structural connections of typical retrofit solutions rarely show a dominate anchor load direction. Tension and shear loads occur in varying portions and in a smeared manner. Further research could shed light on the realistic demand and possible beneficial effect of the shear and tension load interaction on the axial displacement behaviour.

Zusammenfassung (German Summary)

Experimentelles Verhalten und Empfehlungen für die Qualifikation von nachträglich installierten Dübeln im seismischen Anwendungsfall

Kapitel 1 – Einleitung

Die Starkbebenwahrscheinlichkeit ist für weite Teile der Erde vergleichsweise gering. Allerdings hängt das Schadensrisiko nicht nur von der Erdbebenintensität ab, sondern auch von den Vermögenswerten und der Verwundbarkeit des betrachteten Gebiets. Daher ist in vielen vormals als gering erdbebengefährdet eingestuften Gebieten das Potential zu Personen- und Sachschäden tatsächlich erheblich höher als allgemein angenommen. Gerade bei Erdbeben geringer Stärke in Gebieten mit hohem Technologisierungsgrad und empfindlicher Infrastruktur kommt der Erdbebensicherung mittels nachträglich installierter Dübel eine herausragende Bedeutung zu.

Nachträglich installierte Dübel dienen der Befestigung von tragenden und nichttragenden Bauteilen an tragende Betonbauteile. Sie werden während eines Erdbebens extremen Beanspruchungen ausgesetzt, welche im Allgemeinen mit zyklischen Belastungen in Längs- und Querrichtung assoziiert werden. Da man davon ausgehen muss, dass der Dübel sich in einem bereits vorhandenen oder während des Erbebens entstehenden Betonriss befindet, erfährt der Dübel zusätzlich eine Beanspruchung durch den sich zyklisch öffnenden und schließenden Riss. Desweiteren werden seismische Einwirkungen durch große Rissweiten und teilweise schockartige Belastungsgeschwindigkeiten charakterisiert.

Diese besonderen Beanspruchungen werden derzeit bei der Qualifizierung von Dübelsystemen nach den einschlägigen Prüfrichtlinien wie der europäischen *ETAG 001 (2006)* oder der US-amerikanischen *ACI 355.2 (2007)* nicht oder nicht im ausreichenden Maße berücksichtigt. Ziel dieser Dissertation ist es, die Erdbebensicherheit von nachträglich installierten Dübeln zu erhöhen, indem das Verhalten unter Erdbebeneinwirkung umfassend erforscht und Prüfrichtlinien um sinnvolle Testkriterien für die seismische Qualifikation ergänzt werden.

Kapitel 2 – Derzeitiger Stand von Prüfrichtlinien

Kapitel 2 analysiert den derzeitigen Stand des Regelwerks für die Zulassung von Dübeln. Einleitend wird der Zusammenhang von Prüfrichtlinien, Bemessungsrichtlinien und Zulassungen von Dübeln dargelegt. Wichtige Begriffe und die grundsätzliche Vorgehensweise bei Zulassungsverfahren werden erläutert. Die Analyse konzentriert sich auf bestehende europäischer und US-amerikanischer Normen und Richtlinien, wie die *ETAG 001 (2006)* und *ACI 355.2 (2007)* als Prüfrichtlinien und die *CEN/TS 1992-4 (2009)* und *ACI 318 (2011)* als Bemessungsrichtlinien.

Die Diskussion gliedert sich in folgende Aspekte: Belastungsgeschwindigkeit, Dübelduktilität, Dübelgruppen, sowie getrennt oder gleichzeitig wirkende zyklische Lasten und Risse. Die Randbedingungen und Prüfkriterien der entsprechenden Qualifikationstests werden hinsichtlich ihrer Relevanz für die Beurteilung der Erdbebentauglichkeit im Detail bewertet. Kritische Punkte werden herausgearbeitet und Defizite im Verständnis über das Verhalten von nachträglich installierten Dübeln identifiziert. Fragen, die beantwortet werden müssen, um eine seismische Prüfrichtlinie erarbeiten zu können, werden formuliert.

Kapitel 3 – Untersuchungen auf Komponentenebene: Tests unter simulierten Erdbebenbedingungen

Die in Kapitel 3 vorgestellten Forschungsarbeiten dienen der Beseitigung der zuvor identifizierten Defizite. Hierzu wurden umfangreiche Literaturrecherchen sowie theoretische und experimentelle Untersuchungen zu den oben aufgeführten Aspekten durchgeführt:

- Belastungsgeschwindigkeit. Anders als Hinterschnitt-, Schraub- oder Verbunddübel übertragen Spreizdübel die Lasten über Reibung mit Hilfe einer Spreizhülse, in die sich der konisch zulaufende Dübelbolzen beim Belasten zieht. Auszugsversuche an im Riss installierten Spreizdübeln sollten klären, ob es infolge erdbebentypischer Belastungsgeschwindigkeiten zu einer ungünstigen Änderung der Reibungsverhältnisse und Abnahme der Tragfähigkeit kommen kann. Die Versuche zeigten jedoch, dass die Tragfähigkeit tendenziell mit steigender Belastungsgeschwindigkeit zunahm und im Mittel nie unter der quasi-statischen Tragfähigkeit lag. Um sicher zu gehen, dass die gemessenen Laststeigerungen nicht Ausdruck einer zunehmenden inneren Reibung sind und damit die Funktionstüchtigkeit potentiell gefährden, wurden zusätzliche Untersuchungen über die äußere Reibung und den Eindrückwiderstand der Hülse in den Beton durchgeführt. Die Ergebnisse dieser Untersuchungen ergaben, dass die Laststeigerung auf die Erhöhung des Eindrückwiderstands zurückzuführen ist und eine

Verminderung der Tragfähigkeit unter hohen Belastungsgeschwindigkeiten praktisch ausgeschlossen werden kann. Damit haben sich Hochgeschwindigkeitsversuche für die seismische Qualifizierung von nachträglich installierten Dübeln als nicht erforderlich erwiesen.

- Dübelduktilität: Während die Klassifizierung der Duktilität von Dübeln konkrete Auswirkungen auf ihre Bemessung hat, sind die im Ansatz existierenden und auf reiner Materialduktilität beruhenden Definitionen nicht schlüssig. Insbesondere ist in den einschlägigen Prüfrichtlinien bis dato nicht geregelt, wie sich Dübel für eine hinreichende Duktilität qualifizieren können. Um den Begriff der Duktilität in der Dübeltechnologie sinnvoll und quantifizierbar definieren zu können, wurden Duktilitätskriterien entwickelt und auf eine mehrere tausend Lastverschiebungskurven umfassende Versuchsdatenbank angewendet. Die Auswertung hat ergeben, dass die Bewertung des Dübels hinsichtlich der relativen Verschiebekapazität im Sinne eines vom Erdbebeningenieurwesen bekannten Duktilitätsfaktors wenig sinnvoll ist. Mangels eines ausgeprägten Fließpunktes sowie wegen der großen Streuung im abnehmenden Ast der Lastverschiebungskurve sind die ermittelten relativen Verschiebekapazitäten zu gering um relevant sein zu können. Dahingegen ist eine Bewertung des Dübels hinsichtlich der absoluten Verschiebekapazität am Punkt der Höchstlast zuverlässig und charakterisierend für das Verschiebeverhalten des Dübels. Ein neuer Ansatz zur Bestimmung der Dübelduktilität wird vorgeschlagen, der unabhängig von der Versagensart einen Dübel als duktil klassifiziert, wenn die auf seine Verankerungstiefe bezogene Verschiebung bei Höchstlast mindestens genauso groß ist wie die geforderte prozentuale Längung des Dübelwerkstoffes in einem Zugversuch.
- Dübelgruppen: Während in der Vergangenheit das Lastverschiebungsverhalten von Einzelbefestigungen weitestgehend untersucht worden ist, gilt dies nicht für Mehrfachbefestigungen. Aus der systematischen Betrachtung der bei Mehrfachbefestigungen relevanten Randbedingungen und die zielgerichtete Auswertung vorhandener numerischer Versuche konnte geschlussfolgert werden, dass Dübelgruppen unter Einhaltung eines maximal zulässigen Variationskoeffizienten für die Verschiebung nach erdbebenbedingter Risszyklen von 30 % auch unter Erdbebeneinwirkung eine Tragfähigkeit von mindestens 85 % der Summe der Einzeltragfähigkeiten aufweisen. Allerdings wurde in den bisherigen Untersuchungen die bei öffnenden und schließenden Rissen zu erwartende Lastumverteilung nicht ausreichend berücksichtigt. Um das Tragverhalten von Mehrfachbefestigungen, deren Dübel sich teilweise in einem sich zyklisch öffnenden Riss befinden, besser zu verstehen, wurden Versuche an Zwei- und

Vierfachbefestigungen unter exakt definierten Randbedingungen durchgeführt. Bei diesen experimentellen Versuchen wurde unter extremen Anforderungen an die Mess- und Steuertechnik ein in der experimentellen Dübelforschung bisher nicht dagewesenes Komplexitätsniveau erreicht. Die dabei insbesondere für drehsteife Anschlüsse beobachteten Umlagerungseffekte wirkten sich positiv auf das Lastverschiebungsverhalten aus. Die Tragfähigkeit von mindestens 85 % der Summe der Einzeltragfähigkeiten konnte bestätigt werden; und die Verschiebungen fielen im Vergleich zu den gelenkigen Anschlüssen erheblich geringer aus. Das durch die Versuche vertiefte Verständnis erlaubte es ferner, ein analytisches Modell zu entwickeln, das die Umlagerungseffekte innerhalb von Dübelgruppen simulieren und so die äußerst aufwendigen Gruppenversuche zukünftig ersetzen kann.

- Zyklische Lasten: Das Verhalten von nachträglich installierten Dübeln unter schrittweise ansteigenden Dübellasten wurde anhand diverser Dübeltypen und -produkte untersucht. Dabei hat sich gezeigt, dass in Längsrichtung belastete Dübel die 36 Lastzyklen generell und unabhängig von der Versagensart überstehen und die Umhüllende der zyklischen Lastverschiebungskurven der mittleren monotonen Auszugskurve folgt. Damit wurden für mechanische Dübel bereits vorher getätigte Beobachtungen bestätigt und auf Verbunddübel ausgedehnt. In Querrichtung belastete Dübel zeigen einige Dübeltypen mehr oder weniger ausgeprägtes Ermüdungsverhalten im Zuge dessen sich die Umhüllende der zyklischen Lastverschiebungskurven von der mittleren monotonen Auszugskurve löst und der Dübel vor Erreichen der angestrebten Last bzw. Lastwechselanzahl versagt. Dübel, die in Rahmen von Tastversuchen nicht last- sondern wegkontrolliert belastet wurden, haben im Prinzip das gleiche Verhalten und die gleiche Grenztragfähigkeit aufgewiesen. Da jedoch wegkontrolliert abgefahrenen Lastwechsel zu unregelmäßigen Lastamplituden führen, ist der lastkontrollierten Durchführung der Qualifikationstests den Vorzug zu geben. Desweiteren haben die Versuche gezeigt, dass eine vollständige Abfahrung der vorgegebenen Lastwechselanzahl für eine Auswertung der Grenztragfähigkeit unabdingbar ist. Damit kann die während der Lastwechsel maximal erreichte Last nicht für die Auswertung der Grenztragfähigkeit herangezogen werden und der Test ist in diesem Fall auf einem niedrigeren Niveau zu wiederholen.
- Zyklische Risse: Auch das Verhalten unter schrittweise ansteigenden Rissweiten wurde anhand diverser Dübeltypen und -produkte untersucht. Dabei kam erstmalig ein Versuchsaufbau zum Einsatz, der unter gleichzeitiger exakter Einhaltung der Dübellast die rissweitenkontrollierte Abfahrung komplexer Testprotokolle erlaubte. Die Steuerung und Auswertung der Tests

im Bereich weniger hundertstel Millimeter stellt neue Herausforderung an die Prüfkörper und technischer Ausstattung der Prüflabore dar. Die Versuchsergebnisse haben verdeutlicht, dass Risszyklusversuche wegen der dabei auftretenden Dübelverschiebungen eine extreme Anforderung an die Dübel darstellen, die im Allgemeinen für die seismische Grenztragfähigkeit und Gebrauchstauglichkeit in Längsrichtung maßgeblich ist. Die Größe der Dübelverschiebung richtet sich nach dem Lastübertragungsmechanismus. Verbunddübel zeigen erheblich geringere Verschiebungen als mechanische Dübel, jedoch neigt dieser Dübeltyp dazu, vor Ablauf aller 32 Risszyklen schlagartig zu versagen und muss daher als ungeeignet für diese Art der Belastung angesehen werden. Zusätzliche Versuche mit einer erhöhten Anzahl an Rissöffnungen haben den erheblichen Einfluss der oberen Rissweitenamplituden auf das Verschiebeverhalten herausgestellt und verdeutlicht, dass die Differenzierung des Gebrauchstauglichkeits- und Grenztragfähigkeitsniveaus sich nicht nur in der Maximalamplitude, sondern auch in der Anzahl der Zyklen widerspiegeln muss.

- Gleichzeitig wirkende zyklische Lasten und Risse: Das getrennte Testen zyklischer Lasten und zyklischer Risse ist im Allgemeinen konservativ. Für Risszyklusversuche, bei denen die Rissweite gezykelt und der Dübel mit einer konstanten Dauerlast in Höhe der maximalen Bemessungslast belastet wird, kann dieser Ansatz zu unrealistischen Bedingungen und sehr ungünstigen Versuchsergebnissen führen. Daher wurde in mehreren Testreihen untersucht, wie sich gleichzeitiges Last- und Risszykeln in unterschiedlichen Phasenlagen das Verschiebeverhalten eines Dübels beeinflusst. Die Ergebnisse zeigten deutlich, dass die Verschiebungen für Zyklen in Phase, Zyklen außer Phase und Zyklen bei unterschiedlichen Frequenzen zunehmend geringer werden. Unter der Annahme, dass eine Belastung im ungünstigsten Fall einer Befestigung tragender Bauteile in Phase auftritt, kann man die Dauerlast während der Testphase auf Gebrauchstauglichkeitsniveau auf 80 % der Bemessungstragfähigkeit reduzieren, die während der Testphase auf Grenztragfähigkeitsniveau angesetzt wird. Da die Versuche mit Kopfbolzendübel ausgeführt wurden, die eine geringe Streuung in den Verschiebungen aufweisen, konnte gezeigt werden, dass sich die Dübelverschiebung proportional zum akkumulierten Schadenspotential entwickelt. Dieses Schadenspotential (engl. Accumulated Damage Potential, ADP) ist definiert als das Produktintegral aus Rissweite und Lastniveau über den Risszyklus. Zwar sind Versuche mit gleichzeitig wirkenden zyklische Lasten und Risse zur Qualifizierung von Dübeln nicht erforderlich. Jedoch zeigen diese Versuche, dass insbesondere bei Befestigungen nicht tragender Bauteile und der hierbei anzunehmenden Außerphasigkeit von Last und Riss

die konstante Dauerlast reduziert werden könnte, um bei Risszyklusversuchen realistische Verhältnisse zu replizieren.

Zusammenfassend konnte gezeigt werden, anhand welcher Testtypen im Rahmen von Zulassungsverfahren die Qualifikation von nachträglich installierten Dübeln für die Verwendung in Erdbebengebieten erfolgen sollte: Tragfähigkeitsversuche unter Hochgeschwindigkeit, gesonderte Tests zur Feststellung der Dübelduktilität sowie Tests zur Bestimmung der Dübelgruppentragfähigkeit sind zur Beurteilung der Eignung nicht erforderlich. Zukünftige seismische Prüfrichtlinien sollten im Wesentlichen auf Lastzyklus- und Risszyklusversuche basieren. Schrittweise ansteigende Last- und Risszyklusprotokolle erlauben eine gute Beurteilung des seismischen Verhaltens und sollten die bei Erdbeben auftretenden Belastungen auf Gebrauchstauglichkeits- und Grenztragfähigkeitsniveau realistisch abbilden. Dabei sind Testprozeduren zu wählen, die reproduzierbare Ergebnisse liefern, gleichzeitig jedoch den Testaufwand so gering wie möglich halten.

Kapitel 4 – Ergänzung der Prüfrichtlinien für seismische Anwendungen

In Kapitel 4 werden die Untersuchungen vorgestellt, mit deren Hilfe die weiter entwickelten Testprotokolle und -prozeduren für die seismische Qualifizierung von nachträglich installierten Dübeln überprüft wurden. Für die Lastzyklus- und Risszyklusversuche wurden zunächst die Prüfbedingungen für separate und kombinierte Testprotokolle auf Gebrauchstauglichkeits- und Grenztragfähigkeitsniveau definiert.

Separate Testprotokolle erlauben die Überprüfung des Verhaltens von nachträglich installierten Dübeln getrennt auf dem Gebrauchstauglichkeitsniveau und dem Grenztragfähigkeitsniveau. Da getrennte Tests grundsätzlich zu einer erhöhten Anzahl an durchzuführenden Tests führen, wurde die Beurteilung der Eignung und Bestimmung der charakteristischen Bemessungswerte auf Grundlage eines kombinierten Testprotokolls angestrebt. Die Gleichwertigkeit der separaten und kombinierten Testprotokolle konnte anhand von Vergleichsversuchen verifiziert werden. Dabei konnte auch gezeigt werden, dass bei zyklischen Querlastversuchen die Reduzierung der hohen Anzahl an kleinen Lastamplituden zu Beginn des Testprotokolls eine erhebliche Testzeitverkürzung ohne Auswirkung auf das Testergebnis erlaubt.

Ferner wurde überprüft, ob vereinfachte Testprotokolle mit konstanter Anzahl je Amplitudenstufe ohne signifikante Änderung der Versuchsergebnisse möglich sind. Zwar haben diese Untersuchungen gezeigt, dass die Unterschiede gering sind, jedoch ist der Gewinn durch vereinfachte Protokolle zu gering, um diese zu rechtfertigen. Im Gegensatz dazu stellt die Annäherung der Sinusschwingungen durch dreiecksförmige Zeitverläufe eine erhebliche Vereinfachung und

Beschleunigung dar, so dass diese Lösung ausdrücklich zur Aufnahme in den Prüfrichtlinien empfohlen wird.

Ergänzend zu den Prüfbedingungen wurden auf Grundlage der bis dato vorhandenen Erkenntnisse sinnvolle Bewertungskriterien bezüglich der Dübelverschiebung, der Abminderung der Tragfähigkeit sowie der dazugehörigen Streuungen hergeleitet. Die gesammelten Untersuchungsergebnisse resultierten dann in einem Vorschlag über die Prüfbedingungen, Versuchsdurchführung und Bewertungskriterien für die seismische Ergänzung von Prüfrichtlinien.

Kapitel 5 – Untersuchungen auf Systemebene: Rütteltischversuche

Die in Kapitel 3 und 4 präsentierte Forschung wurde am isolierten Dübel, auf der so genannten Komponentenebene, unter simulierten Erdbebenbedingungen durchgeführt. Bei den in Kapitel 5 vorgestellten Forschungsarbeiten ist das Verhalten des Dübels als Teil eines Systems Gegenstand der Untersuchungen. Hierzu wurden Rütteltischversuche durchgeführt, bei denen ein Gewicht über Kopf mittels vier nachträglich installierter Dübel in eine Betonplatte befestigt wurde. Die Betonplatte wurde über den Rütteltisch nach Beschleunigungszeitverläufen realer Erdbeben angeregt, gleichzeitig wurden die Risse, in denen die Dübel zur Befestigung gesetzt wurden, nach korrespondierenden Verkrümmungszeitverläufen geöffnet und geschlossen. Hierbei kamen ein relativ steifer Hinterschnittdübel sowie ein verschiebungsfähiger Spreizdübel zum Einsatz. Die Tests waren die ersten ihrer Art und ermöglichten die genaue Untersuchung des Tragverhaltens von Dübeln bei der Befestigung nicht tragender Bauteile unter realen Bedingungen. Ferner ermöglichte der direkte Vergleich das Bestätigen zahlreicher auf Komponentenebene getätigter Beobachtungen. Das Testprogramm bestand im Wesentlichen aus folgenden Testtypen:

- Korrelationstests haben gezeigt, dass bei dieser Konfiguration Dübellast und Rissweite nur eine geringe Korrelation zeigen. Das heißt, dass maximale Dübellast und maximale Rissweite nur selten zusammentreffen. Statistisch liegt die Dübellast unabhängig von der Rissweite bei im Schnitt 20 % der Bemessungstragfähigkeit. Daraus lässt sich ableiten, dass die Dauerlast in Risszyklusversuchen zumindest bei der Prüfung von Befestigungen nichttragender Elemente deutlich reduziert werden könnte.
- Verschiebungstests erlaubten den direkten Vergleich mit den Dübelverschiebungen, die in den seismischen Qualifikationstests gemessen wurden. Aufgrund des relativ geringen Dübellastniveaus fielen die Verschiebungen bei den Rütteltischversuchen erheblich kleiner aus. Setzt man jedoch die Verschiebungen im Verhältnis zu den akkumulierten Schadenspotentialen der Qualifikationstests (Kapitel 4) und den der

Rütteltischversuche, so kann gezeigt werden, dass sich die Verschiebungen in der gleichen Größenordnung bewegen.

- Versagenstests hatten das Ziel, den Versagensmechanismus von Überkopfinstallationen zu untersuchen. Die Höhe der wechselseitig auftretenden Lasten wurde von den erdbebenbedingten Trägheitskräften dominiert; die bei Überkopfinstallationen zusätzlich wirkenden Gravitationslasten spielten dahingegen eine untergeordnete Rolle. Das Versagen von zwei der vier Dübel führte nicht zum Totalversagen des Anschlusses, auch weil die Dübel von dem nach dem Teilversagen veränderten statischen System profitierten. Da die Risse zum Zeitpunkt der maximalen Lasten weitestgehend geschlossen waren, wurden die in den unter Kapitel 4 durchgeführten Qualifikationstest ermittelten Grenztragfähigkeiten überschritten. Insofern können die Qualifikationstests als ausreichend konservativ angesehen werden.

Ferner hat die detaillierte Analyse der Kraft-, Verschiebungs- und Beschleunigungsdaten ergeben, dass das Schwingverhalten des montierten Gewichts in erster Linie von der Eigenfrequenz dieses abhängt und nicht von dem Niveau der Dübellasten oder der Rissweiten. Die Nichtlinearität des Systems führt zu einer Reduzierung der Lastanforderungen an die Dübel bei hohen Horizontal-beschleunigungen. Zwar sind hierfür eine Lockerung der Befestigung und die einhergehende Verlängerung der Schwingperiode erforderlich, jedoch ist die Nichtlinearität unabhängig vom Dübeltyp und dessen charakteristischen, mit den Dübelduktilitäten assoziierten (Kapitel 3) Verformungsverhalten. Die in den Tests gemessenen Belastungsgeschwindigkeiten bestätigten den Geschwindigkeits-bereich, der zuvor bei den Hochgeschwindigkeitsversuchen (Kapitel 3) als erdbebenrelevant angesehen wurde.

Kapitel 6 – Empfehlungen für Prüf- und Bemessungsrichtlinien

Aus den gewonnenen Erkenntnissen vorgenannter Untersuchungen werden folgende Empfehlungen für Prüf- und Bemessungsrichtlinien vorgeschlagen:

- Generell wird empfohlen, bestimmte Randbedingungen der Qualifikationstests detaillierter zu definieren, um eine gute Reproduzierbarkeit der Testergebnisse zu gewährleisten. Dies gilt unter anderem für die Prüfkörpergeometrie und -bewehrung, die Generierung der Risse, sowie der Testaufbau insbesondere bei Querkraftversuchen.
- Hochgeschwindigkeitsversuche müssen in den Versuchskatalog zur Qualifizierung von Dübeln für den Verwendung in Erdbebengebieten nicht aufgenommen werden.

- Die Dübelduktilität sollte grundsätzlich im Rahmen von Zulassungsverfahren bestimmt werden, auch wenn sie für die seismische Qualifizierung keine besondere Relevanz hat. Hierfür wird vorgeschlagen, dass ein Dübel, der unabhängig von der Versagensart eine auf die Verankerungstiefe bezogene Verschiebung bei Höchstlast in Größe der geforderten prozentuale Längung des Dübelwerkstoffes in einem Zugversuch erreicht, als duktil klassifiziert wird. Die plastische Bemessung von Befestigungen tragender Bauteile gemäß *CEN/TS 1992-4 (2009)* Annex B und die in *ACI 318 (2011)* Appendix D für duktile Befestigungen angegebenen Teilsicherheitsbeiwerte sollten unter diesem Gesichtspunkt überprüft werden.
- Die Tragfähigkeiten von Dübelgruppen und deren Abminderung infolge von geringen Dübelabständen werden grundsätzlich nach der Concrete Capacity (CC) Methode bei Betonversagen und des Uniform Bond (UB) Modells bei Verbundversagen ermittelt. Der zur vollen Übertragung der Tragfähigkeit eines Einzeldübels erforderliche Mindestabstand von $3\,h_{ef}$ hat sich in der Vergangenheit bestätigt. Damit erscheinen Gruppenversuche, wie sie im Gegensatz zum *ACI 355.2 (2007)* laut *ETAG 001 (2006)* noch Bestandteil des Testprogramms sind, als nicht erforderlich. Falls jedoch Gruppenversuche durchgeführt werden, sollten diese unter klar definierten Randbedingungen erfolgen, da die Drehsteifigkeit einen erheblichen Einfluss auf das Tragverhalten haben kann. Mit Einführung eines zusätzlichen Gruppenabminderungsfaktors von 0.85 für die Berücksichtigung ungünstiger Einflüsse bei seismischen Anwendungen kann der bestehende, nicht näher definierte seismische Abminderungsfaktor von 0.75 nach *CEN/TS 1992-4 (2009)* und *ACI 318 (2011)* entfallen.
- Zyklische Lastversuche in Längs- und Querrichtung bilden einen zentralen Bestandteil der seismischen Qualifikation von nachträglich installierten Dübeln. Diese folgen einem schrittweise ansteigenden Amplitudenprotokoll mit 75 Lastwechseln, deren Maximaldübellast bei Längskraft 75 % und bei Querkraft 85 % der mittleren monotonen Tragfähigkeit entspricht. Gebrauchstauglichkeits- und Grenztragfähigkeitsniveau werden in einem Testdurchgang getestet. Das Gebrauchstauglichkeitsniveau wird jeweils bei 50 % der Maximallast erreicht. Die Rissweite beträgt 0.5 mm auf Gebrauchstauglichkeitsniveau und 0.8 mm auf Grenztragfähigkeitsniveau. Nach Durchfahren aller Amplituden wird die Resttragfähigkeit in einem Auszugsversuch ermittelt. Weitere Empfehlungen werden im Kapitel 4 gegeben. Insbesondere gilt es, den Versuchsaufbau bei zyklischen Querkraftversuchen genauer zu definieren.
- Zyklische Rissversuche bilden den zweiten zentralen Bestandteil der seismischen Qualifikation von nachträglich installierten Dübeln. Diese folgen

einem schrittweise ansteigenden Amplitudenprotokoll mit 59 Rissöffnungen, deren Maximalrissweite 0.8 mm beträgt. Gebrauchstauglichkeits- und Grenztragfähigkeitsniveau werden in einem Testdurchgang getestet. Gebrauchstauglichkeitsniveau wird bei einer Rissweite von 0.5 mm erreicht. Die Dübellast beträgt während des Testens auf Grenztragfähigkeitsniveau 50 % der mittleren monotonen Tragfähigkeit und wird während des Testens auf Gebrauchstauglichkeitsniveau auf 80 % dieses Wertes reduziert. Nach Durchfahren aller Amplituden wird die Resttragfähigkeit in einem Auszugsversuch ermittelt. Weitere Empfehlungen werden im Kapitel 4 gegeben. Besondere Aufmerksamkeit ist bei zyklischen Rissversuchen der genauen Messung der Rissweiten und Dübelverschiebungen zu schenken.

Die seismische Qualifikation von nachträglich installierten Dübeln ist also durch zyklische Lastversuche und zyklische Rissversuche zu erlangen. Die oben beschriebenen Versuche bilden den Kern eines Vorschlags für die seismische Ergänzung der europäischen Prüfrichtlinie *ETAG 001 (2006)*. Da bei der Festlegung der Randbedingungen für die im Rahmen dieser Dissertation durchgeführte Forschung nicht nur bestehende Bestimmungen europäischer Richtlinien, sondern auch die der US-amerikanischen berücksichtigt wurden, lassen sich die Empfehlungen auch in das US-amerikanische Normenwesen übertragen.

Kapitel 7 – Modell zur Berechnung der Dübelverschiebung

Die Auswirkung von zyklischen Rissen auf die axiale Dübelverschiebung ist ein zentrales Thema dieser Dissertation. Große Verschiebungen sind ein kritischer Parameter bei der Bestimmung der seismischen Tragfähigkeit. Risszyklusversuche sind technisch aufwendig und wegen ihres hohen Zeitaufwandes auch sehr teuer. Daher ist eine näherungsweise Abschätzung der zu erwartenden Verschiebung auf Grundlage vorgegebener Last- und Rissregime erstrebenswert. Das hierfür entwickelte Modell ermöglicht dies auf Grundlage des ADP Ansatzes und monotoner Auszugskurven, deren charakteristische Verschiebungsverhalten zur Ermittlung eines Verschiebungsinkrements ausgewertet werden.

Anhand vorhandener Lastverschiebungskurven konnte gezeigt werden, dass mit diesem Ansatz eine Berechnung der akkumulierten Verschiebung grundsätzlich möglich ist. Die Lastverschiebungskurven aus dem Testprogramm der zyklischen Rissversuche mit 32 Rissöffnungen konnten mit Hilfe des Modells gut dargestellt werden. Die Simulation der Lastverschiebungskurven der seismischen Qualifikationstests mit 59 Rissöffnungen lieferte nicht ganz so gute Ergebnisse. Diese waren jedoch vor dem Hintergrund, dass die vorgestellte Methode nicht als Ersatz sondern als Ergänzung von Zulassungsversuchen dienen soll, immer noch

zufriedenstellend, gerade in Anbetracht der mit Rissöffnungsversuchen verbundenen extrem großen Streuungen.

Kapitel 8 – Zusammenfassung und offene Fragen

Die vorliegende Dissertation stellt eine umfassende Behandlung des Verhaltens und Qualifizierung von nachträglich installierten Dübeln für seismische Anwendungen dar. Hierzu wurden umfangreiche Untersuchungen auf Komponenten- und Systemebene durchgeführt, deren wesentliche Ergebnissen in Kapitel 8 zusammengefasst sind. Alle Fragestellungen, deren Beantwortung für eine seismische Ergänzung der europäischen Prüfrichtlinie unabdingbar war, konnten abschließend behandelt werden.

Darüber hinaus wurden Testmethoden und Modelle entwickelt, die für weiterführende Untersuchungen verwendet werden können. Als untersuchungswert wurden folgende Punkte identifiziert:

- Weitere Forschung ist erforderlich, um den Zusammenhang von lokaler Dübelduktilität und globaler Bauwerksduktilität zu verstehen. Hierzu bieten sich numerische Simulationen an. Außerdem sind zusätzliche Querkraftversuche unter genau definierten Randbedingungen hilfreich, um den Parameterbereich der Querverschiebungen genauer zu quantifizieren.
- Zusätzliche Gruppentests mit weiteren Dübelprodukten sind notwendig, um eine generelle Gültigkeit des vorgeschlagenen seismischen Gruppenfaktors zu zeigen. Hierzu bieten sich Simulationen auf Grundlage des entwickelten Modells zur Lastumverlagerung an. Bei in Querrichtung belasteten Gruppen spielt die Lastumverlagerung infolge erdbebenbedingter Risszyklen keine Rolle, jedoch findet hier eine Umverlagerung infolge unterschiedlichen Lochspiels statt. Bevor eine weitere Untersuchung dieses Effekts erfolgt, sollte die Frage nach dem Verfüllen des Lochspiels adressiert werden.
- Die zyklischen Tests haben gezeigt, dass grundsätzlich jeder Dübeltyp für den seismischen Einsatz geeignet ist. Dies gilt allerdings für Verbunddübel nur eingeschränkt, da diese einer größeren Anzahl an Risszyklen nicht standhalten. Da der Einsatz von Klebstoffen in der Befestigungstechnik grundsätzlich vielversprechend ist, sollte das Verhalten von Verbundspreizdübeln näher untersucht werden. Hinsichtlich der zyklischen Querkraftbelastung sollten die kritischen Parameter für das Ermüdungsverhalten näher untersucht werden.
- Theoretische Überlegungen haben gezeigt, dass Befestigungen tragender Bauteile bezüglich der Belastung aus zyklischen Lasten und Rissen kritischer einzustufen sind als Befestigungen nicht tragender Bauteile. Diese Hypothese

sollte durch bauwerksdynamische Simulationen und experimentelle Versuche bestätigt werden. Ferner sollte untersucht werden, ob gleichzeitig auftretende Längs- und Querkraftzyklen einen potentiell positiven Effekt auf die axiale Verschiebung des Dübels im Riss haben.

Literature

DIN 1045 (2001): Tragwerke aus Beton, Stahlbeton und Spannbeton: Teil 1 Bemessung und Konstruktion; Teil 2 Festlegung, Eigenschaften, Herstellung und Konformität (Concrete, reinforced concrete and prestressed concrete structures: Part 1, design and construction; Part 2, regulation, properties, production and conformity). Deutsches Institut für Normung (in German)

DIN 1048 (1991): Prüfverfahren für Beton (Test methods for concrete). Deutsches Institut für Normung (in German)

DIN 4149 (2005): Bauten in deutschen Erdbebengebieten: Lastannahmen, Bemessung and Ausführung üblicher Hochbauten, (Construction in German earthquake regions: Loading assumptions, design and execution of typical tall structures). Deutsches Institut für Normung (in German)

DoD 6055.9 (2004): DoD Directive 6055.9-STD: Ammunition and explosives safety standard. Department of Defense

AC156 (2007): Acceptance criteria for seismic qualification testing of nonstructural components. International Code Council Evaluation Service, Inc. (ICC-ES), Whittier, California

AC193 (2010): Acceptance criteria for mechanical anchors in concrete elements. International Code Council Evaluation Service, Inc. (ICC-ES), Whittier, California

AC308 (2009): Acceptance criteria for post-installed adhesive anchors in concrete elements. International Code Council Evaluation Service, Inc. (ICC-ES), Whittier, California

ACI 318 (2002): Building code requirements for structural concrete (ACI 318-02) and commentary (ACI 318R-02), American Concrete Institute, Farmington Hills, Michigan

ACI 318 (2008): Building code requirements for structural concrete (ACI 318-08) and commentary (ACI 318R-08), American Concrete Institute, Farmington Hills, Michigan

ACI 318 (2011): Building code requirements for structural concrete (ACI 318-11) and commentary (ACI 318R-11), American Concrete Institute, Farmington Hills, Michigan

ACI 349 (2006): Code Requirements for nuclear safety-related concrete structures (ACI 349-06) and commentary (ACI 349R-06), American Concrete Institute, Detroit, Michigan

ACI 355.2 (2001): Qualification of post-installed mechanical anchors in concrete (ACI 355.2-01) and commentary, American Concrete Institute (ACI), Farmington Hills, Michigan

ACI 355.2 (2007): Qualification of post-installed mechanical anchors in concrete (ACI 355.2-07) and commentary, American Concrete Institute (ACI), Farmington Hills, Michigan

ACI 355.4 (2010): Acceptance criteria for qualification of post-installed adhesive anchors in concrete (ACI 355.4-10) and commentary (ACI 355.4R-10) (Provisional Standard), American Concrete Institute (ACI), Farmington Hills, Michigan

Ammann, W. (1992): Fastening systems under seismic loading conditions. Proceedings of the 10th World Conference on Earthquake Engineering, Madrid 1992, Vol. 9, 5247-5252

ASCE 7 (2010): Minimum design loads for buildings and other structures: Revision of ANSI/ASCE 7-10, American Society of Civil Engineers (ASCE), Reston, Virginia

Asmus, J. (1999): Bemessung von zugbeanspruchten Befestigungen bei der Versagensart Spalten des Betons (Design of tension loaded fastenings for splitting of the concrete). Dissertation, Institut für Werkstoffe im Bauwesen, Universität Stuttgart (in German)

ASTM A307 (1997): Standard specification for carbon steel bolt and studs, 60 000 psi tensile strength, American Society for Testing and Materials (ASTM), ASTM International, West Conshohocken, PA

ASTM F606 (1998): Standard test methods for determining the mechanical properties of externally and internally threaded fasteners, washers, direct tension indicators, and rivets. American Society for Testing and Materials (ASTM), ASTM International, West Conshohocken, PA

ATC-24 (1992): Guidelines for cyclic seismic testing of components of steel structures, Applied Technology Council (ATC)

ATC-29-1 (1998): Proceedings of seminar on seismic design, retrofit; performance of nonstructural components, Applied Technology Council (ATC)

ATC-40 (1996): Seismic evaluation and retrofit of concrete buildings: Volumes 1; 2, Applied Technology Council (ATC)

ATC-58 (2004): Project task report: Phase 2. Task 2.2 (Engineering demand parameters for structural framing systems) and Task 2.3 (Engineering demand parameters for nonstructural components), Applied Technology Council (ATC)

Bachmann, H. (1995): Erdbebensicherung von Bauwerken (Earthquake Guarding of Buildings). Birkhäuser Verlag, Basel (in German)

Bergmeister, K. (1988): Stochastik in der Befestigungstechnik mit realistischen Einflussgrößen (Stochastic in fastening technology under realistic variables). Dissertation, Universität Innsbruck

Bergmeister, K.; Rieder, A. (2009): Crack cycling tests for ASPC2, Presentation to EOTA Working Group 06.01/03, EOTA Meeting Rome, December 15, 2009, not published

Block, K.; Dreier, F. (1998): Die Ermüdungsfestigkeit zuverlässig und kostengünstig ermitteln (Reliable and economic determination of fatigue strength). Materialprüfung 1998;40 (in German)

Block, K.; Dreier, F. (2002): Dübelbefestigungen bei ermüdungsrelevanten Einwirkungen. DIBt Mitteilungen 4/2002, 98-105

BM Bau (1981): Nachweis der Schocksicherheit von Einbauteilen in Schutzräumen (Verification of resistance against impact loading on components in shelters). Bundesministerium für Raumordnung, Bauwesen und Städtebau (BM Bau) (in German)

Bowden, P.; Tabor, D. (1959): Reibung und Schmierung fester Körper (Friction and lubrication of solids). Springer-Verlag Berlin (in German)

Brunet, R. (2002): Lignes de force de l'espace europeen (Lines of force in the European region). Mappe Monde 66 (2002.2) 14-19 (in French)

Fib Bulletin No. 58 (2011): Design of anchorages in concrete. Guide to good practice. Bulletin No. 58, Fédération International du Béton (fib)

BZS (1980): Technische Weisung für die Schocksicherheit von Einbauteilen in Zivilschutzbauten (Technical advice on resistance against impact loading of components in shelters). Eidgenössisches Justiz- und Polizeidepartment, Bundesamt für Zivilschutz (in German)

CAN/CSA-N287.2-M91 (1991): Material requirements for concrete containment structures for CANDU nuclear power plants, Canadian Standards Association (CSA) (reaffirmed 2003)

CAN3-N289.4-M86 (1986): Testing procedures for seismic qualification of CANDU nuclear power plants, Canadian Standards Association (CSA) (reaffirmed 2003)

Cattaneo, S. (2007): Wedge-type expansion anchors in high-performance concrete. ACI Structural Journal, March-April 2007, Vol. 104, No. 2, 191-198

CEB Bulletin d'information No. 158 (1984): CEB-Manual Cracking and Deformation. Bulletin d'information Nr. 158, Comité Euro-International du Béton (CEB), London

CEB Bulletin d'information No. 187 (1988): Concrete structures under impact and impulsive loading. Bulletin d'information Nr. 187, Comité Euro-International du Béton (CEB), London

CEB Bulletin d'information No. 216 (1994): Fastenings to concrete and masonry structures. Bulletin d'information Nr. 216, Comité Euro-International du Béton (CEB), London

CEB Design Guide (1997): Design of fastenings in concrete. Design Guide, Comité Euro-International du Béton (CEB), London

CEB State of the Art Report (1996): Fastenings for seismic retrofitting, State-of-the-art report on design and application, Comité Euro-International du Béton (CEB), London

CEN/TS 1992-4 (2009): Design of fastenings for use in concrete – Part 4-1 – 4-5. Technical Specification, European Committee for Standardization (CEN), Brussels

Chopra, A. (2007): Dynamics of structures – Theory and applications to earthquake engineering. 3rd Edition, Pearson Prentice Hall

CICHE 401 (1996): Reinforced concrete design code and commentary (CICHE 401-96). Chinese Institute of Civil and Hydraulic Engineering (CICHE), Taipei, Taiwan

Cook, R.; Collins, D.; Klingner, R.; Polyzois, D. (1992): Load-deflection behavior of cast-in-place and retrofit concrete anchors. ACI Structural Journal, November-December 1992, Vol. 89, No. 6, 639-649

Cook, R.; Kunz, J.; Fuchs, W.; Konz, R. (1998): Behavior and design of single adhesive anchors under tensile load in uncracked concrete, ACI Structural Journal, Januar-February 1998, Vol. 95, No. 1, 9-26

CUAP Concrete Screw (2003): CUAP Concrete screw for anchorage in normal weight concrete. Drafted by DIBt

Czichos, H.; Habig, K.-H. (1992): Reibung und Verschleiß; Systemanalayse, Prüftechnik, Werkstoffe und Konstruktionselemente (Friction and wear; System analysis, testing methods, materials and elements). Vieweg Verlag Braunschweig und Wiesbaden (in German)

DIBt KKW Leitfaden (1998): Verwendung von Dübeln in Kernkraftwerken und kerntechnischen Anlagen, Leitfaden zur Beurteilung von Dübelbefestigungen bei der Erteilung von Zustimmungen im Einzelfall nach den Landesbauordnung der Bundesländer (Use of anchors in nuclear power plants and nuclear technology installations, guideline for evaluating fastenings for granting permission in individual cases according to the state structure regulations of the federal states of Germany), Deutsches Institut für Bautechnik (DIBt), Berlin (in German)

DIBt KKW Leitfaden (2010): Leitfaden für Dübelbefestigungen in Kernkraftwerken und anderen kerntechnischen Anlagen (Guideline for fastenings in nuclear power plants and other nuclear technical facilities), Deutsches Institut für Bautechnik (DIBt), Berlin (in German)

Dutta, A.; Mander, J. (2001): Energy based methodology for ductile design of concrete columns. ASCE Journal of Structural Engineering, December 2001, Vol. 127, No. 12, 1374-1381

EERI SER Christchurch (2011): The M 6.3 Christchurch, New Zealand, Earthquake of February 22. Special Earthquake Report, Earthquake Engineering Research Institute (EERI), Oakland, California

EERI SER Maule (2010): The Mw 8.8 Chile Earthquake of February 27, 2010. Special Earthquake Report, Earthquake Engineering Research Institute (EERI), Oakland, California

Eibl, J.; Keintzel, E. (1989a): Verhalten von Dübeln unter hoher Stoß- und Wechselbeanspruchung (Behaviour of anchors under high speed impact and reversed cyclic loads). IMB, Universität Karlsruhe (TH) (in German)

Eibl, J.; Keintzel, E. (1989b): Zur Beanspruchung von Befestigungsmitteln bei dynamischen Lasten (Loading of fastenings under dynamic loads). IMB, Universität Karlsruhe (TH) (in German)

Eligehausen, R.; Balogh, T. (1995): Behavior of fasteners loaded in tension in cracked reinforced concrete. ACI Structural Journal, May-June 1995, Vol. 92, No. 3, 365-379

Eligehausen, R.; Hutchinson, T.; Mahrenholtz, P.; Mahrenholtz, C.; Wood, R. (2010): Load and cyclic crack protocol for anchorage - Part 2: Alternate proposal. Presentation to EOTA WG 06.01/03 Meeting July 27, 2010 Stuttgart

Eligehausen, R.; Lotze, D.; Sawade, G. (1986): Untersuchungen zur Frage der Wahrscheinlichkeit, mit der Dübel in Rissen liegen (Investigation of the probability that anchors are located in cracks). Report No. 1/20-86/17, Institut für Werkstoffe im Bauwesen, Universität Stuttgart, not published (in German)

Eligehausen, R.; Mallée, R.; Silva, J. (2006): Anchorage in concrete construction. Ernst & Sohn, Berlin

EOTA TR 029 (2010): Design of bonded anchors. Technical Report 029

ETAG 001 (1997): Guideline for European technical approval of metal anchors for use in concrete, Parts 1 – 6. European Organization of Technical Approvals (EOTA), Brussels

ETAG 001 (2006): Guideline for European technical approval of metal anchors for use in concrete, Parts 1 – 6. European Organization of Technical Approvals (EOTA), Brussels

Eurocode 0 (2002): Basis of structural design. European Committee for Standardization (CEN); DIN EN 1990-: 2002

Eurocode 2 (2005): Design of concrete structures. European Committee for Standardization (CEN); DIN EN 1992: 2005

Eurocode 8 (2006): Design of structures for earthquake resistance. European Committee for Standardization (CEN); DIN EN 1998: 2006

Eurocode 8 / NA (2009): Design of structures for earthquake resistance – National Annex. European Committee for Standardization (CEN); DIN EN 1998: 2009/NA (draft)

FEMA-273 (1997): NEHRP guidelines for the seismic rehabilitation of buildings. Federal Emergency Management Agency (FEMA)

FEMA-356 (2000): Prestandard and commentary for the seismic rehabilitation of buildings. Prepared for the Federal Emergency Management Agency (FEMA) by the American Society of Civil Engineers (ASCE). Federal Emergency Management Agency (FEMA)

FEMA-461 (2007): Interim testing protocols for determining the seismic performance characteristics of structural and nonstructural components. Federal Emergency Management Agency (FEMA)

Fischer, L. (1995): Bestimmung des 5%-Quantils im Zuge der Bauwerksprüfung – Bezugnahme auf DIN-Normen und Eurocodes (Evaluation of 5%-Quantile in the course of Structural Inspection. Reference to DIN-Standards and EURO-Codes). Bautechnik 72, Heft 11, 712-722

Franchi, A.; Rosati, G.; Cattaneo, S.; Crespi, P.; Muciaccia, G. (2009): Experimental investigation on post-installed metal anchors subjected to seismic loading in R/C members. Studi e ricerche - Politecnico di Milano. Scuola di specializzazione in construzioni in cemento armato, Volume 29

Fuchs, W.; Eligehausen, R. (1995): Das CC-Verfahren für die Berechnung der Betonausbruchlast von Verankerungen (CC-method for determination of the concrete failure load of fastenings). Beton- und Stahlbetonbau, 1995, No. 1, 6-9, No. 2, 38-44, No. 3, 73-76 (in German)

Fujikake, K.; Nakayama, J.; Sato, H.; Mindess, S.; Ishibashi, T. (2003): Chemically bonded anchors subjected to rapid pullout loading. ACI Materials Journal, May-June 2003, Vol. 100, No. 3, 246-252

Furche, J. (1994): Zum Trag- und Verschiebungsverhalten von Kopfbolzen bei zentrischem Zug (Load-bearing and displacement behavior of headed bolts under centric tension load). Dissertation, University of Stuttgart.

Genesio, G. (2007): Tragverhalten von Befestigungen unter wechselnder Querzugbeanspruchung im gerissenen Beton (w=0,8mm) (Load-bearing behaviour of fasteners under alternating shear loading in cracked concrete (w=0.8mm)). Test Report WS 212/19-07/08, Institut für Werkstoffe im Bauwesen, Universität Stuttgart, not published (in German)

Gergely, P.; Lutz, L. (1968): Maximum crack width in reinforced concrete flexural members. Causes, Mechanisms and Control of Cracking in Concrete, ACI, SP-20, 87-117

Ghobarah, A. (2001): Performance-based design in earthquake engineering: state of development. Engineering Structures 23, 878-884

Ghobarah, A.; Aziz, T. (2004): Seismic qualification of expansion anchors to Canadian nuclear standards. Nuclear Design and Engineering, Vol. 228, 377-392

Götz, A. (2003): Erdbeben – die unterschätzte Naturgefahr. Aquaterra 2/2003, Schweizer Bundesamt für Wasser und Geologie

Gould, N.; Griffin, M. (2003): Earthquake performance of nonstructural components. ABS Consulting, January 2003, International Risk Management Institute, Inc. http://www.irmi.com/Expert/Articles/2003/Gould01.aspx (Date accessed: June 6, 2009)

Griffin, M.; Winn, V. (2009): Nonstructural seismic performance for facilities in seismic regions: is the expected earthquake performance really being achieved. Proceedings of the ATC & SEI 2009 Conference on Improving the Seismic Performance of Existing Buildings and Other Structures, San Francisco

Grünthal, G.; Arvidsson, R.; Bosse, C. (2004): Earthquake model for the European-Mediterranean Region for the purpose of GEM1. Scientific Technical Report STR10/04, Deutsches Geoforschungszentrum (GFZ)

Guillet, T. (2011): Behavior of metal anchors under combined tension and shear cycling loads. ACI Structural Journal, May-June 2011, Vol. 108, No. 3, 315-323

Gurbuz, T.; Ilki, A. (2011): Pullout performance of fully and partially bonded retrofit anchors in low-strength concrete. ACI Structural Journal, January-February 2011, Vol. 108, No. 1, 61-70

Hegger, J.; Döinghaus, P.; Sedlacek, G.; Trumpf, H. (2003): Untersuchungen zur Duktilität der Verbundmittel bei Anwendung von hochfestem Stahl und hochfestem Beton: Forschungsbericht (Investigations on the ductility of dowels for applications in high strength steel and high strength concrete). Düsseldorf Verlags- und Vertriebsgesellschaft (Forschung für die Praxis) (in German)

Herdman, R. (1995): Reducing Earthquake Losses. U.S. Congress, Office of Technology Assessment, OTA-ETI-623

Hoehler, M. (2006): Behavior and testing of fastenings to concrete for use in seismic applications. Dissertation, University of Stuttgart, 2006

Hoehler, M.; Dowell, R.; Watkins, D. (2011): Shear and axial load measurement device for anchorages in concrete. ASTM Journal of Testing and Evaluation, Vol. 39, Issue 4, July 2011

Hoehler, M.; Mahrenholtz, P.; Eligehausen, R. (2011): Behavior of anchors in concrete at seismic-relevant loading rates. ACI Structural Journal, March-April 2011, Vol. 108, No. 2, 238-247

Hoehler, M.; Silva, J.; Floriani, L.; Bourgund, U.; Gassner, H.; Restrepo, J. I.; Panagiotou, M. (2007): Full-scale shake table test of pipes anchored in a 7-

story RC building. Proceedings of the 2nd RILEM International Symposium on Connections between Steel and Concrete, Stuttgart

Hoehler, M.; Silva, J.; Mahrenholtz, P. (2011): Testing and assessment of anchor ductility. Proceedings of the fib Symposium, 543-546, Praha

Hunziker, P. (1999): Shocktesting of concrete anchor bolts for shock resistant applications in protective structures. Proceedings of the 3rd International Conference on Shock & Impact Loads on Structures, Singapore

Hutchinson, T.; Wood, R. (2010): Load and cyclic crack protocol for anchorage - Part 1: Background. Presentation to EOTA WG 06.01/03 Meeting July 27, 2010 Stuttgart

IBC (2009): International Building Code (IBC). International Code Council (ICC), 2010

ISO 2566-1 (1999): Conversion of elongation values – Part 1: Carbon and low alloy steels

ISO 6892-1 (2009): Metallic materials – Tensile testing – Part 1: Method of test at room temperature

Kim, S.-Y.; Yu, C.-S.; Yoon, Y.-S. (2004): Sleeve-type expansion anchor behavior in cracked and uncracked concrete. Nuclear Engineering and Design, Vol. 228, 273-281

Klingner, R. (1993): The role of plastic design approaches in connections to concrete for seismic loads. Structural Engineers Association of Southern California (SEAOSC) Anchorage to Concrete Seminar, April, 1993

Klingner, R.; Gross, J.; Lotze, D.; Park, H.-G.; Rodriguez, M.; Zhang, Y-G. (1998): Anchor bolt behavior and strength during earthquakes, U.S. Nuclear Regulatory Commission, NUREG/CR-5434

Klingner, R.; Mendonca, J.; Malik, J. (1982): Effect of reinforcing details on the shear resistance of anchor bolts under reversed cyclic loading. ACI Journal Proceedings, January 1982, Vol. 79, No. 1, 471-479

KTA 3205.3 (2006): Komponentenstützkonstruktionen mit nichtintegralen Anschlüssen, Teil 3: Serienmäßige Standardhalterungen (Connections of components, Part 3: Standard mount). Sicherheitstechnische Regel des kerntechnischen Ausschusses (KTA) (in German)

Küenzlen, J. (2005): Tragverhalten von Schraubdübeln unter statischer Zugbelastung (Load behaviour of screw anchors for static tensile loading). Dissertation, University of Stuttgart, 2005 (in German)

Kunnath, S.; Chai, Y.-H. (2004): Cumulative damage-based inelastic cyclic demand spectrum. Earthquake Engineering and Structural Dynamics, Vol. 33, No. 4, 499-520

Lehmann, R. (1992): Tragverhalten von Metallspreizdübeln im ungerissenen und gerissenen Beton bei der Versagensart Herausziehen (Load bearing behaviour of mechanical expansion anchors in uncracked and cracked concrete in case of pullout failure). Dissertation, University of Stuttgart (in German)

Lieberum, K.-H. (1989): Das Tragverhalten von Beton bei extremer Teilflächenbelastung (Resistance of concrete to external partial area loading). Dissertation, TH Darmstadt

Lotze, D. (1986): Tragverhalten von Dübeln unter nicht vorwiegend ruhender Belastung – Tragverhalten von Mehrfachbefestigungen (Load-beaing behaviour of anchors under non-predemoninantly static loads - Load-bearing behaviour of multiple connections). Bericht Nr. 11/3-86/11, Institut für Werkstoffe im Bauwesen, Universität Stuttgart, not published (in German)

Lotze, D. (1987): Untersuchungen zur Frage der Wahrscheinlichkeit, mit der Dübel in Rissen liegen - Einfluß der Querbewehrung (Investigations on the Probability of Fasteners being Located in Cracks – Influence of Transverse Reinforcement). Bericht Nr. 1/24-87/6, Institut für Werkstoffe im Bauwesen, Universität Stuttgart, not published (in German)

Lotze, D. (1993): Tragverhalten und Anwendung von Dübeln unter oftmals wiederholter Belastung (Load bearing behavior and applications for anchors under frequently repeated loads). Dissertation, University of Stuttgart, 1993 (in German)

Mahrenholtz, C. (2009): Cyclic crack tests on post-installed and cast-in anchors – Test and summary report. HS II/09-09/06, Institut für Werkstoffe im Bauwesen, Universität Stuttgart, not published

Mahrenholtz, C. (2010): Cyclic crack tests – Literature review. HS III/12-10/02, Institut für Werkstoffe im Bauwesen, Universität Stuttgart, not published

Mahrenholtz, C. (2012): Seismic bond model for concrete reinforcement and the application to column-to-foundation connections. Dissertation, University of Stuttgart, 2012

Mahrenholtz, C.; Eligehausen, R.; Sharma, A. (2010): Behavior of post-installed concrete undercut anchors subjected to high loading rate and crack cycling frequency. Proceedings of the 9th U.S. National and 10th Canadian Conference on Earthquake Engineering, Paper No 1589, Toronto

Mahrenholtz, C.; Silva, J.; Eligehausen, R.; Hofmann, J. (2012): Testing anchors in cyclic cracks: Guidance for testing laboratories on how to generate cracks and cycle crack widths. Concrete International (in preparation)

Mahrenholtz, P. (2007a): Effect of high loading rates on friction – Literature review. HS II/01-07/01, Institut für Werkstoffe im Bauwesen, Universität Stuttgart, not published

Mahrenholtz, P. (2007b): High loading rate tests on torque-controlled expansion anchors – Test report. HS II/03-07/03, Institut für Werkstoffe im Bauwesen, Universität Stuttgart, not published

Mahrenholtz, P. (2008): Anchor groups – Literature review. HS I/02-08/08, Institut für Werkstoffe im Bauwesen, Universität Stuttgart, not published

Mahrenholtz, P. (2009): Cyclic tensile and shear tests on post-installed anchors – Test and summary report. HS II/08-09/05, Institut für Werkstoffe im Bauwesen, Universität Stuttgart, not published

Mahrenholtz, P. (2010a): Anchor ductility – Literature review and exploratory tensile tests. HS III/07-10/01, Institut für Werkstoffe im Bauwesen, Universität Stuttgart, not published

Mahrenholtz, P. (2010b): Group tests on post-installed anchors – Summary test report. HS I/05-10/03, Institut für Werkstoffe im Bauwesen, Universität Stuttgart, not published

Mahrenholtz, P. (2010c): Dübelgruppen unter seismischer Beanspruchung (Anchor groups under seismic loading). DFG Antrag, Institut für Baustoffe im Bauwesen, Universität Stuttgart, not published (in German)

Mahrenholtz, P. (2010d): Cyclic shear and cyclic crack tests on undercut anchors, expansion anchors, and headed bolts – Test and Summary Report. HS II/14-10/05, Institut für Werkstoffe im Bauwesen, Universität Stuttgart, not published

Mahrenholtz, P. (2011a): Anchor behavior under high loading rates – Summary report and discussion. EII/07-A/01, Institut für Werkstoffe im Bauwesen, Universität Stuttgart, not published

Mahrenholtz, P. (2011b): Anchor ductility – Development of ductility parameters and evaluation of data base. HS III/08-11/02, Institut für Werkstoffe im Bauwesen, Universität Stuttgart, not published

Mahrenholtz, P. (2011c): True and pseudo displacement-controlled tests – Test report. HS II/15-11/01, Institut für Werkstoffe im Bauwesen, Universität Stuttgart, not published

Mahrenholtz, P. (2011d): Investigation on the behaviour of rotation-restrained anchor groups by means of multi-axes servo-hydraulic control system. Annual Report 2008/10, 77-84 of the Institut für Werkstoffe im Bauwesen (IWB), Universität Stuttgart

Mahrenholtz, P. (2012): Behaviour of post-installed expansion anchor under high loading rates. Proceedings of the 9th fib International PhD Symposium in Civil Engineering, 673-678, Karlsruhe

Mahrenholtz, P.; Asmus, J.; Eligehausen, R. (2011): Post-installed anchors in nuclear power plants: Performance and qualification. Proceedings of the 21st International Conference on Structural Mechanics in Reactor Technology (SMiRT 21), Proceeding Div-V: Paper ID# 072, New Delhi

Mahrenholtz, P.; Eligehausen, R. (2010): Behavior of anchor groups installed in cracked concrete under simulated seismic actions. Proceeding of the Conference on Fracture Mechanics of Concrete Structures (FraMCoS 7), 816-822, Jeju

Mahrenholtz, P.; Eligehausen, R. (2012): Seismic design – αeq reduction factors. Presentation to fib SAG Fastening Meeting 2012, Kyoto, not published

Mahrenholtz, P.; Eligehausen, R.; Hofmann, J. (2011): Ductility of post-installed anchors. Proceedings of the Conference on Advances in Structural Engineering and Mechanics (ASEM11+), 1660-1675, Seoul

Mahrenholtz, P.; Hutchinson, T.; Eligehausen, R. (2012): Shake table tests on anchors connecting suspended components to cyclically cracked concrete. SSRP–12/01, UCSD

Mahrenholtz, P.; Hutchinson, T.; Eligehausen, R.; Hofmann, J. (2012): Shake table tests: Seismic performance of anchors connecting nonstructural components. Proceedings of the 15th World Conference on Earthquake Engineering (15WCEE), Paper #2751, Lisbon

Mahrenholtz, P.; Mahrenholtz, C. (2010): Cyclic crack tests on headed bolts –Test and summary report. HS II/13-10/04, Institut für Werkstoffe im Bauwesen, Universität Stuttgart, not published

Mahrenholtz, P.; Mahrenholtz, C.; Sharma, A.; Eligehausen, R. (2012): Concrete undercut anchors: Performance under dynamic actions in the context of qualification for use in NPP. Engineering Structures (in preparation)

Malhotra, P. (2002): Cyclic-demand spectrum. Earthquake Engineering and Structural Dynamics, Vol. 31, No. 7, 1441-1457

Malhotra, P.; Senseny, P.; Braga, A.; Allard, R. (2003): Testing of sprinkler-pipe seismic-brace components. Earthquake Spectra, Vol. 19, No. 1, 87-109

Mallée, R.; Fuchs, W.; Eligehausen, R. (2012): Befestigungstechnik (Fastening technology). Beton-Kalender 2012, Part 2, 93-173, Ernst & Sohn, Berlin

Martin, H.; Schießl, P.; Schwarzkopf, M. (1980): Ableitung eines allgemein gültigen Berechnungsverfahren für Rissbreiten aus Lastbeanspruchung auf der Grundlage von theoretischen Erkenntnissen und Versuchsergebnissen (A general method for the calculation of crack widths under loading based on theoretical and experimental studies). Forschung Straßenbau und Straßenverkehrstechnik, 309, 33-36 (in German)

Marxer, G.; Kunz, J.; Schoch, M.; Schuler, D. (2003): Earthquake resistant installations: Guideline for earthquake resistant design of installations and nonstructural elements, Hilti, December 2003

Masek, J.; Ridge, R. (2009): Identification of methods to achieve successful implementation of nonstructural and equipment seismic restraints. Report, Earthquake Engineering Research Institute (EERI), Oakland, California

Matsuzaki, Y.; Akiyama, T. (2008): Design of fasteners under seismic excitations - Section 4: Anchor design for seismic actions. Science University of Tokyo, Japan

Mayer, B. (1990): Funktionsersatzprüfung für die Beurteilung der Eignung von kraftkontrolliert spreizenden Dübeln (Functions substitution test for the assessment of the suitability of torque-controlled expansion anchors). Dissertation, Institut für Werkstoffe im Bauwesen, Universität Stuttgart (in German)

Mayer, B.; Eligehausen, R. (1983): Mehrfachbefestigungen mit kraftkontrolliert spreizenden Dübeln in der Betonzugzone (Multiple connections with force controlled expansion anchors located in tensioned concrete: Report on conducted tests). Bericht Nr. 1/3-83/13, Institut für Werkstoffe im Bauwesen, Universität Stuttgart, not published (in German)

Mayer, B.; Eligehausen, R. (1984): Ankergruppen mit Dübeln in der Betonzugzone: Bericht über durchgeführte Versuche (Anchor groups with anchors located in tensioned concrete: Report on conducted tests). Bericht Nr. 1/4 - 84/8, Institut für Werkstoffe im Bauwesen, Universität Stuttgart, not published (in German)

Menzel, K. (1995): Korrosion hinter vorgehängten Fassaden (Corosion behind facades). Industriebau 3/88, 208-211 (in German)

Meskouris, K.; Hinzen, K.-G. (2003): Bauwerke und Erdbeben (Structures and earthquakes). Vieweg-Verlag Wiesbaden, 2003 (in German)

Mészároš, J. (2002): Tragverhalten von Einzelverbunddübeln unter zentrischer Kurzzeitbelastung (Short-term load behavior of adesive anchors under tension). Dissertation, University of Stuttgart (in German)

Miner, M. (1945): Cumulative damage in fatigue. Journal of Applied Mechanics (ASME), Vol. 12, 159-164

Nch433Of (1996): Diseño sísmico de Edificios (Nch433Of.1996). Norma Chilena Oficial (NChOf), Santiago, Chile (in Spanish)

Newmark, N.; Hall, W. (1982): Earthquake spectra and design. EERI Monograph

Nürnberger, U. (1990): Spannungsrißkorrosion an Bauteilen aus nichtrostendem Stahl in Schwimmbadhallen (Stress cracking corrosion of elements made of noncorroding steel in roof constructions of indoor swimming pools). Stahl und Eisen 110 (1990) Nr. 6 (in German)

Nuti, C.; Santini, S. (2008): Fastening technique in seismic areas: A critical review. Proceedingof the Conference on Tailor Made Concrete Structures, 899-905, Roma

NZS 3101 (2006): Concrete structures standard. Part 1: The Design of Concrete Structure. Part 2: Commentary on the Design of Concrete Structures. New Zealand Standard Council, Wellington

Oh, B.-H.; Kang, Y.-J. (1987): New formulas for maximum crack width and crack spacing in reinforced concrete flexural members. ACI Structural Journal, March-April 1987, Vol. 85, No. 2, 103-112

Okelo, R. (1996): The influence of the scatter of the load displacement curves of individual anchors on the bearing capacity of a quadruple anchor group. Report No. 20/29-96/34, Institut für Werkstoffe im Bauwesen, Universität Stuttgart, not published (in German)

OSHPD Database (2009): Database of equipment/components with Office of Statewide Health Planning and Development (OSHPD) Special Seismic Certification Preapproval (OSP). Available at: http://www.oshpd.ca.gov/fdd/Pre-Approval/special_seismic_cert_pre-approval.html

Park, R. (1989): Evaluation of ductility of structures and structural assemblages from laboratory testing. Bulletin of the New Zealand National Society for Earthquake Engineering, Vol. 22, No. 3, 155–66, 1989

Paulay, T.; Bachmann, H.; Moser, K. (1990): Erdbebenbemessung von Stahlbetonhochbauten, Christchurch/Zürich, Verlag Birkhäuser

Paulay, T.; Priestley, N. (1992): Seismic design of reinforced concrete and masonry buildings. John Wiley & Sons, Inc.

PEER Database (2010): Strong Motion Database of the Pacific Earthquake Engineering Research Center (PEER). Available at: http://peer.berkeley.edu/smcat/

Penelis, G.; Kappos, A. (1997): Earthquake Resistant Concrete Structures, E&FN Spon

Periskic, G. (2009): Numerical investigations of multiple anchors connected by a common, rigid plate (flexible or hinged) with anchor spacing s ≥ scr under seismic loading conditions – Report. Institut für Werkstoffe im Bauwesen, Universität Stuttgart

prEN 1992-1 (2002): Eurocode 2: Design of concrete structures – Part 1 General rules and rules for buildings. prEN 1992--1--1: 2002

Priestley, N.; Calvi, G.; Kowalsky, M. (2007): Displacement-based seismic design of structures. IUSS Press, Pavia, Italy

Proposal for ETAG 001 Seismic Amendment (2011): Guideline for European Technical Approval of metal anchors for use in concrete: Assessment of metal anchors under seismic actions. Draft March 2011

Proposal for ETAG 001 Seismic Amendment (2012): Guideline for European Technical Approval of metal anchors for use in concrete - Annex E: Assessment of metal anchors under seismic actions. Draft April 2012

Rabinowicz, E. (1965): Friction and wear of materials. Department of Mechanical Engineering, Massachusetts Intitute of Technology, Wiley Series on the Science and Technology of Materials

Rehm, G.; Lehmann, R. (1982): Untersuchungen mit Metallspreizdübeln in der gerissenen Zugzone von Stahlbetonbauteilen (Investigations with metal expansion anchors in cracked reinforced concrete). Fraunhofer Society Research Report V. 1015 (in German)

Reitherman, R. (2006): Robert Park & Thomas Paulay. The EERI Oral History Series, published by the Earthquake Engineering Research Institute (EERI)

Rieder, A. (2002): Ductility – a basic requirement for seismic performance of fasteners. Proceedings of the 4th International PhD Symposium in Civil Engineering, 164-171, München

Rieder, A. (2009): Seismic response of post-installed anchors. Dissertation, Institut für konstruktiven Ingenieurbau der Universität für Bodenkultur, Wien

Rodriguez, M.; Lotze, D.; Gross, J.; Zhang, Y.-G.; Klingner, R.; Graves, H. (2001): Dynamic behavior of tensile anchors to concrete. ACI Structural Journal, July-August 2001, Vol. 98, 511-524

Salim, H.; Dinan, R.; Shull, J.; Townsend, P. (2005): Shock load capacity of concrete expansion anchoring systems in uncracked concrete, ASCE Journal of Structural Engineering, August 2005, V. 131, No. 8, 1206-1215

Schuler, D. (2007): Erdbebensicherheit von nichtragenden Bauteilen, Installationen und Einrichtungen (Earthquake resistance of nonstructural components). Tag der Befestigungstechnik, 01.03.2007, Zürich (in German)

Schwarz, J.; Langhammer, T.; Maiwald, H.; Smolka, A. (2004): Comparative seismic risk studies for German earthquake regions – damage and loss assessment for the city cologne. Proceedings of 13th World Conference on Earthquake Engineering, Vancouver

Schwarz, J.; Maiwald, H.; Langhammer, T. (2005): Erdbebenszenarien für deutsche Großstadträume und Quantifizierung der Schadenspotentiale. D-A-CH Mitteiliungsblatt 80, März 2005, Bauingenieur (in German)

SEAOC (1995a): Performance based seismic engineering of buildings, Structural Engineers Association of California (SEAOC), Whittier, California, April 1995

SEAOC (1995b): Vision 2000 - A Framework for Performance Based Earthquake Engineering. Vol. 1

SEAOSC (1997): Standard method of cyclic load test for anchors in concrete or grouted masonry, Structural Engineers Association of Southern California (SEAOSC), Whittier, California, April 1997

Seghezzi, H. (1985): Wechselbeziehungen zwischen Prüftechnik und Entwicklung von Befestigungselementen (Interactions between testing technology and development of fastening elements). Presentation 15.01.1985, Stuttgart

Sharma, A.; Mahrenholtz, C.; Eligehausen, R.; Reddy, G.; Vaze, K.; Ghosh, A.; Kushwawa, H. (2010): Evaluation of load on anchor for concrete structures corresponding to maximum crack width – A probabilistic approach. International Journal of Earth Sciences and Engineering, Vol. 3, No. 4, 798-811

SIA 261 (2003): Schweizer Norm (SN) 505 261: Einwirkungen auf Tragwerke (Actions on structures). Schweizerischer Ingenieur- und Architektenverein (in German)

SIA 262 (2003): Schweizer Norm (SN) 505 262: Betonbau (Concrete structures). Schweizerischer Ingenieur- und Architektenverein (in German)

Silva, J. (2001): Test methods for seismic qualification of post-installed anchors. Proceedings of the Symposium on Connections between Steel and Concrete, 2001, Stuttgart

Silva, J. (2007): Open questions in the field of anchorage to concrete. Beton- und Stahlbetonbau 102, Special Edition

Silva, J.; Eligehausen, R.; Hoehler, M. (2006): Seismic design requirements for anchor bolts – a fresh perspective. Proceedings of the 8th National Conference on Earthquake Engineering, San Francisco

Smith, J.; Dowell, R. (2008): Nonstructural component amplification. Final report for Hilti Corporation, not published

Solomos, G.; Berra, M. (2006): Testing of anchorages in concrete under dynamic tensile loading, RILEM Materials and Structures, Vol. 39, No. 7, 2006, 695-706

Taghavi, S.; Miranda, E. (2003): Response assessment of nonstructural building elements. PEER 2003/05, Pacific Earthquake Engineering Research Center, University of California, Berkeley College of Engineering

Tang, J.; Deans, J. (1983): Test criteria and method for seismic qualification of concrete expansion anchors. Proceedings of the 4th Canadian Conference on Earthquake Engineering, 58-69, University of British Columbia, Vancouver

Usami, S.; Abe, U.; Matsuzaki, Y. (1981): Experimental study on the strength of bonded anchors under alternate shear load and combined load. Proceedings of the Annual Meeting of the Kantou Branch of the Architectural Institute of Japan, 1981

Vintzeleou, E.; Eligehausen, R. (1981): Behavior of fasteners under monotonic or cyclic displacements. Anchors in Concrete – Design and Behavior. ACI Special Publication SP 130, 181-204

Watkins, D.; Chui, L.; Hutchinson, T.; Hoehler, M. (2009): Survey and characterization of floor and wall mounted mechanical and electrical equipment in buildings. SSRP-2009/11, UCSD

Watkins, D.; Hutchinson, T. (2011): Seismic performance of nonstructural components anchored in concrete with cyclic cracks. SSRP–2010/07, UCSD

Weigler, H.; Lieberum, K. H. (1984): Belastungsprüfungen an Liebig-Einspannankern ultra-plus M16, verankert in kreuzartig gerissenen Betonprobkörpern bei stoßartiger und statischer Belastung (Load tests on Liebig restraining anchor Ultra-plus M16, anchored in concrete specimens with intersecting cracks under impact and static loads). Report, Institute für Massivbau, TH Darmstadt (in German)

Wesche, K.; Krause, K. (1972): Der Einfluss der Belastungsgeschwindigkeit auf Druckfestigkeit und Elastizitätsmodul von Beton (The influence of the loading rate on the compressive strength and elasticity modulus of concrete). Materialprüfung 14, Nr. 7, 212-218 (in German)

Whittaker, A.; Soong, T. (2003): An overview of nonstructural components research at three U.S. Earthquake Engineering Research Centers. Proceedings of Seminar on Seismic Design Performance; Retrofit of Nonstructural Components in Critical Facilities, 271-280, Newport Beach

Wood, R.; Hutchinson, T.; Hoehler, M. (2010): Cyclic load and crack protocols for anchored nonstructural components and systems. SSRP-2009/12, UCSD

Appendix A: External and Internal Friction Test Data

The following data are extracted from *Mahrenholtz, P. (2011a)*.

Table A.1 External friction

Anchor Type	Anchor Size	Angle of Cone	Concrete Grade	Preset Expansion Load [kN]	Preset Loading Rate [mm/min]	External Friction Coefficient μ [-] Test Number 1	2	3	4	5	$\mu=\frac{N/F_{exp} - \pi \cdot \tan\alpha}{\pi + N/F_{exp} \cdot \tan\alpha}$
EAs1'	M12	13°	C20/25	5.00	2.0	0.30	0.40	-	-	-	
					30,000	0.22	0.33	0.46	-	-	
EAb1'	M12	11°	C20/25	5.00	2.0	0.17	0.36	-	-	-	
					30,000	0.36	0.45	0.28	-	-	
EAb1'	M12	11°	C20/25	15.00	2.0	0.16	0.12	0.12	0.14	0.30	
					30,000	0.12	0.10	0.15	0.21	0.11	
EAb1'	M12	11°	C50/60	15.00	2.0	0.24	0.30	0.12	0.25	0.33	
					30,000	0.26	0.37	0.26	0.16	0.16	

Table A.2 Internal friction

Anchor Type	Dice Diameter	Dice Length	Concrete Grade	Preset Indentation [mm]	Preset Loading Rate [mm/min]	Increase in Compressive Force between 1 and 2 mm [kN] Test Number 1	2	3	4	5	6	Mean
EAs1	18	200	C20/25	1.0	1.0	21.00	19.00	20.20	20.60	21.70	16.00	19.75
					30,000	31.00	29.60	28.50	31.90	30.50	26.30	29.63
											normalised	1.51
EAb1'	6	150	C20/25	1.0	1.0	16.00	16.90	18.30	16.90	19.10	-	17.44
					30,000	25.30	19.10	29.90	27.30	29.30	23.80	25.78
											normalised	1.48

The make of EAb1' (metric size) anchor is similar to that of EAb1 (imperial size) anchor.

Appendix B: Numerical Group Test Data

Table B.1 Results of numerical tests extracted from *Periskic, G. (2009)*

Reduction Factors given as calculated group load divided by four times the capacity of a single anchor loacted in a crack and cycled crack, respectively

Headed Stud = HS
Expansion Anchor = EA

	HS	EA
$F_{u,m,uncracked}$	79.1	48.4
$F_{u,m,cracked}$	52.8	33.1
$F_{u,m,cycled\ crack}$	42.4	25.8
$F_{u,m,cracked}/F_{u,m,}$	0.80	0.78

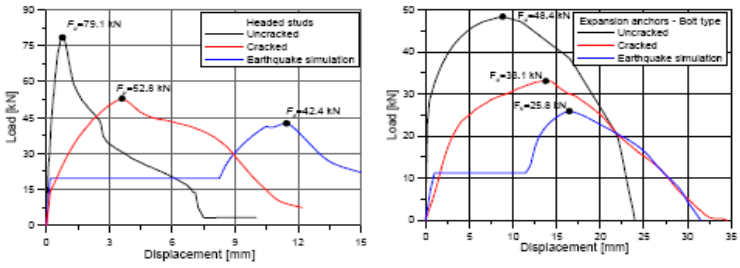

Fig. 8: Employed load-displacement curves for investigated anchors

Basic Investigation: Static; $F_u/F_{u,all\ cracked}$

		HS	EA
Rotation-**unrestrained**	Crack Case **1**	1.24	1.25
	Crack Case **2**	1.02	1.21
	Crack Case **3**	1.04	1.05
	Crack Case **4**	0.97	0.97
Rotation-**restrained**	Crack Case **1**	1.22	1.33
	Crack Case **2**	0.97	1.22
	Crack Case **3**	0.97	1.22
	Crack Case **4**	0.88	1.10

Basic Investigation: Cyclic; $F_u/F_{u,all\ cracked}$

		HS	EA
Rotation-**unrestrained**	Crack Case **1**	0.98	1.15
	Crack Case **2**	0.94	1.00
	Crack Case **3**	0.87	0.84
	Crack Case **4**	0.59	0.69
Rotation-**restrained**	Crack Case **1**	1.22	1.21
	Crack Case **2**	0.93	0.99
	Crack Case **3**	0.93	0.99
	Crack Case **4**	0.65	0.88

Basic Investigation: Cyclic; $F_u/F_{u,all\ seismic\ crack}$

		HS	EA
Rotation-**unrestrained**	Crack Case **1**	1.22	1.48
	Crack Case **2**	1.17	1.28
	Crack Case **3**	1.08	1.08
	Crack Case **4**	0.73	0.88
Rotation-**restrained**	Crack Case **1**	1.52	1.55
	Crack Case **2**	1.16	1.27
	Crack Case **3**	1.16	1.27
	Crack Case **4**	0.81	1.13

Investigation Scatter: Static; $F_u/F_{u,all\ cracked}$

			HS	EA
Rotation-**unrestrained**	Crack Case **3**		1.04	1.05
	K_{ucr}/K_{cr}	+40%	1.06	1.07
		-40%	1.03	1.04
	$N_{u,cr}$	+20%	1.22	1.24
		-20%	0.88	0.84
	Crack Case **4**		0.97	0.97
	K_{ucr}/K_{cr}	+40%	0.94	0.99
		-40%	0.93	0.95
	$N_{u,cr}$	+20%	1.12	1.17
		-20%	0.97	0.79
Rotation-**restrained**	Crack Case **3**		0.97	1.22
	K_{ucr}/K_{cr}	+40%	1.08	1.24
		-40%	0.93	1.24
	$N_{u,cr}$	+20%	1.04	1.31
		-20%	0.93	1.10
	Crack Case **4**		0.88	1.10
	K_{ucr}/K_{cr}	+40%	0.85	1.05
		-40%	0.97	1.13
	$N_{u,cr}$	+20%	1.04	1.25
		-20%	0.73	0.86

Investigation Scatter: Cyclic; $F_u/F_{u,all\ cracked}$

				HS	EA
Rotation-**unrestrained**	Crack Case **3**				
	same	1+1		0.84	0.85
		2+2		0.87	0.87
		3+3		0.89	0.87
		4+4		-	0.84
	different	1+2		0.69	0.80
		1+3		0.77	0.69
		2+3		0.77	0.81
		1+4		-	0.78
		2+4		-	0.68
Rotation-**unrestrained**	Crack Case **4**				
	same	1+1+1		-	0.66
		2+2+2		-	0.62
		3+3+3		-	0.63
		4+4+4		-	0.73
	different	1+1+4		-	0.83
		1+1+3		-	0.59
		3+3+1		-	0.60
		3+3+2		-	0.62
		4+4+1		-	0.83

Investigation Scatter: Cyclic; $F_u/F_{u,all\ seismic\ crack}$

				HS	EA
Rotation-**unrestrained**	Crack Case **3**				
	same	1+1		1.05	1.09
		2+2		1.08	1.11
		3+3		1.11	1.12
		4+4		-	1.08
	different	1+2		0.86	1.02
		1+3		0.96	0.88
		2+3		0.96	1.04
		1+4		-	1.00
		2+4		-	0.87
Rotation-**unrestrained**	Crack Case **4**				
	same	1+1+1		-	0.85
		2+2+2		-	0.80
		3+3+3		-	0.81
		4+4+4		-	0.94
	different	1+1+3		-	1.07
		1+1+4		-	0.76
		3+3+1		-	0.77
		3+3+2		-	0.79
		4+4+1		-	1.06

Expansion anchor

N_{gr} = 19.20 kN

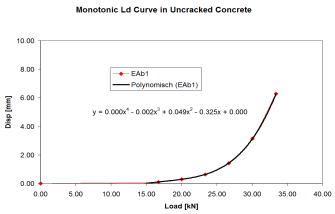

Initial load		Stiffness [kN/mm]	Displacement [mm]	Load [kN]
Anchor 1	k_{uncr}^0 =	120.00	0.14	16.46
Anchor 2	k_{cr}^0 =	20.00	0.14	2.74
				19.20

Cycling		Stiffness [kN/mm]
Anchor 1	k_{uncr} =	f(F_1)
Anchor 2	k_{cr} =	130

Displacement rate per cycle with reference to load	[mm/kN]
$\Delta s_{cr,diff,n}/N$ =	0.115
$\Delta s_{uncr,diff,n}/N$ =	0.01

n	N_{uncr}^0	N_{cr}^0	k_{uncr}	k_{cr}	$\Delta s_{cr,diff,n,i}$	$\Delta N_{gr,n,i}$	$\Delta N_{gr,n,i} \cdot k_{uncr}$	N_{uncr}^n	N_{cr}^n	$\Delta s_{uncr,diff,n}$	$\Delta s_{gr,n}$	$\Sigma \Delta s_{gr,n}$
								0.00	0.00	0.00		0
0	-	-	-	-	0.000	-	-	16.46	2.74			0.14
1	16.46	2.74	20.00	130	0.158	2.73	0.14	19.19	0.01	0.05	0.19	0.33
2	19.19	0.01	16.67	130	0.001	0.01	0.00	19.20	0.00	0.06	0.06	0.39
3	19.20	0.00	16.65	130	0.000	0.00	0.00	19.20	0.00	0.06	0.06	0.46
4	19.20	0.00	16.65	130	0.000	0.00	0.00	19.20	0.00	0.06	0.06	0.52
5	19.20	0.00	16.65	130	0.000	0.00	0.00	19.20	0.00	0.06	0.06	0.59
6	19.20	0.00	16.65	130	0.000	0.00	0.00	19.20	0.00	0.06	0.06	0.65
7	19.20	0.00	16.65	130	0.000	0.00	0.00	19.20	0.00	0.06	0.06	0.71
8	19.20	0.00	16.65	130	0.000	0.00	0.00	19.20	0.00	0.06	0.06	0.78
9	19.20	0.00	16.65	130	0.000	0.00	0.00	19.20	0.00	0.06	0.06	0.84
10	19.20	0.00	16.65	130	0.000	0.00	0.00	19.20	0.00	0.06	0.06	0.91

Figure B.1 Exemplary calculation of load redistribution for expansion anchor

Undercut anchor

N_{gr} = 36.40 kN

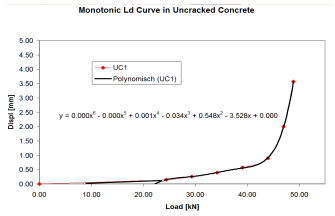

Initial load		Stiffness [kN/mm]	Displacement [mm]	Load [kN]
Anchor 1	k_{uncr}^0 =	80.00	0.28	22.40
Anchor 2	k_{cr}^0 =	50.00	0.28	14.00
				36.40

Cycling		Stiffness [kN/mm]
Anchor 1	k_{uncr} =	f(F_1)
Anchor 2	k_{cr} =	70

Displacement rate per cycle with reference to load	[mm/kN]
$\Delta s_{cr,diff,n}/N$ =	0.027
$\Delta s_{uncr,diff,n}/N$ =	0.003

n	N_{uncr}^0 [kN]	N_{cr}^0 [kN]	k_{uncr} [kN/mm]	k_{cr} [kN/mm]	$\Delta s_{cr,diff,n,i}$ [mm]	$\Delta N_{gr,n,i}$ [kN]	$\Delta N_{gr,n,i} \cdot k_{uncr}$ [mm]	N_{uncr}^n [kN]	N_{cr}^n [kN]	$\Delta s_{uncr,diff,n}$ [mm]	$\Delta s_{gr,n}$	$\Sigma \Delta s_{gr,n}$ [mm]
								0.00	0.00			0.00
0	-	-	-	-	0.000	-	-	22.40	14.00			0.28
1	22.40	14.00	70.00	70	0.189	6.62	0.09	29.02	7.39	0.02	0.12	0.40
2	29.02	7.39	54.39	70	0.100	3.05	0.06	32.07	4.33	0.03	0.09	0.48
3	32.07	4.33	31.59	70	0.059	1.27	0.04	33.34	3.06	0.03	0.07	0.55
4	33.34	3.06	28.39	70	0.041	0.83	0.03	34.17	2.23	0.03	0.06	0.62
5	34.17	2.23	27.76	70	0.030	0.60	0.02	34.77	1.63	0.03	0.06	0.67
6	34.77	1.63	27.93	70	0.022	0.44	0.02	35.21	1.19	0.03	0.05	0.72
7	35.21	1.19	28.37	70	0.016	0.32	0.01	35.53	0.87	0.04	0.05	0.77
8	35.53	0.87	28.86	70	0.012	0.24	0.01	35.77	0.63	0.04	0.04	0.81
9	35.77	0.63	29.32	70	0.008	0.17	0.01	35.95	0.45	0.04	0.04	0.86
10	35.95	0.45	29.69	70	0.006	0.13	0.00	36.08	0.32	0.04	0.04	0.90

Figure B.2 Exemplary calculation of load redistribution for undercut anchor

Appendix C: Experimental Test Data – Component Level

Appendix C.1 High loading rate tests

The following data are extracted from *Mahrenholtz, P. (2007b)*.

Table C.1 Key test results of high loading rate tests (0.8 mm crack)

Anchor Type, Anchor Size, Emb. Depth	Crack Width w	Loading Rate[(1)]	Mean Rise Time to Ultimate Load, sec Ultimate Load N_u, kN Displacement at Ultimate Load $s(N_u)$, mm						
			1	2	3	4	5	Mean	CV
EAb1';	0.8 mm	QS	Pt	Pt	-	-	-		
M12			190	108	-	-	-	149	38.9 %
90 mm			23.18	23.25	-	-	-	23.21	0.2 %
			17.17	10.02	-	-	-	14.1	40.9 %
		LB	Pt	Pt	Pt	-	-		
			0.47	0.61	0.66	-	-	0.58	17.0 %
			24.95	25.65	27.39	-	-	25.99	4.8 %
			13.11	19.65	14.59	-	-	17.20	21.1 %
		UB	Pt	Pt	Pt	-	-		
			0.064	0.054	0.039	-	-	0.052	24.0 %
			18.11	25.81	25.15	-	-	23.02	18.5 %
			12.11	11.60	17.30	-	-	17.99	38.6 %
EAb2;	0.8 mm	QS	Pt	Pt	Pt	Pt	Pt		
M12;			149	111	117	119	99	119	15.5 %
68 mm			12.51	14.10	11.31	11.41	12.53	12.37	9.1 %
			13.83	9.54	10.85	12.48	9.53	11.25	16.8 %
		LB	Pt	Pt	Pt	Pt	Pt		
			0.28	0.26	0.90	0.68	0.76	0.58	49.9 %
			17.94	18.21	14.05	17.63	16.03	16.77	10.4 %
			7.68	5.18	13.98	10.08	11.46	9.68	35.1 %
		UB	Pt	Pt	Pt	Pt	Pt		
			0.026	0.029	0.037	0.025	0.037	0.031	19.0 %
			17.88	17.80	18.60	13.92	19.69	17.58	12.4 %
			6.60	7.36	11.69	5.27	12.26	8.64	36.4 %
EAb3;	0.8 mm	QS	Pt	Po	Pt	Pt	Pt		
M12;			224	190	226	164	105	181	27.5 %
68 mm			21.81	20.71	18.24	19.23	18.63	19.72	7.6 %
			16.80	14.03	17.86	12.91	7.23	13.77	30.3 %
		LB	Pt	Pt	Pt	Pt	Pt		
			0.25	0.44	0.50	0.35	0.58	0.42	30.3 %
			24.87	20.60	18.15	21.40	21.52	21.31	11.3 %
			8.11	12.10	14.94	9.32	17.22	12.34	30.8 %
		UB	Pt	Pt	Pt	Pt	Pt		
			0.041	0.047	0.031	0.049	0.053	0.044	19.4 %
			17.49	21.02	19.33	21.64	19.22	19.74	8.3 %
			14.84	17.27	8.34	16.13	17.71	14.86	25.6 %
EAs1;	0.8 mm	QS	C	C	C	C	C		
M12;			85	91	123	72	70	88	24.2 %
80 mm			34.86	32.95	29.88	31.53	33.11	32.47	5.7 %
			8.33	7.95	11.58	5.93	4.95	7.74	33.0 %
		LB	C	C	C	C	C		
			0.17	0.50	0.97	0.58	0.73	0.59	50.0 %
			40.76	34.25	35.85	37.56	40.46	37.78	7.5 %
			6.86	5.39	9.80	4.86	6.50	6.68	28.8 %
		UB	C	C	C	C	C		
			0.054	0.046	0.049	0.043	0.044	0.047	9.4 %
			44.95	39.94	43.61	39.24	39.63	41.47	6.3 %
			10.83	10.09	9.38	8.69	8.61	9.52	9.9 %

(1) QS = Quasi-static loading rate; LB = Lower bound and UB = Upper bound of earthquake relevant loading rate

The following data are extracted from *Mahrenholtz, P. (2011a)*.

Table C.2 Key test results of high loading rate tests (0.5 mm crack)

Anchor Type, Anchor Size, Emb. Depth	Crack Width w	Loading Rate[1]	Mean Rise Time to Ultimate Load, sec Ultimate Load N_u, kN Displacement at Ultimate Load $s(N_u)$, mm						
			1	2	3	4	5	Mean	CV
EAb1';	0.5 mm	QS	Pt	Pt	Pt	Pt	Pt		
M12;			136	165	128	99	236	153	34.1 %
85 mm			24.08	24.12	23.70	26.45	24.44	24.56	4.4 %
			12.83	16.25	12.29	8.79	15.80	13.19	22.9 %
		LB	Pt	Pt	Pt	Pt	Pt		
			0.44	0.55	0.45	0.56	0.53	0.51	11.0 %
			33.02	28.60	27.36	25.89	30.55	29.08	9.6 %
			12.26	15.81	12.41	16.35	14.63	14.29	13.2 %
		UB	Pt	Pt	Pt	Pt	Pt		
			0.066	0.092	0.055	0.055	0.051	0.064	26.2 %
			32.19	29.76	30.18	25.51	21.13	27.75	16.0 %
			16.32	22.46	15.27	12.17	14.66	26.18	23.7 %

(1) QS = Quasi-static loading rate; LB = Lower bound and UB = Upper bound of earthquake relevant loading rate

Appendix C.2 True and pseudo displacement controlled tests

The following data are extracted from *Mahrenholtz, P. (2011c)*.

Table C.3 Key test results of true and pseudo displacement controlled tests

Anchor Type, Anchor Size, Emb. Depth	Crack Width w	Loading Rate[1]	Failure Mode Ultimate Load N_u, kN Displacement at Ultimate Load $s(N_u)$, mm Ultimate Displacement s_u at 0.85 N_u post-peak, mm						
			1	2	3	4	5	Mean	CV
SA2;	0.0 mm	True	Po/C	Po/C	Po/C	Po/C	Po/C		
∅12;			34.00	39.29	35.76	34.56	33.53	35.43	6.5 %
75 mm			0.67	0.98	0.70	0.63	0.64	0.72	20.2 %
			1.44	1.34	1.06	1.06	1.18	1.22	13.9 %
		Pseudo	Po/C	Po/C	Po/C	Po/C	Po/C		
			38.67	35.46	39.15	37.18	37.91	37.67	3.8 %
			1.03	1.32	1.13	1.17	0.97	1.12	11.9 %
			1.39	2.39	2.00	1.51	1.74	1.81	22.2 %
EAb5;	0.0 mm	True	Pt	Pt	Pt	Pt	Pt		
M16;			49.53	46.91	47.59	47.18	49.86	48.21	2.9 %
100 mm			11.39	10.88	11.39	11.53	13.72	11.78	9.5 %
			18.45	19.10	16.63	19.39	19.60	18.63	6.4 %
		Pseudo	Pt	Pt	Pt	Pt	Pt		
			42.30	51.91	47.54	49.62	49.43	48.16	7.5 %
			9.76	10.77	13.16	13.39	11.80	11.78	13.2 %
			21.40	15.66	19.39	19.66	17.18	18.66	12.1 %
BA4;	0.0 mm	True	S	S	S	S	-		
M12			75.42	75.61	73.15	75.70	-	74.97	1.6 %
threaded rod;			4.12	3.69	3.58	3.86	-	3.81	0.0 %
85 mm			7.06	6.85	6.52	7.03	-	6.87	0.0 %
		Pseudo	S	S	S	S	-		
			81.90	74.62	76.54	77.44	-	77.63	4.0 %
			3.35	3.91	2.81	3.43	-	3.38	13.2 %
			5.82	6.56	5.29	6.28	-	5.99	9.3 %

(1) True = True displacement controlled tests; Pseudo = Pseudo displacement controlled tests

Appendix C.3 Group tests

The following data are extracted from *Mahrenholtz, P. (2010b)*.

Table C.4 Key test results of reference tests

Anchor Type; Anchor Size; Emb. Depth; Perm. Load	Crack Width	Crack Type	Failure Mode Ultimate Load N_u, kN Displacement at 50% Mean Ultimate Load $s(0.5N_{u,m})$, mm Displacement at Ultimate Load $s(N_u)$, mm Displacement after Cycling s_{cyc}, mm					
			1	2	3	4	Mean	CV
UC1;	w = 0.0 mm	Uncracked	S	-	-	-		
M10;			48.89	-	-	-	48.89	-
90 mm			0.20	-	-	-	0.20	-
			3.52	-	-	-	3.52	-
	w = 0.8 mm	Cracked	S	S	S	-		
			42.72	49.31	44.46	-	45.50	7.5 %
			1.98	1.30	2.28	-	1.85	27.1 %
			6.25	6.27	5.65	-	6.06	5.8 %
N_w = 18.2 kN	w_1 = 0.8 mm	Cycled	S	S	S	-		
	w_2 = 0.0 mm	Cracked	48.41	48.18	48.83	-	48.48	0.7 %
			0.99	1.01	1.23	-	1.08	12.4 %
			6.17	7.11	6.88	-	6.72	7.3 %
			5.48	6.34	6.10	-	5.97	7.4 %
UC1;	w = 0.0 mm	Uncracked	C	C	C	-		
M10;			48.91	46.51	39.27	-	44.90	11.2 %
60 mm			0.84	0.82	0.69	-	0.75	10.4 %
			4.82	3.76	1.50		3.36	50.5 %
	w = 0.8 mm	Cracked	C	C	C	-		
			32.19	34.52	33.0	-	33.24	3.6 %
			1.07	1.47	0.89	-	1.14	26.0 %
			4.65	3.69	3.89	-	4.08	12.4 %
N_w = 13.3 kN	w_1 = 0.8 mm	Cycled	C	C	C	-		
	w_2 = 0.0 mm	Cracked	31.51	36.94	23.74	-	30.73 %	21.6 %
			0.51	0.99	0.49	-	0.66	42.7 %
			1.67	1.01	0.68	-	1.12	45.0 %
			5.39	2.96	4.32	-	4.22	28.8 %
SA1;	w = 0.0 mm	Uncracked	Po/C	Po/C	-	-		
∅16;			40.75	45.81	-	-	43.28	8.3 %
105 mm			0.16	0.24	-	-	0.20	28.0 %
			1.00	1.01	-	-	1.01	0.7 %
	w = 0.8 mm	Cracked	Po/C	Po/C	Po/C	-		
			22.46	15.43	18.69	-	18.86	18.7 %
			0.77	0.50	0.69	-	0.66	21.1 %
			3.61	4.21	2.99	-	3.60	16.9 %
N_w = 7.6 kN	w_1 = 0.8 mm	Cycled	Po/C	Po/C	Po/C	-		
	w_2 = 0.0 mm	Cracked	-	-	12.67	-	12.67	-
			-	-	0.40	-	0.40	-
			-	-	0.80	-	0.80	-
			6.01(1)	5.99(1)	3.29	-	5.10	30.7 %
EAb1';	w = 0.0 mm	Uncracked	C	C	C	C		
M12;			33.32	31.33	35.28	33.58	33.38	4.8 %
70 mm			0.08	0.08	0.06	0.10	0.08	21.1 %
			7.86	5.55	5.47	6.46	6.34	17.5 %
	w = 0.8 mm	Cracked	Pt	Pt	Pt	Pt		
			26.66	18.48	27.35	23.15	23.91	17.0 %
			1.38	3.82	1.88	2.23	2.33	45.1 %
			10.03	11.27	9.30	7.77	9.59	15.2 %
N_w = 9.6 kN	w_1 = 0.8 mm	Cycled	Po/C	Po/C	Po/C	Po/C		
	w_2 = 0.0 mm	Cracked	11.89	14.25	10.65	6.47	10.82	30.1 %
			1.52	0.81	1.04	1.93	1.33	37.7 %
			3.52	1.91	1.78	4.19	2.85	41.9 %
			25.00	21.87	19.37	25.01	22.81	12.0 %

(1) Anchor failed during last cycle, displacement after cycling taken as displacement at the moment of failure

Table C.5 Key test results of group tests

Anchor Type, Anchor Size; Emb. Depth; Configuration; Perm. Load	Anchor in Uncr. Conc.: Nos; Failure Mode; Crack Width	Anchor in Crack: Nos; Failure Mode; Crack Width	Ultimate Load $N_{u,group}$, kN Ultimate Load $N_{u,group,i}$, kN (Anchor in Uncracked Concrete) Ultimate Load $N_{u,group,i}$, kN (Anchor in Crack) Displacement after Cycling $s_{cyc,group}$, mm Displacement after Cycling $s_{cyc,group,i}$, mm (Anchor in Uncracked Concrete) Displacement after Cycling $s_{cyc,group,i}$, mm (Anchor in Crack)					
			1	2	3	4	Mean	CV
UC1;	1	1	95.57	89.82	89.53	-	91.64	3.7 %
M10;	S	-	47.89	47.93	48.53	-		
90 mm;	w = 0.0 mm	w_1 = 0.8 mm	47.68	41.88	41.00	-		
2 RR[(1)];		w_2 = 0.0 mm	0.90	0.95	0.78	-	0.88	10.0 %
N_w = 36.4 kN			0.90	0.95	0.78	-		
			0.89	0.95	0.78	-		
UC1;	1	1	54.47	60.00	61.15	-	58.54	6.1 %
M10;	C	-	41.06	43.18	39.72	-		
60 mm;	w = 0.0 mm	w_1 = 0.8 mm	13.40	16.82	21.44	-		
2 RR[(1)];		w_2 = 0.0 mm	1.20	1.07	1.29	-	1.19	9.3 %
N_w = 26.2 kN			1.20	1.07	1.29	-		
			1.20	1.07	1.29	-		
SA1;	1	1	60.27	57.81	67.62	-	61.9	8.2 %
∅16;	Po/C	-	50.00	41.21	48.77	-		
105 mm;	w = 0.0 mm	w_1 = 0.8 mm	10.26	16.60	18.85	-		
2 RR[(1)];		w_2 = 0.0 mm	0.07	0.01	0.14	-	0.07	88.7 %
N_w = 15.2 kN			0.07	0.01	0.14	-		
			0.07	0.01	0.14	-		
EAb1';	1	1	50.71	51.88	52.72	-	51.77	1.9 %
M12;	Pt	-	32.89	33.69	30.62	-		
70 mm;	w = 0.0 mm	w_1 = 0.8 mm	17.83	18.19	22.01	-		
2 RR[(1)];		w_2 = 0.0 mm	0.83	1.02	0.97	-	0.94	10.5 %
N_w = 19.2 kN			0.83	1.02	0.97	-		
			0.83	1.02	0.97	-		
EAb1';	1	1	44.28	52.59	45.84	40.33	45.76	11.2 %
M12;	-	Pt	23.62	27.14	26.12	23.23		
70 mm;	w = 0.0 mm	w_1 = 0.8 mm	19.31	24.61	19.61	17.80		
2; RU[(1)];		w_2 = 0.0 mm	5.34	5.00	7.08	6.75	6.04	10.5 %
N_w = 19.2 kN			0.19	2.59	0.03	0.14		
			10.48	11.32	14.13	13.35		
EAb1';	2	2	78.63	78.31	78.28	76.32	77.9	1.4 %
M12;	-	Pt	20.65	19.66	23.02	23.82		
70 mm;	w = 0.0 mm	w_1 = 0.8 mm	21.94	22.21	22.23	19.94		
4 RU[(1)];		w_2 = 0.0 mm	16.39	18.95	16.75	14.88		
N_w = 38.4 kN			19.25	17.07	17.49	17.58		
			5.00	6.22	4.65	4.59	5.12	11.3 %
			0.01	0.11	0.73	0.21		
			0.42	0.22	0.76	0.18		
			9.35	16.69	8.78	9.60		
			10.22	7.86	8.34	9.85		

(1) Nos of anchors and base plate configuration: RR = Rotational-restrained; RU = Rotational-unrestrained

Appendix C.4 Load cycling tests

The following data and figures are extracted from *Mahrenholtz, P. (2009)*.

Table C.6 Key test results of tension load cycling tests – Mechanical anchors

Anchor Type; Anchor Size; Emb. Depth	Crack Width w	Load Type[(1)]	Failure Mode Ultimate Load N_u, kN Displacement at 50% Mean Ultimate Load $s(0.5N_{u,m})$, mm Displacement at Ultimate Load $s(N_u)$, mm				
			1	2	3	Mean	CV
UC1;	0.5 mm	monotonic	C	C	C		
M10;			37.9	44.3	36.0	39.4	11.0 %
90 mm			0.37	0.10	0.67	0.38	74.6 %
			1.78	3.09	6.83	3.90	67.2 %
		cyclic	C	C	C		
			42.9	43.6	46.9	44.5	4.8 %
			0.84	0.86	0.87	0.86	1.4 %
			3.95	2.76	7.63	4.78	53.1 %
	0.8 mm	monotonic	C	C	C		
			36.4	33.0	33.1	34.2	5.7 %
			0.19	0.25	0.32	0.25	25.9 %
			1.85	1.47	1.60	1.64	11.8%
		cyclic	C	C	C		
			42.4	28.6	39.0	36.7	19.6 %
			0.25	1.15	1.56	0.99	67.5 %
			2.71	2.92	6.14	3.92	49.0 %
EAs1;	0.5 mm	monotonic	C	C	C		
M12;			37.0	45.6	34.2	38.9	15.3 %
80 mm			0.25	0.90	0.69	0.61	54.0 %
			5.67	10.99	2.95	6.54	62.6 %
		cyclic	C	C	C		
			38.4	37.7	35.6	37.2	3.9 %
			0.88	0.93	0.67	0.83	16.6 %
			6.51	3.16	2.81	4.16	49.1 %
EAs2;	0.5 mm	monotonic	C	C	C		
5/6";			21.4	24.3	24.5	23.4	7.4 %
85 mm			2.58	1.21	0.41	1.40	78.5 %
			8.26	8.67	7.93	8.29	4.5 %
		cyclic	C	C	C		
			27.0	25.7	26.4	26.4	2.5 %
			1.16	1.06	0.86	1.03	14.5 %
			4.74	8.99	4.70	6.14	40.1 %
EAb1;	0.5 mm	monotonic	Pt	Pt	Pt		
1/2";			25.0	23.7	27.0	25.2	6.6 %
83 mm			2.40	2.51	1.19	2.03	35.8 %
			7.30	9.13	7.38	7.94	13.0 %
		cyclic	Pt	Pt	Pt		
			25.6	26.3	22.0	24.6	9.4 %
			1.36	0.93	2.42	1.57	48.9 %
			12.33	7.55	9.23	9.70	25.0 %
	0.8 mm	monotonic	Pt	Pt	Pt		
			20.9	20.8	23.6	21.8	7.3 %
			3.91	3.97	2.87	3.58	17.2 %
			9.87	11.00	12.08	10.98	10.1 %
		cyclic	Pt	Pt	Pt		
			23.7	22.8	24.0	23.5	2.7 %
			4.08	3.87	1.83	3.26	38.0 %
			14.16	14.06	12.35	13.52	7.5 %

Table C.7 Key test results of tension load cycling tests – Adhesive anchors

Anchor Type; Anchor Size; Emb. Depth	Crack Width w	Load Type[1]	Failure Mode Ultimate Load N_u, kN Displacement at 50% Mean Ultimate Load $s(0.5N_{u,m})$, mm Displacement at Ultimate Load $s(N_u)$, mm				
			1	2	3	Mean	CV
BA1;	0.5 mm	monotonic	P	P	P		
M12			72.6	85.1	77.0	78.2	8.1 %
threaded rod			0.24	0.29	0.52	0.35	41.7 %
96 mm			0.87	1.17	1.58	1.21	29.5 %
		cyclic	P	P	P		
			81.6	72.6	75.0	76.4	6.1 %
			0.39	0.43	-[!]	0.41	6.9 %
			1.52	1.21	-[!]	1.37	16.1 %
	0.8 mm	monotonic	P	P	P		
			64.9	55.3	67.6	62.6	10.3 %
			0.18	0.70	0.47	0.45	58.3 %
			1.60	2.56	1.44	1.87	32.5 %
		cyclic	P	P	P		
			77.1	68.6	56.5	67.4	15.4 %
			0.40	0.53	0.49	0.47	14.0 %
			1.42	1.41	2.31	1.71	30.2 %
BA2;	0.5 mm	monotonic	P	P	P		
M12			48.5	35.7	48.3	44.2	16.6 %
threaded rod			0.31	0.35	0.28	0.31	11.4 %
96 mm			0.85	0.64	1.00	0.83	21.8 %
		cyclic	P	P	P		
			45.6	46.0	46.9	46.2	1.4 %
			0.17	0.30	0.22	0.23	29.3 %
			0.44	0.89	0.51	0.61	39.5 %

(1) Anchor displacement not correctly recorded

Table C.8 Key test results of shear load cycling tests– Mechanical anchors

Anchor Type; Anchor Size; Emb. Depth	Crack Width w	Load Type	Failure Mode Ultimate Load V_u, kN Displacement at 50% Mean Ultimate Load $s(0.5V_{u,m})$, mm Displacement at Ultimate Load $s(V_u)$, mm				
			1	2	3	Mean	CV
UC1;	0.8 mm	monotonic	S	S	S		
M10;			85.3	88.7	93.6	89.2	4.7 %
90 mm			5.41	5.19	6.60	5.73	13.3 %
			22.25	34.34	36.95	31.18	25.2 %
		cyclic	S	S	S		
			61.1	59.4	49.6	56.7	10.9 %
			6.09	5.40	5.15	5.55	8.8 %
			19.66	21.73	17.74	19.71	10.1 %
SA1;	0.8 mm	monotonic	S	S	S		
M10;			63.8	58.6	56.6	59.7	6.2 %
90 mm			4.19	4.06	4.62	4.29	6.8 %
			13.03	15.10	14.94	14.36	8.0 %
		cyclic	S	S	S		
			57.4	58.8	64.1	50.1	5.9 %
			5.21	4.70	3.90	4.60	14.4 %
			11.67	12.39	12.13	12.06	3.0 %
EAs1;	0.8 mm	monotonic	S	S	S		
M12;			73.5	65.5	65.2	68.1	6.9 %
80 mm			4.95	3.14	5.48	4.52	27.1 %
			19.52	20.01	23.852	21.12	11.1 %
		cyclic	S	S	S		
			42.3	55.4	49.4	49.0	13.4 %
			7.27	5.47	4.61	5.78	23.4 %
			14.75	15.52	11.23	13.83	16.5 %
EAb1;	0.8 mm	monotonic	S	S	S		
1/2";			33.0	33.5	30.7	32.4	4.6 %
83 mm			5.14	4.58	5.34	5.02	7.9 %
			11.67	9.87	12.09	11.21	10.5 %
		cyclic	S	S	S		
			27.3	26.6	26.1	26.7	2.3 %
			9.19	10.38	8.45	9.34	10.4 %
			11.71	13.15	12.25	12.37	5.9 %

Table C.9 Key test results of shear load cycling tests– Adhesive anchors

Anchor Type; Anchor Size; Emb. Depth	Crack Width w	Load Type	Failure Mode Ultimate Load V_u, kN Displacement at 50% Mean Ultimate Load s($0.5V_{u,m}$), mm Displacement at Ultimate Load s(V_u), mm				
			1	2	3	Mean	CV
BA1;	0.8 mm	monotonic	S	S	S		
M12			32.2	35.6	32.4	33.4	5.7 %
threaded rod			1.65	5.69	2.82	3.39	61.4 %
96 mm			7.79	12.21	10.94	10.31	22.1 %
		cyclic	S	S	S		
			33.1	34.9	33.4	33.8	2.9 %
			3.59	1.75	2.65	2.66	34.7 %
			12.08	8.75	8.23	9.69	21.6 %

Appendix C.5 Crack cycling tests

The following data and figures are extracted from *Mahrenholtz, C. (2009)*.

Table C.10 Key test results of crack cycling tests – Mechanical anchors – Part 1

Anchor Type; Anchor Size; Emb. Depth; Perm. Load	Crack Width w	Load Type[(1)]	Failure Mode Ultimate Load N_u, kN Displacement at 50% Mean Ultimate Load s($0.5N_{u,m}$), mm Displacement at Ultimate Load s(N_u), mm				
			1	2	3	Mean	CV
UC1;	0.8 mm	monotonic	C	C	C		
M10;			36.4	33.0	33.1	34.2	5.7 %
90 mm;			0.19	0.25	0.32	0.25	25.9 %
			1.85	1.47	1.60	1.64	11.8%
N_w = 13.7 kN		cyclic	C	C	C		
			44.2	45.1	38.4	42.6	8.5 %
			2.72	2.00	2.35	2.36	15.2 %
			7.47	5.24	6.34	6.35	17.6 %
SA1;	0.5 mm	monotonic	Po/C	Po/C	Po/C		
M10;			33.6	36.1	33.1	34.3	4.7 %
90 mm;			0.41	0.87	0.83	0.70	36.0 %
			1.61	3.41	3.06	2.69	35.4 %
N_w = 14.4 kN		cyclic	Po/C	Po/C	Po/C		
			18.8	19.4	20.4	19.5	4.1 %
			3.78	3.10	2.59	3.16	18.9 %
			4.42	3.95	3.65	4.01	9.7 %
	0.8 mm	monotonic	Po/C	Po/C	Po/C		
			12.2	21.0	24.5	19.2	33.0 %
			1.27	0.43	0.35	0.68	74.9 %
			2.75	3.27	3.20	3.07	9.2 %
N_w = 7.7 kN		cyclic	Po/C	Po/C	Po/C		
			21.8	13.9	15.3	17.0	24.8 %
			1.33	3.18	0.91	1.80	66.9 %
			3.69	4.01	3.19	3.63	11.4 %

Table C.11 Key test results of crack cycling tests – Mechanical anchors – Part 2

Anchor Type; Anchor Size; Emb. Depth; Perm. Load	Crack Width w	Load Type[1]	Failure Mode Ultimate Load N_u, kN Displacement at 50% Mean Ultimate Load $s(0.5N_{u,m})$, mm Displacement at Ultimate Load $s(N_u)$, mm				
			1	2	3	Mean	CV
EAs1;	0.5 mm	monotonic	C	C	C		
M12;			37.0	45.6	34.2	38.9	15.3 %
80 mm;			0.25	0.90	0.69	0.61	54.0 %
			5.67	10.99	2.95	6.54	62.6 %
N_w = 15.6 kN		cyclic	C	C	C		
			39.8	39.4	34.5	37.9	7.8 %
			3.77	3.45	5.34	4.19	24.1 %
			8.40	8.48	12.41	9.76	23.5 %
	0.8 mm	monotonic	C	C	C		
			29.9	26.7	26.0	27.5	7.6 %
			0.97	1.24	1.32	1.18	15.6 %
			10.39	4.73	3.23	6.12	61.7 %
N_w = 11.0 kN		cyclic	C	C	C		
			27.8	32.6	29.3	29.9	8.2 %
			13.21	10.46	10.54	11.40	13.7 %
			17.18	17.51	14.15	16.28	11.4 %
EAb1;	0.5 mm	monotonic	Pt	Pt	Pt		
1/2";			25.0	23.7	27.0	25.2	6.6 %
83 mm;			2.40	2.51	1.19	2.03	35.8 %
			7.30	9.13	7.38	7.94	13.0 %
N_w = 10.1 kN		cyclic	Pt	Pt	Pt		
			17.6	24.9	28.8	23.8	23.9%
			9.69	7.56	8.25	8.50	12.8 %
			13.55	18.58	14.57	15.57	17.1 %
	0.8 mm	monotonic	Pt	Pt	Pt		
			20.9	20.8	23.6	21.8	7.3 %
			3.91	3.97	2.87	3.58	17.2 %
			9.87	11.00	12.08	10.98	10.1 %
N_w = 8.7 kN		cyclic	Pt	Pt	Pt		
			18.9	17.5	19.2	18.5	4.9 %
			12.98	9.29	13.37	11.88	19.0 %
			18.83	16.06	26.04	20.31	25.4 %
EAb4;	0.8 mm	monotonic	Pt	Pt	Pt		
1/2";			15.7	16.66	16.50	16.3	3.2 %
86 mm;			1.38	2.99	2.64	2.34	36.2 %
			10.75	8.81	12.26	10.61	16.3 %
N_w = 6.7 kN		cyclic	Pt	Pt	Pt		
			13.1	16.0	11.8	13.6	15.8 %
			7.08	8.37	16.33	10.59	47.3 %
			13.22	16.06	21.81	17.03	25.7 %

Table C.12 Key test results of crack cycling tests – Adhesive anchors – Part 1

Anchor Type; Anchor Size; Emb. Depth; Perm. Load	Crack Width w	Load Type[1]	Failure Mode Ultimate Load N_u, kN Displacement at 50% Mean Ultimate Load $s(0.5N_{u,m})$, mm Displacement at Ultimate Load $s(N_u)$, mm				
			1	2	3	Mean	CV
BA1;	0.5 mm	monotonic	P	P	P		
M12			72.6	85.1	77.0	78.2	8.1 %
threaded rod			0.24	0.29	0.52	0.35	41.7 %
96 mm;			0.87	1.17	1.58	1.21	29.5 %
N_w = 31.3 kN		cyclic	P	P	P		
			31.9	-[1]	38.1	35.0	12.5 %
			1.37	-[1]	1.95	1.66	24.7 %
			3.16	-[1]	2.89	3.00	6.3 %
	0.8 mm	monotonic	P	P	P		
			64.9	55.3	67.6	62.6	10.3 %
			0.18	0.70	0.47	0.45	58.3 %
			1.60	2.56	1.44	1.87	32.5 %
N_w = 25.0 kN		cyclic	P	P	P		
			-[1]	18.5	-[1]	18.5	-
			-[1]	3.5	-[1]	3.5	-
			-[1]	5.3	-[1]	5.3	-

(1) Anchor did not complete crack cycles

Table C.13 Key test results of crack cycling tests – Adhesive anchors – Part 2

Anchor Type; Anchor Size; Emb. Depth; Perm. Load	Crack Width w	Load Type[1]	Failure Mode Ultimate Load N_u, kN Displacement at 50% Mean Ultimate Load $s(0.5N_{u,m})$, mm Displacement at Ultimate Load $s(N_u)$, mm				
			1	2	3	Mean	CV
BA2; M12 threaded rod 96 mm; N_w = 17.5 kN	0.8 mm	monotonic	P	P	P		
			46.4	42.9	34.9	41.4	14.2 %
			0.23	0.14	0.13	0.17	32.1 %
			0.79	0.89	1.24	0.97	24.3 %
		cyclic	P	P	P		
			39.9	25.9	17.7	27.8	32.6 %
			0.96	2.04	2.10	1.70	37.7 %
			3.06	2.89	2.81	2.98	5.5 %
BA3; M12 threaded rod 96 mm; N_w = 12.4 kN	0.8 mm	monotonic	P	P	P		
			32.1	28.0	28.1	29.4	8.0 %
			0.16	0.36	0.17	0.23	50.3 %
			1.20	1.26	0.96	1.14	13.9 %
		cyclic	P	P	P		
			19.2	19.3	14.8	17.8	14.5 %
			0.21	1.16	1.15	0.84	65.0 %
			0.96	1.90	2.70	1.85	47.0 %

Appendix C.6 Simultaneous load and crack cycling tests

The following data and figures are extracted from *Mahrenholtz, P.; Mahrenholtz, C. (2010)*.

Table C.14 Key test results of simultaneous load and crack cycling tests

Test Series	Crack Width Time History	Anchor Load Time History	Displacement after Cycling s_{cyc}, mm				
			1	2	3	Mean	CV
HB constant	10 cycles; w_{max} = 0.8 mm	Constant; N_{max} = 27.8 kN	3.00	4.89	3.38	3.76	26.6 %
HB in-phase	10 cycles; w_{max} = 0.8 mm	10 cycles; N_{max} = 27.8 kN	3.10	2.94	2.87	2.97	4.0 %
HB out-of-phase	10 cycles; w_{max} = 0.8 mm	10 cycles; N_{max} = 27.8 kN	1.46	1.51	-	1.49	2.4 %
HB different frequencies	10 cycles; w_{max} = 0.8 mm	2.5 cycles; N_{max} = 27.8 kN	2.17	-	-	2.17	-

Appendix D: Experimental Test Data – Seismic Qualification

Appendix D.1 Verification tests with separate and unified protocols

The following data and figures are extracted from *Mahrenholtz, P. (2010d)*.

Table D.1 Key test results of verification tests (load cycling)

Anchor Type; Anchor Size; Emb. Depth	Prot. Type[1]	Num. of Cycles	Crack Width w	Target Load V_{max}	Failure Mode Ultimate Load V_u, kN Displacement after Cycling s_{cyc}, mm, Serviceability Level Displacement after Cycling s_{cyc}, mm, Suitability Level						
					1	2	3	4	5	Mean	CV
UC1; M10; 90 mm;	P50	118			S	S	S	S	S		
			0.8 mm		93.5	97.3	79.4	86.9	102.3	91.9	9.8 %
		118	0.8 mm	24.3 kN	4.56	4.85	4.98	5.08	5.02	4.90	4.2 %
					-	-	-	-	-	-	-
	P90	212			S						
			0.8 mm		Failure in cycle 201						
		212	0.8 mm	75.8 kN	(90% level)						
	P90, 1st reduction	212			S						
			0.8 mm		Failure in Cycle 204						
		212	0.8 mm	60.7 kN	(90% level)						
	P90, 2nd reduction	212			S	S	S	S	S		
			0.8 mm		100.4	82.5	80.9	95.7	105.6	93.0	11.7 %
					-	-	-	-	-	-	-
		212	0.8 mm	48.6 kN	8.09	9.99	(14.9)[2]	10.76	10.93	9.95	13.3 %
	Uni	75			S	S	S	S	S		
			0.8 mm		87.1	111.3	102.5	90.4	65.6	91.4	18.9 %
		50	0.8 mm	24.3 kN	4.62	5.42	4.94	5.40	5.13	5.10	6.6 %
		25	0.8 mm	48.6 kN	9.75	10.85	9.11	13.49	18.48	12.34	30.9 %
	SUni	45			S	S	S	S	S		
			0.8 mm		85.8	87.6	95.7	80.9	92.2	88.4	6.5 %
		20	0.8 mm	24.3 kN	4.35	3.80	5.01	5.80	6.68	5.13	22.3 %
		25	0.8 mm	48.6 kN	11.93	13.85	13.25	14.24	13.76	13.41	6.7 %
EAb1; 1/2"; 83 mm	Uni, 1st reduction	75			S						
			0.8 mm		Failure in						
		50	0.8 mm	13.8 kN	Cycle 69						
		25	0.8 mm	27.5 kN	(90% level)						
	Uni, 2nd reduction	75			S	S					
			0.8 mm		27.1	Failure in					
		50	0.8 mm	11.0 kN	3.68	Cycle 70					
		25	0.8 mm	22.0 kN	10.65	(100% level)					
	Uni	75			S	S	S	S	S		
			0.8 mm		30.2	31.0	31.5	28.3	32.0	30.6	4.7 %
		50	0.8 mm	9.9 kN	3.40	3.89	3.21	4.02	3.76	3.66	9.3 %
		25	0.8 mm	19.8 kN	6.00	6.11	5.81	7.39	6.22	6.31	9.9 %
	SUni	45			S	S	S	S	S		
			0.8 mm		33.3	(24.3)[3]	32.1	30.3	32.2	32.0	3.9 %
		20	0.8 mm	9.9 kN	4.28	(5.2)[3]	3.17	3.89	4.14	3.87	12.8 %
		25	0.8 mm	19.8 kN	7.05	(11.4)[3]	6.39	7.13	6.71	6.32	20.6 %

(1) Protocol Type: Uni = Unified Protocol; SUni = Simple Unified Protocol
(2) Servo control error during cycling caused load overshooting and increased displacement
(3) Outlier

Table D.2 Key test results of verification tests (crack cycling)

Anchor Type; Anchor Size; Emb. Depth	Prot. Type[1]	Num. of Cycles	Perm. Load N_w	Crack Width w_{max}	Failure Mode Ultimate Load N_u, kN Displacement after Cycling s_{cyc}, mm, Serviceability Level Displacement after Cycling s_{cyc}, mm, Suitability Level						
					1	2	3	4	5	Mean	CV
HB1;	P50	40			C	C	C	C	-		
M20;				0.5 mm	75.6	73.3	71.2	67.1	-	71.8	5.0 %
100 mm;		40	28.6 kN	0.5 mm	3.02	2.94	2.37	2.64	-	2.74	10.8 %
					-	-	-	-	-	-	-
	P90	66			C	C	C	C	-		
				0.8 mm	69.0	52.9	53.0	64.7	-	59.9	13.7 %
					-	-	-	-	-	-	-
		66	35.7 kN	0.8 mm	6.09	5.51	5.65	6.35	-	5.90	6.6 %
	Uni	59			C	C	C	C	-		
				0.8 mm	71.4	71.9	58.8	49.1	-	62.8	17.4 %
		45	28.6 kN	0.5 mm	2.60	2.97	3.09	2.81	-	2.87	7.4 %
		14	35.7 kN	0.8 mm	6.34	6.98	7.67	6.47	-	6.87	8.8 %
	SUni	59			C	C	C	C	-		
				0.8 mm	68.1	45.4	45.0	57.5	-	54.0	20.5 %
		45	28.6 kN	0.5 mm	2.65	2.20	3.84	3.00	-	2.92	23.7 %
		14	35.7 kN	0.8 mm	6.55	5.03	7.89	6.43	-	6.48	18.1 %
EAb1;	Uni, 1st	59			Pt						
1/2";	reduction				Failure in						
83 mm		45	9.7 kN	0.5 mm	Cycle 57						
		14	12.1 kN	0.8 mm	(100% level)						
	Uni	59			Pt	Pt	Pt	Pt	Pt		
				0.8 mm	28.0	19.7	18.0	31.5	(11.1)[2]	24.3	26.7 %
		45	8.5 kN	0.5 mm	8.06	9.76	8.78	7.90	8.08	8.52	9.1 %
		14	10.6 kN	0.8 mm	22.84	28.33	25.44	16.11	(-)[2]	23.18	22.5 %
	SUni	39			Pt	Pt	Pt	Pt	Pt		
				0.8 mm	15.9	17.4	(-)[3]	20.7	14.0	17.0	16.7 %
		25	8.5 kN	0.5 mm	9.78	11.12	9.01	8.29	5.99	8.84	21.6 %
		14	10.6 kN	0.8 mm	24.96	30.63	(-)[3]	22.97	27.33	26.47	12.4 %

(1) Protocol Type: Uni = Unified Protocol; SUni = Simple Unified Protocol
(2) Failure during last cycle
(3) Servo control system got out of control when increasing load to N_{w2}

Appendix E: Experimental Test Data – System Level

Appendix E.1 Shake table tests

The following data and figures are extracted from *Mahrenholtz, P.; Hutchinson, T.; Eligehausen, R. (2012)*.

Table E.1 Key test results of Correlation Tests

Anchor Type; Anchor Size; Crack Width	NCS Type	Floor Motion	Scale Factor, %	Accumulated Anchor Displacement during Shaking, mm				Maximum Anchor Load during Shaking, kN			
				1 (SW)	2 (NW)	3 (SE)	4 (NE)	1 (SW)	2 (NW)	3 (SE)	4 (NE)
UC1; M10; 0.8 mm	Heavy	FM02	20	0.57	0.36	0.58	0.42	14.0	14.8	11.9	9.7
		FM03	21	0.51	0.55	0.32	0.66	12.4	12.5	11.7	8.5
		FM05	42	0.97	0.38	1.23	0.43	8.2	10.3	7.6	9.0
		FM08	26	1.08	0.26	1.43	0.18	12.6	19.8	12.7	14.8
		FM12	50	0.41	0.49	0.67	0.49	10.6	12.5	7.6	10.8
		FM13	29	0.18	0.48	0.65	0.39	10.6	8.2	6.7	6.6
		FM14	28	0.37	0.45	0.33	0.49	11.0	12.0	9.1	9.8
		FM16	39	0.40	1.00	0.71	0.23	9.0	14.0	8.2	10.0
		FM18	23	0.28	0.43	1.03	0.53	11.7	7.7	8.1	7.2
		FM19	30	0.36	0.04	0.49	0.52	11.4	8.3	9.7	6.7
		FM20	58	0.44	0.37	0.51	0.52	11.3	14.5	7.7	12.5
	Light	FM02	50	2.00	1.61	4.07	1.63	7.7	10.5	12.2	10.4
		FM03	58	0.58	-(1)	-(1)	0.37	13.0	11.0	9.9	8.6
		FM05	86	0.64	0.56	-(1)	0.64	11.9	13.4	7.3	6.8
		FM08	87	0.44	0.58	0.82	0.47	12.7	13.3	7.8	6.8
		FM12	100	0.36	0.25	0.44	0.27	6.2	5.8	5.4	5.1
		FM13	160	0.29	0.67	1.53	0.63	15.6	19.7	11.3	12.2
		FM14	130	0.30	-(1)	0.20	0.46	11.6	15.9	8.3	11.9
		FM16	100	0.33	0.29	0.31	0.21	6.5	6.3	5.0	5.3
		FM18	127	0.30	0.29	0.37	0.14	9.8	6.9	6.8	5.8
		FM19	126	0.40	0.28	0.50	0.40	11.6	8.1	7.6	6.8
		FM20	100	0.65	0.20	0.31	0.41	5.5	5.3	5.2	5.4

(1) Displacement sensor detached during shaking

Table E.2 Key test results of Failure Tests

Anchor Type; Anchor Size; NCS Type	Crack Width, mm	Floor Motion	Scale Factor, %	Accumulated Anchor Displacement during Shaking, mm				Maximum Anchor Load during Shaking, kN			
				1 (SW)	2 (NW)	3 (SE)	4 (NE)	1 (SW)	2 (NW)	3 (SE)	4 (NE)
UC1; M10; Heavy	0.8	FM02	40	1.94	-(1)	1.95	2.31	29.4	40.1	28.1	24.3
			70	1.48	3.07	1.40	1.89	36.1	40.9	32.2	32.3
			100	4.16	6.47	3.60	5.16	40.2	44.4	47.3	43.2
			130	7.69	-(1)	8.21	-(1)	40.1	43.1	45.5	45.9
EAb1; 1/2"; Heavy	0.8	FM02	20	4.37	3.23	3.25	2.29	9.5	9.4	11.9	8.7
			40	7.04	6.84	6.81	3.33	24.8	30.8	36.5	28.1
			60	-(1)	35.00	9.44	17.40	31.8	35.3	41.2	33.8

(1) Displacement sensor detached during shaking

Table E.3 Key test results of Displacement Tests

Anchor Type; Anchor Size; NCS Type	Crack Width, mm	Floor Motion	Scale Factor, %	Accumulated Anchor Displacement during Shaking, mm				Maximum Anchor Load during Shaking, kN			
				1 (SW)	2 (NW)	3 (SE)	4 (NE)	1 (SW)	2 (NW)	3 (SE)	4 (NE)
UC1; M10; Heavy	0.5	FM02	31	0.25	0.66	0.33	0.51	26.8	26.2	22.2	18.9
		FM03	48	0.43	1.25	0.29	0.72	30.9	24.7	27.8	22.1
		FM05	90	2.06	0.38	1.34	0.54	29.2	25.9	24.1	27.1
		FM08	34	0.55	0.09	0.50	0.20	15.1	18.4	9.5	7.9
		FM12	103	1.50	1.41	1.29	1.24	23.4	28.5	17.5	24.6
		FM13	96	1.27	0.84	0.84	0.60	37.6	26.2	33.8	30.0
		FM14	67	3.08	3.57	1.73	3.86	38.9	36.4	40.6	38.7
		FM16	74	-(1)	0.18	0.69	0.12	22.7	27.8	17.5	25.1
		FM18	59	0.40	0.49	0.47	0.38	33.4	27.2	27.7	24.8
		FM19	74	0.48	0.81	0.40	0.39	35.4	19.7	29.1	25.2
		FM20	101	0.38	0.06	0.40	0.24	15.9	21.5	26.1	14.0
	0.8	FM02	31	1.44	1.22	1.05	1.50	17.0	18.1	19.4	17.3
		FM03	48	-(1)	-(1)	1.50	5.18	20.3	19.0	18.4	22.3
		FM05	90	2.63	1.17	3.00	1.07	22.1	33.3	30.2	31.5
		FM08	34	2.51	1.32	2.14	0.75	25.6	21.0	17.2	25.7
		FM12	103	2.42	1.65	2.44	0.47	19.2	23.6	17.9	28.1
		FM13	96	3.11	2.38	5.12	1.46	35.2	26.2	25.3	35.7
		FM14	67	6.80	6.33	5.82	5.07	40.8	28.6	22.9	39.9
		FM16	74	5.40	3.09	4.19	1.19	25.5	31.2	27.9	37.6
		FM18	59	3.15	3.76	2.18	2.25	28.1	23.3	25.8	29.4
		FM19	74	0.92	1.74	0.86	1.21	30.9	28.2	39.3	23.2
		FM20	101	0.86	0.30	0.99	0.22	13.9	23.5	26.5	14.5
	0.8*	FM02	31	-(1)	0.44	-(1)	1.12	17.4	21.6	-(2)	18.5
		FM03	48	0.55	0.42	0.98	0.35	13.4	17.3	23.3	20.5
		FM05	90	1.59	0.01	2.45	0.05	17.6	14.0	29.2	26.4
		FM08	34	1.66	0.63	2.41	0.78	17.0	25.0	24.4	24.6
		FM12	103	0.22	0.35	0.80	0.18	16.1	24.3	27.0	23.2
		FM13	96	1.93	0.43	2.99	0.35	24.1	29.9	32.8	28.5
		FM14	67	5.60	2.28	7.06	2.22	39.4	37.0	43.3	43.6
		FM16	74	4.30	0.27	3.51	1.16	20.8	30.3	-(2)	25.1
		FM18	59	0.82	0.35	1.09	0.83	13.8	19.2	-(2)	19.9
		FM19	74	1.04	0.20	1.33	1.23	18.4	12.4	-(2)	15.4
		FM20	101	-(1)	0.25	2.18	0.59	16.7	28.8	-(2)	20.5
EAb1; 1/2"; Heavy	0.5	FM02	15	0.40	0.96	1.12	1.06	10.6	10.4	9.8	6.9
		FM03	18	-(1)	1.42	1.06	1.35	18.1	11.7	8.9	8.3
		FM05	36	4.26	1.53	5.51	0.71	14.3	19.7	11.8	10.0
		FM08	14	1.20	0.30	2.41	0.58	7.0	11.6	5.9	5.8
		FM12	41	1.33	0.52	1.97	0.72	10.1	14.8	10.7	7.3
		FM13	38	0.76	1.32	1.14	1.17	15.6	16.4	8.6	9.4
		FM14	27	1.30	2.32	1.16	1.22	11.2	19.0	11.6	9.6
		FM16	30	-(1)	0.42	1.41	0.76	8.11	12.1	6.3	8.2
		FM18	24	1.09	0.57	1.45	0.85	10.6	9.5	6.8	7.3
		FM19	30	0.33	1.13	0.68	0.35	14.3	15.5	13.1	6.7
		FM20	40	0.60	0.22	0.84	0.04	8.7	16.7	10	5.5
	0.8	FM02	15	2.74	2.93	4.17	3.56	7.4	12.5	9.8	7.3
		FM03	18	0.96	2.35	2.91	3.75	15.6	12.5	8.8	7.7
		FM05	36	4.63	3.04	7.24	5.33	16.9	18.0	11.0	11.0
		FM08	14	7.24	1.46	8.92	2.58	15.0	16.9	10.6	7.7
		FM12	41	5.12	0.66	8.50	2.11	13.2	19.5	10.4	7.6
		FM13	38	3.45	2.72	3.79	2.35	18.5	21.3	13.6	11.4
		FM14	27	4.38	4.33	3.97	3.33	18.7	22.0	20.3	19.3
		FM16	30	-(1)	0.68	6.54	1.31	12.4	15.8	10.8	10.5
		FM18	24	3.57	1.65	5.17	2.62	15.3	12.0	9.0	8.2
		FM19	30	2.22	1.66	2.18	1.25	8.7	20.1	9.7	9.6
		FM20	40	2.14	0.24	2.42	0.17	9.1	20.7	9.9	10.4

(*) Tests with 2 anchors in crack
(1) Displacement sensor detached during shaking
(2) Load washer defect

Appendix F: Calculated Displacement Data Reference-Test Based Model

a1)

$N_{u,m,cr}$	= 34.2 kN		Ultimate load reference tests
N_w^*	= 0.4 $N_{u,m,cr}$		Reference permanent load level
w_1^*	= 0.5 mm		Reference crack width
$\Delta s_{cyc,n}^*$	= 0.09 mm		Incremental reference anchor displacement
s_i	= 0.30 mm		Initial displacement
cal. $\left(\frac{s(0.5N_{u,m,cr})}{s(0.5N_{u,m,uncr})}\right)$	= 1.5		Data base evaluation

n	$N_{w,n}/N_{u,m,cr}$	$w_{1,n}$	$\Delta s_{cyc,n}$	s_{cyc}	$s_{cyc} + s_i$	$N_{w,n}$
					0.00	0.0
1	0.4	0.08	0.0	0.01	0.31	13.7
2	0.4	0.08	0.0	0.02	0.32	13.7
3	0.4	0.08	0.0	0.03	0.33	13.7
4	0.4	0.08	0.0	0.04	0.34	13.7
5	0.4	0.08	0.0	0.05	0.35	13.7
6	0.4	0.08	0.0	0.05	0.35	13.7
7	0.4	0.08	0.0	0.06	0.36	13.7
8	0.4	0.08	0.0	0.07	0.37	13.7
9	0.4	0.08	0.0	0.08	0.38	13.7
10	0.4	0.08	0.0	0.09	0.39	13.7
11	0.4	0.16	0.0	0.11	0.41	13.7
12	0.4	0.16	0.0	0.13	0.43	13.7
13	0.4	0.16	0.0	0.14	0.44	13.7
14	0.4	0.16	0.0	0.16	0.46	13.7
15	0.4	0.16	0.0	0.18	0.48	13.7
16	0.4	0.16	0.0	0.20	0.50	13.7
17	0.4	0.24	0.0	0.23	0.53	13.7
18	0.4	0.24	0.0	0.25	0.55	13.7
19	0.4	0.24	0.0	0.28	0.58	13.7
20	0.4	0.24	0.0	0.31	0.61	13.7
21	0.4	0.32	0.0	0.34	0.64	13.7
22	0.4	0.32	0.0	0.38	0.68	13.7
23	0.4	0.32	0.0	0.41	0.71	13.7
24	0.4	0.40	0.0	0.46	0.76	13.7
25	0.4	0.40	0.0	0.50	0.80	13.7
26	0.4	0.48	0.1	0.56	0.86	13.7
27	0.4	0.48	0.1	0.61	0.91	13.7
28	0.4	0.56	0.1	0.68	0.98	13.7
29	0.4	0.56	0.1	0.74	1.04	13.7
30	0.4	0.64	0.1	0.81	1.11	13.7
31	0.4	0.72	0.1	0.89	1.19	13.7
32	0.4	0.80	0.1	0.98	1.28	13.7

a2)

$N_{u,m,cr}$	= 19.2 kN		Ultimate load reference tests
N_w^*	= 0.4 $N_{u,m,cr}$		Reference permanent load level
w_1^*	= 0.5 mm		Reference crack width
$\Delta s_{cyc,n}^*$	= 0.23 mm		Incremental reference anchor displacement
s_i	= 0.10 mm		Initial displacement
cal. $\left(\frac{s(0.5N_{u,m,cr})}{s(0.5N_{u,m,uncr})}\right)$	= 1.5		Data base evaluation

n	$N_{w,n}/N_{u,m,cr}$	$w_{1,n}$	$\Delta s_{cyc,n}$	s_{cyc}	$s_{cyc} + s_i$	$N_{w,n}$
					0.00	0.0
1	0.4	0.08	0.02	0.02	0.12	7.7
2	0.4	0.08	0.02	0.05	0.15	7.7
3	0.4	0.08	0.02	0.07	0.17	7.7
4	0.4	0.08	0.02	0.09	0.19	7.7
5	0.4	0.08	0.02	0.12	0.22	7.7
6	0.4	0.08	0.02	0.14	0.24	7.7
7	0.4	0.08	0.02	0.16	0.26	7.7
8	0.4	0.08	0.02	0.18	0.28	7.7
9	0.4	0.08	0.02	0.21	0.31	7.7
10	0.4	0.08	0.02	0.23	0.33	7.7
11	0.4	0.16	0.05	0.28	0.38	7.7
12	0.4	0.16	0.05	0.32	0.42	7.7
13	0.4	0.16	0.05	0.37	0.47	7.7
14	0.4	0.16	0.05	0.41	0.51	7.7
15	0.4	0.16	0.05	0.46	0.56	7.7
16	0.4	0.16	0.05	0.51	0.61	7.7
17	0.4	0.24	0.07	0.58	0.68	7.7
18	0.4	0.24	0.07	0.64	0.74	7.7
19	0.4	0.24	0.07	0.71	0.81	7.7
20	0.4	0.24	0.07	0.78	0.88	7.7
21	0.4	0.32	0.09	0.87	0.97	7.7
22	0.4	0.32	0.09	0.97	1.07	7.7
23	0.4	0.32	0.09	1.06	1.16	7.7
24	0.4	0.40	0.12	1.17	1.27	7.7
25	0.4	0.40	0.12	1.29	1.39	7.7
26	0.4	0.48	0.14	1.43	1.53	7.7
27	0.4	0.48	0.14	1.56	1.66	7.7
28	0.4	0.56	0.16	1.73	1.83	7.7
29	0.4	0.56	0.16	1.89	1.99	7.7
30	0.4	0.64	0.18	2.07	2.17	7.7
31	0.4	0.72	0.21	2.28	2.38	7.7
32	0.4	0.80	0.23	2.51	2.61	7.7

a3)

$N_{u,m,cr}$	= 21.8 kN		Ultimate load reference tests
N_w^*	= 0.4 $N_{u,m,cr}$		Reference permanent load level
w_1^*	= 0.5 mm		Reference crack width
$\Delta s_{cyc,n}^*$	= 1.34 mm		Incremental reference anchor displacement
s_i	= 1.00 mm		Initial displacement
cal. $\left(\frac{s(0.5N_{u,m,cr})}{s(0.5N_{u,m,uncr})}\right)$	= 3.0		Data base evaluation (yielded ~ 5.0, however, limited to 3 with respect to ETAG001, Clause 3.2.1)

n	$N_{w,n}/N_{u,m,cr}$	$w_{1,n}$	$\Delta s_{cyc,n}$	s_{cyc}	$s_{cyc} + s_i$	$N_{w,n}$
					0.00	0.0
1	0.4	0.08	0.13	0.13	1.13	8.7
2	0.4	0.08	0.13	0.27	1.27	8.7
3	0.4	0.08	0.13	0.40	1.40	8.7
4	0.4	0.08	0.13	0.54	1.54	8.7
5	0.4	0.08	0.13	0.67	1.67	8.7
6	0.4	0.08	0.13	0.80	1.80	8.7
7	0.4	0.08	0.13	0.94	1.94	8.7
8	0.4	0.08	0.13	1.07	2.07	8.7
9	0.4	0.08	0.13	1.21	2.21	8.7
10	0.4	0.08	0.13	1.34	2.34	8.7
11	0.4	0.16	0.27	1.61	2.61	8.7
12	0.4	0.16	0.27	1.88	2.88	8.7
13	0.4	0.16	0.27	2.14	3.14	8.7
14	0.4	0.16	0.27	2.41	3.41	8.7
15	0.4	0.16	0.27	2.68	3.68	8.7
16	0.4	0.16	0.27	2.95	3.95	8.7
17	0.4	0.24	0.40	3.35	4.35	8.7
18	0.4	0.24	0.40	3.75	4.75	8.7
19	0.4	0.24	0.40	4.15	5.15	8.7
20	0.4	0.24	0.40	4.56	5.56	8.7
21	0.4	0.32	0.54	5.09	6.09	8.7
22	0.4	0.32	0.54	5.63	6.63	8.7
23	0.4	0.32	0.54	6.16	7.16	8.7
24	0.4	0.40	0.67	6.83	7.83	8.7
25	0.4	0.40	0.67	7.50	8.50	8.7
26	0.4	0.48	0.80	8.31	9.31	8.7
27	0.4	0.48	0.80	9.11	10.11	8.7
28	0.4	0.56	0.94	10.05	11.05	8.7
29	0.4	0.56	0.94	10.99	11.99	8.7
30	0.4	0.64	1.07	12.06	13.06	8.7
31	0.4	0.72	1.21	13.27	14.27	8.7
32	0.4	0.80	1.34	14.61	15.61	8.7

b)

n	$N_{w,n}/N_{u,m,cr}$	$w_{1,n}$	$\Delta s_{cyc,n}$	s_{cyc}	$s_{cyc} + s_i$	$N_{w,n}$
					0.00	0.0
1	0.4	0.10	0.15	0.15	1.15	8.5
2	0.4	0.10	0.15	0.30	1.30	8.5
3	0.4	0.10	0.15	0.45	1.45	8.5
4	0.4	0.10	0.15	0.60	1.60	8.5
5	0.4	0.10	0.15	0.75	1.75	8.5
6	0.4	0.10	0.15	0.90	1.90	8.5
7	0.4	0.10	0.15	1.06	2.06	8.5
8	0.4	0.10	0.15	1.21	2.21	8.5
9	0.4	0.10	0.15	1.36	2.36	8.5
10	0.4	0.10	0.15	1.51	2.51	8.5
11	0.4	0.10	0.15	1.66	2.66	8.5
12	0.4	0.10	0.15	1.81	2.81	8.5
13	0.4	0.10	0.15	1.96	2.96	8.5
14	0.4	0.10	0.15	2.11	3.11	8.5
15	0.4	0.10	0.15	2.26	3.26	8.5
16	0.4	0.10	0.15	2.41	3.41	8.5
17	0.4	0.10	0.15	2.56	3.56	8.5
18	0.4	0.10	0.15	2.71	3.71	8.5
19	0.4	0.10	0.15	2.86	3.86	8.5
20	0.4	0.10	0.15	3.02	4.02	8.5
21	0.4	0.20	0.30	3.32	4.32	8.5
22	0.4	0.20	0.30	3.62	4.62	8.5
23	0.4	0.20	0.30	3.92	4.92	8.5
24	0.4	0.20	0.30	4.22	5.22	8.5
25	0.4	0.20	0.30	4.52	5.52	8.5
26	0.4	0.20	0.30	4.82	5.82	8.5
27	0.4	0.20	0.30	5.13	6.13	8.5
28	0.4	0.20	0.30	5.43	6.43	8.5
29	0.4	0.20	0.30	5.73	6.73	8.5
30	0.4	0.20	0.30	6.03	7.03	8.5
31	0.4	0.30	0.45	6.48	7.48	8.5
32	0.4	0.30	0.45	6.93	7.93	8.5
33	0.4	0.30	0.45	7.39	8.39	8.5
34	0.4	0.30	0.45	7.84	8.84	8.5
35	0.4	0.30	0.45	8.29	9.29	8.5
36	0.4	0.40	0.60	8.89	9.89	8.5
37	0.4	0.40	0.60	9.50	10.50	8.5
38	0.4	0.40	0.60	10.10	11.10	8.5
39	0.4	0.40	0.60	10.70	11.70	8.5
40	0.4	0.40	0.60	11.31	12.31	8.5
41	0.4	0.50	0.75	12.06	13.06	8.5
42	0.4	0.50	0.75	12.81	13.81	8.5
43	0.4	0.50	0.75	13.57	14.57	8.5
44	0.4	0.50	0.75	14.32	15.32	8.5
45	0.4	0.50	0.75	15.08	16.08	8.5
46	0.5	0.60	1.13	16.21	17.21	10.6
47	0.5	0.60	1.13	17.34	18.34	10.6
48	0.5	0.60	1.13	18.47	19.47	10.6
49	0.5	0.60	1.13	19.60	20.60	10.6
50	0.5	0.60	1.13	20.73	21.73	10.6
51	0.5	0.70	1.32	22.05	23.05	10.6
52	0.5	0.70	1.32	23.37	24.37	10.6
53	0.5	0.70	1.32	24.69	25.69	10.6
54	0.5	0.70	1.32	26.00	27.00	10.6
55	0.5	0.70	1.32	27.32	28.32	10.6
56	0.5	0.80	1.51	28.83	29.83	10.6
57	0.5	0.80	1.51	30.34	31.34	10.6
58	0.5	0.80	1.51	31.85	32.85	10.6
59	0.5	0.80	1.51	33.35	34.35	10.6

Figure F.1 Exemplary calculation of displacement: a) Crack cycling tests with stepwise increasing crack protocol (n = 32) – a1) UC1; a2) SA1; a3) EAb1; b) Seismic qualification tests (n = 59) – EAb1

Curriculum Vitae

Personal Data

Philipp Mahrenholtz
Born on the 25th of February, 1974
in Brunswick, Germany.

Education

1980 – 1986	Elementary School, Brunswick
1986 – 1993	Highschool ‘Gymnasium Kleine Burg’, Brunswick
1993 – 1998	University of Aachen (RWTH), Germany
1998	Imperial College of London, United Kingdom
1998	*Diplom-Ingenieur (M.Sc.)*
2006 – 2012	University of Stuttgart, Germany
2010 – 2011	University of California, San Diego, United States
2012	*Doktor-Ingenieur (Ph.D.)*

Experience

1998 – 2002	Züblin AG, Munich and Stuttgart, Germany Site Engineer
2002 – 2003	Züblin International Singapore, Singapore Project Engineer
2003 – 2005	Züblin AG, Munich and Frankfurt, Germany Project Manager
2005 – 2006	Züblin Tunnelling, Cologne, Germany, and Rotterdam, Netherlands Senior Engineer
2006 – 2012	University of Stuttgart, Germany Test Engineer, Teaching Assistant, Research Engineer
2010 – 2011	University of California, San Diego, United States Visiting Researcher
2012	Seoul National University, Seoul, Korea Post-doctoral Researcher

Scholars have the greatest responsibility to the people. Their work can ultimately improve the lives of all people in future. But if an academic becomes lost in his study, he cannot see the benefit of his work. Therefore, like a well balanced fencing stance, or a reasonable argument, the scholar must have a fair and balanced mind.

King Sejong the Great, 1397 – 1450

Hiermit versichere ich, die vorliegende Dissertation ohne Hilfe Dritter nur mit den angegebenen Quellen und Hilfsmitteln angefertigt zu haben. Alle Stellen, die aus den Quellen entnommen wurden, sind als solche kenntlich gemacht worden. Diese Arbeit hat in gleicher oder ähnlicher Form noch keiner Prüfungsbehörde vorgelegen.